UNIVERSITY OF OKLAHOMA

GRADUATE COLLEGE

DESIGN AND SYNTHESIS OF OSW-1 ANALOGS AND OTHER BIOACTIVE SMALL MOLECULES FOR POTENTIAL THERAPEUTIC APPLICATIONS

A DISSERTATION

SUBMITTED TO THE GRADUATE FACULTY

in partial fulfillment of the requirements for the

Degree of

DOCTOR OF PHILOSOPHY

By

ANH THI QUYNH LE
Norman, Oklahoma
2018

DESIGN AND SYNTHESIS OF OSW-1 ANALOGS AND OTHER BIOACTIVE SMALL MOLECULES FOR POTENTIAL THERAPEUTIC APPLICATIONS

A DISSERTATION APPROVED FOR THE
DEPARTMENT OF CHEMISTRY AND BIOCHEMISTRY

BY

Dr. Anthony W. G. Burgett, Chair

Dr. Christina R. Bourne

Dr. Laura E. Bartley

Dr. Daniel T. Glatzhofer

Dr. George B. Richter-Addo

To my grandpa, who taught me patience and perseverance.

Acknowledgements

First and foremost, I would like to thank Dr. Burgett for welcoming me into his lab and giving me opportunities to pursue my scientific curiosity, for his guidance and mentorship, for the encouragement when I faced road blocks, for all the fun and exciting final Friday get-togethers over the years. I also would like to acknowledge my committee members for their support and their time, Dr. Glatzhofer, Dr. Richter-Addo, Dr. Bourne and Dr. Bartley.

I would like to thank all the past and current members of the Burgett's lab. I have learned a lot from all of you. I have special thanks to Rama -for always having my back, to Juan - for showing me the way during my first year here, to Cori - for becoming my partner-in-crime in the organic crew, and to Angel - a honorary Burgett's lab member who published with me and became my one of my best friends.

More than 10 years ago, I came to the US knowing nobody. My host family opened their arms and accepted me to their family. Mom and Poppa, I would not have made it to where I am today without you-Thank you! Thank you to all my host siblings, especially Leah for proof-reading through all my essays regardless the subjects.

I came to Oklahoma as a stranger, but I have built my home and family here. Special thanks to my wonderful husband, Mike, who has been coaching me through grad school, been by my side and helped me believe in myself.

Finally, I would like to thank my family. I would like to thank my sister, Tram, for joining me here in Oklahoma and feeding me when I forget to eat. My biggest thanks go to my parents, for letting me pursuing my dreams, for their endless supports and encouragements.

Table of Contents

Acknowledgements v

List of Tables xi

List of Schemes xii

List of Figures xv

Abstract xviii

Chapter I: Introduction and Background 1

I.1 Plant-derived saponin natural products 1

I.1.1 Isolation and characterization of saponin OSW-1 1

I.1.2 Other cholestane glycosides from *O. saundersiae* bulb 4

I.2 Biological activity of steroidal glycoside OSW-1 and related compounds 6

I.2.1 OSBP/ORP protein family 9

I.2.2 OSBP and ORP4 as therapeutic targets for precision medicine 10

I.3 OSW-1 as a synthetic target 11

I.3.1 Total synthesis of OSW-1 by Yu's group 11

I.3.2 Total synthesis of OSW-1 by Jin's group 16

I.3.3 Total synthesis of OSW-1 by Morzycki's group 19

I.3.4 Total synthesis of OSW-1 by Yu's group 20

I.3.5 Total synthesis of OSW-1 by Tsubuki's group 23

I.3.6 Total synthesis of OSW-1 by Guo's group 24

I.4 Personalized cancer therapy through Single-probe quantitative Single Cell Mass Spectrometry 27

I.5 Precision medicine in myopia: development of selective inhibitor for retinaldehyde dehydrogenase enzymes 27

Chapter II : Synthesis and Characterization of Natural Product OSW-1 Probe Analogs 29

II.1 Introduction 30

II.2 Design of OSW-1 Analogs 31

II.2.1 Deuterated OSW-1: internal standard for MS quantification of OSW-1 31

II.2.2 TBS-OSW-1: a biologically inactive analog as a negative control compound 32

II.2.3 OSW-1 analogs with amine linker 33

II.3 Results and discussion 34

II.3.1 Synthesis of L-arabinose moiety of OSW-1 34

II.3.2 Synthesis of D-xylose and disaccharide moieties of OSW-1 36

II.3.3 Synthesis of deuterated disaccharide glycosyl donor of OSW-1 40

II.3.4 Synthesis of deuterated OSW-1 41

II.3.5 Synthesis of TBS-OSW-1-a biologically inactive OSW-1 analog 46

II.3.6 Synthesis of OSW-1 analogs with amine linker 47

II.4 Conclusions 52

II.5 Experimental section 53

II.5.1 General methods 53

II.5.2 Compound data 54

II.6 Chapter appendix 93

Chapter III : Design and Synthesis of Modified OSW-1 Scaffolds- a Two-component Approach 112
III.1 Introduction and Background 113
III.2 Designs of simplified scaffolds for OSW-1 mimetics 115
III.2.1 Structure-activity relationship (SAR) of the OSW-1 compound 115
III.2.2 Rationale and design of new OSW-1 scaffolds through a two-component approach 116
III.3 Results and discussion 120
III.3.1 Validation of the two-component approach to OSW-1-related scaffolds .. 120
III.3.1.1 Intramolecular hydroalkoxylation reaction 120
III.3.1.2 Tandem carbonyl ene-hydroalkoxylation reaction 122
III.3.2 Synthesis of OSW-1-related analogs with only E-ring modification 124
III.3.2.1 Synthesis of homoallylic alcohols 3.18 125
III.3.2.2 Investigation of pathways to spiro-oxetane product 3.21 128
III.3.2.3 Synthesis of steroidal homoallylic amines 134
III.3.2.4 N-glycosylation to form OSW-1-related analogs: trials and tribulations 137
III.4 Conclusion 147
III.5 Experimental section 147
III.5.1 General methods 147
III.5.2 Compound data 148
III.6 Chapter appendix 192

Chapter IV : Synthesis, Characterization and Evaluation of Stable-isotopically Labeled Anti-cancer Compounds for Precision Medicine 248
IV.1 Introduction 249
IV.1.1 Personalized medicine in cancer therapy 249
IV.1.2 Single Cell Mass Spectrometry and its application in personalized cancer medicine 251
IV.1.3 Anti-cancer compounds used in qSCMS studies 253
IV.2 Results and discussion 254
IV.2.1 Syntheses of stable-isotopically labeled anti-cancer compounds 255
IV.2.1.1 Synthesis and characterization of d-OSW-1 255
IV.2.1.2 Synthesis and characterization of $^{15}N,^{13}C$-labeled Gemcitabine 255
IV.2.1.3 Synthesis and characterization of ^{15}N-labeled Cisplatin 259
IV.2.2 Application of stable-isotopically labeled anti-cancer compounds in qSCMS 260
IV.3 Conclusion 264
IV.4 Experimental section 265
IV.4.1 General methods 265
IV.4.2 Compound data 266
IV.4.3 Cell cytotoxicity assay 270
IV.5 Chapter appendix 272
Chapter V : Synthesis, Characterization and Evaluation of α,α-Dichloro-all-trans-retinone (DAR) as a Selective Inhibitor for Retinaldehyde Dehydrogenase Enzymes 291

V.1 Introduction and background 291
V.2 Results and discussion 294
V.2.1 Structure-based design of DAR 294
V.2.2 Synthesis and characterization of DAR 295
V.2.3 Biological evaluation of DAR 297
V.2.3.1 Effects of DAR on aldehyde dehydrogenase activity 297
V.2.3.2 DAR is an irreversible inhibitor of RALDH2 299
V.2.3.3 DAR inhibits all-*trans*-retinoic acid synthesis in a RALDH2 expressing cell line 300
V.3 Conclusions 303
V.4 Experimental section 303
V.4.1 General methods 303
V.4.2 Compound data 304
V.4.3 LCMS calibration curve for all-*trans*-retinoic acid 308
V.5 Chapter appendix 310
Chapter VI : Conclusions and Outlooks 320
Appendix 324
References 391

List of Tables

Table 1. Condition screening for intramolecular hydroalkoxylation reaction 121

Table 2. Condition screening for tandem carbonyl ene-cyclization reaction 123

Table 3. Condition screening for carbonyl-ene reaction 126

Table 4. Condition screening of Schmidt glycosylation reaction 139

Table 5. Optimization of Fukuyama-Mitsunobu glycosylation reaction with monosaccharide 144

Table 6. Optimization of Fukuyama-Mitsunobu glycosylation reaction with OSW-1 disaccharide moiety 145

Table 7. 2D NMR assignment of spiro-oxetane 3.21 157

List of Schemes

Scheme 1. Total synthesis of OSW-1 by Yu's group 15

Scheme 2. Total synthesis of OSW-1 from Jin's group 18

Scheme 3. Total synthesis of OSW-1 by Morzycki's group 20

Scheme 4. Total synthesis of OSW-1 by Yu's group 22

Scheme 5. Total synthesis of OSW-1 by Tsubuki's group 24

Scheme 6. Total synthesis of OSW-1 by Guo's group 26

Scheme 7. Synthesis of L-arabinose moiety 36

Scheme 8. Synthesis of D-xylose moiety of OSW-1 38

Scheme 9. Synthesis of OSW-1 disaccharide moiety 39

Scheme 10. Synthesis of deuterated disaccharide glycosyl donor of OSW-1 41

Scheme 11. Synthesis of *d*-OSW-1 42

Scheme 12. Synthesis of TBS-OSW-1 46

Scheme 13. Synthesis of diamine linker 47

Scheme 14. Synthesis of OSW-1-linker derivatives 50

Scheme 15. A) Structure of OSW-1; B) proposed OSW-1-related scaffolds; C) the proposed two-component approach to OSW-1-related scaffolds 118

Scheme 16. A) Aldehyde-version of two-component approach; B) OSW-1 analogs with E-ring modification 119

Scheme 17. Intramolecular hydroalkoxylation reaction with sterol 3.10 (TBS = tert-butyldimethylsilyl) 120

Scheme 18. Tandem carbonyl-ene and hydroalkoxylation reactions 123

Scheme 19. Retrosynthesis of OSW-1 analogs with E-ring modification 125

Scheme 20. Carbonyl-ene reaction to form homoallylic alcohols 126

Scheme 21. A) Synthesis of 4-methylpentanal; B) carbonyl-ene reaction with 4-methylpentanal 127

Scheme 22. Reactions of acetylated pregnadiene 3.19 with 4-methylpentanoic acid or acetone 129

Scheme 23. Formation and fragmentation of 4-hydroxy-4-methylpentanoic acid..... 130

Scheme 24. Conversion of dimethyl-γ-butyrolactone to 4-hydroxy-4-methylpentanoic acid 131

Scheme 25. Reactions of diene 3.19 with sodium 4-hydroxy-4-methylpentanoate or 4-hydroxy-4-methylpentanoic acid 133

Scheme 26. Synthesis of homoallylic amines from C-acetylated homoallylic alcohol 3.20 134

Scheme 27. Synthesis of C-3-PMB protected homoallylic amines 136

Scheme 28. Schmidt glycosylation of homoallylic amine 3.28 and disaccharide imidates 43 afforded *O*-glycosylated product 138

Scheme 29. N-glycosylation through Schmidt glycosylation method 139

Scheme 30. A) Reported N-glycosylation of indole derivative and chloro sugar[81]; B) N-glycosylation of homoallylic amines and bromo-L-arabinopyranoside 141

Scheme 31. Synthesis of *N*-2-nitrobenzenesulfonyl-protected amines and 2,3,4-triacetyl-α,β-L-arabinopyranose 142

Scheme 32. Fukuyama-Mitsunobu reaction of Ns-amines and L-arabinosyl hemiacetal 143

Scheme 33. Fukuyama-Mitsunobu reaction with OSW-1 disaccharide moiety..... 145

Scheme 34. Synthesis of OSW-1 mimetics 146

Scheme 35. Synthesis of stable-isotopically labeled Gemcitabine 256

Scheme 36. Synthesis of ^{15}N-labeled cisplatin 259

Scheme 37. Synthesis of α,α-dichloro-all-trans-retinone DAR 295

List of Figures

Figure 1. First natural products isolated from *O. saundersiae* bulb, and numbering system of OSW-1. Figure is adapted from Kubo *et al*.[3] 2

Figure 2. Natural products isolated from *O. saundersiae* bulb. Figure is adapted from Tang *et al*.[4] 6

Figure 3. Chemical structures of ORPphillins: cephalostatin, ritterazine B, stelletin E, OSW-1(2), schweinfurthin A and B. Figure is adapted from Burgett *et al*.[10] 8

Figure 4. OSBP and ORP4L protein domain sequence and homology diagram. Figure is adapted from Juan Nuñez dissertation. 9

Figure 5. A) OSW-1 retrosynthesis; B) *d*-OSW-1 and TBS-OSW-1 analogs 32

Figure 6. OSW-1 analogs with amine linker 33

Figure 7. Possible side products in glycosylation reaction to assemble *d*-OSW-1 43

Figure 8. ^{1}H NMR of OSW-1 (top), 108-*d*-OSW-1 (middle), ^{2}H NMR of d-OSW-1 (bottom) 45

Figure 9. Representative Inhibition Binding Curves of OSBP for the OSW-1 compound (A) and OSW-1 analogs with linker (B, C, and D). Figure is adapted from Juan Nuñez's dissertation. 52

Figure 10. Structure-activity relationship (SAR) of the OSW-1 compound 116

Figure 11. ^{1}H NMR spectra of lactone 3.23, sodium carboxylate 3.24, and hydroxy acid 3.25 132

Figure 12. Set up schematic of a single cell MS analysis [45] 252

Figure 13. Anti-cancer compounds in qSCMS studies and their stable-isotopically labeled analogs 254

Figure 14. ^{1}H NMR spectra of non-labeled gemcitabine (top) and labeled gemcitabine (bottom) 257

Figure 15. Cytotoxicity assay of non-labeled gemcitabine (Gem) and stable-isotopically labeled Gemcitabine (Labeled Gem) on T-24 cell line 258

Figure 16. ^{1}H NMR spectra of ^{15}N-labeled cisplatin (top) and non-labeled cisplatin (bottom) 260

Figure 17. Schematic of real-time SCMS sampling with the Single-probe (courtesy of Shawna Standke) 261

Figure 18. SCMS spectrum of T-24 (bladder cancer) cells after 2 hours treatment of 1µM OSW-1 with 100nM d-OSW-1 in the sampling solvent (courtesy of Shawna Standke and Ryan Bensen) 262

Figure 19. SCMS spectrum of T-24 (bladder cancer) cells after 1-hour treatment of 0.1µM gemcitabine with 100nM labeled gemcitabine in the sampling solvent (courtesy of Shawna Standke and Ryan Bensen) 263

Figure 20. Mass spectrum of gemcitabine and ^{15}N-labeled-gemcitabine (1 µM) from an individual cell isolated from the urine of a bladder cancer patient (courtesy of Shawna Standke and Ryan Bensen) 264

Figure 21. Structures of WIN 18446, all-*trans*-retinaldehyde, and DAR 294

Figure 22. Crystal structure of the covalent adduct between Cys 320 and WIN 18446; proposed mechanism of adduct formation. Figure is adapted from Chen *et al*. [123] 295

Figure 23. Dose response curves to compare the effect of DAR on chick and human RALDH1a isoforms and human mitochondrial ALDH2 (hALDH2). Data points (A-E)

represent the average ± SEM for triplicate samples. Figure is adapted from Harper *et al*.[47] 298

Figure 24. DAR is an irreversible inhibitor of RALDH2. 300

Figure 25. DAR inhibits all-*trans*-retinoic acid (atRA) synthesis in a RALDH2 expressing cell line. 302

Figure 26. all-trans-retinoic acid LCMS calibration curve 309

Abstract

OSW-1 is a cholestane glycoside natural product with potent anti-proliferative activity, broad spectrum anti-viral activity, and a novel mechanism of action. The OSW-1's cellular targets are oxysterol-binding protein (OSBP) and OSBP-related protein 4 (ORP4). Recently, OSBP has been determined to execute an essential role in the proliferation of many classes of pathogenic viruses. ORP4 has been determined, also recently, to be a driver of cellular proliferation and to be a precision cancer target. The main project of this dissertation research is focused on using organic synthesis to produce new synthetic routes to access new OSW-1-derived compounds. To better understand the compound's mechanism of action and molecular pharmacology, a set of OSW-1 probe analogs were designed and produced. To further the potential development of OSW-1-derived therapeutic compounds, a new approach for the rapid and convergent synthesis of a diverse library of OSW-1 analogs based on a new scaffold was developed. This new approach to OSW-1 analogs synthesis will allow for the future production of analogs with selective affinity for OSBP or ORP4 and improved pharmacological properties. Additionally, a set of stable-isotopically-labeled anti-cancer agents were synthesized to allow the absolute quantification of the drug inside the individual cancer cells through a new mass spectrometry technique. The last project describes the design and synthesis of a retinaldehyde's analog with high selectivity for retinaldehydrogenase (RALDH) enzymes. This novel compound could form the basis for the development of new treatments for blindness caused by pathological myopia.

Chapter I: Introduction and Background

I.1 Plant-derived saponin natural products

Saponins constitute an important class of structurally diverse terpenoid plant-derived natural products with a wide range of biological properties.[1] These compounds display a unique physical property of forming a foamy lather upon shaking in aqueous condition.[2] The trivial name for this class of natural products was therefore derived from the Latin *sapo*, meaning soap.[2] Saponins' general structure consists of a skeleton (either a steroidal-C_{27} or a triterpenoid-C_{30}) with varying numbers of sugar residues attached at different positions.[2] Plant saponins have been reported to exhibit a wide range of biological activities, including cytotoxic, anti-inflammatory, hemolytic, anti-fungal, and anti-bacterial properties.[1] These diverse biological activities of plant saponins have attracted considerable interest in structural characterization, total synthesis of saponins and their analogs for the development of potential therapeutic applications.

I.1.1 Isolation and characterization of saponin OSW-1

In 1992, Sashida group from Tokyo College of Pharmacy reported the isolation and characterization of a family of cholestane glycoside compounds, including the OSW-1 compound (**Figure 1**, compound **2**), from the bulbs of the flowering plant *Ornithogalum saundersiae* .[3] This plant species, which produces attractive blooms used as cut flowers, is native to the Highveld region of South Africa and Swaziland.[3,4] The isolation of the cholestane glycoside compounds from the *O. saundersiae* started with refluxing methanol extraction of minced bulb material. The methanol fraction was then extracted with 1-butanol, and the butanol soluble phase was then fractioned through two rounds of silica gel column chromatography using $CHCl_3$-MeOH as eluent.[3] Further compound separation was

done using octadecylsilanzied (ODS) silica gel column chromatography with methanol-water (4:1) followed by preparative HPLC with methanol-water (12:1) and acetonitrile-water (4:1).[3] This purification yielded three acylated cholestane glycoside compounds (**Figure 1**).[3] 16.2 kg of fresh *Ornithogalum saundersiae* bulbs afforded 25 mg of compound **1a**, 439 mg of compound **2** (OSW-1) and 23.5 mg of compound **1b** (**Figure 1**).[3]

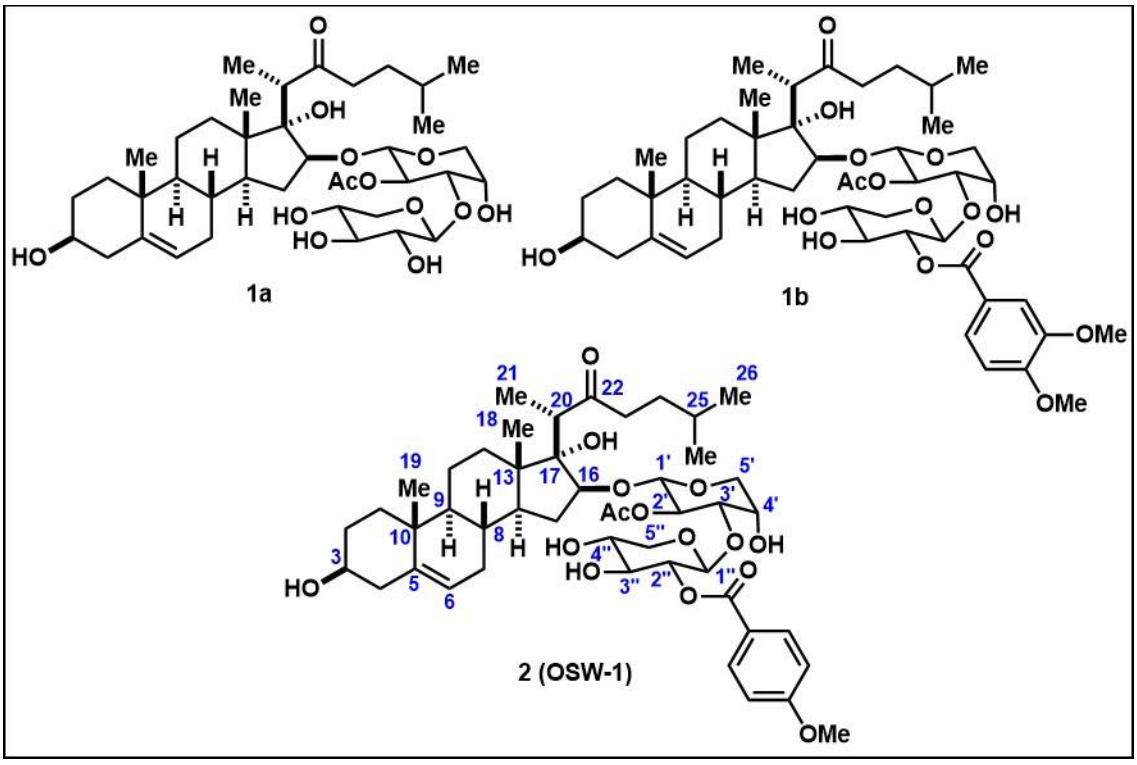

Figure 1. First natural products isolated from *O. saundersiae* bulb, and numbering system of OSW-1. Figure is adapted from Kubo *et al*.[3]

The structural elucidation of the three isolated cholestane glycosides was carried out using a combination of spectroscopic techniques [(mass spectrometry, 1D and 2D-nuclear magnetic resonance spectroscopy (NMR), infrared spectroscopy (IR)] and chemical decomposition. Their molecular formulae were identified through negative-ion fast atom bombardment (FAB) mass spectrometry and ^{13}C NMR.[3] IR absorption bands at 3450 and 1045 cm^{-1} indicated that compound **1a** possesses a glycosidic moiety.[3] The

presence of a carbonyl group in the molecule was shown by the IR (1695 cm^{-1}) and ^{13}C NMR (218.9 ppm) spectra.[3] Furthermore, the IR band at 1740 cm^{-1}, ^{1}H NMR [2.34 ppm (3H, s)] and ^{13}C NMR (170.0 and 21.5 ppm) indicated the presence of an acetyl group.[3] To confirm this, alkaline treatment of compound **1a** with 3% sodium methoxide in methanol resulted in a deacetylated compound.[3]

The ^{13}C NMR spectrum of **1a** showed 27 carbons associated with the aglycon, and 10 carbons associated with the saccharide component.[3] Further analysis of the aglycon carbons by DEPT spectra showed five methyl, nine methylene, eight methine and five quaternary carbon groups.[3] The signals at δ 219.5 (C), 141.9 (C) and 121.2 (CH) were assigned to a carbonyl carbon and a pair of olefinic carbons, respectively.[3] There were three carbons bearing oxygen functions at δ 88.9 (CH), 86.2 (C), and 71.3 (CH).[3] The ^{1}H NMR spectrum of **1a** contained two singlets for tertiary methyl protons at δ 1.08 and 0.94, and three secondary methyl protons at δ 1.32 (*d*, J = 7.4 Hz), 0.92 (*d*, J = 6.4 Hz), and 0.87 (*d*, J = 0.63 Hz).[3] These data together suggested that the structure of **1a** was a cholestane derivative with a carbonyl group and three hydroxy groups, one of which is connected to the carbohydrate moiety.[3]

To characterize the carbohydrate moiety, compound **1a** was subjected to acidic hydrolysis using 1M hydrochloric acid in dioxane-H_2O (1:1).[3] The resulting mixture of sugars was converted to 1-[(S)-N-acetyl-α-methylbenzylamino'-1-deoxyalditol acetate derivatives, then analyzed by HPLC against standards to confirm the absolute configuration [3]. L-arabinose and D-xylose was determined to be the carbohydrate composition of the compounds.[3] By comparing the ^{13}C signals of the sugars with those of reference methyl glycosides, the glycosidic bond was revealed to be β-D-xylopyranosyl-

(1→3)-α-L-arabinopyranose.[3] The position of the acetyl group attachment as being on the C-2 of the arabinose was elucidated by comparing the proton chemical shifts of compound **1a** with the deacetylated compound.[3] In addition to this, the ^{13}C signals of the arabinose C-1 and C-3 of compound **1a** was shifted upfield by 4.0 ppm and 3.7 ppm, respectively, as compared with those of the deacetylated compound.[3]

Compound **2** (later termed OSW-1) had spectral data that were essentially analogous with those of compound **1a** with one exception.[3] In addition to the acetyl group, the spectral data suggested the presence of a 4-methoxybenzoyl group through IR [1690 cm^{-1} (C=O); 1600 and 1510 cm^{-1} (aromatic ring)], UV (λ_{max} 259 nm), ^1H NMR [δ 8.32 and 7.08 (each 2H, *d*, *J* = 8.9 Hz); δ 3.75 (3H, *s*)] and ^{13}C NMR [δ 123.0 (C), 132.4 (CH) x 2, 114.2 (CH) x 2, 163.9 (C), 165.5 (C), and 55.5 (CH_3)] spectra.[3] Furthermore, alkaline hydrolysis of **2** with 4% potassium hydroxide in ethanol yielded **1a** and 4-methoxybenzoic acid. In the ^1H NMR spectrum of **2**, the signal due to the xylose H-2 were shifted downfield by 1.68 ppm as compared with those of **1a** to appear at δ 5.67 (dd, J = 8.9, 7.6 Hz)[3]. Also, the ^{13}C signal due to the xylose C-1 and C-3 were shifted upfield by 3.2 and 3.0 ppm respectively. These data suggested that the 4-methoxybenzoyl group is linked to the C-2 of xylose. The structure of **2** (i.e. OSW-1) was determined to be 3β,16β,17α-trihydroxycholest-5-en-22-one-16-*O*-(2-*O*-4-methoxybenzoyl-β-D-xylopyranosyl)-(1→3)-(2-*O*-acetyl-α-L-arabinopyranoside).

I.1.2 Other cholestane glycosides from *O. saundersiae* bulb

In the years subsequent to the isolation of OSW-1 (1992-2017), over 40 additional structurally diverse cholestane glycoside compounds have been discovered in *Ornithogalum saundersiae* extracts (see **Figure 2** for partial representative of natural

products isolated from *O. saundersiae* bulbs).[4,5] All of these OSW-1-related compounds were identified from either the methanol or n-butanol extracts of the bulb. These natural product compounds, despite sharing the general structure similarity of being cholestane glycosides, differ in the composition of the cholestane steroidal core, the aliphatic side chains, and the composition of glycoside moiety.

The cholestane glycoside most closely related to OSW-1 retain the 3β,16β,17α-trihydroxyl cholestane aglycon linked with glycoside moiety (mainly L-arabinose and D-xylose) through C-16 hydroxyl group (**Figure 2**). In these related compounds, the C-3 position is either a free hydroxyl or, in the case of **1d** and **1e**, the C-3 hydroxyl is glycosylated with β-D-glucopyranoside. Remaining differences are observed within the D-xylopyranosyl moiety.[4] The benzoate portion on C-2 have different substitution patterns ranging from different numbers of methoxy groups on the benzoate moiety (mono-, di-, or tri-methoxybenzoate) to different aromatic motifs (benzoate vs. cinnamoyl). C-3 hydroxyl of D-xylose moiety remained free hydroxyls. C-4 hydroxyl, in two instances in compound **1f** and **1g**, is linked to β-D-glycopyranoside through a glycosidic link.[4]

Some of the isolated compounds have a monosaccharide component (L-rhamnopyranoside) instead of the disaccharide moiety similar to OSW-1.[6] Compounds **3a-3f** shared the same polyhydroxylated cholestane steroidal core with 3β, 11α, 16β-hydroxyls.[7] The hydroxyl group at C-2 of L-rhamnopyranoside can sometimes be acetylated.[7] The C-3 hydroxyl group of L-rhamnopyranoside either exists as free hydroxyl, or capped as either acetate or 3,4,5-trimethoxybenzoate group.[8] It is interesting to note that the steroidal core of this group of compounds lacks the C-17 hydroxyl group, and C-22 in the aliphatic sidechain exists as an alcohol as compared to ketone in OSW-1.[4] Compounds

4a-4c are very similar to compound **3**-subfamily, but have an olefin at C-24 and C-25 of the aliphatic chain.[7,8] Compound **5**, even though isolated from the same source, has quite a different structure compared to OSW-1.[8] C-1 in the steroidal core of **5** is bulkier with the appended β-D-glycopyranosyl moiety.[8] The aliphatic side chain of **5** is not functionalized at C-22, but possesses C-23-C-24 olefin and C-25 hydroxyl group.[8] Compound **5** only has a monosaccharide of L-arabinopyranoside with 3,4,5-trimethoxybenzoate group on C-2.[8]

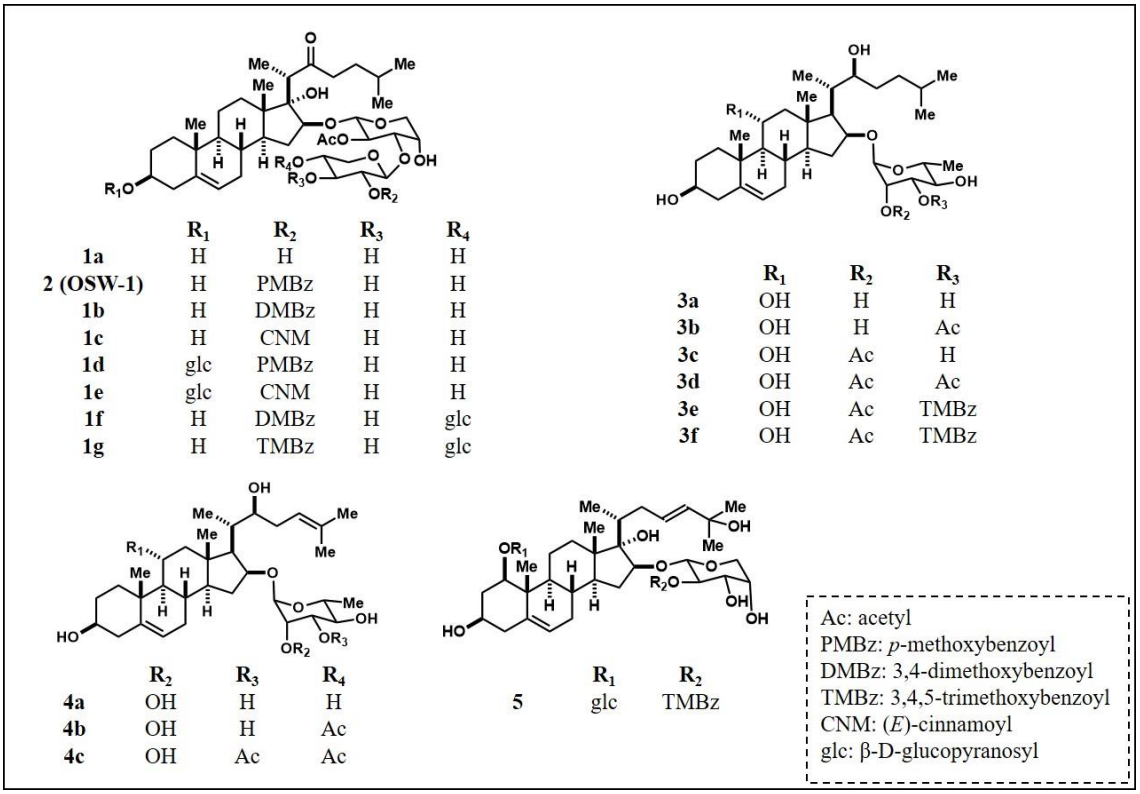

Figure 2. Natural products isolated from *O. saundersiae* bulb. Figure is adapted from Tang *et al.*[4]

I.2 Biological activity of steroidal glycoside OSW-1 and related compounds

The biological activity of the OSW-1 compound has been the subject of extensive research.[4,9–11] Although upon isolation, OSW-1 was identified as a micromolar inhibitor of 3',5'-cyclic adenosine monophosphate (cAMP) phosphodiesterase activity. OSW-1 was

later determined to have potent anti-proliferative activity. [4,9] cAMP plays an important role as a "second messenger" in various biological processes, therefore screening for cAMP phosphodiesterase inhibitory activity serves as a useful tool for the screening of biologically active compounds in natural sources.[12] Following the isolation of natural products from *O. saundersiae* bulbs, they were examined for their cAMP phosphodiesterase inhibitory activity.[3] Compared to the activity of a known cAMP phosphodiesterase inhibitor, papaverine (IC_{50} = 3.0 x 10^{-5} M), OSW-1 exhibited a comparable cAMP phosphodiesterase activity (IC_{50} = 5.0 x 10^{-5} M) [3]. Compound **1a** that was missing the benzoate moiety on the disaccharide showed a much weaker inhibitory effect (IC_{50} = 23.0 x 10^{-5} M) [3].

Further investigation into OSW-1 biological activity showed that it exhibited potent anti-tumor activity.[4,9] OSW-1, compound **1b** and **1c** strongly inhibited the growth of leukemia HL-60 cells with the IC_{50} values ranging between 0.1 to 0.3 nM, which was much more potent than the clinically applied anti-cancer agents used as positive controls (etoposide-IC_{50} = 25 nM, Adriamycin-IC_{50} = 7.2 nM and methotrexate-IC_{50} = 12 nM).[9] Moreover, OSW-1 was found to have exceptionally potent cytostatic activities on many malignant tumor cells such as mouse mastrocarcinoma, human pulmonary adenocarcinoma, human pulmonary large cell carcinoma, and human pulmonary squamous cell carcinoma including ADM-resistant P388 leukemia and camptothecin (CPT)-resistant P388 [9]. The anti-cancer activities of OSW-1 are around 10 to 100 times more potent than the clinically used anti-cancer agents such as mitomycin C, cisplatin and taxol, but it showed little toxicity to normal human pulmonary cells.[9] OSW-1 showed exceptionally

potent cytostatic activities in the U.S. National Cancer Institute 60 cancer cell lines (NCI-60) in vitro screen, with the mean IC_{50} of 0.78 nM.[9]

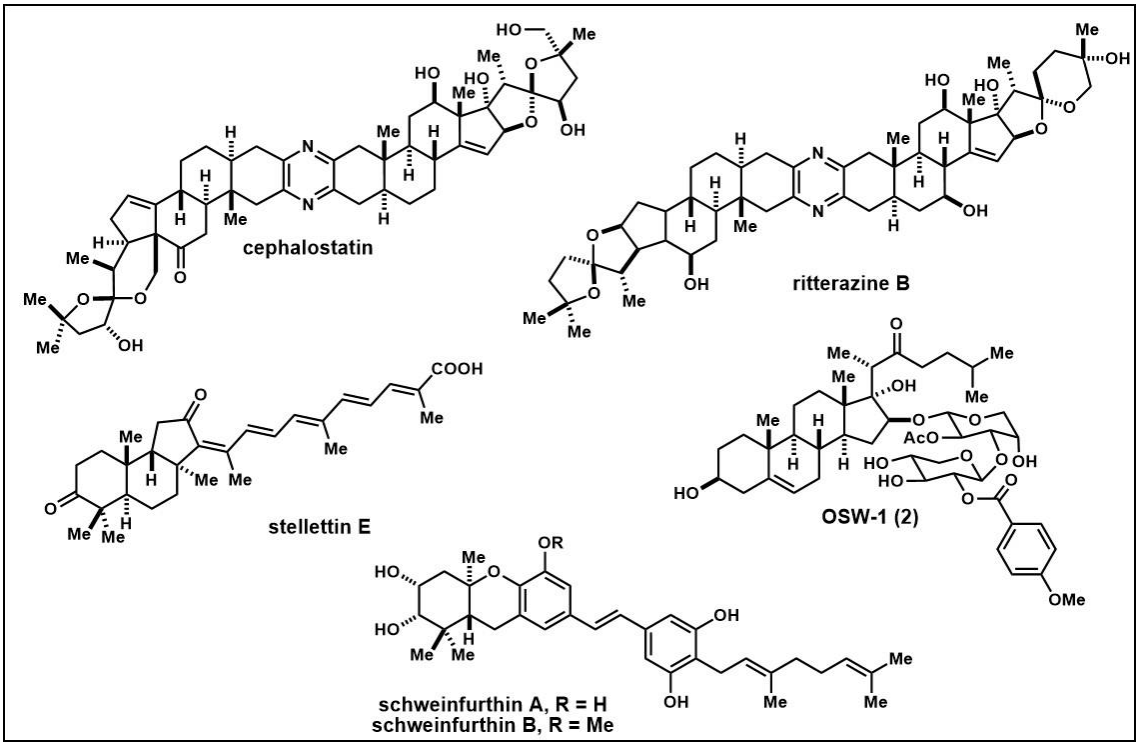

Figure 3. Chemical structures of ORPphillins: cephalostatin, ritterazine B, stelletin E, OSW-1(2), schweinfurthin A and B. Figure is adapted from Burgett *et al*.[10]

OSW-1 was associated with a group of structurally diverse natural products sharing a similar and unique pattern of sensitivity against the NCI-60 cell line panel, as identified through the NCI-DTP COMPARE algorithm (**Figure 3**).[10] This algorithm expressed the similarity in NCI-60 profiles through Pearson correlation coefficients (*r*). Compounds with high COMPARE correlation ($r > 0.6$) tend to have related mechanisms of action [13]. Through COMPARE analysis, the high correlation values of OSW-1, cephalostatin[14], ritterazine B [15], schweinfurthin A [16], schweinfurthin B [16] and stellettin E [17] suggest that all six natural products share a common but unidentified cellular target [13]. Through an affinity purification and proteomic analysis of an OSW-1 affinity resin, Burgett *et al*. determined

that OSW-1, cephalostatin, ritterazine B and schweinfurthin A share cellular targets of oxysterol binding protein (OSBP) and its closest paralog, OSBP-related protein 4L (ORP4L).[10] Hence, these natural products (**Figure 3**) were named the ORPphillins, based on their ability to interact with OSBP and OSBP-related proteins (i.e., ORPs).[10] The cellular targets of OSW-1 being OSBP and ORP4L were further supported through extensive biological experimentations including measurement of high affinity binding between OSW-1 compound and the OSBP and ORP4 proteins.[10]

I.2.1 OSBP/ORP protein family

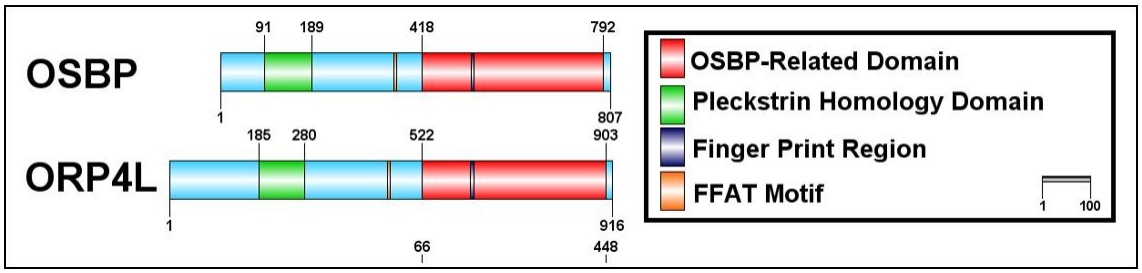

Figure 4. OSBP and ORP4L protein domain sequence and homology diagram. Figure is adapted from Juan Nuñez dissertation.

OBSP and ORP4L belongs to the family of oxysterol-binding proteins that is conserved in all eukaryotic cells, from yeast to humans.[18,19] Oxysterol-binding protein (OSBP) was the first identified[20] and the most well-studied of this protein family in humans. Through genomic analysis it was revealed that beside OSBP, the family consists of 11 other OSBP-related proteins (ORPs) [21]. All members of OSBP/ORPs family have a conserved feature of carboxy-terminal OSBP-related ligand-binding domain (ORD) (~50 kDa) (**Figure 4**).[19] The ORD is capable of binding oxysterols and potentially other lipid ligands.[19] A highly conserved "OSBP-fingerprint" sequence, EQVSHHPP, is present in all OSBP/ORPs in the ORD.[19] Different OSBP/ORP family members possess different

regulatory domains such as a pleckstrin homology (PH) domain, a cluster of ankyrin repeats, or "two phenylalanines ina an acidic tract" (FFAT) sequence motif, along with the conserved sterol binding domain[19]. The definitive cellular functions of the individual OSBP/ORPS are the focus of extended research.[22,23] The OBSP/ORP proteins are believed to serve as lipid sensors and lipid transport proteins, based on the conversed sterol binding domain to bind and transport small lipid molecules (e.g. oxysterols).[19] Furthermore, members of the protein family have been shown to bind ligands other than oxysterols, including phosphatidylserine[24] and phosphoinositides[25].

I.2.2 OSBP and ORP4 as therapeutic targets for precision medicine

OSBP and ORP4 belong to the same subfamily I of the OSBP/ORP family, and both have been shown to interact with ORPphillin compounds (**Figure 3**). These two proteins share a 59% overall sequence identity, including a 68% sequence identity in the sterol binding domain (ORD) (**Figure 4**).[26] In addition, OBSP and ORP4 share the same regulatory domains such as PH and FFAT domain. Despite sharing a strong sequence similarity, OSBP and ORP4 have very different biological roles and functions. OSBP is expressed ubiquitously in all tissues, while ORP4 has been shown to be expressed in only a few selective tissues in the body such as retina, testes and parts of the brain.[21,27] OSBP and ORP4 have been shown to have different cellular localization patterns and disease relevance.[10,28] OSBP was demonstrated to play a critical role in the replication of a broad spectrum of clinically-important human pathogens that belong to the *Enterovirus* genus such as common cold, myocardial infections, hand, foot, mouth disease (HFMD), and several neurologic diseases.[11,29–31] Inhibition of OSBP with itraconazole, an anti-viral compound, blocked the replication of *Flavivirun* pathogens dengue virus and Zika virus.[32]

ORP4L (one major variant of ORP4) was shown to be overexpressed and essential for cancer cell viability in T-cell acute lymphoblastic leukemia (T-ALL).[33,34] Inhibition of ORP4L expression in T-ALL cells led to cancer cell death.[34] Thus, ORP4L can serve as a precision cancer therapeutic target.

Even though both OSBP and ORP4L binds ligands with similar affinity, such as 25-hydroxycholesterol and OSW-1, in some instances, the proteins exhibit differences in ligand selectivity.[10] More specifically, schweinfurthin A (**Figure 3**) was shown to bind to OSBP with a much greater affinity (Ki = 68 ± 23 nM) than ORP4L (Ki = 2600 ± 570 nM).[10] In Burgett's laboratory, the difference in binding affinity of ligands to OSBP or ORP4L have been demonstrated (Juan Nuñez's doctoral work). These results together indicate that analogs derived from the OSW-1 compound can be developed with selective affinity to OSBP for anti-viral activity, or to ORP4L for anti-cancer therapeutic agents.

I.3 OSW-1 as a synthetic target

When the potent cytotoxicity activity of the OSW-1 compound was recognized, many chemists from around the world undertook the synthesis of the molecule. The common strategy of OSW-1 disconnection into two parts (the cholestane aglycon and the disaccharide moiety) was adopted by the majority of laboratories. Here, the different synthetic approaches to each part of OSW-1 from different groups are highlighted.

I.3.1 Total synthesis of OSW-1 by Yu's group

Seven years after its isolation, OSW-1 was first synthesized by Yu's group from Chinese Acedemy of Sciences in 1999 (**Scheme 1**). The group assembled OSW-1 from cholestane aglycon **14** and the functionalized disaccharide trichloroacetimidates **25**. The protecting group strategy of hydroxyl groups (silyl ether) and ketone group (ethylene

glycol ketal) were carefully thought out. These protecting groups can be removed late stage in very mild conditions that would not affect other functional groups in the assembled molecule.[4] Cholestane aglycon **14** was synthesized from the commercially available *trans*-dehydroandrosterone **6**. Wittig olefination installed C-20 and C-21, followed by protection of C-3 hydroxyl group as tert-butyldiphenylsilyl (TBDPS) ether (70% yield over 2 steps).[35] The diene **7** then participated in an ene reaction with paraformaldehyde in the presence of catalytic amount of $BF_3{\cdot}Et_2O$ to generate the homoallylic alcohol stereoselectively to set C-20 stereocenter.[35] The homoallylic alcohol was then oxidized to aldehyde **8** with Dess-Martin periodinane in good yield (65% over 2 steps). The aliphatic side chain was appended through Grignard reaction of aldehyde **8** and 3-methylbutylmagnesium bromide to yield alcohol **9** with the indicated stereoisomer in high yield (96%).[35] C-22 alcohol was oxidized to the ketone using PDC reagent. The C-22 ketone was protected as ethylene glycol ketal under very mild conditions with a long reaction time (4 days) to give compound **10** in satisfactory yield (80% through 2 steps). The silyl ether protecting group on C-3 hydroxyl was switched from tert-butyldiphenyl to a more labile tert-butyldimethyl silyl (TBS) ether to avoid the possible complications associated with acyl group migration and cleavage in the final removal of the TBDPS ether under TBAF or HF/Pyr.[35] The diene **11** was subjected to dihydroxylation condition with OsO_4 (1.2 equiv) to give the corresponding 16α, 17α-diol **12** in moderate yield (41%). The authors commented that the reaction resulted in more polar byproducts, perhaps from dihydroxylation of C-5-C-6 alkene, along with starting material.[35] The stereochemistry at C-17 hydroxyl group was inverted through Swern oxidation of diol **12** to afford ketone **13**, which was then reduced

with $NaBH_4/CeCl_3$ to afford the desired 16β-OH aglycon **14** exclusively. The group successfully synthesized aglycon **14** of OSW-1 in 12 steps and 10% yield overall from **6.**[35]

The glycon part of OSW-1 was constructed from D-xylose and L-arabinose. The xylosyl donor **17** was synthesized from D-xylose in 5 steps as shown in **Scheme 1**. First, the anomeric hydroxyl group was protected as a benzyl ether. Then, the 4-methoxybenzoyl group was installed regioselectively on C-2 through a reaction of triol **15** with 4-methoxybenzoyl chloride/pyridine. The free hydroxyl groups on C-3 and C-4 were masked as the bis-TES ether to afford compound **16** in 60% yield.[35] The anomeric benzyl ether was removed in hydrogenolysis condition, then the resulting hemiacetal was converted to the corresponding mixture of trichloroacetimidates **17.**[35] In the meantime, the arabinosyl acceptor **20** was prepared in 4 steps from L-arabinose. After the anomeric benzylation, isopropylidenation of C-3 and C-4, followed by acetylation at C-2 afforded compound **19**[35] The isopropyliden moiety was then removed to reveal hydroxyl groups on C-3 and C-4 in arabinosyl acceptor **20**. Schmidt glycosylation of trichloroacetimidates **17** and diol **20** in presence of $BF_3{\cdot}Et_2O$ as the catalyst at low temperature gave the desired 1→3-linked disaccharide **22** as the major product, along with the isomer 1→4-linked disaccharide **21** as the minor product, which were not separable through silica gel column chromatography.[35] The mixture of **21** and **22** was reacted with TESOTf to mask the free hydroxyl, affording disaccharides **23** (21%) and **24** (70%) separately after silica gel column chromatography. Hydrogenolysis of disaccharide **24** resulted in the corresponding hemiacetal, which was converted to the trichloroacetimidates **25** to serve as glycosyl donor in the following Schmidt glycosylation.[35]

The aglycon acceptor **14** and glycosyl donor **25** was joined together through Schmidt glycosylation reaction under the promotion of trimethylsilyl triflate (TMSOTf) at low temperature to produce the fully protected OSW-1 **26** in satisfactory yield (69%).[35] Finally, all the protecting groups (one TBS group, three TES groups and one ethylene glycol ketal group) were removed cleanly in a single step with $Pd(MeCN)_2Cl_2$ as the catalyst to furnish the final target OSW-1 in good yield (79%). Overall, Yu's group accomplished the first total synthesis of OSW-1 through 27 steps, with the longest linear sequence being 14 steps, and in 6% overall yield.[35]

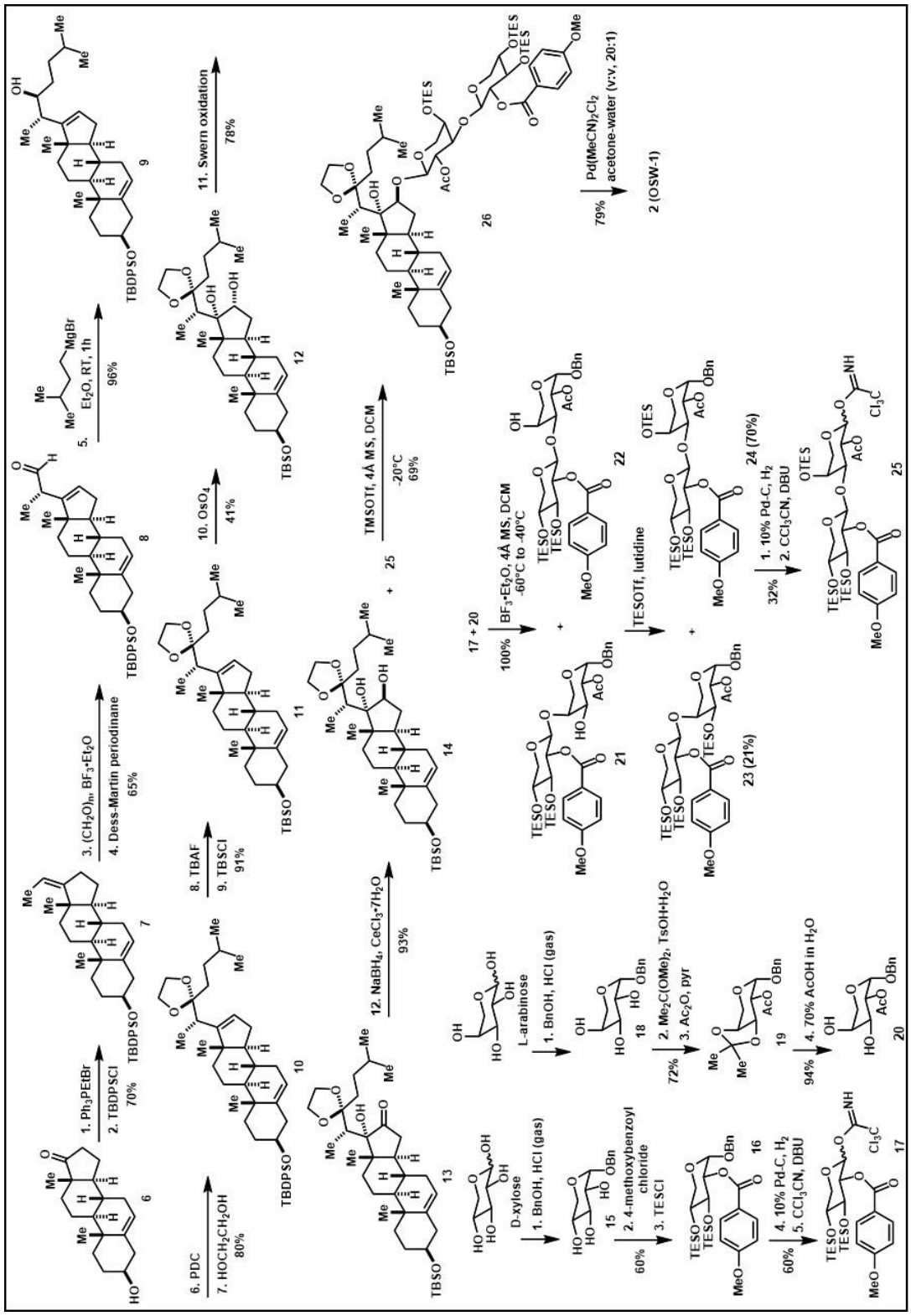

Scheme 1. Total synthesis of OSW-1 by Yu's group. Figure is adapted from Deng *et al*.[35]

I.3.2 Total synthesis of OSW-1 by Jin's group

Shortly after Yu's group published the first OSW-1 total synthesis, another elegant route to OSW-1 was published in 2002 by Jin's research lab from the University of Iowa. The retrosynthesis approach followed the same strategy of independent construction of OSW-1 aglycon and glycon moieties, which were joined late stage through Schmidt glycosylation reaction. The authors constructed the OSW-1 aglycon through a key stereoselective 1,4-addition of α-alkoxyvinyl cuprate to a steroid $\Delta^{17(20)}$-en-16-one.[36] *Trans*-dehydroandrosterone **6** (**Scheme 2**) was converted to diene **27** in high yield (94%) through masking C-3 hydroxyl group as TBS ether and Wittig olefination. Diene **27** was then subjected to a highly regio- and stereoselective selenium dioxide-mediated allylic hydroxylation to afford allylic alcohol **28** in great yield (97%).[36] This alcohol underwent Swern oxidation to afford enone **29** in nearly quantitative yield (96%). TMSCl-activated stereoselective 1,4-addition of α-cyclohexyloxy vinyl cuprate **30** to enone **29** went smoothly to give silyl enol ether **31** *in situ*, which was converted to enol acetate **32**. The conversion of silyl enol ether to enol acetate allowed the group to achieve chemoselective transformation of the enol ether at C-22 to ethylene glycol ketal **33.**[36] Potassium *tert*-butoxide generated an enolate from **33**, which then underwent stereoselective α-hydroxylation by Davis reagent to afford α-hydroxy ketone **13.**[36] C-17 ketone **13** was reduced stereoselectively with LAH in THF at -78°C to provide the desired *trans*-16β,17α-diol **14**. Overall, the aglycon moiety was assembled in eight operations with 48.4% yield.[36]

The disaccharide moiety of OSW-1 was synthesized from tetraacetyl-L-arabinose **34** and tetraacetyl-D-xylose **38** as starting points. Thioglycoside **35** was obtained from **34** through glycosylation reaction in presence of tin (IV) chloride as the promoter and the

removal of the remaining acetate groups.[36] C-3 and C-4 hydroxyl groups were converted to an acetonide, which allowed selective protection of C-2 hydroxyl as an acetate group in **36**. The acetonide was deprotected and C-4 hydroxyl was re-protected selectively with TESOTf and lutidine at low temperature to afford glycosyl acceptor **37.**[36]

Tetraacetyl-D-xylopyranoside **38** was converted to thio ortho ester **39** through bromo-glycoside intermediate in moderate yield (75%). Protecting group manipulation gave compound **40**, followed by zinc chloride-promoted ring opening of thio ortho ester yielded thioglycoside **41.**[36] The 4-methoxybenzoate moiety was installed on C-2 after deacetylation step. The thioglycoside **42** was converted to first a hemiacetal, then trichloroacetimidates to serve as glycosyl donor **43** in the construction of disaccharide moiety.[36]

Glycosylation of **37** and **43** with $BF_3{\cdot}Et_2O$ catalyst at low temperature afforded the desired β-disaccharide **44** in excellent yield (93%), which was converted to glycosyl donor **45** after two steps.[36] Schmidt glycosylation of aglycon acceptor **14** and disaccharide donor **45** in presence of catalyst TMSOTf at low temperature gave the fully protected OSW-1 **46** in moderate yield. The *p*-methoxybenzyl protection groups were cleaved with 2,3-dichloro-5,6-dicyanobenzoquinone (DDQ); the silyl ethers and acetonide was removed in presence of $Pd(CN)_2Cl_2$ to accomplish the target OSW-1. Overall, OSW-1 was synthesized in 28 steps with the reported yield of 6.5%.[36].

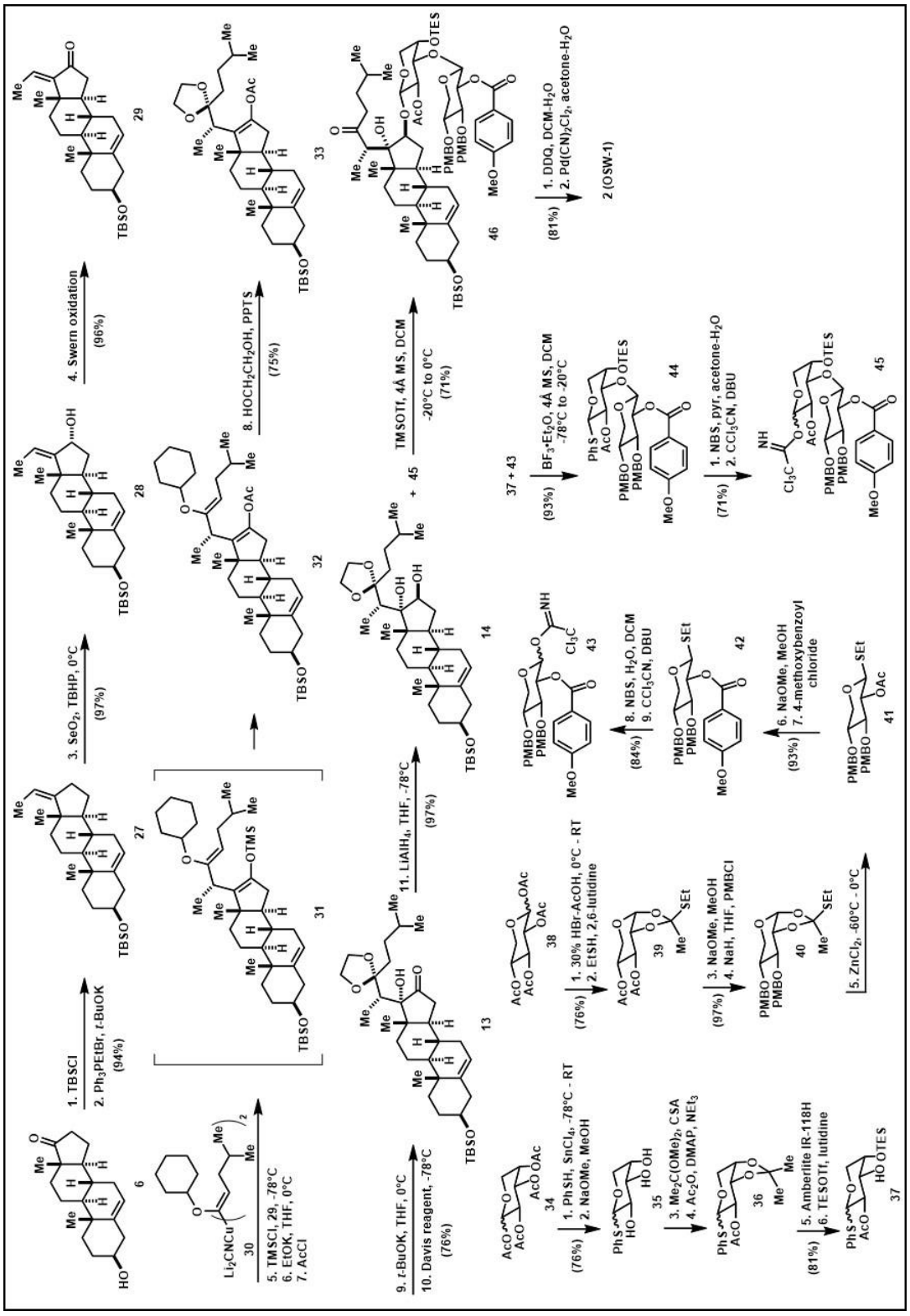

Scheme 2. Total synthesis of OSW-1 from Jin's group. Scheme is adapted from Yu *et al*.[36]

I.3.3 Total synthesis of OSW-1 by Morzycki's group

In 2002, Morzycki's group at University of Bialystok, Poland reported their take on OSW-1 total synthesis. The overall approach still followed assembling OSW-1 through Schmidt glycosylation of aglycon and glycone moiety. However, the group realized that 16β,17α-diol motif in the steroidal moiety of OSW-1 can be accessed from ring opening of 16α,17α-epoxide with oxygen nucleophiles[37], which would eliminate the use of expensive and toxic OsO_4 and the lengthy process to set the desired stereochemistry at C-16 in the other OSW-1 syntheses. *trans*-dehydroandrosterone **6** underwent Horner-Wadsworth-Emmons reaction with triethyl phosphonoacetate to produce (*E*)-α,β-enonate **47** (**Scheme 3**), which was alkylated at C-20 to install C-21 methyl group.[38] The 3β-hydroxyl group and the olefin in B-ring was protected as an *i*-steroid ether **49**, which allowed C-16-C-17 alkene to be transformed to epoxide **50** in presence of m-CPBA in good yield (76%).[37] Epoxy-ester **50**, when subjected to lithium hydroperoxide afforded dihydroxy-acid **51**, which spontaneously cyclized to lactone **52** upon removal of solvent after purification.[37] Treatment of **52** with isoamyl lithium installed the aliphatic side chain of OSW-1 in lactol **53**, which was reduced with $LiAlH_4$ to afford triol **54.**[37] C-22 hydroxyl group was protected as benzyl ether **55**. This aglycon acceptor **55** was joined with disaccharide trichloroacetimidates **25** in Schmidt glycosylation conditions to afford protected OSW-1 56 in moderate yield (59%).[39] The C-22 benzyl ether was removed via hydrogenolysis to afford C-22 free hydroxyl, which was oxidized to C-22 keto with PDC.[39] Finally, all the protection groups (3α,5α-cyclo-6β-methoxy and TES ether groups) were removed with a soft Lewis acid – $Pd(MeCN)_2Cl_2$ at ambient temperature, or alternatively with catalytic amound of p-TsOH in dioxane/water at 75°C to afford the target OSW-1.[39]

The highlight of the synthesis reported by Morzycki's group was the direct installation of 16β,17α-diol motif without utilization of extremely toxic OsO_4.

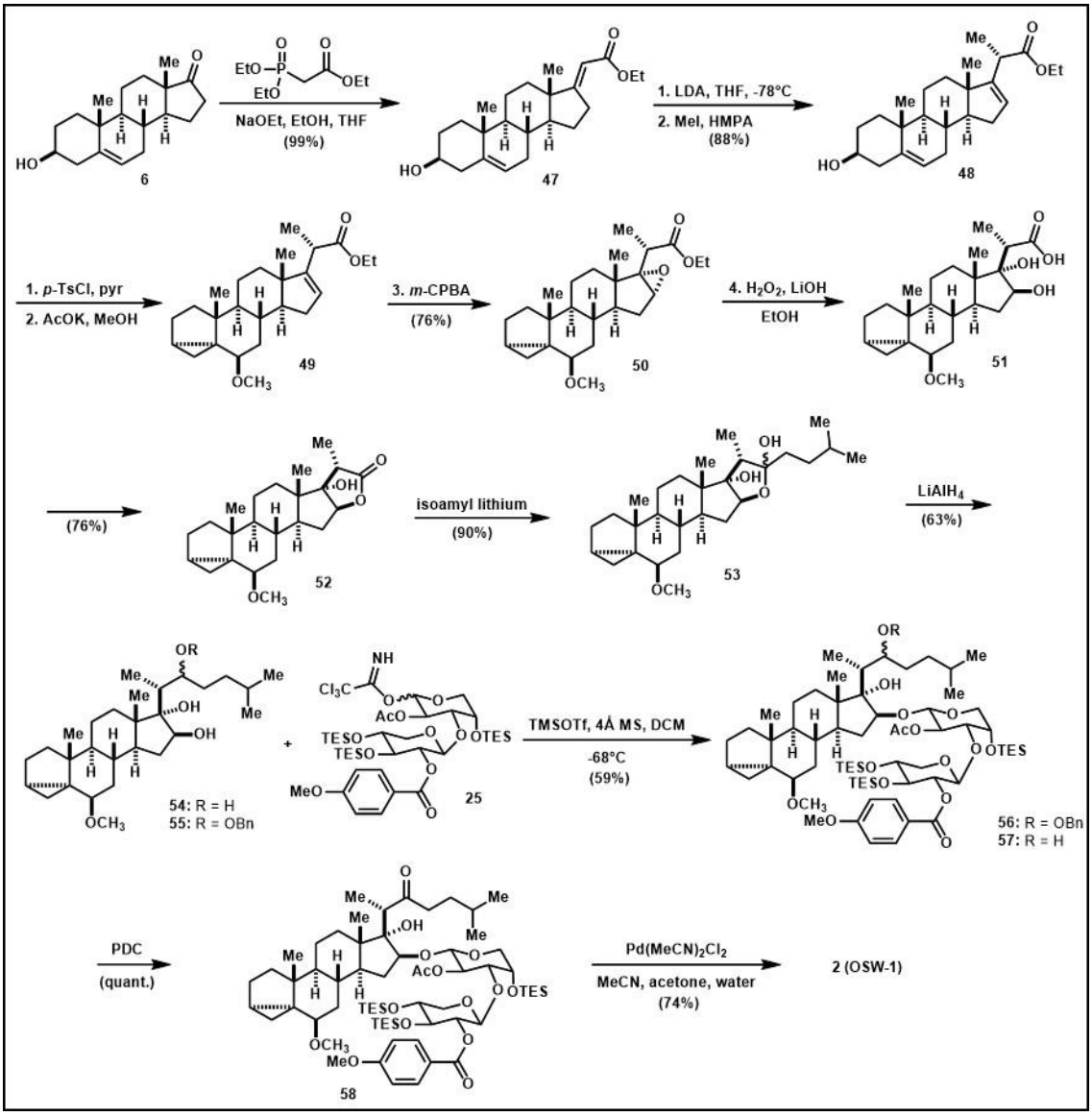

Scheme 3. Total synthesis of OSW-1 by Morzycki's group. Scheme is adapted from Morzycki *et al*.[40]

I.3.4 Total synthesis of OSW-1 by Yu's group

In 2005, Yu's group from Chinese Academy of Sciences published another total synthesis of OSW-1, after their first one in 1999, described an aldol approach to the

stereoselective construction of the 16α,17α-dihydroxycholest-22-one structure (**Scheme 4**).[41] Bromination of acetylated trans-dehydroandrosterone **59** yielded 16α-bromine **60**. C-3 hydroxyl was re-protected as a TBS ether.[41] Under alkaline condition, epimerization between 16α-bromide and its 16β isomer took place readily. The only 16β-bromide underwent S_N2 displacement with hydroxide to stereospecifically formed 16α-ol **62** in great yield (95%).[41] 17-ketone **62** was subjected to aldol condensation condition with lithium *E*-enolate of ethyl propionate in THF at low temperature afford desired 20S-aldol adduct **63** in good yield (75%).[41] Oxidation of C-16 alcohol in presence of tetrapropylammonium perruthenate (TPAP) and *N*-methyl-morpholine N-oxide (NMO) resulted in ketone **64** in excellent yield (93%). Reduction of ketone **64** with $NaBH_4/CeCl_3$ led stereoselectively to 16β,17α-diol **66**. However, only intramolecular lactonization product **65** could be isolated when this reaction was quenched at room temperature with addition of methanol and water. Ester **66** can be isolated when the reduction reaction was quenched at low temperature.[41] Both lactone **65** and ester **66** can be converted to lactol **67** in presence of isoamyl lithium. Reduction of lactol **67** with $LiAlH_4$ resulted in triol **68**, then C-22 hydroxyl group was selectively protected as 2-(azidomethyl)benzoyl (AZMB) ester in slightly low yielding reaction to afford aglycon acceptor **69**.[41] Schmidt glycosylation of **69** and disaccharide donor **25** yielded protected OSW-1 **70**. The 22-O-AZMB was removed with PBu_3 to provide 22-ol, which was subsequently oxidized to 22-keto with PDC in great yield (97%).[41] Finally, the silyl protecting groups were removed in mild condition with $Pd(MeCN)_2Cl_2$ to achieve the target OSW-1. This synthetic route allowed also the synthesis of OSW-1 analogs with a C-22-ester side chain.[41]

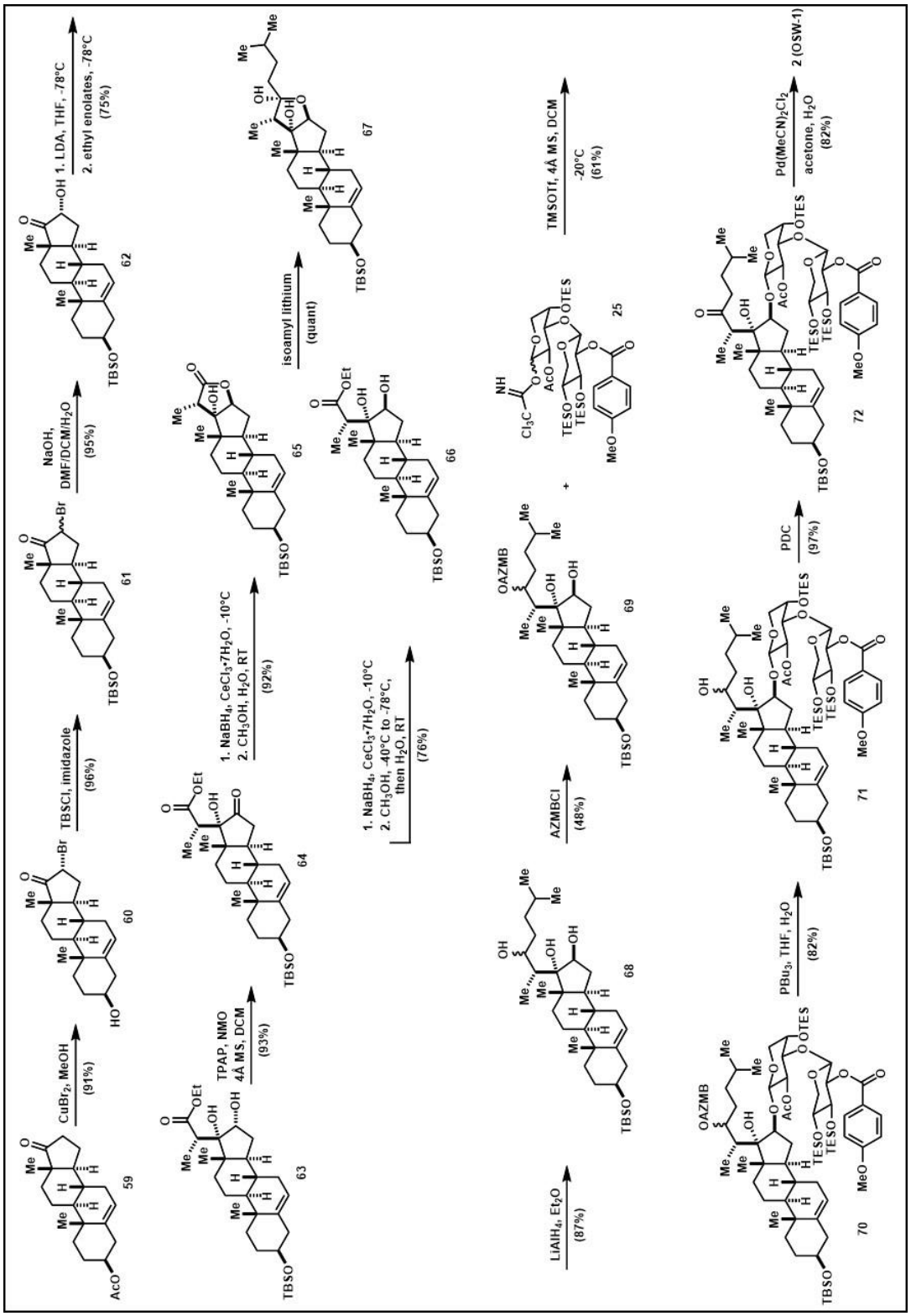

Scheme 4. Total synthesis of OSW-1 by Yu's group. Scheme is adapted from Shi *et al*.[41]

I.3.5 Total synthesis of OSW-1 by Tsubuki's group

Tsubuki's group at Hoshi University in Japan reported their unique synthesis of OSW-1 in 2008 through the means of Wittig rearrangement of allyl thiophenemethyl ether for the construction of (*20S*)-22-hydroxy steroidal side chain.[42] The group aimed at synthesized OSW-1 analogs incorporating heterocyclic rings, such as thiophene and thiazole, at the side chain for SAR study of OSW-1 (**Scheme 5**). Starting from the readily prepared allylic alcohol **73**, thiophene-yl methyl ether **74** was prepared by etherification with (4-methyl-2-thiphene-yl) methyl bromide in great yield (92%).[42] Treatment of **74** with *t*-BuLi in THF at low temperature gave [2,3]-rearranged product **75** (22α- and 22β-alcohols in ratio of 78:22) in moderate yield (59%).[42] C-22 alcohol was oxidized to ketone **76** with Dess-Martin periodinane. Then the olefin in D-ring was subjected to *syn*-hydroxylation condition with $OsO_{4..}$[42] The stereochemistry at C-16 alcohol of **77** was inverted through oxidation-stereoselective reduction sequence to afford the desired *trans*-diol **79**, which acted as aglycon acceptor for Schmidt glycosylation reaction with disaccharide donor **25** in presence of promoter TMSOTf.[42] The glycosylated product **80** was obtained in good yield (72%). All the protecting groups (one MOM and three TES) were cleanly removed by treatment of **80** with TMSBr to give OSW-1 thiophene analog **81.**[42] Lastly, thiophene ring in **81** was reductively desulfurized with W-2 Raney Nickel under an atmosphere of hydrogen to give the target OSW-1 in 79% yield.[42]

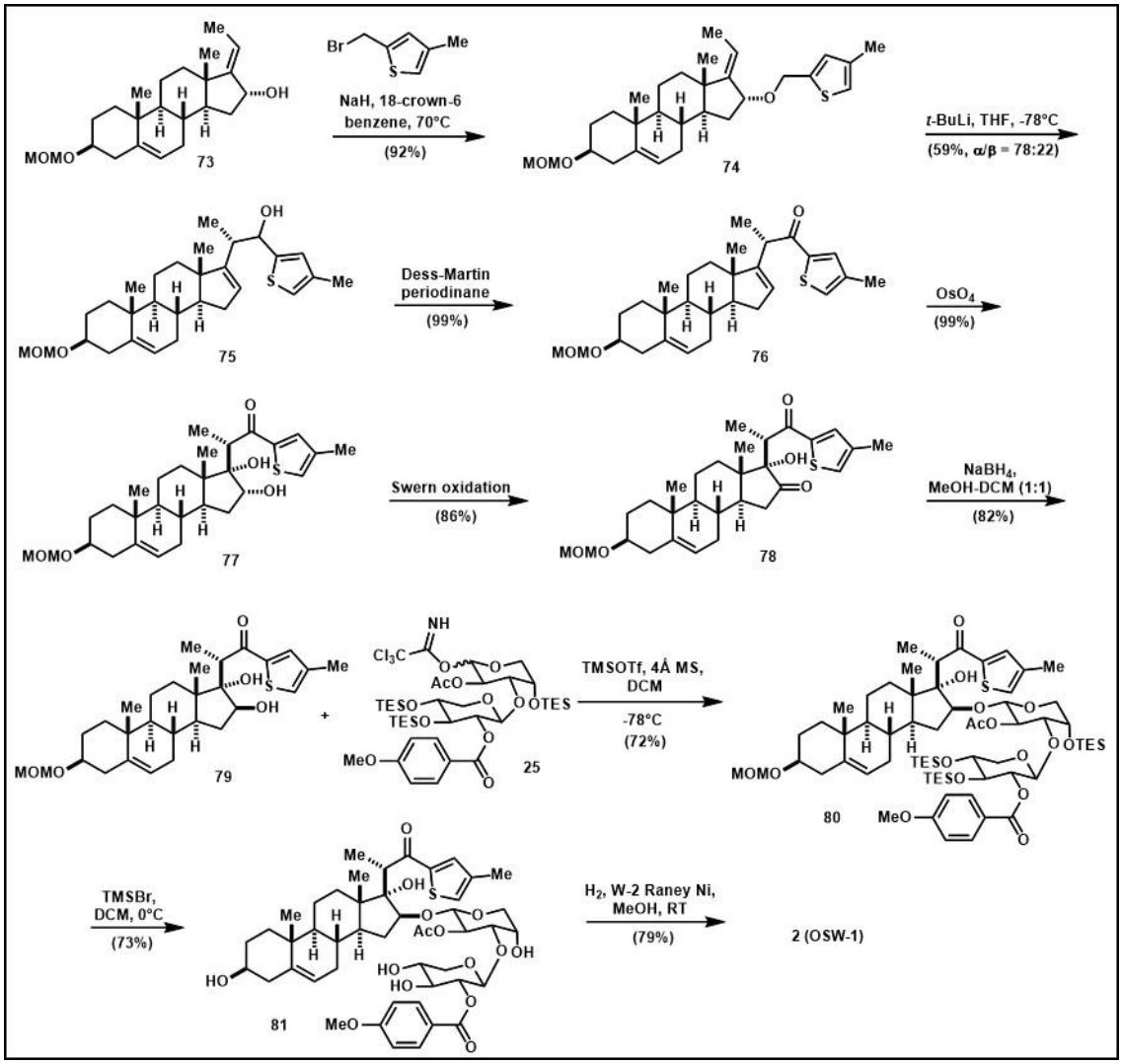

Scheme 5. Total synthesis of OSW-1 by Tsubuki's group. Scheme is adapted from Tsubuki *et al*.[42]

I.3.6 Total synthesis of OSW-1 by Guo's group

Most recently, also in 2008, Guo's group from Wayne State University in Michigan reported a total synthesis of OSW-1 that they carried out in gram scale (**Scheme 6**).[43] *trans*-dehydroandrosterone **6** underwent an aldol condensation with propanenitrile in presence of LDA at low temperature to obtain an epimeric mixture **82** with excellent yield after recrystallization.[43] The aliphatic side chain was installed with a Grignard reagent in

refluxing benzene to give ketone **83**. Protection of C-3 OH group as TBS ether, and C-22 ketone as acetonide went smoothly to afford compound **11**. From here, as seen from some previous OSW-1 syntheses, C 16-C-17 alkene underwent *syn*-dihydroxylation, then the C-16 stereocenter was inverted to afford aglycon **14**.[43]

The synthesis of L-arabinose moiety was slightly different from what had been done previously. Tetraacetylate-L-arabinose was converted to 1,2-*O*-(1-methoxyethylidene)-α-L-arabinose **85** after deacetylation through bromide glycoside intermediate.[43] Ortho ester **85** was *p*-methoxybenzylated regioselectively with the assistance of dibutyltin complex to afford **86**, which was subjected to acetolysis to give arabinosyl acceptor **87**. Schmidt glycosylation of **87** and xylosyl donor **43** with $BF_3{\cdot}Et_2O$ promotor afforded desired disaccharide moiety **88** in good yield (80%).[43] Anomeric deacetylation of **88** with benzyl amine gave hemiacetal, which was immediately converted to trichloroacetimidate **89** for the last Schmidt glycosylation with aglycon acceptor **14** to yield protected OSW-1 **90** in moderate yield (58%).[43] Global deprotection of **90** was accomplished in two separate steps. First, TBS ether and acetonide protecting group were removed under mild acidic condition. Then PMB protecting group on disaccharide moiety were removed with DDQ to afford target OSW-1 with the overall yield of 6.4%.[43]

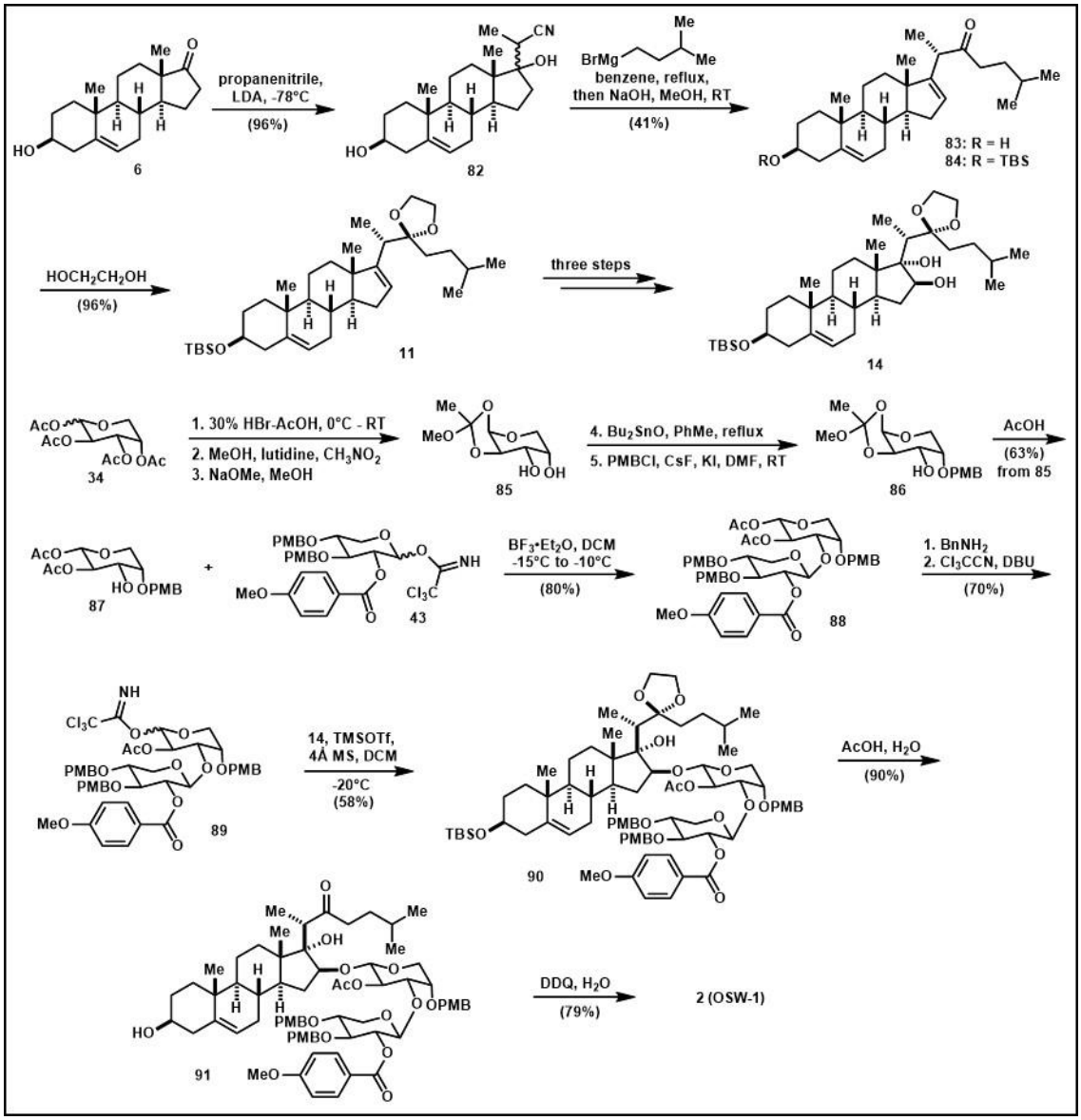

Scheme 6. Total synthesis of OSW-1 by Guo's group. Scheme is adapted from Xue *et al*.[43]

The synthetic strategies presented in this section (Section **I.3**) have provided background and insights for the derivatization of OSW-1 with selective affinity to OSBP or ORP4 proteins for the development of anti-viral and anti-cancer therapeutic agents.

I.4 Personalized cancer therapy through Single-probe quantitative Single Cell Mass Spectrometry

Personalized cancer medicine has emerged as a targeted and tailored treatment approach to maximize the treatment efficacy and reduce toxicity for individual patients.[44] The conventional administration of cancer chemotherapy drugs follows non-personalized protocols that bases on the patient's physical characteristics, but does not take into account patient's individual rate of drug metabolism. This is mainly due to the lack of bioanalytical capabilities to provide timely and meaningful feedback from the patient's well-being throughout the course of treatment. In hope to advance personalized cancer therapy, Single-probe quantitative Single Cell Mass Spectrometry (qSCMS) was developed from the collaboration of Dr. Burgett's and Dr. Yang's laboratories at the University of Oklahoma as a robust bioanalytical method that allows the MS analysis of the intracellular constituents of live single eukaryotic cells in real-time[45]. Furthermore, this technology is able to measure the absolute concentration of small molecules in the cellular contents of the single cells with the use of internal standards. Chapter IV will describe the synthesis and characterization of stable-isotopically labeled analogs of anti-cancer drugs (i.e. gemcitabine and cisplatin) as internal standards for Single-probe qSCMS studies of mammalian single cells.

I.5 Precision medicine in myopia: development of selective inhibitor for retinaldehyde dehydrogenase enzymes

The retinaldehyde dehydrogenase (RALDH) enzyme subfamily (including RALDH1, RALDH2, and RALDH3) catalyzes the irreversible oxidation of retinaldehyde to all-*trans*-retinoic acid (atRA).[46] Despite the importance of RALDH enzymes in embryonic

development and their disease relevance, there is currently no commercially available inhibitor that target these enzymes selectively. Applying structure-based design strategy, α,α-dichloro-all-*trans*-retinone (DAR) was designed based on the structure of the enzymes' natural substrate retinaldehyde.[47] Chapter V describes the synthesis, characterization and evaluation of first inhibitor, α,α-dichloro-all-*trans*-retinone (DAR), that exhibits selectivity for RALDH1, 2, and 3 proteins.

Chapter II : Synthesis and Characterization of Natural Product OSW-1 Probe Analogs

Abstract

Determining the molecular pharmacology of complex, bioactive natural products led to many important discoveries of cellular biology and biochemical processes. The elucidation of a natural product's mechanism of action is often achieved through a use of its probe analogs. The probe analog compounds, which carry different functionalities such as biotin units or a radioactive-label, allow for the cellular function of a compound to be fully understood. Probe analogs can be used to determine the interactions of the natural product compound with its cellular target and to understand how the compound causes a cellular phenotype. This chapter focuses on the development of probe analogs of OSW-1, a natural product with potent anti-cancer and anti-viral activities. The design, syntheses and characterization of the following OSW-1 probe analogs will be reported: 1) a deuterated OSW-1 analog useful for mass spectrometry (MS) quantification of OSW-1;2) a biologically inactive OSW-1 analog useful for serving as a negative control compound, and 3) a series of OSW-1 analogs with an introduced amine linker that retains the biological activity of OSW-1 while allowing for direct further derivatization. These compounds were prepared through both the direct derivatization of the OSW-1 as well as through the total synthesis of the OSW-1 compound. This set of OSW-1 probe analogs are powerful reagents to fully elucidate the OSW-1 molecular pharmacology, cellular biology and potential for drug development.

II.1 Introduction

Determining the biological activity of natural products compounds has profoundly advanced the understanding of cellular biology and inspired therapeutic drug development in a wide array of human diseases. Through investigation of many natural products' mechanism of action, several biochemical processes were discovered and better understood. For example, discovery of natural product rapamycin's target led to understanding of Target of Rapamycin (TOR) signaling pathway.[48] Investigation into the biological effect of paclitaxel revealed the importance of targeting microtubules for anti-cancer therapy.[49] Natural products hold great potential to guide our understanding of many unique and complicated biochemical processes. Hence, research focused on the molecular pharmacology of complex and bioactive natural products will likely continue to expand our understanding in cellular biology and the development of new therapeutic agents.

The identification of a natural product compound's cellular target or the elucidation of its mechanism of action usually requires the use of analogs that can serve as biochemical probes. These probes are often derivatives of natural products with specific add-on features such as a biotin or radioactive-label, and the probe analogs are the used to define the connection between a compound and its reported phenotype.[50] The production of a natural product compound through an adaptable and convergent total synthesis allows for the freedom and flexibility in designing analogs suitable for the desired studies. An adaptable synthetic approach that allows for modifications at multiple positions on the structure at different stages of the synthesis is ideal for incorporation functionalities useful for probing biological activities. With a set of probe analogs, the molecular pharmacology of a molecule could be investigated and its mechanism of action determined.

The OSW-1 natural product compound causes its cellular effects through interacting with oxysterol binding protein (OSBP) and OBSP-related protein 4 (ORP4)[10], but the cellular mechanism of action through which OSW-1 interacting with OSBP and ORP4 causes the observed phenotype is not elucidated. OSW-1 has been the target of extensive total synthesis approaches (see Chapter I.3), and this research provides a foundation of the production of probe OSW-1 analogs. Additionally, reaction methodology can be used to directly derivatize the OSW-1 compound into new probe analogs. This chapter describes the design and synthesis of multiple OSW-1 probe analogs that will be employed to study how OSW-1 interacts its cellular targets OSBP and ORP4 and how the compound induces its cellular effects.

II.2 Design of OSW-1 Analogs

II.2.1 Deuterated OSW-1: internal standard for MS quantification of OSW-1

A fundamental requirement to determine the biological activity of a compound is the ability to measure the concentration of a compound in a biological or cellular sample. Therefore, it is imperative to develop a methodology that can directly quantify the concentration of the small molecule and follow its metabolites inside the cells after treatment. Single Cell Mass Spectrometry (SCMS) with the Single-probe technology developed by Dr. Yang's lab at University of Oklahoma has the ability to measure in real time the concentration of small molecules inside living, in-tact single cells with excellent sensitivity.[45] Quantification of an analyte through mass spectrometry requires an internal standard-a molecule with slightly different molecular mass but yet similar in structure and ionization ability. This is usually accomplished through use of a stable isotopically-labeled analog compound. Herein, deuterated OSW-1 (or *d*-OSW-1, **108, Figure 5B**) was

synthesized via total synthesis (Section II.3.1 through II.3.4). The deuterium label (-CD_3) is introduced on the benzoate moiety of xylose sugar of OSW-1 (**Figure 5B**).

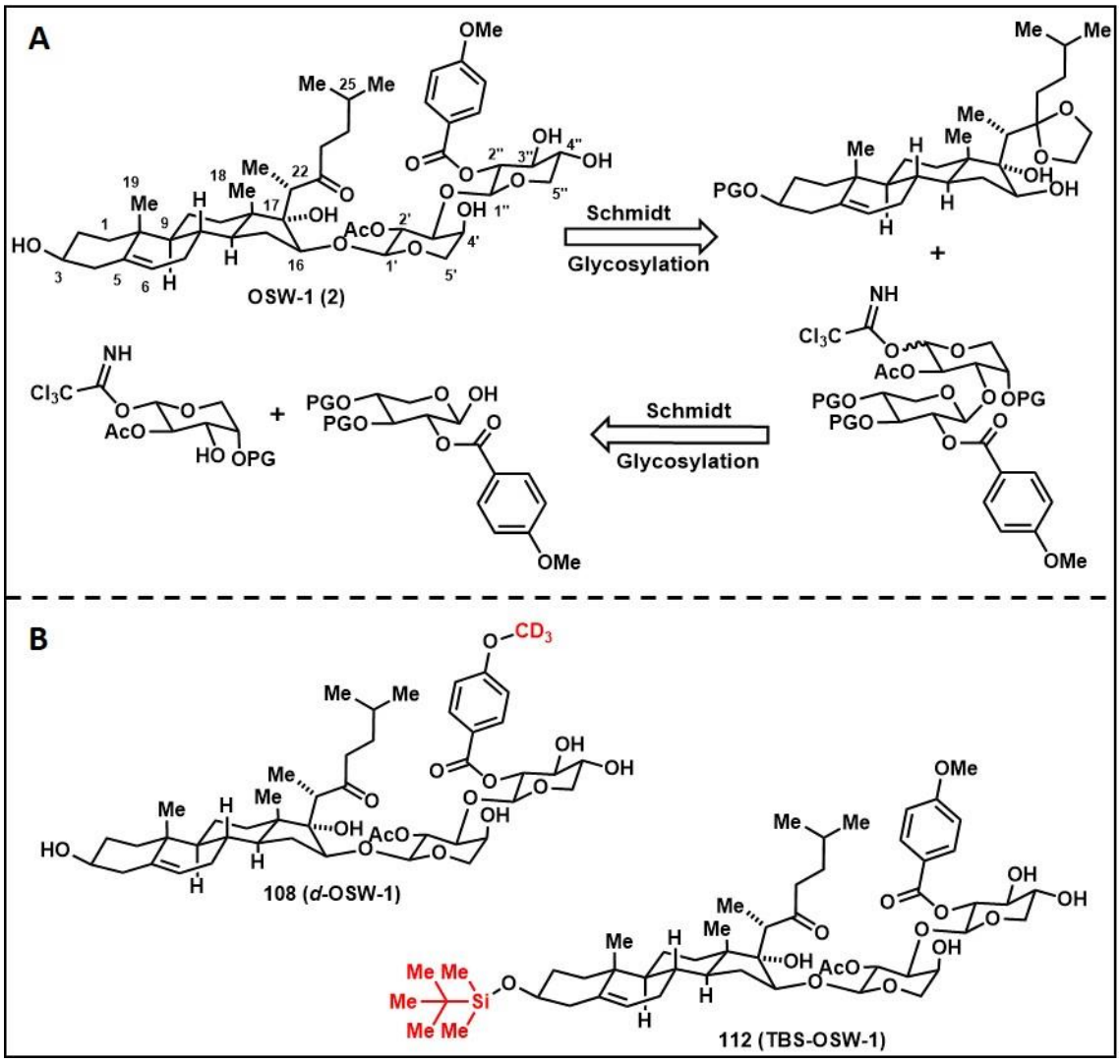

Figure 5. A) OSW-1 retrosynthesis**; B)** *d*-OSW-1 and TBS-OSW-1 analogs

II.2.2 TBS-OSW-1: a biologically inactive analog as a negative control compound

Structural-activity-relationship (SAR) studies of OSW-1 revealed the importance of the C-3 hydroxyl group in its bioactivity.[4] When the hydroxyl group was substituted with large groups, OSW-1's bioactivity is significantly reduced.[10] A key probe analog to evaluate bioactivity of OSW-1 and its analogs is a negative control compound - a

compound that is structurally highly similar to, but lacks the potent OSW-1 bioactivity. For this purpose, a sterically-large tert-butyldimethylsilyl (TBS) group was installed to deactivate the C-3 hydroxyl group in compound **112** (TBS-OSW-1, **Figure 5B**). The synthesis of this compound is reported in Section II.3.5.

II.2.3 OSW-1 analogs with amine linker

The ability to add structural features to a compound while fully retaining the biological activity is a useful approach to producing new probe analogs. Burgett *et al*. reported the synthesis and utilization of OSW-1 analogs with an introduced diamine linker, and one of the OSW-1-amine linker analog was key to identify the OSW-1 cellular target.[10] Following this report, OSW-1 analogs with a versatile amine linker were synthesized (**Figure 6**). Section II.3.6 describes the installation of the linker on the 3" or 4'' position in the disaccharide moiety of OSW-1 through a carbamate functional group with an amine handle for further derivatization.

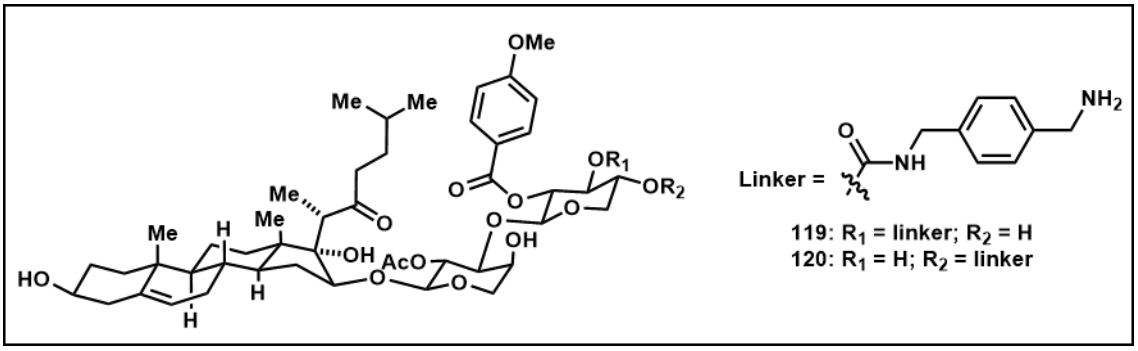

Figure 6. OSW-1 analogs with amine linker

With the free amine handle installed, the potent anti-cancer molecule OSW-1 can be conjugated to an antibody that specifically targets cancer cells, allowing the selective delivery of OSW-1 to cancer cells in the Antibody-Drug Conjugate approach (ADC). Besides the ability to be conjugated to antibodies, the amine functional group will pave the

way for synthesis of different OSW-1 analogs for various biological studies. A fluorescent tag could be attached through the linker to allow for the evaluation of OSW-1 localization in cell. On the other hand, OSW-1's drug-like property can be enhanced by transforming the free amine to quaternary ammonium salt to increase its hydrophilicity.

II.3 Results and discussion

II.3.1 Synthesis of L-arabinose moiety of OSW-1

With the OSW-1 aglycon moiety **14** (**Scheme 11**) already synthesized by Dr. Gopal Peddabudi (a former postdoctoral fellow in Dr. Burgett's lab), the synthesis of deuterated OSW-1 started with the construction of disaccharide moiety from monosaccharide (L-arabinose and D-xylose) pieces.

The L-arabinose moiety was accessed in seven steps (**Scheme 7**) starting from L-arabinose, with the sequence similar to Guo's OSW-1 synthesis[43], with an improved acetylation procedure and overall yield. L-arabinose was subjected to acetylation conditions to afford peracetylated product **34** (**Scheme 7**). Two acetylation conditions were investigated. The first condition consisted of acetic anhydride and used pyridine as the base and solvent. The work-up procedure for this condition was quite involved as saturated copper (II) sulfate solution was used to wash the organic phase multiple times to completely remove the pyridine. ^{1}H NMR analysis of crude product revealed a complex mixture of products, which included the following regio- and stereo-isomers: α-, β-L-arabinofuranoside **34a** and α-, β-L-arabinopyranoside **34**. The complicated product mixture and the use of toxic pyridine prompted the exploration of alternative method to achieve the peracetylated product. A report by Burns' group at University of Louisville showed that acetylation reaction can be carried out in DCM as the solvent, with more benign triethyl

amine as the base and 4-(*N, N*-dimethylamino)pyridine (DMAP) as the catalyst.[51] When this condition was used for the acetylation of L-arabinose, the ^{1}H NMR of crude mixture showed mainly tetraacetyl-α-L-arabinopyranoside (>90%) and β-anomer as the minor product. The physical appearance of crude product differed vastly, from sticky and thick gel of the pyridine method to an easier-to-handle slight sticky solid of the triethylamine/DMAP method. Both acetylation methods proceeded smoothly with almost quantitative yield.

The peracetylated L-arabinose was then transformed to bromo-glycoside **92**, preparing the stage for formation of ortho ester **93** (**Scheme 7**). Treatment of **34** with a hydrobromic solution in acetic acid (33%) at ambient temperature overnight resulted in mainly 2,3,4-tri-*O*-acetyl-β-L-arabinopyranosyl bromide **92**, due to the anomeric effect. When the mixture of tetraacetyl-α-, β-L-arabinofuranoside **34a** and α-, β-L-arabinopyranoside **34** was subjected to bromination condition, only thermodynamic product **92** was obtained. Bromo-glycoside **92** was converted to methyl ortho ester **93** in the presence of methanol, with 2,6-lutidine as the base and nitromethane as the solvent. Compound **93** was purified by flash chromatography with a triethyl amine additive to the eluent (3% NEt_3 in hexanes) to prevent the degradation of ortho ester. With C-1 and C-2 hydroxyl groups tied together in an ortho ester functionality, protecting groups on C-3 and C-4 hydroxyls can be manipulated. Deacetylation of **93** with a catalytic amount of sodium methoxide in methanol gave diol **85**.

The key step in the synthesis of L-arabinose moiety was the regioselective protection of C-4 hydroxyl, which was achieved in high yield and selectivity through the assistance of dibutyltin (IV) oxide. Diol **85** formed a stannylene acetal when it was heated

in reflux toluene in the presence of dibutyltin (IV) oxide (**Scheme 7**). It was postulated that the fluoride anion (from CsF) attacked tin atom of the stannylene acetal to form the pentacoordinated complex, which can reversibly dissociate into a highly reactive alkoxide ion to participate in p-methoxybenzylation with PMBCl.[52] Only mono-PMB protected **86** was observed, possibly due to the less sterically hindered C-4 hydroxyl of L-arabinose.[43] Compound **86** was directly subjected to acetolysis in glacial acetic acid to cleave the ortho ester, resulting in the desired glycosyl acceptor **87**. When "wet" acetic acid was used (presence of water), a mixture of products was observed including a hemiacetal (hydroxyl group at C-1 instead of an acetyl group). Overall, the L-arabinose moiety was synthesized in seven steps with a 26% yield.

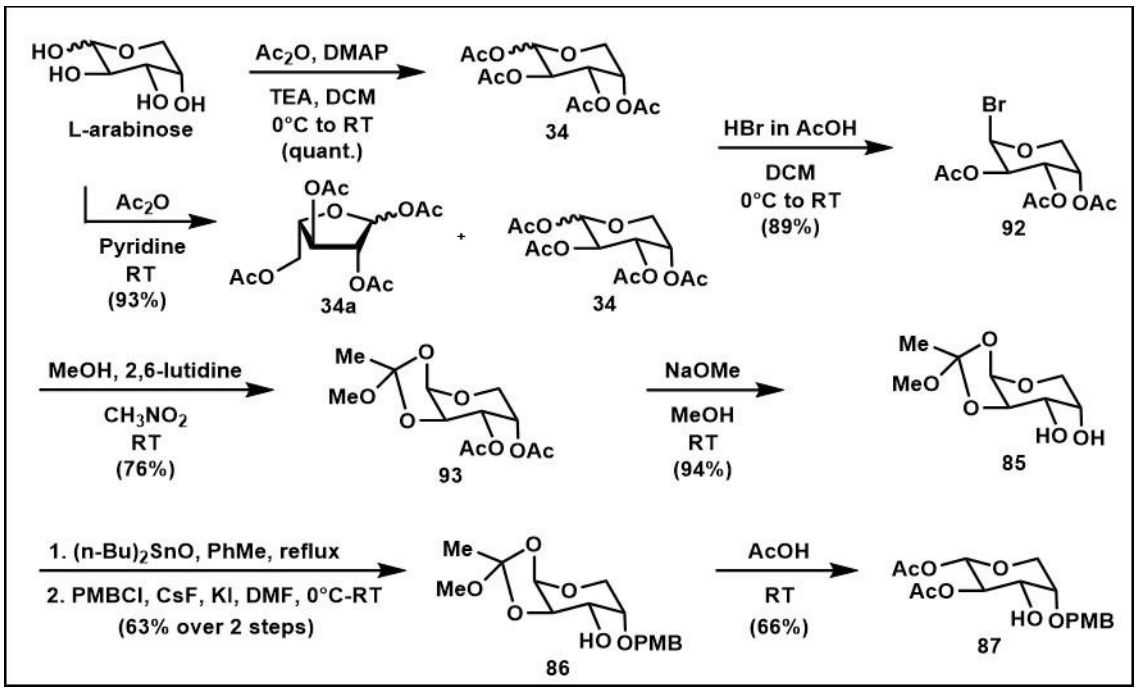

Scheme 7. Synthesis of L-arabinose moiety

II.3.2 Synthesis of D-xylose and disaccharide moieties of OSW-1

While the L-arabinose moiety was prepared, the D-xylose moiety was also being assembled. Since the deuterium label was planned for the D-xylose moiety, the regular D-

xylose moiety was synthesized first to pave the way for installation of the more expensive deuterated label (**Scheme 8**).

2,3,4-tri-O-acetyl-α-D-xylopyranosyl bromide **94** was synthesized employing the same reaction sequence that was used in the L-arabinose moiety synthesis (i.e. peracetylation followed by anomeric bromination). Thio ortho ester **39** arose from treatment of **94** with ethane thiol in presence of 2,6-lutidine and polar aprotic solvent nitromethane. With C-1 and C-2 hydroxyl groups incorporated in the thio ortho ester, manipulation of protecting groups was carried out on C-3 and C-4 hydroxyls to afford di-PMB protected compound **40**. Intramolecular ring opening promoted by zinc chloride at low temperature resulted in thioglycoside **41**. Deacetylation of **41** revealed the C-2 hydroxyl group in **96**, this allowed for the installation of the biologically important benzoate moiety through a straight-forward esterification reaction. Dethiolation of **42** with N-bromosuccinimide (NBS) afforded hemiacetal **97**, which was converted to glycosyl donor trichloroacetimidate **43** in good yield (80%).

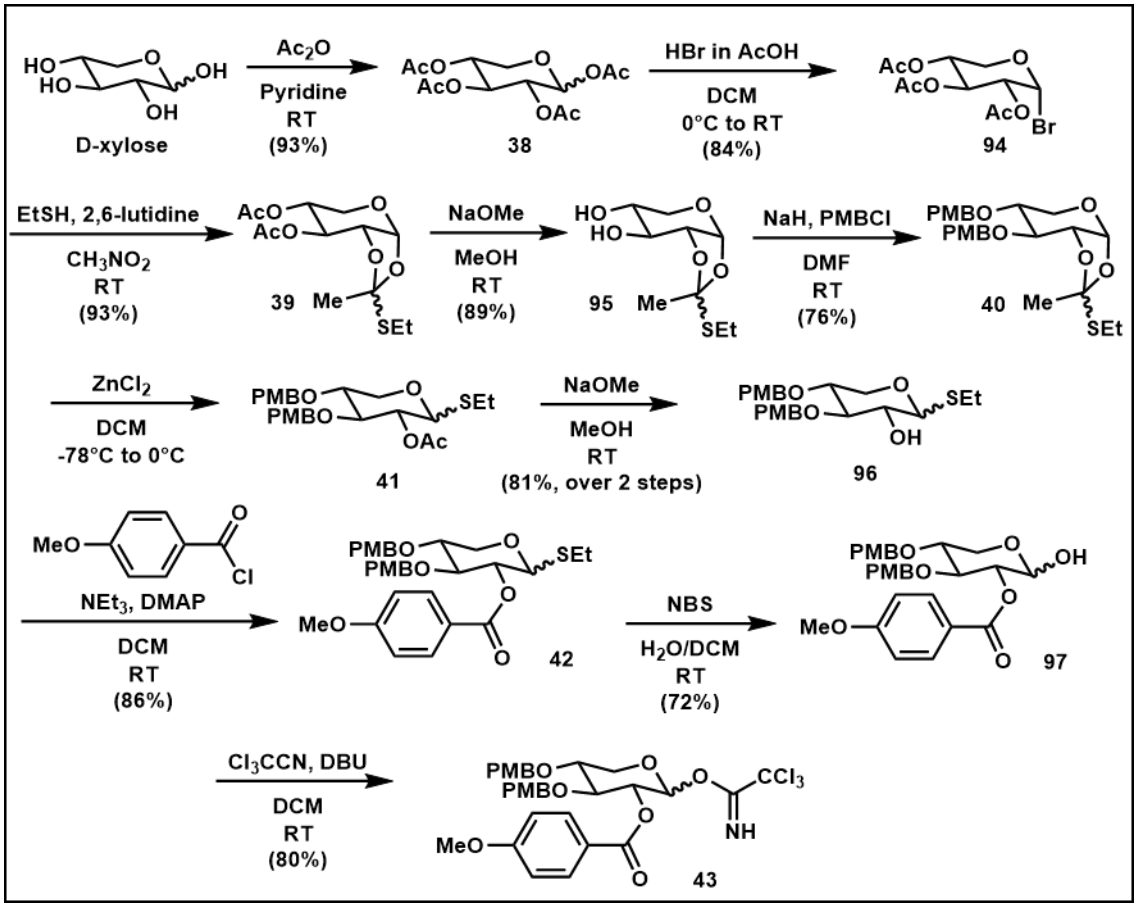

Scheme 8. Synthesis of D-xylose moiety of OSW-1

With both acceptor and donor for the glycosylation reaction ready, the Schmidt glycosylation reaction was attempted and optimized. After various screening of temperature, amount of Lewis acid, ratio of donor and acceptor, the optimal condition was realized. Schmidt glycosylation of acceptor **87** (1.7 equiv) and donor **43** (1.0 equiv) with catalytic amount of Lewis acid $BF_3{\cdot}Et_2O$ (0.3 equiv) at low temperature afforded the desired 1→3 β-glycosidic linkage to assemble the disaccharide moiety of OSW-1 in moderate yield (70%) (**Scheme 9**). Even though donor **43** was set as the limiting reagent, it was never completely consumed based on TLC analysis of the reaction. Attempts to push the reaction to completion (higher temperature or more Lewis acid) resulted in the

degradation of the product. Presence of unreacted acceptor **87** in the crude reaction mixture added difficulty to purification process of the pure desired product **88** since both of them possessed similar polarity. At last, disaccharide **88** was purified away from acceptor **87** with flash chromatography using the atypical mixture of acetone and benzene as the eluent.

Disaccharide **88** was converted to disaccharide trichloroacetimidate **89** through two steps (**Scheme 9**). First, the acetyl group at the anomeric position was selectively removed. In Guo's synthesis, this step was reported with benzyl amine [43]. However, the reaction of **88** with benzyl amine was found to be very sluggish and low yield. Morpholine was used as a replacement of benzyl amine in excess (8 equiv.) to afford the desired hemiacetal **98** over 24-48 hours in moderate yield (74%). Hemiacetal **98** was converted to trichloroacetimidate **89** with treatment of trichloroacetonitrile and catalytic amount of DBU with decent yield (65%).

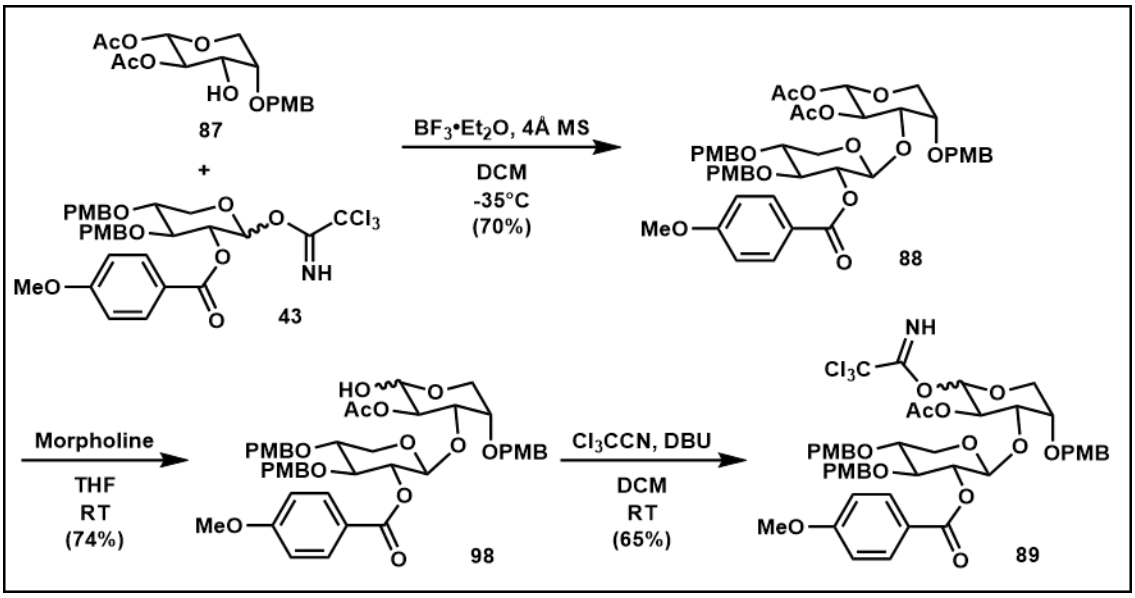

Scheme 9. Synthesis of OSW-1 disaccharide moiety

II.3.3 Synthesis of deuterated disaccharide glycosyl donor of OSW-1

With the OSW-1 disaccharide moiety having been successfully synthesized, and the reaction conditions optimized, efforts were then focused on incorporating a deuterium label to the disaccharide moiety, more specifically the benzoate moiety of D-xylose (**Scheme 10)**. 4-methoxybenzoyl chloride-D_3 (**101**) was readily synthesized from commercially available material with high yield. The hydroxyl group on methyl 4-hydroxybenzoate was alkylated with iodomethane-D_3 in presence of NaH to afford methyl 4-methoxybenzoate-D_3 **99**. Saponification of **99** in basic conditions gave carboxylic acid **100**, which was converted to 4-methoxybenzoyl-D_3 chloride **101** by refluxing with thionyl chloride in good yield (85% over 3 steps).

Esterification of thioglycoside **96** with benzoyl chloride **101** installed the deuterium label on D-xylose moiety. Dethiolation of **102** with NBS gave hemiacetal **103**, then trichloroacetimidate formation afforded **104** as glycosyl donor in good yield. Glycosylation of **104** with arabinosyl acceptor **87** in Schmidt conditions yielded disaccharide **105**. Disaccharide donor **106** was accessed in two steps: anomeric deacetylation in morphiline, and trichloroacetimidate formation.

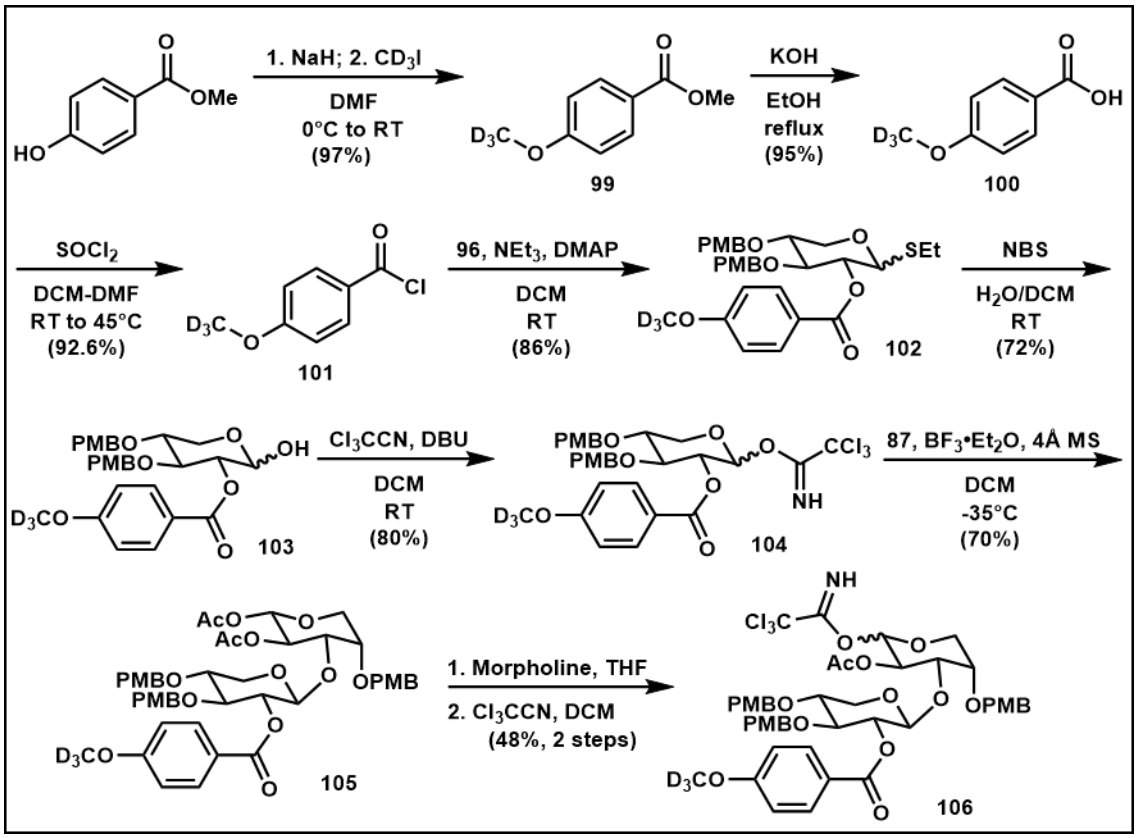

Scheme 10. Synthesis of deuterated disaccharide glycosyl donor of OSW-1

II.3.4 Synthesis of deuterated OSW-1

The stage was set for assembling deuterated OSW-1 with both halves ready: deuterated disaccharide donor **106** and aglycon acceptor **14** (synthesized by Dr. Gopal Peddabudi- a former postdoctoral fellow) (**Scheme 11**). Schmidt glycosylation conditions to couple these moieties have been reported in almost all OSW-1 total syntheses to consist of Lewis acid trimethylsilyl trifluoromethanesulfonate (TMSOTf) in anhydrous DCM at low temperature.[4] The reported yields for the glycosylation reaction ranged from moderate (58%) to good (72%)[4], but this did not reflect the use of excess disaccharide moiety which required almost 20 steps to synthesize. With the materials ready, the glycosylation reaction to assemble *d*-OSW-1 commenced (**Scheme 11**).

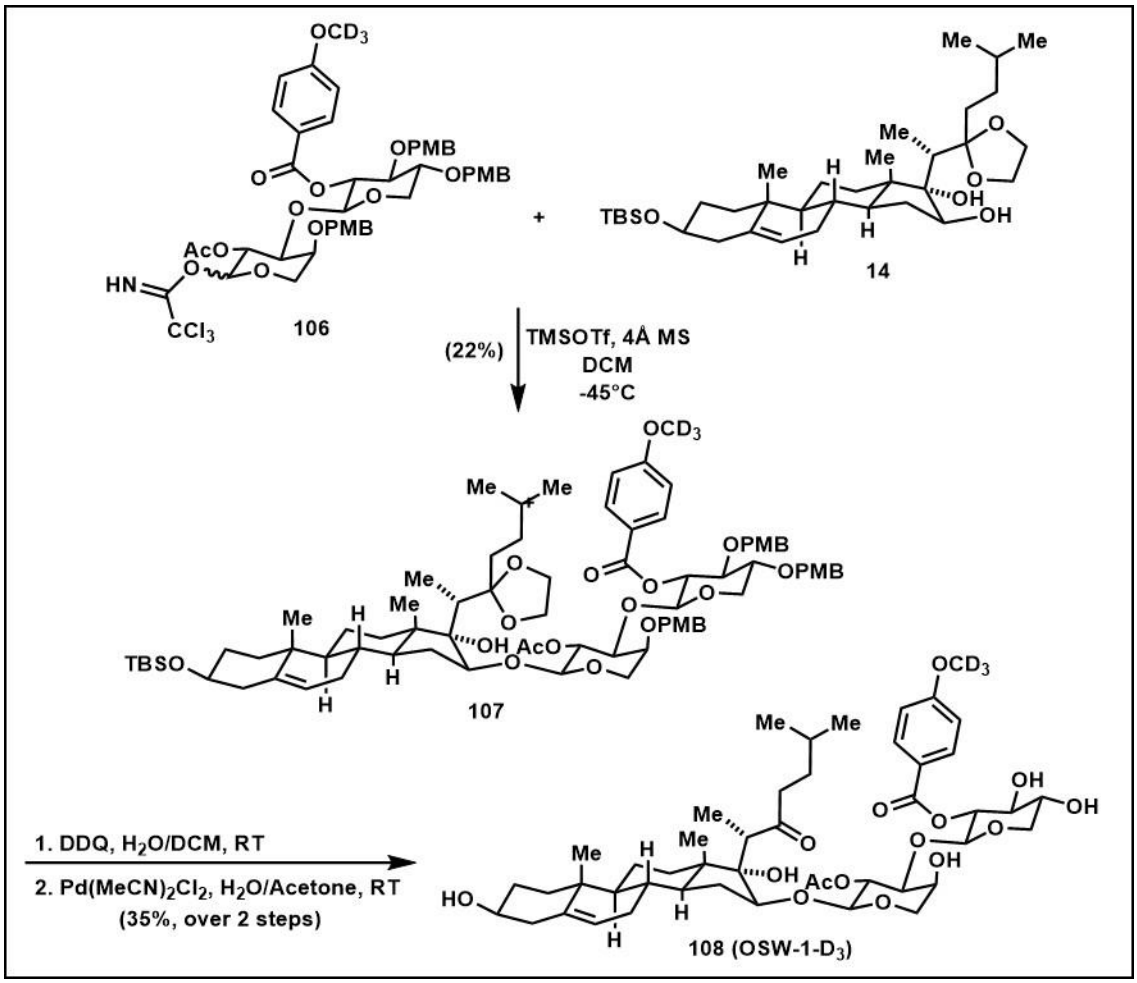

Scheme 11. Synthesis of *d*-OSW-1

First, the inverse addition procedure of glycosylation was investigated. The inverse procedure in glycosylation reaction was first introduced by Schmidt in 1991 to increase the reaction efficiency when reactive glycosyl donors were employed [53]. Here, the glycosyl acceptor **14** was allowed to interact with the promoter TMSOTf before the reactive glycosyl trichloroacetimidate **106** was introduced. When this method was applied to glycosylation to assemble *d*-OSW-1, TLC analysis of the glycosyl donor **14** and TMSOTf mixture showed new spots (2 to 3 spots) with R_f values higher than acceptor **14**, which suggested the presence of less polar side products. In presence of a strong Lewis acid such

as TMSOTf, it could be hypothesized that the acetonide protecting group in **14** was cleaved, exposing the C-22 ketone giving compound **109** (**Figure 7**). The C-16 hydroxyl group could then condense with the C-22 ketone to produce lactol **67** (**Figure 7**). Both **109** and **67** seemed to be less polar than acceptor **14**, and could be the side products observed in TLC analysis. These products were attempted to be purified and characterized, but due to the small scale, the ^{1}H NMR spectrum did not give enough structural information, only that they were not the same as acceptor **14**.

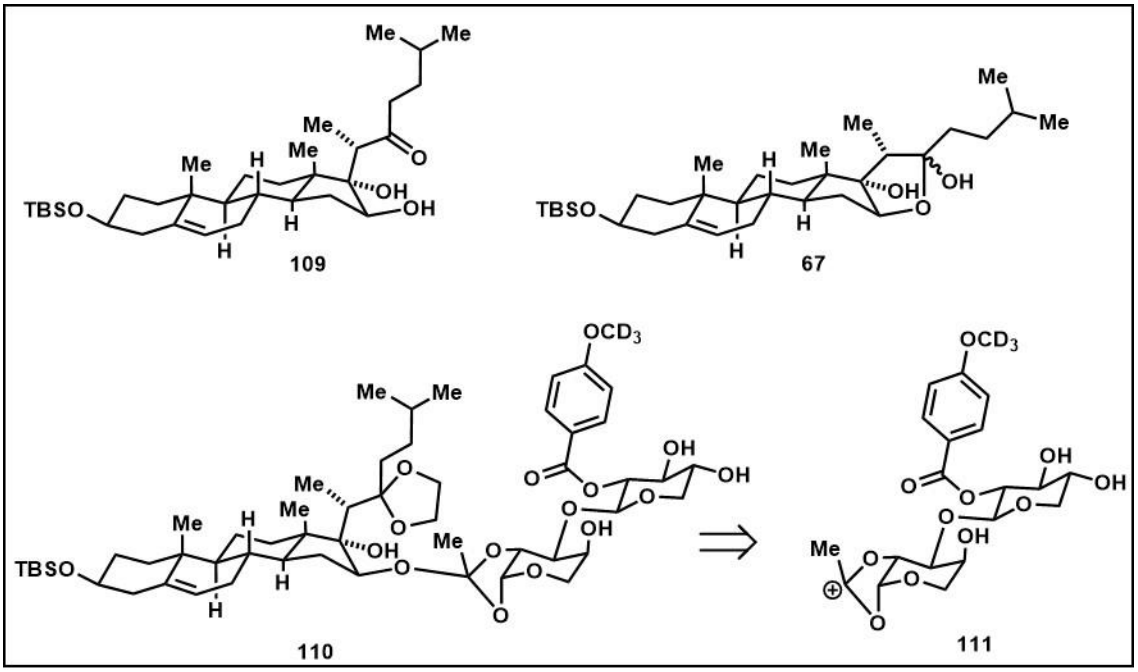

Figure 7. Possible side products in glycosylation reaction to assemble *d*-OSW-1

Addition of glycosyl donor **106** to the mixture of acceptor **14** and TMSOTf produced multiple new compounds on TLC analysis. Addition of more TMSOTf reagent in order to advance a stalled reaction led to some decomposition of the desired product. The main product was isolated and characterized to be the desired glycosylated product **107** (**Scheme 11**) in low yield, along with a small amount of side product that showed

signals for both steroidal and disaccharide moieties on the ^{1}H NMR spectrum. This side product, even though it was not characterized fully due to small quantity, was hypothesized to be ortho ester **110** (**Figure 7)**. This product could have been formed when intermediate **111** (**Figure 7**) was trapped by nucleophilic attack of acceptor **14**. This intermediate resulted from the interaction of carbonyl oxygen of the C-2 acetate group and the oxonium ion formed after the trichloroacetimidate group left (neighboring group participation effect)[54]. Presence of **111** also explained the stereoselectivity of this glycosylation reaction. Due to the neighboring group participation of the C-2 acetate group, only β-glyosidic linkage was observed in product **107** (**Scheme 11**)[54].

In the inverse procedure, presence of only TMSOTf seemed to degrade acceptor **14**, so the glycosylation reaction was carried out in the normal procedure, in which the promoter was added to the mixture of glycosyl donor **106** and acceptor **14** at low temperature. This reaction condition gave a similar TLC profile as when it was carried out with the inverse procedure, but the observed amount of side product **67** and **109** (**Figure 7**) was smaller, with the desired protected *d*-OSW-1 as the main product. Even though in published OSW-1 syntheses, the yield of this glycosylation reaction ranged from high 50% to low 70%; in my hands, this glycosylation reaction was low-yielding and gave a complex mixture of products. The relatively small scale of the reaction (between 2 to 20 μmol) due to the availability of both pieces added difficulties to separate and purify multiple products from the complex reaction mixture. In the end, the desired glycosylated product **107** was obtained in 25% (based on recovered starting material-borsm) yield to carry the synthesis of *d*-OSW-1 forward.

Intermediate compound **107** (**Scheme 11**) required two deprotection steps to produce deuterated OSW-1 analog. The *p*-methoxybenzyl ether protecting groups on the disaccharide moiety were cleaved oxidatively in the reaction with 2,3-dichloro-5,6-dicyano-p-benzoquinone (DDQ). Then TBS ether and acetonide was removed in a mildly acidic aqueous condition containing bis(Acetonitrile)dichloropalladium (II) [$Pd(MeCN)_2Cl_2$] to afford the target *d*-OSW-1 **108** in 35% yield after two steps and HPLC purification.

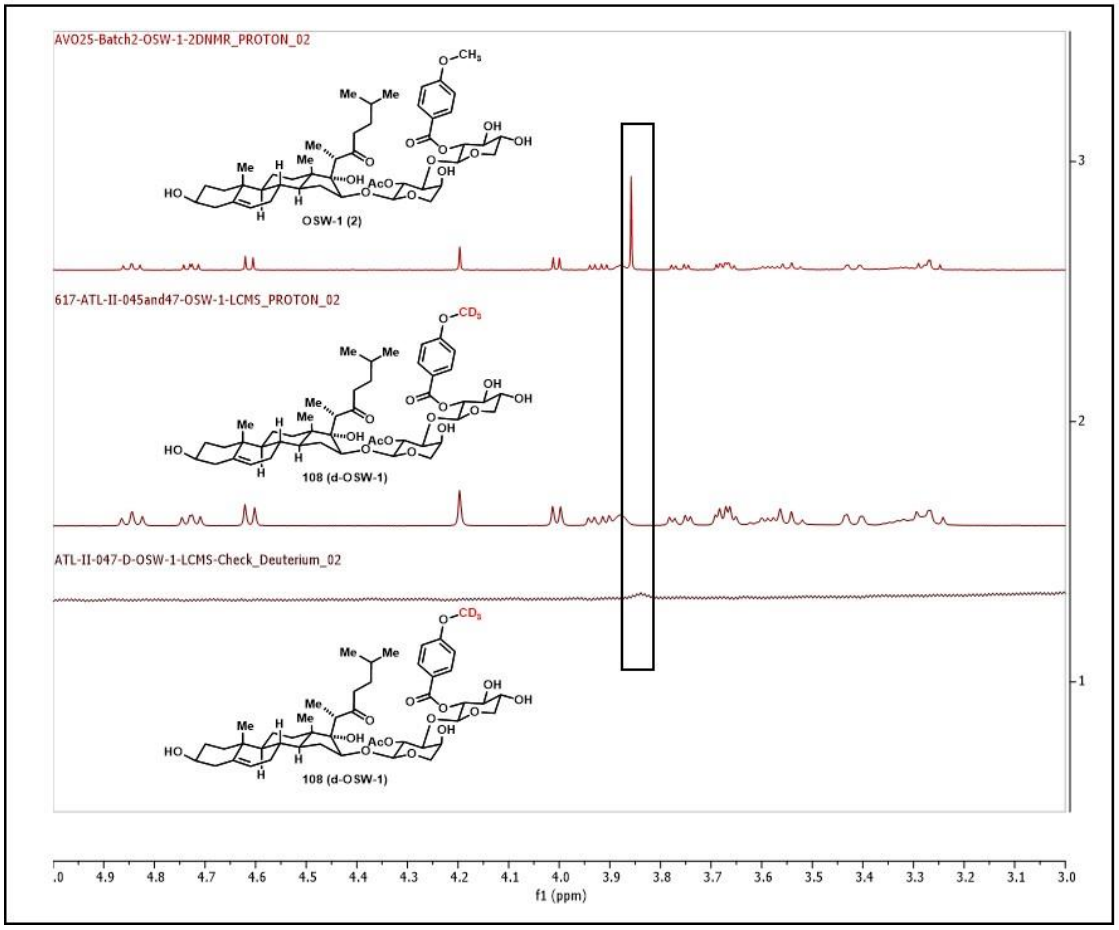

Figure 8. ^{1}H NMR of OSW-1 (top), **108**-*d*-OSW-1 (middle), ^{2}H NMR of d-OSW-1 (bottom)

d-OSW-1 **108** was characterized by NMR and HR-MS (see Chapter appendix). The ^{1}H NMR spectrum of **108** was almost identical to that of OSW-1 (**Figure 8**). The singlet at 3.86 ppm that corresponded to the *p*-methoxy of benzoate moiety was absent in the ^{1}H NMR of **108**, since deuterium can't be observed in proton's resonance frequency. Furthermore, the chemical shift scales are the same for ^{2}H and ^{1}H, so when **108** was analyzed by ^{2}H NMR, a singlet was observed at 3.86 ppm. This observation, along with high resolution mass spectrometry analysis, confirmed that the deuterium labeled was installed correctly on *d*-OSW-1.

In conclusion, deuterated OSW-1 was successfully synthesized and characterized in a small quantity (~1.5 mg). This material has been used as the internal standard for Single Cell Mass Spectrometry, as it will be discussed in more details in Chapter III.

II.3.5 Synthesis of TBS-OSW-1-a biologically inactive OSW-1 analog

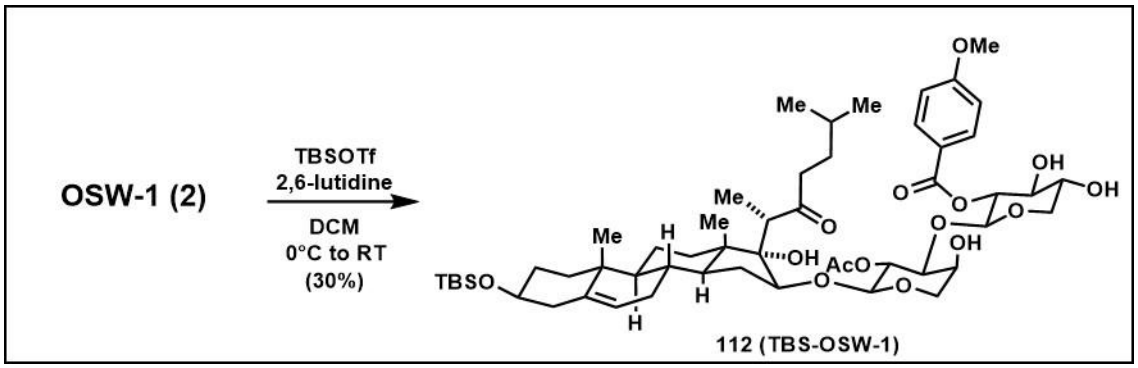

Scheme 12. Synthesis of TBS-OSW-1

The biologically inactive OSW-1 analog,TBS-OSW-1 (**112**), was synthesized following the established procedure from Burgett's report in 2011 (**Scheme 12**).[10] OSW-1 (1 equiv.) was treated with tert-butyldimethylsilyl trifluoromethanesulfonate (TBSOTf, 1.3 equiv) in the presence of 2,6-lutidine as a base at 0°C for 15 minutes. Only one product was observed on the TLC plate, along with the starting OSW-1. When additional TBSOTf

(0.5 equiv) was added, side products started to emerge. After isolation and HPLC purification, the major product was characterized as TBS-OSW-1 **112**.

The yield of the reaction was relatively low, but it was an acceptable outcome considering there were four hydroxyl groups that could undergo the etherification transformation (C-3 hydroxyl group, along with 3 hydroxyl groups on the disaccharide moiety). The controlled reaction condition (low temperature, limited amount of TBSOTf, short reaction time) allowed the most reactive and exposed hydroxyl group – C-3-OH to undergo the reaction selectively. The side products observed when additional TBSOTf was added could be attributed to other hydroxyl groups participating in the reaction when more TBSOTf was available.

The TBS-OSW-1 was prepared as 10 mM stock solution in DMSO, aliquoted and passed on to the biochemists for utilization as negative control in biochemical assays.

II.3.6 Synthesis of OSW-1 analogs with amine linker

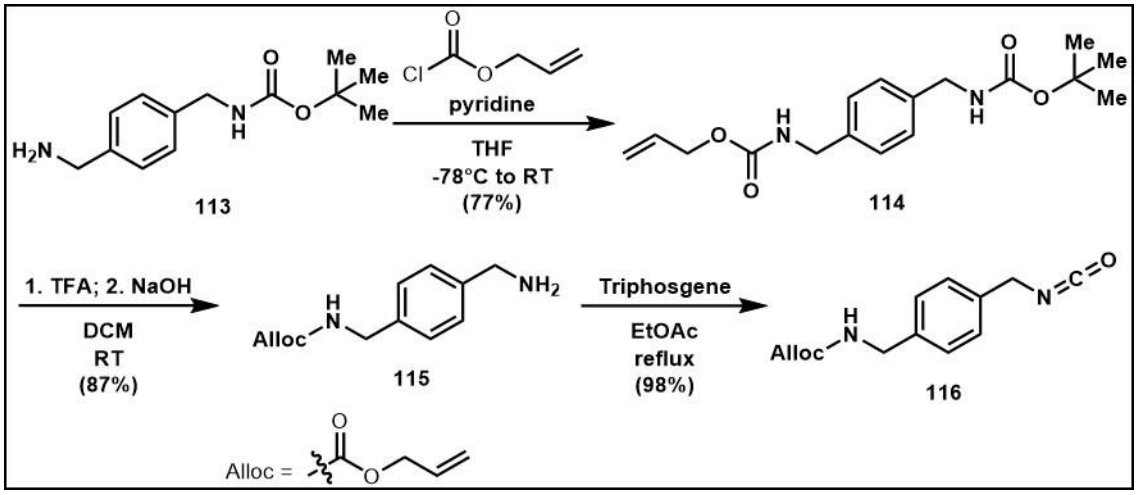

Scheme 13. Synthesis of diamine linker

The introduction of the versatile amine linker to OSW-1 analogs that retain OSW-1 bioactivity will allow for further derivatization of the analogs to produce different probes

for biological studies. The diamino linker was first synthesized for the preparation of this group of OSW-1 derivatives (**Scheme 13**). *p*-xylylene diamine is an excellent reagent because it possesses two amino functional groups that can participate in various chemical reactions making it easy to manipulate chemically. Compound **113**, with one amine group capped with the tert-butyloxycarbonyl (Boc) protecting group underwent a stable allyloxycarbonyl (Alloc) protection at the remaining free amine group to afford bis-protected amine **114** in moderate yield (77%). Then, the Boc group was removed in acidic condition with trifluoroacetic acid to reveal the free amine **115**, which was converted to isocyanate **116** in presence of triphosgene in refluxing ethyl acetate. Compound **116** was used in the subsequence reaction without purification due to the instability of the isocyanate group. The isocyanate functional group served as the reactive handle to functionalize OSW-1.

The linker **116** was installed on OSW-1 through a carbamate formation between the OSW-1 hydroxyl group and isocyanate on the linker (**Scheme 14**). The carbamate formation reaction proceeded smoothly to afford C-3'' (**117**) and C-4'' (**118**) carbamate in ~30% borsm yield for each compound after preparative TLC and HPLC purifications. When more than 2 equivalents of isocyanate were used, bis-carbamate was observed. In presence of copper (I) chloride, only hydroxyl groups on the D-xylose moiety underwent the transformation. The C-3 hydroxyl group on the A ring of the steroid, being the most reactive hydroxyl group as observed in the synthesis of TBS-OSW-1, did not participate in this carbamate formation reaction. It was plausible that Lewis-acidic copper (I) chloride interacts with Lewis-basic and accessible C-3-OH group, which reduced the nucleophilicity of the hydroxyl group to react with the isocyanate moiety. Dr. Burgett had

observed that in absence of copper (I) chloride, the reaction of OSW-1 with isocyanate **116** produced mainly carbamate at the C-3 hydroxyl. In addition, no carbamate formation on C-3' of the L-arabinose moiety was observed. This group could be sterically unavailable in the OSW-1 structure, which could provide limited access for the interaction with the isocyanate linker.

Removal of the Alloc group mediated by tetrakis(triphenylphosphine)palladium (0) [$Pd(PPh_3)_4$] and morpholine afforded free amines **119** and **120** in low (21%) to moderate yield (40%) (**Scheme 14**). The free amines had very limited solubility, which made handling difficult and possibly reduced the reaction yield. HPLC purification gave amines **119** and **120** in analytical purity.

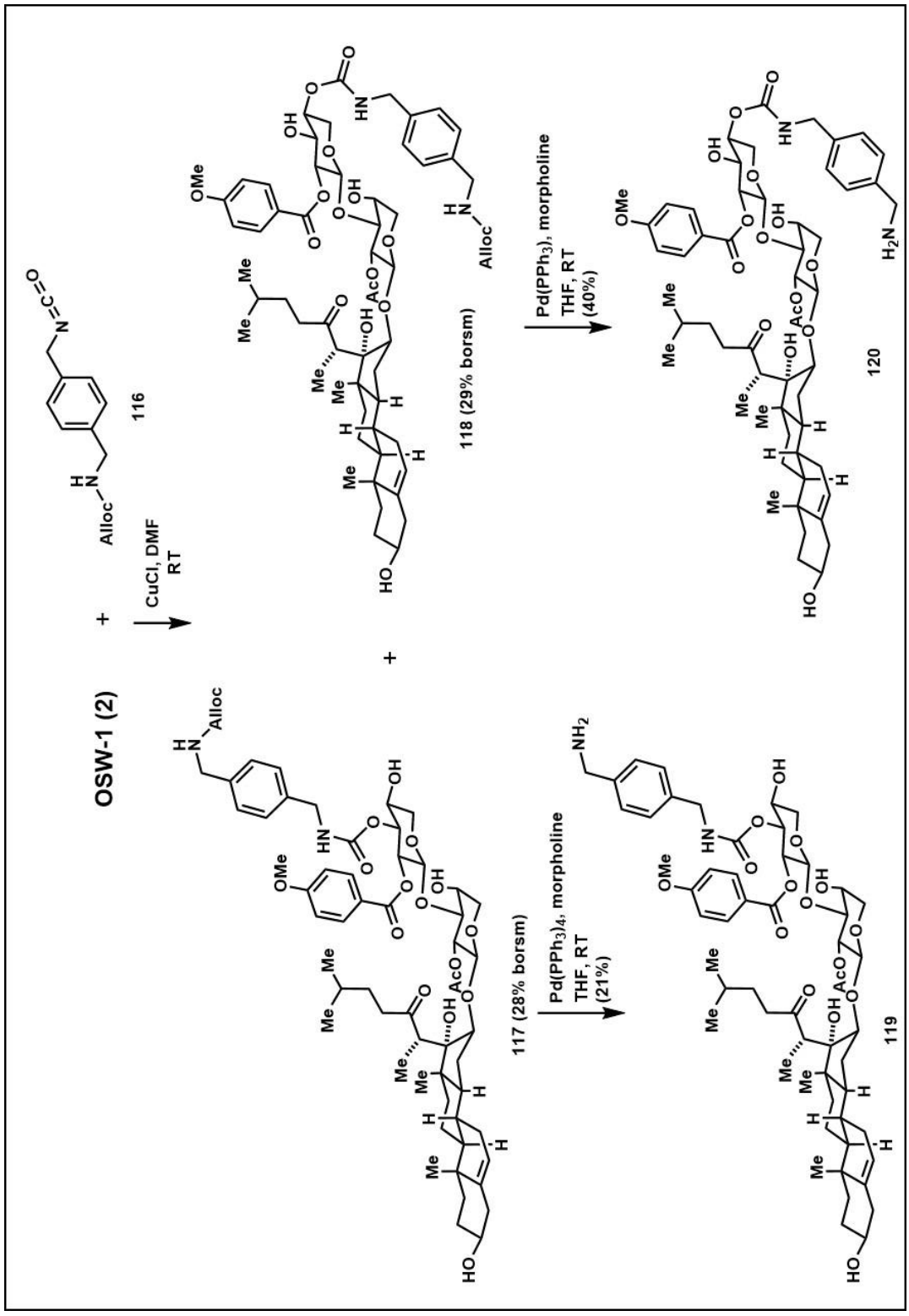

Scheme 14. Synthesis of OSW-1-linker derivatives

The OSBP-binding affinity of the amine analogs was evaluated through binding assays with OSBP to determine whether the addition of the linker affects the interaction of the compound and the target protein (**Figure 9**). These high through-put binding assays were performed by another member of the lab, Juan Nuñez. The binding affinity can be interpreted through inhibition constant, Ki value. The lower Ki value of a compound indicates that it binds to the protein with high affinity. Amine **119** (**Figure 9B**) with the linker attached to C-3'' of xylose moiety showed the apparent Ki value of 40 nM, which was comparable with OSW-1 (29 nM) (**Figure 9A**). Amine **120**, however, exhibited the apparent Ki value of 226 nM (**Figure 9C**), which was about 8-fold higher than the value obtained from OSW-1. Furthermore, the carbamate **117** also had a comparable Ki value with OSW-1 (**Figure 9D**). Taken together, the information suggested that C-3'' position on the D-xylose moiety could be solvent-exposed while bound the OSBP and ORP4 proteins, and therefore these proteins can tolerate the introduction of a sterically bulky group without compromising the potent bioactivity of OSW-1.

The free amine, after being installed on OSW-1 with the linker, can be transformed to analogs for different purposes. The primary goal for installing the amine linker was to develop OSW-1 into an Antibody-Drug-Conjugate. The amine can be used to conjugate the OSW-1 molecule with antibodies that are specific to the target cancer type. Furthermore, the amine can be linked to a fluorescent tag that can be used to study the localization of the molecule once it gets inside the cell. Being so versatile, the free amine could also be converted to a quaternary ammonium salt to increase the hydrophilicity of the saponin OSW-1.

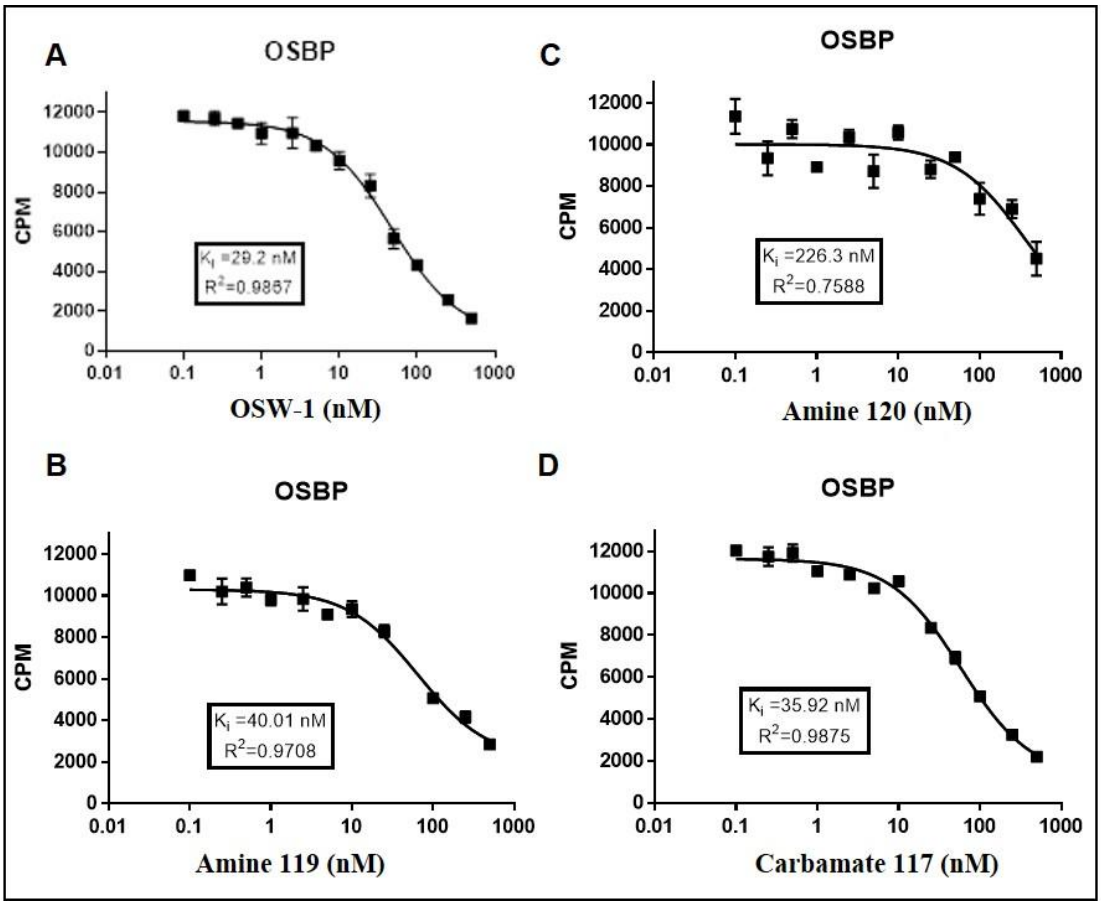

Figure 9. Representative Inhibition Binding Curves of OSBP for the OSW-1 compound (A) and OSW-1 analogs with linker (B, C, and D). Figure is adapted from Juan Nuñez's dissertation.

II.4 Conclusions

A set of OSW-1 probe analogs including deuterated OSW-1, TBS-OSW-1 and OSW-1 analogs with an amine linker were successfully synthesized and characterized. Deuterated OSW-1 was utilized as internal standard to timely quantify the concentration of OSW-1 inside individual treated cells. TBS-OSW-1 acted as a negative control and confirmed the SAR of the C-3 hydroxyl group of OSW-1. OSW-1 analog **119** (**Scheme 14**) with the amine linker on the C-3'' position retained the bioactivity of OSW-1 and can be further derivatized for different purposes. These OSW-1 probe analogs will be powerful

reagents to help elucidate the molecular pharmacology and cellular biology of the OSW-1 compound in cells.

II.5 Experimental section

II.5.1 General methods

All reactions were performed in oven-dried glassware under a positive pressure of nitrogen unless noted otherwise. Flash column chromatography was performed as described by Still *et al*.[55] employing E. Merck silica gel 60 (230-400 mesh ASTM). TLC analyses and preparative TLC (pTLC) purification was performed on 250µm Silica Gel 60 F254 plates purchased from EM Science and Fluka Analytical. All solvents and chemicals were used as purchased without further purification. Solvents used in the reactions were collected under nitrogen from a Pure Solv 400-5-MD Solvent Purification System (Innovative Technology). Infrared spectra were recorded on a Shimadzu IRAffinity-1 instrument, or Bruker Tensor 27 spectrometer, and IR spectra peaks are reported in terms of frequency of absorption (cm^{-1}). ^{1}H and ^{13}CNMR spectra were recorded on VNMRS 300, VNMRS 400, VNMRS 500 or VNMRS 600 MHz-NMR Spectrometer. Chemical shifts for proton and carbon resonances are reported in ppm (δ) relative to the residual proton or the specified carbon in chloroform (δ 7.26, proton; 77.16, carbon). High-resolution mass spectrometry (HRMS) analysis was performed using Agilent 6538 high-mass-resolution QTOF mass spectrometer. HPLC purification was performed on Shimadzu LCMS 2020 system [LC-20AP (pump), SPD-M20A (diode array detector), LCMS-2020 (mass spectrometer)]. Semi-preparative HPLC purification was performed using Phenomenex Luna C-18(2) column, 5µm particle size (250 mm x 4.6 mm), supported by Phenomenex Security Guard cartridge kit C18 (4.0 mm x 3.0 mm); Phenomenex Luna C-8(2) column,

5µm particle size (250 mm x 4.6 mm), supported by Phenomenex Security Guard cartridge kit C8 (4.0 mm x 3.0 mm) and HPLC-grade solvents.

II.5.2 Compound data

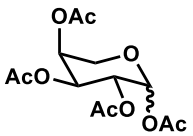

34

Compound **34** was synthesized as describe previously.[51] A suspension of L-arabinose (5.0 g, 33.3 mmol), DMAP (406.8 mg, 3.33 mmol), triethylamine (37.1 mL, 266.4 mmol) in anhydrous DCM (25 mL, 1.33 M) was stirred at 0°C for 30 minutes. To the reaction mixture was then added Ac_2O (22 mL, 233.1 mmol) dropwise slowly over 1 hour using an addition funnel. The mixture was stirred at 0°C for 1 hour, then at RT overnight to afford a clear, dark yellow solution. The reaction progress was monitored by TLC (10% MeOH/DCM, $KMnO_4$ stain). The reaction mixture was cooled to 0°C for 20 minutes, quenched with chilled DI H_2O (50 mL), stirred at 0°C for additional 30 minutes. The bi-phasic, yellow mixture was transferred to a separatory funnel, extracted with DCM (40 mL x 3). The combined organic phase was washed with 1N HCl (40 mL x 4), chilled DI H_2O (30 mL x 3), sat'd $NaHCO_3$ (30 mL x 3), chilled DI H_2O (30 mL x 2), and brine (50 mL), dried over Na_2SO_4, and filtered. The solvent was removed *in vacuo* to afford desired product **34** as a light yellow, sticky solid (10.6 g). The desired product was used in subsequent reaction without further purification. ^{1}H NMR (500 MHz, Chloroform-d) δ 6.35 (d, J = 3.1 Hz, 1H), 5.42 – 5.32 (m, 3H), 4.06 (dd, J = 12.9, 1.5 Hz, 1H), 3.82 (dd, J = 13.2, 2.0 Hz, 1H), 2.15 (d, J = 1.6 Hz, 6H), 2.02 (s, 6H). ^{13}C NMR (126 MHz, Chloroform-d) δ 170.4, 170.3, 170.0, 169.3, 90.3, 68.6, 67.2, 66.8, 62.9, 21.0, 21.0, 20.84, 20.7. See **Appendix** for NMR spectra.

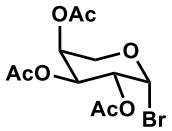

92

Compound **92** was synthesized as describe previously. [56] To a solution of **34** (10.6 g, 33.3 mmol) in anhydrous DCM (33.5 mL, 1M) at 0°C was added HBr in AcOH solution (18.1 mL, 99.9 mmol) dropwise over 1 hour using an addition funnel. The reaction mixture was stirred at 0°C for 1 hours, then at RT for 3 hours. The reaction progress was monitored by TLC (5% MeOH/DCM, $KMnO_4$ stain). After completion, the reaction mixture was quenched with DI H_2O (50 mL). The organic phase was then added to chilled, sat'd $NaHCO_3$ solution (50 mL). The mixture was stirred for 10 minutes. The aqueous phase was extracted with DCM (30 mL x 2). The combined organic phase was washed with sat'd $NaHCO_3$ solution (30 mL x 4), DI H_2O (40 mL), and brine, dried over Na_2SO_4, and filtered. The solvent was removed *in vacuo* to afford desired product **92** as a light-yellow solid (10.1 g, 89%). The desired product was used in subsequent reaction without further purification. ^{1}H NMR (500 MHz, Chloroform-d) δ 6.69 (d, J = 3.8 Hz, 1H), 5.44 – 5.35 (m, 2H), 5.08 (ddd, J = 11.7, 3.9, 1.5 Hz, 1H), 4.20 (dt, J = 13.2, 1.0 Hz, 1H), 3.93 (dd, J = 13.4, 1.8 Hz, 1H), 2.15 (s, 3H), 2.11 (s, 3H), 2.02 (s, 3H). ^{13}C NMR (126 MHz, Chloroform-d) δ 170.2, 170.2, 169.9, 89.8, 68.1, 68.0, 67.7, 64.8, 21.0, 20.9, 20.8. See **Appendix** for NMR spectra.

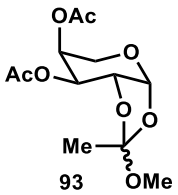

93

Compound **93** was synthesized as describe previously.[56] To a clear, yellow solution of **92** (10.1 g, 29.8 mmol) in nitromethane (30 mL, 1M) at RT under N_2 was added 2,6-lutidine

(8.7 mL, 74.7 mmol) and anhydrous MeOH (8.5 mL, 209.0 mmol). The reaction mixture was stirred at RT, the reaction progress was monitored by TLC (60% EtOAc/hexanes with 3% NEt_3, UV, CAM stain, TLC plates were pre-eluted before sample spotted). The reaction was completed after 20 hours based on TLC. The reaction was quenched with sat'd $NaHCO_3$ solution (30 mL). The aqueous phase was extracted with DCM (30 mL x 3). The combined organic phase was washed with DI H_2O (50 mL x 3), sat'd $CuSO_4$ solution (to removed 2,6-lutidine, continuous washing until $CuSO_4$ solution color remained unchanged), DI H_2O (50 mL), brine, and dried over Na_2SO_4, and filtered. The solvent was removed *in vacuo* to afford crude mixture as an orange/brown, clear oil (7.4 g). The crude mixture was purified by flash chromatography (Biotage, 50g column x 3, EtOAc/hexanes with 3% NEt_3 gradient -7% to 60%) to afford the desired mixture of ortho esters **93** as a clear, light-yellow gel (6.6 g, 76 %). ^{1}H NMR spectrum of **93** showed a mixture of two isomers. ^{1}H NMR (500 MHz, Chloroform-d) δ 5.56 (d, J = 3.9 Hz, 1H), 5.41 – 5.36 (m, 1H-minor isomer), 5.33 – 5.29 (m, 1H-minor isomer), 5.29 – 5.22 (m, 2H), 5.16 (dd, J = 9.5, 7.0 Hz, 1H-minor isomer), 5.02 (dd, J = 9.4, 3.5 Hz, 1H-minor isomer), 4.32 (d, J = 7.0 Hz, 1H-minor isomer), 4.29 (dd, J = 5.1, 3.9 Hz, 1H), 4.16 (d, J = 1.5 Hz, 1H-minor isomer), 4.09 – 4.05 (m, 1H-minor isomer), 4.02 (dd, J = 12.4, 4.5 Hz, 2H), 3.79 – 3.75 (m, 1H-minor isomer), 3.73 (dd, J = 12.5, 4.9 Hz, 1H), 3.62 (dd, J = 13.1, 1.8 Hz, 1H-minor isomer), 3.48 (s, 1H), 3.36 (s, 1H), 3.27 (s, 3H), 2.14 – 2.08 (m, 5H), 2.08 – 2.03 (m, 5H), 2.03 – 1.99 (m, 2H). ^{13}C NMR (126 MHz, Chloroform-d) δ 170.4, 170.3, 169.9, 169.9, 123.2, 102.0, 97.3, 96.7, 76.1, 75.6, 70.4, 70.0, 69.3, 69.2, 67.8, 66.7, 66.2, 63.3, 63.1, 62.5, 60.5, 56.9, 50.4, 50.0, 23.9, 23.4, 21.1, 21.0, 20.9, 20.89, 20.8, 14.3. See **Appendix** for NMR spectra.

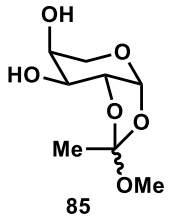

85

Compound **85** was synthesized as describe previously.[56] To a clear, light-yellow solution of **93** (6.6 g, 22.8 mmol) in anhydrous MeOH (76 mL, 0.3 M) was added NaOMe (61.6 mg, 1.14 mmol) at RT. The reaction mixture was stirred at RT under N_2, the reaction progress was monitored by TLC (50% EtOAc/hexanes with 3% NEt_3, UV, CAM stain, TLC plates were pre-eluted before sample spotted). The reaction was completed after 6 hours based on TLC. The solvent was removed *in vacuo* to afford the desired mixture of isomers **85** as a clear, light-yellow gel (4.4 g, 94%). The desired product was used in the subsequent reaction without further purification. ^{1}H NMR (600 MHz, Chloroform-d) δ 5.52 (d, J = 3.6 Hz, 1H), 5.33 (d, J = 3.6 Hz, 1H-minor isomer), 4.29 (t, J = 3.6 Hz, 1H), 4.21 (t, J = 3.7 Hz, 0H), 4.14 (t, J = 3.7 Hz, 1H), 4.12 – 4.08 (m, 1H), 4.05 (dt, J = 7.6, 4.0 Hz, 1H-minor isomer), 4.01 – 3.98 (m, 1H), 3.96 (dd, J = 12.8, 2.5 Hz, 1H-minor isomer), 3.92 (d, J = 2.7 Hz, 1H-minor isomer), 3.79 (dd, J = 12.0, 4.6 Hz, 1H), 3.71 (dd, J = 11.7, 7.4 Hz, 1H-minor isomer), 3.67 (dd, J = 11.8, 6.9 Hz, 1H), 3.62 (dd, J = 4.4, 1.6 Hz, 1H), 3.56 – 3.48 (m, 6H), 3.47 (s, 1H), 3.40 (s, 1H-minor isomer), 3.37 (s, 1H), 3.28 (s, 3H). ^{13}C NMR (151 MHz, Chloroform-d) δ 123.2, 122.8, 104.4, 96.9, 95.5, 78.7, 78.6, 73.0, 71.5, 69.0, 68.5, 68.3, 66.2, 65.9, 65.3, 63.3, 63.1, 57.2, 50.9, 50.3, 50.0, 23.8, 23.5. See **Appendix** for NMR spectra.

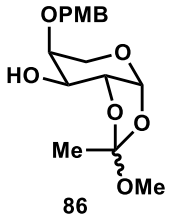

86

Compound **86** was synthesized as describe previously.[56] To a solution of **85** (3.3 g, 16.1 mmol) in anhydrous toluene (60 mL, 0.27 M) was added dibutyltin (IV) oxide (4.22 g, 16.96 mmol). The reaction mixture was heated under reflux for 3 hours using a Dean Stark trap to remove water. The solvent was removed *in vacuo* to afford crude mixture as a light brown, waxy solid. To the flask containing this crude mixture was added CsF (4.5 g, 29.8 mmol), KI (4.0 g, 23.9 mmol) and anhydrous DMF (32.3 mL, 0.5 M). The reaction mixture was then cooled to 0°C. To the reaction mixture was added p-methoxybenzyl chloride solution (2.6 mL, 19.2 mmol, dissolved in 5 mL DMF) dropwise. The reaction mixture was stirred at 0°C for 2 hours, then at RT overnight. The reaction progress was monitored by TLC (60% EtOAc/hexanes with 3% NEt_3, UV, CAM stain, TLC plates were pre-eluted before sample spotted). The reaction was completed after 16 hours by TLC. The reaction mixture was diluted with DCM (30 mL), washed with DI H_2O (30 mL). The aqueous phase was extracted with DCM (10 mL x 2). The combined organic phase was washed with DI H_2O (20 mL x 4), brine (20 mL x 2), dried over Na_2SO_4, and filtered. The solvent was removed *in vacuo* to afford crude mixture as white solid suspension in yellow oil (8.0 g). The crude mixture was purified by flash chromatography (Biotage, 50g column x 3, EtOAc/hexanes with 3% NEt_3 gradient -15% to 60%) to afford the desired mono-PMB protected sugar **86** as an off-white, waxy solid (3.28 g, 63 % over 2 steps). ^{1}H NMR (500 MHz, Chloroform-d) δ 7.28 – 7.23 (m, 2H), 6.92 – 6.86 (m, 2H), 5.49 (d, J = 3.0 Hz, 1H), 5.27 (d, J = 3.0 Hz, 1H-minor isomer), 4.55 (s, 2H), 4.29 (dq, J = 6.5, 3.2 Hz, 2H), 4.07 (t,

J = 3.1 Hz, 1H-minor isomer), 3.81 (s, 3H), 3.79 – 3.71 (m, 2H), 3.67 (dd, J = 10.9, 7.5 Hz, 1H), 3.36 (s, 1H), 3.28 (s, 3H). ^{13}C NMR (126 MHz, Chloroform-d) δ 159.7, 129.6, 129.6, 129.5, 123.0, 114.2, 96.8, 94.8, 78.5, 78.1, 72.2, 71.8, 71.6, 71.5, 66.8, 66.2, 60.3, 60.2, 55.4, 49.9, 24.3, 23.8. See **Appendix** for NMR spectra.

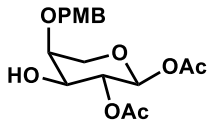

87

Compound **87** was synthesized as describe previously.[43] To a RBF containing **86** (1.58 g, 4.8 mmol) under N_2 was added glacial AcOH (9 mL) at RT. The clear, colorless solution was stirred at RT. The reaction progress was monitored by TLC (60% EtOAc/hexanes with 3% NEt_3, UV, CAM stain, TLC plates were pre-eluted before sample spotted; TLC plates were placed under vacuum after sample spotted to reduce streaking). After 40 minutes, the reaction was completed base on TLC. The reaction mixture was diluted with EtOAc (50 mL). The organic phase was washed with DI H_2O (until the aqueous phase was not acidic anymore by pH paper), brine, dried over Na_2SO_4, and filtered. The solvent was removed *in vacuo* to afford crude mixture as off-white, waxy solid (1.4 g). The crude mixture was purified by flash chromatography (Biotage, 50g column, EtOAc/hexanes gradient -30% to 100%) to afford the desired product **87** as an off-white, waxy solid (1.14 g, 66 %). ^{1}H NMR (500 MHz, Chloroform-d) δ 7.27 (d, J = 8.7 Hz, 2H), 6.89 (d, J = 8.5 Hz, 2H), 5.59 (d, J = 6.6 Hz, 1H), 5.11 (dd, J = 7.9, 6.7 Hz, 1H), 4.66 (d, J = 11.4 Hz, 1H), 4.48 (d, J = 11.4 Hz, 1H), 4.08 (dd, J = 12.8, 3.7 Hz, 1H), 3.81 (s, 3H), 3.79 – 3.71 (m, 2H), 3.53 (dd, J = 12.9, 1.9 Hz, 1H), 2.11 (s, 3H), 2.09 (s, 3H). ^{13}C NMR (126 MHz, Chloroform-d) δ 170.3, 169.6, 165.1, 129.7, 129.4, 114.8, 92.1, 74.0, 71.5, 71.4, 70.7, 62.4, 55.5, 26.1, 21.1, 21.0. See **Appendix** for NMR spectra.

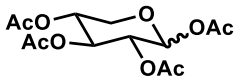

38

Compound **38** was synthesized as describe previously.[43] To a mixture of D-xylose (5.0 g, 33.3 mmol) in pyridine (48.0 mL, 0.7 M) was added Ac_2O (18.9 mL, 199.8 mmol) fast dropwise under N_2. The reaction mixture was stirred at RT. The reaction progress was monitored by TLC (10% MeOH/DCM, $KMnO_4$ stain). After 2 hours, the reaction was completed based on TLC. The reaction was quenched with DI H_2O (3 mL), neutralized with sat'd $NaHCO_3$ solution (160 mL), extracted with EtOAc (40 mL x 3). The organic phase was washed with sat'd $NaHCO_3$ solution (50 mL x 3), sat'd $CuSO_4$ solution (washed until the color of $CuSO_4$ remained the same to remove pyridine), brine (50 mL x 2), dried over Na_2SO_4, and filtered. The solvent was removed *in vacuo* to afford desired products **38** (a mixture of α and β-furanose and α and β-pyranose) as a clear, light yellow thick gel (10.1 g, 95 %). ^{1}H NMR (500 MHz, Chloroform-d) δ 6.25 (d, J = 3.7 Hz, 1H), 5.71 (d, J = 6.9 Hz, 1H), 5.45 (t, J = 9.8 Hz, 1H), 5.19 (t, J = 8.3 Hz, 1H), 5.05 – 4.99 (m, 3H), 5.00 – 4.94 (m, 1H), 4.16 – 4.08 (m, 1H), 3.92 (dd, J = 11.2, 5.9 Hz, 1H), 3.73 – 3.67 (m, 1H), 3.52 (dd, J = 12.0, 8.5 Hz, 1H), 2.16 (s, 3H), 2.12 – 2.07 (m, 3H), 2.05 – 2.02 (m, 12H), 2.01 (s, 3H). See **Appendix** for NMR spectra.

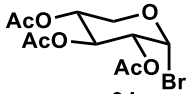

94

Compound **94** was synthesized as describe previously.[43] To a solution of **38** (9.86 g, 31.0 mmol) in anhydrous DCM (140 mL, 0.22M) at 0°C under N_2 was added HBr in AcOH solution (16.3 mL, 30% w/v, 93.0 mmol) dropwise over 30 minutes. The reaction mixture was stirred at 0°C for 1.5 hours, then at RT for 2.5 hours. The reaction progress was

monitored by TLC (5% MeOH/DCM, $KMnO_4$ stain). The reaction was completed after 4 hours based on TLC. The reaction mixture was washed with DI H_2O (75 mL). The aqueous phase was extracted with DCM (50 mL x 3). The combined organic phase was washed with sat'd $NaHCO_3$ solution (50 mL x 3), brine (50 mL x 2), dried over Na_2SO_4, and filtered. The solvent was removed *in vacuo* to afford desired product **94** as a white solid (9.4 g, 89%). ^{1}H NMR (300 MHz, Chloroform-d) δ 6.58 (d, J = 4.0 Hz, 1H), 5.56 (t, J = 9.8 Hz, 1H), 5.04 (ddd, J = 10.9, 9.6, 6.0 Hz, 1H), 4.77 (dd, J = 9.9, 4.0 Hz, 1H), 4.05 (dd, J = 11.4, 6.0 Hz, 1H), 3.88 (td, J = 11.2, 0.7 Hz, 1H), 2.12 – 2.08 (m, 3H), 2.08 – 2.04 (m, 6H). See **Appendix** for NMR spectra.

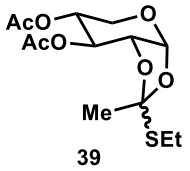

39

Compound **39** was synthesized as describe previously.[43] To a solution of **94** (14.1 g, 41.5 mmol) in anhydrous CH_3NO_2 (75.0 mL, 0.55 M) at RT under N_2 was added EtSH (6.14 mL, 82.9 mmol) and 2,6-lutidine (9.66 mL, 82.9 mmol) slowly. The reaction mixture was stirred at RT. The reaction progress was monitored by TLC (30% EtOAc/hexanes with 3% NEt_3, TLC plates were pre-eluted before sample spotting). After 24 hours, the reaction was completed based on TLC. The reaction was quenched with sat'd $NaHCO_3$ solution (30 mL). The reaction mixture was diluted with DCM (70 mL), washed with DI H_2O (50 mL). The aqueous phase was extracted with DCM (50 mL x 3). The combined organic phase was washed with sat'd $CuSO_4$ solution (washed until the color of $CuSO_4$ remained the same to remove 2,6-lutidine), brine, dried over Na_2SO_4, and filtered. The solvent was removed *in vacuo* to afford desired product **39** as a yellow, thick gel (12.87 g, 95%). The product was used in the subsequent reaction without further purification, but alternatively,

the product can be purified by silica gel column chromatography with EtOAc/hexanes with 3% NEt_3 gradient. ^{1}H NMR (300 MHz, Chloroform-d) δ 5.58 (d, J = 4.8 Hz, 1H), 5.24 (t, J = 2.6 Hz, 1H), 4.89 (dddd, J = 9.3, 6.4, 2.7, 1.1 Hz, 1H), 4.38 (ddd, J = 4.8, 2.6, 1.1 Hz, 1H), 3.95 (dd, J = 11.9, 6.4 Hz, 1H), 3.62 (ddd, J = 11.8, 8.5, 0.6 Hz, 1H), 2.62 (q, J = 7.5 Hz, 2H), 2.12 (s, 3H), 2.08 (s, 3H), 1.95 (s, 3H), 1.25 (t, J = 7.5 Hz, 3H). See **Appendix** for NMR spectra.

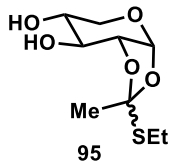

95

Compound **95** was synthesized as describe previously.[43] To a clear, light-yellow solution of acetylated thio ortho ester **39** (5.74 g, 17.9 mmol) in anhydrous MeOH (110 mL, 0.16 M) at 0˚C under N_2 was added NaOMe (48.3 mg, 0.893 mmol) dissolved in MeOH (9 mL) slowly. The reaction mixture was stirred at RT; the reaction progress was monitored via TLC (30% EtOAc/hexanes with 3% NEt_3, TLC plates were pre-eluted before sample spotting). The reaction mixture appearance did not change. After 2 hours, the reaction was completed based on TLC. The solvent was removed *in vacuo* to afford desired product **95** as a yellow oil, which turned into a yellow waxy solid under high vacuum (4.0g, 95% yield). ^{1}H NMR (500 MHz, Chloroform-d) δ 5.50 (d, J = 3.5 Hz, 1H), 4.31 (td, J = 3.5, 1.1 Hz, 1H), 4.16 (s, 1H), 3.96 (dd, J = 12.0, 3.3 Hz, 1H), 3.76 – 3.70 (m, 1H), 3.70 – 3.63 (m, 1H), 2.66 (q, J = 7.5 Hz, 2H), 1.96 (s, 3H), 1.26 (t, J = 7.5 Hz, 3H). See **Appendix** for NMR spectra.

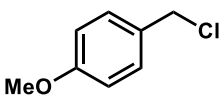

PMB-Cl

4-methoxybenzyl chloride (PMB-Cl): To a 100mL-RBF was added 4-methoxybenzyl alcohol (20.79 g, 143.6 mmol), a stir bar, 37% HCl solution (~38 mL). The flask was sealed and vented with a needle. The reaction mixture was biphasic, one was milky white and the other one was clear, light yellow. The reaction mixture was stirred at RT the reaction progress was monitored by TLC (30% EtOAc/hex with NEt_3). After 1.5hr, the reaction was completed based on the absence of SM on TLC. To the reaction mixture was added hexane (50 mL) and DI H_2O (50mL). The aqueous layer was extracted with hexane (50 mL x 2). The combined organic layer was washed with DI H_2O (50 mL x 3), dried with Na_2SO_4, and concentrated *in vacuo* to afford desired. product as a clear oil (22 g, 97% yield). The product was stored at -20˚C with K_2CO_3 as a stabilizer. The NMR data agreed with the published reference found on Sigma-Aldrich website. ^{1}H NMR (400 MHz, Chloroform-d) δ 7.36 – 7.31 (m, 2H), 6.92 – 6.87 (m, 2H), 4.58 (s, 2H), 3.82 (s, 3H).

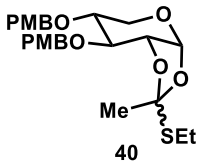

40

Compound **40** was synthesized as describe previously.[43] To a clear, yellow solution of de-protected thio ortho ester **95** (1.4 g, 5.92 mmol) in anhydrous DMF (30 mL, 0.2 M) at RT under N_2 atmosphere was wadded NaH (1.02 g, 23.7 mmol, 60% suspension in mineral oil). The cloudy, grayish mixture was stirred at RT for 10 minutes, then PMB-Cl solution (2.3 g, 14.8 mmol, diluted in 10 mL anhydrous DMF) was added dropwise. The reaction mixture was stirred at RT; the reaction progress was monitored by TLC (30% EtOAc/hexanes with 3% NEt_3, TLC plates were pre-eluted before sample spotting). After ~ 5 hours, no PMB-Cl was observed on TLC. To the reaction was added more PMB-Cl (0.58 g, 3.7 mmol, dissolved in 2 mL DMF). After 6 hours, the reaction was completed

based on TLC. The reaction was quenched with sat'd $NaHCO_3$ solution (40 mL). The aqueous phase was extracted with EtOAc (30 mL x 3). The combined organic phase was washed with brine, dried over Na_2SO_4, filtered, and the solvent was removed *in vacuo* to afford crude mixture. The mixture was purified through silica gel column chromatography (Biotage, 50 g column x 2, EtOAc/hexanes with 3% NEt_3 gradient) to afford the desired PMB-protected thio ortho ester **40** (2.0 g, 70.8 %). ^{1}H NMR (500 MHz, Chloroform-d) δ 7.29 – 7.24 (m, 2H), 7.23 – 7.19 (m, 2H), 6.91 – 6.84 (m, 4H), 5.60 (d, J = 5.1 Hz, 1H), 4.63 – 4.58 (m, 1H), 4.55 – 4.49 (m, 2H), 4.48 – 4.42 (m, 2H), 3.84 (dd, J = 4.1, 2.7 Hz, 1H), 3.81 (s, 3H), 3.80 (s, 3H), 3.77 (dd, J = 11.2, 5.7 Hz, 1H), 3.65 (ddd, J = 9.8, 5.6, 4.1 Hz, 1H), 3.56 (dd, J = 11.2, 9.5 Hz, 1H), 2.62 (q, J = 7.5 Hz, 2H), 1.91 (s, 3H), 1.26 (t, J = 7.4 Hz, 3H). See **Appendix** for NMR spectra.

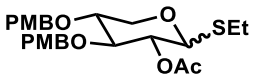

41

Compound **41** was synthesized as describe previously.[43] To a solution of **40** (2.1 g, 4.41 mmol) in anhydrous DCM (18 mL, 0.25 M) at -78°C was added $ZnCl_2$ solution (40 mg, 0.29 mmol, dissolved in 2 mL anhydrous THF). The clear, light yellow solution was stirred at - 78°C for 45 minutes, then at 0°C for 2h15m. The reaction progress was monitored by TLC (30% EtOAc/hexanes with 3% NEt_3, TLC plates were pre-eluted before sample spotting). After 3 hours, the reaction mixture was warmed up to RT, diluted with DCM (50 mL), washed with sat'd NH_4Cl solution (40 mL), sat'd $NaHCO_3$ solution (40 mL), and DI H_2O (40 mL). The combined aqueous phase was back extracted with DCM (10 mL x 2). The combined organic phase was washed with brine, dried over Na_2SO_4, and filtered. The solvent was removed *in vacuo* to afford crude product **41** as a tan, thick gel (2.06 g, 98%).

The crude product was used in the subsequent reaction without further purification. ^{1}H NMR (500 MHz, Chloroform-d) δ 7.25 – 7.19 (m, 4H), 6.90 – 6.83 (m, 4H), 4.92 (dd, J = 9.1, 8.3 Hz, 1H), 4.74 (d, J = 11.2 Hz, 1H), 4.65 – 4.60 (m, 2H), 4.53 (d, J = 11.3 Hz, 1H), 4.36 (d, J = 9.1 Hz, 1H), 4.02 (dd, J = 11.6, 4.9 Hz, 1H), 3.80 (d, J = 1.0 Hz, 6H), 3.61 (ddd, J = 9.3, 8.3, 4.9 Hz, 1H), 3.55 (t, J = 8.3 Hz, 1H), 3.24 (dd, J = 11.6, 9.4 Hz, 1H), 2.71 – 2.59 (m, 2H), 2.01 (s, 3H), 1.23 (t, J = 7.5 Hz, 3H). See **Appendix** for NMR spectra.

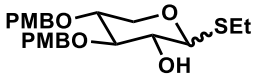

96

Compound **96** was synthesized as describe previously.[43] To a mixture of **41** (2.06 g, 4.32 mmol) in anhydrous MeOH (22 mL, 0.2 M) at RT under N_2 was added NaOMe (94 mg, 1.73 mmol). The reaction mixture was stirred at RT; the reaction progress was monitored by TLC (30% EtOAc/hexanes with 3% NEt_3). After 14 hours, the reaction as not completed, so to the reaction mixture was added more NaOMe (94 mg, 1.73 mmol). After 38 hours, the reaction was completed based on TLC. The solvent was removed to afford crude mixture, which was purified by silica gel column chromatography to afford desired product **96** as a white solid (1.47 g, 78.3 %). ^{1}H NMR (400 MHz, Chloroform-d) δ 7.32 – 7.27 (m, 2H), 7.25 – 7.20 (m, 2H), 6.90 – 6.84 (m, 4H), 4.76 – 4.69 (m, 2H), 4.63 – 4.51 (m, 3H), 4.11 (dd, J = 11.9, 3.6 Hz, 1H), 3.81 (s, 6H), 3.59 – 3.48 (m, 2H), 3.38 – 3.31 (m, 1H), 2.90 (d, J = 4.5 Hz, 1H), 2.68 (qd, J = 7.4, 5.0 Hz, 2H), 1.29 (t, J = 7.4 Hz, 3H). ^{13}C NMR (101 MHz, Chloroform-d) δ 159.6, 159.5, 130.6, 130.0, 129.7, 129.7, 114.0, 114.0, 86.5, 80.9, 76.3, 74.0, 72.5, 71.7, 65.1, 55.4, 25.2, 15.4. See **Appendix** for NMR spectra.

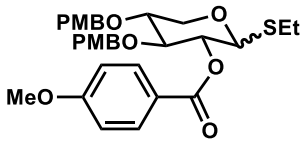

42

Compound **42** was synthesized as describe previously.[43] To a mixture of **96** (970.0 mg, 2.23 mmol), DMAP (27.3 mg, 0.223 mmol), NEt_3 (466.7 μ, 3.35 mmol) in anhydrous DCM (8.9 mL, 0.25 M) at RT was added 4-methoxybenzoyl chloride solution (761.6 mg, 4.46 mmol, dissolved in 8 mL anhydrous DCM). The clear, light-yellow reaction mixture was stirred at RT; the reaction progress was monitored by TLC (5% EtOAC/DCM, or DCM, UV, CAM stain). After 22 hours, the reaction was completed based on TLC. The reaction was quenched with sat'd $NaHCO_3$ (30 mL), diluted with DCM (50 mL). The organic phase was washed with sat'd $NaHCO_3$ (20 mL x 2), DI H_2O (20 mL x 2). The combined aqueous phase was back extracted with DCM (10 mL x 2). The combined organic phase was washed with brine, dried over Na_2SO_4, and filtered. The solvent was removed *in vacuo* to afford crude mixture as a yellow gel. The crude mixture was purified by silica gel column chromatography (eluted with EtOAC/DCM gradient from 0 to 5%) to afford desired product **42** as a clear, sticky gel (1.15 g, 90 %). ^{1}H NMR (400 MHz, Chloroform-d) δ 7.95 (d, J = 8.9 Hz, 1H), 7.24 (d, J = 8.6 Hz, 2H), 7.09 (d, J = 8.6 Hz, 2H), 6.89 (d, J = 8.9 Hz, 2H), 6.86 (d, J = 8.6 Hz, 2H), 6.68 (d, J = 8.6 Hz, 2H), 5.17 (t, J = 8.3 Hz, 1H), 4.71 – 4.59 (m, 3H), 4.58 – 4.52 (m, 2H), 4.09 (dd, J = 11.6, 4.4 Hz, 1H), 3.86 (s, 3H), 3.80 (s, 3H), 3.72 (s, 3H), 3.70 – 3.61 (m, 2H), 3.36 – 3.29 (m, 1H), 2.74 – 2.59 (m, 2H), 1.21 (t, J = 7.4 Hz, 3H). ^{13}C NMR (101 MHz, Chloroform-d) δ 165.1, 163.6, 159.5, 159.2, 132.1, 130.3, 130.3, 129.8, 129.7, 122.5, 114.0, 113.8, 113.7, 84.1, 81.2, 77.1, 74.3, 73.0, 71.5, 67.1, 55.6, 55.4, 55.2, 24.3, 21.2, 15.0, 14.3. See **Appendix** for NMR spectra.

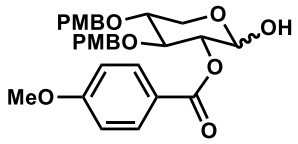

97

Compound **97** was synthesized as describe previously.[43] To a mixture of **42** (1.13 g, 1.99 mmol) in DCM (13.2 mL, 0.15 M) and DI H_2O (1.3 mL, 1.5 M) at RT was added NBS (389.0 mg, 2.19 mmol) as a solid. The reaction mixture was stirred at RT under N_2. The reaction progress was monitored by TLC (30% EtOAc/hexanes, UV, CAM stain). The appearance of the reaction mixture changed from clear, light yellow to cloudy, dark orange after 15 minutes, when the reaction was completed based on TLC. The reaction was quenched with sat'd $Na_2S_2O_3$ solution (20 mL). The reaction mixture was diluted with DCM (50 mL), washed with sat'd $Na_2S_2O_3$ solution (20 mL x 2). The combined aqueous phase was back extracted with DCM (10 mL x 2). The combined organic phase was washed with DI H_2O (20 mL x 2), brine, dried over Na_2SO_4, and filtered. The solvent was removed *in vacuo* to afford crude mixture as a clear gel. The crude mixture was purified by silica gel column chromatography (eluted with EtOAc/hexanes gradient, 30% to 80%) to afford desired mixture of products **97** (α and β anomers) as a clear, thick gel (722.6 mg, 69%).[1]H NMR (500 MHz, Chloroform-d) δ 8.02 – 7.91 (m, 4H), 7.26 – 7.21 (m, 3H), 7.17 – 7.11 (m, 3H), 6.95 – 6.83 (m, 7H), 6.77 – 6.72 (m, 3H), 5.41 (t, J = 3.9 Hz, 1H), 4.99 (ddd, J = 9.3, 3.5, 1.0 Hz, 1H), 4.95 (dd, J = 8.4, 7.0 Hz, 1H), 4.79 – 4.64 (m, 5H), 4.64 – 4.54 (m, 3H), 4.04 (ddd, J = 16.9, 10.6, 6.6 Hz, 2H), 3.93 – 3.85 (m, 7H), 3.84 – 3.78 (m, 6H), 3.77 – 3.74 (m, 5H), 3.71 (dd, J = 11.3, 5.2 Hz, 1H), 3.69 – 3.60 (m, 2H), 3.38 (dd, J = 12.0, 9.0 Hz, 1H), 2.76 (dd, J = 4.3, 1.1 Hz, 1H). [13]C NMR (126 MHz, Chloroform-d) δ 165.8, 159.6, 132.2, 132.1, 130.6, 130.4, 129.8, 129.7, 129.7, 129.6, 122.2, 114.1, 114.0, 114.0, 113.9,

113.8, 113.82, 96.2, 91.0, 79.4, 78.0, 74.9, 74.7, 74.57, 73.4, 73.1, 72.9, 63.3, 60.7, 55.6, 55.6, 55.4, 55.3. See **Appendix** for NMR spectra.

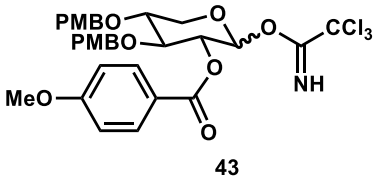

43

Compound **43** was synthesized as describe previously.[43] To a solution of **97** (718.0 mg, 1.37 mmol) in anhydrous DCM (9.1 mL, 0.15 M) under N_2 at RT was added trichloroacetonitrile (686 µL, 6.84 mmol) and DBU (20.4 µL, 0.136 mmol). The reaction color changed from light to dark yellow. The reaction mixture was stirred at RT. The reaction progress was monitored by TLC (30% EtOAc/hexanes with 3% NEt_3, TLC plates were pre-eluted before sample spotting). After 1.5 hours, an aliquot of the reaction was analyzed by ^{1}H NMR to show the completion of the reaction. The solvent was removed *in vacuo* to afford crude mixture as a yellow, thick gel. The crude mixture was purified by silica gel column chromatography (eluted with EtOAc/hexanes with 3% NEt_3 gradient) to afford desired mixture of products **43** (α and β anomers) as a light yellow, thick gel (881.0 mg, 96 %). ^{1}H NMR (400 MHz, Chloroform-d) δ 8.58 (s, 1H), 8.48 (s, 1H), 7.91 (dt, J = 9.1, 2.6 Hz, 3H), 7.29 – 7.20 (m, 3H), 7.14 (t, J = 8.5 Hz, 3H), 6.91 – 6.82 (m, 6H), 6.75 – 6.68 (m, 3H), 6.46 (d, J = 3.6 Hz, 1H), 5.97 (d, J = 5.7 Hz, 1H), 5.41 (dd, J = 7.0, 5.7 Hz, 1H), 5.21 (dd, J = 9.9, 3.6 Hz, 1H), 4.82 – 4.73 (m, 1H), 4.73 – 4.66 (m, 3H), 4.66 – 4.53 (m, 3H), 4.17 – 4.08 (m, 2H), 3.89 – 3.83 (m, 5H), 3.83 – 3.75 (m, 7H), 3.75 – 3.70 (m, 5H), 3.62 (dd, J = 11.9, 7.2 Hz, 1H). See **Appendix** for NMR spectra.

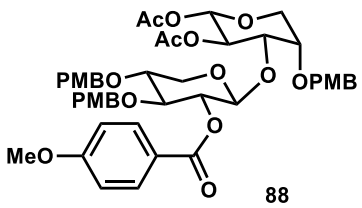

88

Compound **88** was synthesized as describe previously.[43] A mixture of imidates **43** (306.0 mg, 0.457 mmol), L-arabinose moiety **87** (95.4 mg, 0.269 mmol) and 4Å molecular sieves powder (400 mg) in anhydrous DCM (2.7 mL, 0.1 M) was stirred at RT under N_2 for 1 hour, then cooled down to -35°C. To the reaction was added $BF_3{\cdot}Et_2O$ (10.0 µL, 0.0807 mmol, dissolved in 100 µL of anhydrous DCM). The reaction mixture was stirred at -35°C. The reaction progress was monitored by TLC (55% EtOAc/hexanes with 3% NEt_3, UV, CAM stain). After 30 minutes, the reaction mixture was allowed to warm up to -20°C. After 1 hour, since not much change was observed by TLC, the reaction was quenched with NEt_3 (100 µL). The reaction mixture was warmed up to RT, filtered through celite. The solvent was removed *in vacuo* to afford crude mixture as a yellow gel. The crude mixture was purified by silica gel column chromatography (eluted with acetone/benzene gradient from 0% to 8%) to afford desired product **88** as a white, foamy solid (193.0 mg, 83%). ^{1}H NMR (500 MHz, Chloroform-d) δ 7.85 – 7.79 (m, 2H), 7.19 – 7.12 (m, 4H), 7.02 – 6.94 (m, 2H), 6.81 – 6.71 (m, 6H), 6.58 (d, J = 8.6 Hz, 2H), 5.43 (d, J = 5.8 Hz, 1H), 5.08 (ddd, J = 12.9, 7.2, 5.8 Hz, 2H), 4.62 – 4.49 (m, 6H), 4.48 – 4.42 (m, 1H), 3.88 (dd, J = 11.9, 4.2 Hz, 1H), 3.83 (dd, J = 12.1, 5.2 Hz, 1H), 3.78 – 3.72 (m, 4H), 3.71 (s, 3H), 3.70 – 3.66 (m, 4H), 3.65 – 3.55 (m, 6H), 3.40 (dd, J = 12.1, 2.4 Hz, 1H), 3.23 (dd, J = 11.7, 7.8 Hz, 1H), 1.86 (s, 3H), 1.69 (s, 3H). ^{13}C NMR (126 MHz, Chloroform-d) δ 169.7, 169.1, 164.8, 163.6, 159.5, 159.3, 159.2, 132.0, 130.4, 130.2, 130.1, 129.8, 129.74, 129.73, 129.71, 129.7, 128.4, 122.3, 114.0, 113.7, 113.7, 113.69, 101.9, 92.1, 79.1, 77.4, 76.7, 73.8,

72.74, 72.70, 71.9, 71.6, 69.8, 63.0, 55.5, 55.38, 55.36, 55.2, 20.8, 20.6. See **Appendix** for NMR spectra.

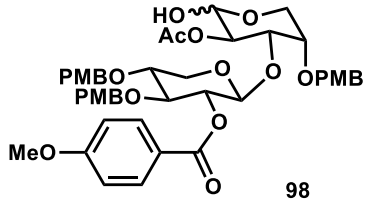

98

To a clear, colorless solution of **88** (193.0 mg, 0.224 mmol) in anhydrous THF (2.5 mL, 0.1 M) at RT under N_2 was added morpholine (154.7 µL, 1.79 mmol). The reaction mixture was stirred at RT. The reaction progress was monitored by TLC (70% EtOAc/hexanes, UV, CAM stain). After 19 hours, TLC showed only 50% conversion. To the reaction mixture was added more morpholine (70.0 µL, 0.81 mmol). After 48 hours, the reaction was mostly completed based on TLC. The solvent was removed *in vacuo* to afford crude mixture, which was purified by silica gel column chromatography (EtOAc/hexanes gradient- 20% to 100%) to afford desired mixture of products **98** (α and β anomers) as a white powder (119.0 mg, 65%). ^{1}H NMR (400 MHz, Chloroform-d) δ 7.94 – 7.87 (m, 2H), 7.30 – 7.21 (m, 4H), 7.09 (dd, J = 8.9, 2.7 Hz, 2H), 6.91 – 6.81 (m, 6H), 6.71 – 6.64 (m, 2H), 5.25 – 5.13 (m, 2H), 5.04 (dd, J = 9.1, 3.1 Hz, 1H), 4.94 (td, J = 9.1, 8.4, 6.0 Hz, 0H), 4.78 – 4.47 (m, 10H), 4.11 – 4.06 (m, 1H), 4.02 – 3.86 (m, 2H), 3.87 – 3.83 (m, 4H), 3.81 – 3.80 (m, 3H), 3.79 (s, 6H), 3.75 – 3.69 (m, 6H), 3.68 – 3.57 (m, 1H), 1.76 (s, 3H). ^{13}C NMR (101 MHz, Chloroform-d) δ 171.3, 170.2, 164.8, 163.57, 159.5, 159.3, 159.22, 159.21, 132.0, 131.9, 130.7, 130.3, 130.2, 130.1, 129.8, 129.78, 129.75, 129.6, 122.4, 114.0, 113.8, 113.77, 113.75, 113.72, 113.6, 102.2, 91.1, 80.0, 76.6, 74.5, 74.1, 72.9, 72.6, 72.1, 70.8, 63.4, 61.9, 60.5, 55.5, 55.4, 55.38, 55.24, 55.22, 21.2, 20.7, 20.7, 14.3. See **Appendix** for NMR spectra.

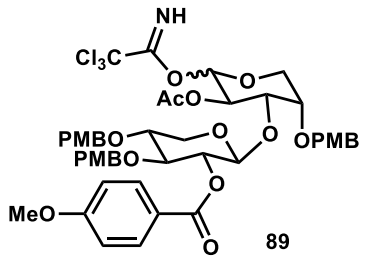

89

Compound **89** was synthesized as describe previously.[43] To a solution of **98** (71.4 mg, 0.087 mmol) in anhydrous DCM (0.58 mL, 0.15 M) under N_2 at RT was added trichloroacetonitrile (61.2 µL, 0.61 mmol) and DBU (1.3 µL, 0.0087 mmol). The reaction color changed from light to dark yellow. The reaction mixture was stirred at RT. The reaction progress was monitored by TLC (30% EtOAc/hexanes with 3% NEt_3, TLC plates were pre-eluted before sample spotting). After 1.5 hours, an aliquot of the reaction was analyzed by ^{1}H NMR to show the completion of the reaction. The solvent was removed *in vacuo* to afford crude mixture as a yellow, thick gel. The crude mixture was purified by silica gel column chromatography (eluted with EtOAc/hexanes with 3% NEt_3 gradient) to afford desired mixture of products **89** (α and β anomers) as a light yellow, thick gel (68.0 mg, 81 %). The products were used in the subsequent reaction as a mixture of anomers. α-anomer: ^{1}H NMR (500 MHz, Chloroform-d) δ 8.48 (s, 1H), 7.93 – 7.88 (m, 2H), 7.31 – 7.23 (m, 4H), 7.12 – 7.06 (m, 2H), 6.86 (td, J = 8.7, 6.7 Hz, 6H), 6.71 – 6.65 (m, 2H), 6.43 (d, J = 3.5 Hz, 1H), 5.34 (dd, J = 10.3, 3.5 Hz, 1H), 5.20 (dd, J = 8.0, 6.5 Hz, 1H), 4.78 – 4.72 (m, 2H), 4.70 – 4.54 (m, 5H), 4.15 – 4.08 (m, 2H), 3.96 (dd, J = 11.8, 4.5 Hz, 1H), 3.92 – 3.88 (m, 2H), 3.87 – 3.84 (m, 4H), 3.81 (s, 3H), 3.81 – 3.77 (m, 4H), 3.77 – 3.65 (m, 6H), 3.34 (dd, J = 11.8, 8.2 Hz, 1H), 1.61 (s, 3H). β-anomer: ^{1}H NMR (500 MHz, Chloroform-d) δ 8.55 (s, 1H), 7.96 – 7.89 (m, 2H), 7.30 – 7.27 (m, 2H), 7.24 – 7.19 (m, 2H), 7.16 – 7.10 (m, 2H), 6.90 – 6.80 (m, 6H), 6.73 – 6.68 (m, 2H), 5.72 (d, J = 5.9 Hz,

1H), 5.42 (dd, J = 8.0, 5.9 Hz, 1H), 5.22 (dd, J = 6.9, 5.3 Hz, 1H), 4.81 (d, J = 5.3 Hz, 1H), 4.73 – 4.48 (m, 7H), 4.06 (ddd, J = 11.8, 4.5, 2.4 Hz, 2H), 3.95 – 3.91 (m, 1H), 3.88 – 3.82 (m, 5H), 3.82 – 3.77 (m, 7H), 3.76 – 3.70 (m, 4H), 3.63 (dt, J = 6.9, 3.4 Hz, 1H), 3.59 (dd, J = 12.1, 2.4 Hz, 1H), 3.38 (dd, J = 11.9, 7.3 Hz, 1H), 1.79 (s, 3H). See **Appendix** for NMR spectra.

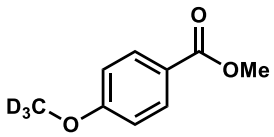

99

To a clear, colorless solution of methyl 4-hydroxybenzoate (1.0 g, 6.57 mmol) in anhydrous DMF (13.1 mL, 0.5 M) at 0°C under N_2 was added NaH (315.5 mg, 7.9 mmol, 60% dispersion in oil) in portion. The mixture was then stirred at RT for 45 minutes, then cooled back down to 0°C. To the reaction mixture was added CD_3I (0.9 mL, 14.45 mmol) dropwise. The reaction mixture was stirred at RT. The reaction progress was monitored by TLC (20% EtOAc/hexanes, UV). After 2 hours 45 minutes, the reaction mixture was diluted with $CHCl_3$ (40 mL), washed with brine (50 mL x 3). The aqueous layer was extracted with $CHCl_3$ (20 mL). The combined organic layer was washed with brine, dried over Na_2SO_4, and filtered. The solvent was removed *in vacuo* to afford desired product **99** as a white, waxy solid (1.07 g, 97%). The NMR data agreed with that of methyl *p*-methoxybenzoate with the absence of the singlet due to the deuterium moiety. ^{1}H NMR (400 MHz, Chloroform-d) δ 7.99 (d, J = 9.2 Hz, 2H), 6.91 (d, J = 8.9 Hz, 2H), 3.88 (s, 3H). See **Chapter appendix** for NMR spectra.

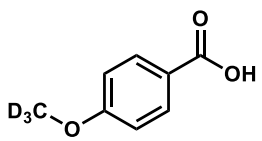

100

To a clear, colorless solution of **99** (1.07 g, 6.35 mmol) in 200-proof ethanol (42.3 mL, 0.14 M) was added KOH (534.7 mg, 9.53 mmol, dissolved in the minimum amount of DI H_2O). The reaction mixture was heated under reflux for 3 hours. Then the solvent was removed *in vacuo* to afford a white solid, which was dissolved in DI H_2O and cooled to 0°C. The solution was made acidic with 6N HCl added dropwise, which resulted in white precipitation. The precipitation was filtered and dried under vacuum to afford the desired product **100** as a white solid (950.0 mg, 96%). The NMR data agreed with that of *p*-methoxybenzoic acid with the absence of the singlet due to the deuterium moiety. ^{1}H NMR (400 MHz, Chloroform-d) δ 8.06 (d, J = 8.9 Hz, 2H), 6.95 (d, J = 8.9 Hz, 2H). See **Chapter appendix** for NMR spectra.

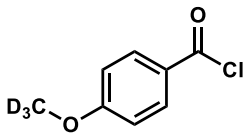

101

To a mixture of acid **100** (500.0 mg, 3.22 mmol) in anhydrous DCM (6.4 mL, 0.5 M) at RT under N_2 was added $SOCl_2$ (0.7 mL, 9.67 mmol) dropwise. The reaction mixture was heated under reflux for 3 hours. The solvent was then removed in vacuo to afford desired product **101** as an off-white, waxy solid (555.0 mg, 98 %). The product was used in subsequent reaction without further purification. The NMR data agreed with that of *p*-methoxybenzoyl chloride with the absence of the singlet due to the deuterium moiety. ^{1}H NMR (400 MHz, Chloroform-d) δ 8.07 (d, J = 9.0 Hz, 2H), 6.96 (d, J = 9.0 Hz, 2H). ^{13}C NMR (101 MHz, Chloroform-d) δ 167.24, 165.52, 134.12, 125.54, 114.35. See **Chapter appendix** for NMR spectra.

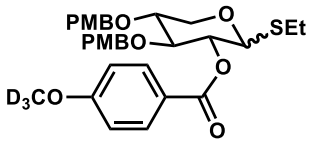

102

To a mixture of **96** (453.9mg, 1.04 mmol), DMAP (19.5 mg, 0.159 mmol), NEt_3 (218.0 µL, 1.57 mmol) in anhydrous DCM (3.5 mL, 0.29 M) at RT was added 4-methoxybenzoyl chloride-D_3 **101** solution (442.7 mg, 2.55 mmol, dissolved in 1 mL anhydrous DCM). The clear, light-yellow reaction mixture was stirred at RT; the reaction progress was monitored by TLC (5% EtOAC/DCM, or DCM, UV, CAM stain). After 4 days, the reaction was completed based on TLC. The reaction was quenched with sat'd $NaHCO_3$ (30 mL), diluted with DCM (50 mL). The organic phase was washed with sat'd $NaHCO_3$ (20 mL x 2), DI H_2O (20 mL x 2). The combined aqueous phase was back extracted with DCM (10 mL x 2). The combined organic phase was washed with brine, dried over Na_2SO_4, and filtered. The solvent was removed *in vacuo* to afford crude mixture as a yellow gel. The crude mixture was purified by silica gel column chromatography (eluted with EtOAC/DCM gradient from 0 to 5%) to afford desired product **102** as a clear, sticky gel (513.6 mg, 86 %). The NMR data agreed with that of compound **42** with the absence of the singlet due to the deuterium moiety. ^{1}H NMR (400 MHz, Chloroform-d) δ 7.95 (d, J = 8.9 Hz, 2H), 7.25 – 7.21 (m, 2H), 7.12 – 7.05 (m, 2H), 6.91 – 6.81 (m, 4H), 6.68 (d, J = 8.7 Hz, 2H), 5.17 (t, J = 8.2 Hz, 1H), 4.71 – 4.59 (m, 3H), 4.58 – 4.51 (m, 2H), 4.12 – 4.06 (m, 1H), 3.80 (s, 3H), 3.72 (s, 3H), 3.70 – 3.60 (m, 1H), 3.33 (dd, J = 11.5, 8.6 Hz, 1H), 2.76 – 2.57 (m, 2H), 1.21 (t, J = 7.4 Hz, 3H). See **Chapter appendix** for NMR spectra.

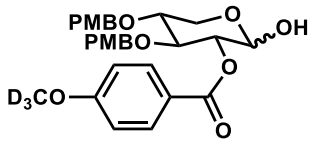

103

To a mixture of **102** (513.6 mg, 0.898 mmol) in DCM (5.4 mL, 0.15 M) and DI H_2O (0.54 mL, 1.5 M) at RT was added NBS (180.0 mg, 1.01 mmol) as a solid. The reaction mixture was stirred at RT under N_2. The reaction progress was monitored by TLC (30% EtOAc/hexanes, UV, CAM stain). The appearance of the reaction mixture changed from clear, light yellow to cloudy, dark orange after 15 minutes, when the reaction was completed based on TLC. The reaction was quenched with sat'd Na2S2O3 solution (10 mL). The reaction mixture was diluted with DCM (25 mL), washed with sat'd $Na_2S_2O_3$ solution (10 mL x 2). The combined aqueous phase was back extracted with DCM (5 mL x 2). The combined organic phase was washed with DI H_2O (10 mL x 2), brine, dried over Na_2SO_4, and filtered. The solvent was removed *in vacuo* to afford crude mixture as a clear gel. The crude mixture was purified by silica gel column chromatography (eluted with EtOAc/hexanes gradient, 30% to 80%) to afford desired mixture of products **103** (α and β anomers) as a clear, thick gel (320.5 mg, 67%). The NMR data agreed with that of compound **97** with the absence of the singlet due to the deuterium moiety. ^{1}H NMR (400 MHz, Chloroform-d) δ 8.04 – 7.91 (m, 2H), 7.33 – 7.21 (m, 2H), 7.18 – 7.10 (m, 2H), 6.96 – 6.83 (m, 6H), 6.79 – 6.70 (m, 2H), 6.29 (d, J = 2.8 Hz, 1H), 5.41 (d, J = 3.4 Hz, 1H), 4.99 (dd, J = 9.3, 3.5 Hz, 1H), 4.88 (d, J = 11.0 Hz, 1H), 4.80 – 4.63 (m, 4H), 4.63 – 4.53 (m, 1H), 4.06 (dd, J = 9.3, 8.2 Hz, 1H), 3.90 – 3.82 (m, 1H), 3.82 – 3.79 (m, 5H), 3.75 (s, 3H), 3.73 – 3.60 (m, 2H), 3.38 (dd, J = 12.0, 9.0 Hz, 0H), 2.74 (s, 1H). See **Chapter appendix** for NMR spectra.

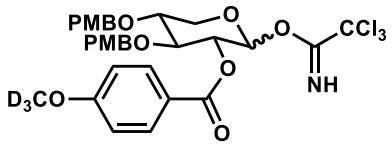

104

To a solution of **103** (314.0 mg, 0.595 mmol) in anhydrous DCM (4.0 mL, 0.15 M) under N_2 at RT was added trichloroacetonitrile (298.4 µL, 2.98 mmol) and DBU (4.5 µL, 0.030 mmol). The reaction color changed from light to dark yellow. The reaction mixture was stirred at RT. The reaction progress was monitored by TLC (30% EtOAc/hexanes with 3% NEt_3, TLC plates were pre-eluted before sample spotting). After 1.5 hours, an aliquot of the reaction was analyzed by ^{1}H NMR to show the completion of the reaction. The solvent was removed *in vacuo* to afford crude mixture as a yellow, thick gel. The crude mixture was purified by silica gel column chromatography (eluted with EtOAc/hexanes with 3% NEt_3 gradient) to afford desired mixture of products **104** (α and β anomers) as a light yellow, thick gel (342.3 mg, 85 %). The NMR data agreed with that of compound **43** with the absence of the singlet due to the deuterium moiety. ^{1}H NMR (400 MHz, Chloroform-d) δ 8.58 (s, 1H), 8.48 (s, 1H), 7.94 – 7.86 (m, 2H), 7.25 – 7.20 (m, 2H), 7.18 – 7.10 (m, 2H), 6.90 – 6.80 (m, 4H), 6.75 – 6.67 (m, 2H), 6.46 (d, J = 3.6 Hz, 1H), 5.97 (d, J = 5.7 Hz, 1H), 5.41 (dd, J = 7.0, 5.7 Hz, 1H), 5.21 (dd, J = 9.9, 3.6 Hz, 1H), 4.81 – 4.51 (m, 5H), 4.17 – 4.08 (m, 1H), 3.84 – 3.78 (m, 5H), 3.78 – 3.69 (m, 5H), 3.62 (dd, J = 11.9, 7.3 Hz, 1H). See **Chapter appendix** for NMR spectra.

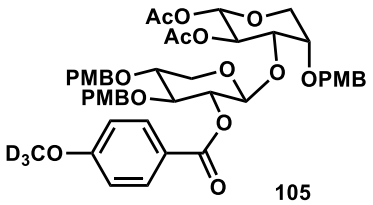

105

A mixture of imidates-D_3 **104** (74.0 mg, 0.110 mmol), L-arabinose moiety **87** (26.0 mg, 0.0734 mmol) and 4Å molecular sieves powder (100 mg) in anhydrous DCM (734 µL, 0.1 M) was stirred at RT under N_2 for 1 hour, then cooled down to -35°C. To the reaction was added $BF_3{\cdot}Et_2O$ (2.8 µL, 0.022 mmol, dissolved in 50 µL of anhydrous DCM). The reaction mixture was stirred at -35°C. The reaction progress was monitored by TLC (55% EtOAc/hexanes with 3% NEt_3, UV, CAM stain). After 30 minutes, the reaction mixture was allowed to warm up to -20°C. After 1 hour, since not much change was observed by TLC, the reaction was quenched with NEt_3 (20 µL). The reaction mixture was warmed up to RT, filtered through celite. The solvent was removed *in vacuo* to afford crude mixture as a yellow gel. The crude mixture was purified by silica gel column chromatography (eluted with EtOAc/hexanes with 3% NEt_3 gradient from 18% to 70%) to afford desired product **105** as a white, foamy solid (55.0 mg, 86%). The NMR data agreed with that of compound **88** with the absence of the singlet due to the deuterium moiety. ^{1}H NMR (400 MHz, Chloroform-d) δ 7.95 – 7.86 (m, 2H), 7.29 – 7.21 (m, 4H), 7.13 – 7.07 (m, 2H), 6.92 – 6.79 (m, 6H), 6.71 – 6.64 (m, 2H), 5.53 (d, J = 5.7 Hz, 1H), 5.18 (dt, J = 13.3, 6.5 Hz, 2H), 4.73 – 4.50 (m, 7H), 3.98 (dd, J = 11.8, 4.0 Hz, 1H), 3.93 (dd, J = 12.0, 5.2 Hz, 1H), 3.84 (dd, J = 7.7, 3.1 Hz, 1H), 3.81 (s, 3H), 3.80 (s, 3H), 3.79 – 3.74 (m, 1H), 3.73 – 3.64 (m, 5H), 3.50 (dd, J = 11.9, 2.5 Hz, 1H), 3.33 (dd, J = 11.6, 7.4 Hz, 2H), 1.96 (s, 3H), 1.80 (s, 3H). See **Chapter appendix** for NMR spectra.

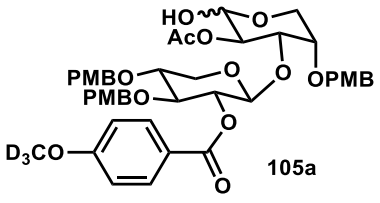

105a

To a clear, colorless solution of **105** (52.0 mg, 0.060 mmol) in anhydrous THF (0.60 mL, 0.1 M) at RT under N_2 was added morpholine (45.0 µL, 0.48 mmol). The reaction mixture was stirred at RT. The reaction progress was monitored by TLC (70% EtOAc/hexanes, UV, CAM stain). After 48 hours, the reaction was mostly completed based on TLC. The solvent was removed *in vacuo* to afford crude mixture, which was purified by silica gel column chromatography (EtOAc/hexanes gradient- 20% to 100%) to afford desired mixture of products **105a** (α and β anomers) as a clear gel (36.7 mg, 74%). The NMR data agreed with that of compound **98** with the absence of the singlet due to the deuterium moiety. ^{1}H NMR (400 MHz, Chloroform-d) δ 7.94 – 7.87 (m, 2H), 7.29 – 7.20 (m, 4H), 7.12 – 7.06 (m, 2H), 6.92 – 6.81 (m, 6H), 6.72 – 6.61 (m, 2H), 5.26 – 5.12 (m, 2H), 5.04 (dd, J = 8.9, 3.1 Hz, 1H), 4.95 (dd, J = 7.5, 5.0 Hz, 1H), 4.77 – 4.49 (m, 9H), 4.09 (dd, J = 9.0, 3.0 Hz, 1H), 4.02 – 3.83 (m, 3H), 3.81 (s, 3H), 3.80 – 3.77 (m, 5H), 3.73 – 3.70 (m, 4H), 3.69 – 3.65 (m, 1H), 3.62 (dd, J = 11.9, 4.2 Hz, 1H), 3.47 (dd, J = 12.2, 2.9 Hz, 0H), 3.37 – 3.27 (m, 1H), 2.44 (d, J = 4.3 Hz, 1H), 1.85 (s, 1H), 1.78 (s, 3H). See **Chapter appendix** for NMR spectra.

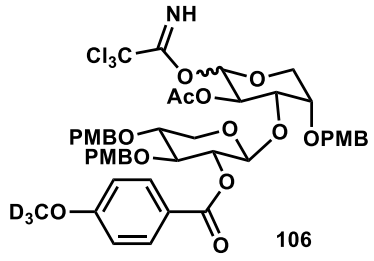

106

To a solution of **105a** (36.7 mg, 0.045 mmol) in anhydrous DCM (0.30 mL, 0.15 M) under N_2 at RT was added trichloroacetonitrile (22.4 µL, 0.22 mmol) and DBU (0.33 µL, 0.0022 mmol). The reaction color changed from light to dark yellow. The reaction mixture was stirred at RT. The reaction progress was monitored by TLC (30% EtOAc/hexanes with 3%

NEt_3, TLC plates were pre-eluted before sample spotting). After 1.5 hours, an aliquot of the reaction was analyzed by ^1H NMR to show the completion of the reaction. The solvent was removed in vacuo to afford crude mixture as a yellow, thick gel. The crude mixture was purified by silica gel column chromatography (eluted with EtOAc/hexanes with 3% NEt_3 gradient) to afford desired mixture of products **106** (α and β anomers) as a light yellow, thick gel (25.5 mg, 60 %). The products were used in the subsequent reaction as a mixture of anomers. ^1H NMR signals with integration of 0H correspond to the minor anomer. The NMR data agreed with that of compound **89** with the absence of the singlet due to the deuterium moiety. ^1H NMR (400 MHz, Chloroform-d) δ 8.55 (s, 1H), 8.48 (s, 0H), 7.96 – 7.88 (m, 2H), 7.30 – 7.24 (m, 2H), 7.23 – 7.19 (m, 2H), 7.16 – 7.11 (m, 2H), 6.90 – 6.80 (m, 6H), 6.73 – 6.66 (m, 2H), 6.42 (d, J = 3.5 Hz, 0H), 5.72 (d, J = 5.9 Hz, 1H), 5.42 (dd, J = 8.0, 5.9 Hz, 1H), 5.22 (dd, J = 6.8, 5.3 Hz, 1H), 4.80 (d, J = 5.3 Hz, 1H), 4.75 – 4.48 (m, 7H), 4.09 – 4.03 (m, 2H), 3.96 – 3.88 (m, 1H), 3.88 – 3.82 (m, 1H), 3.80 (s, 3H), 3.79 (s, 3H), 3.76 – 3.70 (m, 4H), 3.66 – 3.56 (m, 2H), 3.46 – 3.34 (m, 2H), 1.79 (s, 3H). See **Chapter appendix** for NMR spectra.

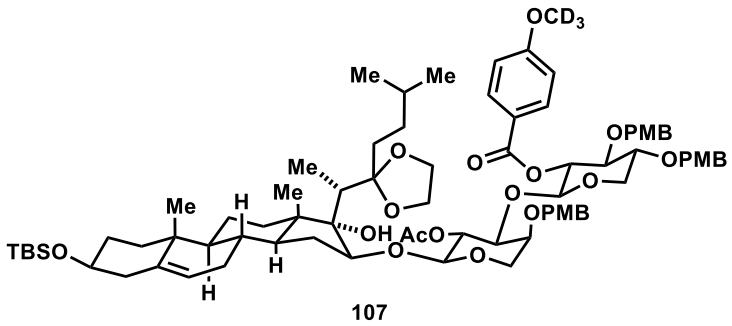

107

Compound **107** was synthesized with the procedure adapted from Xue *et al*.[43] A mixture of disaccharide imidates **106** (22.5 mg, 0.0233 mmol), aglycone **14** (12.5 mg, 0.0211 mmol) and 4Å molecular sieve powder (60 mg) in anhydrous DCM (266 µL, 0.08M) was stirred at RT under N_2 for 30 minutes before cooling to -45°C. To the reaction mixture was

added TMSOTf (0.38 µL in 9.6 µL solution in anhydrous DCM, 0.0021 mmol). The reaction mixture was stirred at -45°C. The reaction progress was monitored by TLC (40% EtOAc/hexanes, UV, CAM stain). After 25 minutes, no further progress was observed. To the reaction mixture was added more TMSOTf (0.12 µL in 3.0 µL solution in anhydrous DCM, 0.66 µmol). After 50 minutes, no further progress was observed. The reaction was quenched with sat'd $NaHCO_3$ solution (1 mL). The reaction mixture was diluted with DCM (10 mL). The organic phase was washed with sat'd $NaHCO_3$ solution (10 mL x 3). The combined aqueous phase was back extracted with DCM (5 mL x 2). The combined organic phase was washed with brine, dried over Na_2SO_4, and filtered. The solvent was removed *in vacuo* to afford crude mixture as a white foamy solid. The crude mixture was purified by pTLC (eluted with 30% EtOAc/hexanes) to afford desired product **107** (6.3 mg, 21%). ^{1}H NMR (400 MHz, Chloroform-d) δ 7.96 (d, J = 8.8 Hz, 2H), 7.30 – 7.22 (m, 4H), 7.17 (d, J = 8.5 Hz, 2H), 6.85 – 6.77 (m, 6H), 6.73 (d, J = 8.5 Hz, 2H), 5.29 – 5.21 (m, 2H), 5.12 – 5.07 (m, 1H), 5.03 (s, 1H), 4.76 (d, J = 11.3 Hz, 1H), 4.66 – 4.42 (m, 6H), 4.43 – 4.25 (m, 2H), 4.17 – 4.07 (m, 2H), 4.00 – 3.82 (m, 3H), 3.81 – 3.78 (m, 3H), 3.77 (s, 3H), 3.76 – 3.68 (m, 5H), 3.58 – 3.42 (m, 3H), 2.65 (q, J = 7.3 Hz, 1H), 2.30 – 2.21 (m, 1H), 2.18 – 2.09 (m, 2H), 1.98 (s, 3H), 1.85 – 1.64 (m, 5H), 1.64 – 1.50 (m, 2H), 1.50 – 1.34 (m, 5H), 1.32 – 1.17 (m, 4H), 1.13 (d, J = 7.4 Hz, 3H), 1.09 – 0.94 (m, 2H), 0.92 (s, 3H), 0.89 (s, 9H), 0.86 (s, 3H), 0.67 (d, J = 6.2 Hz, 3H), 0.58 (d, J = 6.2 Hz, 3H), 0.06 (s, 6H). See **Chapter appendix** for NMR spectra.

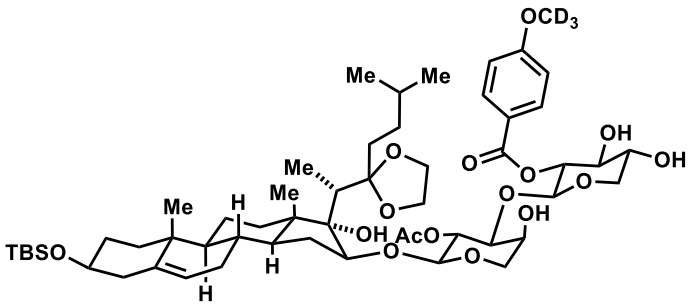

107a

Compound **107a** was synthesized with the procedure adapted from Xue *et al*.[43] To a stirring solution of **107** (3.9 mg, 0.0028 mmol) in H_2O/DCM (1:10, 0.28 mL) at RT under N_2 was added DDQ (2.3 mg, 0.01 mmol). The reaction mixture changed color from colorless to dark green to yellow with dark red water droplets. The reaction progress was monitored by TLC (4% MeOH/DCM) until the starting material was all consumed. The reaction mixture was then diluted in DCM (5 mL), washed with sat'd $NaHCO_3$ solution (5 mL x 3). The combined dark orange aqueous phase was back extracted with DCM (5 mL x 2). The combined light tan organic layer was washed with brine, dried over Na_2SO_4, and filtered. The solvent was removed *in vacuo* to afford crude mixture as a tan gel, which was then separated on pTLC (1/2 plate, 4% MeOH/DCM, 1 elution) to afford desired product **107a** as a colorless film (1.5 mg, 52 % yield). ^{1}H NMR (400 MHz, Chloroform-d) δ 8.00 (d, J = 8.8 Hz, 2H), 6.93 (d, J = 8.8 Hz, 2H), 5.33 – 5.28 (m, 1H), 5.08 – 5.04 (m, 1H), 5.01 (d, J = 4.0 Hz, 1H), 4.96 (t, J = 4.8 Hz, 1H), 4.70 – 4.68 (m, 1H), 4.28 (dd, J = 12.2, 3.3 Hz, 1H), 4.10 (s, 1H), 4.04 – 3.83 (m, 7H), 3.82 – 3.73 (m, 2H), 3.58 – 3.43 (m, 3H), 3.09 (s, 1H), 2.92 (s, 1H), 2.70 – 2.62 (m, 1H), 2.51 (d, J = 7.3 Hz, 1H), 2.32 – 2.19 (m, 2H), 2.19 – 2.13 (m, 1H), 2.01 – 1.92 (m, 2H), 1.80 (d, J = 13.3 Hz, 2H), 1.75 – 1.64 (m, 4H), 1.52 – 1.37 (m, 2H), 1.37 – 1.27 (m, 2H), 1.28 – 1.21 (m, 4H), 1.20 – 1.09 (m, 1H), 1.04 (d, J =

7.5 Hz, 3H), 1.03 – 0.99 (m, 4H), 0.91 (s, 3H), 0.89 (s, 9H), 0.77 (d, J = 6.6 Hz, 3H), 0.71 (d, J = 6.6 Hz, 3H), 0.05 (s, 6H). See **Chapter appendix** for NMR spectra.

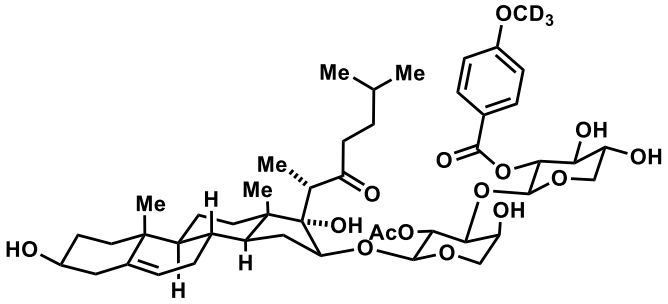

108 (*d*-OSW-1)

Stock solution of $Pd(MeCN)_2Cl_2$ was prepared (0.9 mg dissolved in 0.24 mL acetone). To a stirring solution of **107a** (0.9 mg, 0.87 μmol) in H_2O/acetone (1:20, 100.0 μL total) at RT under N_2 was added $Pd(MeCN)_2Cl_2$ solution (53 μL solution, 0.19 mg, 0.72 μmol). The reaction was stirred at RT. The reaction progress was monitored by TLC (10% MeOH/DCM). After 10 hours, the reaction was completed based on TLC. The solvent was then removed *in vacuo* to afford crude product as a yellow film. The crude product was purified by HPLC (85% MeCN/H_2O) to afford desired **108** *d*-OSW-1 (0.5 mg, 66% yield). ^{1}H NMR (400 MHz, Acetonitrile-d3) δ 8.02 (d, J = 9.0 Hz, 2H), 7.02 (d, J = 8.9 Hz, 2H), 5.31 (d, J = 4.9 Hz, 1H), 4.84 (t, J = 8.2 Hz, 1H), 4.73 (dd, J = 8.3, 6.2 Hz, 1H), 4.61 (d, J = 7.7 Hz, 1H), 4.20 (s, 1H), 4.01 (d, J = 6.2 Hz, 1H), 3.92 (dd, J = 11.5, 4.9 Hz, 1H), 3.88 (s, 1H), 3.76 (dd, J = 12.4, 4.2 Hz, 1H), 3.67 (dt, J = 8.2, 4.2 Hz, 2H), 3.64 – 3.50 (m, 2H), 3.42 (dd, J = 12.4, 2.3 Hz, 1H), 3.38 – 3.22 (m, 2H), 2.86 (q, J = 7.3 Hz, 1H), 2.69 (s, 1H), 2.46 (ddd, J = 18.2, 9.0, 6.5 Hz, 1H), 2.23 – 2.08 (m, 5H), 1.99 – 1.90 (m, 1H), 1.85 – 1.76 (m, 1H), 1.75 – 1.68 (m, 2H), 1.67 (s, 3H), 1.64 – 1.38 (m, 5H), 1.32 (dt, J = 13.1, 6.6 Hz, 1H), 1.29 – 1.14 (m, 3H), 1.07 (d, J = 7.4 Hz, 3H), 1.04 – 1.01 (m, 1H), 1.00 (s, 3H), 0.94 – 0.83 (m, 1H), 0.82 – 0.74 (m, 9H). ^{13}C NMR (101 MHz, Acetonitrile-d3) δ 220.09,

187.51, 169.95, 165.66, 164.73, 143.45, 142.44, 132.79, 123.33, 121.86, 118.31, 114.81, 102.92, 100.98, 88.19, 86.20, 80.82, 75.74, 74.47, 71.90, 71.72, 70.49, 67.67, 66.46, 65.22, 50.89, 49.20, 46.94, 46.54, 43.07, 39.71, 38.13, 37.35, 35.74, 33.19, 32.86, 32.69, 32.63, 32.37, 28.19, 22.88, 22.67, 21.34, 21.04, 19.79, 13.56, 12.16, 1.94, 1.73. ^{2}H NMR (77 MHz, Acetonitrile-d3) δ 3.85. HRMS calcd for $C_{47}H_{65}D_3O_{15}Na$: 898.4639 $[M + Na]^+$, found 898.4611. See **Chapter appendix** for NMR spectra.

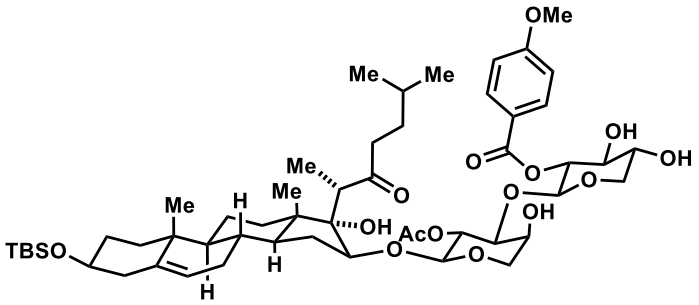

112 (TBS-OSW-1)

Compound **112** was synthesized as describe previously.[10] Under N_2, OSW-1 **2**(5.4 mg, 0.0062 mol) was dissolved in dry DCM (0.125 mL). The solution was cooled in an ice bath. 2,6-lutidine (0.7 µL, 0.0062 mmol) was added via syringe. Tert-Butyldimethylsilyltrifluoromethane sulfonate (2.1 µL, 0.0093 mmol) was then added via syringe. After 5 minutes, the ice bath was removed, and the reaction was allowed to warm to ambient temperature- the total reaction time was 15 minutes. The reaction progress was monitored via TLC (7.5% MeOH/DCM, UV and CAM stain). The reaction was diluted in $CHCl_3$ (5 mL), washed with sat'd aqueous $NaHCO_3$ solution (5 mL) and DI H_2O (5 mL x 2). The combined aqueous layer was back extracted with $CHCl_3$ (2 mL x 2). The combined organic layer was washed with brine, dried over Na_2SO_4, and filtered. The solvent was removed *in vacuo* to afford crude product. The crude product was purified by preparative-TLC, eluted with 5% MeOH/DCM to afford desired product **112** as a white solid (1.8 mg,

30% yield). The desired product was further purified by HPLC (Luna C8(2) column; flow rate of 2.2mL/min; isocratic of 95% MeOH/water in 10 minutes, gradient from 95% MeOH/water to 100% MeOH in 2 minutes, isocratic at 100% MeOH for 6 minutes before re-equilibrating at 95% MeOH/water for 7 minutes. Retention time of desired compound was at 14.1 minutes). 2.5 mg of compound 2 (combination from ATL-III-081 and ATL-III-085) was purified through HPLC, and 1.4 mg was obtained as analytical pure compound. ^{1}H NMR (500 MHz, Acetonitrile-d3) δ 8.04 – 7.98 (m, 2H), 7.05 – 6.99 (m, 2H), 5.31 (d, J = 5.0 Hz, 1H), 4.84 (dd, J = 8.9, 7.7 Hz, 1H), 4.73 (dd, J = 8.3, 6.2 Hz, 1H), 4.61 (d, J = 7.7 Hz, 1H), 4.20 (s, 1H), 4.00 (d, J = 6.2 Hz, 1H), 3.92 (dd, J = 11.6, 5.1 Hz, 1H), 3.90 – 3.83 (m, 4H), 3.76 (dd, J = 12.4, 4.3 Hz, 1H), 3.72 – 3.64 (m, 2H), 3.62 – 3.51 (m, 2H), 3.51 – 3.39 (m, 2H), 3.27 (dd, J = 11.6, 9.7 Hz, 2H), 2.86 (q, J = 7.4 Hz, 1H), 2.46 (ddd, J = 18.2, 9.2, 6.4 Hz, 1H), 1.83 – 1.76 (m, 1H), 1.74 – 1.65 (m, 5H), 1.63 – 1.39 (m, 7H), 1.32 (dp, J = 13.4, 6.7 Hz, 1H), 1.27 – 1.15 (m, 3H), 1.07 (d, J = 7.4 Hz, 3H), 1.05 – 0.98 (m, 4H), 0.88 (s, 9H), 0.81 – 0.75 (m, 9H), 0.04 (d, J = 1.7 Hz, 6H). 13C NMR (101 MHz, Acetonitrile-d3) δ 220.15, 170.00, 164.76, 142.42, 132.84, 123.44, 122.09, 114.86, 102.97, 101.04, 88.21, 86.25, 75.90, 75.77, 75.12, 74.51, 73.54, 71.76, 70.46, 66.52, 56.40, 50.95, 49.26, 48.32, 47.05, 46.59, 43.65, 39.71, 38.10, 37.38, 35.81, 33.24, 33.04, 32.91, 32.66, 28.25, 26.32, 22.95, 22.74, 21.38, 21.11, 19.87, 13.62, 13.25, 12.23, -4.34. HRMS (TOF): calculated for $C_{53}H_{82}NaO_{15}Si$ [M+Na+]: 1009.5321; found: 1009.5348; Δ = 2.67ppm. See **Appendix** for NMR spectra.

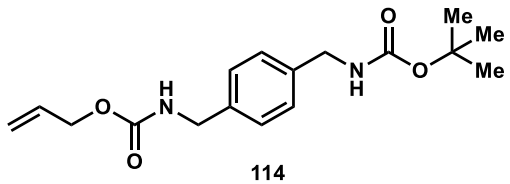

114

Compound **114** was synthesized as describe previously.[10] 1-(N-Boc-aminomethyl)-4-(aminomethyl) benzene **113** (200 mg, 0.85 mmol) was partially dissolved in dry THF (3.0 mL, 0.28M) to create a yellow suspension. Pyridine (68.5 µL, 0.85 mmol) was added via syringe, and then the reaction was cooled to -78°C. Allyl chloroformate (90.3 µL, 0.85 mmol) was added fast drop-wise. After 10 minutes, the reaction was allowed to warm to room temperature and stirred for ~ 2.5 hours. The reaction progress was monitored by TLC (10% MeOH/DCM, I_2 stain). After 2.5 hours, more white precipitation was observed, and TLC indicated the reaction completion. The reaction was then stopped via addition of methanol (3mL), and then concentrated *in vacuo*. The crude reaction mixture was purified by silica gel column chromatography (15g silica, MeOH/DCM gradient- 2% to 5% in 250 mL total, crude mixture was loaded in 5%MeOH/DCM as a slurry). The purification yielded 2 fractions. Fraction 1 (130 mg) had TLC of multiple spots, and ^{1}H NMR of mainly desired product. Fraction 2 (106 mg) had TLC of less spots than fraction 1, and ^{1}H NMR of mainly desired product. Each fraction was purified again by silica gel column chromatography (2.5% MeOH/DCM) to afford pure desired product **114** (210 mg, 77% yield). ^{1}H NMR (500 MHz, Chloroform-d) δ 7.28 – 7.24 (m, 4H), 5.99 – 5.89 (m, 1H), 5.36 – 5.28 (m, 1H), 5.23 (d, J = 10.4 Hz, 1H), 5.02 (bs, 1H), 4.83 (bs, 1H), 4.61 (d, J = 5.6 Hz, 2H), 4.37 (d, J = 6.0 Hz, 2H), 4.30 (d, J = 5.9 Hz, 2H), 1.47 (s, 9H). See **Appendix** for NMR spectra.

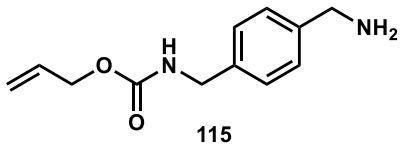

115

Compound **115** was synthesized as describe previously.[10] At room temperature, 1-(N-Alloc-aminomethyl)-4-(N-Boc-aminomethyl) benzene **114** (78.9 mg, 0.246 mmol) was

partially dissolved in DCM (990 µL, 0.25M). TFA (380 µL, 4.93 mmol) was added fast drop-wise to produce a yellow homogenous solution. After 1 hour, the solution was directly concentrated *in vacuo* to afford crude mixture as a thick yellow oil, which was dried on high vacuum for 1 hour. The crude reaction mixture was dissolved in chloroform (10 mL) and washed with 0.2M NaOH solution (5 mL x 3). The aqueous layer was back extracted once with chloroform (5 mL x 2), and the combined organic layer was washed with brine, dried over Na_2SO_4, and filtered. The solvent was removed *in vacuo* to afford desired product **115** as a thick yellow oil (47.2 mg, 87% yield). The desired product was used directly for the next reaction without further purification. ^{1}H NMR (500 MHz, Chloroform-d) δ 7.31 – 7.22 (m, 4H), 5.93 (ddt, J = 16.7, 11.0, 5.8 Hz, 1H), 5.30 (d, J = 17.2 Hz, 1H), 5.21 (d, J = 10.4 Hz, 1H), 5.03 (s, 1H), 4.59 (d, J = 5.6 Hz, 2H), 4.36 (d, J = 6.0 Hz, 2H), 3.85 (s, 2H). See **Appendix** for NMR spectra.

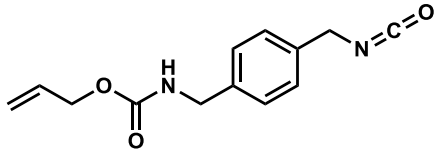

116

Compound **116** was synthesized as describe previously.[10] Alloc-(N) diaminomethyl benzene **115** (43.0 mg, 0.195 mmol) under N_2 was partially dissolved in dry EtOAc (1.6 mL, 0.12M). Solid triphosgene (36.2 mg, 0.122 mmol) was added, and the reaction was heated to 88°C under reflux condition for 5 hours. The reaction mixture turned clearer, but still slightly cloudy. The solvent was evaporated during the reaction period, so EtOAc was added. After cooling, the solvent was removed *in vacuo* and the crude mixture was dried on high vacuum to afford crude product **116** as a yellow paste (47.3mg, 98% yield). ^{1}H NMR (500 MHz, Chloroform-d) δ 5.92 (ddd, J = 16.4, 10.8, 5.4 Hz, 1H), 5.31 (d, J = 17.1

Hz, 1H), 5.22 (d, J = 10.0 Hz, 1H), 4.60 (d, J = 5.7 Hz, 2H), 4.48 (s, 2H), 4.37 (dd, J = 11.5, 6.2 Hz, 2H). IR (NaCl, cm-1): 3329 (Csp3-H), 2921 (Csp2-H), 2360 (O=C=O), 2341 (O=C=O), 2263 (N=C=O), 1702 (amide C=O), 1515 (C-H benzene), 1508 (C-H benzene), 1248 (C-O). See **Appendix** for NMR spectra.

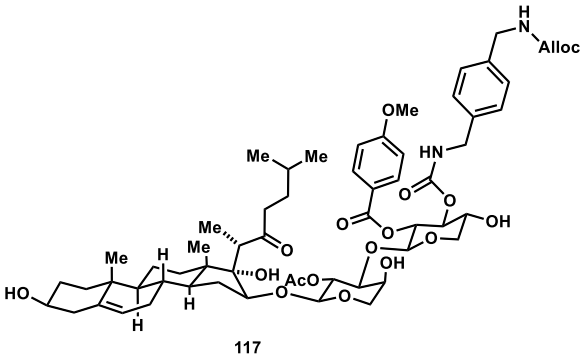

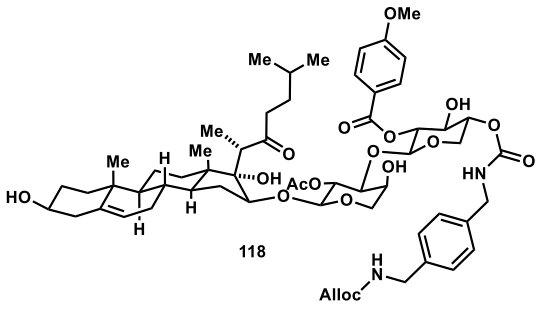

Compound **117** and **118** was synthesized as describe previously.[10] OSW-1 (50 mg, 0.057 mmol) under N_2 was dissolved in anhydrous DMF (0.9 mL). In a nitrogen glove bag, copper (I) chloride (18 mg, 0.18 mmol) was added to a flask containing Alloc-(N)-dimaminomethyl benzene isocyanate (43 mg, 0.18 mmol), then the mixture was dissolved in DMF (1.7 mL) to make a reagent stock solution. 1.1 mL of the reagent stock solution (copper (I) chloride 11.4 mg (0.114 mmol), Alloc-(N)-diaminomethyl benzene isocyanate 28.2 mg, (0.114 mmol)) was added to the OSW-1 solution via syringe at ambient temperature and stirred for 5 hours. The reaction was diluted with $CHCl_3$ (30 mL), washed twice with sat'd $NaHCO_3$ solution. The blue aqueous layer was back extracted twice with $CHCl_3$, and the combined yellow organic layer was washed with brine. The organic layer was dried over Na_2SO_4, filtered and reduce *in vacuo* to produce a yellow crude oil in residual DMF, which was evaporated to a crude solid mixture after 4 hours on the high vacuum pump. A mixture of OSW-1 carbamate **117** and **118** were produced, with

recovered unreacted OSW-1. Both OSW-1 carbamate compounds were purified via pTLC (three plates) eluted with 7.5% MeOH/CH_2Cl_2. Carbamate **117** was obtained as a white solid (9.0 mg, 14%, 28% borsm). Carbamate **118** was obstained as a white solid (9.2mg, 14%, 29% borsm). Both carbamate were purified to analytical purity via HPLC (Luna C18(2) column, 2.4 mL/min, isocratic 75% acetonitrile/(0.1% formic acid in water) for 16 minutes, 100% acetonitrile wash for 8 minutes, re-equilibriate at 75% acetonitrile/(0.1% formic acid in water) for 8 minutes). Retention time of carbamate **117** was 19.9 min, and of carbamate **118** was 23.1 min. The NMR data agreed with the published reference.[10]

Carbamate **117**: ^{1}H NMR (500 MHz, Acetonitrile-d3) δ 7.98 – 7.92 (m, 2H), 7.10 – 6.86 (m, 6H), 6.02 – 5.88 (m, 2H), 5.33 – 5.15 (m, 2H), 5.01 – 4.91 (m, 2H), 4.75 – 4.69 (m, 2H), 4.53 (dt, J = 5.4, 1.6 Hz, 2H), 4.20 (s, 2H), 4.17 (d, J = 6.5 Hz, 2H), 4.01 (d, J = 6.4 Hz, 1H), 3.99 – 3.93 (m, 1H), 3.91 – 3.85 (m, 4H), 3.80 – 3.72 (m, 2H), 3.71 – 3.64 (m, 2H), 3.62 (d, J = 5.0 Hz, 1H), 3.46 – 3.25 (m, 3H), 3.21 (d, J = 4.4 Hz, 1H), 2.85 (q, J = 7.3 Hz, 1H), 2.71 (d, J = 4.6 Hz, 1H), 2.47 (dt, J = 16.8, 8.0 Hz, 1H), 1.84 – 1.77 (m, 1H), 1.74 – 1.66 (m, 1H), 1.64 (s, 2H), 1.62 – 1.56 (m, 0H), 1.56 – 1.48 (m, 3H), 1.47 – 1.38 (m, 1H), 1.33 (dp, J = 13.2, 6.2 Hz, 1H), 1.28 – 1.15 (m, 3H), 1.07 (d, J = 7.4 Hz, 3H), 1.03 (dd, J = 13.9, 3.6 Hz, 1H), 0.99 (s, 3H), 0.88 (td, J = 12.3, 11.4, 4.7 Hz, 1H), 0.79 (dd, J = 6.6, 1.7 Hz, 6H), 0.75 (s, 3H). Low resolution MS: calculated for $C_{60}H_{86}N_3O_{18}$ [M+NH_4^+]: 1136.59; found: 1136.35; calculated for $C_{61}H_{83}N_2O_{20}$ [M+CO_2H^-]: 1163.5545; found: 1163.35. Carbamate **118**: ^{1}H NMR (500 MHz, Acetonitrile-d3) δ 8.04 – 7.97 (m, 2H), 7.22 (s, 4H), 7.03 – 6.97 (m, 2H), 6.10 – 6.01 (m, 2H), 5.92 (ddt, J = 16.3, 10.6, 5.4 Hz, 1H), 5.17 (d, J = 10.5 Hz, 1H), 4.93 (dd, J = 8.2, 6.8 Hz, 1H), 4.75 (dd, J = 8.2, 6.0 Hz, 1H), 4.70 (d, J = 6.7 Hz, 1H), 4.63 (td, J = 8.2, 4.9 Hz, 1H), 4.51 (dt, J = 5.3, 1.5 Hz, 2H), 4.30

– 4.19 (m, 5H), 4.10 (dd, J = 11.8, 4.9 Hz, 1H), 4.04 (d, J = 6.0 Hz, 1H), 3.90 (s, 1H), 3.85 (s, 3H), 3.83 – 3.73 (m, 2H), 3.69 (td, J = 8.0, 4.0 Hz, 2H), 3.46 – 3.35 (m, 2H), 3.32 (p, J = 6.0 Hz, 1H), 3.25 (s, 1H), 2.91 (q, J = 7.2 Hz, 1H), 2.71 (s, 1H), 2.51 (dt, J = 18.1, 7.9 Hz, 1H), 1.84 – 1.78 (m, 1H), 1.74 – 1.67 (m, 4H), 1.63 – 1.48 (m, 3H), 1.48 – 1.38 (m, 1H), 1.33 (dq, J = 13.2, 6.8 Hz, 1H), 1.29 – 1.18 (m, 3H), 1.08 (d, J = 7.3 Hz, 3H), 1.06 – 0.97 (m, 4H), 0.92 – 0.85 (m, 1H), 0.81 – 0.76 (m, 9H). Low resolution MS: calculated for $C_{60}H_{86}N_3O_{18}$ [M+NH_4^+]: 1136.59; found: 1136.35; calculated for $C_{61}H_{83}N_2O_{20}$ [M+CO2H-]: 1163.5545; found: 1163.35. See **Chapter appendix** for NMR spectra.

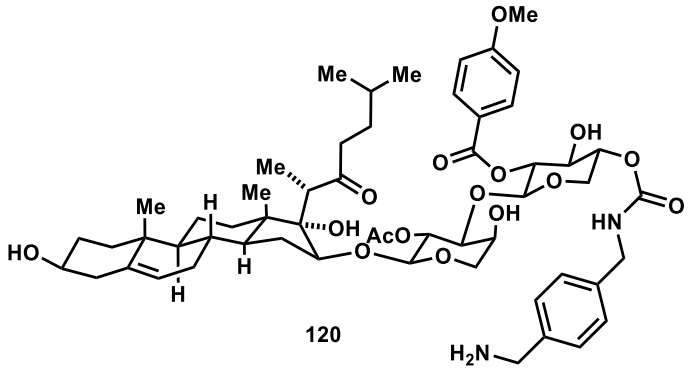

120

Compound **120** was synthesized with the procedure adapted from Burgett *et al.*[10] Carbamate **118** (3.5 mg, 0.0031 mmol) was dissolved in anhydrous THF (0.24 mL) under N_2. Morpholine (1.8 µL, 0.021 mmol) was added via syringe. In a glove bag, $Pd(PPh_3)_4$ (13.8 mg) was dissolved in anhydrous THF (0.51 mL) to make a 27 mg/mL reagent stock solution (20 µL = 15 mol%). To the reaction mixture at RT was added $Pd(PPh_3)_4$ solution in 15 mol% portions, with reaction progress being monitored by TLC (10% MeOH/DCM, UV and CAM stain) after each addition. Overall, 65 µL (48.8 mol%) of $Pd(PPh_3)_4$ was added over 2 hours. The reaction was quenched by three drops of water, and then was concentrated *in vacuo*. Amine **120** was purified to analytical purity from crude mixture via HPLC (Luna C8(2) column, 1.2 mL/min, gradient from 65% methanol/(0.1% formic acid

in water) to 82% methanol/(0.1% formic acid in water) in 4 minutes, isocratic 82% methanol/(0.1% formic acid in water) for 13 minutes, 100% methanol wash for 10 minutes, re-equilibriate at 65% methanol/(0.1% formic acid in water) for 17 minutes). Retention time of amine **120** was 16.7 min. Amine **120** was obtained as a white solid (1.1mg, 40%). The NMR data agreed with the published reference[10]. ^{1}H NMR (500 MHz, 25% Methanol-d4 in Acetonitrile-d3) δ 8.04 – 7.96 (m, 2H), 7.32 – 7.13 (m, 4H), 6.98 (dd, J = 8.6, 5.7 Hz, 2H), 5.30 (d, J = 5.0 Hz, 1H), 4.92 (dd, J = 8.1, 6.4 Hz, 1H), 4.77 (dd, J = 8.2, 6.1 Hz, 1H), 4.70 (d, J = 6.5 Hz, 1H), 4.65 – 4.56 (m, 1H), 4.32 – 4.18 (m, 2H), 4.13 – 4.07 (m, 1H), 4.06 (d, J = 6.1 Hz, 1H), 3.89 (s, 1H), 3.84 (s, 3H), 3.82 – 3.73 (m, 2H), 3.69 (dd, J = 8.1, 4.2 Hz, 2H), 3.45 – 3.40 (m, 1H), 3.40 – 3.34 (m, 5H), 2.95 – 2.88 (m, 1H), 2.57 – 2.47 (m, 1H), 2.28 – 2.05 (m, 4H), 1.84 – 1.78 (m, 2H), 1.74 – 1.68 (m, 4H), 1.61 – 1.47 (m, 3H), 1.41 (qd, J = 14.7, 12.3, 6.0 Hz, 3H), 1.36 – 1.29 (m, 1H), 1.29 – 1.19 (m, 5H), 1.08 (d, J = 7.4 Hz, 3H), 1.03 (dd, J = 13.7, 3.9 Hz, 1H), 0.98 (s, 3H), 0.87 (dq, J = 11.8, 5.6 Hz, 2H), 0.82 – 0.74 (m, 9H). Low resolution MS: calculated for $C_{56}H_{79}N_2O_{16}$ [M+H$^+$]: 1035.5424; found: 1035.55; calculated for $C_{57}H_{79}N_2O_{18}$ [M+CO_2H^-]: 1079.5333; found: 1080.35. See **Chapter appendix** for NMR spectra.

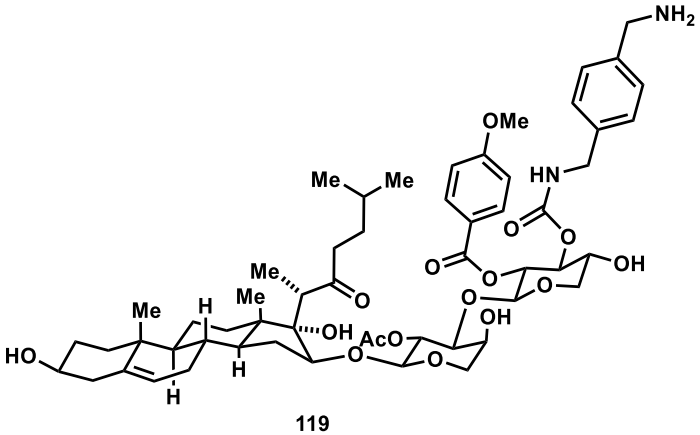

119

Compound **119** was synthesized with the procedure adapted from Burgett *et al.*[10] Carbamate **117** (4.8 mg, 0.0043 mmol) was dissolved in anhydrous THF (0.32 mL) under N_2. Morpholine (2.5 µL, 0.029 mmol) was added via syringe. In a glove bag, $Pd(PPh_3)_4$ (13.8 mg) was dissolved in anhydrous THF (0.37 mL) to make a 37 mg/mL reagent stock solution (20 µL = 15 mol%). To the reaction mixture at RT was added $Pd(PPh_3)_4$ solution in 15 mol% portions, with reaction progress being monitored by TLC (10% MeOH/DCM, UV and CAM stain) after each addition. Overall, 90 µL (67 mol%) of $Pd(PPh_3)_4$ was added over 1.5 hours. The reaction was quenched by three drops of water, and then was concentrated *in vacuo*. Amine **119** was purified to analytical purity from crude mixture via HPLC (Luna C8(2) column, 1.2 mL/min, gradient from 65% methanol/(0.1% formic acid in water) to 82% methanol/(0.1% formic acid in water) in 4 minutes, isocratic 82% methanol/(0.1% formic acid in water) for 13 minutes, 100% methanol wash for 10 minutes, re-equilibrate at 65% methanol/(0.1% formic acid in water) for 17 minutes). Retention time of amine **119** was 16.1 min. Amine **119** was obtained as a white solid (1.0 mg, 21%). The NMR data agreed with the published reference[10]. ^{1}H NMR (500 MHz, , 25% Methanol-d4 in Acetonitrile-d3) δ 7.97 – 7.91 (m, 2H), 7.07 (d, J = 8.0 Hz, 1H), 7.02 – 6.96 (m, 4H), 5.30 (d, J = 5.0 Hz, 1H), 4.99 – 4.91 (m, 2H), 4.75 (dd, J = 8.8, 6.7 Hz, 1H), 4.71 – 4.67 (m, 1H), 4.18 – 4.11 (m, 1H), 4.06 – 4.00 (m, 2H), 3.96 (dd, J = 11.7, 5.4 Hz, 1H), 3.92 – 3.87 (m, 1H), 3.85 (s, 4H), 3.76 (dd, J = 12.6, 3.7 Hz, 1H), 3.69 (ddt, J = 12.6, 8.8, 4.7 Hz, 2H), 3.45 – 3.34 (m, 2H), 2.87 (q, J = 7.4 Hz, 1H), 2.50 (dt, J = 16.8, 7.9 Hz, 1H), 2.25 – 2.06 (m, 5H), 1.83 – 1.76 (m, 1H), 1.74 – 1.64 (m, 2H), 1.62 (s, 3H), 1.59 – 1.46 (m, 2H), 1.46 – 1.38 (m, 1H), 1.34 (dq, J = 13.1, 6.6 Hz, 1H), 1.30 – 1.17 (m, 4H), 1.07 (d, J = 7.4 Hz, 3H), 1.02 (dd, J = 13.9, 3.8 Hz, 1H), 0.97 (s, 3H), 0.86 (p, J = 6.7, 6.2 Hz, 1H), 0.79

(dd, J = 6.6, 1.1 Hz, 6H), 0.74 (s, 3H). Low resolution MS: calculated for $C_{56}H_{79}N_2O_{16}$ $[M+H^+]$: 1035.5424; found: 1035.50; calculated for $C_{57}H_{79}N_2O_{18}$ $[M+CO_2H^-]$: 1079.5333; found: 1079.35. See **Chapter appendix** for NMR spectra.

II.6 Chapter appendix

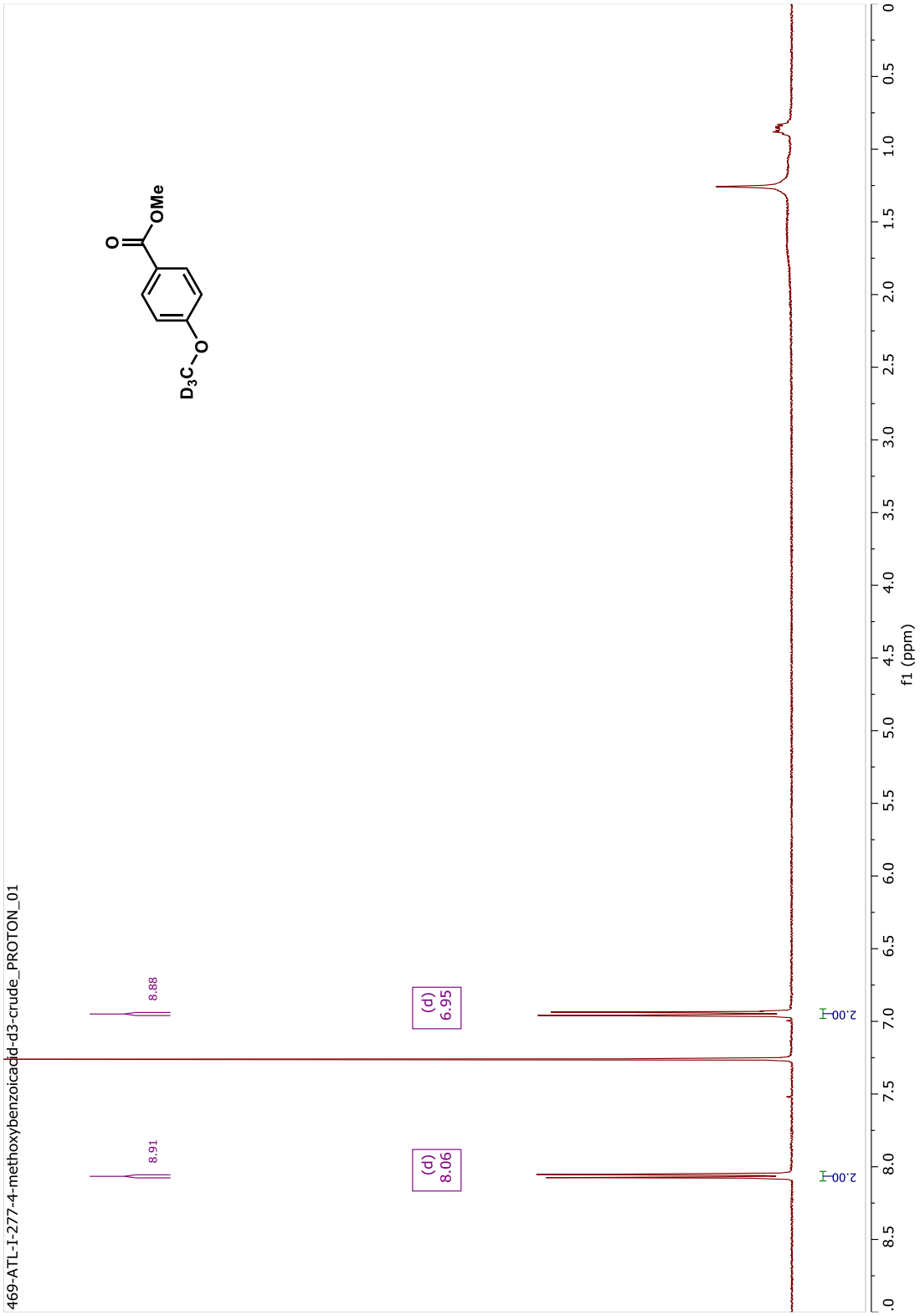

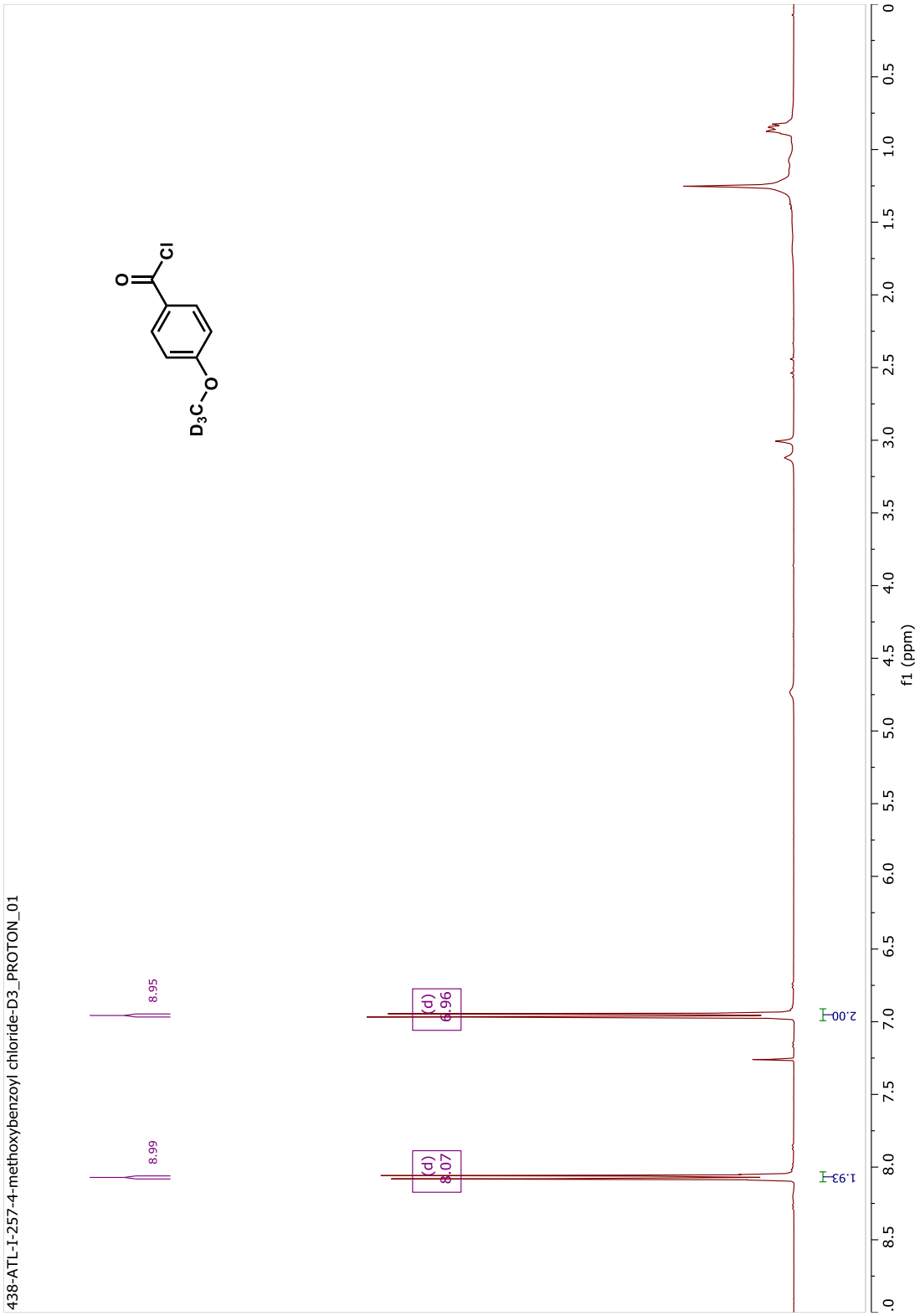
438-ATL-I-257-4-methoxybenzoyl chloride-D3_PROTON_01
O
Cl
D3C
O
8.95
8.99
(d)
8.07
(d)
6.96
2.00
1.93
0
0.5
1.0
1.5
2.0
2.5
3.0
3.5
4.0
4.5
5.0
5.5
6.0
6.5
7.0
7.5
8.0
8.5
.0
f1 (ppm)

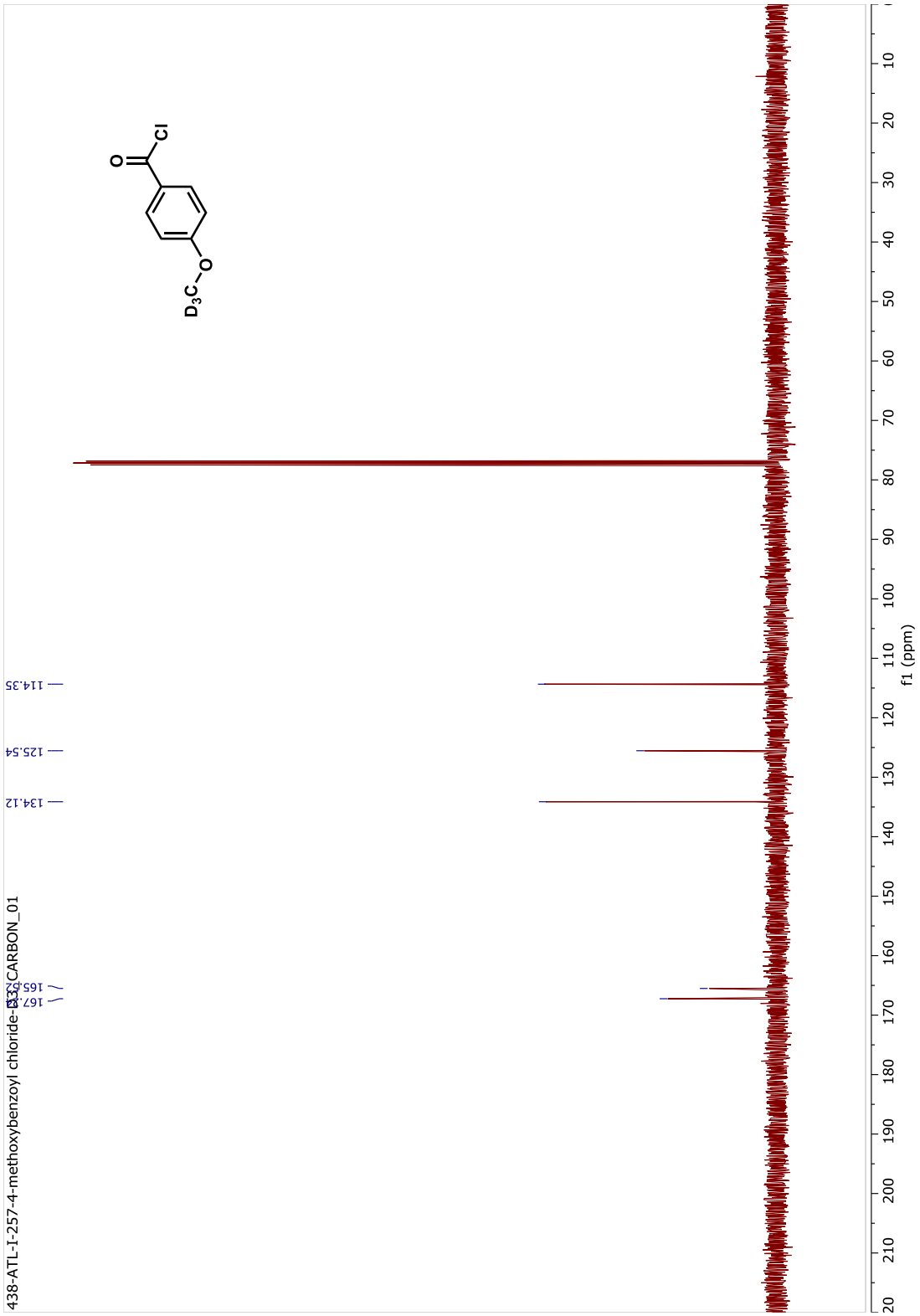
438-ATL-I-257-4-methoxybenzoyl chloride-13CCARBON_01
167.33
165.52
134.12
125.54
114.35
f1 (ppm)
O
Cl
D3C
O

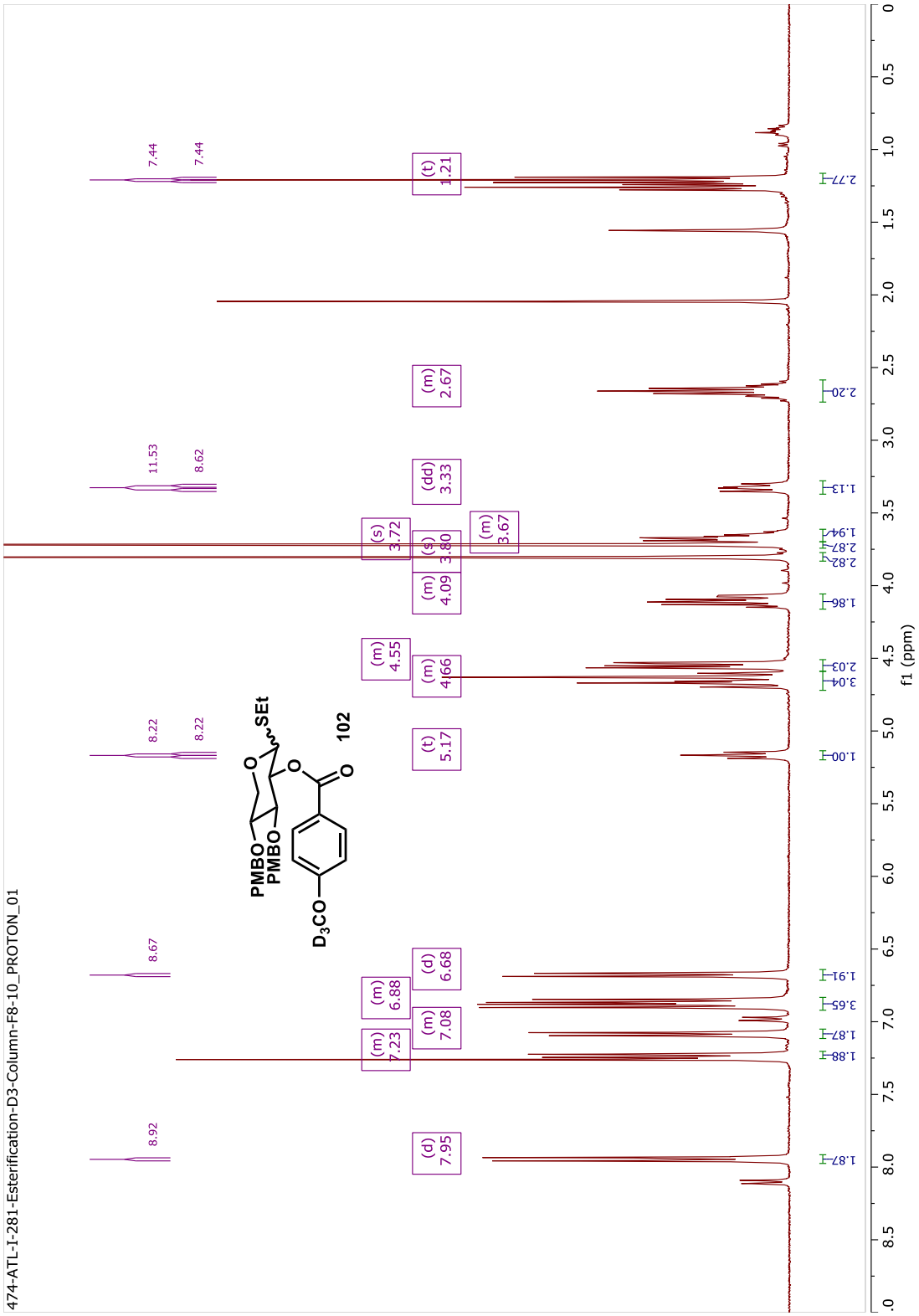
474-ATL-I-281-Esterification-D3-Column-F8-10_PROTON_01
PMBO
PMBO
SEt
O
O
O
O
D3CO
102
8.92
8.67
8.22
8.22
11.53
8.62
7.44
7.44
(d) 7.95
(m) 7.23
(m) 7.08
(m) 6.88
(d) 6.68
(t) 5.17
(m) 4.66
(m) 4.55
(m) 4.09
(s) 3.80
(s) 3.72
(m) 3.67
(dd) 3.33
(m) 2.67
(t) 1.21
1.87
1.88
1.87
3.65
1.91
1.00
2.03
3.04
1.86
2.82
2.87
1.94
1.13
2.20
2.77
f1 (ppm)

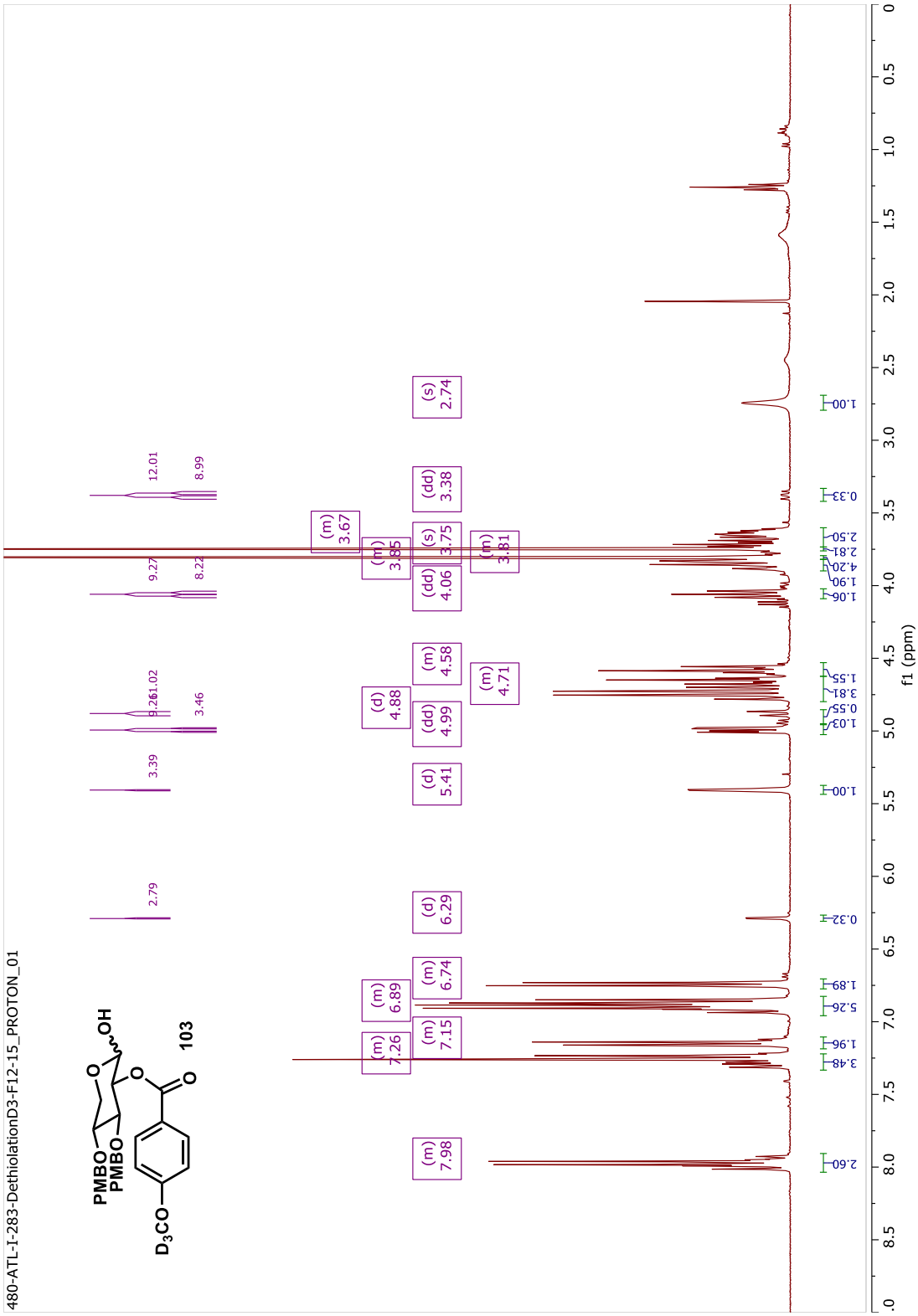
480-ATL-I-283-DethiolationD3-F12-15_PROTON_01
PMBO
PMBO
OH
O
O
O
O
D3CO
103
f1 (ppm)

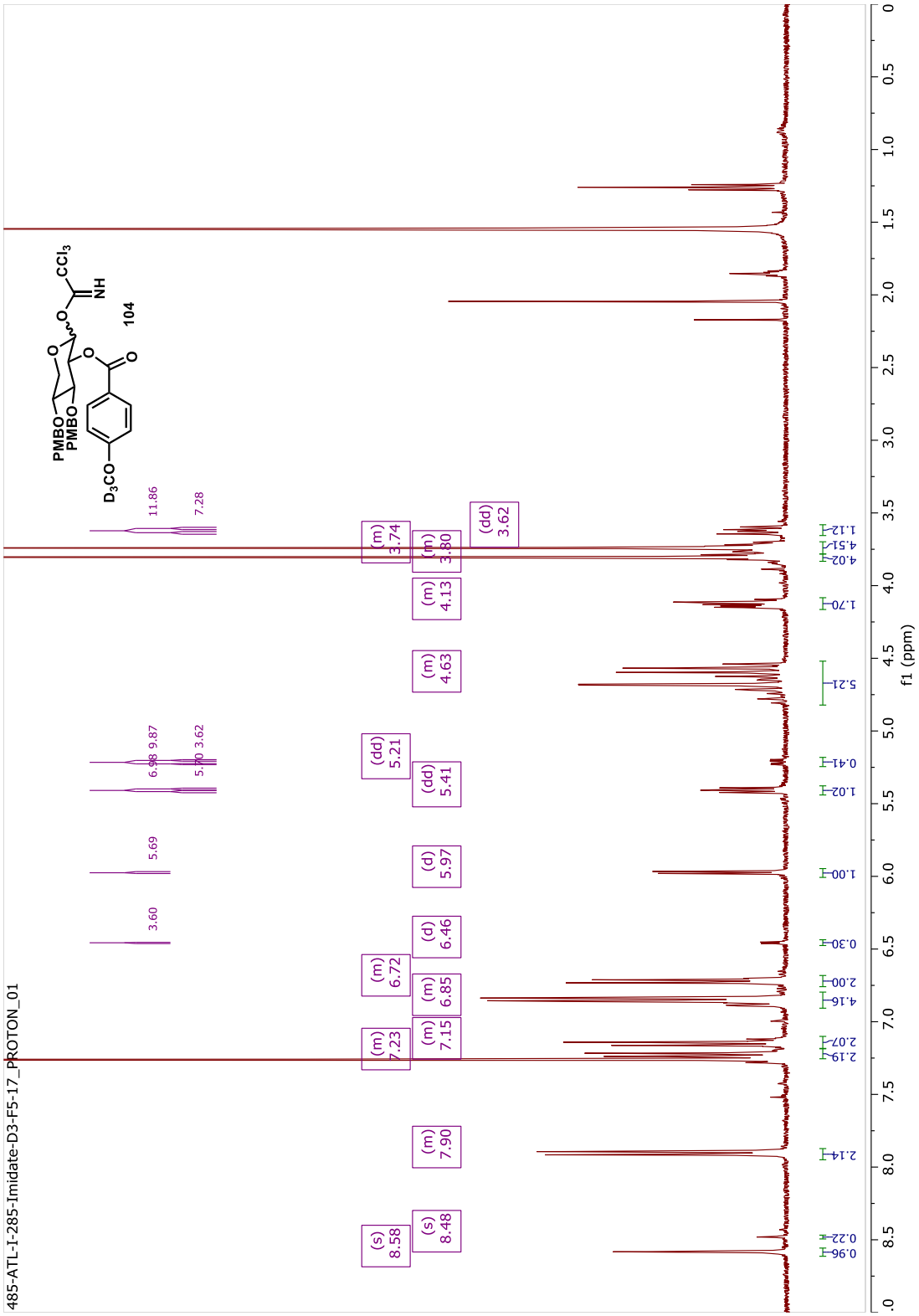
485-ATL-I-285-Imidate-D3-F5-17_PROTON_01
PMBO
PMBO
D3CO
CCl3
NH
104
11.86
7.28
6.98 9.87
5.70 3.62
5.69
3.60
(s) 8.58
(s) 8.48
(m) 7.90
(m) 7.23
(m) 7.15
(m) 6.85
(m) 6.72
(d) 6.46
(d) 5.97
(dd) 5.41
(dd) 5.21
(m) 4.63
(m) 4.13
(m) 3.80
(m) 3.74
(dd) 3.62
0.96
0.22
2.14
2.19
2.07
4.16
2.00
0.30
1.00
1.02
0.41
5.21
1.70
4.02
4.51
1.12
f1 (ppm)

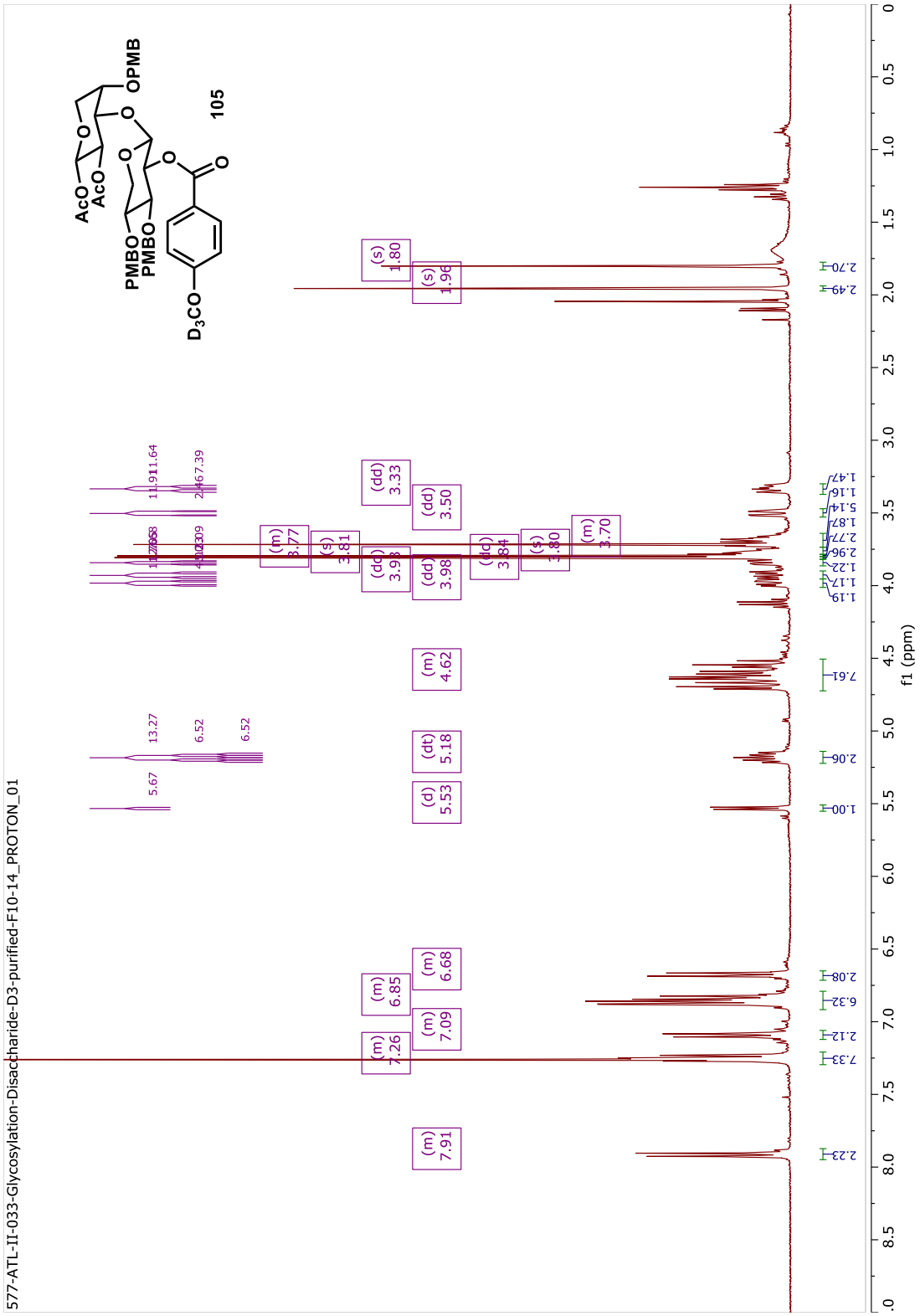
577-ATL-II-033-Glycosylation-Disaccharide-D3-purified-F10-14_PROTON_01
105
AcO
AcO
PMBO
PMBO
OPMB
D3CO
f1 (ppm)

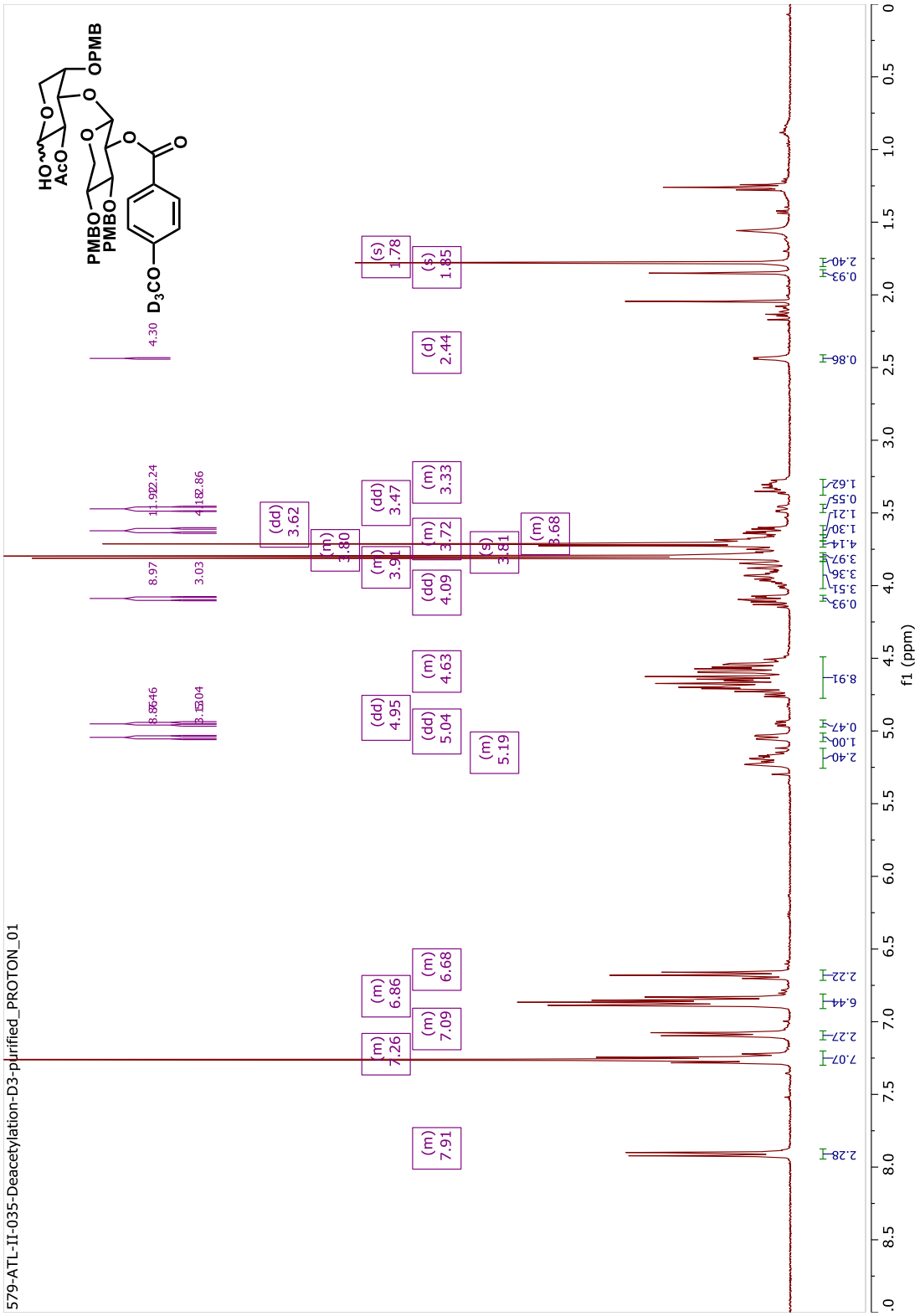
579-ATL-II-035-Deacetylation-D3-purified_PROTON_01
HO
AcO
OPMB
PMBO
PMBO
D3CO
f1 (ppm)

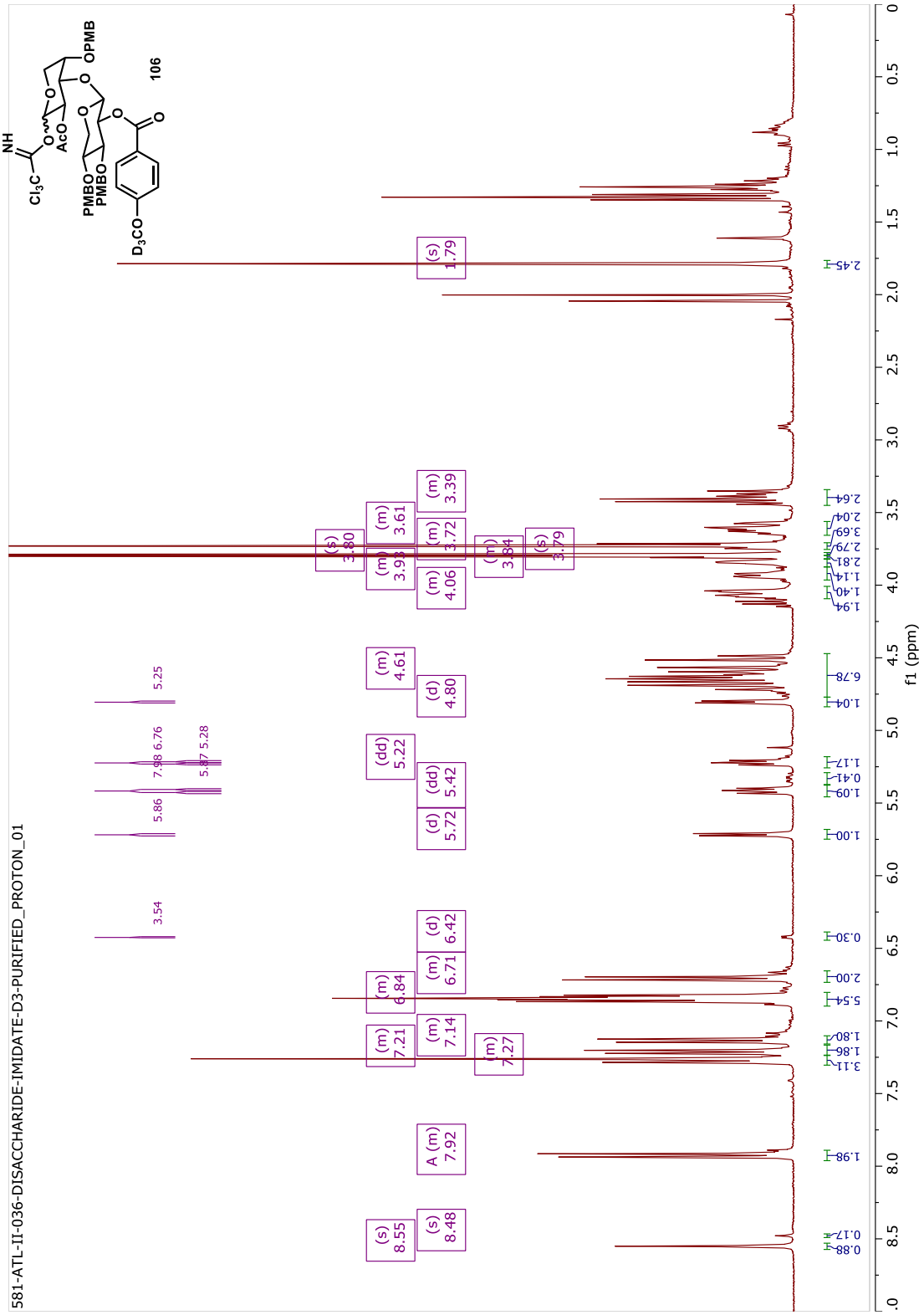
581-ATL-II-036-DISACCHARIDE-IMIDATE-D3-PURIFIED_PROTON_01
106
f1 (ppm)

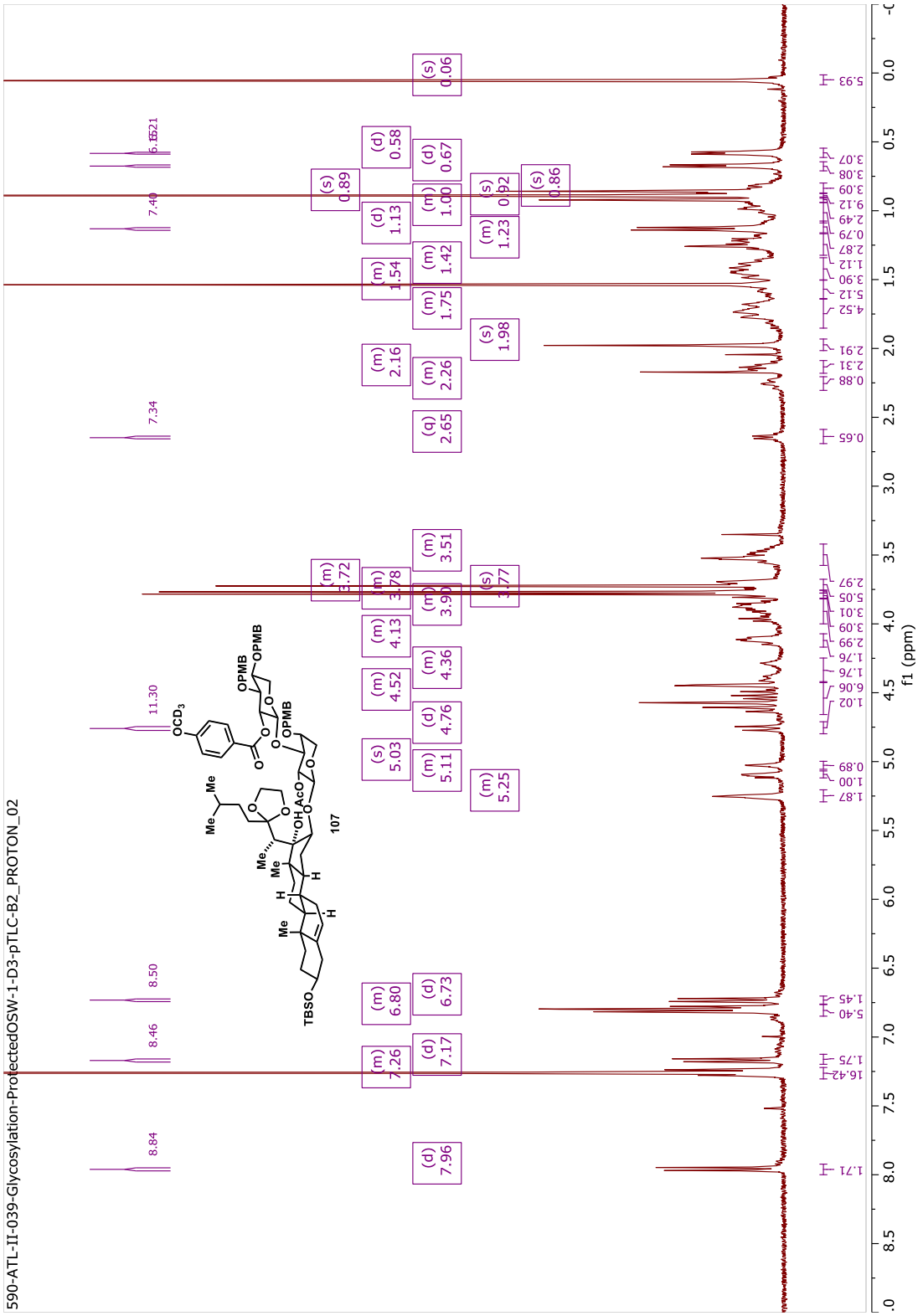
590-ATL-II-039-Glycosylation-ProtectedOSW-1-D3-pTLC-B2_PROTON_02
f1 (ppm)
OPMB
OPMB
OPMB
OCD3
OAc
OH
TBSO
Me
Me
Me
Me
H
H
H
107

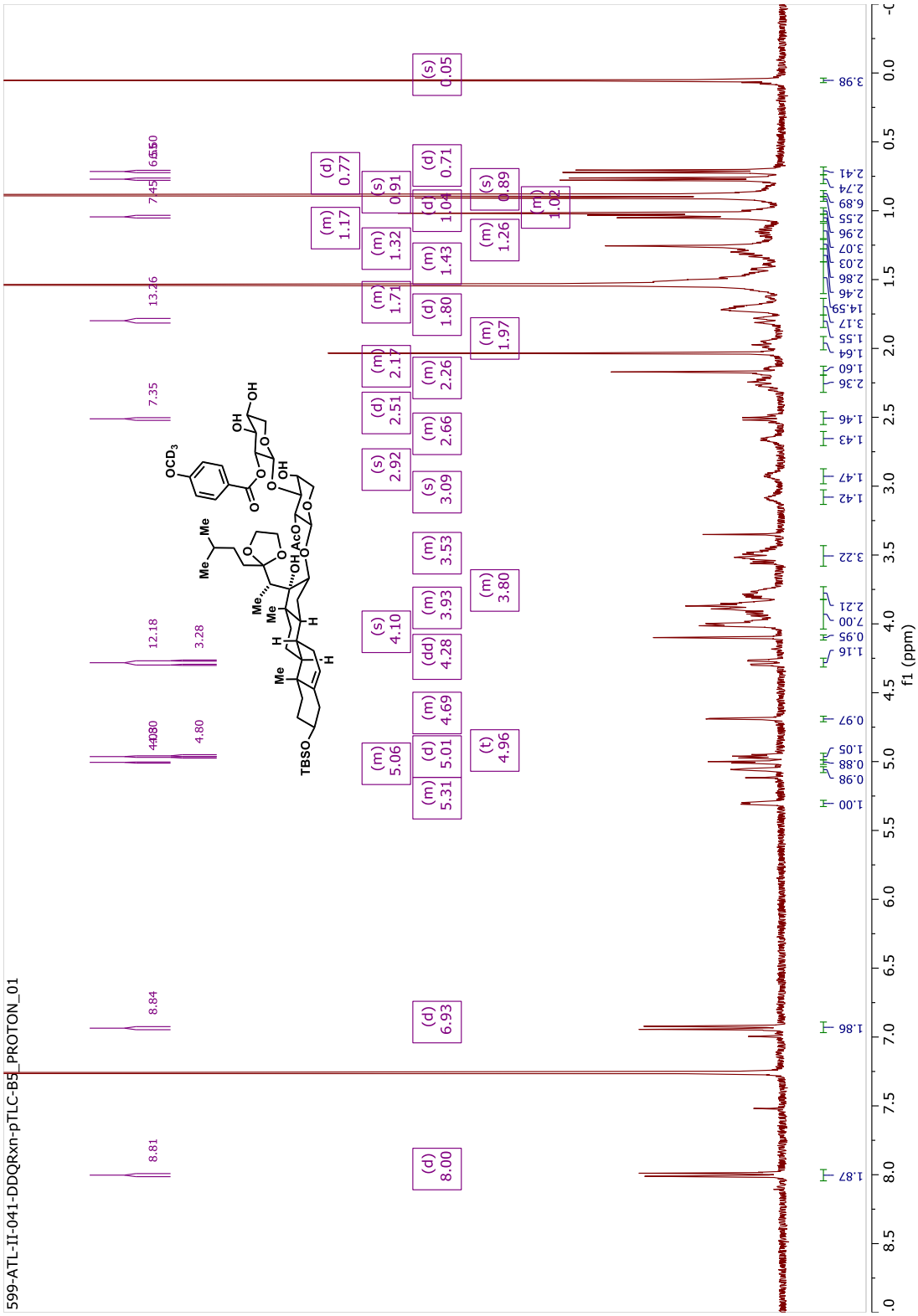
599-ATL-II-041-DDQRxn-pTLC-B5_PROTON_01
f1 (ppm)

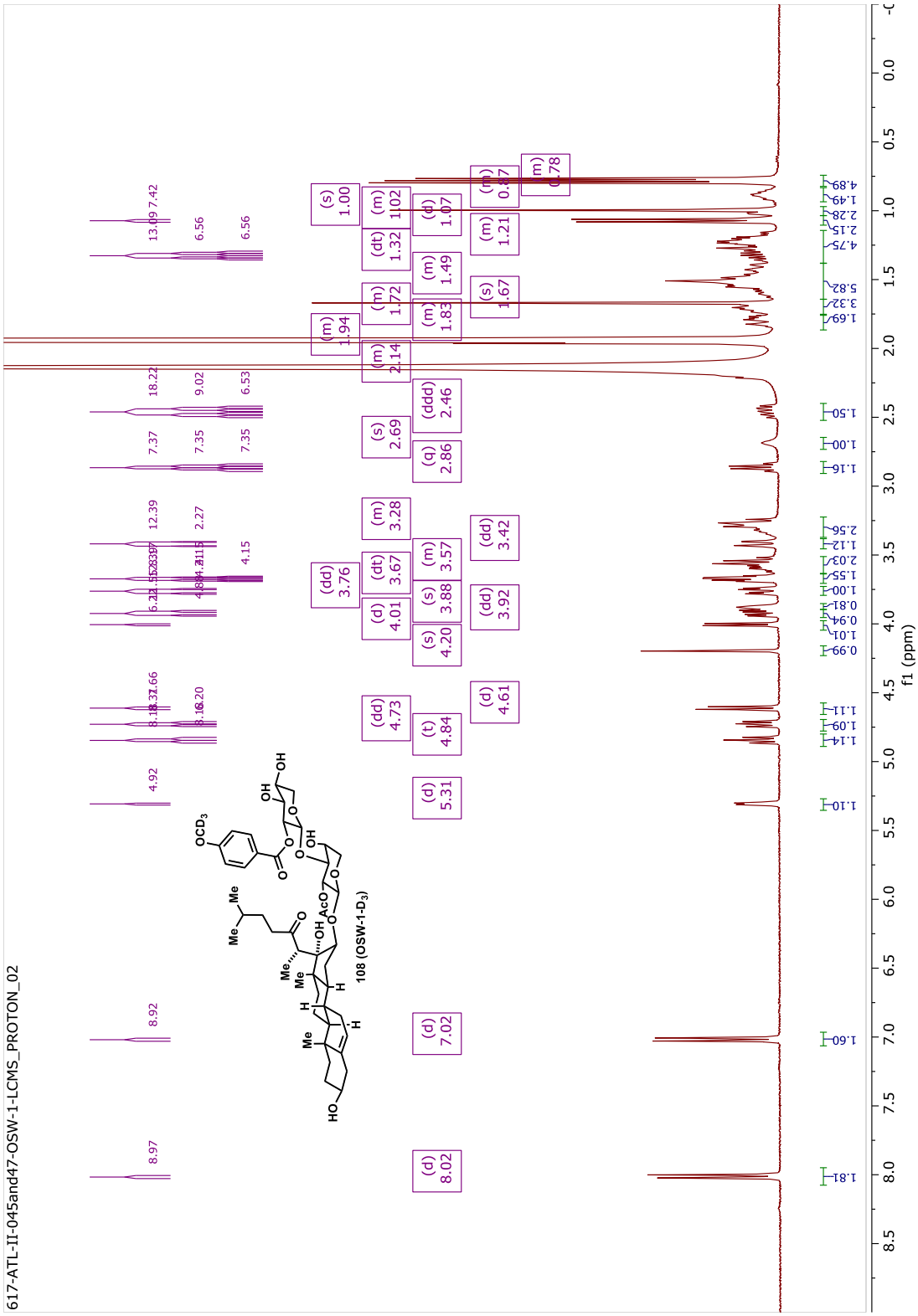
617-ATL-II-045and47-OSW-1-LCMS_PROTON_02
108 (OSW-1-D3)
f1 (ppm)

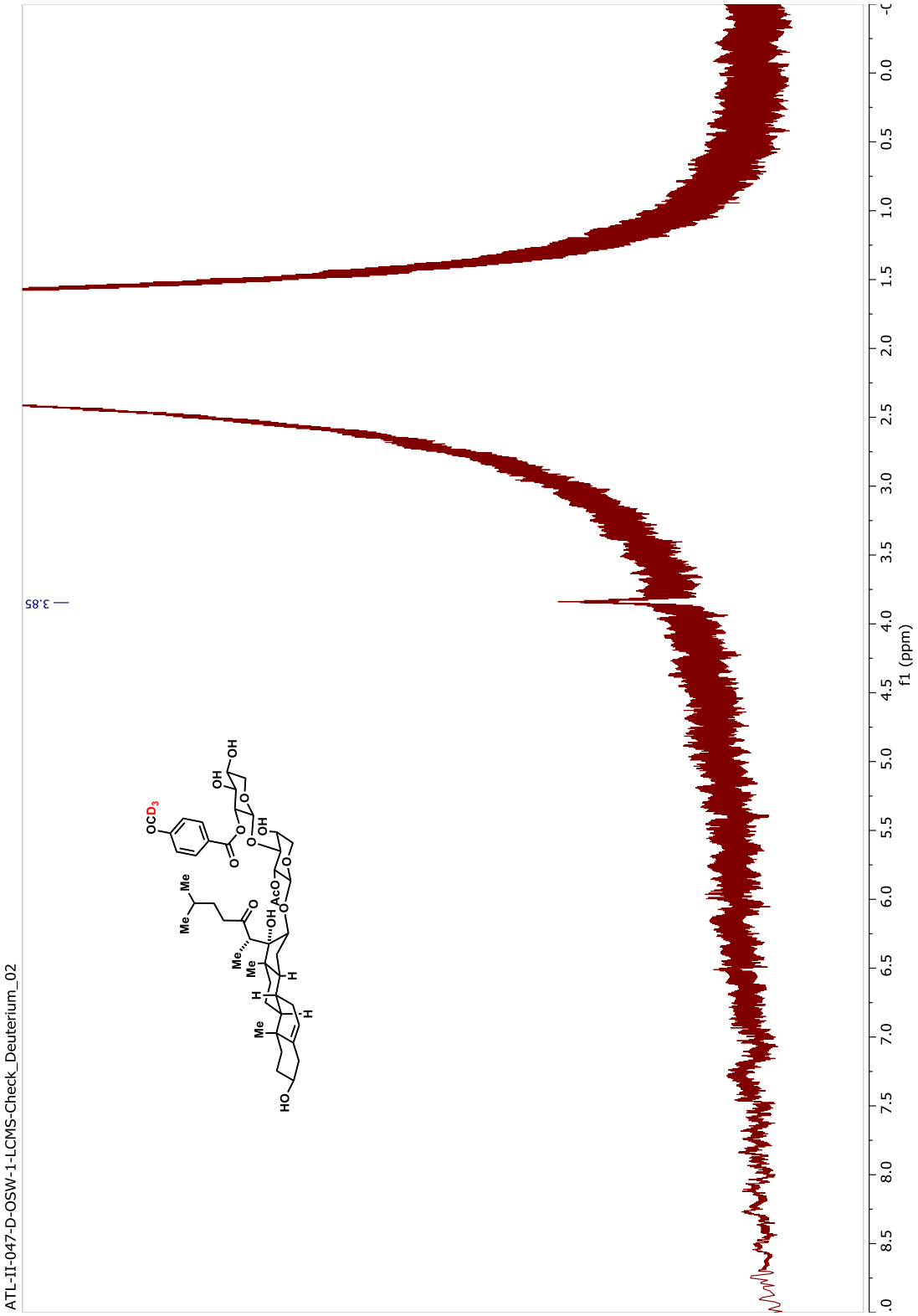
ATL-II-047-D-OSW-1-LCMS-Check_Deuterium_02
3.85
f1 (ppm)

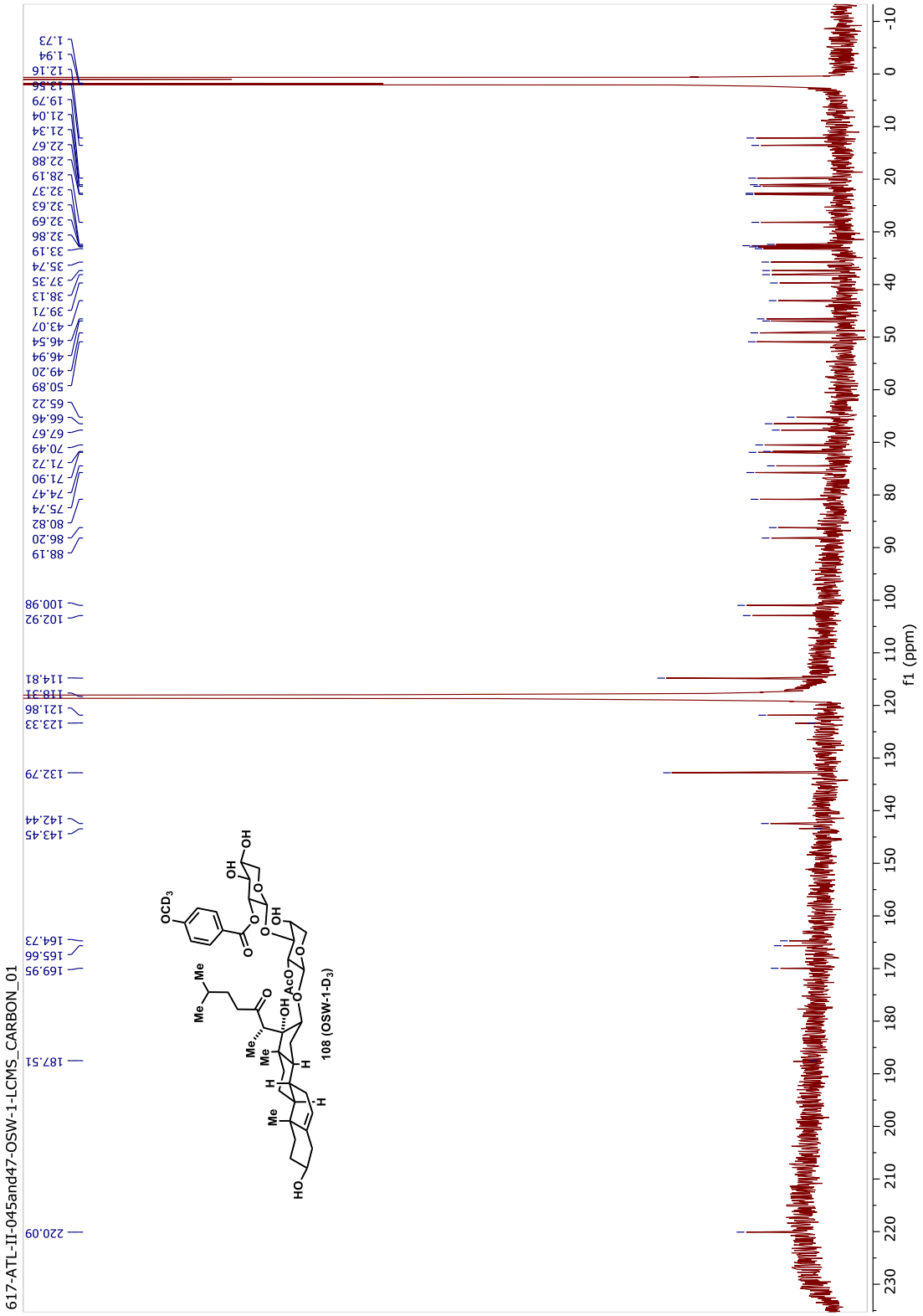
617-ATL-II-045and47-OSW-1-LCMS_CARBON_01
f1 (ppm)
108 (OSW-1-D3)

Sample Name	ATL-II-045+047	**Position**	P1-E1	**Instrument Name**	Instrument MS	**User Name**	Foster
Inj Vol	5	**InjPosition**		**SampleType**	Sample	**IRM Calibration Status**	All Ions Missed
Data Filename	11734AWB0002.d	**ACQ Method**		**Comment**	1x	**Acquired Time**	3/7/2016 10:54:51 AM

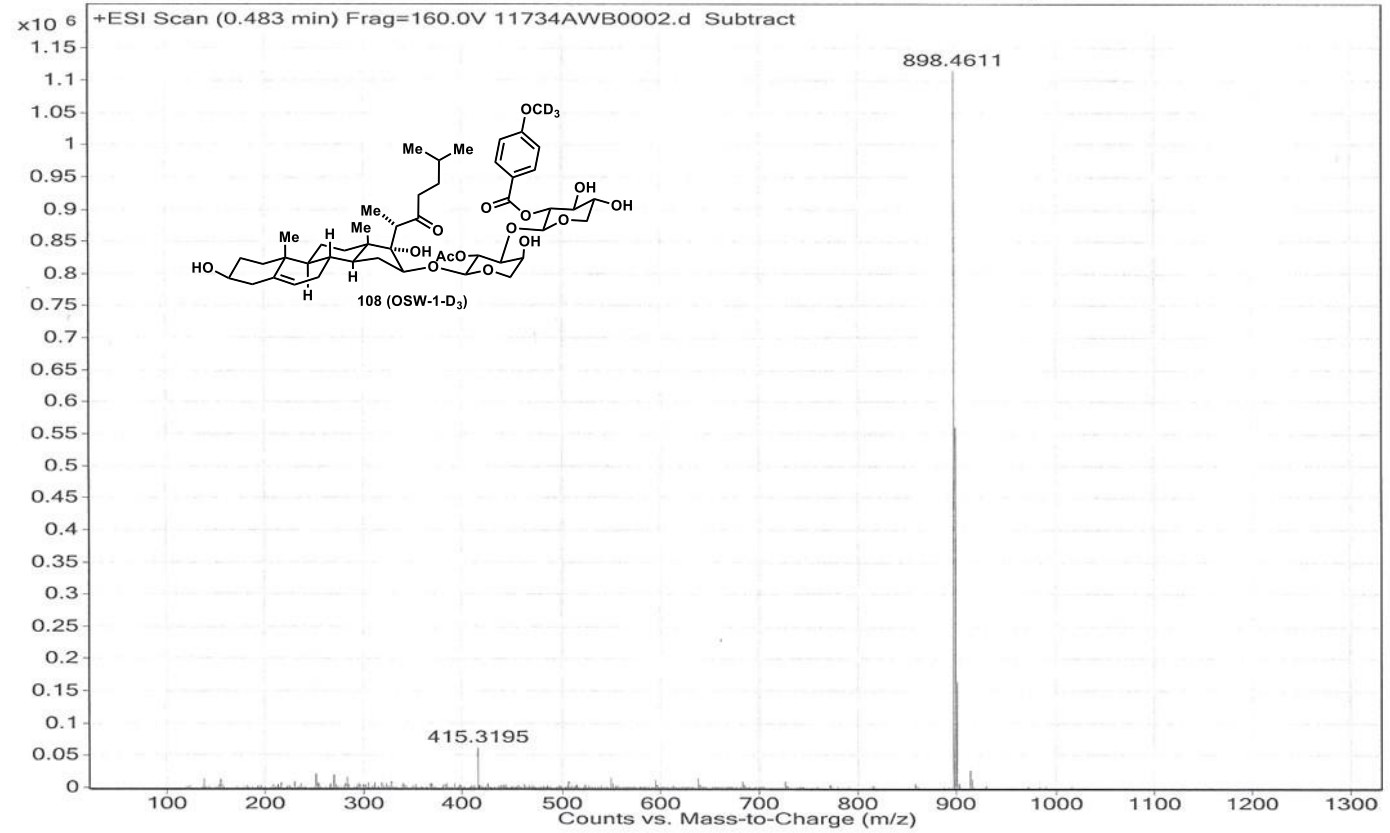

Calculated $(M+Na)^+$ = 898.4639

measured " = 898.4611

∴ error = 3.17 ppm

$C_{47}H_{65}D_3NaO_{15}$

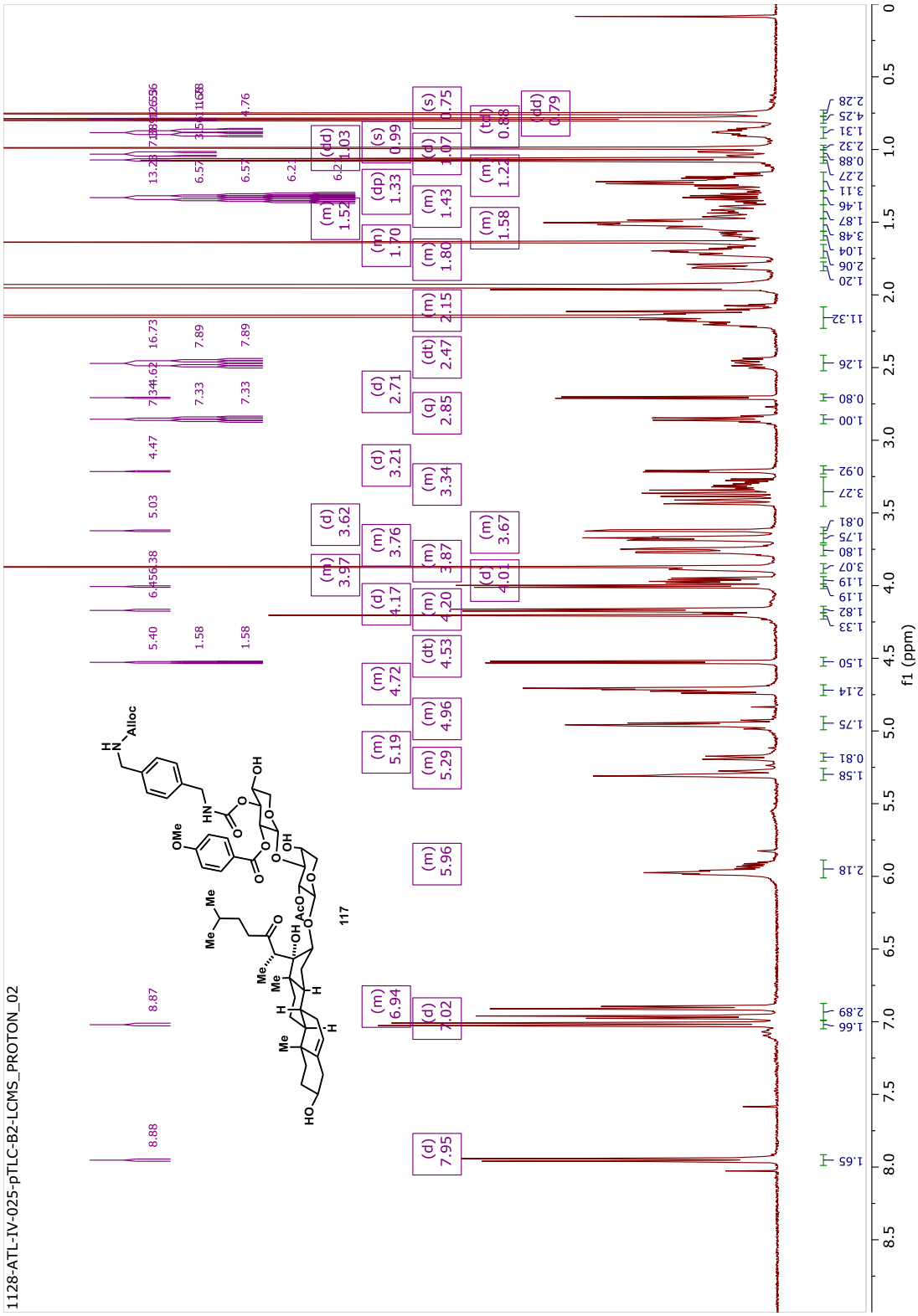
1128-ATL-IV-025-pTLC-B2-LCMS_PROTON_02
f1 (ppm)
117

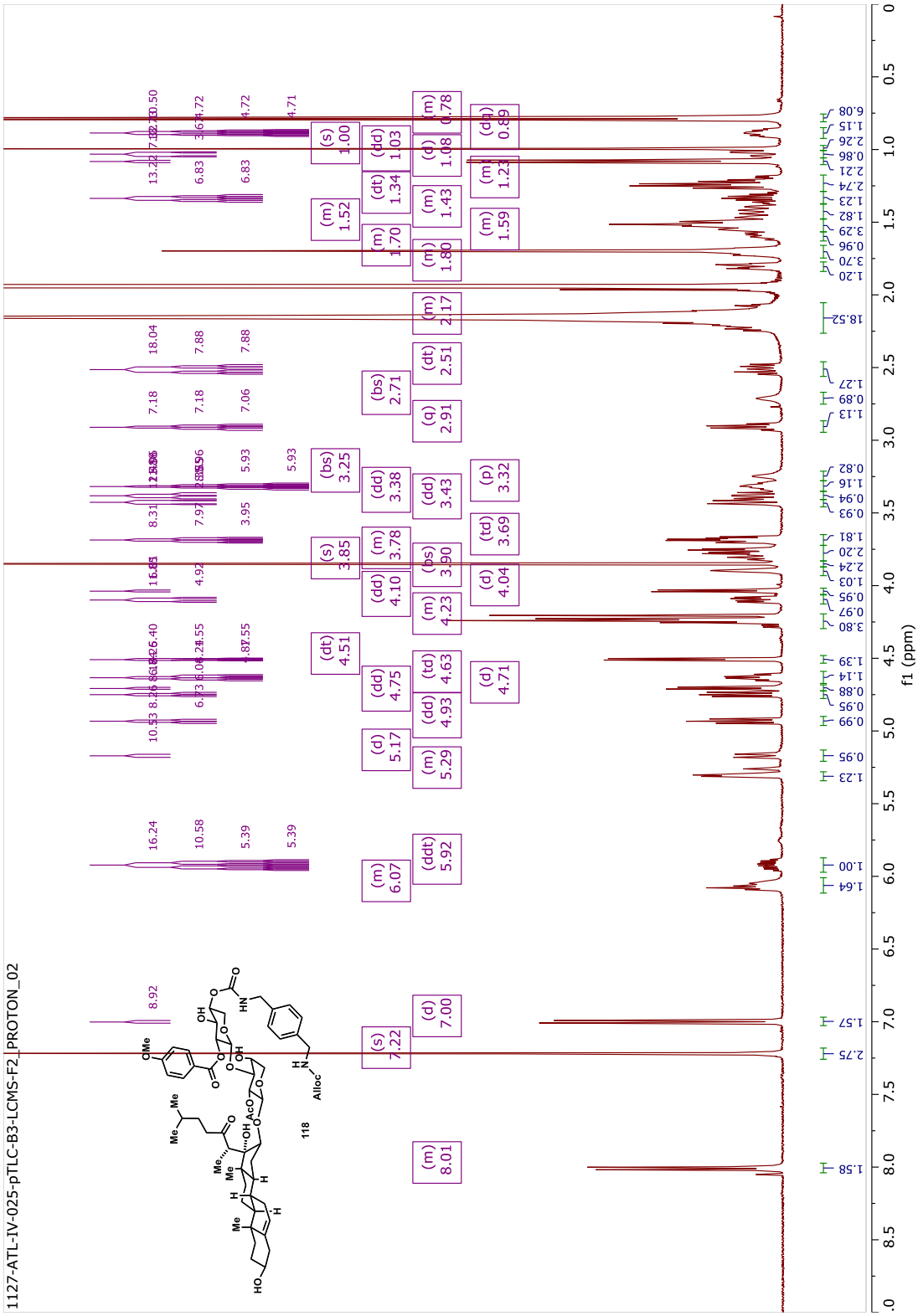
1127-ATL-IV-025-pTLC-B3-LCMS-F2_PROTON_02
f1 (ppm)

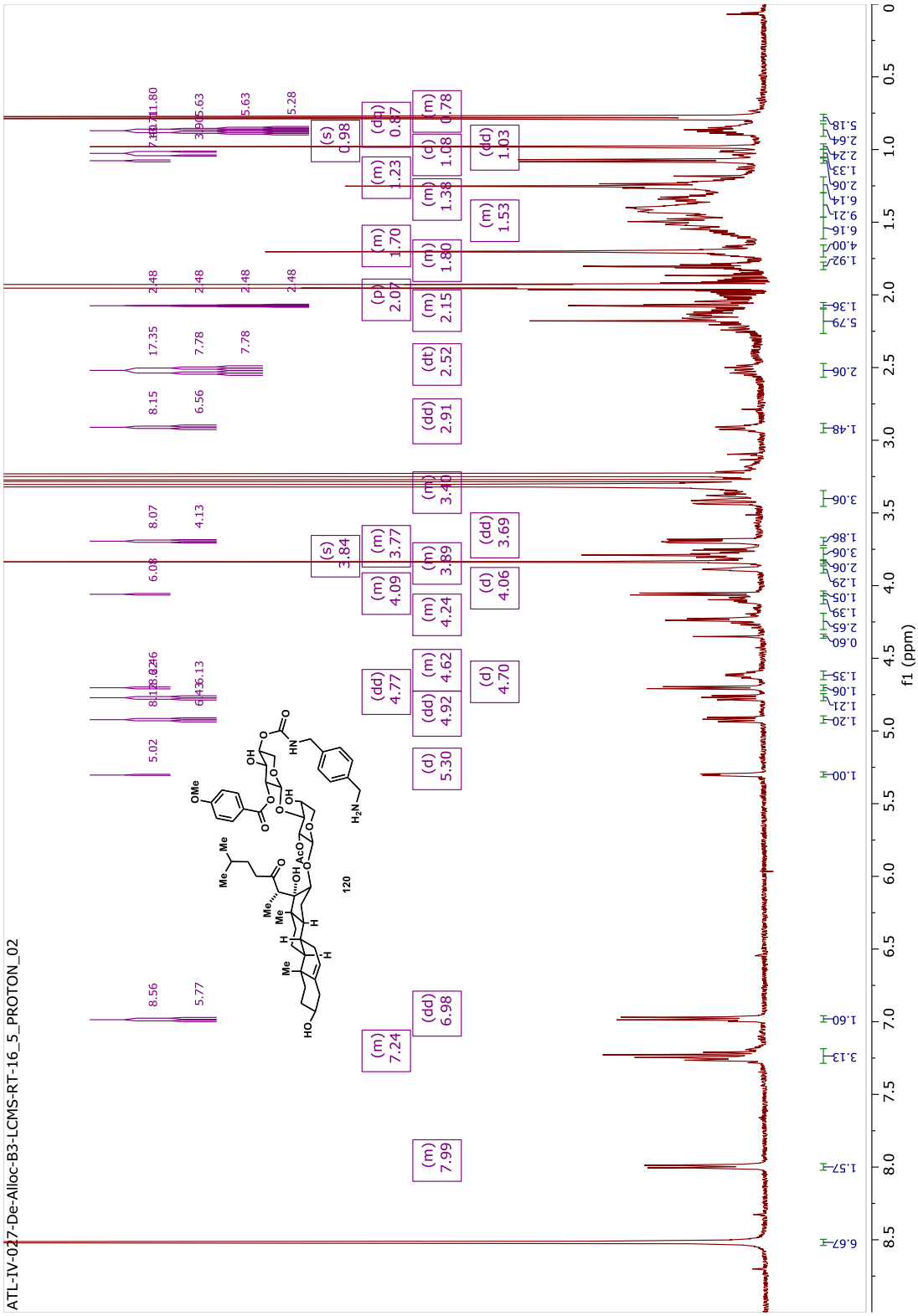
ATL-IV-027-De-Alloc-B3-LCMS-RT-16_5_PROTON_02
f1 (ppm)

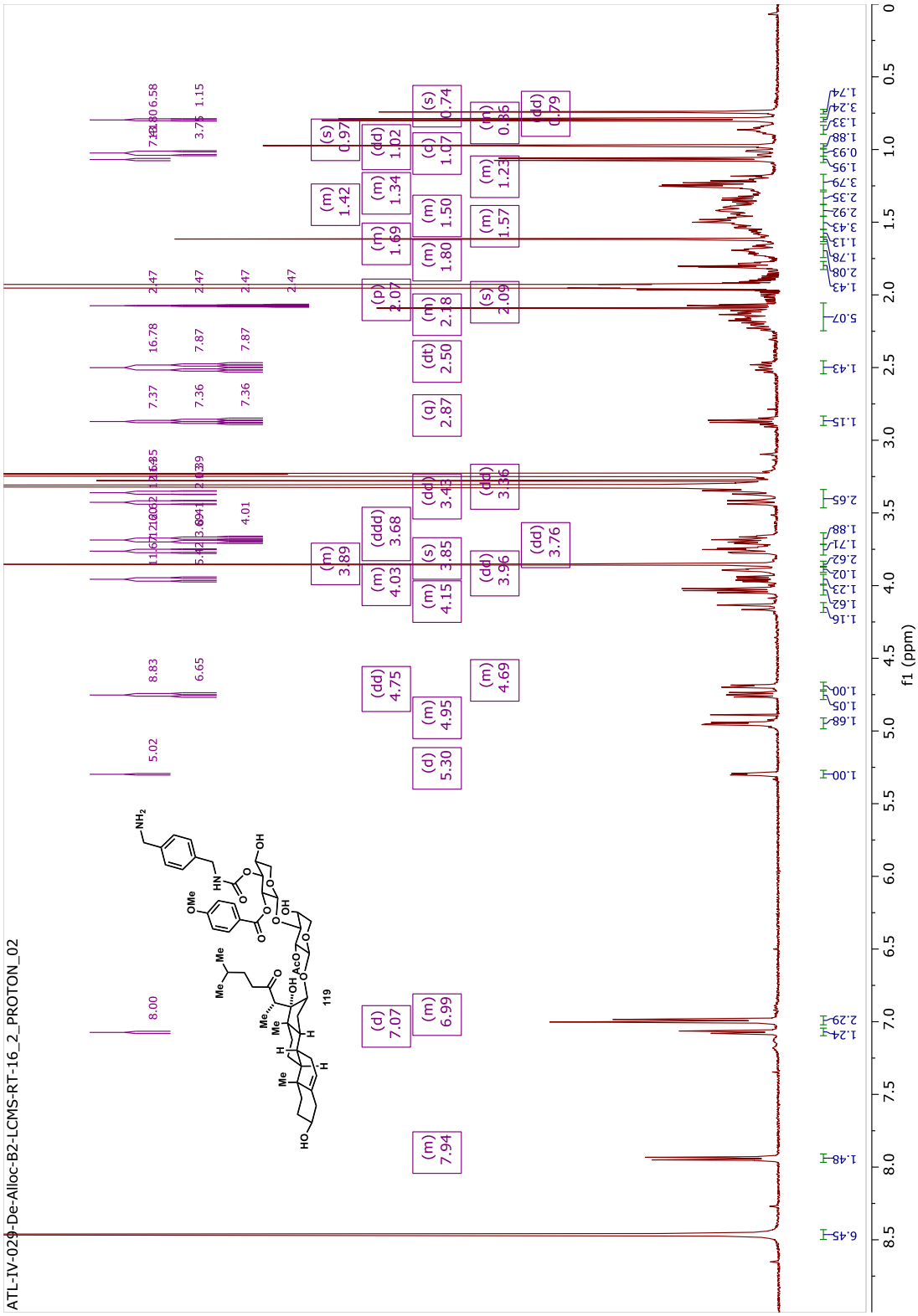
ATL-IV-029-De-Alloc-B2-LCMS-RT-16_2_PROTON_02
f1 (ppm)

Chapter III : Design and Synthesis of Modified OSW-1 Scaffolds- a Two-component Approach

Abstract

Since the identification of OSW-1's cellular targets as OSBP and ORP4, the natural product OSW-1 has shown significant potential for therapeutic applications. The OSW-1 compound exhibits broad spectrum anti-viral activity through its inhibition of OSBP, and potent anti-proliferative activity through its interaction with ORP4. OSBP and ORP4 are closely related members of the oxysterol binding protein family. Despite their sequence similarity, the two proteins possess different cellular function and disease relevance. The comparable binding affinities of OSW-1 to OSBP and ORP4 thereby hinder the use of OSW-1 as the molecular probe to determine the proteins' biological activities, as well as examined its therapeutic potentials. Hence, the development of OSBP- or ORP4-selective OSW-1 analog is important and would allow for the selective studies of each protein's function and disease relevance. The low-yield and non-convergent established syntheses of OSW-1 (as discussed in **Section I.3**) do not allow for the rapid construction and diverse derivatization of OSW-1 analogs, therefore a concise and convergent approach to synthesis OSW-1 analogs is desired. We have developed an efficient two-component approach to the OSW-1 scaffolds. The OSW-1 side chain and disaccharide moiety will compose the imine component, and this will join the steroidal alkene component through a tandem ene-cyclization operation. This will result in a heterocyclic E-ring that appends on the steroidal core. This approach was demonstrated successfully here with the aldehyde-ene reaction version with only the side chain attached, while the imino-ene type is under investigation. Furthermore, a set of OSW-1-related analogs with the E-ring is being synthesized through

the conventional OSW-1 syntheses to determine the effect of these new scaffolds on the biological activity of OSW-1.

III.1 Introduction and Background

The emergence of precision medicine as an evolving approach to cancer treatment requires the identification and characterization of new, druggable and cancer-specific therapeutic targets, along with the customizable and responsive course of treatment.[57] Developments in high-throughput genomic sequencing, bioanalysis, identification of diagnostic and prognostic biomarkers [58] have allowed the characterization of individual patient's unique state of disease. This information can be used along with molecularly targeted therapies to provide the patient with the most effective treatment. To date, many targeted therapies have been approved for patient treatment with several types of cancer, along with many more that are being developed. Despite this, there are still needs for the continuing identification and development of new precision therapeutic targets to treat deadly cancers.

As described in Section I.2.2, the major variant ORP4L of the protein ORP4 has recently been validated as an anti-cancer precision medicine target.[34,59] ORP4L was first identified as a general molecular marker for blood dissemination of solid tumors in the peripheral blood.[60] Later, ORP4 mRNA levels were reported to be expressed in myeloid cells of chronic myeloid leukemia (CML) patients.[61] In 2014, ORP4L's expression and cellular function were demonstrated to be important in cancer cell proliferation and viability.[33] In 2016, Zhong *et al.* showed that ORP4L is selectively expressed and is crucial for T-cell acute lymphoblastic leukemia (T-ALL) cell survival.[34] In this report, ORP4L expression was not detected in normal T-cells, but was at a high level in isolated leukemia

cells from a panel of T-ALL patients; and inhibition of ORP4L expression in T-ALL cells led to cancer cell death.[34] Furthermore, another report demonstrated the similar role of ORP4L in the survival of cervical carcinoma cell lines.[59] These results, together with the discovery of OSBP/ORP4 as cellular targets of the anti-cancer natural product compounds (the ORPphillins-**Figure 3**), present ORP4L as a potential druggable precision cancer therapeutic target.

Recently, OSBP was implicated as an important host factor for enterovirus replication through its discovery as the cellular target responsible for the observed anti-viral activity of itraconazole – an antifungal agent.[29,62,63] Itraconazole was identified as a broad-spectrum inhibitor of enteroviruses[29], polioviruses[62] and rhinoviruses[63]. The natural product compound OSW-1, a high affinity ligand of OSBP, has also been demonstrated to exhibit anti-viral activity through its interaction with OSBP.[11,29] Therefore, OSW-1 analogs with high selectivity to OSBP can be developed to effective anti-viral therapeutic agents.

The natural product OSW-1 can serve as a starting point for development of precision cancer therapeutic agent, however it cannot itself be a lead compound for ORP4 drug development. The OSW-1 compound causes its cellular effects through interacting with OBSP and ORP4; but it shows approximately similar binding affinities for OSBP as it does for ORP4.[10] This non-selective interaction would damper the proposed idea of ORP4 being a precision cancer protein target since OSW-1 can interact with OBSP in non-cancer cells.[21] Ligands with binding selectivity with ORP4 should be attainable since schweinfurthin A compound (**Figure 3**) exhibits binding affinity to OSBP at ~ 40 fold higher than to ORP4.[10]

Using OSW-1's structure as a starting point, a series of modified OSW-1 scaffolds can be designed for rapid assembly of a focused OSW-1 analog library, then the analogs will be evaluated for their selective binding to ORP4 over OSBP and anti-proliferative activity against ORP4-dependent cancer cell lines. Multiple total syntheses of OSW-1 have been reported with very similar synthetic strategy (Section I.3).[35,36,39,41–43] Many OSW-1 analogs have been reported, but the OSW-1 analog development has largely been driven by derivatization that was synthetically convenient during the total synthesis route, as opposed to a directed effort to identify the crucial pharmacophore for OSW-1.[4] This chapter describes the efforts and advances made in the design and synthesis of OSW-1-related scaffolds.

III.2 Designs of simplified scaffolds for OSW-1 mimetics

III.2.1 Structure-activity relationship (SAR) of the OSW-1 compound

The limited on-target structure-activity relationship (SAR) of compound OSW-1 provides guidance for the design for new and improved OSW-1 scaffolds.[4,10] Even though several OSW-1 analogs have been synthesized, their biological evaluation did not provide useful comparative activity information since they were not evaluated against the same cancer cell lines.[4] Thus far, there has been only one report that provided the SAR information of the OSW-1 compound based on its direct cellular targets.[10] The on-target SAR for the OSW-1 compound (**Figure 10**) demonstrated that: 1) sterically bulky substituents at the 3-hydroxyl position of the steroidal core block OSBP/ORP4 binding and therefore limit all biological activity (**Section II.2.2**); 2) the C-2' arabinosyl acetate and C-2" xylosyl benzoate are important for high affinity binding and potent cytotoxic activity;

and 3) introduction of large groups at C-3" hydroxyl of xylose did not affect OSBP/ORP4 binding affinity or cytotoxicity (**Section II.3.6**).[10]

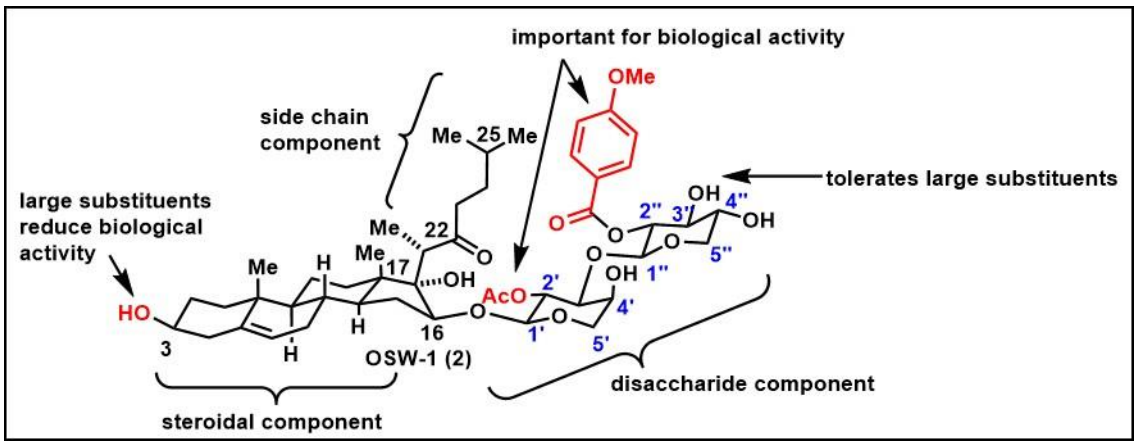

Figure 10. Structure-activity relationship (SAR) of the OSW-1 compound

III.2.2 Rationale and design of new OSW-1 scaffolds through a two-component approach

Based on the SAR information for OSW-1 presented above along with the close examination of the known protein structures of the yeast OSBP/ORP homologs[25], the key components of the OSW-1 compound that make direct contact with the OSBP/ORP4 proteins are hypothesized to be the 1) steroidal core, 2) side chain and 3) benzoate group on C-2" of xylosyl moiety. In the working hypothesis, the steroidal aglycon loads into the binding pocket of the proteins produced by the conserved sterol binding domain (**Figure 4**, **Section I.2.1**), with the side chain and disaccharide units extending out of the binding pocket making contact with other regions of the protein. This brings the side chain and benzoate moiety to close proximity (**Figure 10**). Since the side chain is hypothesized to make contact with other regions of the proteins outside of the conserved binding pocket, modifications to the side chain could be critical for the enhanced selectivity of the analogs to ORP4 over OSBP. The arabinose and likely the xylose moieties are hypothesized to

serve as a spacer for the extension of the critical benzoate moiety to the desired position near the side chain component, while the C-17 hydroxyl, C-22 ketone and the acetate moiety on the arabinose participate in a hydrogen-bonding network to provide the optimal conformation of the OSW-1 molecule. Therefore, a series of OSW-1-related scaffolds that will allow for the rapid generation of analogs with different side chains and simplified spacer units to position the benzoate into the optimal location and orientation are desired.

The established total syntheses of OSW-1[35,36,39,41–43] are unsuitable for the rapid generation of the proposed analogs for the identification of ORP4-selective lead compounds. The published syntheses of OSW-1 mainly follow a 3-component strategy (i.e., steroidal aglycon, L-arabinose and D-xylose moieties), with each component requires 8 to 10 steps of preparation (**Section I.3**). The L-arabinose and D-xylose components are combined through a Schmidt glycosylation reaction to form the disaccharide moiety; then the steroidal aglycon and disaccharide moiety are combined through a late-stage, low yielding Schmidt glycosylation reaction. This Schmidt glycosylation reaction to produce protected OSW-1 were problematic in my hands, with low yield and no recovery of starting materials (**Section II.3.4**). Therefore, any modification to the side chain or disaccharide unit will require several steps, capped by a very low-yield glycosylation reaction.

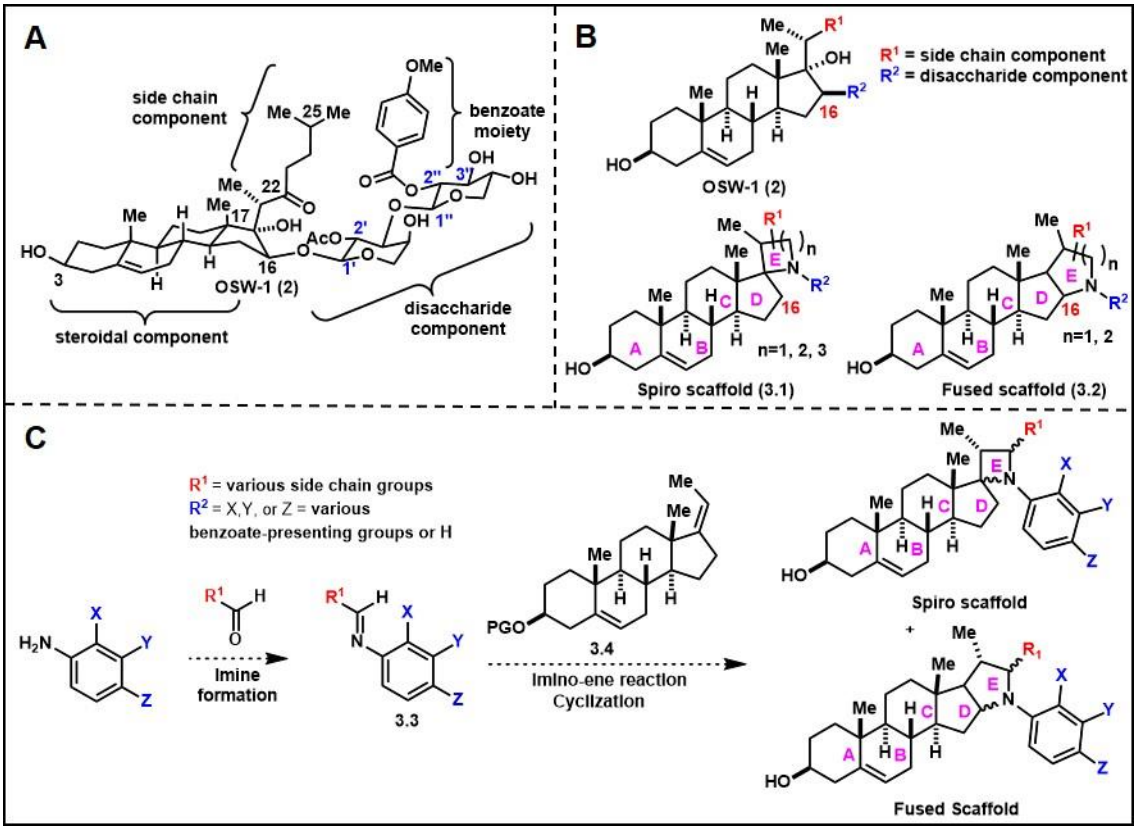

Scheme 15. A) Structure of OSW-1**; B)** proposed OSW-1-related scaffolds**; C)** the proposed two-component approach to OSW-1-related scaffolds

The proposed series of OSW-1-related scaffolds are envisioned to arise from a two-component combination synthesis strategy, with the side chain and the disaccharide units' attachment to the steroidal aglycon through an E-ring bridge – a heterocyclic expansion on the steroidal aglycon (**Scheme 15B**). In this approach, the side chain and disaccharide replacement units can first be combined to form one component, and then that component will merge with the aglycon component to make the E-ring bridge. This approach will allow for rapid and convergent synthesis of OSW-1 analog compounds, since various side chain and disaccharide modifications can be prepared separately in the form of imines (compound **3.3**, **Scheme 15B**), then this imine component can be combined with an alkene protected sterol **3.4** via a Lewis-acid mediated imino-ene type reaction (**Scheme 15C**).

Moreover, the size and stereochemistry of the appended E-ring bridge introduces rigidity and a new dimension of subtle modification to the relative position of the side chain and disaccharide to the aglycon moiety. Both spiro and fused substituted azacycle E-rings can possibly be constructed through the careful choice of Lewis acid. This reaction can both link and cyclize the two components in a one-pot operation. The aldehyde ene version of this reaction on sterol **3.4** has been successfully demonstrated (**Scheme 16B**, Section **III.3.1**). The screening of Lewis acid to activate the imino-ene reaction is being investigated by another lab member – Cori Malinky. In the meantime, it is critical to evaluate the effect of the introduction of the E-ring bridge on the biological activity of OSW-1-analogs. Therefore, OSW-1-closely-related analogs with only E-ring modification were synthesized and characterized (**Scheme 16B**, **Section III.3.2.4**).

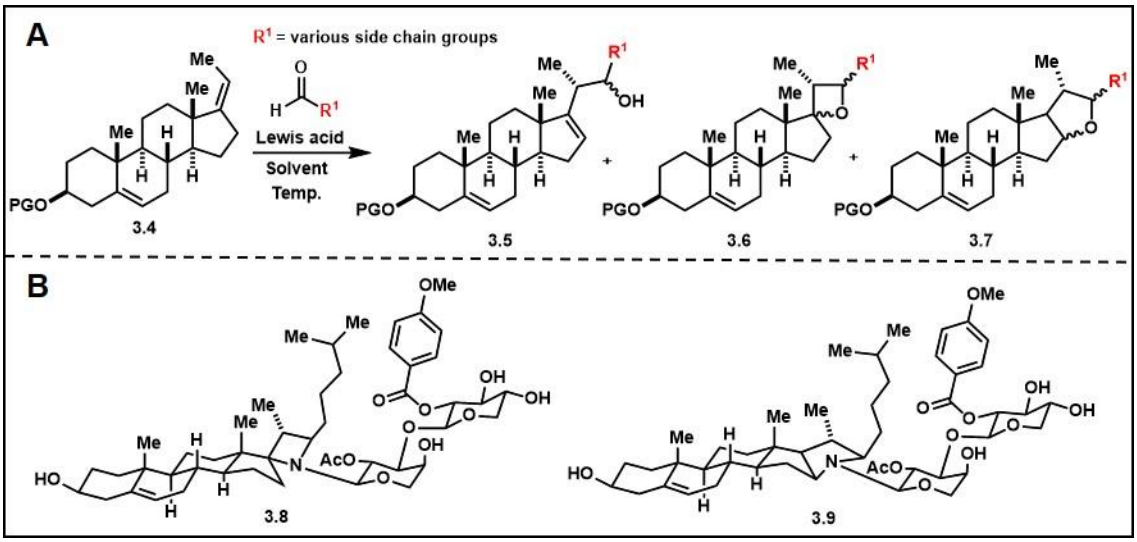

Scheme 16. A) Aldehyde-version of two-component approach**; B)** OSW-1 analogs with E-ring modification

III.3 Results and discussion

III.3.1 Validation of the two-component approach to OSW-1-related scaffolds

The validation of the two-component approach to OSW-1-related scaffolds started with aldehydes instead of imines as one of the components, since one intermediate, namely homoallylic alcohol **3.10a** (**Scheme 17**), was synthesized from paraformaldehyde during the OSW-1 steroidal aglycon synthesis (performed by Dr. Peddabudi). This homoallylic alcohol provided a great starting point for the investigation of intramolecular addition of C-22 alcohol to C16-17 alkene to form the appended E-ring (**Scheme 17**). Depending on the mechanism that the Lewis-acid mediated reaction proceeds through, spiro-oxetane **3.11** (Markovnikov, **Scheme 17**) product or fused-tetrahydrofuran **3.12** (anti-Markovnikov, **Scheme 17**) product can be obtained. Both products will provide useful knowledge once they are evaluated for their biological activity.

III.3.1.1 Intramolecular hydroalkoxylation reaction

Several Lewis acids have been reported to catalyze this intramolecular hydroalkoxylation of inert alkenes.[64–66] Some Lewis acids were examined for their ability to form the desired E-ring on the homoallylic alcohol **3.10** (Error! Reference source not f ound.).

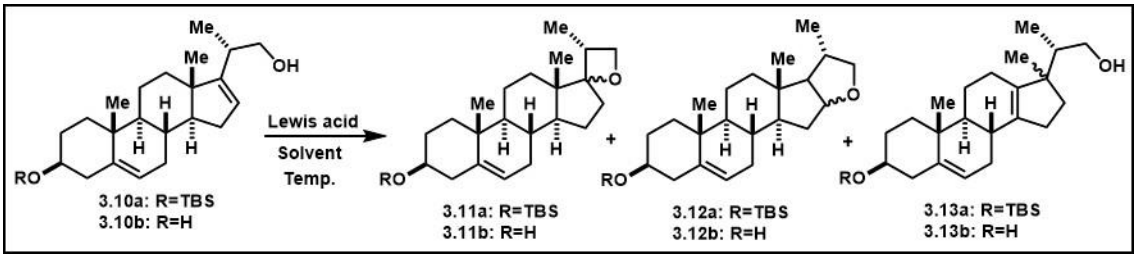

Scheme 17. Intramolecular hydroalkoxylation reaction with sterol **3.10** (TBS = *tert*-butyldimethylsilyl)

Table 1. Condition screening for intramolecular hydroalkoxylation reaction

Entry	Compound	Reagent(s)	Temp.	Time	Results
1	**3.10a**	$Sc(OTf)_3$ (5 mol%), DCE	50°C	12h	**3.10b** (28%), **3.11a** (7%),**3.11b** (trace),
2	**3.10a**	AgOTf (5 mol%), DCE	50°C-70°C	48h	**3.11a** (10%), **3.11b** (12%), **3.13b** (27%)
3	**3.10a**	$BF_3{\cdot}Et_2O$ (1.2 equiv), DCM	0°C	1h	**3.10b** (49%)
4	**3.10a**	I_2 (10 mol%), $PhSiH_3$ (20 mol%), DCM	RT	22h	No reaction
5	**3.10b**	AgOTf (5 mol%), DCE	50°C	8h	**3.11b** (17%), **3.13b** (21%)
6	**3.10b**	$BF_3{\cdot}Et_2O$ (2.4 equiv), DCM	0°C-RT	2h	**3.11b** (45%), **3.13b** (19%)

Lewis acids scandium (III) trifluoromethanesulfonate [$Sc(OTf)_3$], and silver (I) trifluoromethanesulfonate (AgOTf), in the presence of TBS-protected sterol **3.10a** produced the spiro-oxetane product **3.11a** and **b** along with a mixture of undesired side products (entry **1-2**, Error! Reference source not found.), while silane-iodine failed to give a ny cyclized product (entry **4**, Error! Reference source not found.) and boron trifluoride diethyl etherate ($BF_3{\cdot}Et_2O$) mainly deprotected sterol **3.10a** (entry **3**, Error! Reference s ource not found.) . The TBS group seemed labile in the presence of Lewis acids, as seen in the observed deprotected starting material sterol **3.10b** and deprotected spiro-oxetane product **3.11b**. The report by Yang *et al*. showed that both $Sc(OTf)_3$ and AgOTf catalyzes the anti-Markovnikov intramolecular hydroalkoxylation, with AgOTf giving higher yield of the cyclized product.[64] When the conditions were applied to TBS-protected sterol **3.10a**, mainly spiro-oxetane product (Markovnikov) was observed, possibly due to Baldwin's rule for cyclization. The cyclization to produce the spiro-oxetane product is classified as 4-exo-trig, which is favored as compared to the unfavored 5-endo-trig for the case of fused-

tetrahydrofuran ring. $Sc(OTf)_3$ gave the spiro-oxetane product **3.11a** in 7% yield, and a trace amount of deprotected spiro-oxetane product **3.11b**, along with deprotected sterol **3.10a** (28%) (entry **1**, Error! Reference source not found.). AgOTf afforded higher yields o f both protected (**3.11a**, 10%) and deprotected spiro-oxetane (**3.11b**, 12%) (entry **2**, Error! Reference source not found.). The sterol **3.10a** showed rearrangement in presence of AgOTf to compound **3.13b** (27%). This type of rearrangement has been observed in steroid structures before[67,68], where C16-17 olefin migrates to C13-14, and C18 methyl group shifts from C13 to C17. It was speculated that upon Lewis acid coordination with olefin, the olefin rearranged to a more stable tetrasubstituted position after a 1,2-methyl shift.

Since the TBS group on C-3 seemed to interfere with the cyclization reaction and resulted in a complicated mixture of products, it was removed to afford compound **3.10b**, which was then subjected to the intramolecular hydroalkoxylation condition (entry **5-6**, Error! Reference source not found.). $BF_3{\cdot}Et_2O$ produced the spiro-oxetane **3.11b** at a higher y ield (45%) as compared to AgOTf (17%). The unwanted rearranged sterol **3.13a** was observed in both cases. This section demonstrated the ability of homoallylic alcohol **3.10** to undergo cyclization for the formation of E-ring.

III.3.1.2 Tandem carbonyl ene-hydroalkoxylation reaction

During the synthesis of OSW-1 aglycon, homoallylic alcohol **3.10** was formed through a Lewis acid-mediated carbonyl-ene reaction of (*Z*)-3β-hydroxyl-5,17(20)-pregnadiene **3.4** with paraformaldehyde. Since both carbonyl-ene and intramolecular hydroalkoxylation reactions involve Lewis-acid, performing these reactions in tandem would allow for the rapid assembly of the side chain and formation of the E-ring bridge in one operation (**Scheme 18**).

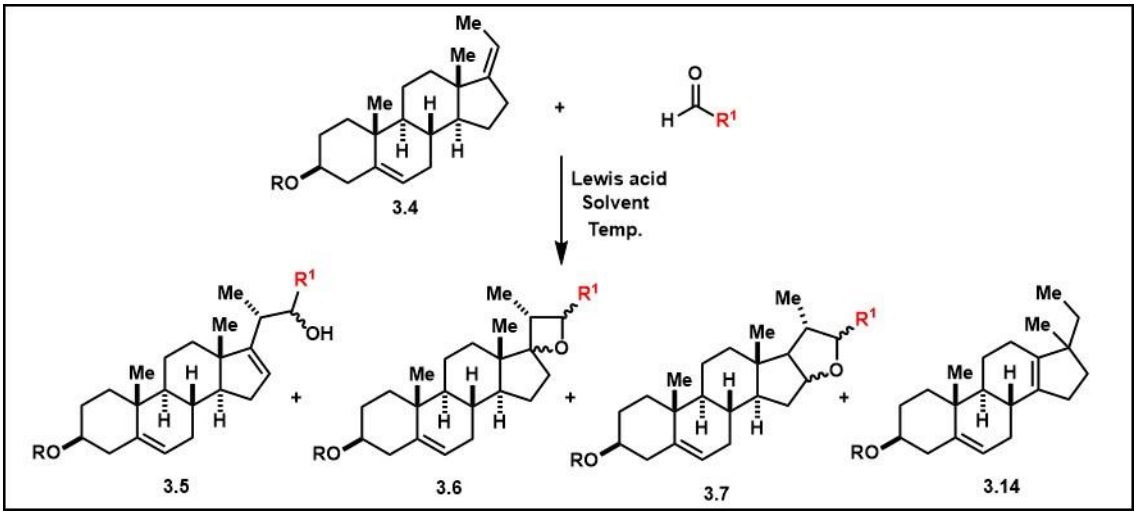

Scheme 18. Tandem carbonyl-ene and hydroalkoxylation reactions

Table 2. Condition screening for tandem carbonyl ene-cyclization reaction

Entry	R	R_1	Lewis acid	Solvent	Temp.	Results
1	H	H (2 eqv)	$BF_3{\cdot}Et_2O$ (3.2 eqv)	DCM	-10°C	**3.5** (16%), **3.6** (22%), **3.14** (11%)
2	H	$CH_2CH_2CH_2CH_2CH_3$ (1 eqv)	$BF_3{\cdot}Et_2O$ (4.5 eqv)	DCM	-10°C	Complex mixture
3	H	$CH_2CH_2CH_2CH_2CH_3$ (1 eqv)	$BF_3{\cdot}Et_2O$ (2 eqv)	DCM	-78°C	**3.14** (trace)
4	Bn	$CH_2CH_2CH_2CH_2CH_3$ (1 eqv)	$BF_3{\cdot}Et_2O$ (2.5 eqv)	DCM	-45°C	**3.5** (16%), **3.6** (trace), **3.14** (24%)
5	Bn	$CH_2CH(CH_3)_2$ (1 eqv)	$BF_3{\cdot}Et_2O$ (2.5 eqv)	DCM	-45°C	**3.5** (8%), **3.6** (23%), **3.7** (15%),**3.14** (23%)

The tandem ene-cyclization reaction was demonstrated successfully with the reaction of pregnadiene **3.4** and paraformaldehyde to produce the homoallylic alcohol **3.5** and spiro-oxetane **3.6** (entry **1**, Error! Reference source not found.). The rearrangement of p regnadiene **3.4** to **3.14** was observed, similar to the rearrangement observed in **Section III.3.1.1**. However, when an aliphatic aldehyde (hexanal, entry **2**, Error! Reference source n

ot found.) was used instead of paraformaldehyde, the reaction resulted in a streaky mixture on TLC analysis, and a complicated mixture of products based on ^{1}H NMR. The free hydroxyl group on C-3 might have undergone addition to the hexanal under Lewis-acidic condition to form a hemiacetal. The streakiness from TLC plate could have resulted from the equilibrium of this hemiacetal formation. When the reaction temperature was lowered to prevent this hemiacetal formation, only rearranged pregnadiene **3.14** was observed in trace amounts (entry **3**, Error! Reference source not found.). When the C-3 hydroxyl group was protected as a benzyl ether, the reaction afforded homoallylic alcohol **3.4**, trace amount of spiro-oxetane **3.5** and rearranged pregnadiene **3.14** (entry **4**, Error! Reference source not found.). Another aliphatic aldehyde (isovaleraldehyde) was examined in this reaction, which resulted in a complex mixture of products (entry **5**, Error! Reference source not found.). The fused-tetrahydrofuran product **3.7** was observed, which suggested the reaction might have proceeded through a slightly different mechanism, since the formation of this product was unfavored according to Baldwin's rule (**Section III.3.1.1**).

Section III.3.1 demonstrated that the E-ring bridge can be constructed rapidly from two components (pregnadiene and aldehyde) in one operation. Even though a mixture of products were observed, the reaction should be tunable with the careful choice of Lewis acid reagents and the reaction conditions. The investigation of imino-ene-cyclization is underway with another lab member-Cori Malinky.

III.3.2 Synthesis of OSW-1-related analogs with only E-ring modification

As the methodology for the two-component approach being developed, it is critical to evaluate the effects of E-ring bridge modification on the biological activity of OSW-1. Therefore, a set of analogs that are closely related to OSW-1 containing the amine on C-

22 and N-glycosidic linkage with OSW-1 disaccharide moiety was synthesized. The retrosynthesis of these analogs is outlined in **Scheme 19**. OSW-1 analogs **3.8** and **3.9** can be accessed through Lewis acid-mediated cyclization of N-linked glycosylated product **3.15**. Compound **3.15** is a glycosylated product of OSW-1 disaccharide **3.17** and homoallylic amine **3.16**. Homoallylic amines **3.16** can be converted from homoallylic alcohols **3.18**, which is the product of carbonyl-ene reaction between pregnadiene **3.14** and 4-methylpentanal similar to the reaction investigated in **Section III.3.1.2**.

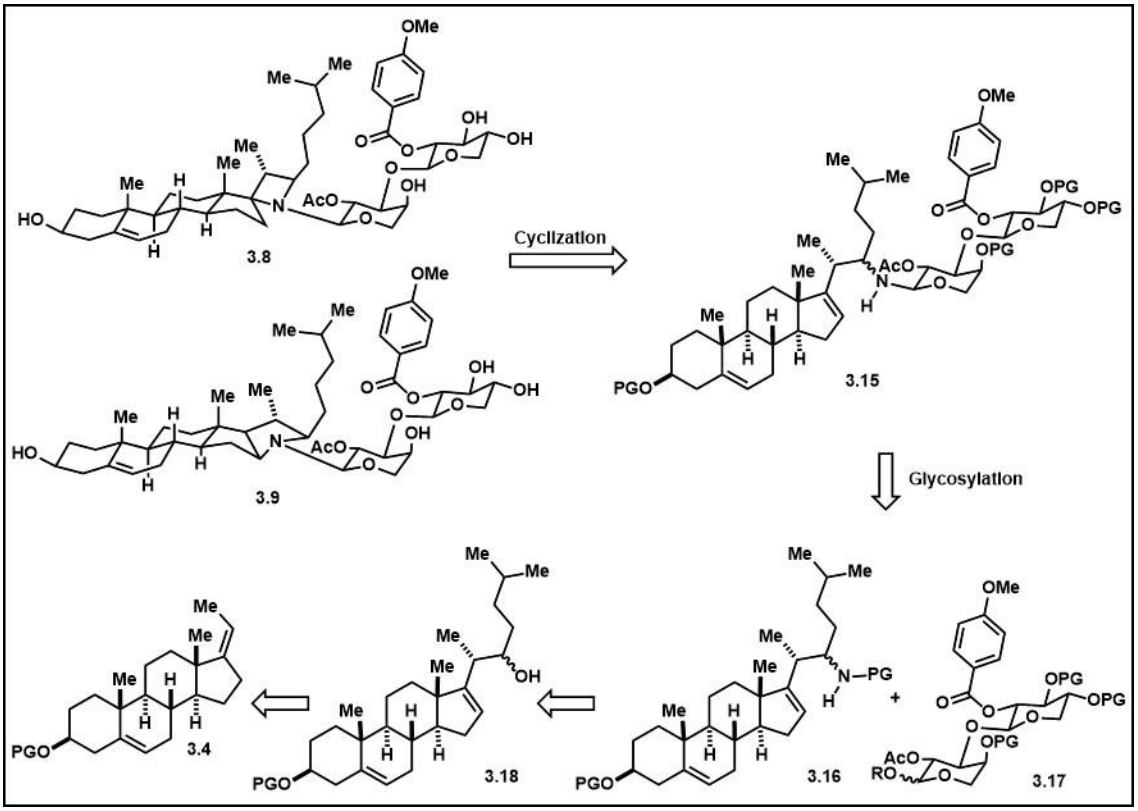

Scheme 19. Retrosynthesis of OSW-1 analogs with E-ring modification

III.3.2.1 Synthesis of homoallylic alcohols 3.18

The carbonyl-ene reaction presented in **Section III.3.1.2** resulted in a mixture of homoallylic alcohols and cyclized products (**Scheme 18**). For the synthesis of these OSW-

1 analogs, only homoallylic alcohols were desired, so the reaction condition was optimized for the production of only homoallylic alcohols.

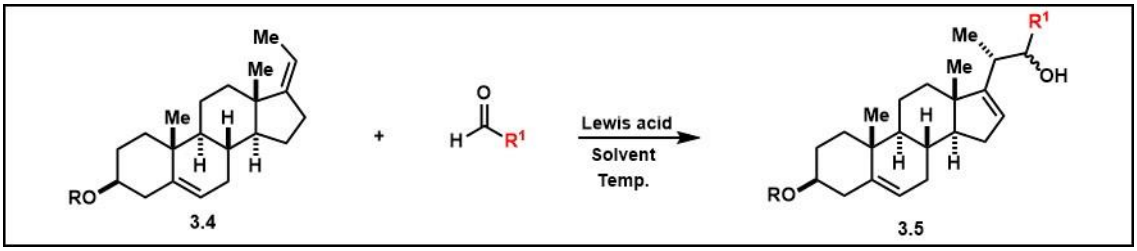

Scheme 20. Carbonyl-ene reaction to form homoallylic alcohols

Table 3. Condition screening for carbonyl-ene reaction

Entry	R	R^2	Lewis acid	Solvent	Temp.	Results
1	Bn	$CH_2CH(CH_3)_2$ (1.1 eqv)	$BF_3{\cdot}Et_2O$ (2.5 eqv)	DCM	-45°C	**3.5** (50% borsm), trace cyclized product
2	Bn	H (5 eqv)	$BF_3{\cdot}Et_2O$ (1.2 eqv)	DCM	RT	**3.5** (76%), trace cyclized product
3	Ac	$CH_2CH(CH_3)_2$ (3 eqv)	Me_2AlCl (5 eqv)	DCM	-78°C - RT	**3.5** (85%)
4	Ac	$CH_2CH_2CH(CH_3)_2$ (3 eqv)	Me_2AlCl (5 eqv)	DCM	-78°C - RT	**3.5** (70%), and side product

The carbonyl-ene reaction was first examined with $BF_3{\cdot}Et_2O$ as the Lewis acid in the presence of 4Å molecular sieves[69], with the pregnadiene **3.4** added to the mixture of aldehyde and Lewis acid to lower the rate of pregnadiene rearrangement. Under these conditions, the reactions produced only homoallylic alcohols with isovaleraldehyde and paraformadedhye in average to good yield (entry **1-2**, Error! Reference source not found.), w ith trace amounts of cyclized products. The benzyl ether protecting group on C-3 hydroxyl was replaced with an acetate group for ease of removal later in the synthesis, since hydrogenolysis of benzyl ether might also reduce the other olefins in the molecule. A report

by Houston *et al*. demonstrated the carbonyl-ene reaction with a more potent Lewis acid-dimethyaluminum chloride (Me_2AlCl) at very low temperature.[70] The carbonyl-ene reaction of acetylated pregnadiene **3.4** with isovaleraldehyde proceeded smoothly to afford the desired homoallylic alcohols **3.5** in great yield (85%), with no cyclized products observed (entry **3**, Error! Reference source not found.).

To synthesize the homoallylic alcohols with the OSW-1 side chain, the aldehyde needed was 4-methylpentanal. However, this was not available commercially, so it was synthesized in the lab form 4-methylpentanoic acid (**Scheme 21A**). 4-methylpentanoic acid was reduced by lithium aluminum hydride to 4-methylpentanol[71], which was selectively oxidized to 4-methylpentanal with pyridinium chlorochromate[72].

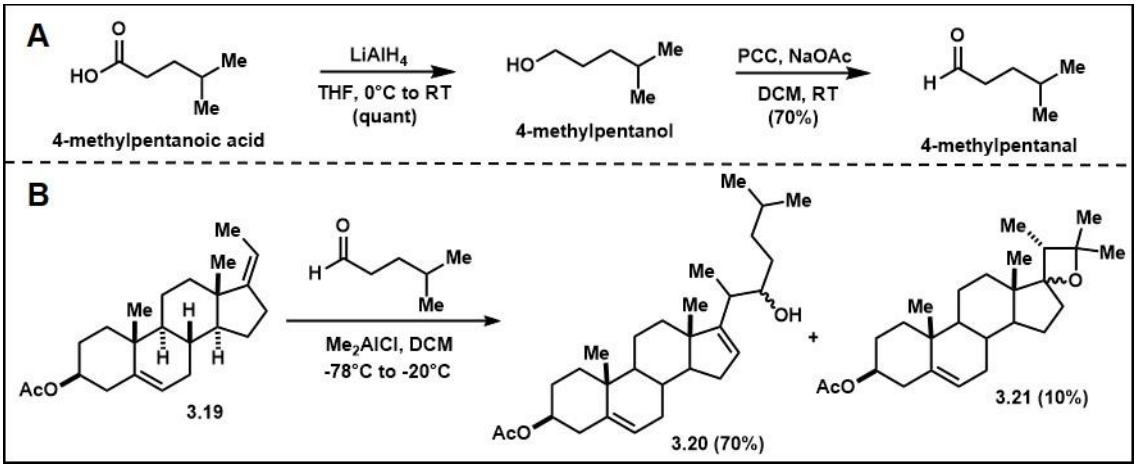

Scheme 21. A) Synthesis of 4-methylpentanal**; B)** carbonyl-ene reaction with 4-methylpentanal

The carbonyl-ene reaction was then carried out with 4-methylpentanal to install the OSW-1 side chain (entry **4**, Error! Reference source not found.). This reaction formed the d esired homoallylic alcohols **3.20** in good yield (70%), along with a side product **3.21** (**Scheme 21B**). The side product had a very similar polarity with the desired homoallylic alcohols, so it was first thought to be one of the homoallylic alcohol isomers. After

extensive purification (through column chromatography with acetone-hexanes mixture eluent, and HPLC), the side product was isolated in 9.7% borsm yield. A full characterization through 2D NMR spectroscopy (HSQC, COSY, and HMBC) revealed the side product as spiro-oxetane **3.21** (see Experimental section for full characterization details-Error! Reference source not found.). This was an unexpected side product. Since t he carbonyl-ene reaction proceeded very cleanly to afford the desired homoallylic alcohols with isovaleraldehyde (entry **3**, Error! Reference source not found.), it was hypothesized t hat the spiro-oxetane side product could have arisen when a contaminant from the synthesis of 4-methylpentanal got carried to the carbonyl-ene reaction. This observation started a small investigation into the formation of the spiro-oxetane (**Section III.3.2.2**).

III.3.2.2 Investigation of pathways to spiro-oxetane product 3.21

Since 4-methylpentanal (also known as isocaproaldehyde) was not available commercially, it was synthesized in our lab. Pyridinium chlorochromate (PCC) oxidized the 4-methylpentanol to the desired aldehyde. ^{1}H NMR spectrum of this crude mixture showed mainly 4-methylpentanl present, along with a small singlet observed at 11.36 ppm (See Chapter appendix). Signals in this region normally correspond to the acidic proton of a carboxylic acid. Even though PCC is mainly employed for the controlled oxidation of a primary alcohol to an aldehyde, there was a possibility of overoxidation to afford carboxylic acid. If water was present, it could react with the aldehyde to form a hydrate adduct. PCC reagent can then oxidize the hydrate to carboxylic acid.

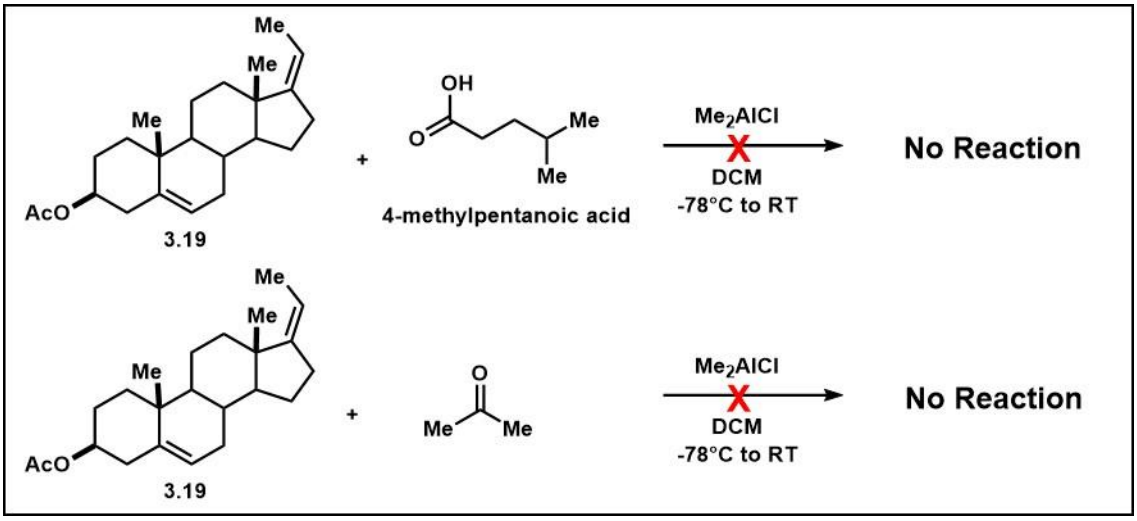

Scheme 22. Reactions of acetylated pregnadiene **3.19** with 4-methylpentanoic acid or acetone

Since a trace amount of carboxylic acid was observed in the ^{1}H NMR spectrum of crude aldehyde product, it was hypothesized that the carboxylic acid could play a role in the formation of the spiro-oxetane product. Moreover, the spiro-oxetane product was essentially a net condensation product of the diene **3.19** and a molecule of acetone. Both of these hypotheses were evaluated by treating the diene **3.19** with 4-methylpentanoic or acetone (**Scheme 22**) in the exact conditions that the carbonyl-ene reaction with 4-methylpentanal was carried out. However, both reactions yielded neither homoallylic alcohols nor spiro-oxetane. The diene **3.19** was recovered fully, without any sign of rearrangement. This was not very surprising, since ketones and carboxylic acids are more electron-rich, due to electron donation from the alkyl and hydroxyl groups, and are therefore are not as reactive as aldehydes in the carbonyl-ene reaction.

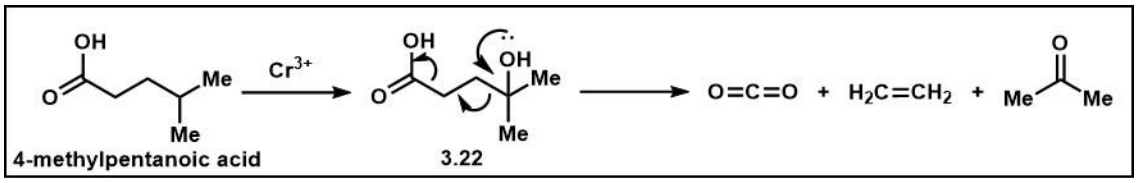

Scheme 23. Formation and fragmentation of 4-hydroxy-4-methylpentanoic acid

Since neither the carboxylic acid nor acetone resulted in spiro-oxetane product, another explanation was sought. In the ^{13}C NMR of the crude aldehyde, a small signal at around 64 ppm was observed (See Chapter III Appendix, #1434). Signals in this chemical shift region are diagnostic for C-O bonds. This signal suggests the possibility that the aldehyde or carboxylic acid underwent a hydroxylation reaction at the tertiary carbon during the oxidation condition. It has been shown that Cr^{3+} species, in acidic condition, could hydroxylate tertiary carbon hydrocarbons.[73,74] If 4-methylpentanoic acid underwent chromium-mediated hydroxylation at its tertiary carbon, it would have been converted to 4-hydroxyl-4-methylpentanoic acid **3.22** (**Scheme 23**). To provide the equivalent of acetone for the formation of the spiro-oxetane **3.21**, the hydroxy acid **3.22** could be envisioned to undergo fragmentation under the carbonyl-ene reaction condition to afford CO_2, ethylene, and an equivalent of acetone (**Scheme 23**). The production of two moles of gas is a great driving force for the fragmentation to proceed, even though two carbon-carbon bonds would be broken. Since the carbonyl-ene reaction of diene **3.19** and acetone did not produce the expected spiro-oxetane, the equivalent of acetone could have been produced and reacted with the participation of the possible remnant chromium species from PCC oxidation. To investigate the role of hydroxy acid in the formation of spiro-oxetane, 4-hydroxy-4-methylpentanoic acid was desired.

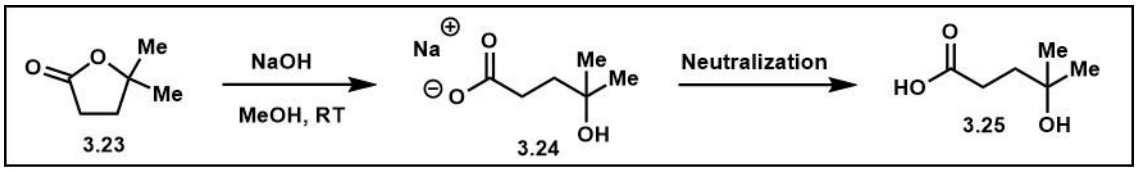

Scheme 24. Conversion of dimethyl-γ-butyrolactone to 4-hydroxy-4-methylpentanoic acid

4-hydroxy-4-methylpentanoic acid **3.25** (**Scheme 24**) was not available commercially, but dimethyl-γ-butyrolactone **3.23** could be purchased. The lactone **3.23** was subjected to mild saponification conditions (NaOH in MeOH) to open the lactone (**Scheme 24**). Neutralization of aqueous phase during the work up afforded an off-white solid, which was characterized as sodium 4-hydroxy-4-methylpentanoate **3.24**.[75] Efforts to obtain free carboxylic acid from the sodium salt using aqueous hydrochloric acid resulted in only lactone **3.23** identified through ^{1}H NMR analysis. Literature suggested that due to the Thorpe-Ingold effect [76], where the geminal dimethyl substituents produce a compression of the internal angle to facilitate the intramolecular cyclization, the molecule was prompted to stay in the cyclized lactone form as compared to the open carboxylic acid form. More specifically, it was demonstrated that in acidic aqueous conditions, the equilibrium ratio of hydroxy acid: lactone for 4-hydroxy-4-methylpentanoic acid was 2:98.[77] This explained the observation of lactone **3.23** when sodium carboxylate **3.24** was neutralized with aqueous HCl. Therefore, anhydrous conditions to convert sodium carboxylate salt to carboxylic acid were investigated. The sodium carboxylate salt was treated with Dowex resin, or dry silica gel, which is weakly acidic in anhydrous tetrahydrofuran (THF). ^{1}H NMR analysis of the resulting mixture from both cases are presented in **Figure 11**. In the ^{1}H NMR spectrum of Dowex treated material, along with signals that were corresponded to lactone, a new set of signals was observed with the

chemical shifts different from that of lactone **3.23** or sodium carboxylate **3.24**. This new set of signals was assigned as 4-hydroxy-4-methylpentanoic acid. The ^{1}H NMR spectrum of silica treated material showed mainly 4-hydroxy-4-methylpentanoic acid. Therefore, dry silica in anhydrous THF seemed to be the best method to convert lactone **3.23** to carboxylic acid **3.25**.

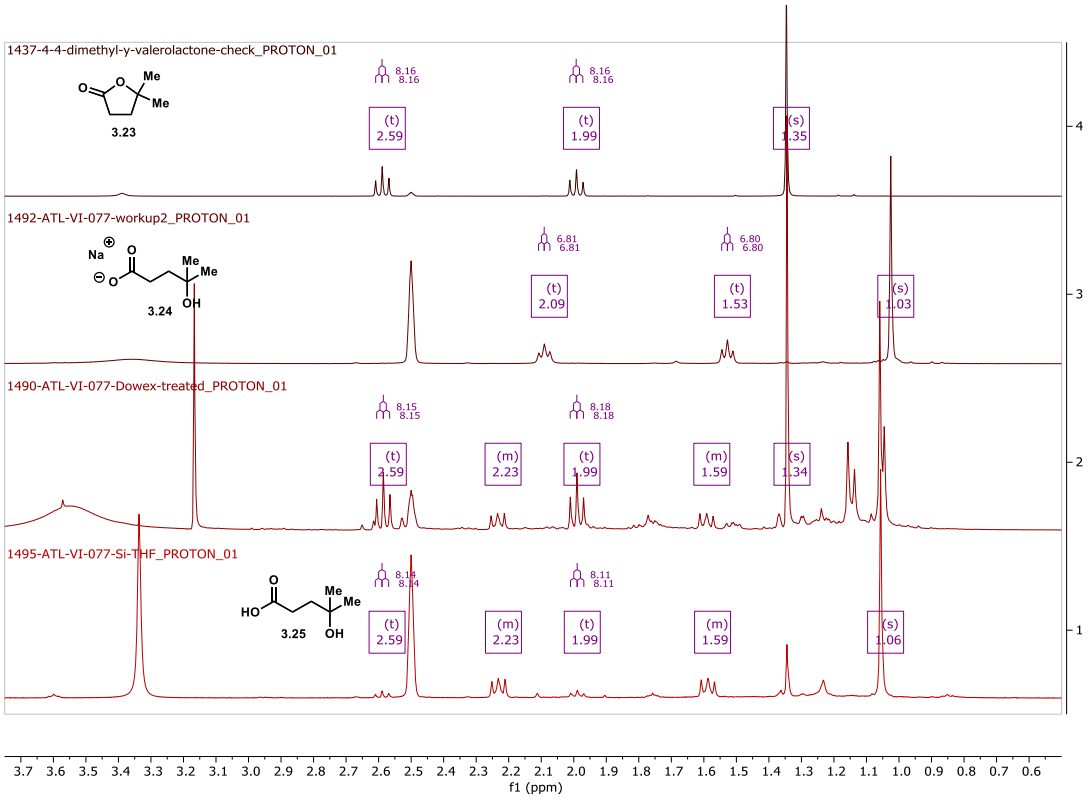

Figure 11. ^{1}H NMR spectra of lactone **3.23,** sodium carboxylate **3.24,** and hydroxy acid **3.25**

The role of carboxylate salt **3.24** and carboxylic acid **3.25** in the formation of the spiro-oxetane product was then investigated. Diene **3.19** was treated with sodium carboxylate **3.24** or carboxylic acid **3.25** in the same condition of the carbonyl-ene reaction that was used before. In both cases, no reaction was observed, the diene was recovered fully. This result suggested that the hydroxy carboxylic acid **3.25** and its derivative **3.24**

alone was not responsible for the formation of the spiro-oxetane **3.21**. It could be the synergistic effect of residual chromium species from PCC oxidation, 4-hydroxy-4-methylpentanoic acid and dimethylaluminum chloride in the carbonyl-ene reaction condition.

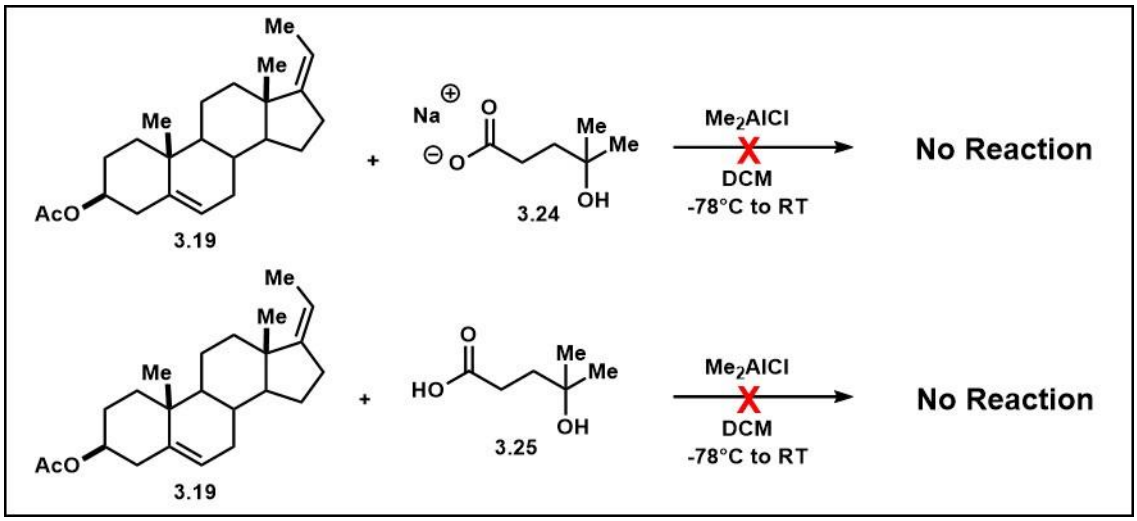

Scheme 25. Reactions of diene **3.19** with sodium 4-hydroxy-4-methylpentanoate or 4-hydroxy-4-methylpentanoic acid

The investigation into possible pathways of spiro-oxetane formation halted here, due to time and resource constraint. The spiro-oxetane side product was observed consistently for multiple carbonyl-ene reactions. Later, a better method was employed for the work-up of the PCC oxidation reaction. This improved work-up passed the crude reaction mixture through a column composed of silica and neutral alumina gel to remove remnant chromium species. The NMR analysis of the resulted aldehyde did not show any signal for carboxylic acid (^{1}H NMR at 11.36 ppm) or hydroxy carboxylic acid (^{13}C NMR at 64 ppm). The carbonyl-ene reaction since then have been proceeded smoothly, with the yield of desired homoallylic alcohols near 85%, and no spiro-oxetane was observed. These observations also strengthen the hypothesis of chromium species involvement in the

formation of spiro-oxetane. Future efforts will be required to develop this potential route to a one-step formation of spiro-oxetane. If successful, this spiro-oxetane reaction would allow for the formation of a complex motif that is important in medicinal chemistry[78] from the simple building blocks of olefins and hydroxy carboxylic acid.

III.3.2.3 Synthesis of steroidal homoallylic amines

The synthesis of OSW-1 analogs continued with the conversion of homoallylic alcohol **3.21** to homoallylic amine **3.28** (**Scheme 26**). Oxidation of homoallylic alcohol **3.20** with pyridinium dichlormate afforded C-22 ketone **3.26** in decent yield (60%). Ketone **3.26** was then transformed to a mixture of oxime isomers **3.27** in good yield (75%), gearing up for the reduction to form homoallylic amines **3.28**.

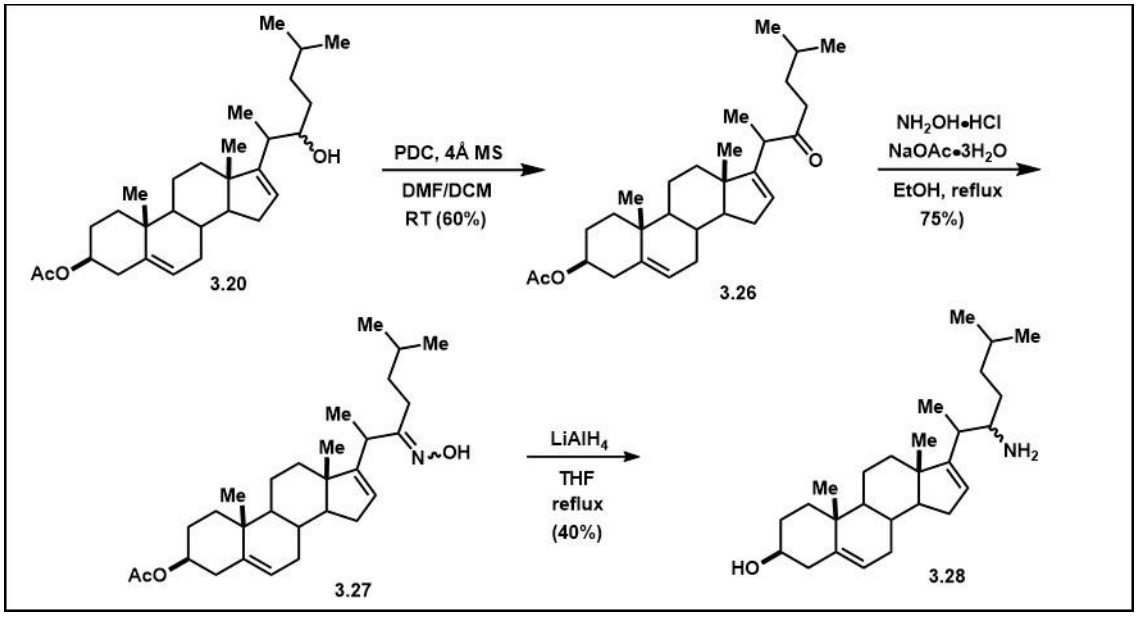

Scheme 26. Synthesis of homoallylic amines from C-acetylated homoallylic alcohol **3.20**

The oximes proved to be resistant to reduction conditions. Several metal-mediated reduction conditions were screened, but only lithium aluminum hydride (10 equiv) in

refluxed tetrahydrofuran produced decent yield of homoallylic amines **3.28**. The acetate group did not survive the reduction condition.

Through the results obtained from screening the reduction of oximes, it was clear that more robust protection group on C-3 hydroxyl would be required to survive the harsh condition of oxime reduction. The acetate group, being an ester, did not survive the LAH reduction condition. The deprotection of C-3 hydroxyl group after the oxime reduction added complications in the subsequence steps, more specifically, the glycosylation reaction. With two competing nucleophiles (C-3 hydroxyl and C-22 amine), the Schmidt glycosylation condition seemed to favor the O-glycosidic linkage formation but not the N-glycosidic bond (**Scheme 22**, **Section III.4.2**). Selective protection of the C-3 hydroxyl group was possible in the presence of free amine through a silyl ether protecting group, but the reaction yield was low (40%) due to difficulties in purification of the desired product. Therefore, to reduce the number of reaction steps and increase the overall yield, a *p*-methoxybenzyl (PMB) group was chosen for the protection of the C-3 hydroxyl group. PMB protecting group is stable towards reduction conditions. Furthermore, the hydroxyl groups on the OSW-1 disaccharide moiety were also protected as a PMB ether. This would allow for one-step global deprotection at the end of the synthesis to yield the desired analogs.

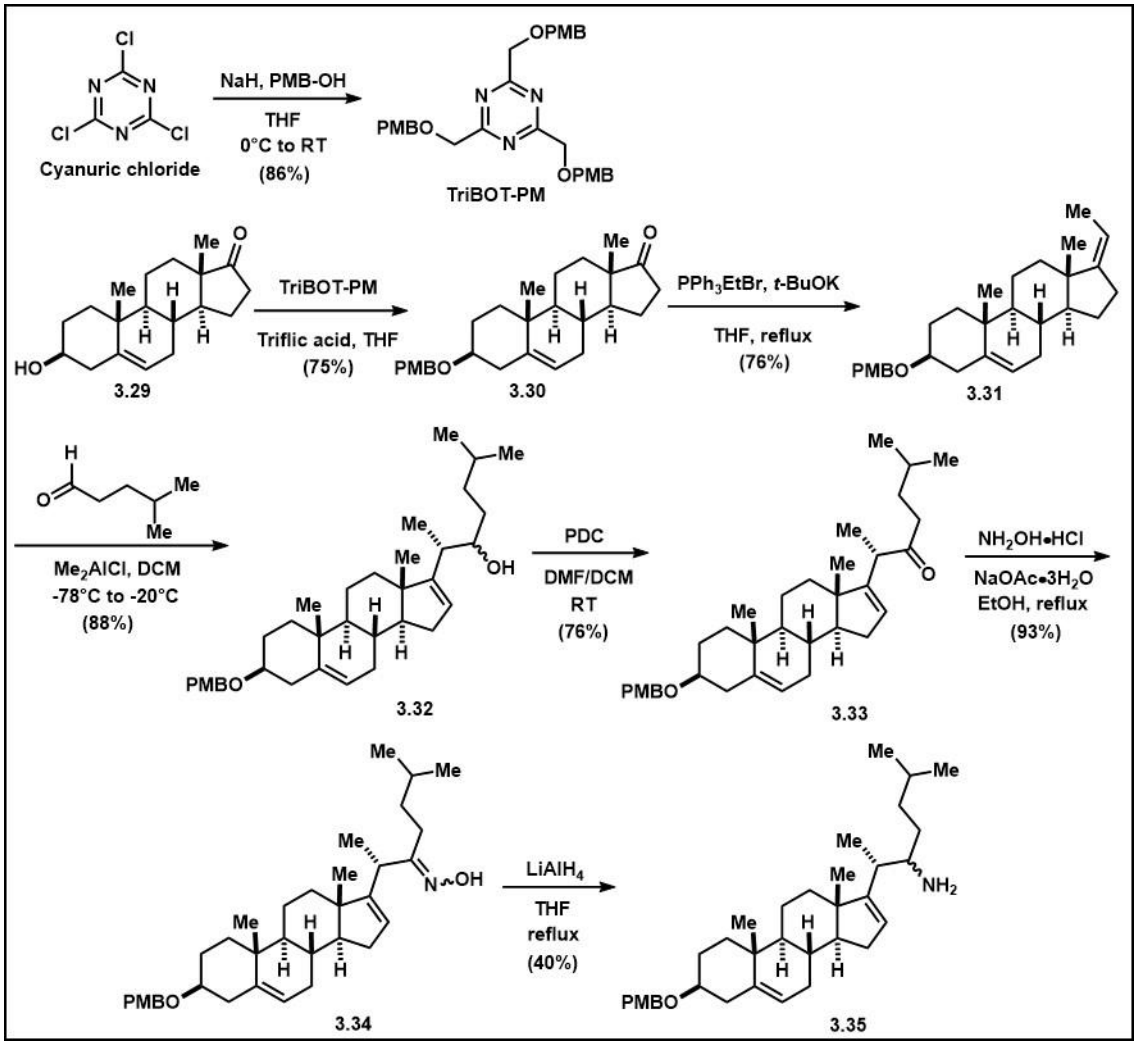

Scheme 27. Synthesis of C-3-PMB protected homoallylic amines

Trans-dehydroandrosterone **3.29** underwent PMB-protection in the presence of 2,4,6-tris(p-methoxybenzyloxy)-1,3,5-triazine (triBOT-PM) reagent.[79] TriBOT-PM can be synthesized on large scale from p-methoxybenzyl alcohol and cyanuric chloride with high yield (86%) (**Scheme 27**).[79] The PMB protection proceeded smoothly with a catalytic amount of trifluoromethanesulfonic acid. The protected product **3.30** was purified through recrystallization in isopropanol, which was beneficial as compared to column chromatography on gram scale. A Wittig reaction converted ketone **3.30** to diene **3.31**,

which was also purified through recrystallization in isopropanol. It seems that the presence of PMB group allowed the molecule to be recrystallized from isopropanol, because attempts to recrystallize the diene **3.19** with acetate protecting group instead of PMB were not successful in purifying the desired product.

Next, the aliphatic side chain was installed through a carbonyl-ene reaction, similar to the synthesis of homoallylic alcohols **3.20** described before. Pregnadiene **3.31** (1 equiv.) was reacted with 4-methylpentanal (3 equiv., synthesized in the lab) in the presence of dimethylaluminum chloride (5 equiv.) at low temperature. The reaction afforded the desired mixture of homoallylic alcohols **3.32** in good yield (88%), with no observation of the side product spiro-oxetane **3.21**. The homoallylic alcohol mixture was oxidized to C-22 ketone **3.33** in the presence of pyridinium dichromate (PDC). Ketone **3.33**, through a reductive amination with oximes **3.34** as an intermediate, was converted to a mixture of homoallylic amine isomers **3.35**. The low yield of oximes reduction was also observed before in the C-3 acetate series. The PMB-protecting group on C-3 of the steroidal core, as predicted, survived the LAH reduction condition. With C-3 hydroxyl protected, the mixture of homoallylic amines proceeded forward to the N-glycosylation reaction with the OSW-1 disaccharide moiety to form the OSW-1 analog for the validation of the proposed two-component approach.

III.3.2.4 N-glycosylation to form OSW-1-related analogs: trials and tribulations

With the homoallylic amines prepared, the key *N*-glycosylation reaction between the homoallylic amines and the disaccharide moiety to assemble OSW-1 mimetics could commence. Although the long-term goal is to replace the OSW-1 disaccharide carbohydrates with isosteric replacement units, the first OSW-1 mimetics will include the

OSW-1 disaccharide linked through the amine. Evaluating these new amine OSW-1 mimetics for biological activity and OSBP/ORP4 binding will be important validation for this overall approach to new OSW-1 analogs. The *O*-glycosylation in the synthesis of deuterated OSW-1 (**Section II.3.4**) had proven to be low-yielding and given a complicated reaction mixture. Different glycosylation methods were investigated and discussed below.

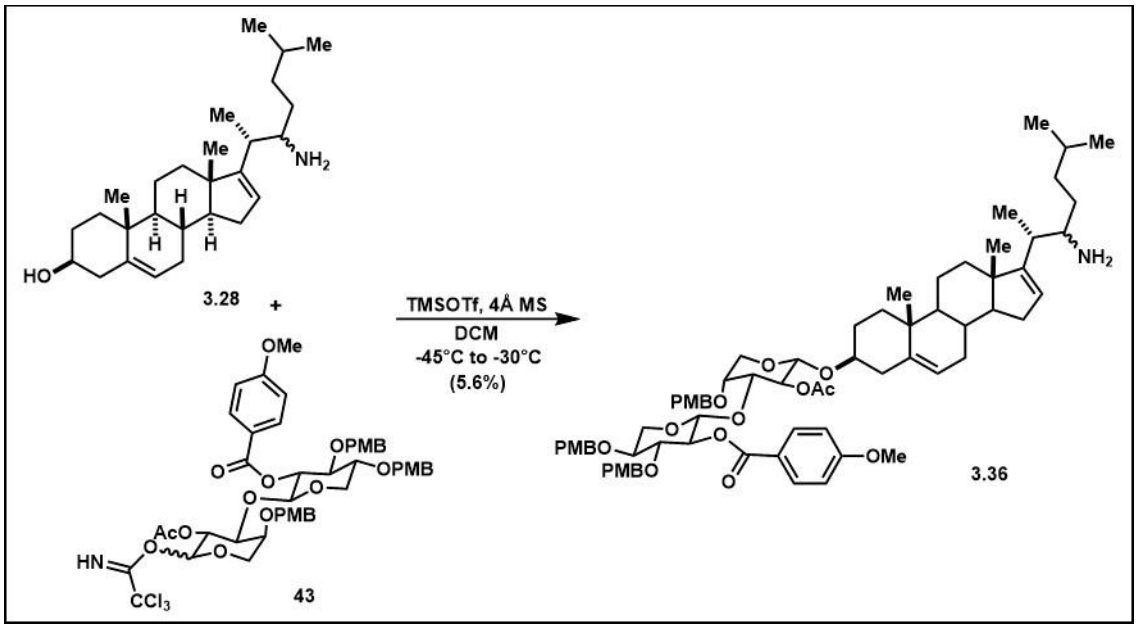

Scheme 28. Schmidt glycosylation of homoallylic amine **3.28** and disaccharide imidates **43** afforded *O*-glycosylated product

First, the Schmidt glycosylation condition that was used to assemble OSW-1 was applied for this N-glycosylation transformation. Steroidal acceptor **3.28** with free C-3 hydroxyl group and C-22-amine was reacted with disaccharide imidates **43** in the presence of TMSOTf promoter at low temperature (**Scheme 28**). This reaction gave a complex mixture of products. Purification through pTLC isolated one glycosylated product, along with products from disaccharide moiety decomposition. This coupled product, however, was characterized as the unwated *O*-glycosylated product **3.36** through 2D NMR analyses. This reaction outcome stressed the importance of a protecting group on the C-3 hydroxy to

eliminate the *O*-glycosylation possibility. Hence, a p-methoxybenzyl (PMB) protecting group was installed on C-3 hydroxyl (compound **3.35**, **Scheme 27**) before the LAH oxime reduction step.

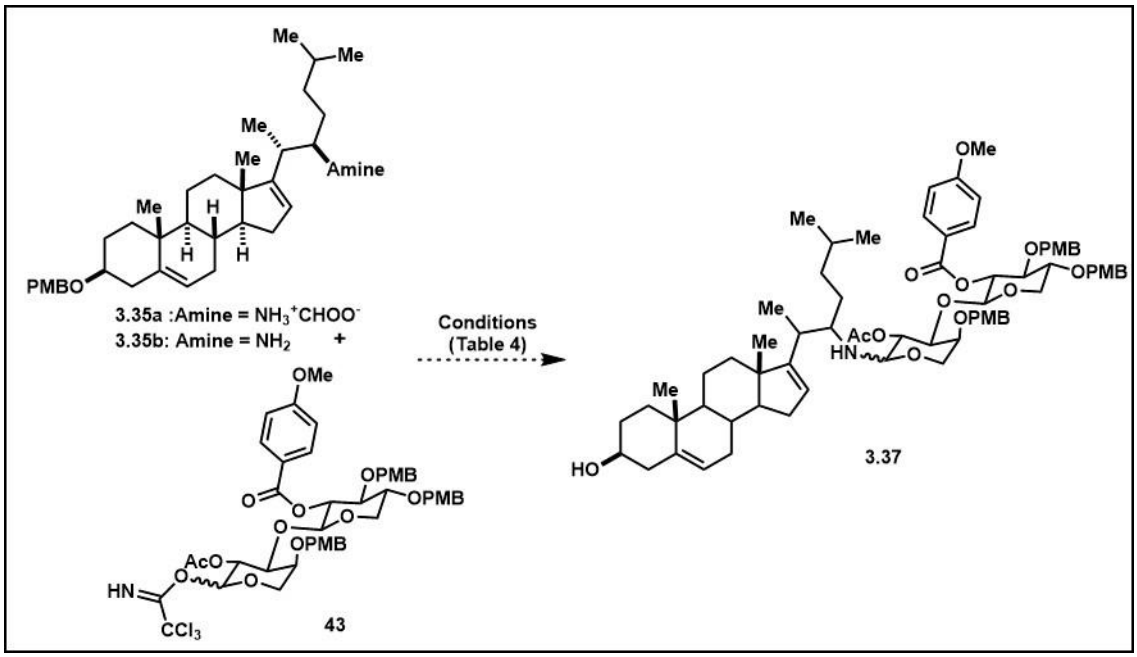

Scheme 29. N-glycosylation through Schmidt glycosylation method

Table 4. Condition screening of Schmidt glycosylation reaction

Entry	Glycosyl acceptor	Glycosyl donor	Reaction conditions	Results
1	**3.35a** (1 equiv)	**43** (1.2 equiv)	1) NEt_3 (0.4 equiv) 2) TMSOTf (1.2 equiv, added in portions), DCM -45°C to -30°C	No glycosylated product **3.37**; decomposition of donor **43**
2	**3.35a** (1 equiv)	**43** (1.2 equiv)	1) NEt_3 (1.5 equiv) 2) TMSOTf (1.4 equiv, added in portions), DCM -45°C to -30°C	No glycosylated product **3.37**; decomposition of donor **43**
3	**3.35a** (1 equiv)	**43** (1.2 equiv)	1) NaH (1.5 equiv) 2) TMSOTf (0.4 equiv, added in portions), DCM -45°C to -30°C	No glycosylated product **3.37**; decomposition of donor **43**
4	**3.35b** (1 equiv)	**43** (1.2 equiv)	TMSOTf (0.6 equiv, added in portions), DCM -45°C to -30°C	No glycosylated product **3.37**; decomposition of donor **43**

The PMB-protected homoallylic amines were purified through HPLC to afford pure isomers for the subsequent optimization of the Schmidt glycosylation reaction. The major isomer (the stereochemistry was later determined to be *R* through X-ray crystallography) was subjected to the Schmidt glycosylation reaction. Since the HPLC purification used a mild, acidic eluent (0.1% formic acid in water), the purified PMB-protected homoallylic amine was characterized as ammonium salt **3.35a** (**Scheme 29**). For the Schmidt glycosylation reactions, the neutralization of the this ammonium salt **3.35a** to reveal the free amine *in situ* was attempted with bases of different activity: 1) a mild non-nucleophilic base-triethyl amine (entry **1** and **2**, Error! Reference source not found.) or 2) a strong base-s odium hydride (entry **3**, Error! Reference source not found.). In all entries, the base was added to deprotonate the ammonium salt and form the free amine, before the disaccharide glycosyl donor **43** and TMSOTf promoter was added. TMSOTf was added in small increments (0.1 equiv) at low temperature and the progress of the reaction was monitored by TLC analysis. Addition of more TMSOTf (entry **2**, Error! Reference source not found.) i n order to accommodate for the presence of the base or advance a stalled reaction led to some decomposition of disaccharide donor **43** based on TLC, and NMR. No desired glycosylated product was observed for entries **1**-**3**, but the homoallylic amine **3.35b** was recovered as the free amine after acid-base work-up of the glycosylation reaction and silica gel column chromatography purification. It was possible that the base present in the glycosylation reaction mixture complexed with the Lewis acid TMSOTf to interfere with the formation of the desired glycosylated product.

Since the deprotonation of the ammonium salt *in situ* did not work as expected, the Schmidt glycosylation condition was attempted again with the purified homoallylic amine

3.35b (**Scheme 29**) recovered from entries **1-3** (entry **4**, Error! Reference source not f ound.). TLC profile of reaction progress was similar to that of entry **1-3**. Once the reaction seemed to halt based on TLC analysis, the reaction was stopped. Upon purification, no desired glycosylated product was observed, but the disaccharide moiety showed decomposition.

The Schmidt glycosylation method was unsuccessful at producing the desired N-linked glycosylated product, possibly due to the different reactivity of the free amine as the glycosyl acceptor. Amines are normally more Lewis basic than oxygen. In this case, the basic primary amine might have acted as a Lewis base rather than nucleophile. The Lewis basicity of amine interferes with the glycosylation reaction through amine interaction with the strong Lewis acid TMSOTf, which prevented the TMSOTf promoter from catalyzing the glycosylation reaction. Searching through literature, there were fewer reports showing the successful N-glycosylation through the Schmidt glycosylation method. Alternative glycosylation methods were then investigated.

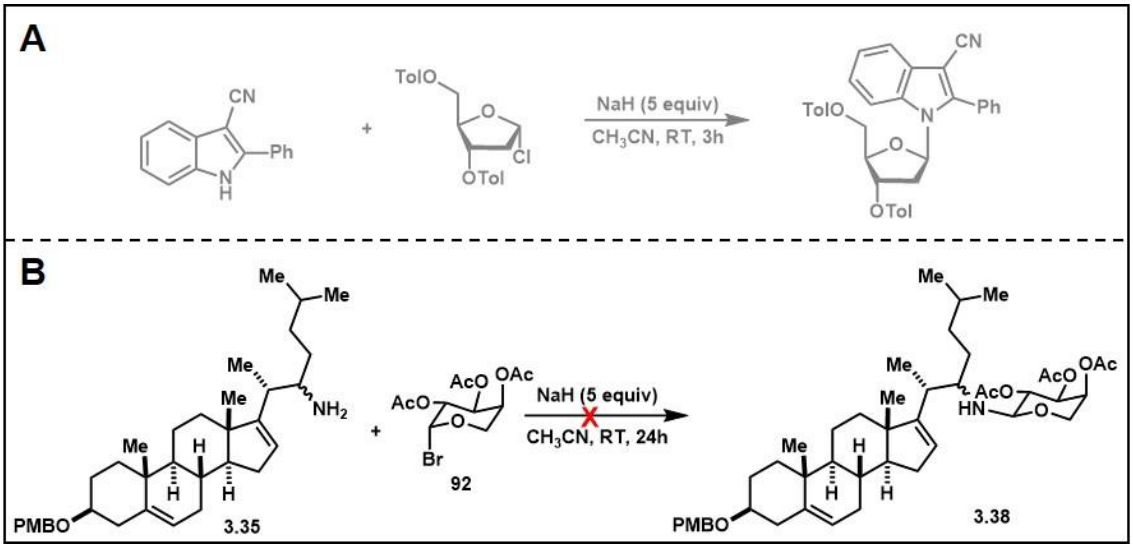

Scheme 30. A) Reported N-glycosylation of indole derivative and chloro sugar[80]**; B)** N-glycosylation of homoallylic amines and bromo-L-arabinopyranoside

A different and simpler glycosyl donor, bromo-L-arabinopyranoside **92**, was employed for the glycosylation condition with the homoallylic amine **3.35** in the presence of sodium hydride (**Scheme 30**). Bromo monosaccharide **92** was an intermediate in the synthesis of the L-arabinose moiety for the total synthesis of the OSW-1 compound (**Section II.3.1**). Li *et al*. demonstrated successful glycosylation reaction between indole, halo sugar in the presence of sodium hydride with high yield (**Scheme 30A**).[80] The reactivity between homoallylic amines **3.35** and indole differ in the elevated acidity of the indole compared to amine **3.35**. The glycosylation reaction produced only recovered starting materials.

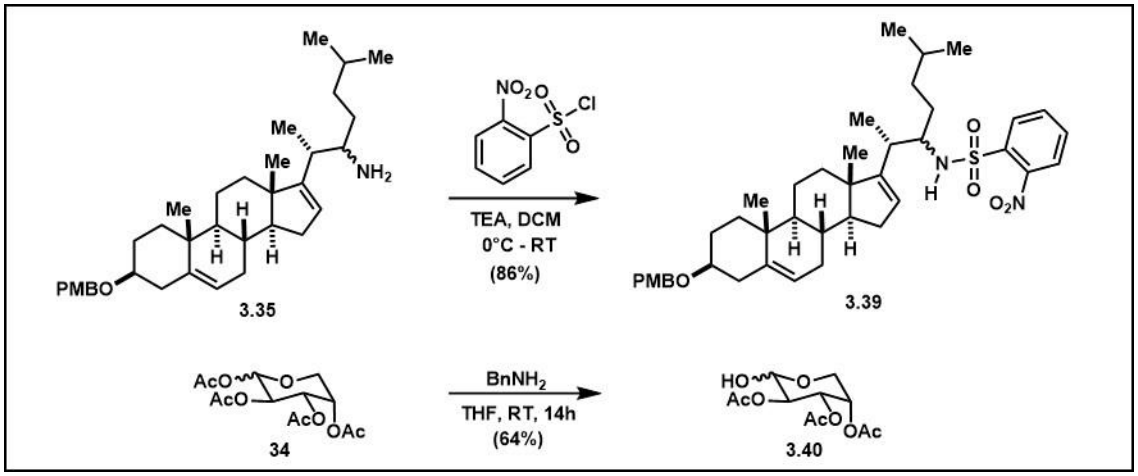

Scheme 31. Synthesis of *N*-2-nitrobenzenesulfonyl-protected amines and 2,3,4-triacetyl-α,β-L-arabinopyranose

A different method, the Fukuyama-Mitsunobu reaction has been shown to successfully form the *N*-glycosidic bond between *N*-2-nitrobenzenesulfonyl-protected amines (i.e. nosyl amines, Ns-amines) and glycosyl donors in their hemiacetal form under mild, near neutral reaction conditions with good yield.[81,82] The reaction was considered for this *N*-glycosylation transformation because of its mild conditions and the lack of a strong Lewis acid to potentially decompose the disaccharide glycosyl donor as occurred during

attempted Schmidt glycosylation. The mixture of homoallylic amines **3.35** were converted to mono-nosylate amines **3.39** smoothly with high yield (**Scheme 31**).[83] The *N*-2-nitrobenzenesulfonyl (nosyl or Ns)group acts as both a protecting and activating group[84]. The nosyl group increases the acidity of the nitrogen's proton which in turn facilitates the Mitsunobu reaction, since the pronucleophile should have pKa below 11 for a successful Mitsunobu reaction.[85] The nosyl group can later be removed easily with soft nucleophiles (such as thiols) in mild condition to give the corresponding secondary amines.[84] The saccharide moiety participates in the Fukuyama-Mitsunobu reaction in their hemiacetal form, which can be easily accessed from the syntheses of either monosaccharide (one step from intermediate **34**[86], **Scheme 7**, **Section II.3.1**) or disaccharide moieties of OSW-1 (compound **98**, **Scheme 9** in **Section II.3.2**).

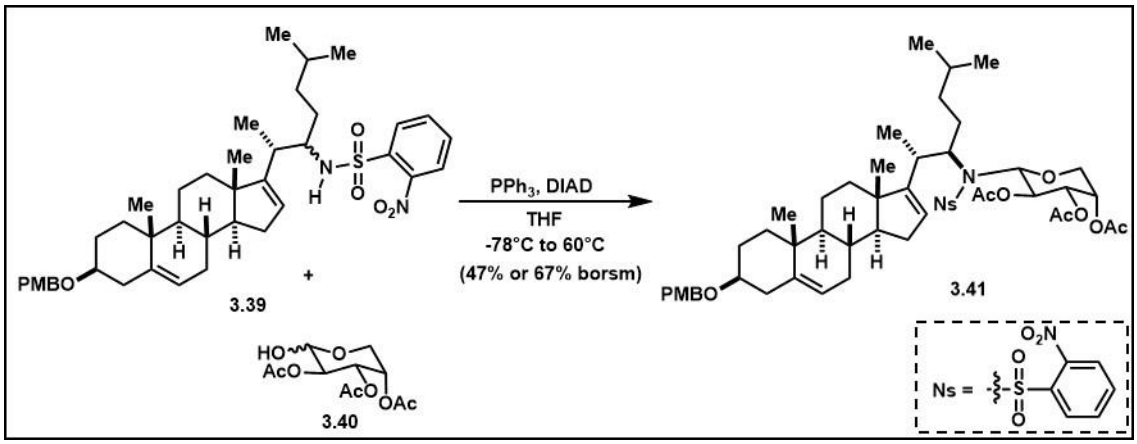

Scheme 32. Fukuyama-Mitsunobu reaction of Ns-amines and L-arabinosyl hemiacetal

Table 5. Optimization of Fukuyama-Mitsunobu glycosylation reaction with monosaccharide

Entry	Glycosyl acceptor	Glycosyl donor	Reaction conditions	Results
1	**3.39** (1 equiv)	**3.40** (2.5 equiv)	PPh_3 (2.5 equiv), DIAD (2.5 quiv), THF, -78°C to RT°C	**3.41** (trace)
2	**3.39** (1 equiv)	**3.40** (2.5 equiv)	PPh_3 (2.5 equiv), DIAD (2.5 quiv), THF, 0°C to RT°C	**3.41** (trace)
3	**3.39** (1 equiv)	**3.40** (5 equiv)	PPh_3 (10 equiv), DIAD (10 quiv), THF, 0°C to RT°C	**3.41** (26% or 45% borsm yield)
4	**3.39** (1 equiv)	**3.40** (3 equiv)	PPh_3 (2.5 equiv), DEAD (2.5 quiv), THF, 0°C to RT°C	**3.41** (trace)
5	**3.39** (1 equiv)	**3.40** (3 equiv)	PPh_3 (5 equiv), DIAD (5 quiv), THF, -78°C to 60°C	**3.41** (47% or 66% borsm yield)

Further optimizations with Ns-amines **3.39** and monosaccharide **3.40** were carried out. Increasing Mitsunobu reagents (triphenylphophine and DIAD) along with more equivalents of monosaccharide **3.40** improved the yield slightly (entry **3**, Error! Reference s ource not found.). When diethyl azodicarboxylate (DEAD) was used instead of DIAD, desired product was formed in trace amount (entry **4**, Error! Reference source not found.). F inally, when the reaction mixture was heated to 60°C for 24 hours after it had warmed up to ambient temperature from -78°C, the desired product was isolated in an acceptable yield (47%, entry **5**, Error! Reference source not found.). Glycosylated product **3.41** was c haracterized through X-ray crystallography to confirm the desired β-N-glycosidic linkage (See **Chapter appendix**). Along with the desired product, another coupled product was observed in trace amount. This side product could be the α-*N*-glycosidic linkage, or the orthoamide that could form when the Ns-amine trapped the reactive intermediate resulting

from the neighboring group participation of C-2 acetate and the anomeric carbon (similar to what was observed during the synthesis of compound *d*-OSW-1-**Section II.3.4**).

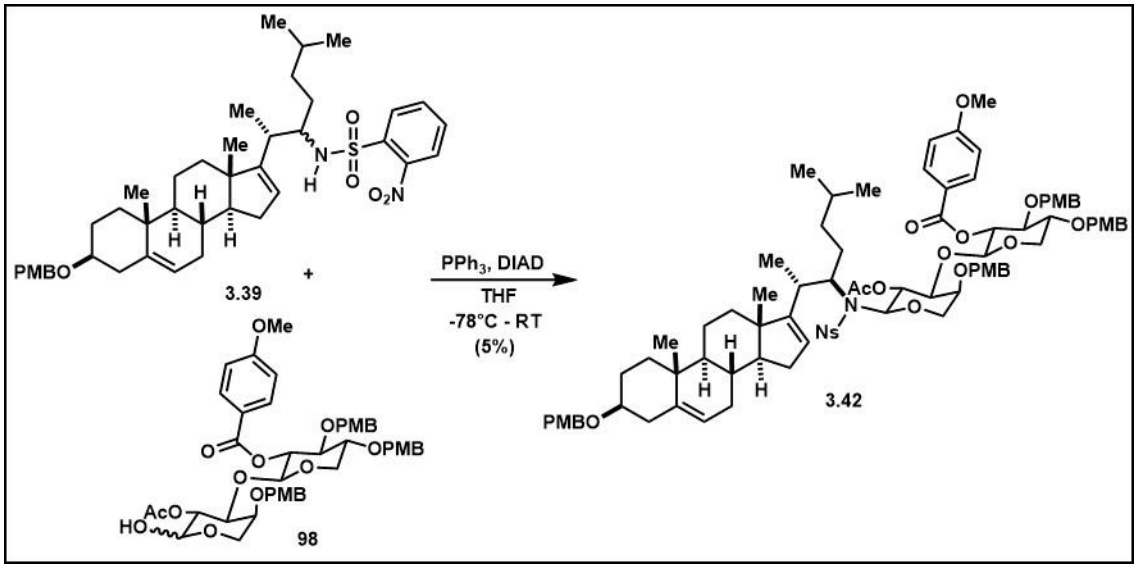

Scheme 33. Fukuyama-Mitsunobu reaction with OSW-1 disaccharide moiety

Table 6. Optimization of Fukuyama-Mitsunobu glycosylation reaction with OSW-1 disaccharide moiety

Entry	Glycosyl acceptor	Glycosyl donor	Reaction conditions	Results
1	**3.39** (1 equiv)	**98** (3 equiv)	PPh_3 (5 equiv), DIAD (5 quiv), THF, -78°C to RT°C	**3.42** (trace)
2	**3.39** (1 equiv)	**98** (3 equiv)	PPh_3 (4 equiv), DIAD (4 quiv), THF, -78°C to 60°C	**3.42** (trace)
3	**3.39** (1 equiv)	**98** (2.5 equiv)	PPh_3 (4 equiv), DIAD (4 quiv), THF, -78°C to 60°C	**3.42** (5% yield-HPLC purified)

Using the optimized Fukuyama-Mitsunobu condition from the reaction with the monosaccharide, the Mitsunobu reaction was attempted with the disaccharide hemiacetal **98** (**Scheme 33**). The desired N-glycosylated product **3.42** was observed, but only in trace amount. The equivalency of disaccharide hemiacetal was lowered slightly due to its

scarcity. When the reaction was carried out on larger scale (entry **1**, Error! Reference source n ot found.), the desired product was isolated in analytical purity through HPLC in low yield (5%). This allowed for the full characterization of **3.42** through 2D NMR spectroscopy (See Chapter III Appendix). The stereochemistry at the anomeric center was putatively assigned as β-linkage based on the similarity between the chemical shifts of anomeric proton and carbon between the glycosylated monosaccharide (compound **3.41**) and the glycosylated disaccharide (compound **3.42**). Attempts at growing crystals for X-ray crystallography analysis have not been successful.

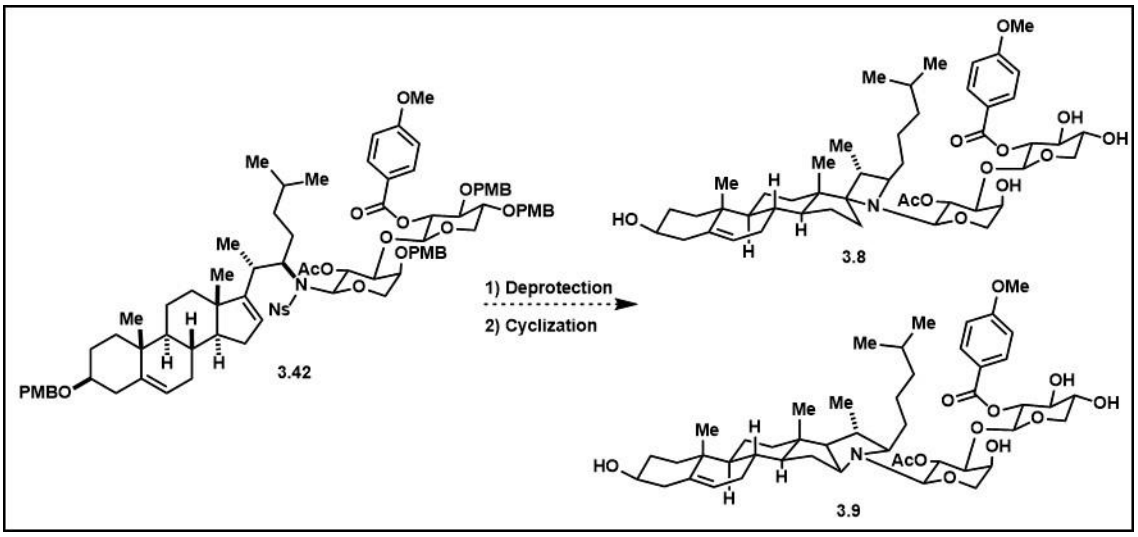

Scheme 34. Synthesis of OSW-1 mimetics

Further optimizations for the Fukuyama-Mitsunobu reaction with the disaccharide moiety will be carried out once more starting materials are available. The *N*-glycosylated product will need to go through two deprotection steps: 1) deprotection with 2,3-dichloro-5,6-dicyano-1,4-benzoquinone (DDQ) to remove PMB protecting groups on C-3 and disaccharide moiety; then 2) deprotection with phenylthiol to remove the nosyl protecting group on the C-22 nitrogen (**Scheme 34**). The fully-deprotected compounds can be

evaluated for its biological activity, or subjected to cyclization condition to produce the proposed E-ring for the validation of the two-component approach of OSW-1-related analogs.

III.4 Conclusion

OSW-1, a natural product with the cellular target of OSBP/ORP4, serves as a good starting point for the development of precision cancer therapeutic agent, since ORP4 protein has recently been validated as a precision cancer therapeutic target for leukemia and cervical cancer.[34,59] Based on the structure of OSW-1, a concise and convergent two-component approach to assemble OSW-1-related scaffolds with the E-ring bridge was developed. The approach was demonstrated through the formation of the E-ring bridge via a tandem carbonyl ene-cyclization reaction of the steroidal core and side chain aldehyde. Along the way, an interesting transformation was observed during the carbonyl-ene reaction to form an unexpected spiro-oxetane product. Lastly, to examine the effects of the new modification on the biological activity of OSW-1, a set of OSW-1-related analogs with E-ring are being assembled through an atypical glycosylation methodology- a Fukuyama Mitsunobu reaction. The biological evaluations of these analogs will provide information to shape the development of future OSW-1 analogs as lead compounds for precision cancer therapeutic agents.

III.5 Experimental section

III.5.1 General methods

All reactions were performed in oven-dried glassware under a positive pressure of nitrogen unless noted otherwise. Flash column chromatography was performed as described by Still *et al.*[55] employing E. Merck silica gel 60 (230-400 mesh ASTM). TLC

analyses and preparative TLC (pTLC) purification was performed on 250µm Silica Gel 60 F254 plates purchased from EM Science and Fluka Analytical. All solvents and chemicals were used as purchased without further purification. Solvents used in the reactions were collected under nitrogen from a Pure Solv 400-5-MD Solvent Purification System (Innovative Technology). Infrared spectra were recorded on a Shimadzu IRAffinity-1 instrument, or Bruker Tensor 27 spectrometer, and IR spectra peaks are reported in terms of frequency of absorption (cm^{-1}). ^{1}H and ^{13}CNMR spectra were recorded on VNMRS 300, VNMRS 400, VNMRS 500 or VNMRS 600 MHz-NMR Spectrometer. Chemical shifts for proton and carbon resonances are reported in ppm (δ) relative to the residual proton or the specified carbon in chloroform (δ 7.26, proton; 77.16, carbon). High-resolution mass spectrometry (HRMS) analysis was performed using Agilent 6538 high-mass-resolution QTOF mass spectrometer. HPLC purification was performed on Shimadzu LCMS 2020 system [LC-20AP (pump), SPD-M20A (diode array detector), LCMS-2020 (mass spectrometer)]. Semi-preparative HPLC purification was performed using Phenomenex Luna C-18(2) column, 5µm particle size (250 mm x 4.6 mm), supported by Phenomenex Security Guard cartridge kit C18 (4.0 mm x 3.0 mm); Phenomenex Luna C-8(2) column, 5µm particle size (250 mm x 4.6 mm), supported by Phenomenex Security Guard cartridge kit C8 (4.0 mm x 3.0 mm) and HPLC-grade solvents.

III.5.2 Compound data

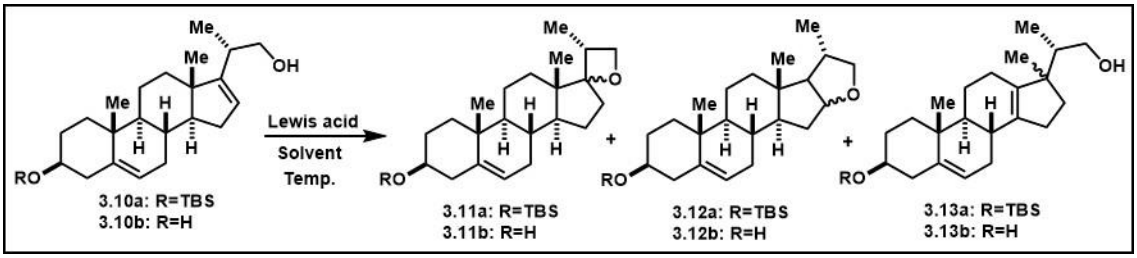

Entry 1,Error! Reference source not found.: representative experimental details. Other e ntries were performed in a similar fashion

To a 5mL pear-shaped flask was added **3.10a** (17mg, 0.0382mmol) and $Sc(OTf)_3$ (1mg, 0.0020mmol). The flask was sealed, purged with N_2, and charged with dry 1,2-dichloroethane (250µL). The reaction mixture was stirred at RT and the progress was monitored by TLC (10% EtOAc/hex). The cloudy, colorless mixture turned to clear, light purple after 15 minutes, and to clear, light orange later. After 42h, the reaction mixture was filtered through a short pipet silica gel column, packed with DCM. The mixture was then diluted in DCM and passed through a short silica pipet column, eluted with DCM (10mL) and EtOAc (10mL) which were collected as two separate fractions. Each fraction (DCM and EtOAc) was separated further through flash chromatography (EtOAc/hexanes gradients) to afford the reported products.

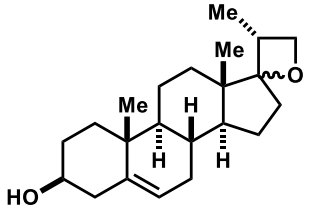

3.11b

3.11b: ^{1}H NMR (400 MHz, Chloroform-d) δ 5.38 – 5.32 (m, 1H), 3.87 (dd, J = 8.5, 6.4 Hz, 1H), 3.53 (ddd, J = 15.8, 10.9, 4.6 Hz, 1H), 3.30 (dd, J = 8.5, 7.2 Hz, 1H), 2.35 – 2.27 (m, 1H), 2.25 – 2.12 (m, 2H), 2.10 – 1.99 (m, 1H), 1.96 – 1.80 (m, 3H), 1.77 – 1.66 (m, 1H), 1.65 – 1.48 (m, 6H), 1.47 – 1.36 (m, 2H), 1.35 – 1.23 (m, 2H), 1.20 – 1.02 (m, 3H), 0.98 (s, 3H), 0.96 (s, 3H), 0.91 (d, J = 7.1 Hz, 3H), 0.89 – 0.79 (m, 1H). ^{13}C NMR (101 MHz, Chloroform-d) δ 140.89, 121.62, 94.16, 72.09, 71.88, 54.48, 52.32, 45.97, 45.40, 42.15, 40.54, 37.68, 37.00, 33.15, 32.93, 31.57, 29.92, 27.09, 20.62, 18.93, 18.48, 13.64. The

structure of **3.11b** was confirmed through 2D NMR analysis. See **Chapter appendix** for ^{1}H and ^{13}C NMR spectra, **Appendix** for 2D NMR spectra.

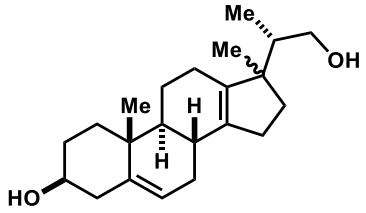

3.13b

3.13b: ^{1}H NMR (600 MHz, Chloroform-d) δ 5.44 – 5.40 (m, 1H), 3.80 (dd, J = 10.6, 3.9 Hz, 1H), 3.57 – 3.51 (m, 1H), 3.40 (dd, J = 10.6, 8.4 Hz, 1H), 2.32 (ddd, J = 12.6, 4.9, 2.3 Hz, 1H), 2.26 – 2.15 (m, 3H), 2.14 – 2.05 (m, 2H), 2.04 – 1.98 (m, 1H), 1.94 (dt, J = 13.3, 3.5 Hz, 1H), 1.89 – 1.74 (m, 4H), 1.67 – 1.48 (m, 4H), 1.41 (ddd, J = 13.1, 9.5, 5.4 Hz, 1H), 1.28 – 1.18 (m, 1H), 1.16 – 1.08 (m, 2H), 1.05 (s, 3H), 0.98 (s, 3H), 0.86 (d, J = 6.8 Hz, 3H). ^{13}C NMR (151 MHz, Chloroform-d) δ 141.54, 140.05, 137.29, 121.99, 72.16, 65.76, 51.44, 49.34, 42.58, 42.31, 37.20, 37.08, 33.28, 32.62, 31.72, 31.65, 31.32, 25.20, 23.38, 23.20, 18.87, 13.05. The structure of **3.13b** was confirmed through 2D NMR analysis. See **Chapter appendix** for ^{1}H and ^{13}C NMR spectra, **Appendix** for 2D NMR spectra.

Entry **1**, Error! Reference source not found.

To a mixture of 4Å MS powder (10mg) in anhydrous DCM (100 µL) was added $BF_3{\cdot}Et_2O$ (7.4 µL, 0.06mmol). The cloudy mixture was stirred at R.T. for an hour. Then, to this mixture was added (*Z*)-3β-hydroxy-5,17(20)-pregnadiene **3.4** (15mg, 0.050 mmol, dissolved in 200 µL anhydrous DCM), and paraformaldehyde (1.5mg, 0.05mmol) respectively. The mixture was then cooled to -10°C (mixture of acetone and dry ice). The reaction progress was monitored by TLC (30%EtOAc/hexanes, CAM stain). There was a new spot with Rf=0.2, consistent with homoallylic alcohol product formed on the TLC

plate. After 1 hour, the reaction seemed to halt. To the mixture was added more paraformaldehyde (1.5mg, 0.05mmol). After 2 hours, to the reaction mixture was added more 4Å MS powder (10mg) and $BF_3{\cdot}Et_2O$ (6.2 µL, 0.05mmol) at -10°C. After 3 hours, to the reaction mixture at -10°C was added $BF_3{\cdot}Et_2O$ (6.2 µL, 0.05mmol). After 3h40m, the mixture had purple residue on the side of the flask. TLC analysis showed another new spot with Rf=0.4. The reaction mixture was stirred at -10°C for another hours, before being quenched by addition of saturated $NaHCO_3$ solution. The mixture was filtered through a pad of celite and rinsed with DCM (5mL). The purple residue disappeared after filtration. The organic layer was washed with saturated $NaHCO_3$ solution (5mL), and DI water (5mL x 2). The combined aqueous layer was back extracted with DCM (5mL). The combined organic layer was washed with brine, dried over Na_2SO_4, and filtered. The solvent was removed to afford the crude mixture was a white foamy solid (13.8mg). The crude mixture was separated by silica gel column chromatography (pipet column, EtOAc/hexanes gradient from 10% to 40%) to afford a rearranged pregnadiene **3.14** (1.7mg, 11% yield), a mixture of products including spiro-oxatane **3.6** (3.7mg, ~22% yield), and desired homoallylic alcohol **3.5** (~2.7mg, 16% yield).

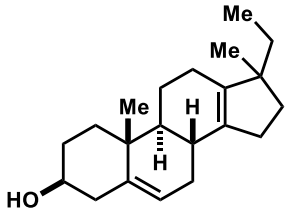

3.14

3.14: ^{1}H NMR (400 MHz, Chloroform-d) δ 5.42 (d, J = 4.9 Hz, 1H), 3.54 (tt, J = 10.8, 4.8 Hz, 1H), 2.38 – 2.28 (m, 1H), 2.27 – 2.01 (m, 4H), 2.02 – 1.90 (m, 2H), 1.90 – 1.69 (m, 4H), 1.66 – 1.46 (m, 7H), 1.35 – 1.19 (m, 4H), 1.17 – 1.00 (m, 3H), 0.99 (s, 3H), 0.97 –

0.95 (m, 3H), 0.75 (t, J = 7.4 Hz, 3H). ^{13}C NMR (101 MHz, cdcl3) δ 141.47, 140.08, 136.64, 122.13, 72.20, 49.39, 49.33, 42.31, 37.18, 37.09, 35.58, 33.12, 32.31, 31.76, 31.64, 30.73, 25.62, 23.20, 22.54, 18.89, 9.20. See **Chapter appendix** for ^{1}H and ^{13}C NMR spectra.

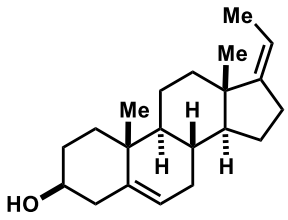

(*Z*)-5,17(20)-pregnadiene

(*Z*)-5,17(20)-pregnadiene was synthesized as describe previously.[70] A bright, orange suspension of PPh_3EtBr (2.57 g, 6.93 mmol) and *t*-BuOK (0.778 g, 6.93 mmol) in anhydrous THF (10 mL) was stirred at RT under N_2 in a 2-neck RBF (fitted with a reflux condenser) for 40 minutes. To the mixture was then added *trans*-dehydroandrosterone **3.29** solution (500.0 mg, 1.73 mmol, dissolved in 6.0 mL of anhydrous THF). The reaction mixture was heated under reflux. The reaction progress was monitored by TLC (30% EtOAc/hexanes, UV, CAM stain). After 2.5 hours, the reaction was completed based on TLC. The reaction mixture was cooled to RT, quenched with sat'd NH_4Cl solution (10 mL). The reaction mixture was diluted with EtOAc (30 mL). The organic phase was washed with sat'd NH_4Cl solution (30 mL), DI H_2O (30 mL x 2). The combined aqueous phase was back extracted with EtOAc (10 mL). The combined organic phase was washed with brine, dried over Na_2SO_4, and filtered. The solvent was removed *in vacuo* to afford crude mixture as a white solid. The crude mixture was purified through flash chromatography (EtOAc/hexanes gradient) to afford desired (*Z*)-5,17(20)-pregnadiene (430.8 mg, 82% yield). ^{1}H NMR (400 MHz, Chloroform-d) δ 5.36 (d, J = 5.0 Hz, 1H), 5.19

– 5.09 (m, 1H), 3.58 – 3.48 (m, 1H), 2.43 – 2.13 (m, 5H), 2.09 – 1.98 (m, 1H), 1.90 – 1.81 (m, 3H), 1.66 (dt, J = 7.1, 2.0 Hz, 3H), 1.64 – 1.57 (m, 2H), 1.57 – 1.45 (m, 6H), 1.30 – 1.04 (m, 3H), 1.02 (s, 3H), 1.01 – 0.93 (m, 1H), 0.90 (s, 3H). See **Chapter appendix** for ^{1}H and ^{13}C NMR spectra.

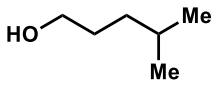

4-methylpentanol

4-methylpentanol was synthesized with an adapted procedure.[71] To a suspension of LiAlH4 (980.2 mg, 25.8 mmol) in anhydrous THF (24 mL) at 0°C was added 4-methylpentanoic acid solution (2.2 mL dissolved in 10 mL THF) slow dropwise. The reaction mixture was stirred at RT for 2 hours, then cooled to 0°C and quenched by addition of EtOAc(10 mL). To the reaction mixture was added a saturated solution of sodium potassium tartrate (200 mL) and Et_2O (100 mL). The mixture was stirred vigorously at RT for 30 minutes. The two phases were then separated. The aqueous phase was extracted with Et_2O (50 mL x 2). The combined organic phase was washed with brine, dried over Na_2SO_4. The solve was removed to afford crude product as a yellow liquid, which was purified through vacuum distillation (T ~ 95°C under house vacuum) to afford desired 4-methylpentanol. The NMR data agreed with the published reference. ^{1}H NMR (400 MHz, DMSO-d6) δ 4.33 (t, J = 5.2 Hz, 1H), 3.36 (td, J = 6.7, 5.2 Hz, 2H), 1.50 (dp, J = 13.3, 6.7 Hz, 1H), 1.44 – 1.36 (m, 2H), 1.19 – 1.11 (m, 2H), 0.85 (d, J = 6.6 Hz, 6H). ^{13}C NMR (101 MHz, DMSO-d6) δ 61.06, 34.83, 30.43, 27.38, 22.52. See **Appendix** for NMR spectra.

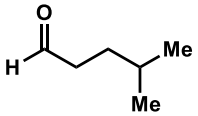

4-methylpentanal

4-methylpentanal was synthesized with an adapted procedure.[72] To a suspension of PCC (2.95 g, 13.7 mmol), anhydrous NaOAc (94.7 mg, 1.37 mmol) and neutral alumina (6.2 g, to aid with work up) in anhydrous DCM (27.4 mL, 0.25M) at 0°C under N_2 atmosphere was added 4-methyl-1-pentanol fast dropwise. The reaction mixture's color changed from light yellow to dark brown within 5 minutes. The reaction mixture was then stirred at RT, and reaction progress was monitored by TLC (5%MeOH/DCM, $KMnO_4$ stain). The reaction was completed after 1.5h. The brown solid was removed by filtration through a short silica gel column, rinsed with DCM (100 mL). The filtrate was then condensed *in vacuo* (water bath temperature around 15°C) to the final volume of 5 mL, light yellow solution. The crude product was used in the subsequent reaction without further purification. ^{1}H NMR (500 MHz, Chloroform-d) δ 9.76 (t, J = 1.9 Hz, 1H), 2.44 – 2.39 (m, 2H), 1.58 (ddt, J = 12.8, 7.6, 6.4 Hz, 1H), 1.54 – 1.49 (m, 2H), 0.90 (d, J = 6.5 Hz, 6H).^{13}C NMR (126 MHz, cdcl3) δ 203.08, 53.57, 42.11, 30.90, 27.79, 22.37. See **Chapter appendix** for NMR spectra.

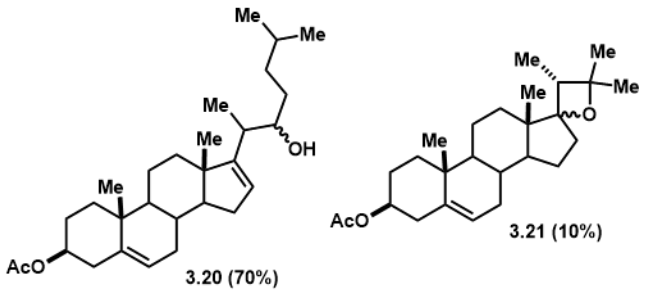

Compound **3.20** was synthesized with an adapted procedure. [70] A solution of anhydrous DCM (10 mL) and 4-methylpentanal (~438 mg, 4.38 mmol, dissolved in 5mL DCM) was stirred under N_2 atmosphere at -78°C for 10 minutes. The mixture was then observed to be cloudy, which might indicate presence of water, so 4ÅMS powder (~200mg) was added. After 10 minutes stirring at -78°C, Me_2AlCl solution (1M solution, 8.8 mL, 8.8 mmol) was

added dropwise over 5 minutes. The mixture was stirred at -78°C for another 10 minutes before acetate-protected pregnadiene **3.19** (511.3 mg, 1.49 mmol, dissolved in 10 mL anhydrous DCM) was added fast dropwise. The reaction mixture was stirred in the cold bath, without additional dry ice added to allow slow warm-up. The reaction progress was monitored by TLC (10% EtOAc/hexanes, UV, CAM stain). After 2.5h, the reaction was warmed up to RT. The reaction was mostly completed based on TLC after 3.5h. The reaction was then quenched by mixture of MeOH: DI H_2O (1:1, 10 mL) at -78°C. The reaction mixture was diluted with DI H_2O (30 mL), extracted with DCM (40 mL x3). The combined organic phase was washed with 1N HCl (50 mL), saturated solution of $NaHCO_3$ (50 mL), DI H_2O (50 mL x2). The combined aqueous phase was back extracted with DCM (15 mL). The combined organic phase was washed with brine, dried over Na_2SO_4. The solvent was removed to afford crude mixture was a yellow gel (720 mg). The crude mixture was then separated through silica gel column (60g Si-gel, 5% acetone/hex (400 mL); 10% acetone/hex (400 mL); 9mL fractions). Some acetate-pregnadiene **3.19** (48.3 mg, 9.4%) was recovered. A mixture of homoallylic alcohols **3.20** was obtained (F31-52, 445.8 mg, 67%, 75% borsm yield). A side product was isolated and identified as spiro-oxetane **3.21** (F22-27, 52.7 mg, 9.7% borsm yield). The NMR data of **3.20** agreed with published reference.[70]

3.20: ^{1}H NMR (500 MHz, Chloroform-d) δ 5.51 – 5.48 (m, 1H), 5.41 – 5.37 (m, 1H), 4.61 (tdd, J = 10.4, 6.2, 4.3 Hz, 1H), 3.63 (dtd, J = 8.0, 4.7, 3.3 Hz, 1H, H-22 of major isomer), 3.57 (tt, J = 8.7, 2.1 Hz, 1H, H-22 of minor isomer), 2.39 – 2.25 (m, 4H), 2.19 – 2.06 (m, 2H), 2.06 – 1.96 (m, 5H), 1.95 – 1.83 (m, 4H), 1.82 – 1.74 (m, 1H), 1.75 – 1.59 (m, 3H), 1.59 – 1.48 (m, 4H), 1.49 – 1.41 (m, 2H), 1.41 – 1.31 (m, 3H), 1.31 – 1.24 (m, 1H), 1.23 –

1.16 (m, 1H), 1.15 – 1.10 (m, 1H), 1.08 – 1.05 (m, 4H), 1.02 (dd, J = 7.0, 1.7 Hz, 3H), 1.01 – 0.98 (m, 1H), 0.92 – 0.87 (m, 13H). See **Chapter appendix** for NMR spectra.

Characterization of spiro-oxetane 3.21

F22-27 that contained **3.21** was purified by HPLC before characterization was carried out. At the beginning, the ^{1}H and ^{13}C NMR of **3.21** were puzzling. According to the ^{1}H NMR, there were only one alkene-proton, and there were no doublets that correspond to the iso-moiety at the end of the side chain. ^{13}C NMR only showed 23 carbons, instead of the expected 26 carbons. The NMR was analyzed in both $CDCl_3$ and benzene-D_6 to eliminate the possibility of signals hidden under the solvent peaks. In the ^{13}C NMR spectrum, two alkene carbons that corresponded to one double bond eliminated the hypothesis of rearrangement of pregnadiene. There was a ^{13}C signal at 93 ppm, which suggested a quaternary C-O that could either be an anomeric carbon, or strained carbon scaffold. Full 2D NMR spectra (COSY, HSQC, HMBC) of **3.21** suggested the structure of spiro-oxetane. With C17 being the carbon at the spiro center, it agreed with the chemical shift of 93 ppm. The stereochemistry of the spiro-oxetane moiety has not been assigned. Attempts at growing crystals for X-ray crystallography did not yield crystals with good quality. HRMS did not resulted in the expected molecular weight, which could be low ionization of the molecule. See **Appendix** for 2D NMR spectra.

Table 7. 2D NMR assignment of spiro-oxetane **3.21**

Atom	Chemical Shift	COSY	HSQC	HMBC
1 C	36.80		1', 1''	18, 9
H'	1.58		1	3, 10
H''	0.89		1	
2 C	28.08		2', 2''	4'
H'	1.84	4', 3	2	
H''	1.55	3	2	3
3 C	73.96		3	1', 2'', 4'
H	4.82	2', 2'', 4', 4''	3	25
4 C	38.49		4', 4''	6
H'	2.48	2', 3	4	3, 2, 5, 6, 10
H''	2.32	3, 6	4	5
5 C	139.58			4'', 4', 7', 7'', 18
6 C	122.91		6	4', 7''
H	5.27	4'', 7', 7''	6	4, 7, 8, 10
7 C	33.82		7', 7''	6
H'	2.05	6, 8	7	5
H''	1.49	6, 8	7	5, 6
8 C	32.62		8	6, 15', 15'', 9
H	1.19	7', 7''	8	
9 C	46.81		9	18, 11', 11''
H	1.06		9	1, 8, 11, 12, 10
10 C	37.74			1', 4', 6, 9, 18
11 C	33.28		11', 11''	9
H'	1.84		11	9, 12
H''	1.65		11	9, 12
12 C	21.82		12', 12''	9, 11', 11''
H'	1.71		12	
H''	1.19		12	
13 C	53.61			15'', 19, 20
14 C	55.34		14	15', 15''
H	1.78		14	17
15 C	25.59		15', 15''	
H'	1.90		15	8, 14
H''	1.32		15	8, 13, 14
16 C	41.95		16', 16''	19, 20
H'	1.38		16	17
H''	1.26		16	19, 17
17 C	93.00			19, 16', 16'', 14
18 C	18.41		18	
H3	0.82		18	1, 5, 9, 10
19 C	20.06		19	16'', 20
H3	0.96		19	13, 20, 16, 17
20 C	54.22		20	19, 23, 24
H	1.69		20	22, 21, 16, 19, 23, 24, 13
21 C	10.93		21	20
H3	0.67		21	22
22 C	81.31			21, 23, 24, 20
23 C	24.85		23	24, 20
H3	1.04		23	22, 20, 24
24 C	29.89		24	23, 20
H3	1.23		24	22, 20, 23
25 C	169.57			3, 26
26 C	21.11		26	
H3	1.75		26	25

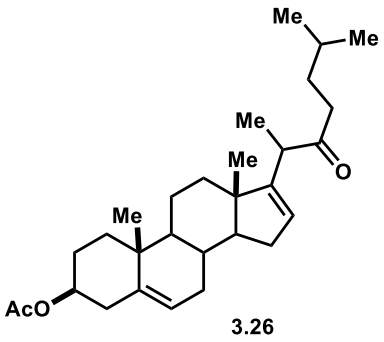

3.26

Compound **3.26** was synthesized with procedure adapted from Deng *et al*.[35] To a solution of homoallylic alcohols **3.20** (333.0 mg, 0.777 mmol) in anhydrous DCM (3.9 mL) and DMF (0.9 mL) at RT under N_2 was added 4Å MS powder (700 mg), PDC (584.5 mg, 1.55 mmol). The brown suspension was stirred at RT, and the reaction progress was monitored by TLC (10% EtOAc/hexanes, UV, CAM stain). After 17h, TLC still showed presence of **3.20**. To the reaction mixture was added more PDC (292.0 mg, 0.77 mmol) and neutral alumna (500 mg). The reaction mixture was stirred at RT for another 24h, when TLC showed the reaction almost completed (~80% conversion). The reaction mixture was filtered through a silica plug, washed with DCM (15 mL). The solvent was removed *in vacuo*. The resulting residue was resuspended in Et_2O (15 mL), washed with DI H_2O (10 mL x 3), brine, dried over Na_2SO_4, and filtered. The solvent was removed *in vacuo* to afford crude mixture, which was purified by flash chromatography (EtOAc/hexanes gradient from 5% to 15%) to afford desired C-22 ketone **3.26** (188.8 mg, 56% yield). The diagnostic NMR data agreed with published reference[35]. ^{1}H NMR (400 MHz, Chloroform-d) δ 5.42 – 5.32 (m, 2H), 4.59 (tdd, J = 10.6, 6.3, 4.2 Hz, 1H), 3.18 (q, J = 6.8 Hz, 1H), 2.47 (dt, J = 15.8, 7.8 Hz, 1H), 2.41 – 2.25 (m, 3H), 2.08 (ddd, J = 15.1, 6.6, 3.2 Hz, 1H), 2.05 – 1.95 (m, 4H), 1.92 – 1.75 (m, 3H), 1.69 – 1.46 (m, 4H), 1.45 – 1.29 (m, 4H), 1.29 – 1.18 (m, 1H), 1.14 (d, J = 7.0 Hz, 3H), 1.09 – 0.97 (m, 4H), 0.91 – 0.81 (m, 9H). ^{13}C NMR (101

MHz, Chloroform-d) δ 211.73, 170.63, 154.37, 140.03, 125.28, 122.48, 73.95, 57.12, 50.59, 47.41, 45.81, 38.35, 38.22, 37.02, 36.91, 34.68, 33.15, 31.60, 31.33, 30.64, 27.84, 27.71, 22.62, 22.36, 21.55, 20.78, 19.34, 16.95, 16.38. See **Chapter appendix** for NMR spectra.

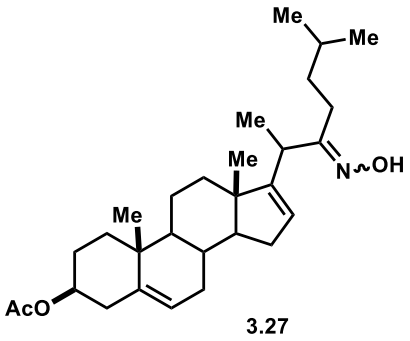

3.27

To a mixture of C-22 ketone **3.26** (56.2 mg, 0.127 mmol) in 200-proof EtOH (1.28 mL) was added hydroxyl amine hydrochloride $NH_2OH{\cdot}HCl$ (35.5 mg, 0.51 mmol) and sodium acetate trihydrates $NaOAc{\cdot}3H_2O$ (104.1 mg, 0.76 mmol). The resulting slurry was heated under reflux. The reaction progress was monitored by TLC (20% EtOAc/hexanes, UV, CAM stain). After 18 hours, the reaction was completed based on TLC. The reaction mixture was diluted with DI H_2O (5 mL). The aqueous phase was extracted with DCM (5 mL x 4). The combined organic phase was washed with brine, dried over Na_2SO_4, and filtered. The solvent was removed *in vacuo* to afford crude mixture as a white solid (58.2 mg). The crude mixture was purified by flash chromatography (EtOAc/hexanes gradient from 5% to 30%) to afford the desired mixture of oxime isomers **3.27** as a white solid (40.0 mg, 70%). Oximes **3.27** were characterized by 2D NMR and HRMS. ^{1}H NMR (500 MHz, Chloroform-d) δ 5.46 (dt, J = 2.9, 1.4 Hz, 1H), 5.42 – 5.37 (m, 1H), 4.65 – 4.55 (m, 1H), 3.12 – 3.07 (m, 1H), 2.37 – 2.29 (m, 2H), 2.29 – 2.23 (m, 1H), 2.17 – 2.05 (m, 2H), 2.03 (s, 3H), 2.00 – 1.96 (m, 1H), 1.91 – 1.82 (m, 4H), 1.72 – 1.44 (m, 7H), 1.42 – 1.23 (m, 3H),

1.20 (d, J = 7.1 Hz, 3H), 1.18 – 1.09 (m, 1H), 1.07 – 0.99 (m, 4H), 0.90 (dd, J = 6.5, 1.8 Hz, 6H), 0.78 (s, 3H). ^{13}C NMR (126 MHz, Chloroform-d) δ 170.68, 164.06, 156.16, 140.11, 125.02, 122.59, 74.07, 57.60, 50.68, 47.02, 38.31, 37.08, 36.97, 35.39, 34.70, 31.70, 31.25, 30.60, 28.90, 27.92, 25.21, 22.55, 22.45, 21.59, 20.83, 19.38, 17.79, 16.27. HRMS: calculated for $C_{29}H_{45}NO_3$ + H^+ -$[M+H]^+$: 456.3478, measured: 456.3469. See **Chapter appendix** for ^{1}H and ^{13}C NMR spectra, **Appendix** for 2D NMR spectra.

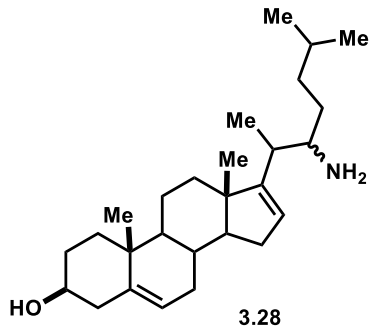

3.28

To a solution of oximes **3.27** (125.0 mg, 0.274 mmol) in anhydrous THF (2.0 mL) at 0°C under N_2 was added a suspension of $LiAlH_4$ (104.1 mg, 2.74 mmol, in 2.7 mL THF) dropwise. The gray suspension was then heated under reflux. The reaction progress was monitored by TLC (5% MeOH/DCM, UV, CAM stain). After 48 hours, TLC showed absence of oximes **3.27**. The reaction was quenched with DI H_2O at 0°C. The reaction mixture was transferred to an Erlenmeyer flask. To it was added 15% NaOH solution (20 mL) and EtOAc (10 mL). The mixture was stirred at RT for 10 minutes. The aqueous phase was extracted with EtOAc (10 mL x 3). The combined organic phase was washed with brine, dried over Na_2SO_4, and filtered. The solvent was removed *in vacuo* to afford crude mixture as a white foamy solid (118.0 mg). The crude mixture was purified by flash chromatography (MeOH/DCM gradient from 0% to 15%) to afford the mixture of

homoallylic amine isomers **3.28** (32.5 mg, 30%). ^{1}H NMR (500 MHz, Chloroform-d) δ 5.40 (dd, J = 3.0, 1.4 Hz, 1H), 5.36 (dt, J = 5.2, 2.0 Hz, 1H), 3.57 – 3.48 (m, 1H), 2.80 (ddt, J = 11.5, 8.9, 5.0 Hz, 1H, H-22 of major isomer), 2.67 – 2.58 (m, 1H, H-22 of minor isomer), 2.30 (ddd, J = 13.1, 5.1, 2.0 Hz, 1H), 2.24 (ddq, J = 15.7, 11.1, 2.6 Hz, 1H), 2.13 – 2.05 (m, 1H), 2.06 – 1.98 (m, 1H), 1.95 – 1.76 (m, 3H), 1.72 – 1.58 (m, 4H), 1.58 – 1.47 (m, 2H), 1.48 – 1.38 (m, 1H), 1.38 – 1.27 (m, 2H), 1.24 – 1.13 (m, 1H), 1.13 – 1.06 (m, 1H), 1.04 (s, 3H), 0.98 (d, J = 6.9 Hz, 3H), 0.93 – 0.86 (m, 6H), 0.83 (s, 3H). See **Chapter appendix** for ^{1}H and ^{13}C NMR spectra.

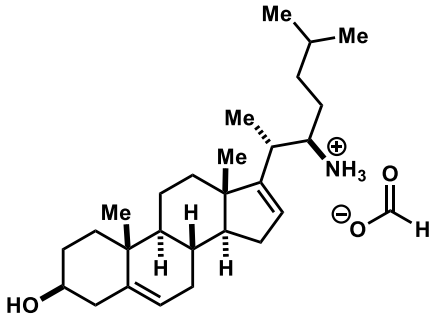

3.28

The mixture of homoallylic amine isomers were purified through HPLC (C8-Phenomenex column, MeOH/0.1% formic acid gradient) to afford the pure major isomer of homoallylic amine in the form of ammonium formate salt. The structure of homoallylic amine **3.28** was confirmed through 2D NMR. However, the absolute stereochemistry at C-22 has been assigned as (*R*), through the X-ray crystallography of compound **3.41**. ^{1}H NMR (500 MHz, Methanol-d4) δ 8.55 (s, 1H), 5.59 (dd, J = 3.1, 1.5 Hz, 1H), 5.37 (dd, J = 4.9, 2.5 Hz, 1H), 3.40 (tt, J = 10.5, 4.9 Hz, 1H), 3.28 (dt, J = 8.2, 4.1 Hz, 1H), 2.45 (p, J = 7.0 Hz, 1H), 2.30 – 2.18 (m, 2H), 2.15 (ddd, J = 15.0, 6.6, 3.3 Hz, 1H), 2.08 – 2.01 (m, 1H), 2.01 – 1.94 (m, 1H), 1.90 – 1.83 (m, 1H), 1.83 – 1.75 (m, 1H), 1.74 – 1.66 (m, 2H), 1.66 – 1.60 (m, 1H), 1.60 – 1.50 (m, 3H), 1.50 – 1.43 (m, 2H), 1.43 – 1.33 (m, 2H), 1.32 – 1.20 (m, 1H), 1.10

(d, J = 6.9 Hz, 3H), 1.09 – 1.00 (m, 4H), 0.95 (dd, J = 6.6, 1.6 Hz, 6H), 0.90 (s, 3H). ^{13}C NMR (126 MHz, Methanol-d4) δ 157.01, 142.58, 126.44, 122.21, 72.38, 59.08, 55.94, 52.23, 48.12, 43.04, 38.49, 37.92, 37.12, 35.97, 35.12, 32.64, 32.29, 32.20, 31.87, 29.41, 28.25, 22.94, 22.60, 21.88, 19.78, 16.70. See **Chapter appendix** for ^{1}H and ^{13}C NMR spectra, **Appendix** for 2D NMR spectra.

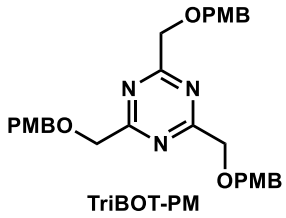

TriBOT-PM

TriBOT-PM was synthesized as described previously. [79] To a suspension of NaH (3.9 g, 97.6 mmol, 60% dispersion in mineral oil) in anhydrous THF (50 mL) at 0°C was added PMB-OH solution (12.34 g, 89.48 mmol, dissolved in 20 mL anhydrous THF) fast dropwise. The gray reaction mixture was stirred at 0°C for 15 minutes, then at RT. After 50 minutes, the reaction mixture was cooled to 0°C, then cyanuric chloride solution (5.0 g, 27.11 mmol, dissolved in 50 mL THF) was added fast dropwise. The reaction mixture was stirred at 0°C for 15 minutes, then a RT for 3 hours. The reaction mixture was then poured slowly to an Erlenmeyer flask containing DI H_2O (100 mL) to quench excess NaH. This mixture was then cooled in an ice bath, which resulted in two layers, not much precipitation. The reaction mixture was filtered through vacuum filtration. During this process, the off-white solid started to form. The filtrated was re-filtered a couple times to collect all of the precipitation. The solid was washed with chilled DI H_2O (100 mL x 2), hexanes (50 mL x 2) and DI H_2O (50 mL). The solid was transferred to a pre-weighted vial and dried on hi-vac to afford desired product at a white powder (11.4 g, 85.9%). ^{1}H NMR (500 MHz, Chloroform-d) δ 7.37 (d, J = 8.7 Hz, 2H), 6.89 (d, J = 8.7 Hz, 2H), 5.38 (s, 2H),

3.81 (s, 3H). ^{13}C NMR (126 MHz, Chloroform-d) δ 173.11, 159.93, 130.37, 127.61, 114.06, 69.86, 55.44. See **Chapter appendix** for NMR spectra.

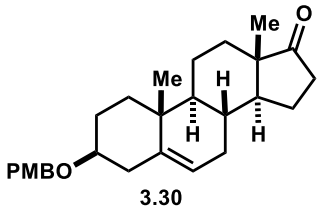

3.30

Compound **3.30** was synthesized with procedure adapted from Yamada *et al*.[79] To a clear, colorless solution of *trans*-dehydroandrosterone **3.29** (2.0 g, 6.93 mmol) in anhydrous THF (17.4 mL, 0.4M) at RT under N_2 atmosphere was added trifluoromethanesulfonic acid solution (18.4 µL, 0.208 mmol dissolved in 100 µL THF). The reaction mixture was stirred at RT for 5 minutes, then TriBOT-PM solution (2.03 g, 4.16 mmol dissolved in 21 mL THF) was added in portions over 40 minutes (~5 mL every 10 minutes). The reaction progress was monitored by TLC every 10 minutes (30% EtOAc/hex, UV, CAM stain). The light yellow, clear reaction mixture was stirred at RT for additional 30 minutes, when TLC profile remained the same. The reaction was quenched by saturated $NaHCO_3$ solution (10 mL). The reaction mixture was diluted with EtOAc (40 mL), washed with saturated $NaHCO_3$ (30 mL), DI H_2O (30 mL x 2). The combined aqueous phase was back extracted with EtOAc (10 mL). The combined organic phase was washed with brine, dried over Na_2SO_4, and filtered. The solvent was removed *in vacuo* to afford crude mixture was a white solid. The pure desired product **3.30** was obtained after two rounds of recrystallization in isopropanol as a white, crystalline powder (2.11 g, 74 % yield). ^{1}H NMR (400 MHz, Chloroform-d) δ 7.30 – 7.24 (m, 3H), 6.90 – 6.85 (m, 2H), 5.37 (dd, J = 4.7, 2.5 Hz, 1H), 4.49 (s, 2H), 3.80 (s, 3H), 3.26 (tt, J = 11.2, 4.5 Hz, 1H), 2.51 – 2.39 (m, 2H), 2.33 – 2.23 (m, 1H), 2.17 – 2.03 (m, 2H), 2.00 – 1.82 (m, 4H), 1.73 – 1.58 (m, 2H),

1.58 – 1.43 (m, 3H), 1.34 – 1.22 (m, 2H), 1.10 – 0.95 (m, 5H), 0.89 (s, 3H). ^{13}C NMR (101 MHz, Chloroform-d) δ 221.27, 159.22, 141.44, 131.23, 129.29, 120.90, 113.94, 78.21, 69.77, 55.44, 51.95, 50.46, 47.70, 39.32, 37.35, 37.19, 36.00, 31.66, 31.61, 30.98, 28.52, 22.03, 20.51, 19.57, 13.71. See **Chapter appendix** for ^{1}H and ^{13}C NMR spectra.

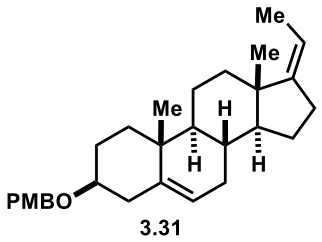

3.31

Compound **3.31** was synthesized with procedure adapted from Houston *et al*.[70] A bright, orange suspension of PPh_3EtBr (6.25 g, 16.83 mmol) and *t*-BuOK (1.89 g, 16.83 mmol) in anhydrous THF (38 mL) was stirred at RT under N_2 in a 2-neck RBF (fitted with a reflux condenser) for 40 minutes. To the mixture was then added PMB-protected dehydroandrosterone **3.30** solution (1.72 g, 4.21 mmol, dissolved in 12 mL of anhydrous THF). The reaction mixture was heated under reflux. The reaction progress was monitored by TLC (10% EtOAc/hexanes, UV, CAM stain). After 3.5 hours, the reaction was completed based on TLC. The reaction mixture was cooled to RT, quenched with sat'd NH_4Cl solution (20 mL). The reaction mixture was diluted with EtOAc (30 mL). The organic phase was washed with sat'd NH_4Cl solution (30 mL), DI H_2O (30 mL x 2). The combined aqueous phase was back extracted with EtOAc (10 mL). The combined organic phase was washed with brine, dried over Na_2SO_4, and filtered. The solvent was removed *in vacuo* to afford crude mixture as a white solid. The pure desired product **3.31** was obtained after two rounds of recrystallization in isopropanol as a white, crystalline powder (1.35 g, 76 % yield). The diagnostic NRM data agreed with published reference[70]. ^{1}H NMR (500 MHz, Chloroform-d) δ 7.30 – 7.25 (m, 2H), 6.90 – 6.85 (m, 2H), 5.35 (dt, J = 5.5, 1.9

Hz, 1H), 5.17 – 5.10 (m, 1H), 4.53 – 4.45 (m, 2H), 3.80 (s, 3H), 3.26 (tt, J = 11.3, 4.5 Hz, 1H), 2.44 – 2.34 (m, 2H), 2.34 – 2.23 (m, 2H), 2.23 – 2.14 (m, 1H), 2.07 – 1.98 (m, 1H), 1.98 – 1.91 (m, 1H), 1.87 (dt, J = 13.5, 3.6 Hz, 1H), 1.66 (dt, J = 7.2, 2.0 Hz, 3H), 1.65 – 1.60 (m, 1H), 1.59 – 1.47 (m, 5H), 1.28 – 1.18 (m, 1H), 1.18 – 1.10 (m, 1H), 1.08 – 1.00 (m, 4H), 0.96 (td, J = 10.9, 4.8 Hz, 1H), 0.90 (s, 3H). ^{13}C NMR (126 MHz, cdcl3) δ 159.19, 150.42, 141.21, 131.30, 129.29, 121.53, 113.92, 113.61, 78.36, 69.72, 56.70, 55.43, 50.36, 44.20, 39.32, 37.36, 37.14, 37.11, 31.91, 31.60, 31.56, 28.59, 24.62, 21.37, 19.51, 16.77, 13.28. See **Chapter appendix** for ^{1}H and ^{13}C NMR spectra.

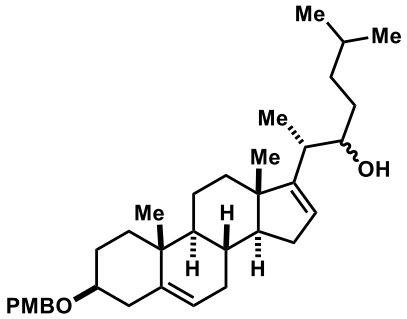

3.32

Compound **3.32** was synthesized with procedure adapted from Houston *et al.*[70] To a solution of 4-methylpentanal (357.2 mg, 3.57 mmol) in anhydrous DCM (15 mL) at -78°C was added dimethylaluminum chloride solution (1M solution, 5.94 mL, 5.94 mmol). The mixture was stirred at -78°C for 15 minutes, then PMB-pregnadiene **3.31** solution (500.0 mg, 1.19 mmol, dissolved in 10 mL anhydrous DCM) was added dropwise. The reaction mixture was stirred in the cold bath, without additional dry ice added to allow slow warm-up. The reaction progress was monitored by TLC (10% EtOAc/hexanes, UV, CAM stain). After 2.5h, the reaction was warmed up to RT. The reaction was mostly completed based on TLC after 4h. The reaction was then quenched by mixture of MeOH: DI H_2O (1:1, 20 mL) at -78°C. The reaction mixture was diluted with DI H_2O (30 mL), extracted with DCM

(15 mL x3). The combined organic phase was washed with 1N HCl (20 mL), saturated solution of $NaHCO_3$ (20 mL), DI H_2O (20 mL x2). The combined aqueous phase was back extracted with DCM (10 mL). The combined organic phase was washed with brine, dried over Na_2SO_4, and filtered. The solvent was removed to afford crude mixture was a white solid (903.8 mg). The crude mixture was then separated through silica gel column (60g Si-gel, Et_2O/hexanes gradient from 5% to 35%) to afford the desired mixture of homoallylic alcohol isomers **3.32** (545.9 mg, 88%). ^{1}H NMR (500 MHz, Chloroform-d) δ 7.30 – 7.23 (m, 2H), 6.90 – 6.84 (m, 2H), 5.49 (dt, J = 3.1, 1.5 Hz, 1H), 5.36 (dd, J = 3.6, 1.9 Hz, 1H), 4.53 – 4.44 (m, 2H), 3.80 (s, 3H), 3.66 – 3.61 (m, 1H,H-22 of major isomer), 3.59 – 3.54 (m, 1H, H-22 of minor isomer), 3.26 (tt, J = 11.2, 4.5 Hz, 1H), 2.42 (ddd, J = 13.3, 4.8, 2.3 Hz, 1H), 2.32 – 2.23 (m, 2H), 2.21 – 2.14 (m, 1H), 2.10 (dddd, J = 15.3, 12.6, 6.5, 3.2 Hz, 1H), 2.02 (ddt, J = 16.9, 5.0, 2.4 Hz, 1H), 1.98 – 1.88 (m, 2H), 1.85 (dt, J = 13.2, 3.7 Hz, 1H), 1.78 (ddd, J = 11.9, 4.6, 2.6 Hz, 1H), 1.72 – 1.59 (m, 3H), 1.59 – 1.46 (m, 3H), 1.47 – 1.38 (m, 1H), 1.38 – 1.24 (m, 3H), 1.24 – 1.13 (m, 1H), 1.05 (d, J = 1.1 Hz, 4H), 1.02 (d, J = 7.0 Hz, 3H), 0.99 (d, J = 6.9 Hz, 2H), 0.92 – 0.86 (m, 9H), 0.83 (s, 1H). See **Chapter appendix** for ^{1}H and ^{13}C NMR spectra.

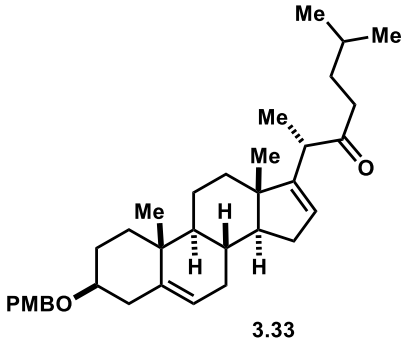

3.33

Compound **3.33** was synthesized with procedure adapted from Deng *et al.*[35] To a suspension of 4Å MS powder (170 mg), PDC (114.1 mg, 0.303 mmol) in anhydrous DCM

(0.160 mL) and DMF (0.170 mL) at RT was added a solution of homoallylic alcohols **3.32** (79.0 mg, 0.151 mmol, dissolved in 1.0 mL DCM). The brown suspension was stirred at RT, and the reaction progress was monitored by TLC (10% EtOAc/hexanes, UV, CAM stain). After 24 hours, the reaction mixture was filtered through a silica plug, washed with DCM (15 mL). The solvent was removed *in vacuo*. The resulting residue was resuspended in Et_2O (7 mL), washed with DI H_2O (3 mL x 3), brine, dried over Na_2SO_4, and filtered. The solvent was removed *in vacuo* to afford crude mixture, which was purified by flash chromatography (EtOAc/hexanes gradient from 5% to 15%) to afford desired C-22 ketone **3.33** (75.7 mg, 76% yield). ^{1}H NMR (500 MHz, Chloroform-d) δ 7.28 (d, J = 8.5 Hz, 2H), 6.91 – 6.84 (m, 2H), 5.40 – 5.34 (m, 2H), 4.50 (s, 2H), 3.81 (s, 3H), 3.27 (tt, J = 11.2, 4.5 Hz, 1H), 3.20 (q, J = 6.8 Hz, 1H), 2.54 – 2.46 (m, 1H), 2.46 – 2.40 (m, 1H), 2.40 – 2.32 (m, 1H), 2.32 – 2.24 (m, 1H), 2.10 (ddd, J = 15.0, 6.5, 3.2 Hz, 1H), 2.06 – 1.99 (m, 1H), 1.99 – 1.93 (m, 1H), 1.92 – 1.83 (m, 2H), 1.81 (ddd, J = 12.1, 4.6, 2.5 Hz, 1H), 1.73 – 1.59 (m, 3H), 1.56 – 1.41 (m, 5H), 1.35 (tt, J = 11.1, 5.4 Hz, 2H), 1.16 (d, J = 6.9 Hz, 3H), 1.09 – 0.98 (m, 5H), 0.93 – 0.82 (m, 9H). See **Chapter appendix** for ^{1}H and ^{13}C NMR spectra.

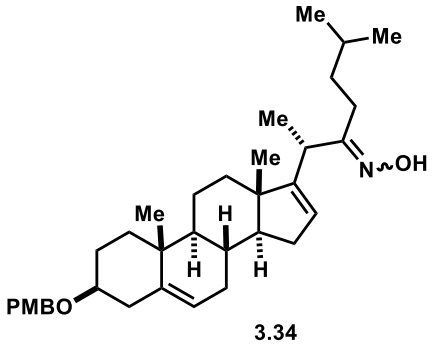

3.34

To a mixture of C-22 ketone **3.33** (270 mg, 0.52 mmol) in 200-proof EtOH (6.0 mL) was added hydroxyl amine hydrochloride $NH_2OH{\cdot}HCl$ (144.7 mg, 2.08 mmol) and sodium acetate trihydrates $NaOAc{\cdot}3H_2O$ (424.9 mg, 3.12 mmol). The resulting slurry was heated

under reflux. The reaction progress was monitored by TLC (20% EtOAc/hexanes, UV, CAM stain). After 5 hours, the reaction was completed based on TLC. The reaction mixture was diluted with DI H_2O (10 mL). The aqueous phase was extracted with DCM (5 mL x 4). The combined organic phase was washed with brine, dried over Na_2SO_4, and filtered. The solvent was removed *in vacuo* to afford a mixture of C-22-oxime isomers **3.34** as a white solid (260.0 mg, 93%). The product was used without further purification. ^{1}H NMR (400 MHz, Chloroform-d) δ 7.27 (d, J = 8.1 Hz, 2H), 6.87 (d, J = 8.6 Hz, 2H), 5.48 – 5.43 (m, 1H), 5.35 (d, J = 5.1 Hz, 1H), 4.49 (s, 2H), 3.80 (s, 3H), 3.25 (td, J = 11.2, 5.5 Hz, 1H), 3.09 (q, J = 7.0 Hz, 1H), 2.41 (dd, J = 13.2, 4.5 Hz, 1H), 2.32 – 2.20 (m, 2H), 2.17 – 2.01 (m, 3H), 2.01 – 1.91 (m, 1H), 1.91 – 1.80 (m, 3H), 1.73 – 1.42 (m, 4H), 1.41 – 1.24 (m, 4H), 1.20 (d, J = 7.0 Hz, 3H), 1.16 (d, J = 7.1 Hz, 1H), 1.03 (d, J = 3.3 Hz, 5H), 0.95 – 0.86 (m, 7H), 0.77 (s, 3H). ^{13}C NMR (101 MHz, Chloroform-d) δ 164.33, 159.20, 156.11, 141.50, 131.29, 129.30, 125.08, 121.44, 113.93, 78.36, 69.73, 57.68, 55.44, 50.83, 47.03, 39.35, 38.28, 37.34, 37.28, 35.35, 34.74, 31.75, 31.26, 30.63, 28.89, 28.59, 25.35, 22.53, 22.43, 20.87, 19.45, 17.78, 16.27. See **Chapter appendix** for ^{1}H and ^{13}C NMR spectra.

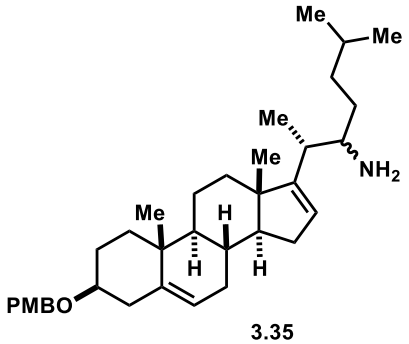

3.35

To a solution of oximes **3.34** (260.0 mg, 0.487 mmol) in anhydrous THF (3.6 mL) at 0°C under N_2 was added a suspension of $LiAlH_4$ (185.0 mg, 4.87 mmol, in 4.9 mL THF) dropwise. The gray suspension was then heated under reflux. The reaction progress was

monitored by TLC (5% MeOH/DCM, UV, CAM stain). After 48 hours, TLC showed absence of oximes **3.34**. The reaction was quenched with DI H_2O at 0°C. The reaction mixture was transferred to an Erlenmeyer flask. To it was added 15% NaOH solution (20 mL) and EtOAc (10 mL). The mixture was stirred at RT for 10 minutes. The aqueous phase was extracted with EtOAc (10 mL x 3). The combined organic phase was washed with brine, dried over Na_2SO_4, and filtered. The solvent was removed *in vacuo* to afford crude mixture as a white foamy solid (200 mg). The crude mixture was purified by flash chromatography (MeOH/DCM gradient from 0% to 10%) to afford the mixture of homoallylic amine isomers **3.35** (100.0 mg, 39%). The ratio between the two isomers were ~ 2:1. ^{1}H NMR (500 MHz, Chloroform-d) δ 7.27 (d, J = 8.7 Hz, 2H), 6.89 – 6.85 (m, 2H), 5.40 (dd, J = 2.8, 1.5 Hz, 1H), 5.36 (dt, J = 5.4, 2.0 Hz, 1H), 4.54 – 4.45 (m, 2H), 3.80 (s, 3H), 3.26 (tt, J = 11.2, 4.5 Hz, 1H), 2.80 (t, J = 8.5 Hz, 1H, H-22 of major isomer), 2.74 – 2.57 (m, 0H-H-22 of minor isomer), 2.42 (ddd, J = 13.2, 4.8, 2.3 Hz, 1H), 2.27 (ddq, J = 16.0, 11.4, 2.7 Hz, 1H), 2.09 (ddd, J = 14.8, 6.6, 3.1 Hz, 1H), 2.02 (dtd, J = 12.5, 4.7, 4.3, 2.2 Hz, 1H), 1.98 – 1.82 (m, 3H), 1.79 (ddd, J = 12.0, 4.4, 2.6 Hz, 1H), 1.73 – 1.57 (m, 3H), 1.57 – 1.47 (m, 3H), 1.46 – 1.24 (m, 4H), 1.24 – 1.12 (m, 2H), 1.08 – 1.01 (m, 4H), 0.98 (d, J = 6.9 Hz, 3H), 0.93 – 0.86 (m, 6H), 0.83 (s, 3H). See **Chapter appendix** for ^{1}H and ^{13}C NMR spectra.

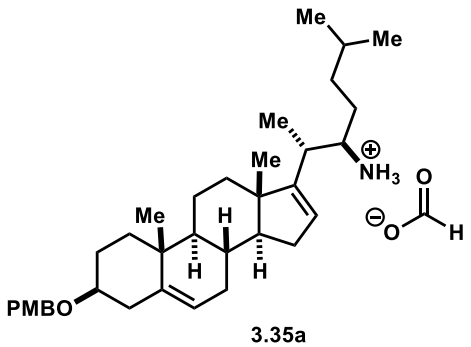

3.35a

The mixture of homoallylic amine isomers were purified through HPLC (C8-Phenomenex column, MeOH/0.1% formic acid gradient) to afford the pure major isomer of homoallylic amine in the form of ammonium formate salt. The absolute stereochemistry at C-22 has been assigned as (*R*), through the X-ray crystallography of compound **3.41**. ^{1}H NMR (500 MHz, Chloroform-d) δ 7.26 (s, 3H), 6.87 (d, J = 8.6 Hz, 2H), 5.50 (s, 1H), 5.35 (d, J = 5.0 Hz, 1H), 4.49 (s, 2H), 3.79 (s, 3H), 3.25 (td, J = 11.1, 5.5 Hz, 1H), 3.09 (s, 1H), 2.44 (dd, J = 19.1, 10.6 Hz, 2H), 2.26 (t, J = 12.5 Hz, 1H), 2.11 (dd, J = 12.6, 6.2 Hz, 1H), 2.05 – 1.87 (m, 3H), 1.82 (t, J = 14.8 Hz, 1H), 1.72 (d, J = 12.7 Hz, 1H), 1.69 – 1.58 (m, 2H), 1.58 – 1.46 (m, 2H), 1.45 – 1.30 (m, 2H), 1.29 – 1.20 (m, 1H), 1.07 (d, J = 6.8 Hz, 3H), 1.03 (s, 3H), 1.02 – 0.96 (m, 1H), 0.89 (dd, J = 6.6, 4.4 Hz, 6H), 0.84 (s, 3H). ^{13}C NMR (126 MHz, Chloroform-d) δ 159.18, 156.90, 141.43, 131.23, 129.30, 124.62, 121.37, 113.92, 78.31, 69.73, 57.71, 55.43, 54.72, 50.78, 47.20, 39.32, 37.30, 37.24, 36.79, 34.75, 34.51, 31.69, 31.42, 30.64, 28.57, 28.19, 27.82, 22.78, 22.35, 20.84, 19.41, 16.42. See **Chapter appendix** for ^{1}H and ^{13}C NMR spectra, **Appendix** for 2D NMR spectra.

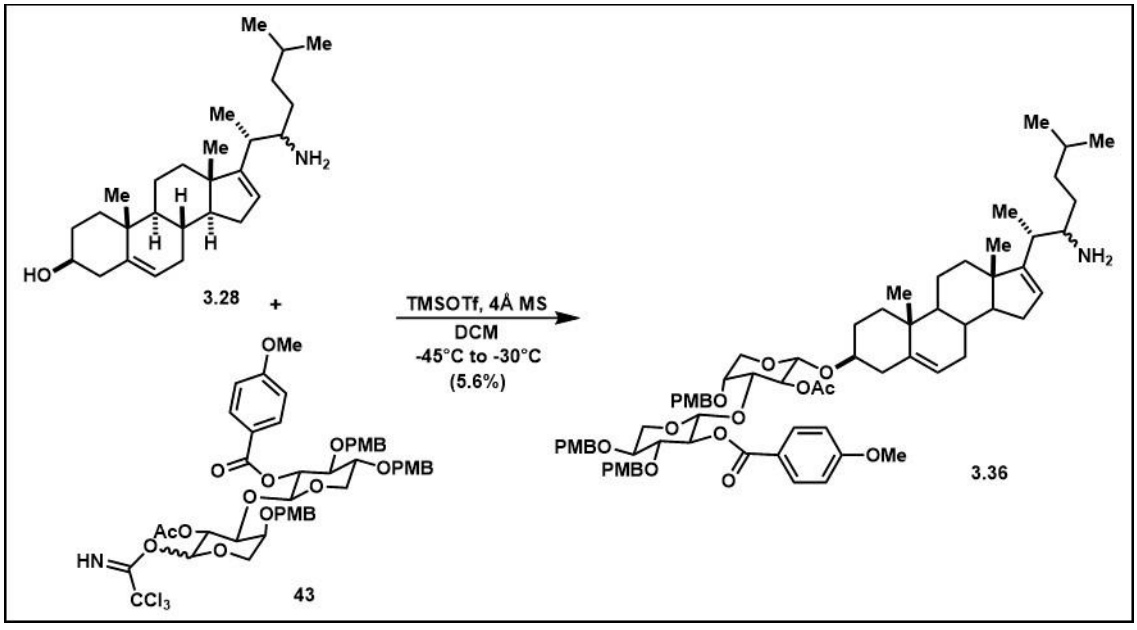

Scheme 28: To a mixture of amine **3.28** (10 mg, 0.0224 mmol) and 4Å MS powder (170 mg) at RT was added dry DCM (1.2 mL) under N_2 atmosphere. To the reaction mixture was then added disaccharide imidates **43** (21.61 mg, 0.0224 mmol, dissolved in 0.4 mL of dry DCM total). The mixture was stirred at RT for 30 minutes. The flask was sonicated in attempt to solubilized small amount of white precipitation observed. After 30 minutes at RT, the reaction mixture was cooled down to -45°C (acetonitrile/dry ice bath). To the reaction mixture was added TMSOTf in portions, while the reaction progress was monitored with TLC (7.5% MeOH/DCM, UV, CAM stain). The reaction temperature was kept within -30°C to -45°C. TMSOTf (0.4 µL, 2.24 µmol) was added at T=0, 15, and 43 minutes. At T=140 minutes, no further progress was observed, so the reaction was quenched by addition of saturated $NaHCO_3$ solution at -30°C. The reaction mixture was then allowed to warm up to RT and stirred for 10 minutes. The aqueous phase was extracted with DCM (5 mL x 3). The combined organic phase was washed with sat'd $NaHCO_3$, DI H_2O, brine, and dried over Na_2SO_4. The solvent was removed to afford crude mixture as a tan, foamy solid (24.8 mg). The crude mixture was separated by pTLC (1 plate, 7.5% MeOH/$CHCl_3$, 3 elutions) to afford 6 bands. Amongst the bands, some unreacted amine **3.28** (2.2 mg), and disaccharide **43** (11.1 mg) were recovered. The most promising band was B4 (1.8 mg 5.6%), which seemed to be the *O*-glycosylated product **3.26** (HMBC spectrum showed correlation of the anomeric proton of arabinose and a ^{13}C signal at 73 ppm; if it were *N*-glycosylated product, it should have been correlated to ^{13}C signal at lower than 70 ppm).

3.26: ^1H NMR (500 MHz, Chloroform-d) δ 7.93 (d, J = 8.8 Hz, 2H), 7.30 – 7.22 (m, 4H), 7.11 (d, J = 8.5 Hz, 2H), 6.87 (dd, J = 8.7, 3.8 Hz, 4H), 6.81 (d, J = 8.5 Hz, 2H), 6.68 (d, J

= 8.6 Hz, 2H), 5.42 (bs, 1H), 5.27 (s, 1H), 5.20 – 5.15 (m, 1H), 5.13 – 5.08 (m, 1H), 4.71 (d, J = 6.1 Hz, 1H), 4.67 (d, J = 11.9 Hz, 1H), 4.63 (s, 2H), 4.62 – 4.57 (m, 2H), 4.53 (d, J = 11.3 Hz, 1H), 4.35 (d, J = 6.4 Hz, 1H), 3.96 (dd, J = 11.8, 4.4 Hz, 1H), 3.90 (dd, J = 12.3, 4.0 Hz, 1H), 3.85 (s, 3H), 3.81 (s, 3H), 3.79 (s, 3H), 3.78 – 3.74 (m, 1H), 3.73 – 3.69 (m, 5H), 3.68 – 3.62 (m, 1H), 3.40 – 3.29 (m, 3H), 2.40 – 2.23 (m, 2H), 2.20 – 1.84 (m, 7H), 1.81 (s, 3H), 1.78 – 1.68 (m, 4H), 1.66 – 1.42 (m, 5H), 1.42 – 1.14 (m, 4H), 1.09 – 0.97 (m, 3H), 0.94 (s, 3H), 0.93 – 0.86 (m, 9H), 0.87 – 0.80 (m, 6H). See **Chapter appendix** for ^{1}H and ^{13}C NMR spectra, **Appendix** for 2D NMR spectra.

Entry 1, Error! Reference source not found.: homoallylic ammonium salt **3.35a** was n eutralized with NEt_3 at RT. Order of addition: homoallylic amine + TMSOTf, then disaccharide imidates **43**; TMSOTf was added more after the reaction started. 0.4 eqv of TMSOTf was used total.

To a solution of ammonium salt **3.35a** (10 mg, 16.6 µmol) in anhydrous DCM (300 µL) was added triethylamine (4 µL, 28.7 µmol). The yellow solution was stirred at RT for 10 minutes, then the solvent was removed. The residue was azeotroped with benzene two times, then dried on hi-vac for one hour. In a 5mL conical flask, a mixture of homoallylic amine, 4Å MS powder (100 mg) in anhydrous DCM (200 µL) was stirred at RT for 5 minutes, then at -35°C for 10 minutes while a solution of TMSOTf was prepared (2.4 µL TMSOTf was dissolved in 97.6 µL of DCM; 10 µL solution contained 0.1 eqv of TMSOTf). To the reaction mixture containing homoallylic amine at -35°C was added TMSOTf (10 µL solution, 0.1 eqv). After 5 minutes, disaccharide imidates **2** (14.9 mg, 15.5 µmol, dissolved in 100 µL DCM). The reaction progress was monitored by TLC (7.5%

MeOH/DCM, UV, CAM stain). The reaction temperature was maintained between -35°C and -20°C. TMSOTf additions are summarized in the table below:

Reagent added	**Time**	**Temperature**
TMSOTf (10 µL solution, 0.1 eqv)	T = 0m	-35°C
TMSOTf (10 µL solution, 0.1 eqv)	T = 35m	-35°C
Fire alarm	T = 50m to 1h20m	-20°C (freezer)
TMSOTf (10 µL solution, 0.1 eqv)	T = 1h40m	-35°C
TMSOTf (10 µL fresh solution, 0.1 eqv)	T = 1h50m	-35°C

After the last addition of TMSOTf, the TLC profile changed significantly. The reaction was quenched by addition of saturated $NaHCO_3$ solution (3 mL) at -30°C. The reaction mixture was then stirred at RT for 10 minutes. The aqueous phase was extracted with DCM (3 mL x 3). The combined organic phase was washed with DI H_2O, brine, and dried over anhydrous Na_2SO_4. The solvent was removed to afford crude mixture as a sticky residue (19.1 mg). The crude mixture was separated by pTLC (3/4 plate, 4% MeOH/DCM, 1 elution). The bands were scraped from the plate in order of increasing Rf value. The silica gel was rinsed with 10% MeOH/DCM. The solvent was removed to afford residue, which was dried on hi-vac and analyzed by ^1H NMR. ^1H NMR spectra of the bands are shown below. From the pTLC results, no glycosylated product was observed. Most of the pTLC bands showed signals of derivative of disaccharide moiety, except for B1, which was the recovered unreacted homoallylic amine.

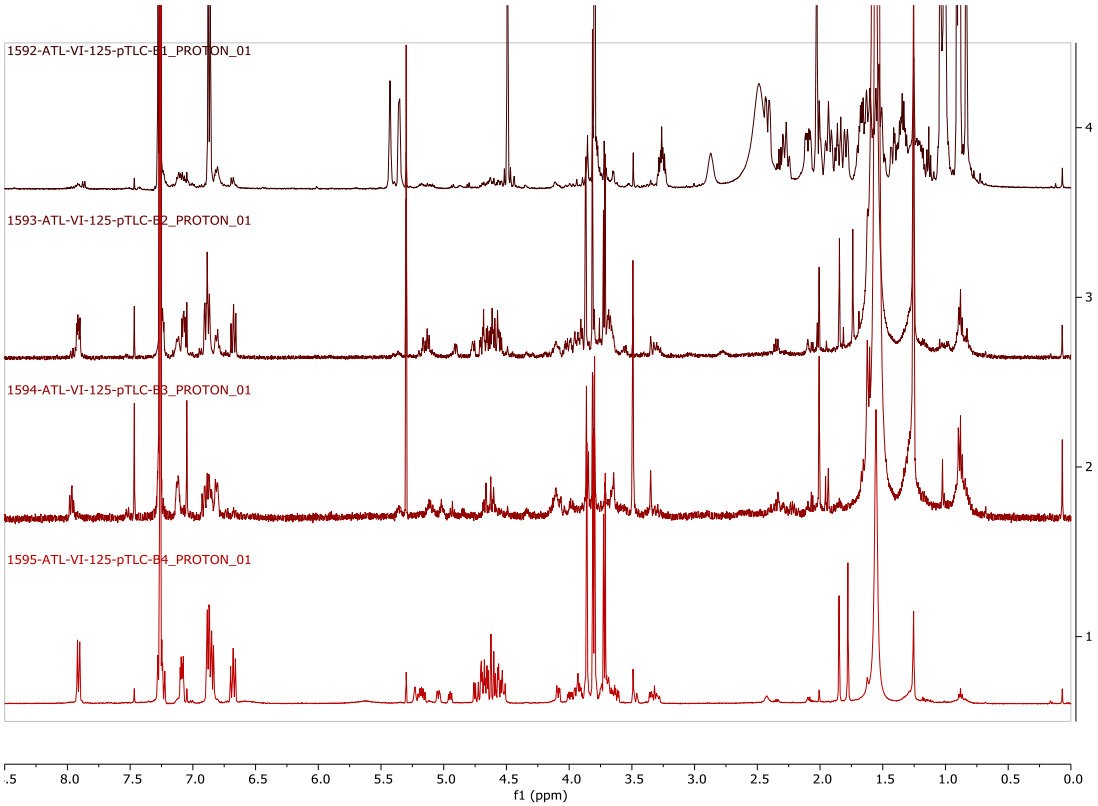
1592-ATL-VI-125-pTLC-B1_PROTON_01
1593-ATL-VI-125-pTLC-B2_PROTON_01
1594-ATL-VI-125-pTLC-B3_PROTON_01
1595-ATL-VI-125-pTLC-B4_PROTON_01
f1 (ppm)

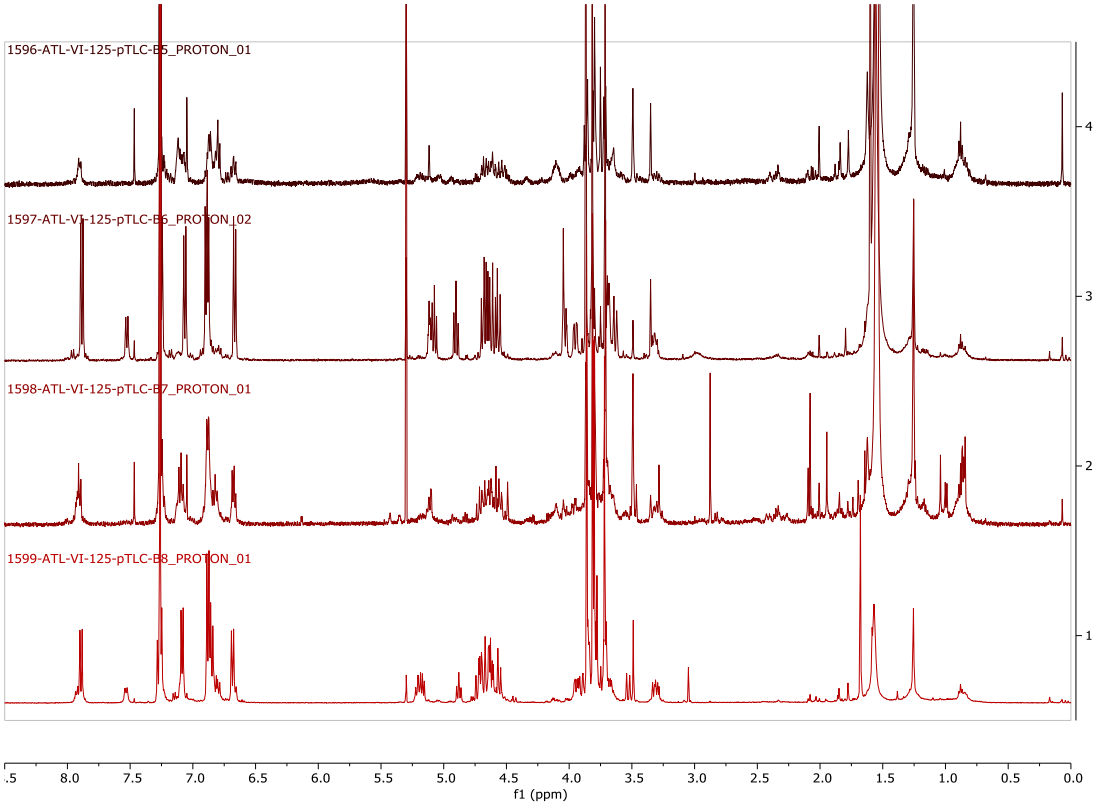
1596-ATL-VI-125-pTLC-B5_PROTON_01
1597-ATL-VI-125-pTLC-B6_PROTON_02
1598-ATL-VI-125-pTLC-B7_PROTON_01
1599-ATL-VI-125-pTLC-B8_PROTON_01
f1 (ppm)

Entry **2**, Error! Reference source not found.: used TEA to neutralize ammonium salt at RT; o rder of addition: disaccharide **43** with TMSOTf, then amine **3.35a** was added; 1.4 eqv TMSOTf used total

To a solution of ammonium salt **1** (7.3 mg, 12.9 µmol) in anhydrous DCM (292 µL) was added triethylamine (2.7 µL, 19.4 µmol). The yellow solution was stirred at RT for 10 minutes, then the solvent was removed. The residue was azeotroped with benzene two times, then dried on hi-vac for one hour. In a 5mL conical flask, a mixture of disaccharide imidates **2** (15.4 mg, 16 µmol) and 4Å MS powder (76 mg) in anhydrous DCM (200 µL) was stirred at RT for 5 minutes, then at -40°C for 10 minutes, while a solution of TMSOTf was prepared (9.3 µL TMSOTf was dissolved in 190.5 µL of DCM). To the reaction flask with disaccharide mixture at -40°C was added TMSOTf (5 µL solution, 0.1 eqv). After 5 minutes, to the reaction flask was added a solution of homoallylic amine **3.35a** (dissolved in 150 µL of anhydrous DCM). The reaction progress was monitored by TLC (7.5% MeOH/DCM, UV, CAM stain). TMSOTf additions are summarized in the table below:

Reagent added	**Time**	**Temperature**
TMSOTf (5 µL solution, 0.1 eqv)	T = 33m	-40°C
TMSOTf (5 µL solution, 0.1 eqv)	T = 45m	-40°C
TMSOTf (5 µL solution, 0.1 eqv)	T = 60m	-40°C
TMSOTf (5 µL solution, 0.1 eqv)	T = 1h14m	-25°C
TMSOTf (5 µL solution, 0.1 eqv)	T = 1h34m	-20°C
TMSOTf (5 µL fresh solution, 0.1 eqv)	T = 1h53m	-20°C
TMSOTf (5 µL fresh solution, 0.1 eqv)	T = 2h7m	-18°C
TMSOTf (5 µL fresh solution, 0.1 eqv)	T = 2h23m	-18°C

TMSOTf (0.2 µL neat, 0.1 eqv)	T = 2h42m	-30°C
Disaccharide imidates **43**	T = 3h	-20°C
TMSOTf (0.5 µL neat, 0.25 eqv)	T = 4h4m	-30°C
TMSOTf (0.5 µL neat, 0.25 eqv)	T = 4h47m	-35°C

At 5h30m, the reaction was quenched by addition of saturated $NaHCO_3$ solution (3 mL) at -30°C. The reaction mixture was then stirred at RT for 10 minutes. The aqueous phsase was extracted with DCM (3 mL x 3). The combined organic phase was washed with DI H_2O, brine, and dried over anhydrous Na_2SO_4. The solvent was removed to afford crude mixture as a tan, foamy solid (23 mg). The crude mixture was separated by pTLC (1 plate, 6% MeOH/DCM, 2 elutions). The bands were scraped from the plate in order of increasing Rf value. The silica gel was rinsed with 10% MeOH/DCM. The solvent was removed to afford residue, which was dried on hi-vac and analyzed by ^1H NMR.

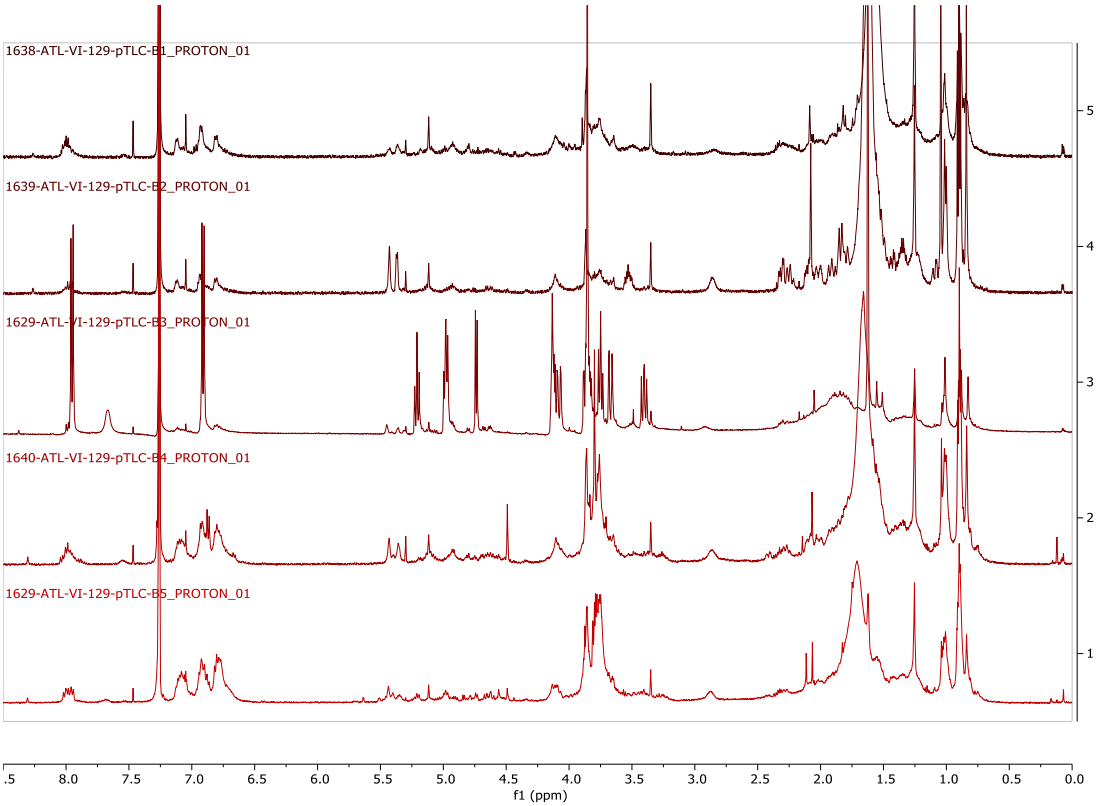
1638-ATL-VI-129-pTLC-B1_PROTON_01
1639-ATL-VI-129-pTLC-B2_PROTON_01
1629-ATL-VI-129-pTLC-B3_PROTON_01
1640-ATL-VI-129-pTLC-B4_PROTON_01
1629-ATL-VI-129-pTLC-B5_PROTON_01
5
4
3
2
1
.5 8.0 7.5 7.0 6.5 6.0 5.5 5.0 4.5 4.0 3.5 3.0 2.5 2.0 1.5 1.0 0.5 0.0
f1 (ppm)

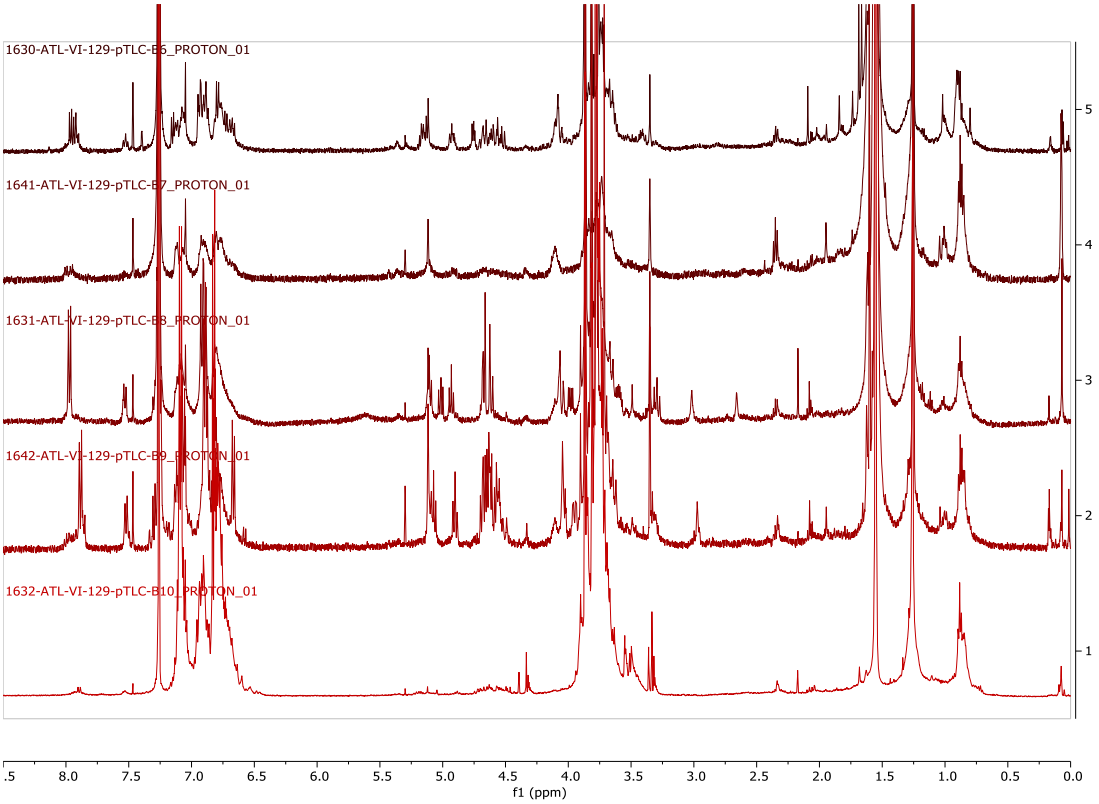
1630-ATL-VI-129-pTLC-B6_PROTON_01
1641-ATL-VI-129-pTLC-B7_PROTON_01
1631-ATL-VI-129-pTLC-B8_PROTON_01
1642-ATL-VI-129-pTLC-B9_PROTON_01
1632-ATL-VI-129-pTLC-B10_PROTON_01
5
4
3
2
1
.5 8.0 7.5 7.0 6.5 6.0 5.5 5.0 4.5 4.0 3.5 3.0 2.5 2.0 1.5 1.0 0.5 0.0
f1 (ppm)

From these NMR spectra, it seems that B4 and B5 might contain some glycosylated product, but it cannot be confirmed, since the NMR spectra looked messy and might contain more than one compound. During the reaction progress, after the last TMSOTf addition (1.4 eqv total), the TLC profile changed significantly. It is possible that too much TMSOTf could degrade the products formed. The TLC of the reaction mixture with disaccharide imidates **43** and TMSOTF showed new spots, but it was not clear if this was the oxonium ion formed once the imidate group left.

Entry **3**, Error! Reference source not found.: used NaH to neutralize the ammonium salt at R T; 0.4 eqv of TMSOTf used total.

To the solution of ammonium salt **3.35a** (7 mg, 12.4 µmol) in anhydrous DCM (150 µL) at RT was added NaH (1.5 mg, 37.2 µmol, 60% suspended in mineral oil). Upon NaH addition, gas evolution was observed. The mixture was stirred at RT for 5 minutes, then disaccharide imidates **43** solution (14.9 mg, 15.5 µmol, dissolved in 150 µL dry DCM) was added fast dropwise at RT. The reaction mixture was stirred at RT, reaction progress was monitored by TLC (8% MeOH/DCM, UV, CAM stain). After 1h15m, 4ÅMS powder (79 mg) was added. At 1h45m, the reaction mixture was cooled down to -40°C, then TMSOTf (0.25 µL, 1.24 µmol) was added every 7 minutes for the total of 1µL of TMSOTf (0.4 eqv). The reaction mixture was analyzed by TLC after each TMSOTf addition. Not much progress was observed, so at 2h30m, the reaction was quenched by addition of saturated $NaHCO_3$ solution (3 mL) at -30°C. The reaction mixture was then stirred at RT for 10 minutes. The aqueous phase was extracted with DCM (3 mL x 3). The combined organic phase was washed with DI H_2O, brine, and dried over anhydrous Na_2SO_4. The solvent was removed to afford crude mixture as a tan, foamy solid (16 mg). The crude mixture was

separated by pTLC (3/4 plate, 3% MeOH/DCM, 2 elutions). The seven bands were scraped from the plate in order of increasing Rf value. The silica gel was rinsed with 10% MeOH/DCM. The solvent was removed to afford residue, which was dried on hi-vac and analyzed by ^{1}H NMR. B1 (2.9 mg), B2 (1.3 mg), B3 (2.5 mg), B4 (1 mg), B5 (0.8 mg), B6 (1.5 mg), B7 (5.1 mg).

Analysis: Out of seven bands obtained from pTLC, only 2 bands (B1 and B7) had NMR signals corresponded to steroidal moiety. The rest of the bands had NMR spectra suggestive of derivatives of disaccharide moiety. This could be explained by the stability of disaccharide imidates. With the excess NaH in the mixture, disaccharide imidates could have been degraded.

B1's NMR spectrum showed the recovered unreacted homoallylic amine. B7's NMR showed signals for both disaccharide and homoallylic amine, along with new signals in 2.2-2.6 ppm region, which could belong to the area around the glycosydic bond if it were formed. LCMS analysis of B7 showed the desired m/z value for the glycosylated product (1320-1321).

B7 material was subjected to a second round of pTLC (1/2 plate, 35% EtOAc/hex, 1 elution). The result of this is showed below. It appeared that no glycosylated product was present. B7-1 through B7-6 showed disaccharide derivatives, while B7-7 and B7-8 showed derivatives of steroidal amines. The homoallylic amine could have cyclized under reaction condition.

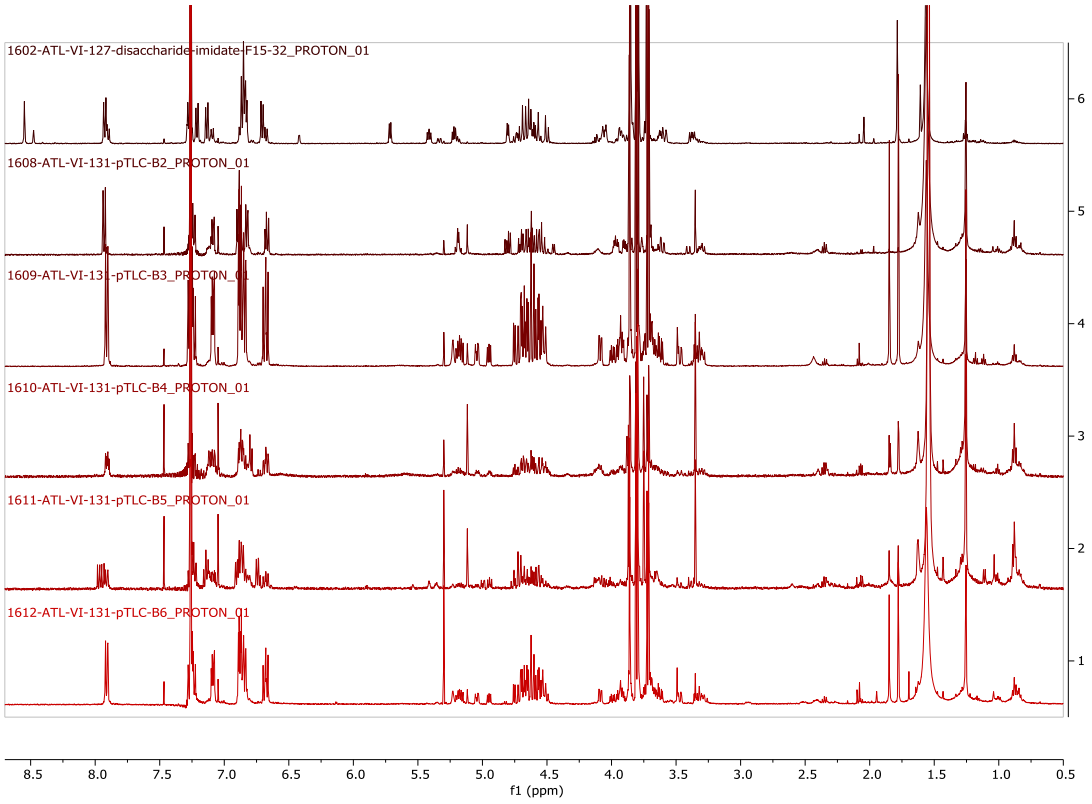
1602-ATL-VI-127-disaccharide-imidate-F15-32_PROTON_01
1608-ATL-VI-131-pTLC-B2_PROTON_01
1609-ATL-VI-131-pTLC-B3_PROTON_01
1610-ATL-VI-131-pTLC-B4_PROTON_01
1611-ATL-VI-131-pTLC-B5_PROTON_01
1612-ATL-VI-131-pTLC-B6_PROTON_01
8.5 8.0 7.5 7.0 6.5 6.0 5.5 5.0 4.5 4.0 3.5 3.0 2.5 2.0 1.5 1.0 0.5
f1 (ppm)

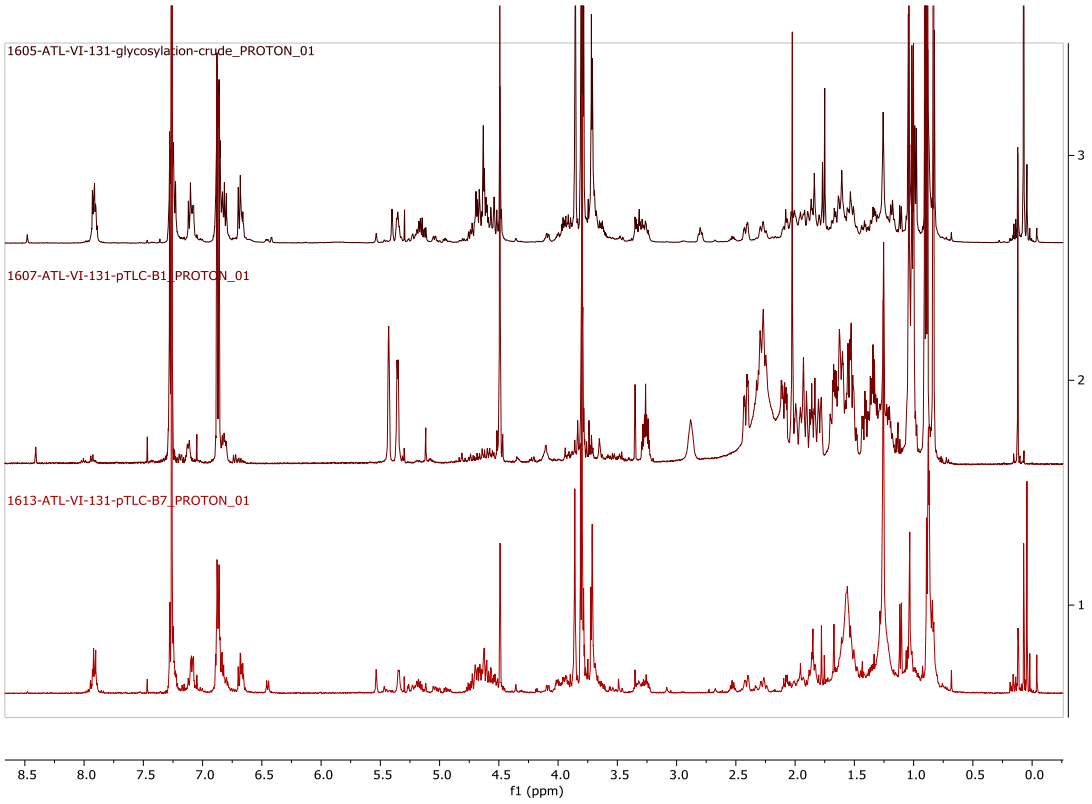
1605-ATL-VI-131-glycosylation-crude_PROTON_01
1607-ATL-VI-131-pTLC-B1_PROTON_01
1613-ATL-VI-131-pTLC-B7_PROTON_01
8.5 8.0 7.5 7.0 6.5 6.0 5.5 5.0 4.5 4.0 3.5 3.0 2.5 2.0 1.5 1.0 0.5 0.0
f1 (ppm)

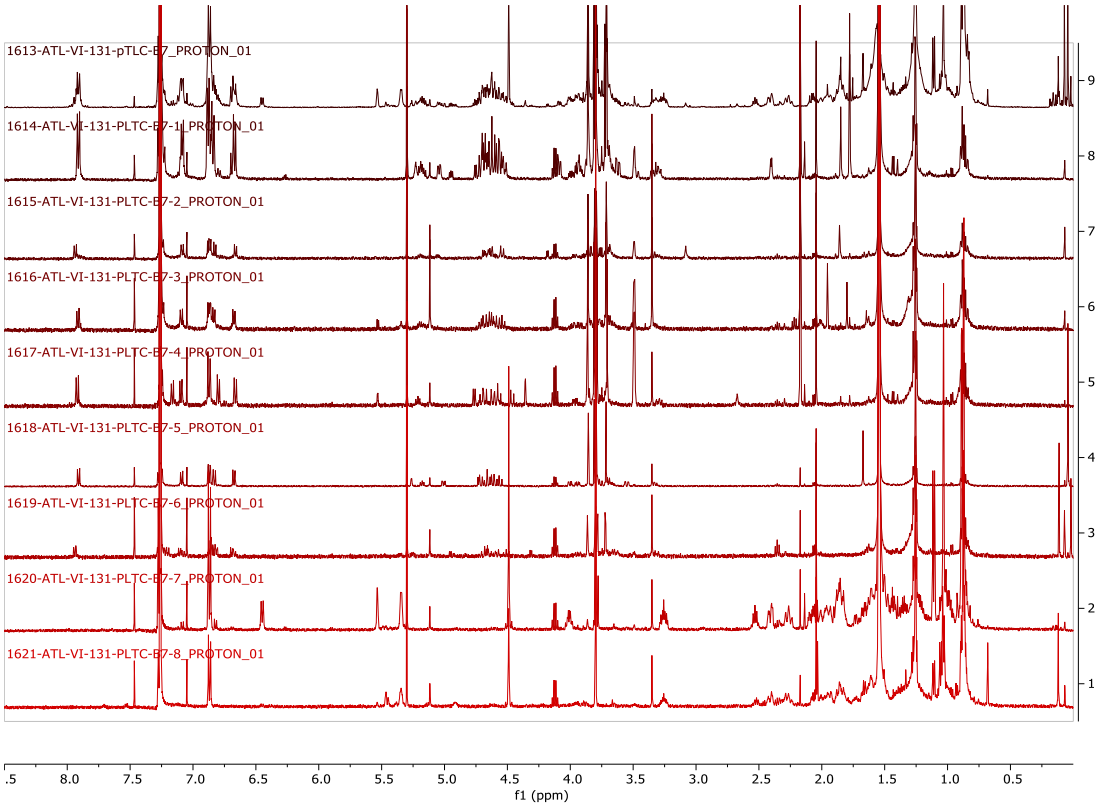

Entry **4**, Error! Reference source not found.: used homoallylic amine recovered from entry **1**-**3**; 0.6 eqv TMSOTf used total

To the solution of homoallylic amine **3.35b** (5.1 mg, 9.81 µmol) in anhydrous DCM (100 µL) and 4ÅMS powder (30 mg) at RT was added disaccharide imidates **43** solution (11.9 mg, 12.4 µmol, dissolved in 150 µL dry DCM. The reaction mixture was stirred at RT for 30 minutes, then cooled to -40°C. A solution of TMSOTf was prepared (7 µL TMSOTf was dissolved in 193 µL of DCM; 5µL solution contained 0.1 eqv). The reaction progress was monitored by TLC (7.5% MeOH/DCM, UV, CAM stain). TMSOTf additions are summarized in the table below:

Reagent added	**Time**	**Temperature**
TMSOTf (5 µL solution, 0.1 eqv)	T = 28m	-40°C
TMSOTf (5 µL solution, 0.1 eqv)	T = 38m	-40°C

TMSOTf (5 µL solution, 0.1 eqv)	T = 48m	-40°C
TMSOTf (0.2 µL neat, 0.11 eqv)	T = 1h8m	-40°C
TMSOTf (0.2 µL neat, 0.11 eqv)	T = 1h20m	-30°C
TMSOTf (0.2 µL neat, 0.11 eqv)	T = 1h31m	-30°C

After the last addition of TMSOTf, the reaction mixture color changed to light purple, and the TLC profile changed significantly. The reaction was quenched by addition of saturated $NaHCO_3$ solution (3 mL) at -30°C. The reaction mixture was then stirred at RT for 10 minutes. The aqueous phase was extracted with DCM (3 mL x 3). The combined organic phase was washed with DI H_2O, brine, and dried over anhydrous Na_2SO_4. The solvent was removed to afford crude mixture as a tan, foamy solid (13 mg). The crude mixture was separated by pTLC (1/2 plate, 6% MeOH/DCM, 1 elution). The bands were scraped from the plate in order of increasing Rf value. The silica gel was rinsed with 10% MeOH/DCM. The solvent was removed to afford residue, which was dried on hi-vac and analyzed by ^1H NMR. All the bands yielded less than 1 mg of material, except B10 (3 mg). The ^1H NMR spectra of the bands are shown below.

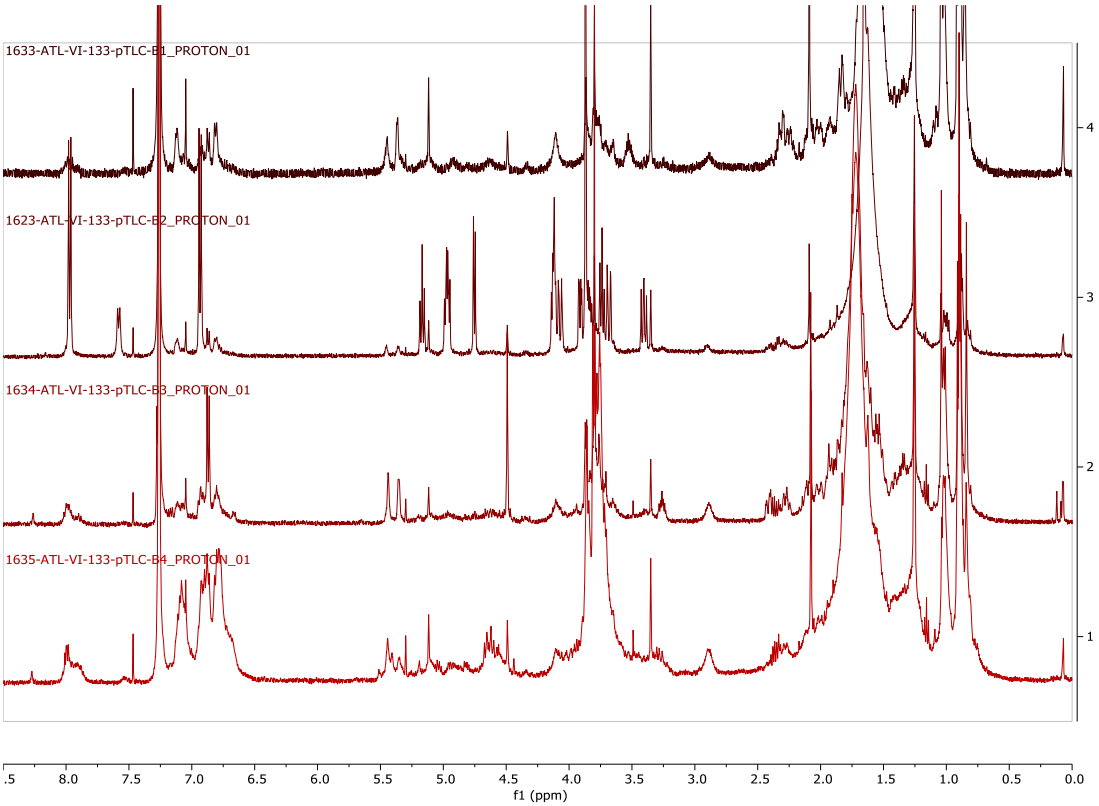
1633-ATL-VI-133-pTLC-B1_PROTON_01
1623-ATL-VI-133-pTLC-B2_PROTON_01
1634-ATL-VI-133-pTLC-B3_PROTON_01
1635-ATL-VI-133-pTLC-B4_PROTON_01
4
3
2
1
.5 8.0 7.5 7.0 6.5 6.0 5.5 5.0 4.5 4.0 3.5 3.0 2.5 2.0 1.5 1.0 0.5 0.0
f1 (ppm)

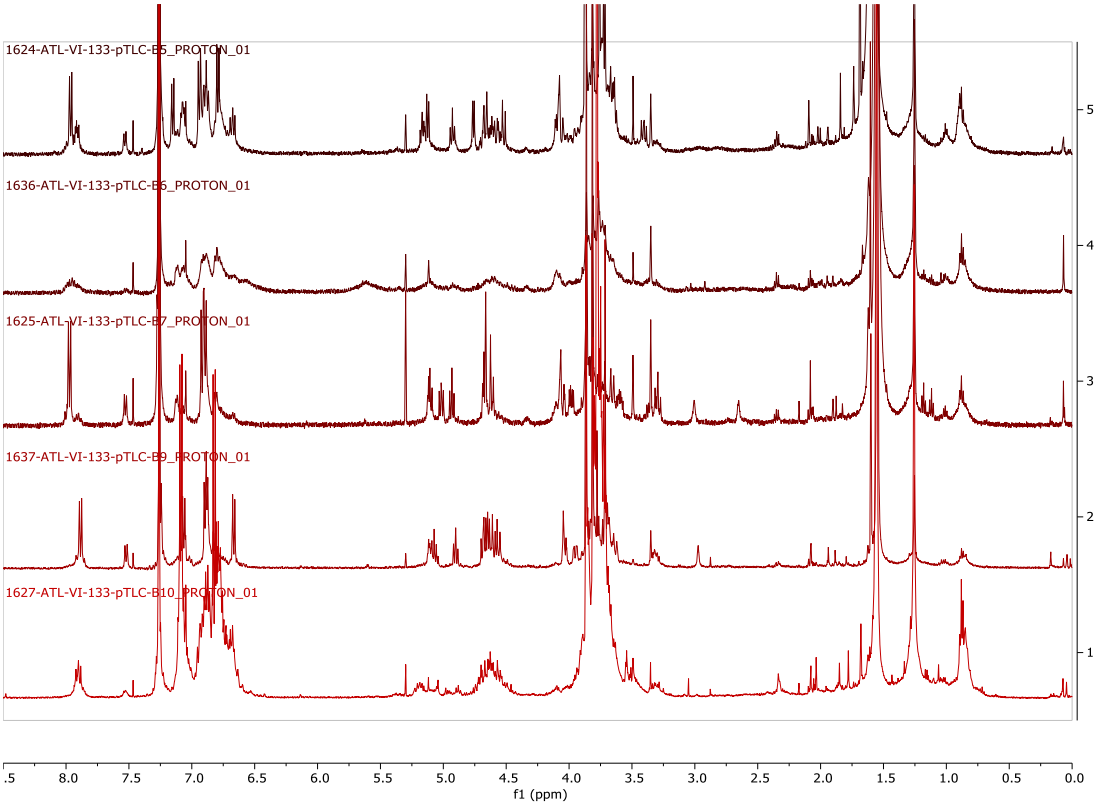
1624-ATL-VI-133-pTLC-B5_PROTON_01
1636-ATL-VI-133-pTLC-B6_PROTON_01
1625-ATL-VI-133-pTLC-B7_PROTON_01
1637-ATL-VI-133-pTLC-B9_PROTON_01
1627-ATL-VI-133-pTLC-B10_PROTON_01
5
4
3
2
1
.5 8.0 7.5 7.0 6.5 6.0 5.5 5.0 4.5 4.0 3.5 3.0 2.5 2.0 1.5 1.0 0.5 0.0
f1 (ppm)

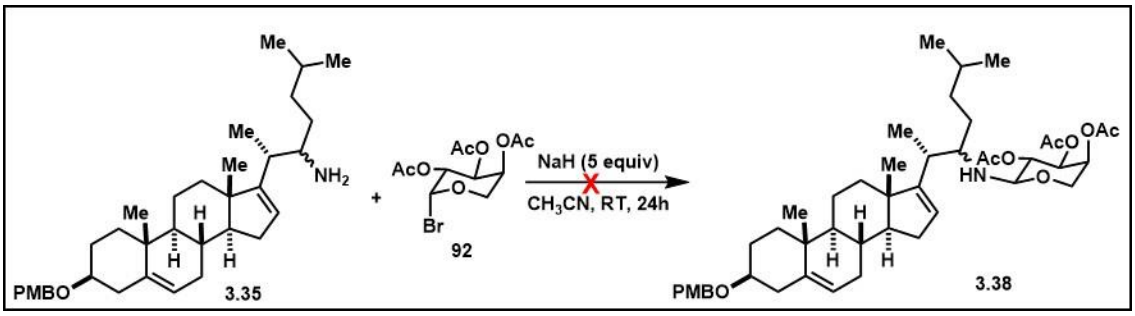

To a solution of homoallylic amines **3.35** (15.0 mg, 0.00288 mmol) in anhydrous acetonitrile (0.2 mL) and DCM (0.1 mL, to help with solubility of amine **3.35**) was added NaH (8.9 mg, 0.217 mmol). The reaction mixture was stirred at RT for 10 minutes, then to it was added compound **92** (14.7 mg, 0.0433 mmol, dissolved in 110 µL anhydrous acetonitrile). The reaction mixture was stirred at RT, and the reaction progress was monitored by TLC (5% MeOH/DCM, UV, CAM stain). After 24h, no changes were observed by TLC. The reaction mixture was neutralized with 1M HCl solution, extracted with EtOAc (5 mL x 3). The combined organic phase was washed with brine, dried over Na_2SO_4, and filtered. The solvent was removed *in vacuo* to afford crude mixture as a tan gel (31.5 mg). ^{1}H NMR analysis did not show any desired product.

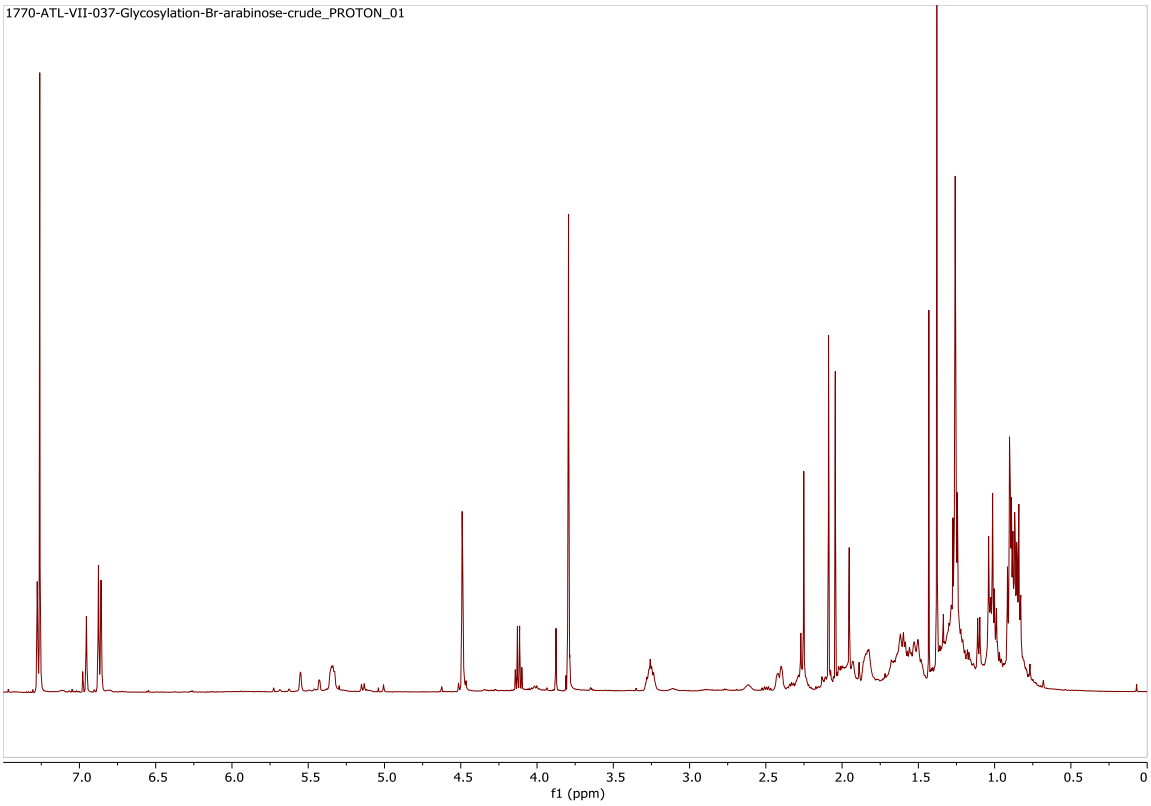

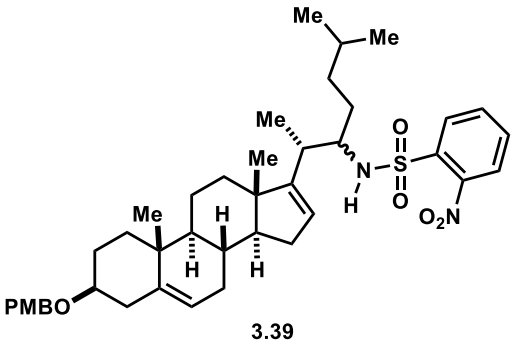

3.39

To a solution of homoallylic amine **3.35** (33.0 mg, 0.0634 mmol) in anhydrous DCM (0.32 mL) was added NEt_3 (8.9 µL, 0.0634 mmol). The reaction mixture was cooled to 0°C in an ice bath. To the reaction mixture was then added 2-nitrobenzenesulfonyl chloride solution (14.1 mg, 0.0634 mmol, dissolved in 70 µL DCM) dropwise. The reaction mixture was stirred at 0°C for 15 minutes, then allowed to warmed up to RT. The reaction progress was monitored by TLC (2.5 % MeOH/DCM/, UV, CAM stain). After 1 hour 10 minutes, TLC showed the reaction was almost completed. The reaction was quenched with 1N HCl

solution (3 mL). The aqueous phase was extracted with DCM (3 mL x 3). The combined organic phase was washed with brine, dried over anhydrous Na_2SO_4. The solvent was removed *in vacuo* to afford crude mixture as a white, foamy solid, which was purified through silica gel column chromatography (eluted with DCM/hexanes gradient from 50% to 100%) to afford the desired Ns-amines **3.39** was a white, foamy solid (38.8 mg, 87% yield). ^{1}H NMR (500 MHz, Chloroform-d) δ 8.18 – 8.08 (m, 0H), 7.91 – 7.85 (m, 0H), 7.72 (pd, J = 7.5, 1.7 Hz, 1H), 5.41 – 5.38 (m, 0H), 5.35 (dd, J = 4.7, 2.7 Hz, 0H), 3.80 (d, J = 1.3 Hz, 1H), 3.26 (tt, J = 10.4, 4.1 Hz, 0H), 2.47 – 2.37 (m, 1H), 2.27 (t, J = 11.5 Hz, 0H), 1.04 (s, 1H), 0.97 (d, J = 7.0 Hz, 1H), 0.79 (s, 1H), 0.72 (dd, J = 17.1, 6.6 Hz, 1H). ^{13}C NMR (101 MHz, Chloroform-d) δ 159.20, 156.76, 147.85, 141.47, 135.70, 133.30, 132.93, 131.27, 130.53, 129.29, 125.43, 125.09, 121.41, 113.93, 78.32, 77.36, 69.73, 58.63, 58.04, 55.43, 50.75, 46.88, 39.34, 37.73, 37.35, 37.26, 34.89, 34.74, 31.68, 31.32, 30.54, 28.58, 27.87, 27.83, 22.74, 22.42, 20.85, 19.44, 16.90, 14.72. Compound **3.39** was characterized fully through 2D NMR. See **Chapter appendix** for ^{1}H and ^{13}C NMR spectra, **Appendix** for 2D NMR spectra.

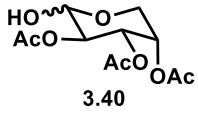

3.40

To a solution of compound **34** (1.0 g, 3.14 mmol) in anhydrous THF (10 mL) under N_2 at RT was added benzyl amine (515.0 µL, 4.71 mmol). The reaction mixture was stirred at RT, and the reaction progress was monitored by TLC (5% MeOH/DCM, UV, KMnO4 stain). After 14h, TLC showed the reaction was almost completed. The reaction mixture was diluted with DCM (10 mL), washed with cold 0.2M HCl (10 mL x 2), then saturated $NaHCO_3$ solution (10 mL), DI H_2O (10 mL), and brine. The organic phase was dried over

anhydrous Na_2SO_4, and filtered. The solvent was removed to afford crude mixture, which was then purified through silica gel column chromatography (eluted with EtOAc/hexanes gradient) to afford desired product **3.40** as a mixture of both anomer (550.0 mg, 63% yield). ^{1}H NMR (500 MHz, Chloroform-d) δ 6.27 (d, J = 3.8 Hz, 1H), 5.48 (s, 1H), 5.41 (dd, J = 10.5, 3.5 Hz, 1H), 5.34 (dt, J = 3.7, 1.9 Hz, 1H), 5.33 – 5.31 (m, 1H), 5.28 (q, J = 2.7, 2.1 Hz, 1H), 5.20 (dd, J = 10.5, 3.5 Hz, 1H), 5.09 – 5.07 (m, 1H), 4.62 (s, 1H), 4.23 – 4.17 (m, 1H), 4.03 (dd, J = 13.4, 2.5 Hz, 1H), 3.99 (d, J = 13.3 Hz, 1H), 3.80 (dd, J = 13.2, 2.1 Hz, 1H), 3.71 (dd, J = 13.0, 2.3 Hz, 1H), 3.69 – 3.65 (m, 1H), 3.54 (d, J = 9.0 Hz, 1H), 2.90 (s, 1H), 2.15 (s, 1H), 2.14 (s, 3H), 2.11 (s, 1H), 2.10 (s, 3H), 2.03 (s, 1H), 2.02 (s, 3H). ^{13}C NMR (126 MHz, Chloroform-d) δ 170.53, 170.48, 170.20, 170.14, 96.34, 91.15, 71.46, 70.11, 69.16, 68.76, 68.74, 68.06, 66.98, 64.27, 60.59, 21.19, 21.09, 21.05, 20.98, 20.87, 20.78, 14.33. Compound **3.40** was characterized fully through 2D NMR. See **Chapter appendix** for ^{1}H and ^{13}C NMR spectra, **Appendix** for 2D NMR spectra.

Entry 5, Error! Reference source not found. (ATL-VII-059)

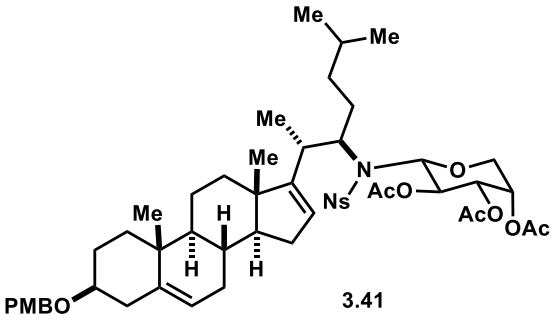

3.41

To a clear, colorless solution of PPh_3 (37.2 mg, 142 µmol) in anhydrous THF (100 µL) at -78°C under N_2 atmosphere was added DIAD solution (28 µL DIAD dissolved in 28 µL anhydrous THF, 142 µmol) dropwise slowly. The bright, clear yellow solution was stirred at -78°C for 40 minutes after which the solution turned cloudy and pale yellow and very thick, then the mixture was allowed to warm up to -40°C. To the reaction mixture was

added L-arabinose hemiacetal **3.40** solution (23.5 mg, 85 µmol, dissolved in 46 µL of THF). The reaction mixture was stirred for 15 minutes at -40°C, then the mixture of homoallylic nosyl amine isomers **3.39** (20.0 mg, 28.4 µmol dissolved in 150 µL THF) was added dropwise. The reaction mixture was stirred at -30°C and allowed to slowly warmed up in the cold bath to RT (the reaction temperature reached 0°C after 2 hours, then up to RT overnight). After 26 hours, the reaction was heated to 50°C for 3 hours, then to 60°C for 11 hours. The reaction mixture was then cooled to RT, the solvent was removed *in vacuo* to afford crude mixture as a tan, sticky gel (101.5 mg). During the reaction time (~60 hours), the reaction progress was monitored by TLC (30% EtOAc, 25% DCM/hexanes, UV, CAM stain).

Purification: The crude mixture was purified through silica gel column chromatography (with EtOAc/hexanes step gradient from 20% to 40%) to afford recovered homoallylic nosyl amines **3.39** (6.0 mg, 30%), a mixture of glycosylated products (13.0 mg, 47%). The mixture of glycosylate products was further purified through HPLC (C8(2) Phenomenex semiprep column, acetonitrile: 0.1% formic acid in water gradient from 65% to 100% acetonitrile. Two main glycosylated products were isolated in small amount. The HPLC sample (prepared in methanol) resulted in crystals that was then analyzed through X-ray crystallography to confirm the product's identity (See **Chapter appendix**).

3.41: ^{1}H NMR (500 MHz, Chloroform-d) δ 8.25 (bs, 1H), 7.68 – 7.57 (m, 2H), 7.41 (bs, 1H), 7.31 – 7.23 (m, 2H), 6.91 – 6.82 (m, 2H), 6.41 (bs, 1H), 5.44 – 5.32 (m, 2H), 5.27 (s, 1H), 4.97 (bs, 1H), 4.62 (bs, 1H), 4.49 (s, 3H), 4.07 (d, J = 11.9 Hz, 1H), 3.98 (bs, 1H), 3.80 (s, 3H), 3.59 (bs, J = 13.1 Hz, 1H), 3.26 (td, J = 11.2, 5.6 Hz, 1H), 2.51 (bs, 1H), 2.45 – 2.38 (m, 1H), 2.32 – 2.21 (m, 5H), 2.12 – 2.05 (m, 5H), 2.03 (s, 5H), 2.01 – 1.98 (m, 1H),

1.98 – 1.89 (m, 2H), 1.85 (d, J = 13.3 Hz, 1H), 1.79 (d, J = 11.8 Hz, 1H), 1.69 (s, 1H), 1.64 – 1.47 (m, 3H), 1.38 – 1.28 (m, 1H), 1.28 – 1.18 (m, 3H), 1.12 (d, J = 7.0 Hz, 3H), 1.05 (s, 3H), 1.03 – 0.93 (m, 2H), 0.87 (s, 3H), 0.67 – 0.55 (m, 6H). See **Chapter appendix** for ^{1}H and ^{13}C NMR spectra, **Appendix** for 2D NMR spectra.

Entry **3**, Error! Reference source not found.

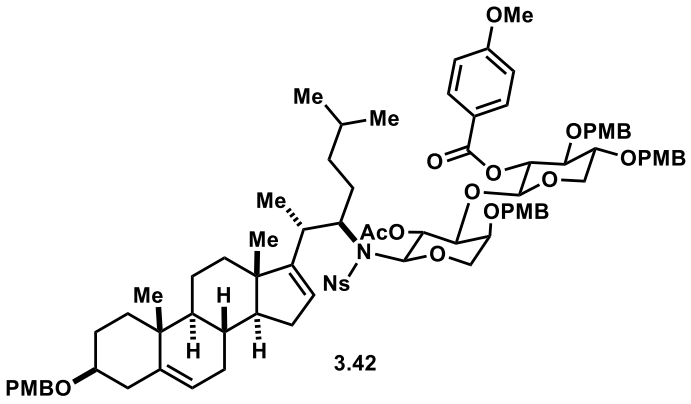

3.42

To a clear, colorless solution of PPh_3 (59.5 mg, 227 µmol) in anhydrous THF (1.0 mL) at -78°C under N_2 atmosphere was added DIAD solution (44.4 µL DIAD dissolved in 55.6 µL anhydrous THF, 227 µmol) dropwise slowly. The bright, clear yellow solution was stirred at -78°C for 40 minutes after which the solution turned cloudy and pale yellow and very thick. To the reaction mixture a mixture of disaccharide hemiacetal **98** (116.2 mg, 141 µmol) and the mixture of homoallylic nosyl amine isomers **3.39** solution (40.0 mg, 56.7 µmol, dissolved in 800 µL THF) was added dropwise slowly. The reaction mixture was stirred at -78°C for 2 hours, then allowed to slowly warmed up in the cold bath to RT (the reaction temperature reached 0°C after 5 hours, then up to RT overnight). The reaction temperature was maintained at RT for 15.5 hours before being heated to 60°C for another 48h. The reaction mixture was then cooled to RT, the solvent was removed *in vacuo* to afford crude mixture as a tan, sticky gel (270 mg). During the reaction time (~74 hours),

the reaction progress was monitored by TLC (30% EtOAc, 25% DCM/hexanes, UV, CAM stain).

Purification: The crude mixture was purified through silica gel column chromatography (with EtOAc/hexanes step gradient from 20% to 100%) to afford recovered homoallylic nosyl amines **3.39** (31.8 mg, 79%), a mixture of glycosylated products (16.4 mg, 19%) and some derivative of disaccharide moiety (75.5 mg). The mixture of glycosylate products was further purified through HPLC (C8(2) Phenomenex semiprep column, acetonitrile: 0.1% formic acid in water gradient from 65% to 100% acetonitrile. Three glycosylated products were isolated (F3-3.9 mg; F4-1.3 mg, F5-1.2 mg). F3 was characterized as the desired glycosylated product **3.42** through HRMS, and 2D NMR (5% yield). The other products have not been definitively characterized due to the small amount of material.

3.42: ^{1}H NMR (500 MHz, Acetonitrile-d3) δ 8.31 (d, J = 8.0 Hz, 1H), 7.98 – 7.92 (m, 2H), 7.74 – 7.63 (m, 2H), 7.48 (d, J = 7.9 Hz, 1H), 7.40 (d, J = 8.2 Hz, 2H), 7.34 – 7.28 (m, 2H), 7.25 (d, J = 8.6 Hz, 1H), 7.03 – 6.97 (m, 4H), 6.94 – 6.86 (m, 5H), 6.67 (d, J = 8.7 Hz, 1H), 6.07 (d, J = 10.0 Hz, 1H), 5.36 (d, J = 5.0 Hz, 1H), 5.02 (dd, J = 8.7, 7.3 Hz, 1H), 4.71 – 4.61 (m, 4H), 4.60 (s, 2H), 4.53 (d, J = 9.2 Hz, 1H), 4.49 (d, J = 10.9 Hz, 1H), 4.45 (s, 2H), 4.03 – 3.96 (m, 2H), 3.87 (s, 4H), 3.79 – 3.77 (m, 4H), 3.74 – 3.70 (m, 1H), 3.69 (s, 3H), 3.68 – 3.62 (m, 1H), 3.48 (d, J = 12.9 Hz, 1H), 3.32 (dd, J = 11.8, 8.7 Hz, 1H), 3.18 (td, J = 11.2, 5.5 Hz, 1H), 2.38 (dd, J = 12.6, 4.3 Hz, 1H), 2.25 (s, 1H), 2.22 – 2.17 (m, 1H), 2.17 – 2.09 (m, 1H), 2.08 – 2.00 (m, 1H), 1.92 – 1.82 (m, 3H), 1.72 – 1.60 (m, 5H), 1.59 – 1.52 (m, 2H), 1.44 (dd, J = 24.8, 11.6 Hz, 3H), 1.30 – 1.23 (m, 1H), 1.20 (t, J = 7.1 Hz, 3H), 1.04 (s, 3H), 1.02 – 0.92 (m, 4H), 0.75 (s, 3H), 0.60 (d, J = 6.6 Hz, 3H), 0.57 (d, J = 6.6 Hz, 3H), 0.37 (s, 1H). HRMS calcd for $C_{85}H_{104}N_2O_{20}S + H^+$- $[M+H]^+$: 1505.6976; found

1505.6943. See **Chapter appendix** for ^{1}H and ^{13}C NMR spectra, **Appendix** for 2D NMR spectra.

III.6 Chapter appendix

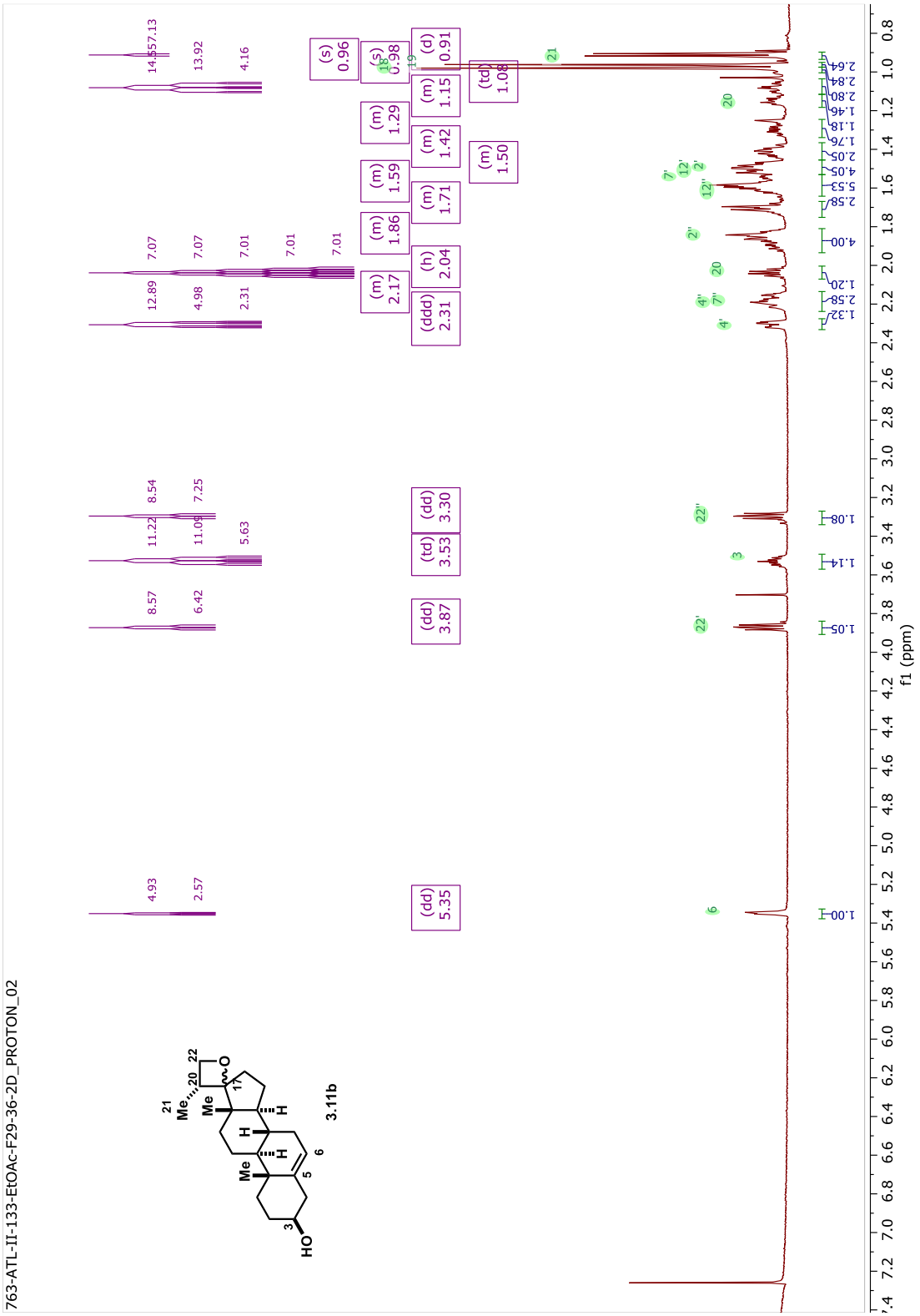

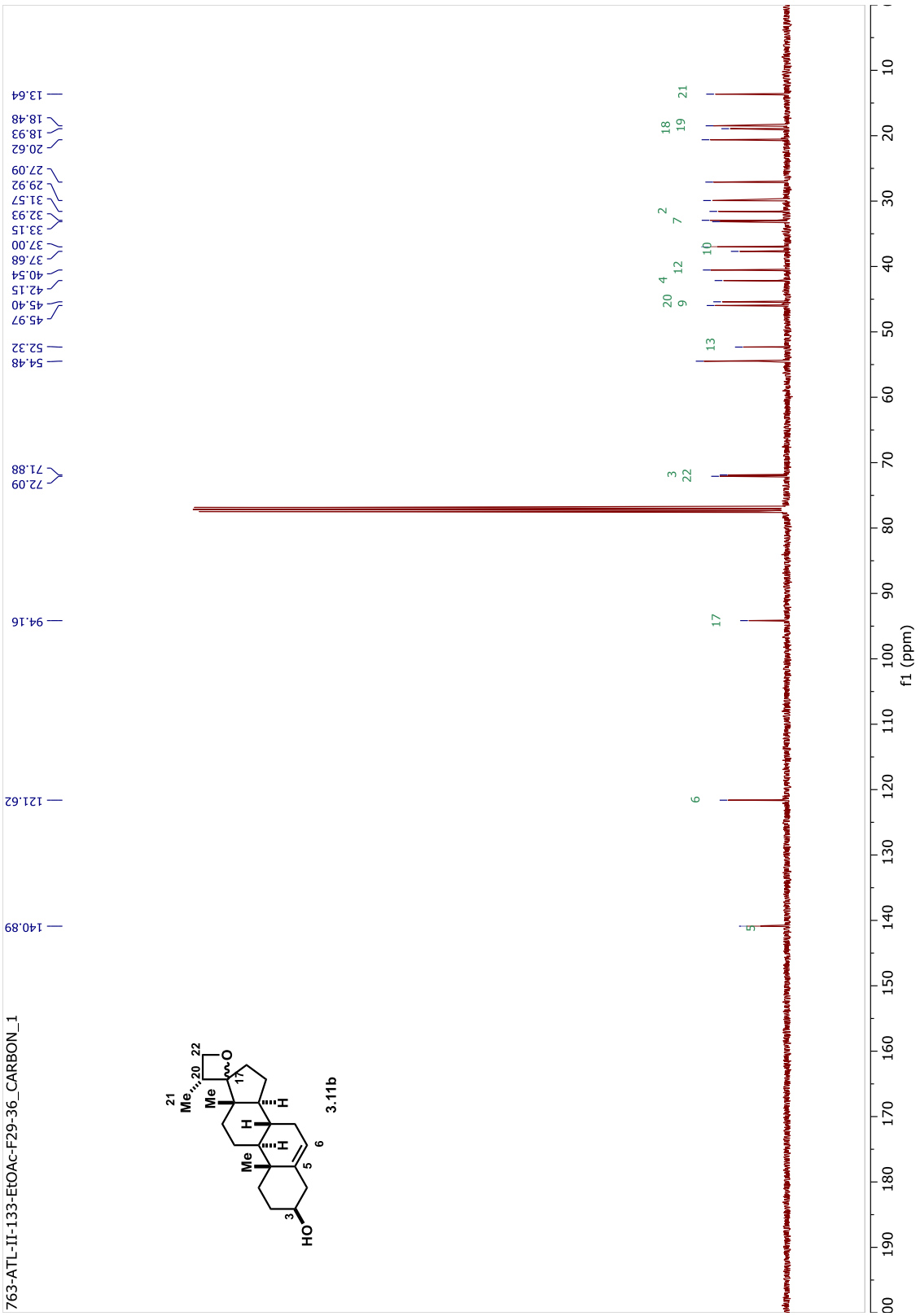
763-ATL-II-133-EtOAc-F29-36_CARBON_1
140.89
121.62
94.16
72.09
71.88
54.48
52.32
45.97
45.40
42.15
40.54
37.68
37.00
33.15
32.93
31.57
29.92
27.09
20.62
18.93
18.48
13.64
3.11b
f1 (ppm)

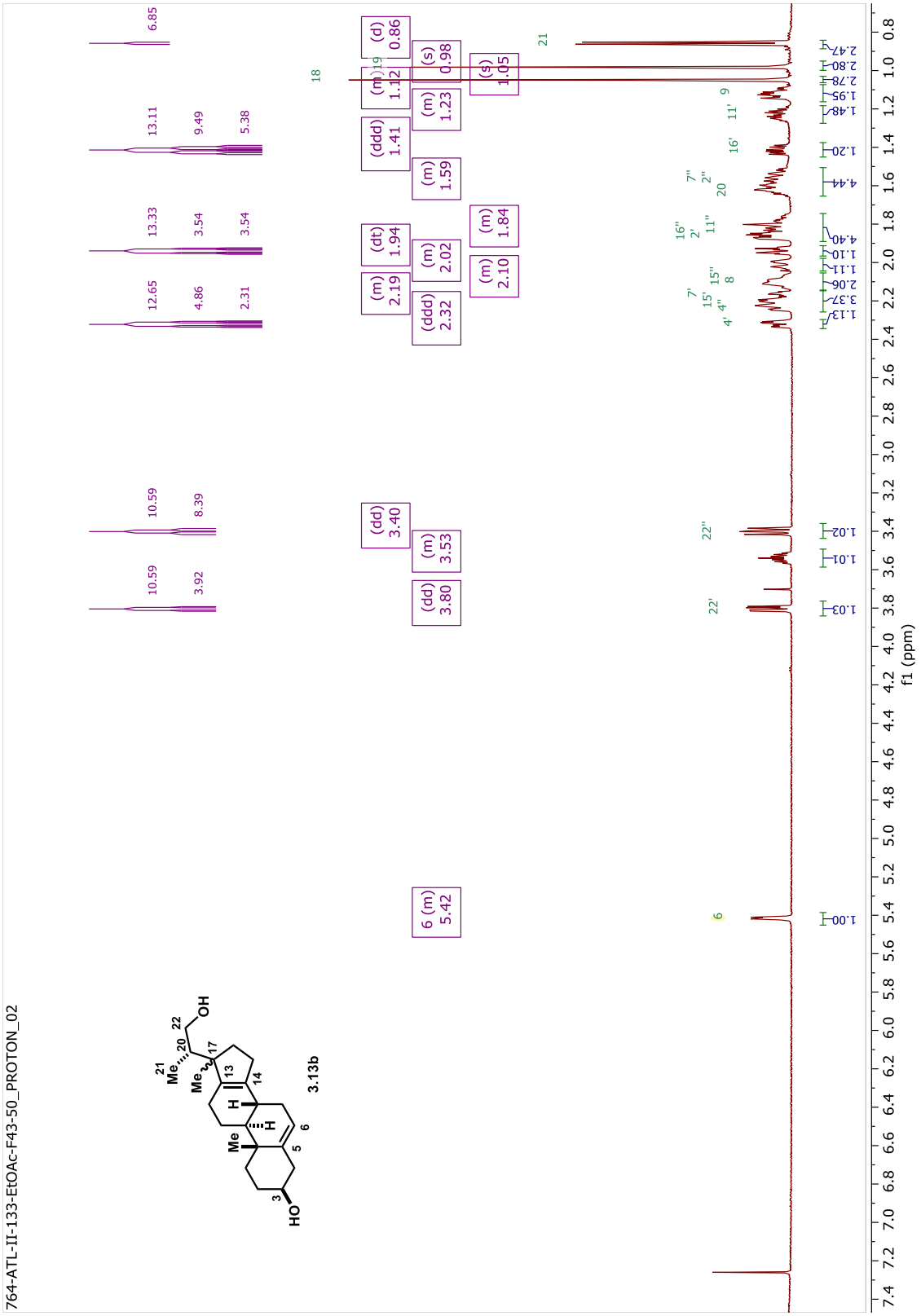
764-ATL-II-133-EtOAc-F43-50_PROTON_02
3.13b
f1 (ppm)

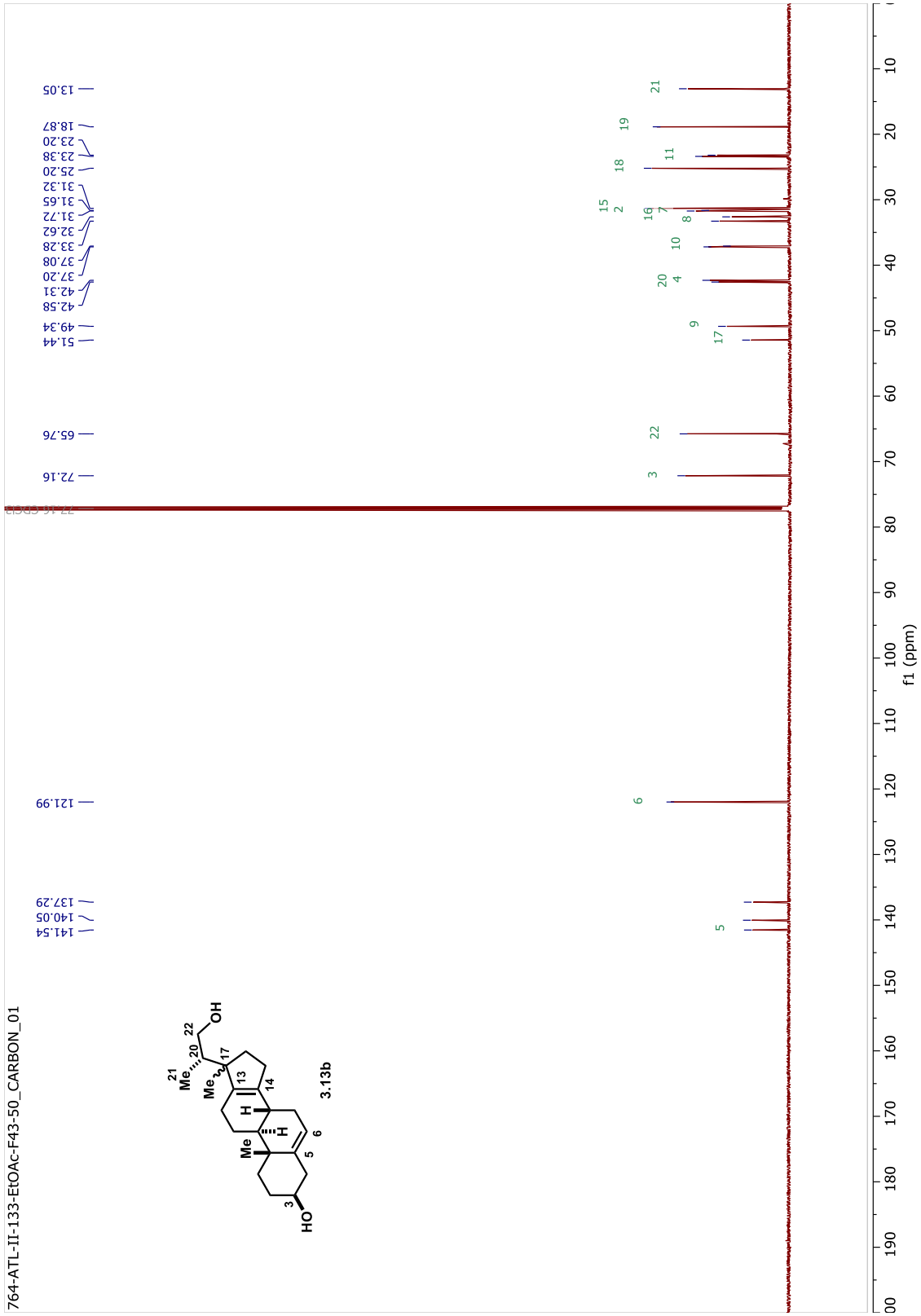
764-ATL-II-133-EtOAc-F43-50_CARBON_01
3.13b
f1 (ppm)

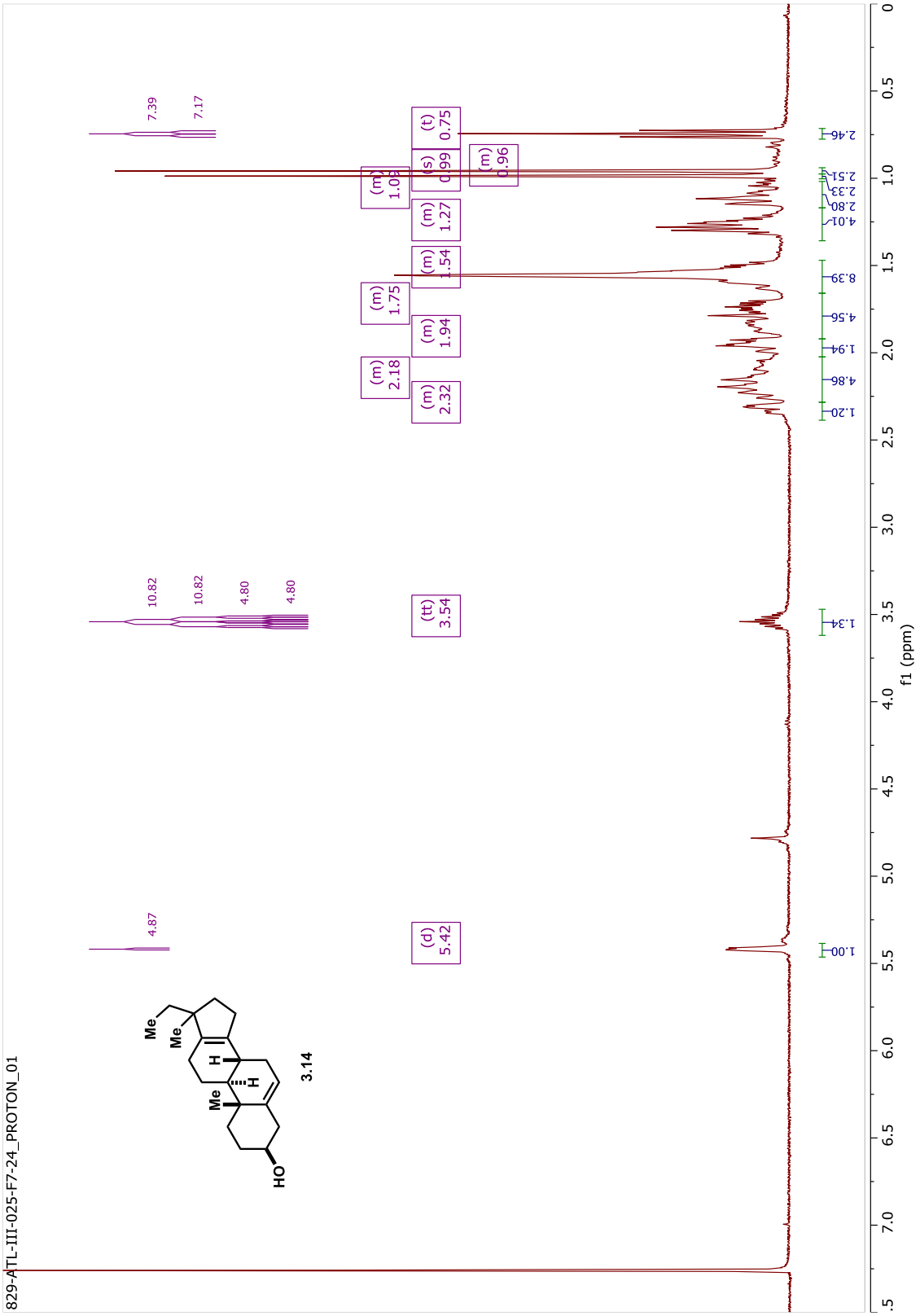
829-ATL-III-025-F7-24_PROTON_01
Me
Me
H
H
Me
HO
3.14
4.87
10.82
10.82
4.80
4.80
7.39
7.17
(d) 5.42
(tt) 3.54
(m) 2.32
(m) 2.18
(m) 1.94
(m) 1.75
(m) 1.54
(m) 1.27
(m) 1.08
(s) 0.99
(t) 0.75
(m) 0.96
1.00
1.34
1.20
4.86
1.94
4.56
8.39
1.54
4.01
2.80
2.33
2.51
2.46
f1 (ppm)

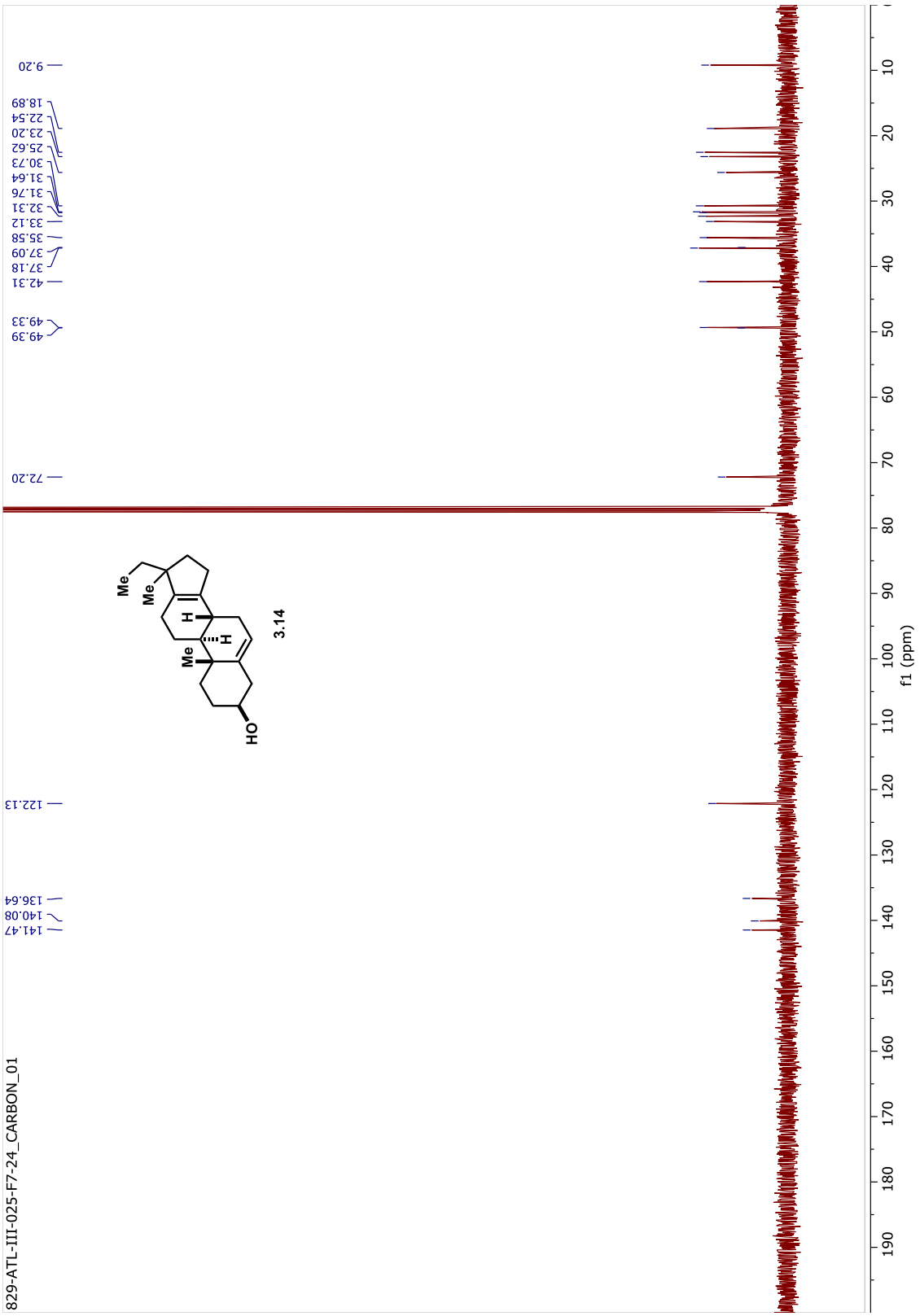
829-ATL-III-025-F7-24_CARBON_01
141.47
140.08
136.64
122.13
72.20
49.39
49.33
42.31
37.18
37.09
35.58
33.12
32.31
31.76
31.64
30.73
25.62
23.20
22.54
18.89
9.20
Me
Me
H
H
Me
HO
3.14
f1 (ppm)

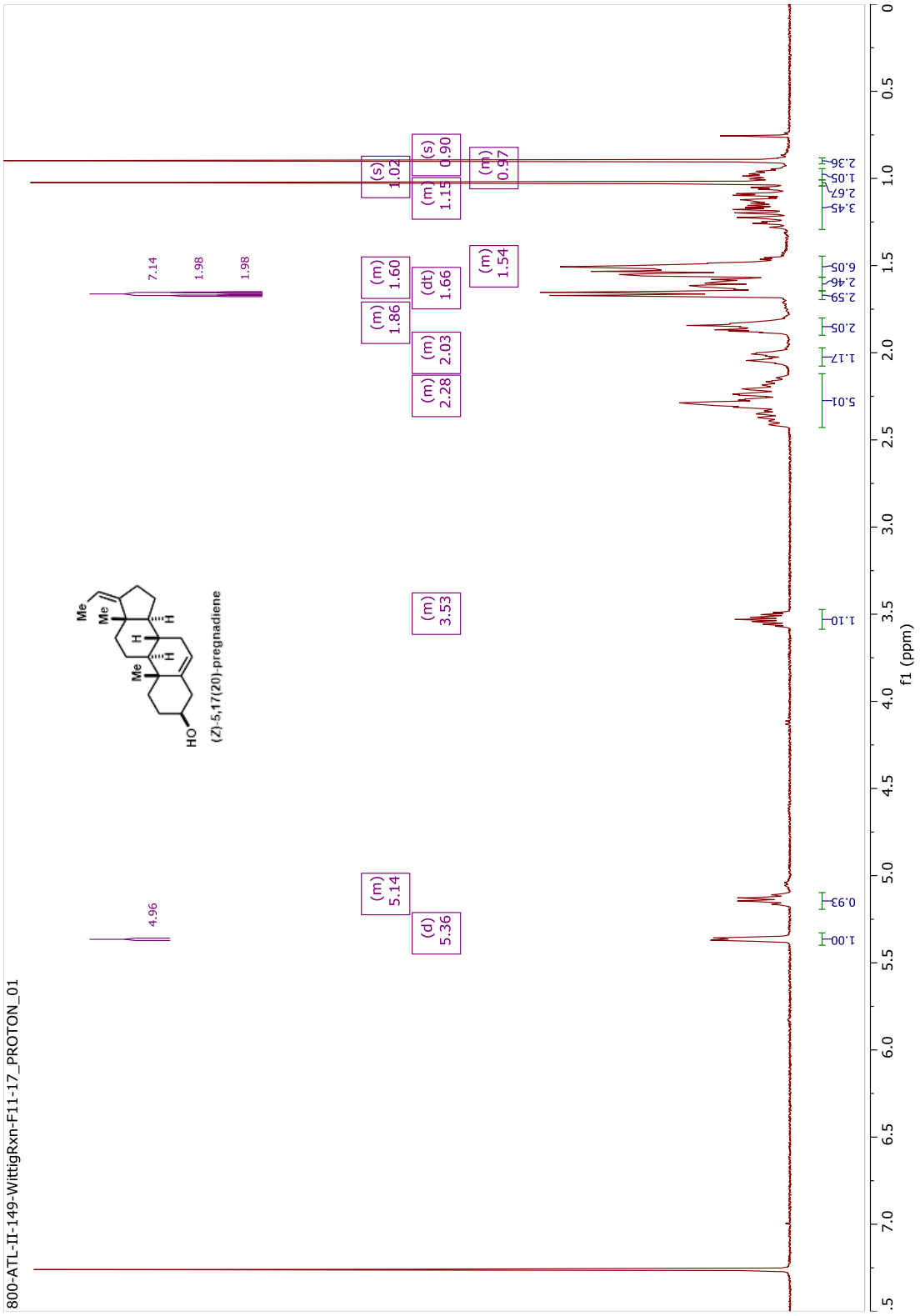
800-ATL-IT-149-WittigRxn-F11-17_PROTON_01
(Z)-5,17(20)-pregnadiene
f1 (ppm)

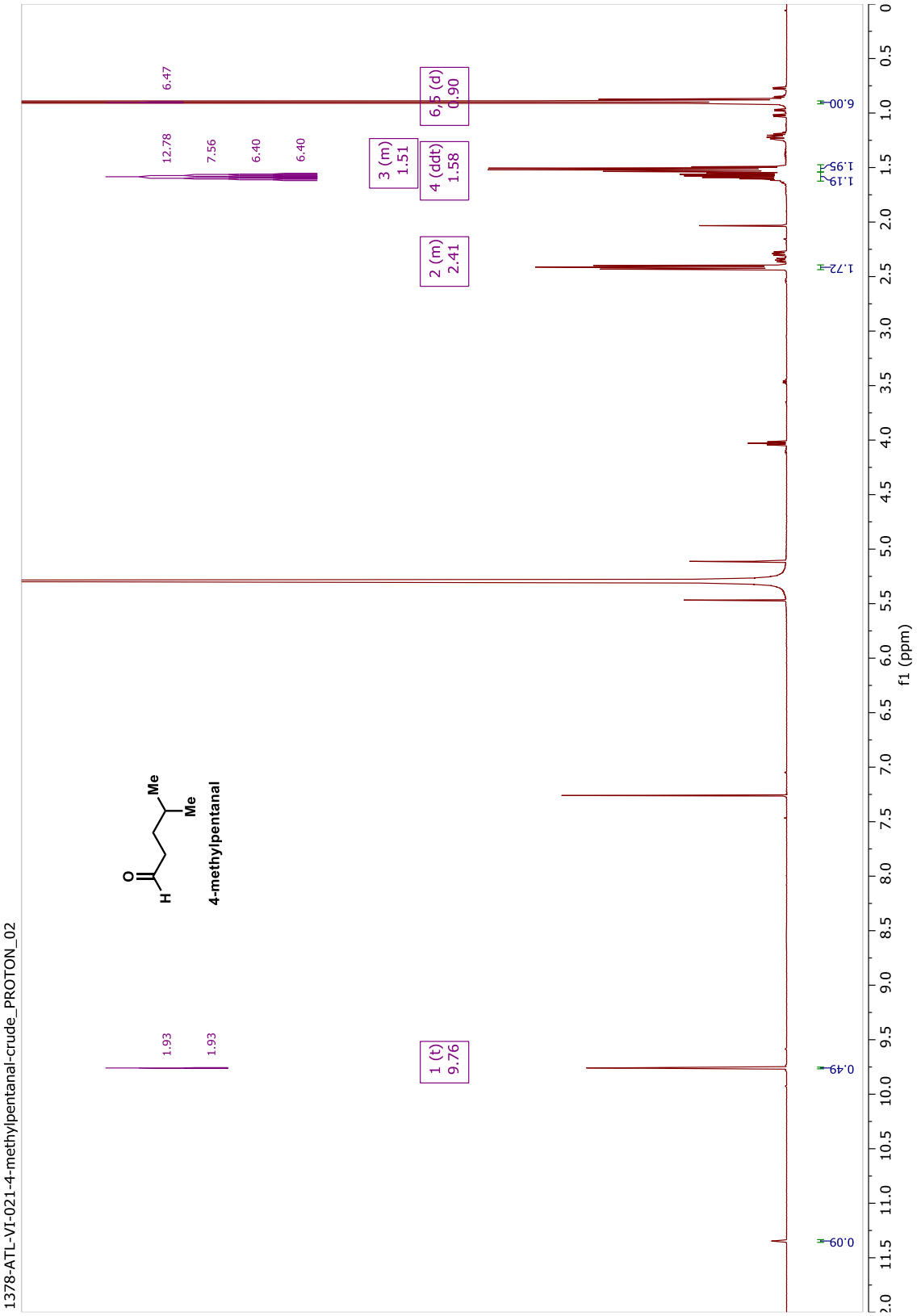
1378-ATL-VI-021-4-methylpentanal-crude_PROTON_02
4-methylpentanal
Me
Me
O
H
1.93
1.93
12.78
7.56
6.40
6.40
6.47
1 (t)
9.76
2 (m)
2.41
3 (m)
1.51
4 (ddt)
1.58
6.5 (d)
0.90
0.49
1.72
1.95
1.19
6.00
0.09
f1 (ppm)

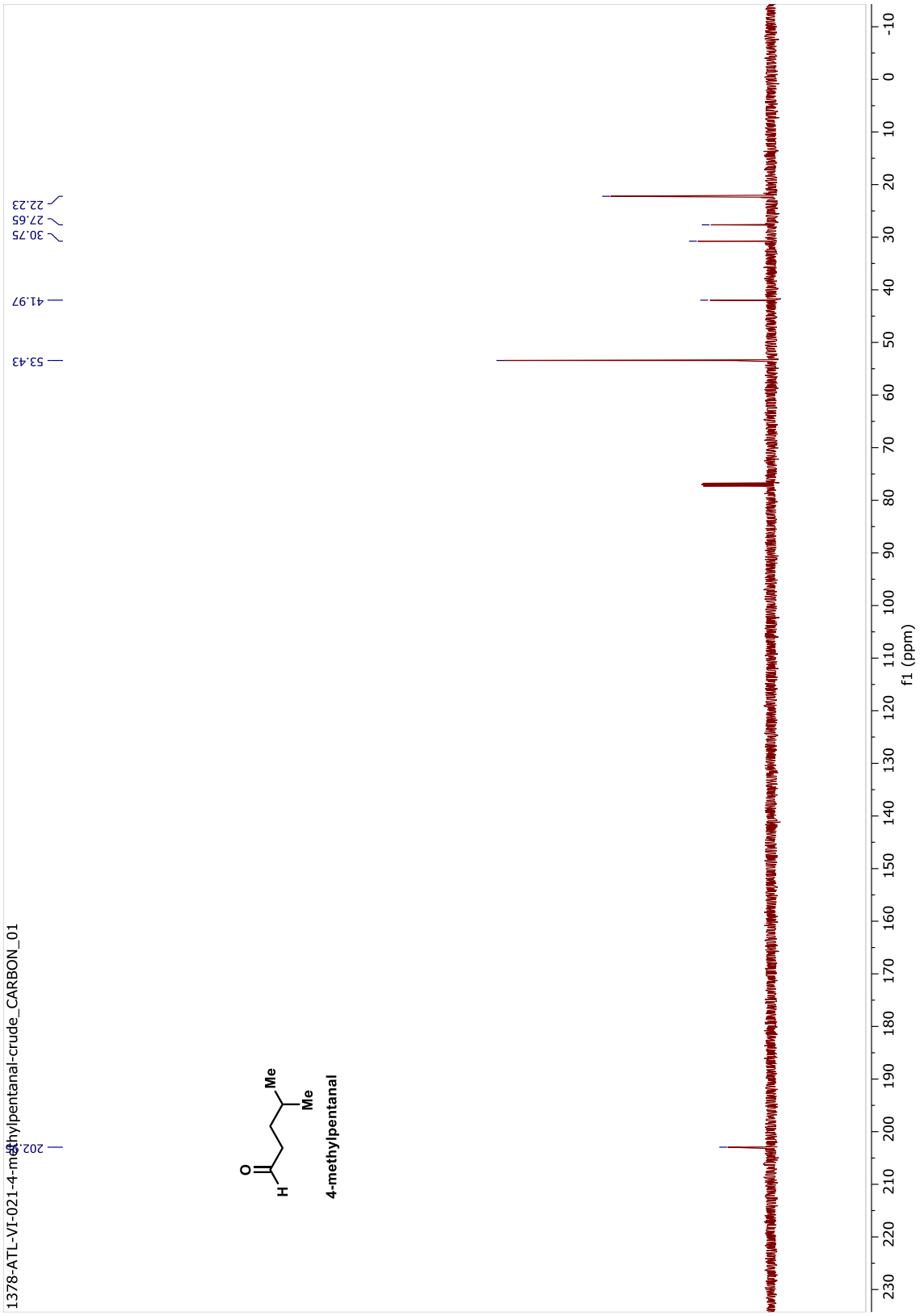
1378-ATL-VI-021-4-methylpentanal-crude_CARBON_01
202.48
53.43
41.97
30.75
27.65
22.23
Me
Me
O
H
4-methylpentanal
f1 (ppm)

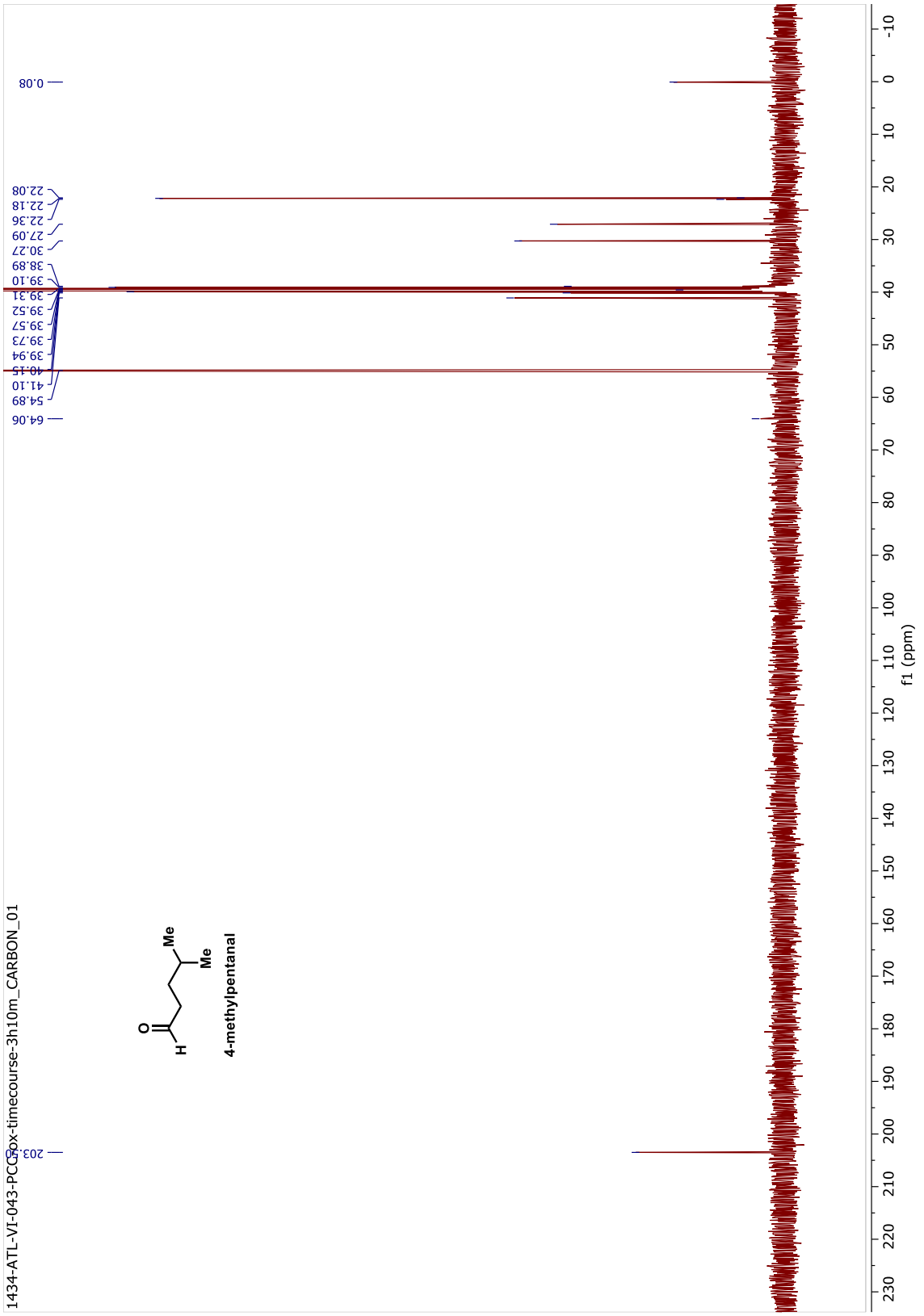
1434-ATL-VI-043-PCCox-timecourse-3h10m_CARBON_01
4-methylpentanal
O
H
Me
Me
203.50
64.06
54.89
41.10
40.15
39.94
39.73
39.57
39.52
39.31
39.10
38.89
30.27
27.09
22.36
22.18
22.08
0.08
f1 (ppm)

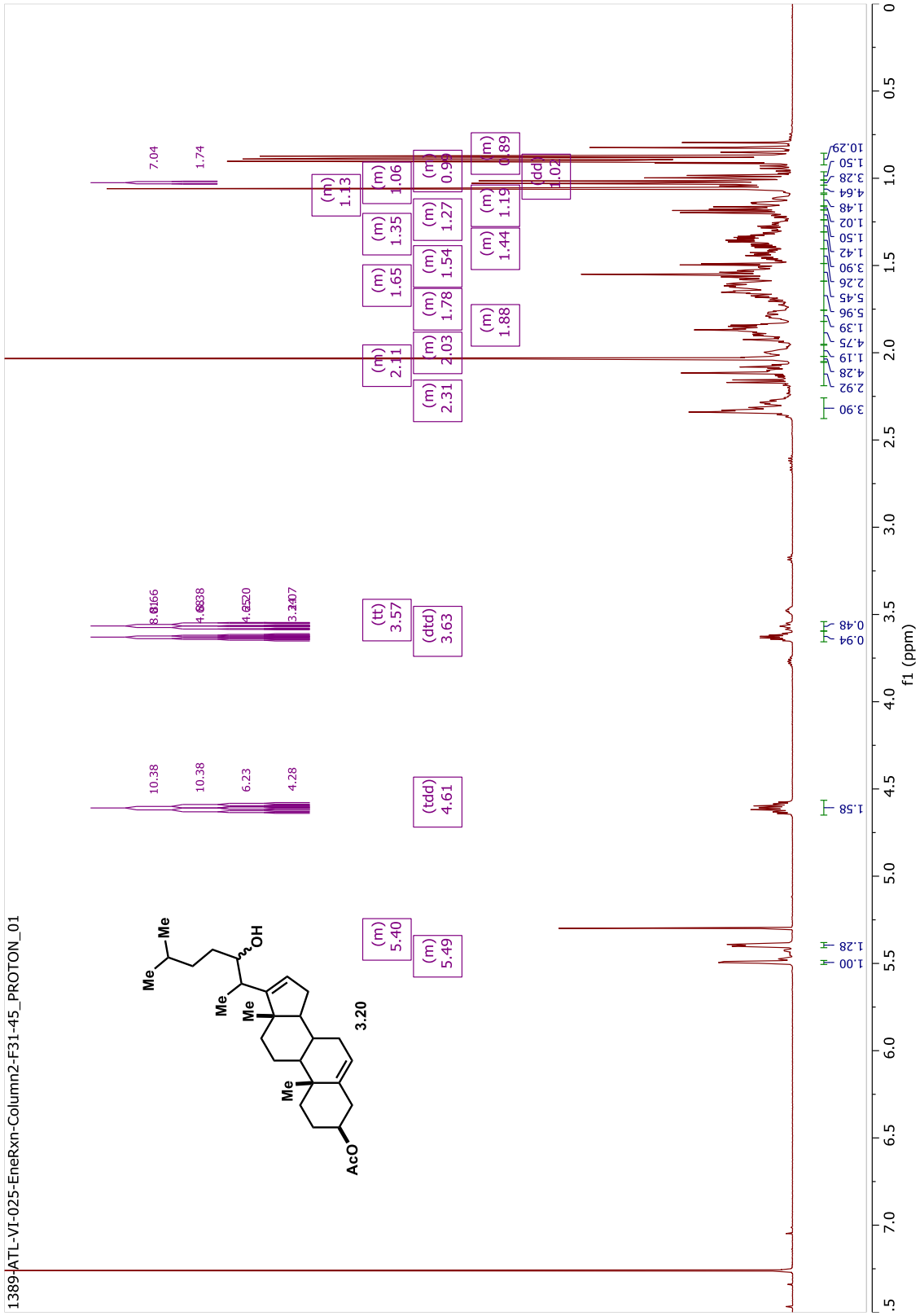
1389-ATL-VI-025-EneRxn-Column2-F31-45_PROTON_01
f1 (ppm)
3.20
AcO
OH
Me
10.38
10.38
6.23
4.28
7.04
1.74
(m) 5.40
(m) 5.49
(tdd) 4.61
(tt) 3.57
(dtd) 3.63
(m) 2.11
(m) 2.03
(m) 2.31
(m) 1.65
(m) 1.78
(m) 1.54
(m) 1.35
(m) 1.27
(m) 1.13
(m) 1.06
(m) 0.99
(m) 1.88
(m) 1.44
(m) 1.19
(m) 0.89
(dd) 1.02
1.58
1.00
1.28
0.94
0.48
3.90
2.92
4.28
1.19
4.75
1.39
5.96
5.45
2.26
3.90
1.42
1.50
1.02
1.48
4.64
3.28
1.50
10.29

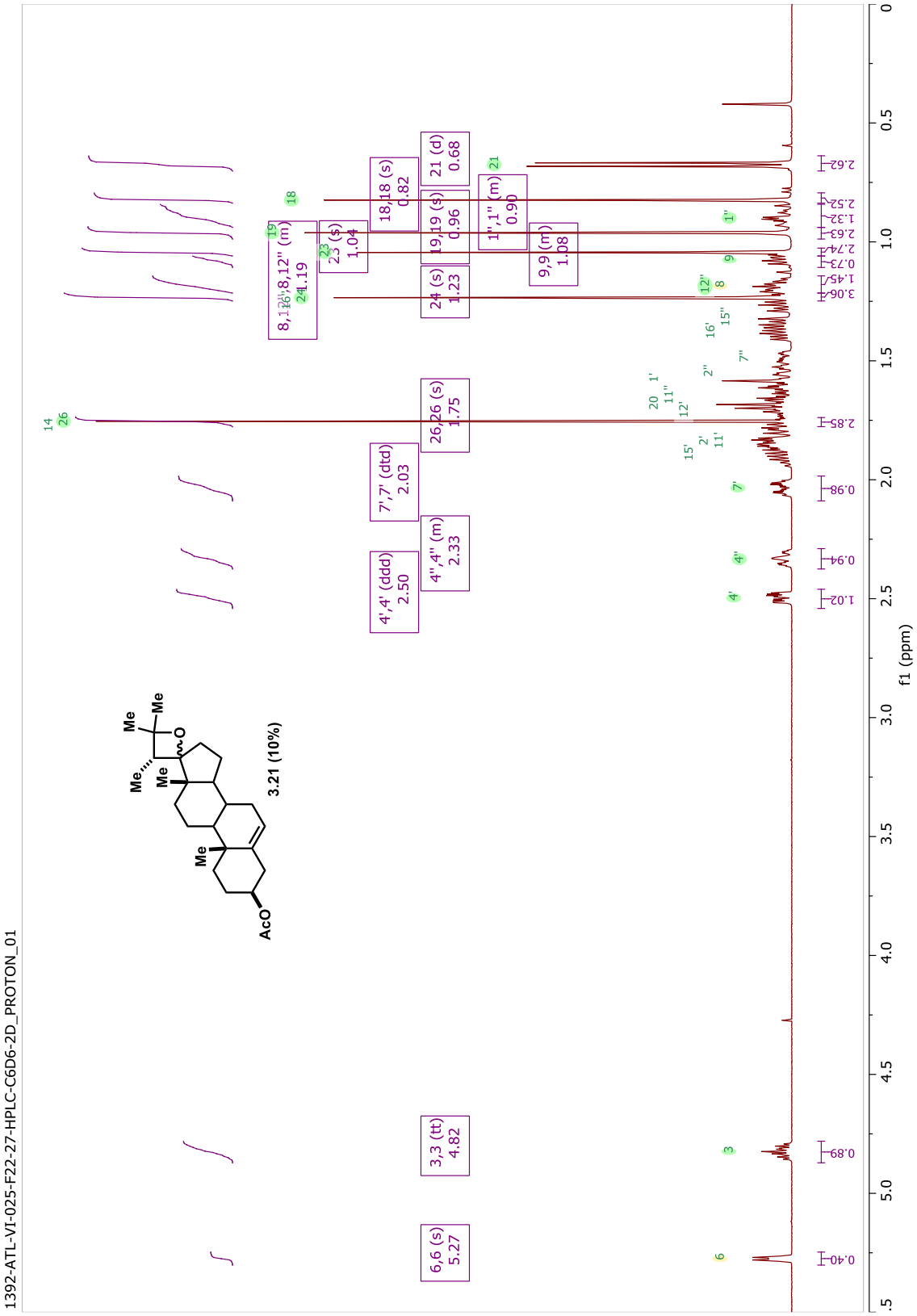
1392-ATL-VI-025-F22-27-HPLC-C6D6-2D_PROTON_01
3.21 (10%)
f1 (ppm)

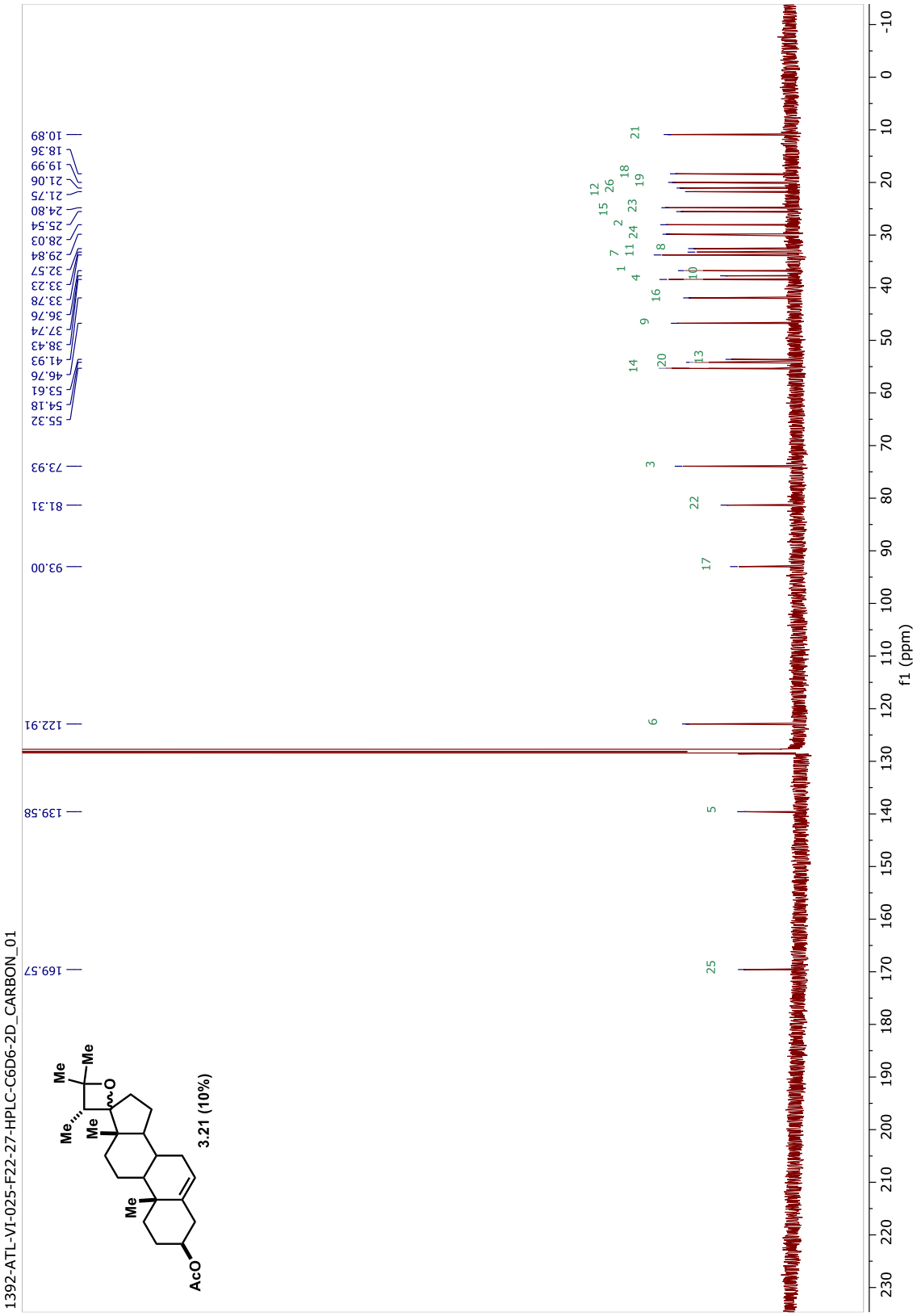
1392-ATL-VI-025-F22-27-HPLC-C6D6-2D_CARBON_01
3.21 (10%)
Me
Me
Me
Me
Me
AcO
O
169.57
139.58
122.91
93.00
81.31
73.93
55.32
54.18
53.61
46.76
41.93
38.43
37.74
36.76
33.78
33.23
32.57
29.84
28.03
25.54
24.80
21.75
21.06
19.99
18.36
10.89
f1 (ppm)

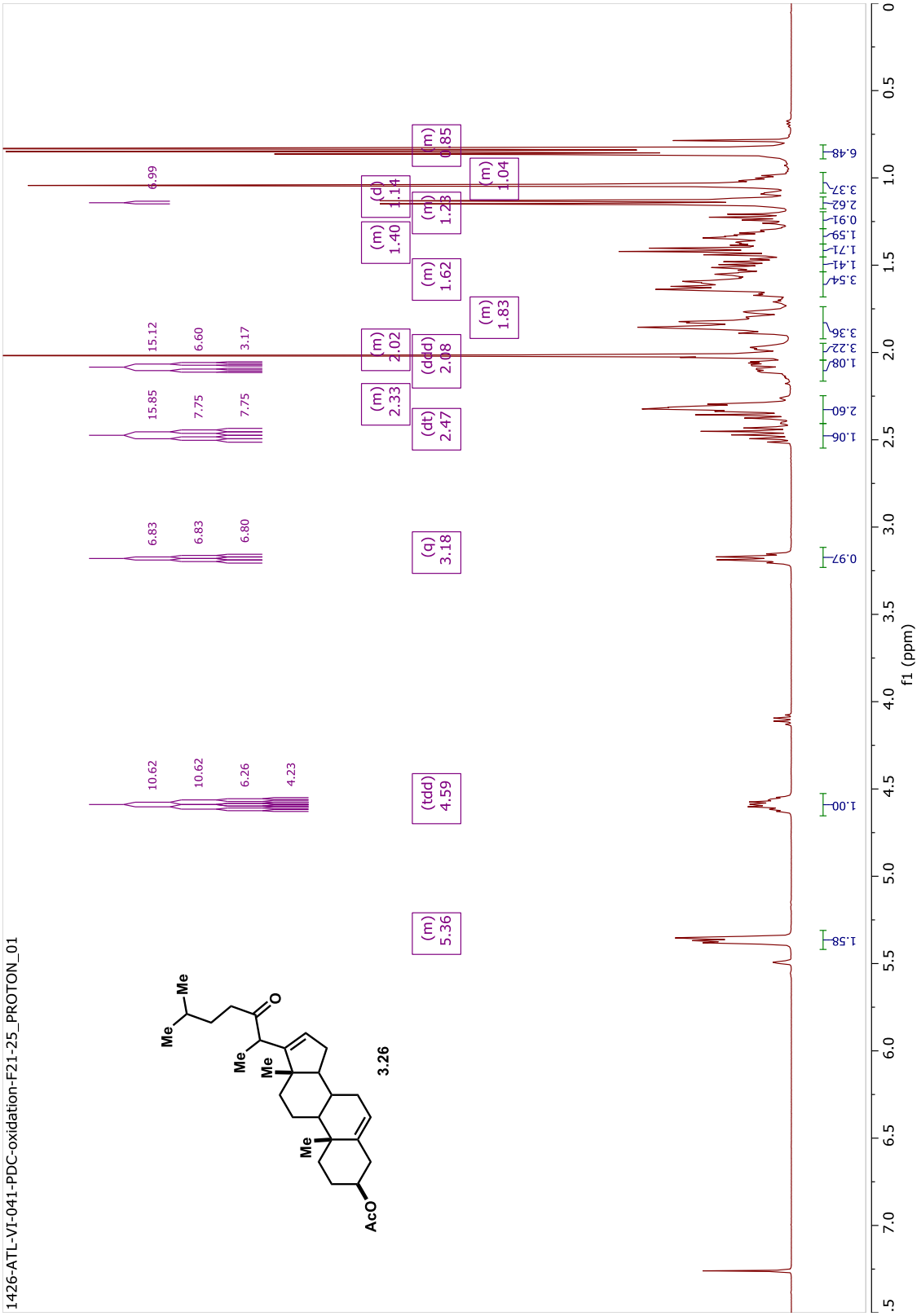
1426-ATL-VI-041-PDC-oxidation-F21-25_PROTON_01
f1 (ppm)
3.26
AcO
Me
Me
Me
Me
Me
O
(m) 5.36
(tdd) 4.59
(q) 3.18
(dt) 2.47
(m) 2.33
(ddd) 2.08
(m) 2.02
(m) 1.83
(m) 1.62
(m) 1.40
(d) 1.14
(m) 1.28
(m) 1.04
(m) 0.85
10.62
10.62
6.26
4.23
6.83
6.83
6.80
15.85
7.75
7.75
15.12
6.60
3.17
6.99
1.00
0.97
1.06
2.60
1.08
3.22
3.36
1.54
1.41
1.71
1.59
0.91
2.62
3.37
6.48
1.58

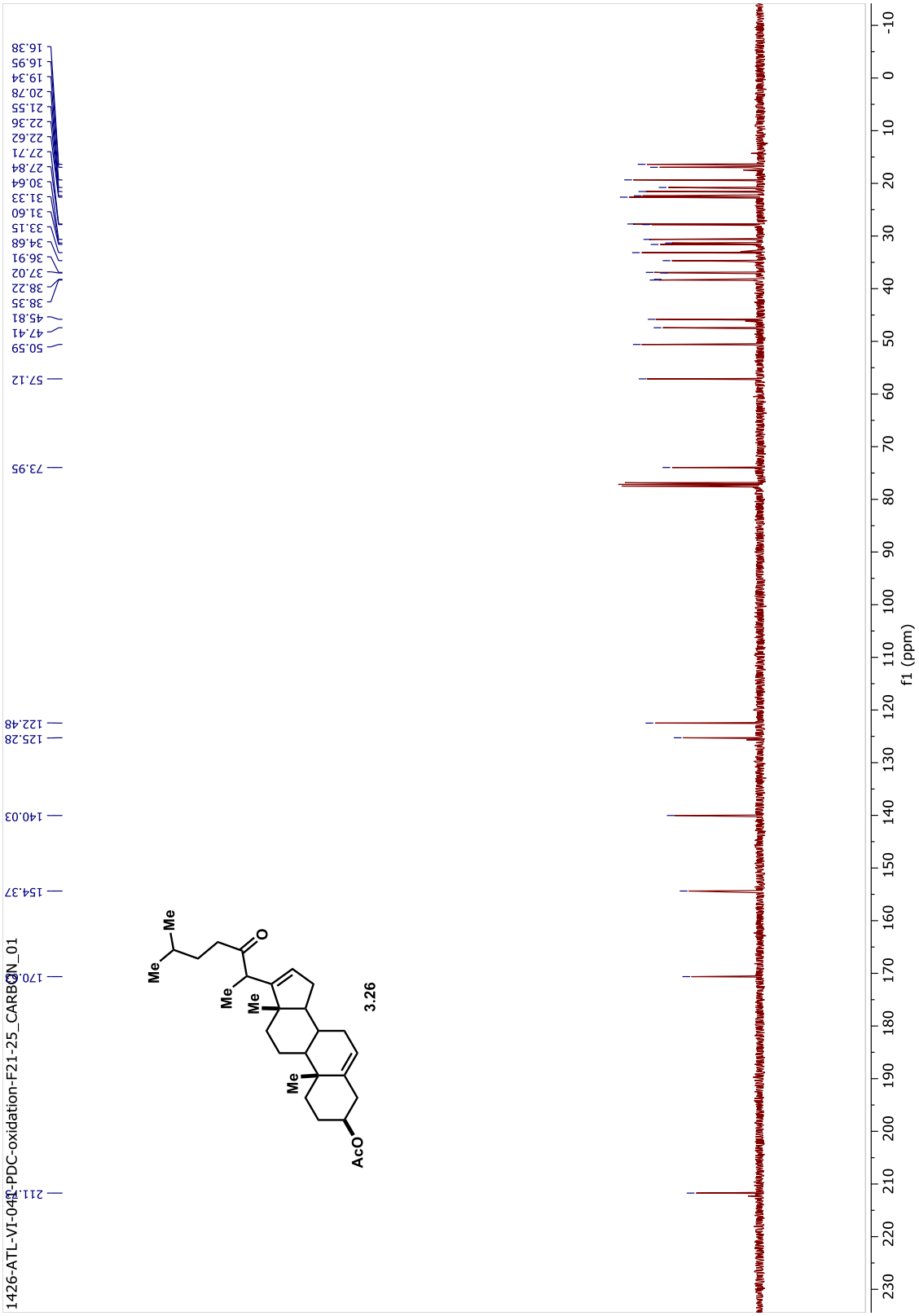
1426-ATL-VI-041-PDC-oxidation-F21-25_CARBON_01
16.38
16.95
19.34
20.78
21.55
22.36
22.62
27.71
27.84
30.64
31.33
31.60
33.15
34.68
36.91
37.02
38.22
38.35
45.81
47.41
50.59
57.12
73.95
122.48
125.28
140.03
154.37
170.29
211.12
Me
Me
Me
Me
Me
O
AcO
3.26
f1 (ppm)

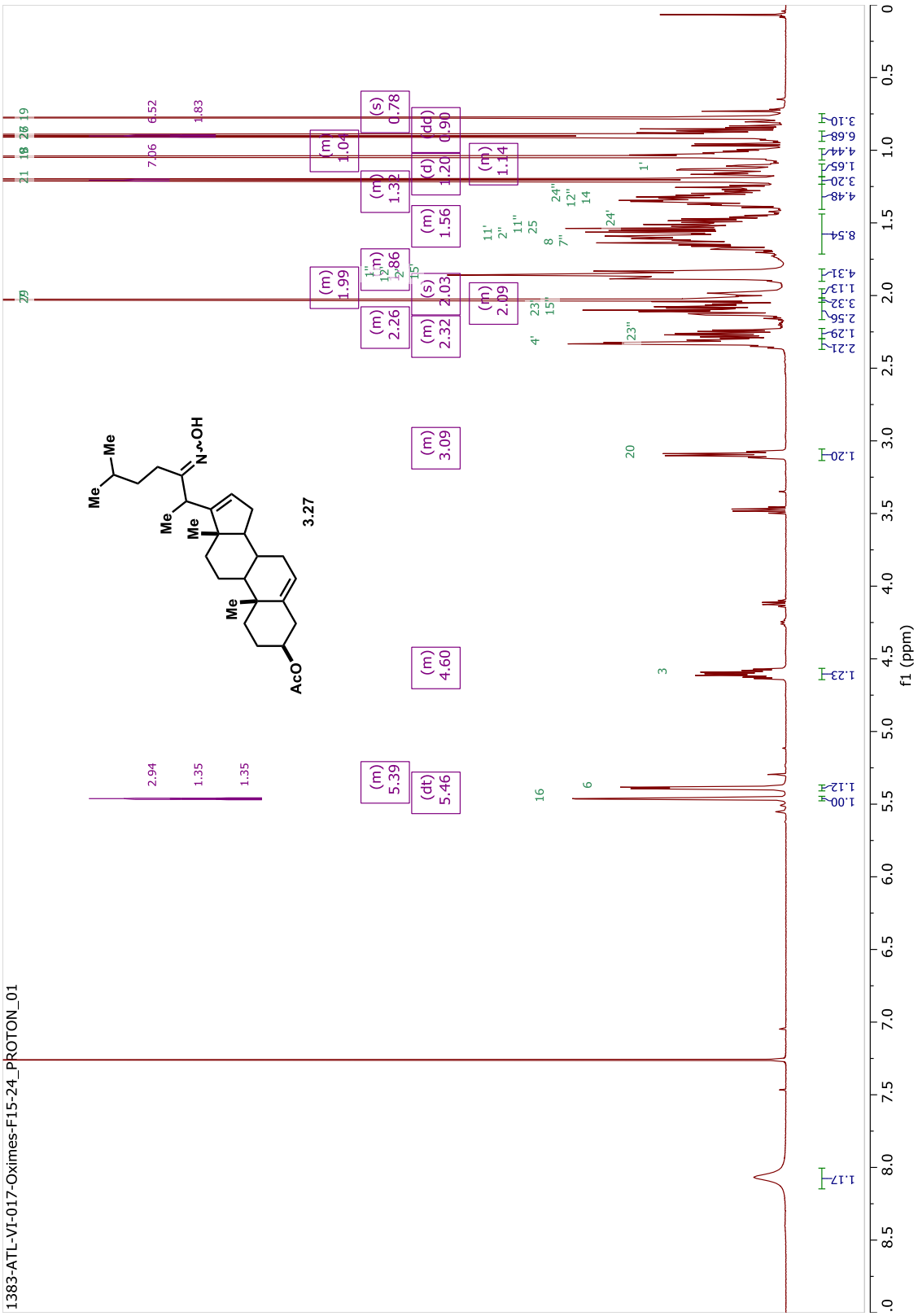
1383-ATL-VI-017-Oximes-F15-24_PROTON_01
3.27
f1 (ppm)

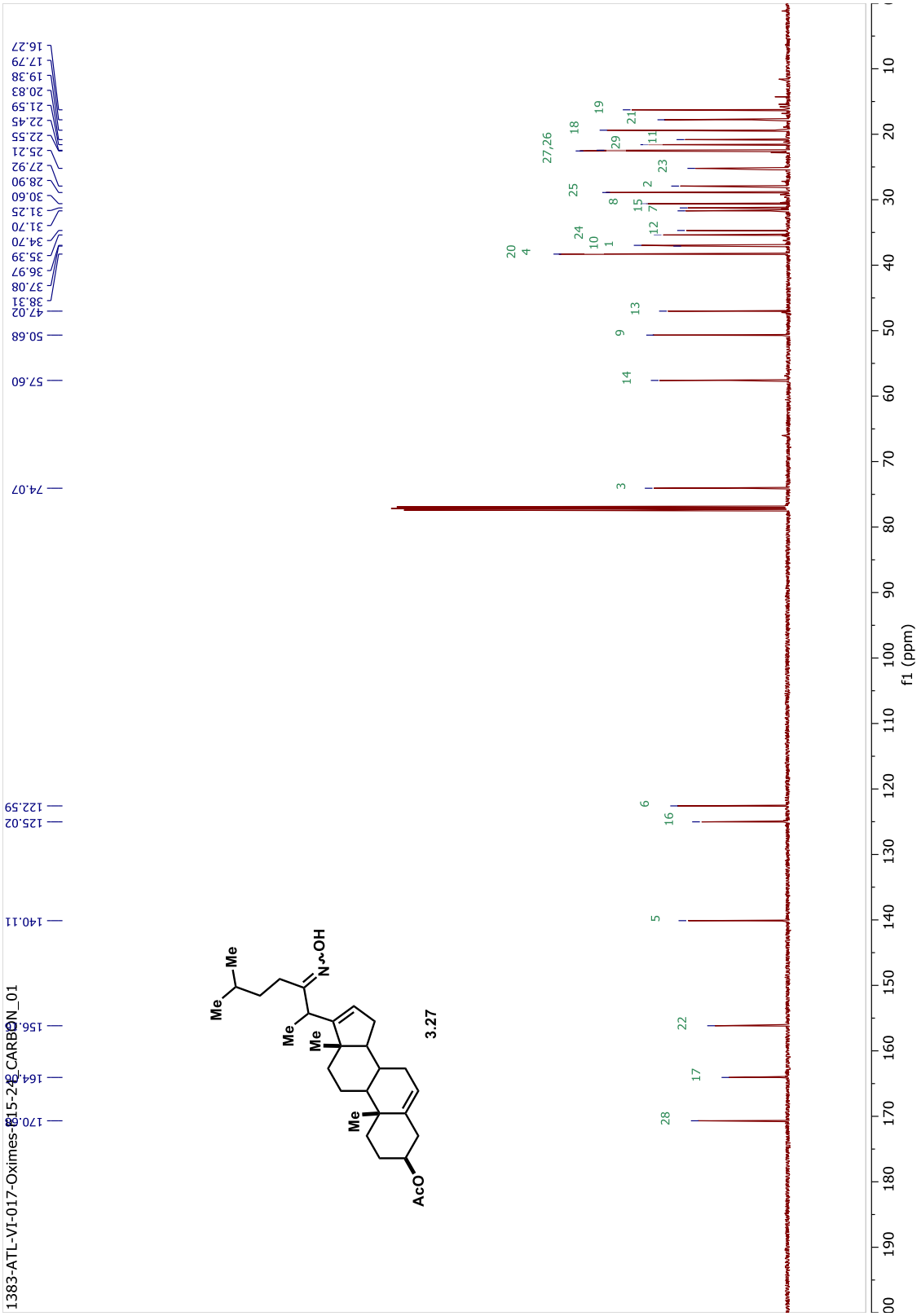
1383-ATL-VI-017-Oximes-815-24-1-13C CARBON_01
3.27
Me
Me
Me
Me
Me
N
OH
AcO
f1 (ppm)

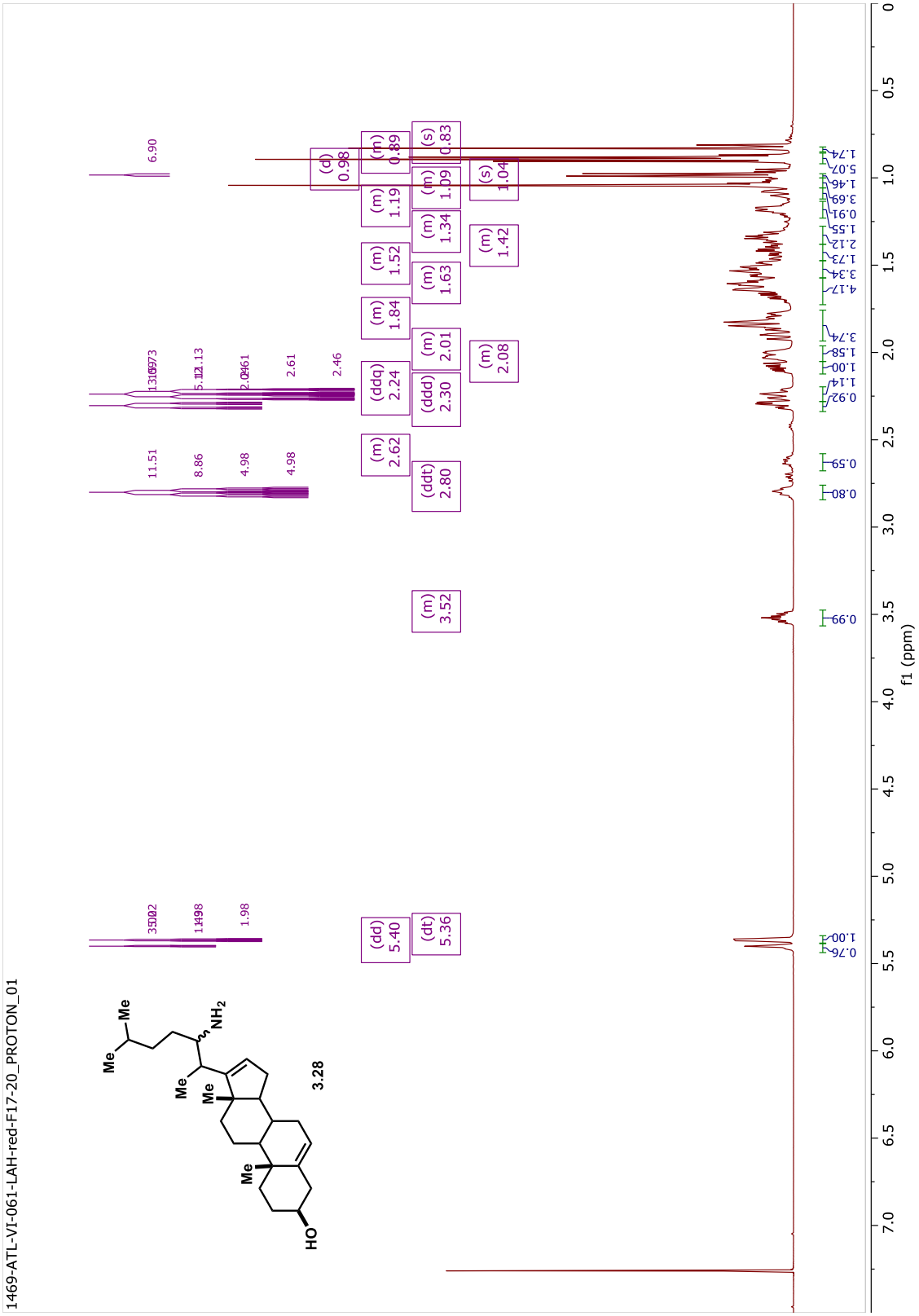
1469-ATL-VI-061-LAH-red-F17-20_PROTON_01
3.28
f1 (ppm)

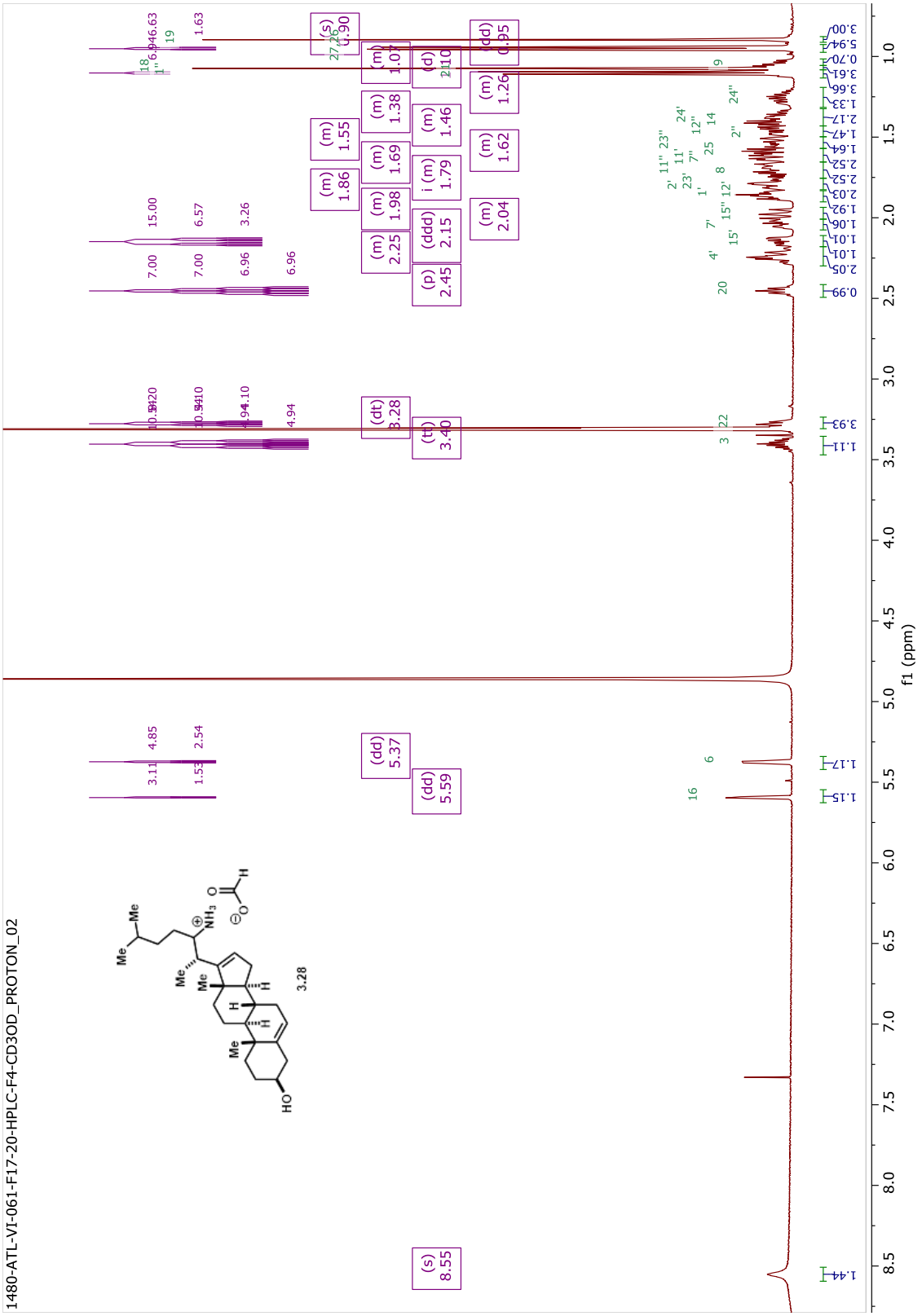
1480-ATL-VI-061-F17-20-HPLC-F4-CD3OD_PROTON_02
f1 (ppm)

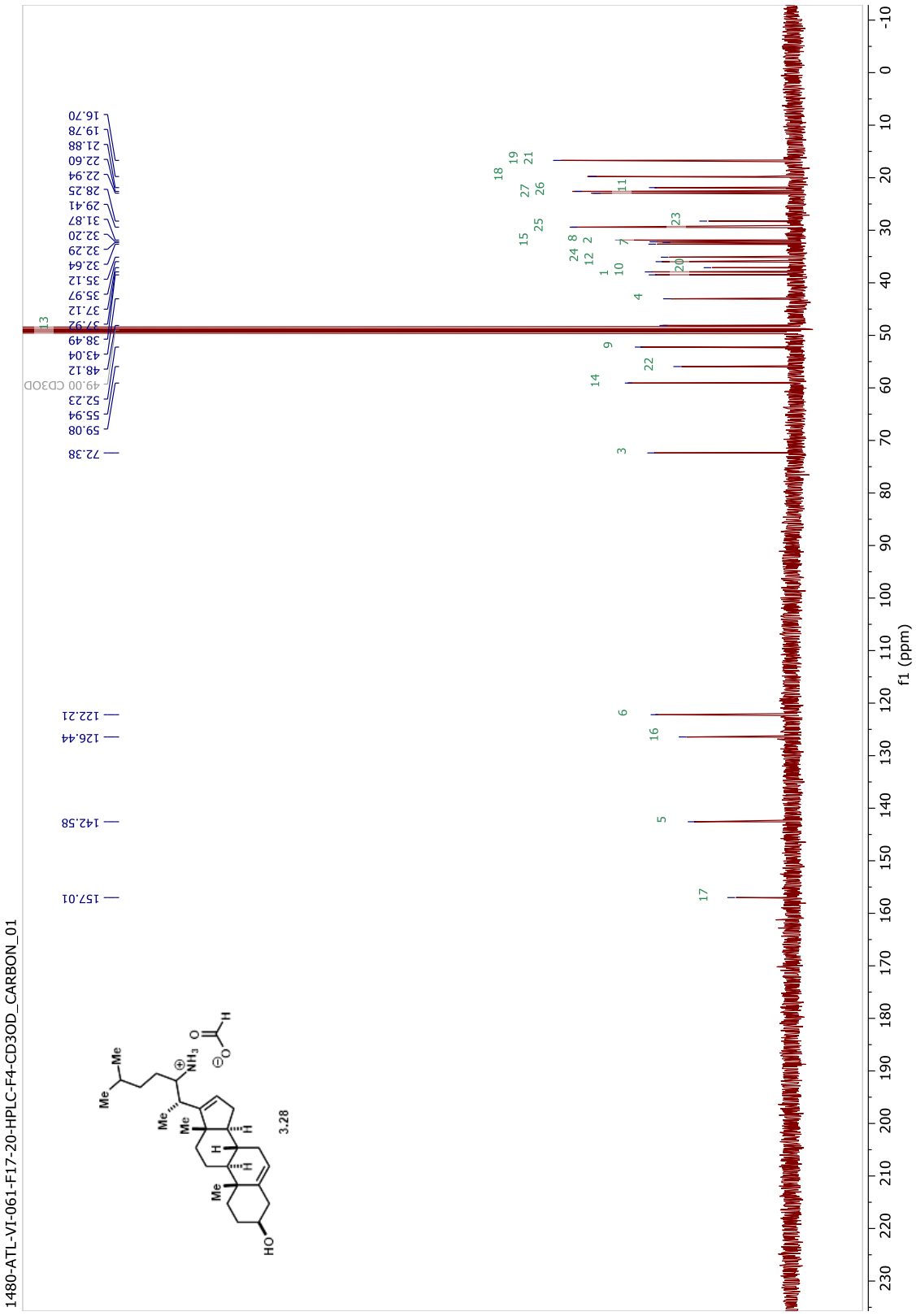
1480-ATL-VI-061-F17-20-HPLC-F4-CD3OD_CARBON_01
f1 (ppm)
3.28

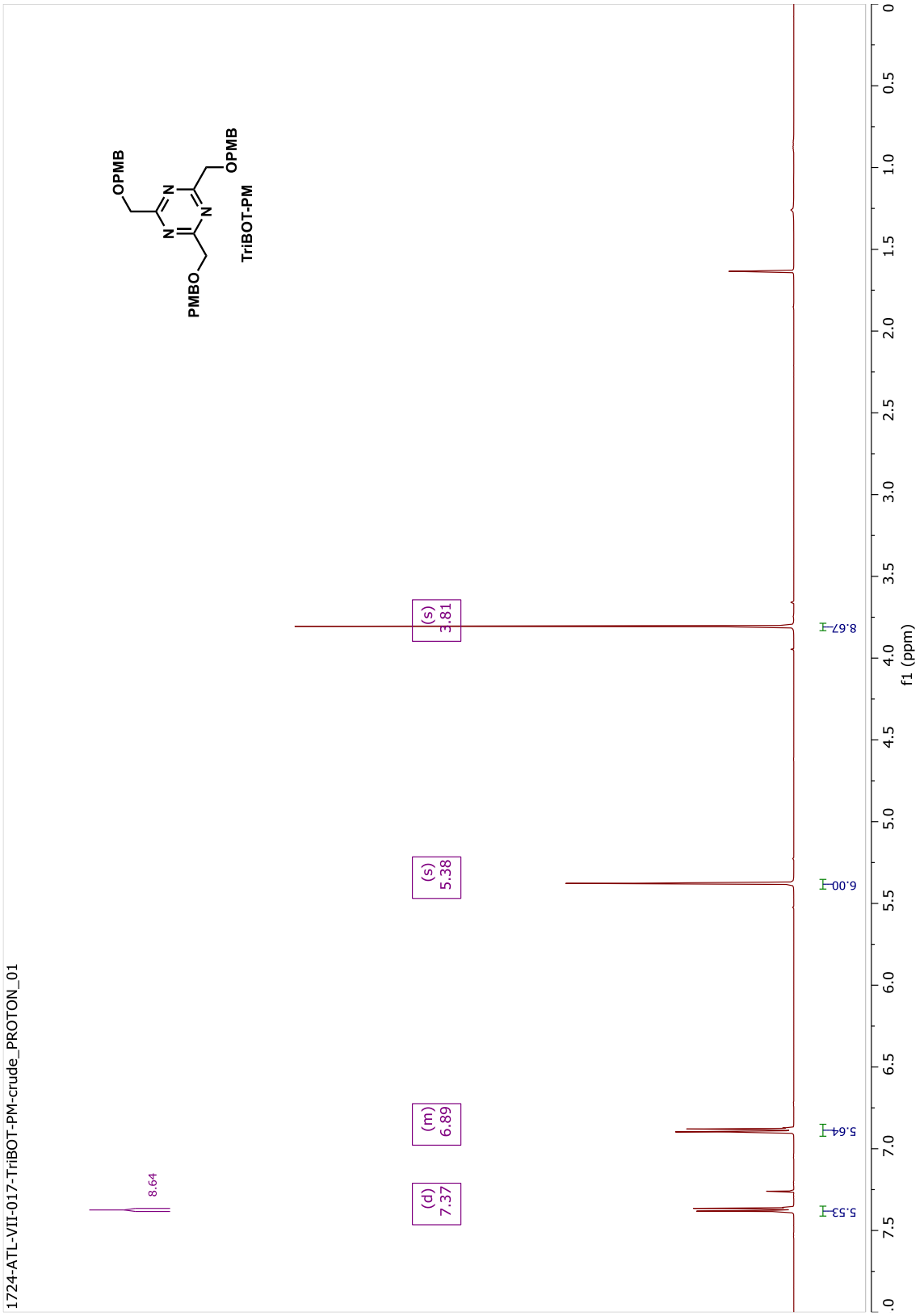
1724-ATL-VII-017-TriBOT-PM-crude_PROTON_01
OPMB
OPMB
PMBO
TriBOT-PM
8.64
(d)
7.37
(m)
6.89
(s)
5.38
(s)
3.81
5.53
5.64
6.00
8.67
f1 (ppm)

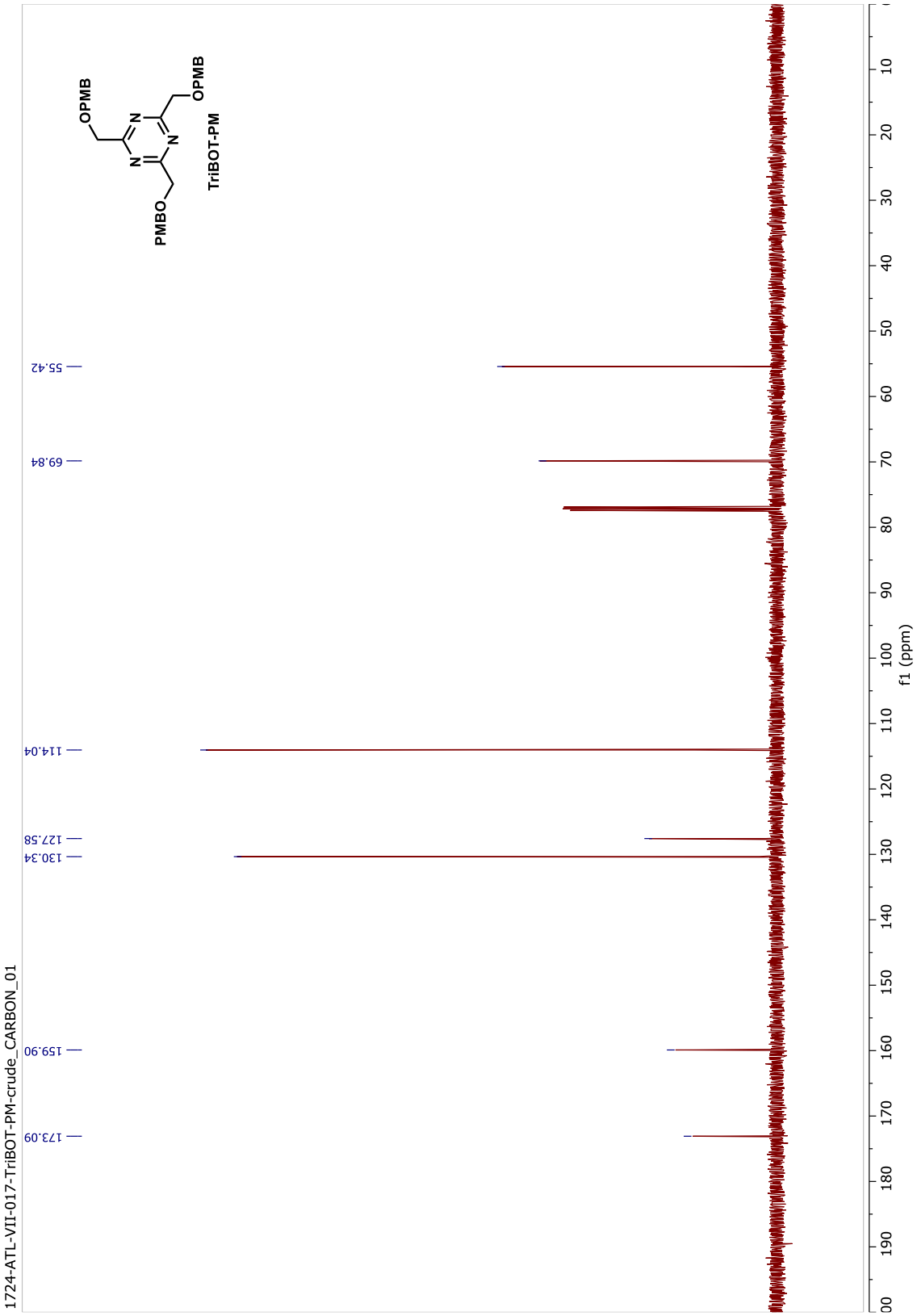
1724-ATL-VII-017-TriBOT-PM-crude_CARBON_01
OPMB
OPMB
PMBO
TriBOT-PM
55.42
69.84
114.04
127.58
130.34
159.90
173.09
f1 (ppm)

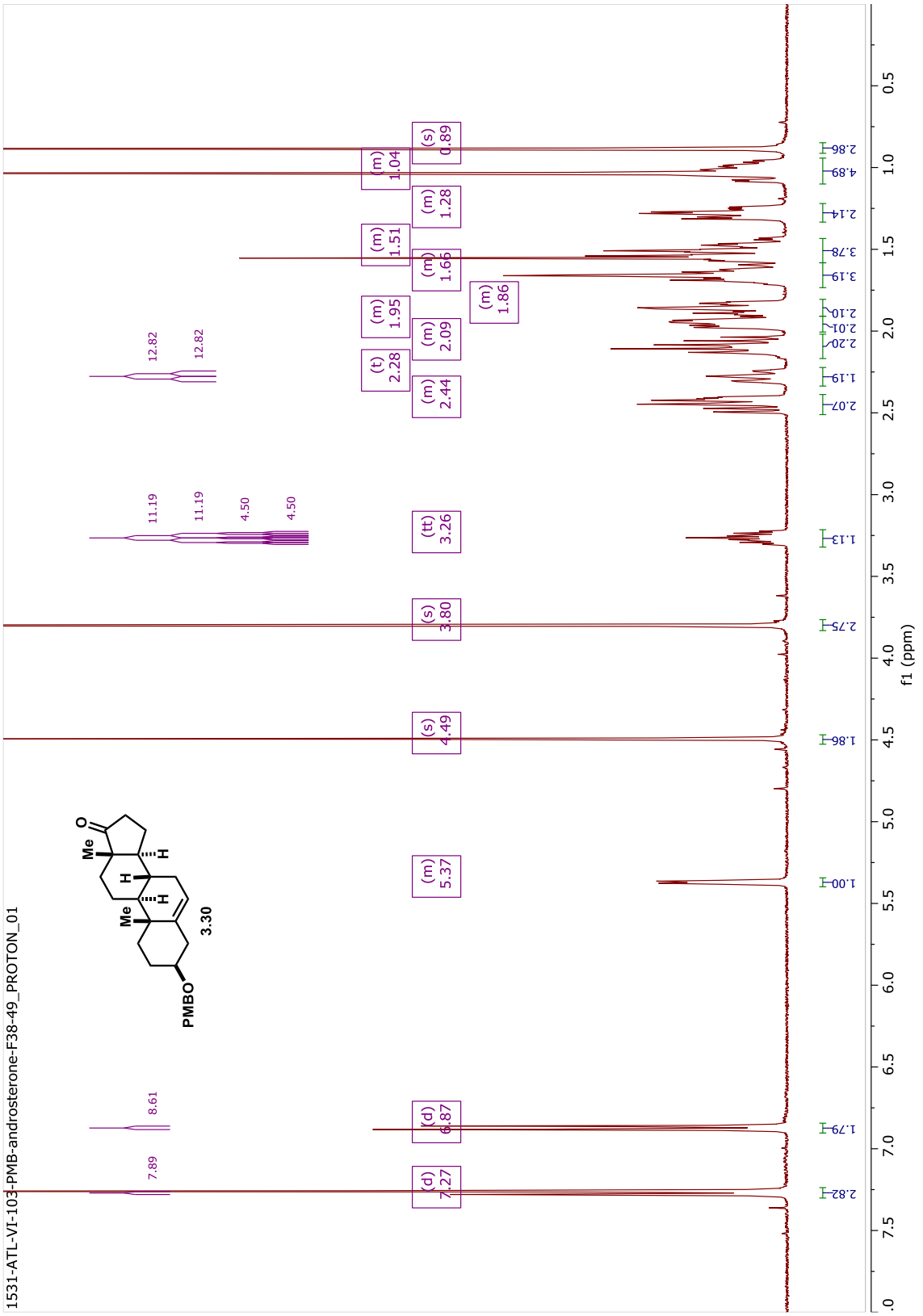
1531-ATL-VI-103-PMB-androsterone-F38-49_PROTON_01
Me
O
H
H
Me
H
PMBO
3.30
8.61
7.89
12.82
12.82
11.19
11.19
4.50
4.50
(d) 7.27
(d) 6.87
(m) 5.37
(s) 4.49
(s) 3.80
(tt) 3.26
(t) 2.28
(m) 2.44
(m) 2.09
(m) 1.95
(m) 1.86
(m) 1.65
(m) 1.51
(m) 1.28
(m) 1.04
(s) 0.89
2.82
1.79
1.00
1.86
2.75
1.13
2.07
1.19
2.20
2.01
2.10
3.19
3.78
2.14
4.89
2.86
f1 (ppm)

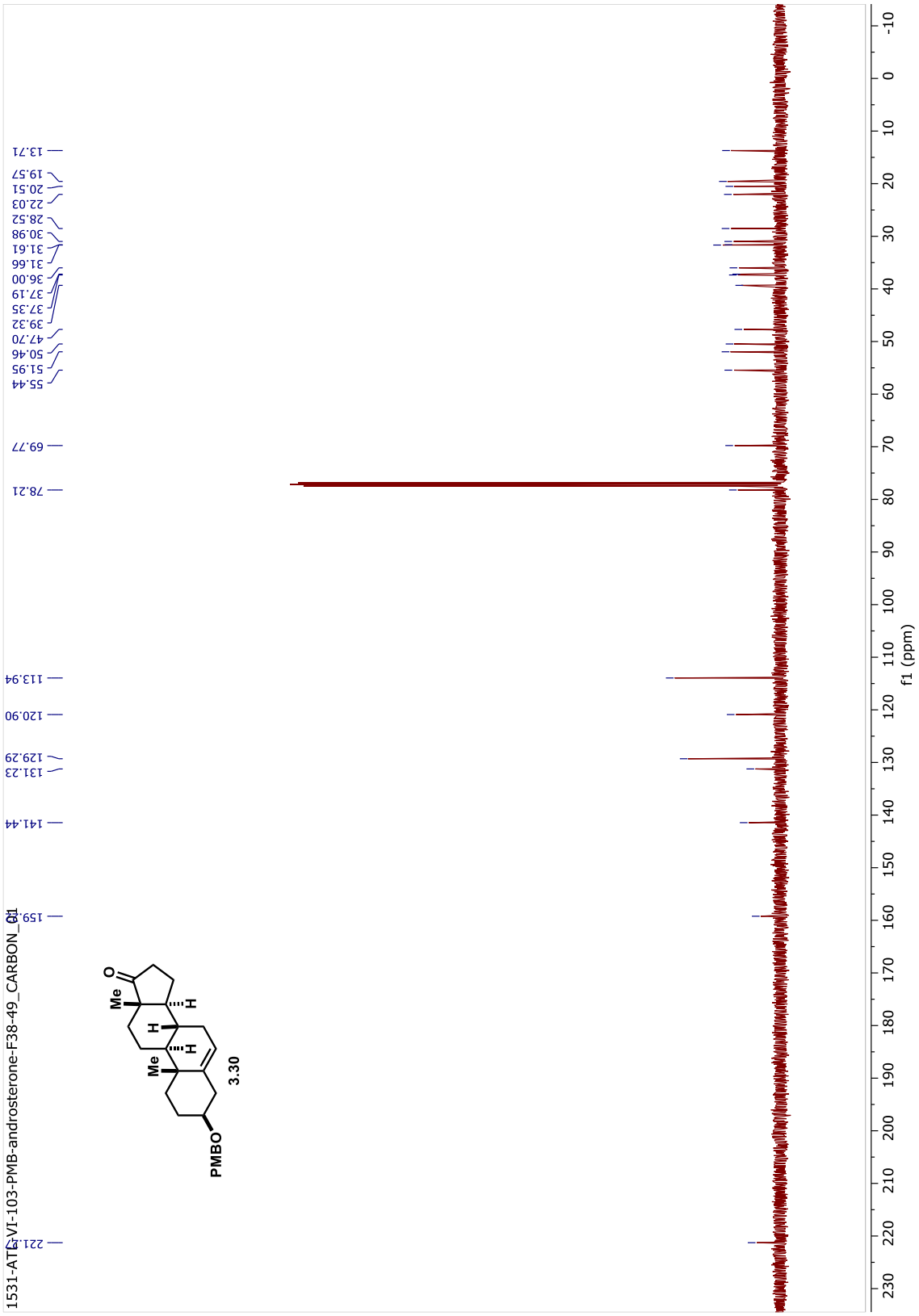
1531-ATG-VI-103-PMB-androsterone-F38-49_CARBON_01
221.12
159.18
141.44
131.23
129.29
120.90
113.94
78.21
69.77
55.44
51.95
50.46
47.70
39.32
37.35
37.19
36.00
31.66
31.61
30.98
28.52
22.03
20.51
19.57
13.71
Me
O
H
H
H
Me
PMBO
3.30
f1 (ppm)

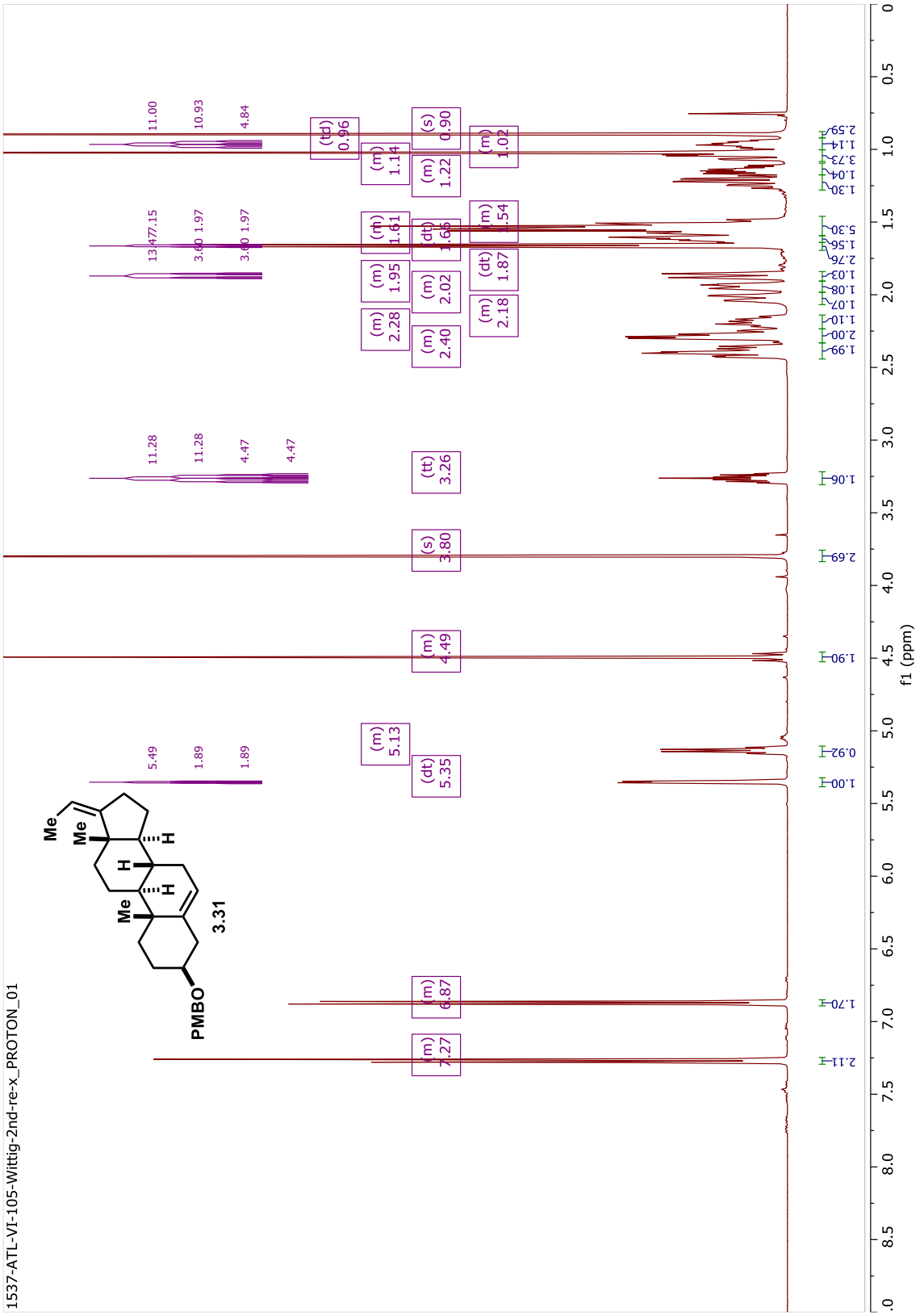
1537-ATL-VI-105-Wittig-2nd-re-x_PROTON_01
PMBO
Me
Me
Me
H
H
H
3.31
f1 (ppm)

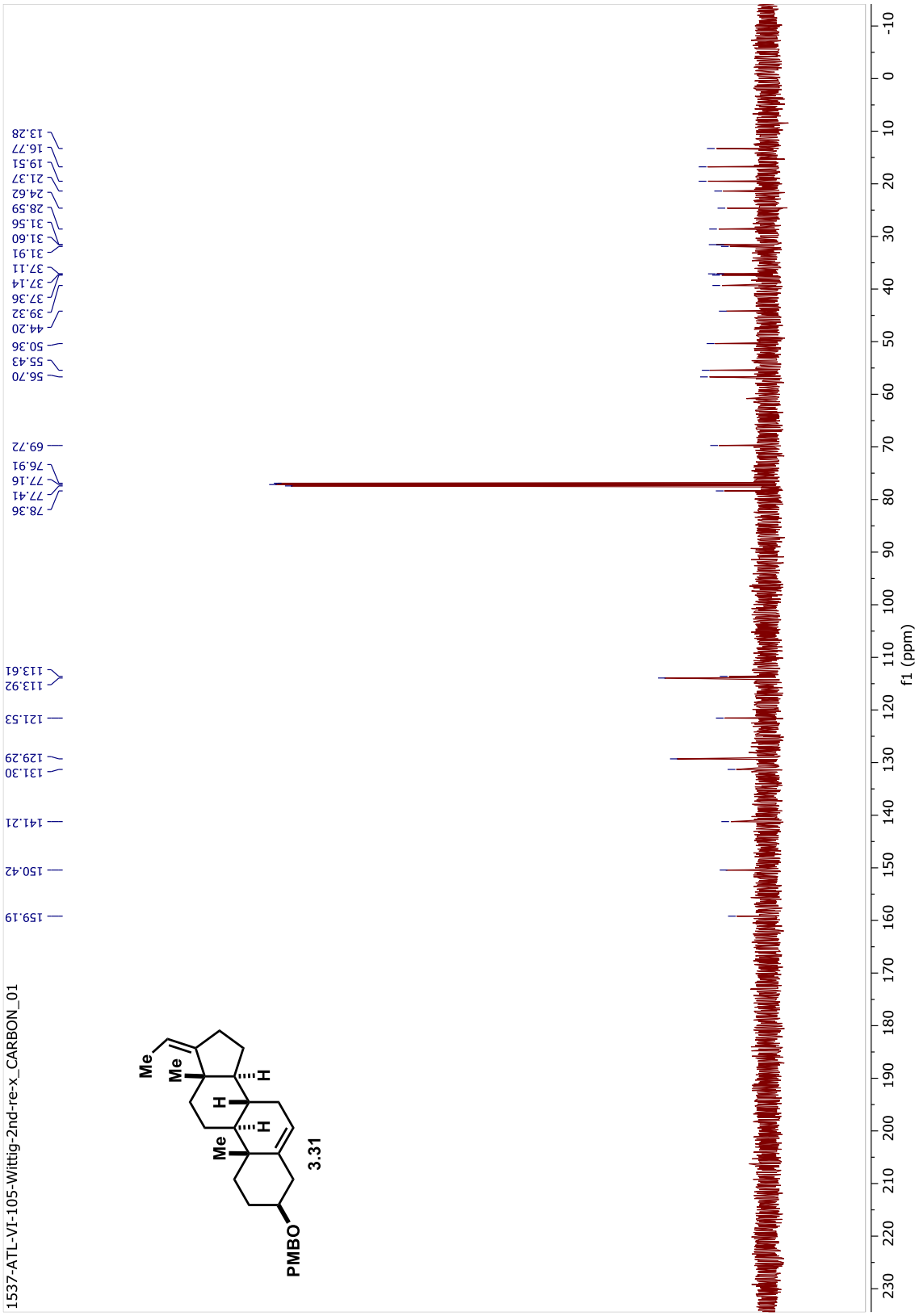
1537-ATL-VI-105-Wittig-2nd-re-x_CARBON_01
159.19
150.42
141.21
131.30
129.29
121.53
113.92
113.61
78.36
77.41
77.16
76.91
69.72
56.70
55.43
50.36
44.20
39.32
37.36
37.14
37.11
31.91
31.60
31.56
28.59
24.62
21.37
19.51
16.77
13.28
Me
Me
H
H
H
Me
PMBO
3.31
f1 (ppm)

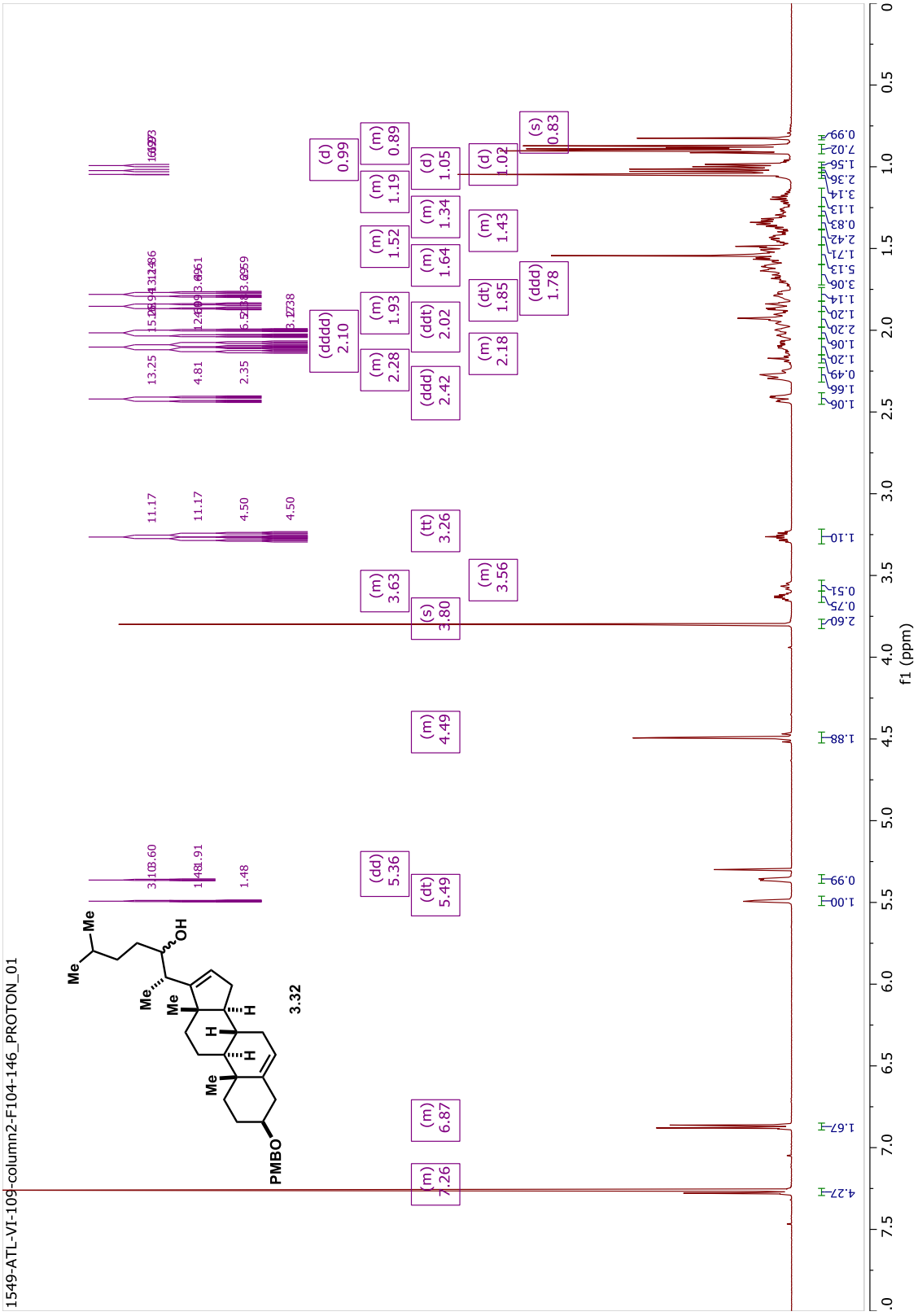
1549-ATL-VI-109-column2-F104-146_PROTON_01
3.32
PMBO
f1 (ppm)

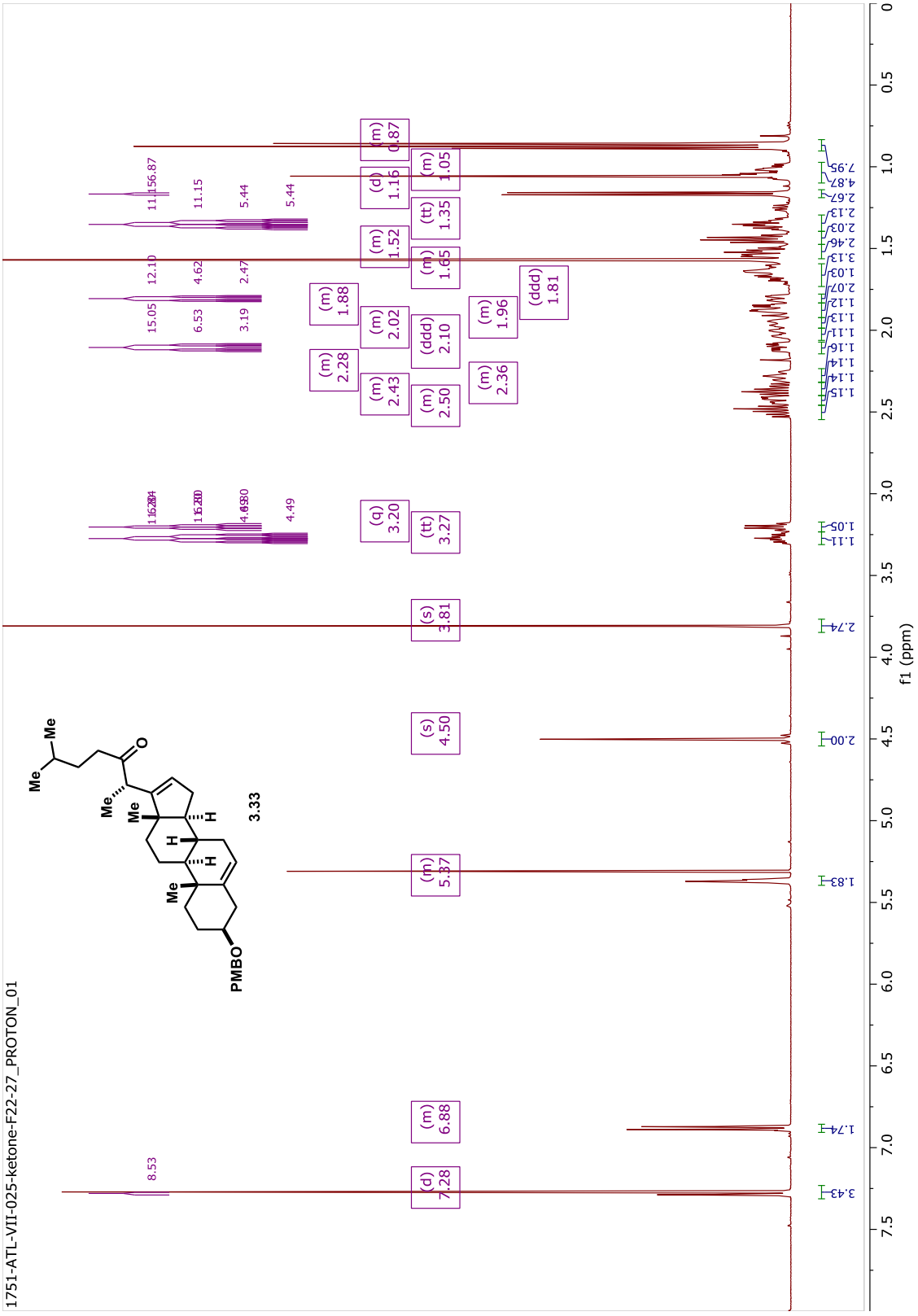
1751-ATL-VII-025-ketone-F22-27_PROTON_01
3.33
PMBO
f1 (ppm)

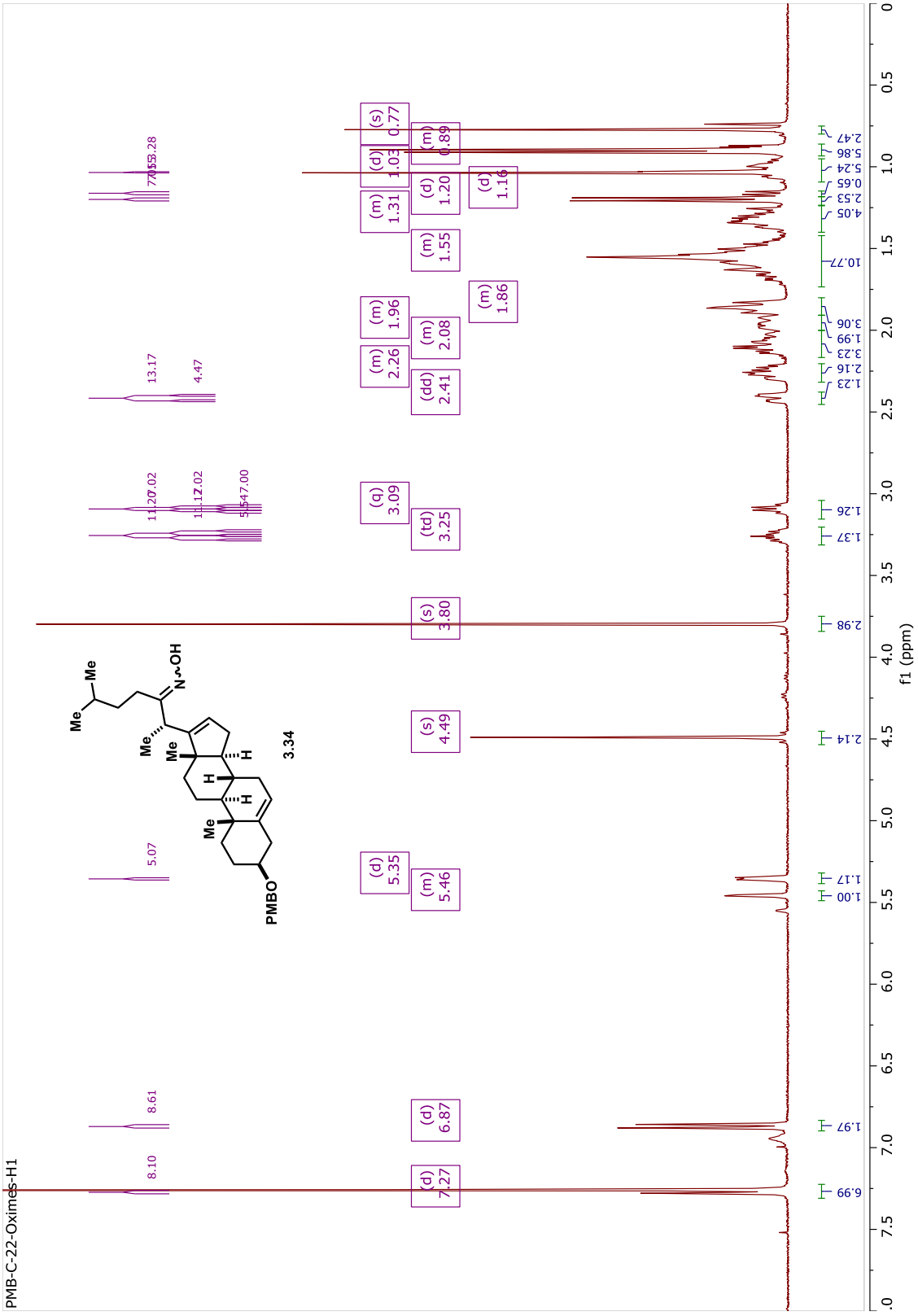
PMB-C-22-Oximes-H1
f1 (ppm)
3.34
PMBO
N-OH
Me
H

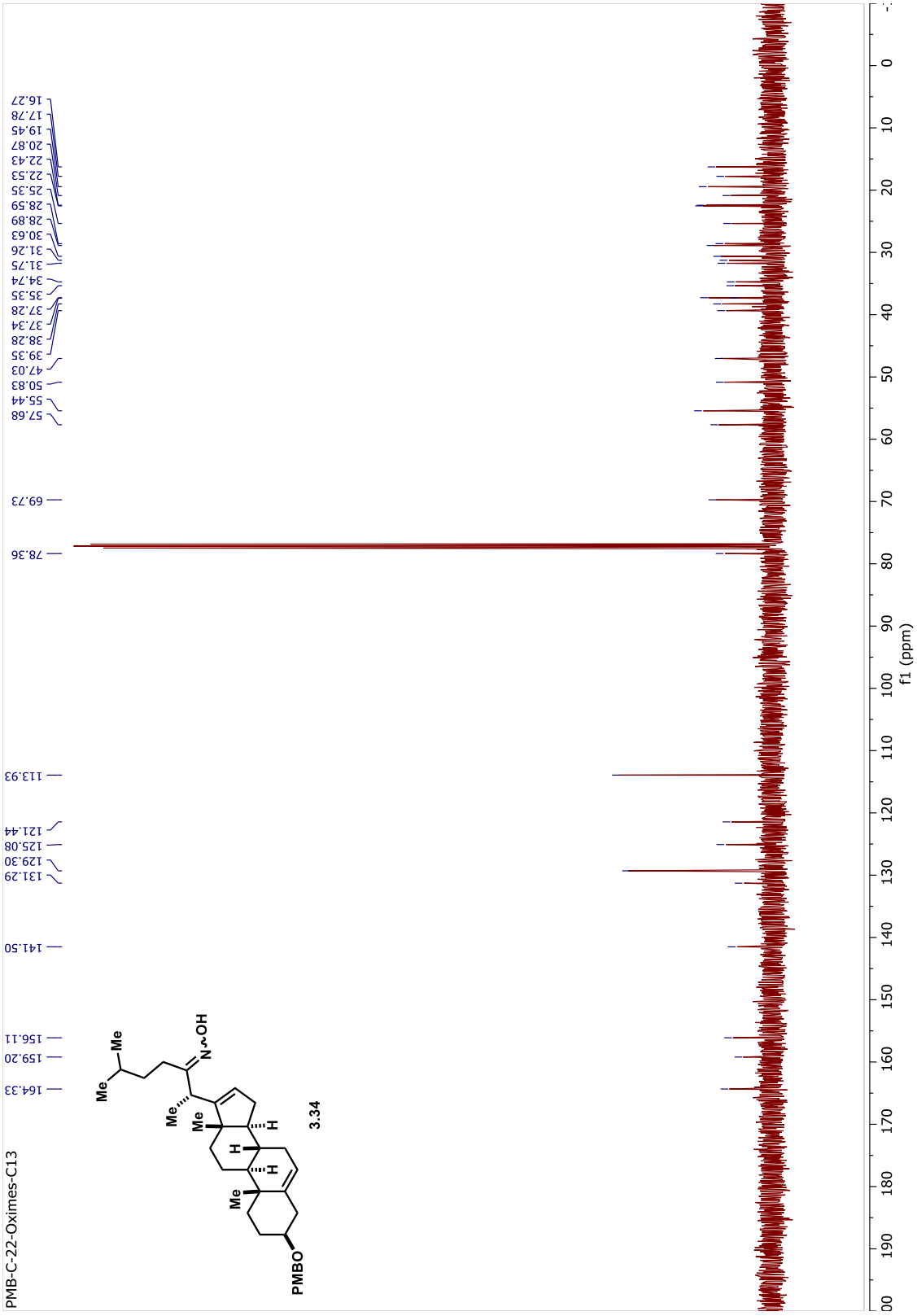
PMB-C-22-Oximes-C13
16.27
17.78
19.45
20.87
22.43
22.53
25.35
28.59
28.89
30.63
31.26
31.75
34.74
35.35
37.28
37.34
38.28
39.35
47.03
50.83
55.44
57.68
69.73
78.36
113.93
121.44
125.08
129.30
131.29
141.50
156.11
159.20
164.33
Me
Me
Me
Me
N
OH
H
H
H
Me
PMBO
3.34
f1 (ppm)

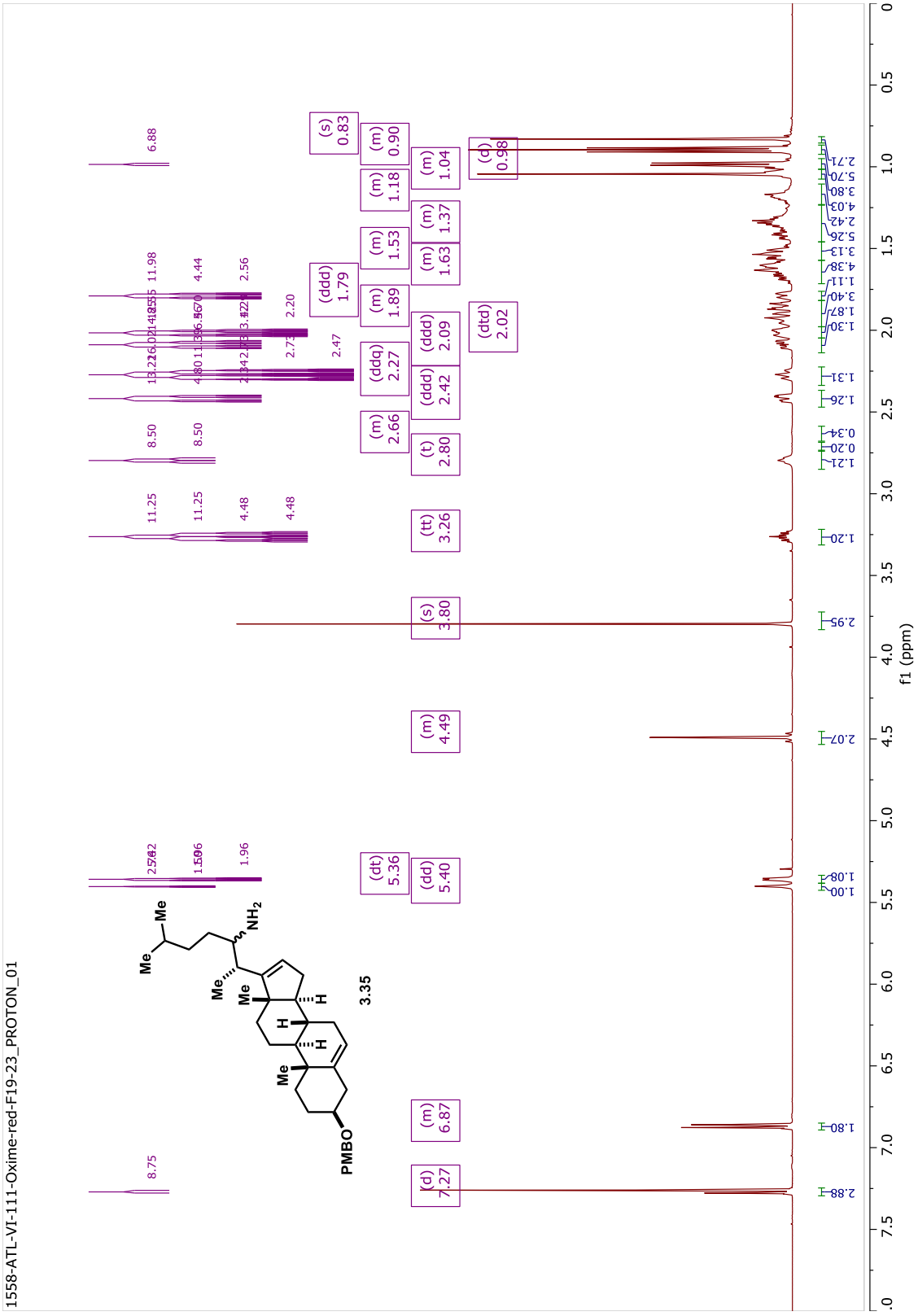
1558-ATL-VI-111-Oxime-red-F19-23_PROTON_01
3.35
PMBO
f1 (ppm)

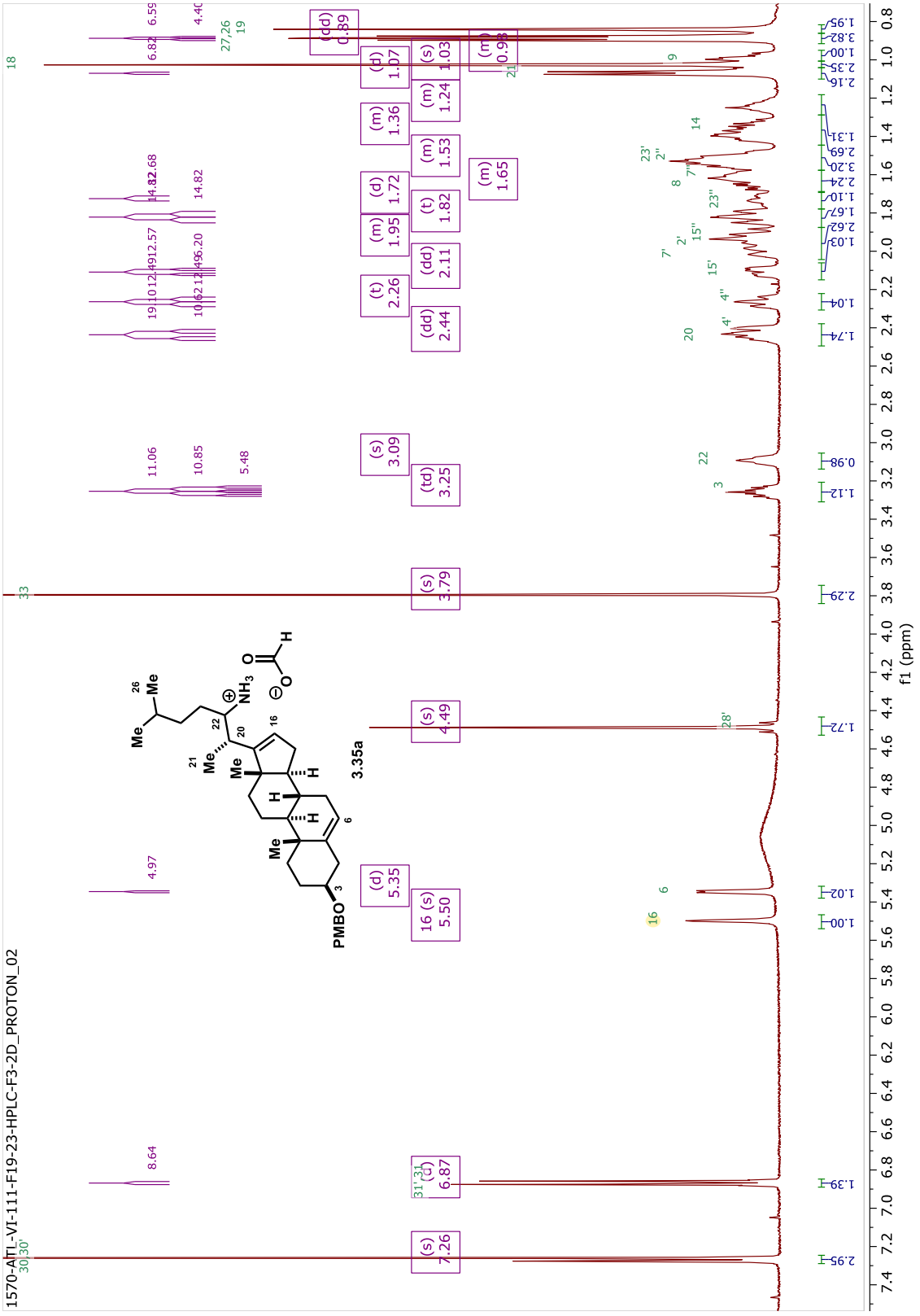
1570-ATL-VI-111-F19-23-HPLC-F3-2D_PROTON_02
f1 (ppm)
PMBO
3.35a
Me
Me
Me
Me
H
H
H
NH3
O
O
H

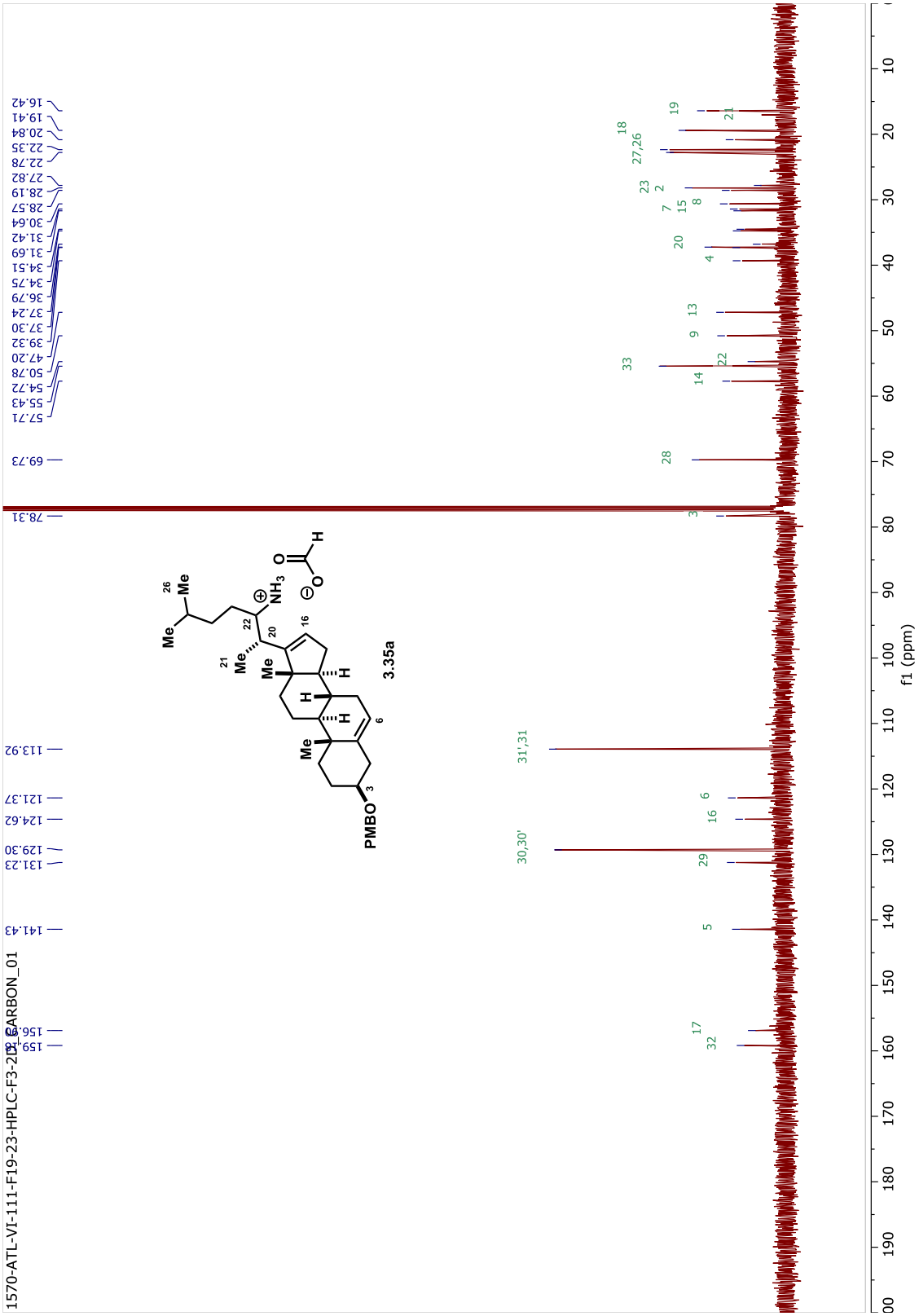
1570-ATL-VI-111-F19-23-HPLC-F3-2D CARBON_01
f1 (ppm)
3.35a
PMBO
NH3
Me
H

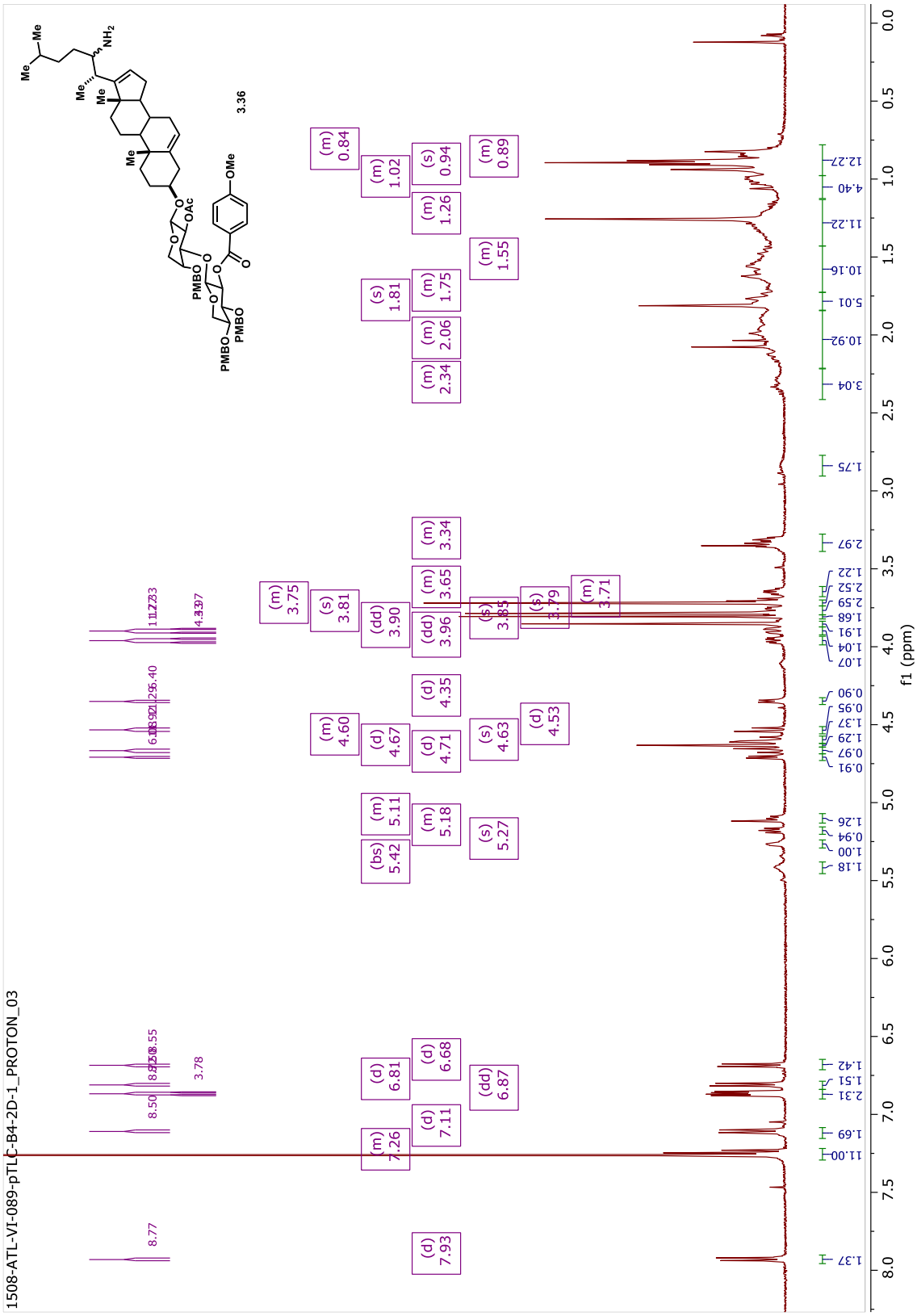
1508-ATL-VI-089-pTLC-B4-2D-1_PROTON_03
f1 (ppm)
Me
Me
NH2
Me
Me
Me
OAc
OMe
PMBO
PMBO
PMBO
3.36

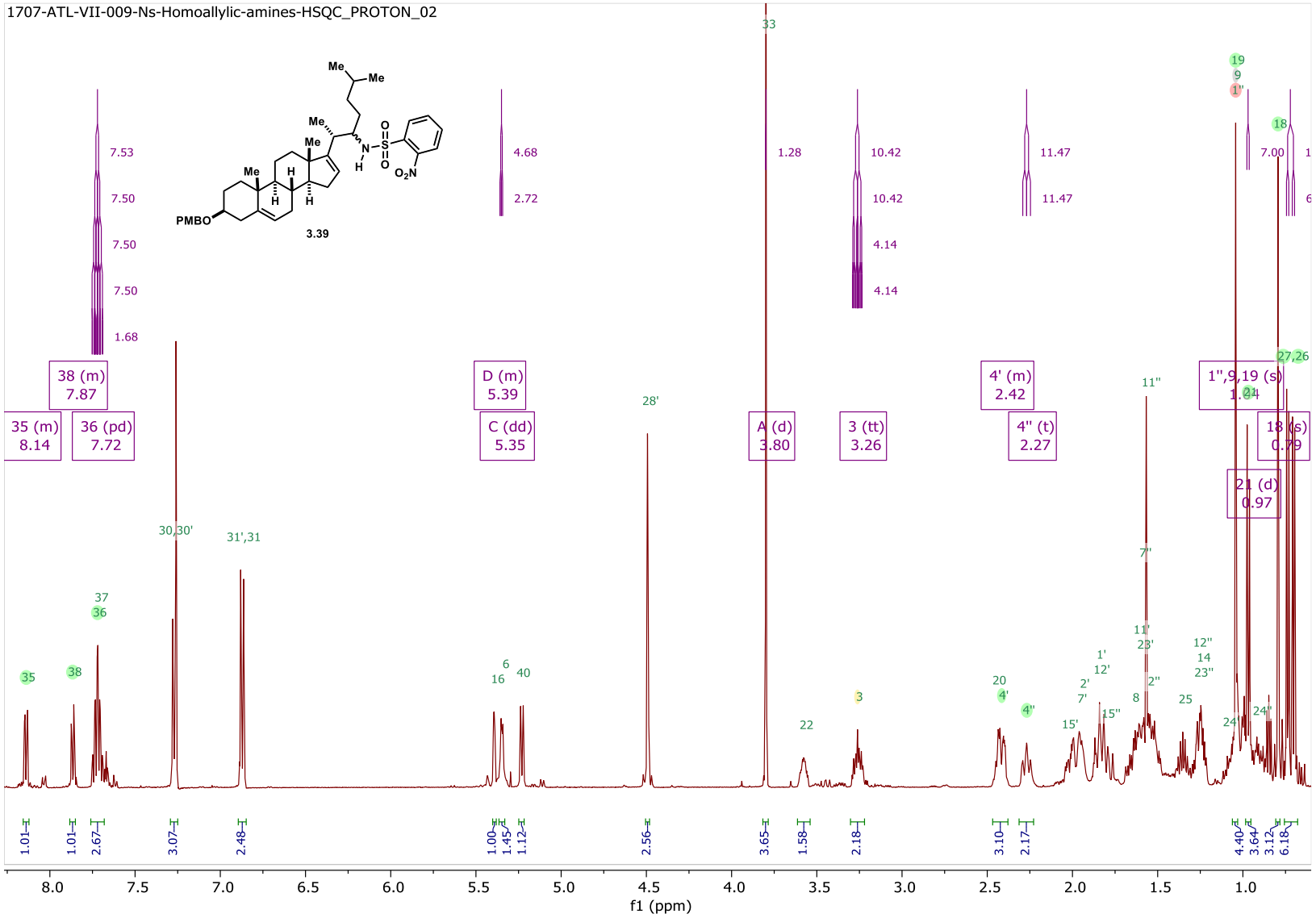
1707-ATL-VII-009-Ns-Homoallylic-amines-HSQC_PROTON_02
PMBO
3.39
38 (m)
7.87
35 (m)
8.14
36 (pd)
7.72
D (m)
5.39
C (dd)
5.35
A (d)
3.80
3 (tt)
3.26
4' (m)
2.42
4" (t)
2.27
1",9,19 (s)
1.24
18 (s)
0.79
21 (d)
0.97
f1 (ppm)

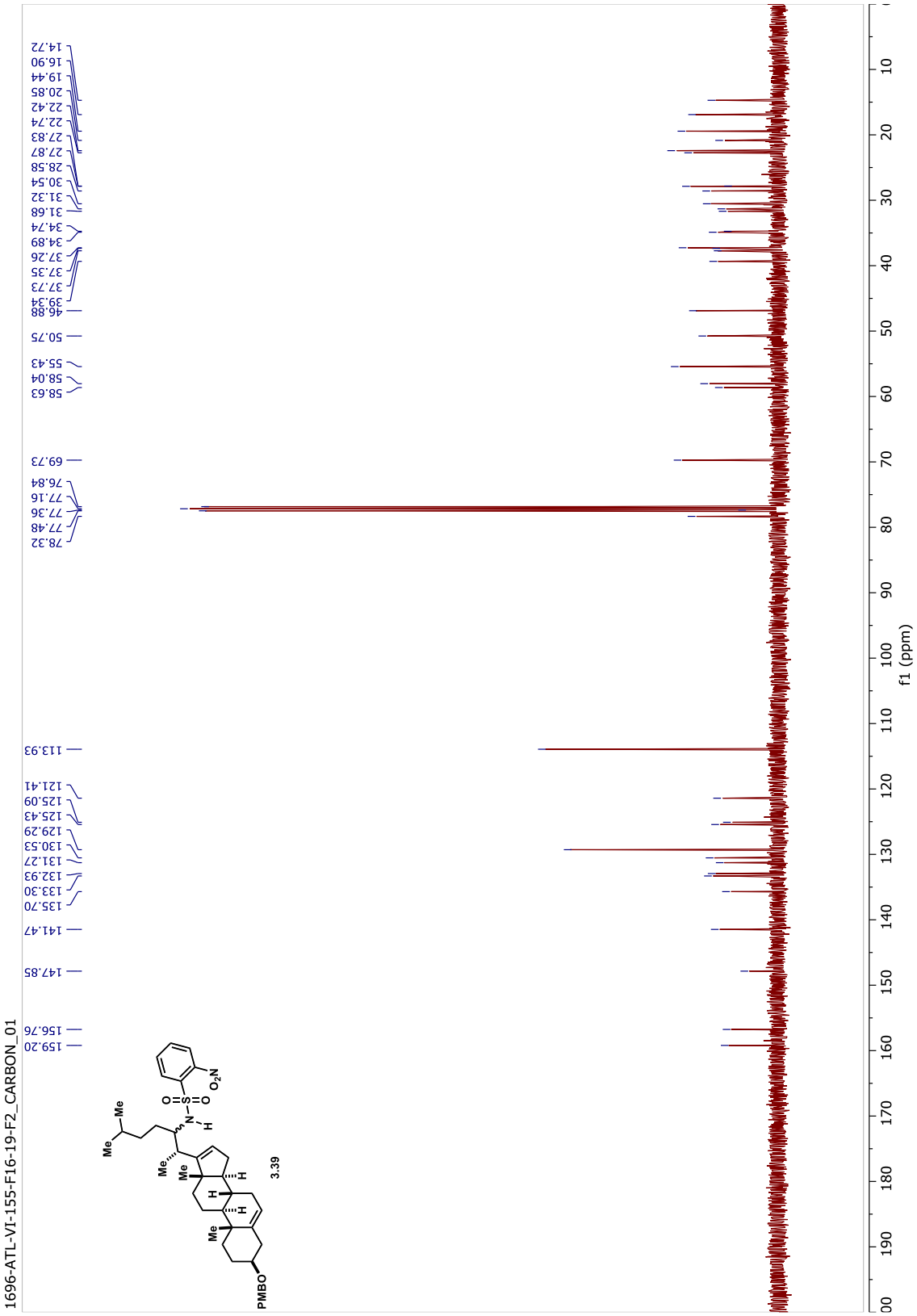
1696-ATL-VI-155-F16-19-F2_CARBON_01
14.72
16.90
19.44
20.85
22.42
22.74
27.83
27.87
28.58
30.54
31.32
31.68
34.74
34.89
37.26
37.35
37.73
39.34
46.88
50.75
55.43
58.04
58.63
69.73
76.84
77.16
77.36
77.48
78.32
113.93
121.41
125.09
125.43
129.29
130.53
131.27
132.93
133.30
135.70
141.47
147.85
156.76
159.20
Me
Me
Me
Me
H
H
H
Me
PMBO
3.39
O
O
S
N
H
O2N
f1 (ppm)

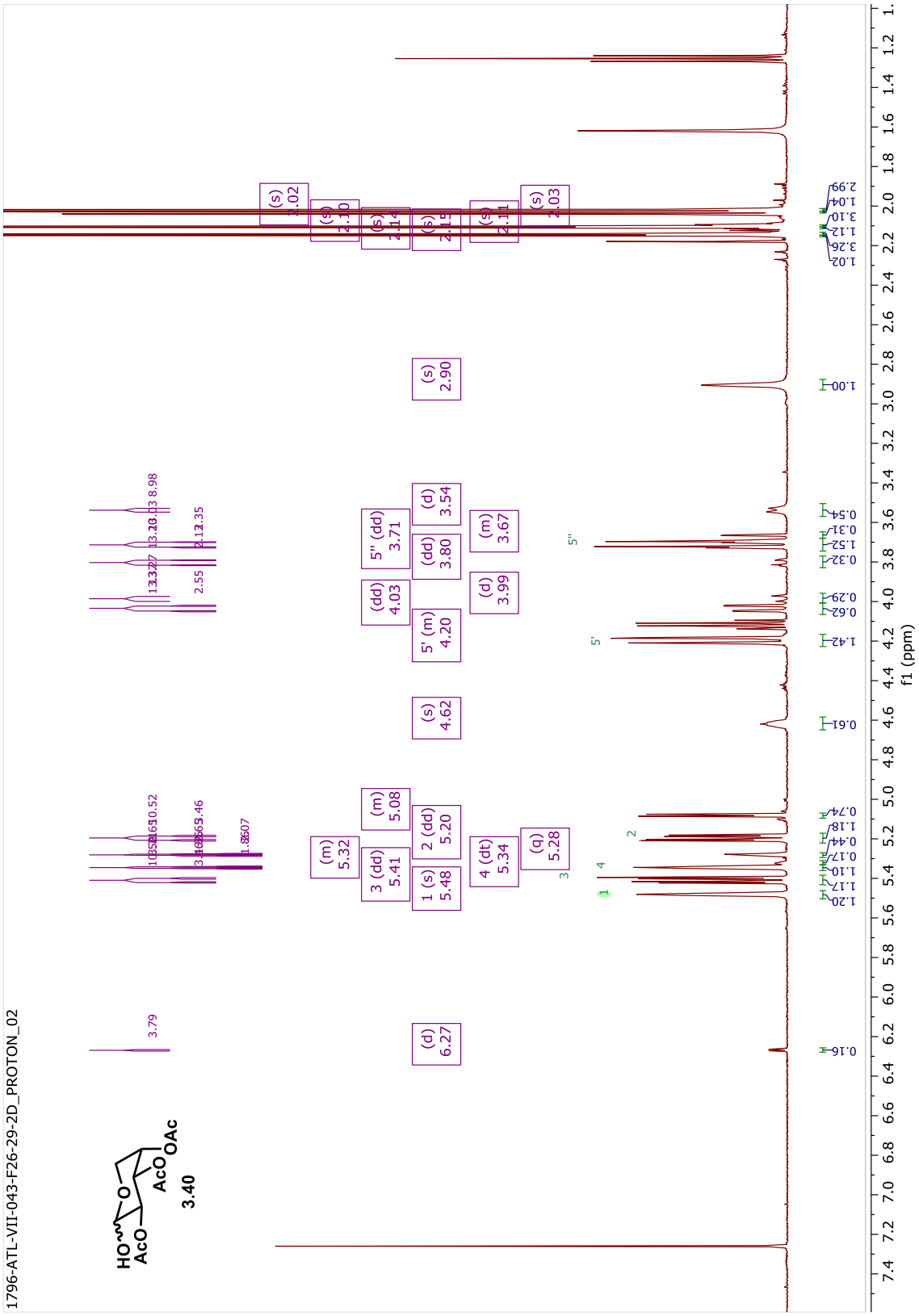
1796-ATL-VII-043-F26-29-2D_PROTON_02
HO
AcO
O
AcO
OAc
3.40
f1 (ppm)

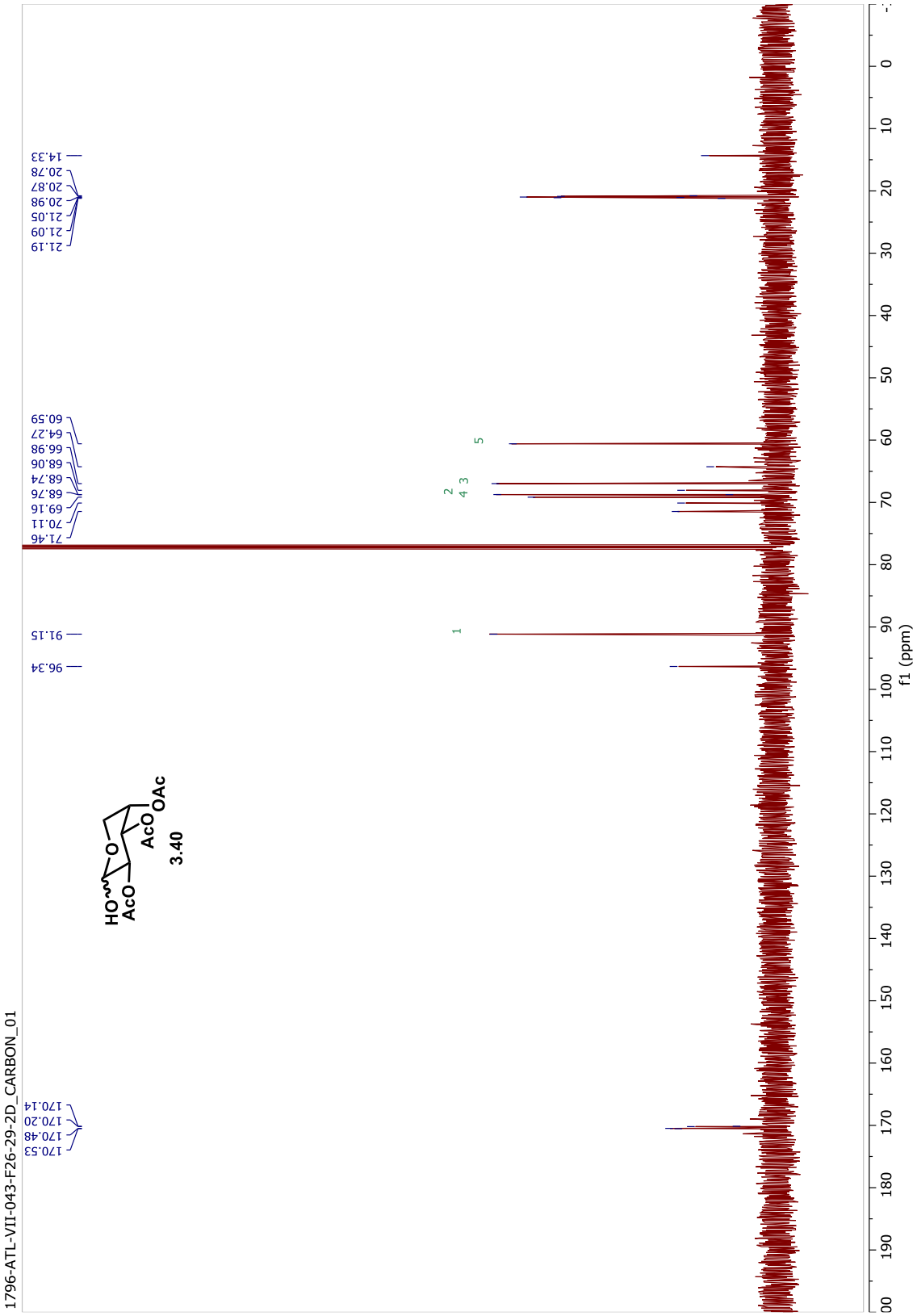
1796-ATL-VII-043-F26-29-2D_CARBON_01
HO
AcO
O
AcO
OAc
3.40
170.53
170.48
170.20
170.14
96.34
91.15
71.46
70.11
69.16
68.76
68.74
68.06
66.98
64.27
60.59
21.19
21.09
21.05
20.98
20.87
20.78
14.33
1
2
4
3
5
f1 (ppm)

N-Glycosylated product **3.41**

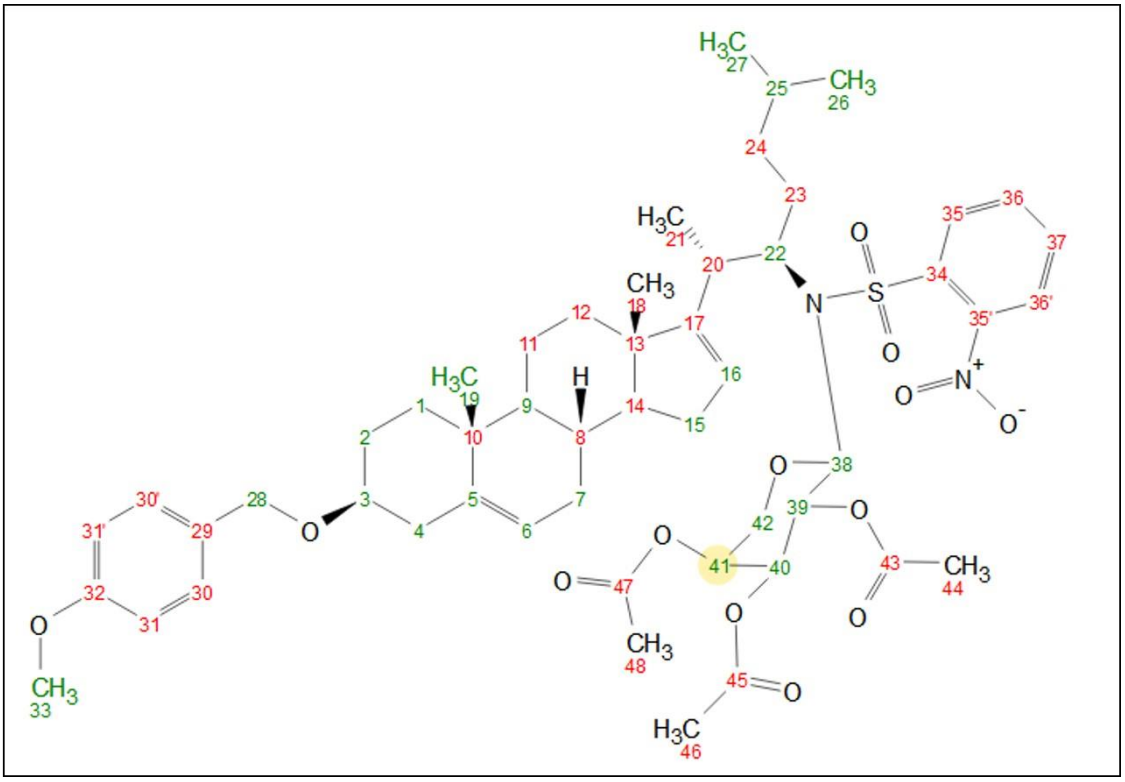

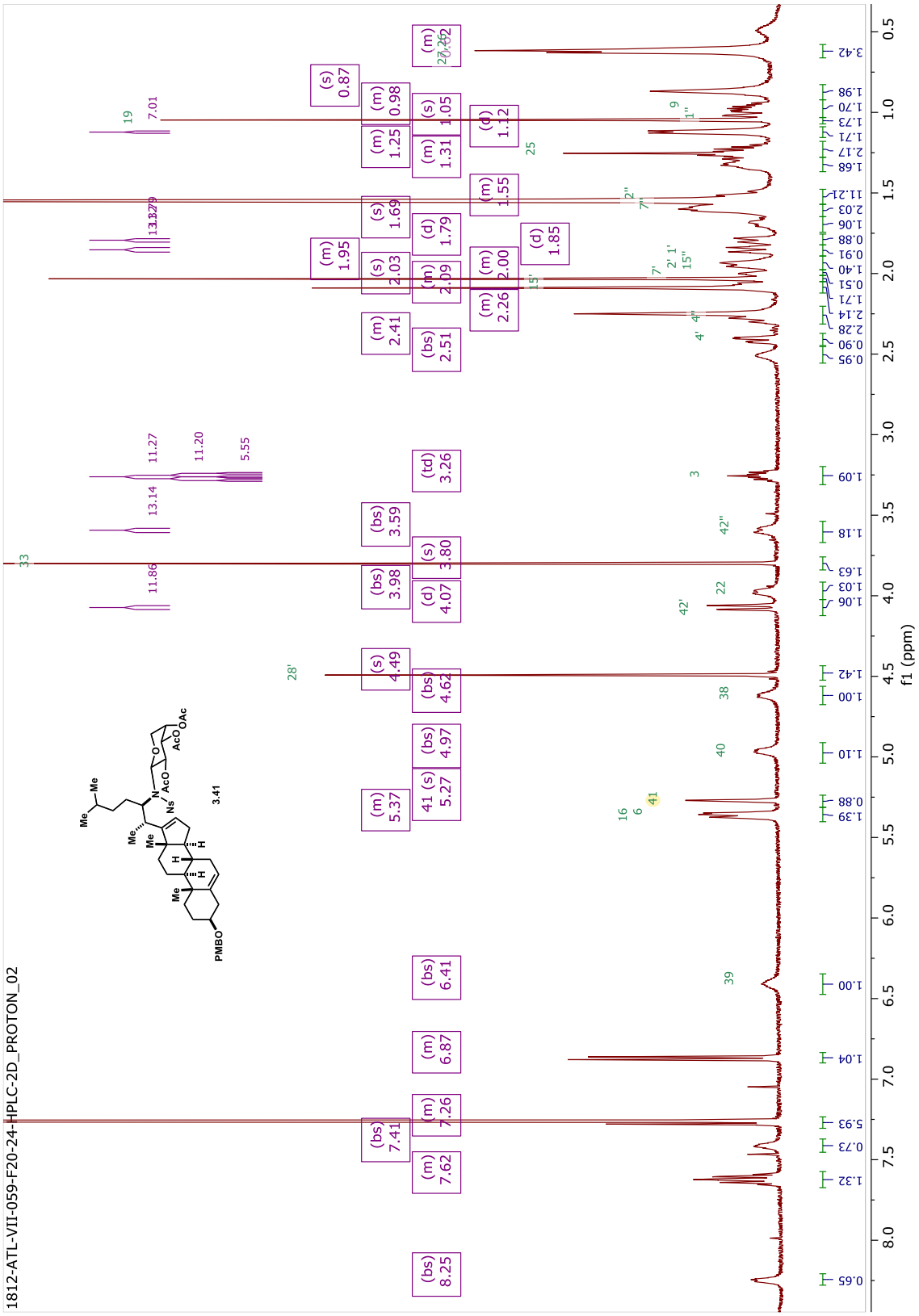
1812-ATL-VII-059-F20-24-HPLC-2D_PROTON_02
f1 (ppm)
PMBO
AcO
OAc
Ns
Me

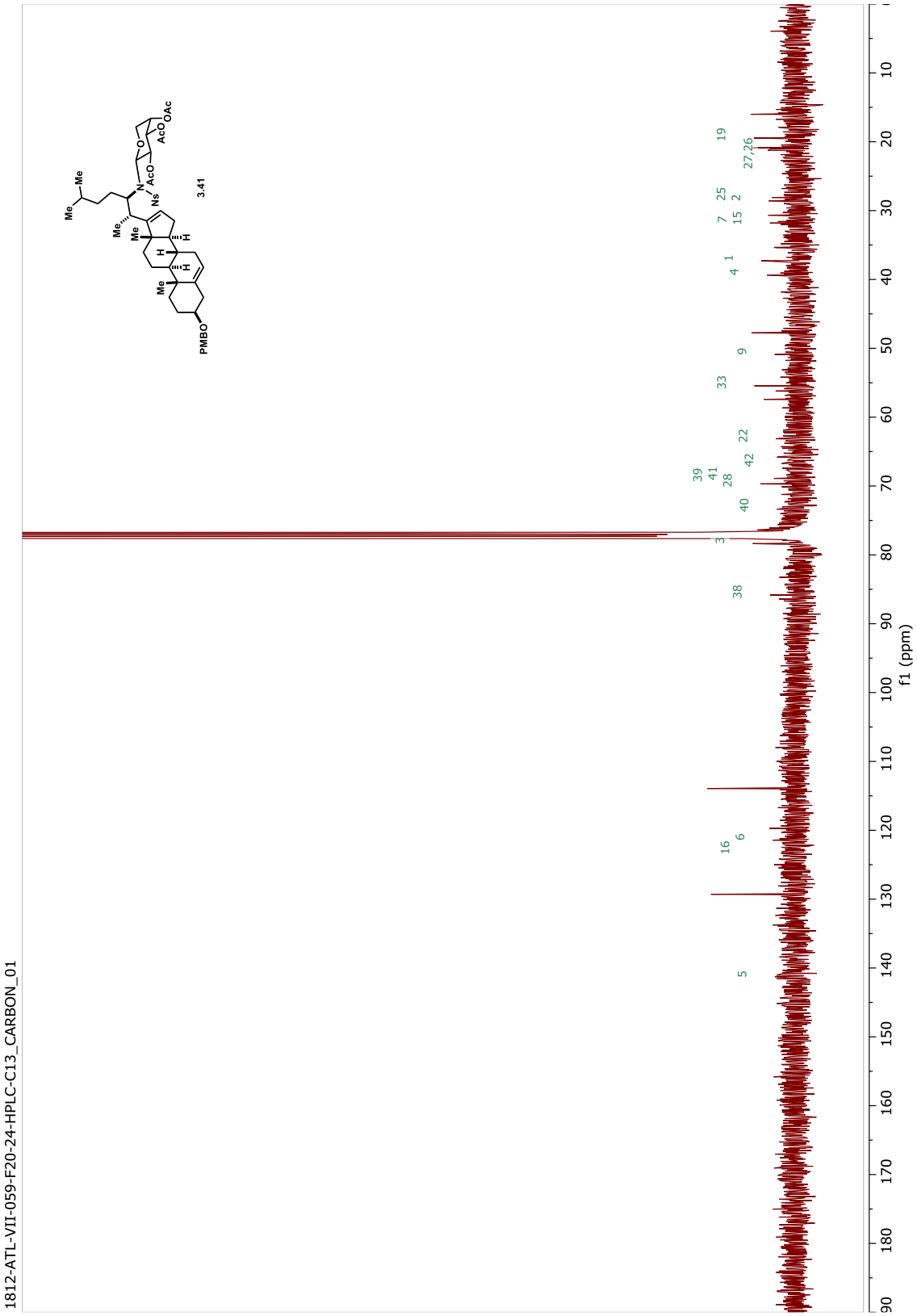
1812-ATL-VII-059-F20-24-HPLC-C13_CARBON_01
3.41
PMBO
AcO
OAc
Ns
Me
f1 (ppm)

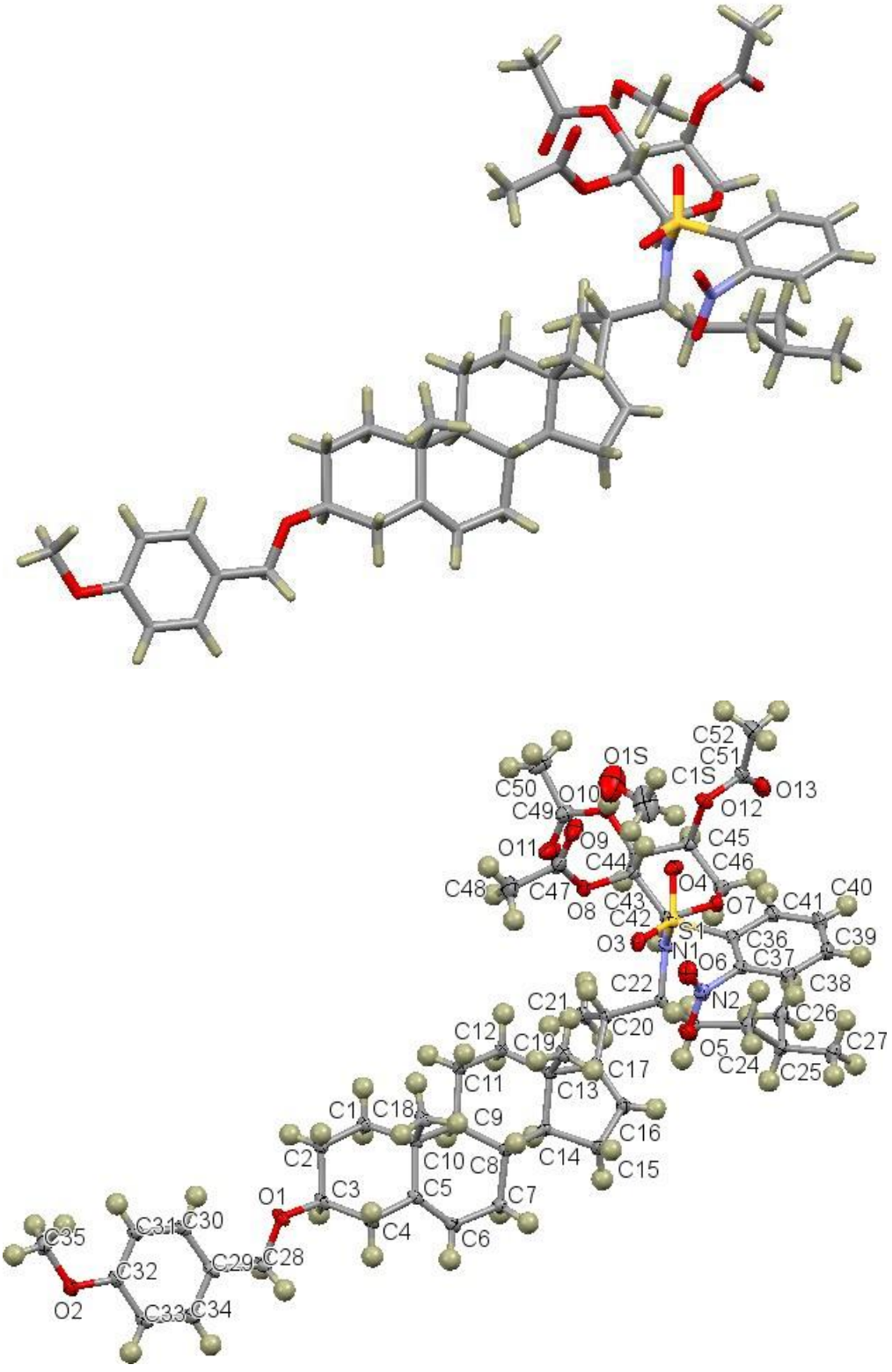
C52
C51
O1S
C1S
C50
O10
O13
C49
O12
O9
C45
O11
C44
C46
C48
C47
O8
C43
O4
O7
C41
C40
C42
S1
O3
N1
O6
C36
C39
C37
C22
C38
N2
C21
C26
C20
C12
C19
O5
C27
C24
C25
C17
C11
C13
C1
C18
C9
C16
C2
C10
C8
C14
C15
O1
C3
C5
C7
C31
C30
C4
C6
C35
C29
C28
C32
O2
C33
C34

X-Ray Crystallography Experimental (Dr. Douglas Powell):

A colorless, plate-shaped crystal of dimensions 0.064 x 0.226 x 0.284 mm was selected for structural analysis. Intensity data for this compound were collected using a D8 Quest diffractometer with a Bruker Photon II ccd area detector (1) and an Incoatec Ims microfocus Mo Ka source (λ = 0.71073 Å). The sample was cooled to 100(2) K. Cell parameters were determined from a least-squares fit of 9979 peaks in the range 2.39 < θ < 27.84°. A total of 80283 data were measured in the range 2.276 < θ < 27.914° using ϕ and ω oscillation frames. The data were corrected for absorption by the empirical method (2) giving minimum and maximum transmission factors of 0.7095 and 0.7456. The data were merged to form a set of 12494 independent data with R(int) = 0.0473 and a coverage of 99.9 %.

The orthorhombic space group $P2_12_12_1$ was determined by systematic absences and statistical tests and verified by subsequent refinement. The structure was solved by direct methods and refined by full-matrix least-squares methods on F^2 (3). The positions of hydrogens bonded to carbons were initially determined by geometry and were refined using a riding model. The hydrogen bonded to O1S was located on a difference map, and its position was refined using a riding model. Non-hydrogen atoms were refined with anisotropic displacement parameters. Hydrogen atom displacement parameters were set to 1.2 (1.5 for methyl) times the isotropic equivalent displacement parameters of the bonded atoms. A total of 631 parameters were refined against 12494 data to give wR(F^2) = 0.0961 and S = 1.010 for weights of w = 1/[σ^2 (F^2) + (0.0550 P)^2 + 1.2500 P], where P = [F_o^2 + 2F_c^2] / 3. The final R(F) was 0.0355 for the 11704 observed, [$F > 4\sigma(F)$], data. The largest shift/s.u. was 0.001

in the final refinement cycle. The final difference map had maxima and minima of 0.242 and -0.302 e/Å^3, respectively. The absolute structure was determined by refinement of the Flack parameter (4).

Table 1. Crystal data and structure refinement for **3.41**

Empirical formula	(C_{52} H_{70} N_2 O_{13} S) · (C	
	H_4 O) C_{53} H_{74} N_2 O_{14} S	
Formula weight	995.20	
Crystal system	orthorhombic	
Space group	$P2_12_12_1$	
Unit cell dimensions	*a* = 11.8174(6) Å	α= 90°
	b = 12.3469(6) Å	β= 90°
	c = 35.8006(18) Å	γ= 90°
Volume	5223.6(5) Å^3	
Z, Z'	4, 1	
Density (calculated)	1.265 Mg/m^3	
Wavelength	0.71073 Å	
Temperature	100(2) K	
F(000)	2136	
Absorption coefficient	0.129 mm^{-1}	
Absorption correction	semi-empirical from equivalents	
Max. and min. transmission	0.7456 and	
0.7095 Theta range for data collection	2.276 to	
27.914° Reflections collected	80283	
Independent reflections	12494 [R(int) = 0.0473]	
Data / restraints / parameters	12494 / 0 / 631	
wR(F^2 all data)	*wR*2 = 0.0961	
R(*F* obsd data)	*R*1 = 0.0355	
Goodness-of-fit on F^2	1.010	
Observed data [I > 2σ(I)]	11704	
Absolute structure parameter	0.00(2)	
Largest and mean shift / s.u	0.001 and 0.000	
Largest diff. peak and hole	0.242 and -0.302 e/Å^3	

$wR2 = \{ \Sigma [w(F_o^2 - F_c^2)^2] / \Sigma [w(F_o^2)^2] \}^{1/2}$

$R1 = \Sigma ||F_o| - |F_c|| / \Sigma |F_o|$

Table 2. Atomic coordinates and equivalent isotropic displacement parameters for compound **3.41** U(eq) is defined as one third of the trace of the orthogonalized U_{ij} tensor.

	x	y	z	U(eq)
S(1)	0.02706(4)	0.57714(4)	0.55595(2)	0.01713(11)
O(1)	0.94094(14)	0.03776(14)	0.69218(4)	0.0239(3)
O(2)	1.42529(14)	-0.17240(14)	0.70177(5)	0.0259(4)
O(3)	0.10633(13)	0.48961(13)	0.55418(5)	0.0225(3)
O(4)	0.02244(15)	0.65427(14)	0.52632(4)	0.0245(3)
O(5)	-0.00385(15)	0.30476(15)	0.59435(5)	0.0306(4)
O(6)	-0.00878(16)	0.28213(15)	0.53403(5)	0.0321(4)
O(7)	-0.06980(13)	0.79590(12)	0.59391(4)	0.0193(3)
O(8)	0.23310(13)	0.78610(13)	0.57478(5)	0.0224(3)
O(9)	0.25102(16)	0.75440(17)	0.51299(5)	0.0366(4)
O(10)	0.17811(14)	1.00586(13)	0.55614(4)	0.0218(3)
O(11)	0.31351(18)	1.03681(18)	0.59914(5)	0.0406(5)
O(12)	-0.04678(14)	0.98600(13)	0.54445(4)	0.0209(3)
O(13)	-0.17844(15)	1.10728(14)	0.56193(5)	0.0280(4)
N(1)	0.04734(15)	0.64249(14)	0.59483(5)	0.0166(4)
N(2)	-0.03915(17)	0.32575(16)	0.56293(6)	0.0228(4)
C(1)	0.74503(18)	0.25580(18)	0.66042(6)	0.0187(4)
C(2)	0.84644(18)	0.1791(2)	0.66097(6)	0.0214(4)
C(3)	0.84562(19)	0.10911(19)	0.69564(6)	0.0206(4)
C(4)	0.7349(2)	0.04696(18)	0.69901(6)	0.0217(4)
C(5)	0.63193(19)	0.11964(17)	0.69626(6)	0.0181(4)
C(6)	0.54783(19)	0.11225(18)	0.72079(6)	0.0198(4)
C(7)	0.44006(19)	0.17628(18)	0.71937(6)	0.0198(4)
C(8)	0.42239(18)	0.23250(17)	0.68170(6)	0.0165(4)
C(9)	0.53610(17)	0.28426(16)	0.66968(6)	0.0152(4)
C(10)	0.62899(18)	0.19831(17)	0.66315(6)	0.0166(4)
C(11)	0.52525(19)	0.36350(18)	0.63646(6)	0.0199(4)
C(12)	0.42898(18)	0.44608(18)	0.64082(6)	0.0200(4)
C(13)	0.31813(18)	0.38733(17)	0.64838(6)	0.0164(4)
C(14)	0.33289(18)	0.32103(17)	0.68453(6)	0.0176(4)
C(15)	0.21074(19)	0.29599(19)	0.69637(7)	0.0229(5)
C(16)	0.15193(19)	0.39811(18)	0.68339(6)	0.0214(4)
C(17)	0.21269(18)	0.45307(17)	0.65844(6)	0.0171(4)
C(18)	0.60776(19)	0.13274(19)	0.62701(6)	0.0209(4)
C(19)	0.2842(2)	0.3172(2)	0.61445(6)	0.0226(4)
C(20)	0.18891(17)	0.55871(17)	0.63828(6)	0.0172(4)
C(21)	0.2409(2)	0.65337(18)	0.66010(7)	0.0237(5)

C(22)	0.06141(17)	0.57345(17)	0.62923(6)	0.0153(4)
C(23)	-0.01101(18)	0.61490(18)	0.66170(6)	0.0176(4)
C(24)	-0.13642(18)	0.58900(19)	0.65736(6)	0.0203(4)
C(25)	-0.21099(19)	0.63232(18)	0.68884(6)	0.0203(4)
C(26)	-0.2111(2)	0.7564(2)	0.68942(8)	0.0270(5)
C(27)	-0.3315(2)	0.5893(2)	0.68428(7)	0.0277(5)
C(28)	0.9862(2)	-0.0005(2)	0.72621(6)	0.0247(5)
C(29)	1.10280(19)	-0.04599(19)	0.71884(6)	0.0208(4)
C(30)	1.1659(2)	-0.01233(18)	0.68821(6)	0.0216(4)
C(31)	1.27411(19)	-0.05222(18)	0.68176(6)	0.0210(4)
C(32)	1.32106(19)	-0.12639(18)	0.70629(6)	0.0204(4)
C(33)	1.2595(2)	-0.16034(19)	0.73727(6)	0.0229(5)
C(34)	1.1512(2)	-0.1207(2)	0.74334(6)	0.0244(5)
C(35)	1.4842(2)	-0.1470(2)	0.66814(8)	0.0299(5)
C(36)	-0.10990(18)	0.51798(18)	0.55853(6)	0.0181(4)
C(37)	-0.13021(18)	0.40723(18)	0.56013(6)	0.0197(4)
C(38)	-0.2391(2)	0.3657(2)	0.55819(6)	0.0237(5)
C(39)	-0.3286(2)	0.4368(2)	0.55452(7)	0.0290(5)
C(40)	-0.3104(2)	0.5472(2)	0.55300(7)	0.0292(5)
C(41)	-0.20155(19)	0.5885(2)	0.55499(7)	0.0234(4)
C(42)	0.04340(18)	0.75948(17)	0.59759(6)	0.0169(4)
C(43)	0.11839(18)	0.82316(18)	0.57019(6)	0.0177(4)
C(44)	0.11373(18)	0.94141(17)	0.58200(6)	0.0182(4)
C(45)	-0.00776(19)	0.98233(18)	0.58275(6)	0.0198(4)
C(46)	-0.08097(19)	0.90644(18)	0.60588(6)	0.0210(4)
C(47)	0.2893(2)	0.7513(2)	0.54391(7)	0.0265(5)
C(48)	0.4028(2)	0.7074(3)	0.55425(10)	0.0425(7)
C(49)	0.2763(2)	1.0496(2)	0.56835(6)	0.0252(5)
C(50)	0.3308(3)	1.1142(3)	0.53815(7)	0.0370(6)
C(51)	-0.1336(2)	1.05463(19)	0.53794(7)	0.0233(5)
C(52)	-0.1639(3)	1.0563(2)	0.49746(8)	0.0357(6)
O(1S)	0.1579(3)	0.6496(3)	0.44607(9)	0.0829(10)
C(1S)	0.0798(3)	0.5639(4)	0.44474(12)	0.0652(11)

Table 3. Bond lengths [Å] and angles [°] for ATL-VII-059-F20-24.

S(1)-O(4)	1.4266(17)	C(7)-H(7AB)	0.9900
S(1)-O(3)	1.4316(17)	C(8)-C(14)	1.524(3)
S(1)-N(1)	1.6266(18)	C(8)-C(9)	1.549(3)
S(1)-C(36)	1.778(2)	C(8)-H(8)	1.0000
O(1)-C(28)	1.412(3)	C(9)-C(10)	1.545(3)
O(1)-C(3)	1.435(3)	C(9)-C(11)	1.545(3)

O(2)-C(32)	1.366(3)	C(9)-H(9)	1.0000
O(2)-C(35)	1.426(3)	C(10)-C(18)	1.547(3)
O(5)-N(2)	1.228(3)	C(11)-C(12)	1.536(3)
O(6)-N(2)	1.220(3)	C(11)-H(11A)	0.9900
O(7)-C(42)	1.417(3)	C(11)-H(11B)	0.9900
O(7)-C(46)	1.437(3)	C(12)-C(13)	1.522(3)
O(8)-C(47)	1.359(3)	C(12)-H(12A)	0.9900
O(8)-C(43)	1.440(3)	C(12)-H(12B)	0.9900
O(9)-C(47)	1.196(3)	C(13)-C(17)	1.530(3)
O(10)-C(49)	1.353(3)	C(13)-C(14)	1.541(3)
O(10)-C(44)	1.439(3)	C(13)-C(19)	1.545(3)
O(11)-C(49)	1.197(3)	C(14)-C(15)	1.536(3)
O(12)-C(51)	1.351(3)	C(14)-H(14)	1.0000
O(12)-C(45)	1.447(3)	C(15)-C(16)	1.513(3)
O(13)-C(51)	1.200(3)	C(15)-H(15A)	0.9900
N(1)-C(42)	1.449(3)	C(15)-H(15B)	0.9900
N(1)-C(22)	1.507(3)	C(16)-C(17)	1.332(3)
N(2)-C(37)	1.476(3)	C(16)-H(16)	0.9500
C(1)-C(2)	1.528(3)	C(17)-C(20)	1.517(3)
C(1)-C(10)	1.547(3)	C(18)-H(18A)	0.9803
C(1)-H(1A)	0.9900	C(18)-H(18B)	0.9799
C(1)-H(1AB)	0.9900	C(18)-H(18C)	0.9799
C(2)-C(3)	1.512(3)	C(19)-H(19A)	0.9802
C(2)-H(2A)	0.9900	C(19)-H(19B)	0.9800
C(2)-H(2AB)	0.9900	C(19)-H(19C)	0.9800
C(3)-C(4)	1.521(3)	C(20)-C(21)	1.534(3)
C(3)-H(3)	1.0000	C(20)-C(22)	1.552(3)
C(4)-C(5)	1.515(3)	C(20)-H(20)	1.0000
C(4)-H(4A)	0.9900	C(21)-H(21A)	0.9800
C(4)-H(4AB)	0.9900	C(21)-H(21B)	0.9800
C(5)-C(6)	1.330(3)	C(21)-H(21C)	0.9801
C(5)-C(10)	1.533(3)	C(22)-C(23)	1.531(3)
C(6)-C(7)	1.500(3)	C(22)-H(22)	1.0000
C(6)-H(6)	0.9500	C(23)-C(24)	1.524(3)
C(7)-C(8)	1.531(3)	C(23)-H(23A)	0.9900
C(7)-H(7A)	0.9900	C(23)-H(23B)	0.9900

C(24)-C(25)	1.527(3)	C(39)-C(40)	1.381(4)
C(24)-H(24A)	0.9900	C(39)-H(39)	0.9500
C(24)-H(24B)	0.9900	C(40)-C(41)	1.386(3)
C(25)-C(27)	1.528(3)	C(40)-H(40)	0.9500
C(25)-C(26)	1.532(3)	C(41)-H(41)	0.9500
C(25)-H(25)	1.0000	C(42)-C(43)	1.538(3)
C(26)-H(26A)	0.9799	C(42)-H(42)	1.0000
C(26)-H(26B)	0.9799	C(43)-C(44)	1.521(3)
C(26)-H(26C)	0.9802	C(43)-H(43)	1.0000

C(27)-H(27A)	0.9801	C(44)-C(45)	1.522(3)
C(27)-H(27B)	0.9801	C(44)-H(44)	1.0000
C(27)-H(27C)	0.9799	C(45)-C(46)	1.521(3)
C(28)-C(29)	1.511(3)	C(45)-H(45)	1.0000
C(28)-H(28A)	0.9900	C(46)-H(46A)	0.9900
C(28)-H(28B)	0.9900	C(46)-H(46B)	0.9900
C(29)-C(30)	1.389(3)	C(47)-C(48)	1.493(4)
C(29)-C(34)	1.396(3)	C(48)-H(48A)	0.9799
C(30)-C(31)	1.390(3)	C(48)-H(48B)	0.9800
C(30)-H(30)	0.9500	C(48)-H(48C)	0.9800
C(31)-C(32)	1.385(3)	C(49)-C(50)	1.490(3)
C(31)-H(31)	0.9500	C(50)-H(50A)	0.9800
C(32)-C(33)	1.391(3)	C(50)-H(50B)	0.9800
C(33)-C(34)	1.388(3)	C(50)-H(50C)	0.9799
C(33)-H(33)	0.9500	C(51)-C(52)	1.493(4)
C(34)-H(34)	0.9500	C(52)-H(52A)	0.9801
C(35)-H(35A)	0.9801	C(52)-H(52B)	0.9800
C(35)-H(35B)	0.9800	C(52)-H(52C)	0.9800
C(35)-H(35C)	0.9800	O(1S)-C(1S)	1.404(5)
C(36)-C(37)	1.390(3)	O(1S)-H(1S)	0.9402
C(36)-C(41)	1.395(3)	C(1S)-H(1SA)	0.9799
C(37)-C(38)	1.387(3)	C(1S)-H(1SB)	0.9799
C(38)-C(39)	1.381(3)	C(1S)-H(1SC)	0.9800
C(38)-H(38)	0.9500		

O(4)-S(1)-N(1)	108.11(10)	C(42)-N(1)-C(22)	120.78(17)
O(3)-S(1)-N(1)	108.41(10)	C(42)-N(1)-S(1)	123.25(15)
O(4)-S(1)-C(36)	106.14(10)	C(22)-N(1)-S(1)	115.79(14)
O(3)-S(1)-C(36)	106.73(10)	O(6)-N(2)-O(5)	125.7(2)
N(1)-S(1)-C(36)	107.06(10)	O(6)-N(2)-C(37)	117.22(19)
C(28)-O(1)-C(3)	115.38(17)	O(5)-N(2)-C(37)	116.99(19)
C(32)-O(2)-C(35)	116.65(19)	C(2)-C(1)-C(10)	114.21(18)
C(42)-O(7)-C(46)	111.12(16)	C(2)-C(1)-H(1A)	108.7
C(47)-O(8)-C(43)	117.89(19)	C(10)-C(1)-H(1A)	108.7
C(49)-O(10)-C(44)	117.81(18)	C(2)-C(1)-H(1AB)	108.7
C(10)-C(1)-H(1AB)	108.7	C(5)-C(10)-C(18)	108.59(17)
H(1A)-C(1)-H(1AB)	107.6	C(9)-C(10)-C(18)	111.78(17)
C(3)-C(2)-C(1)	111.08(18)	C(5)-C(10)-C(1)	108.63(17)
C(3)-C(2)-H(2A)	109.4	C(9)-C(10)-C(1)	108.92(17)
C(1)-C(2)-H(2A)	109.4	C(18)-C(10)-C(1)	109.33(17)
C(3)-C(2)-H(2AB)	109.4	C(12)-C(11)-C(9)	113.80(17)
C(1)-C(2)-H(2AB)	109.4	C(12)-C(11)-H(11A)	108.8
H(2A)-C(2)-H(2AB)	108.0	C(9)-C(11)-H(11A)	108.8
O(1)-C(3)-C(2)	105.96(18)	C(12)-C(11)-H(11B)	108.8
O(1)-C(3)-C(4)	111.84(18)	C(9)-C(11)-H(11B)	108.8
C(2)-C(3)-C(4)	111.03(18)	H(11A)-C(11)-H(11B)	107.7
O(1)-C(3)-H(3)	109.3	C(13)-C(12)-C(11)	109.84(18)

C(2)-C(3)-H(3)	109.3	C(13)-C(12)-H(12A)	109.7
C(4)-C(3)-H(3)	109.3	C(11)-C(12)-H(12A)	109.7
C(5)-C(4)-C(3)	112.75(18)	C(13)-C(12)-H(12B)	109.7
C(5)-C(4)-H(4A)	109.0	C(11)-C(12)-H(12B)	109.7
C(3)-C(4)-H(4A)	109.0	H(12A)-C(12)-H(12B)	108.2
C(5)-C(4)-H(4AB)	109.0	C(12)-C(13)-C(17)	119.34(18)
C(3)-C(4)-H(4AB)	109.0	C(12)-C(13)-C(14)	107.77(17)
H(4A)-C(4)-H(4AB)	107.8	C(17)-C(13)-C(14)	100.16(16)
C(6)-C(5)-C(4)	121.1(2)	C(12)-C(13)-C(19)	110.54(18)
C(6)-C(5)-C(10)	122.51(19)	C(17)-C(13)-C(19)	105.73(17)
C(4)-C(5)-C(10)	116.35(19)	C(14)-C(13)-C(19)	113.07(18)
C(5)-C(6)-C(7)	125.2(2)	C(8)-C(14)-C(15)	121.74(18)
C(5)-C(6)-H(6)	117.4	C(8)-C(14)-C(13)	113.80(17)
C(7)-C(6)-H(6)	117.4	C(15)-C(14)-C(13)	103.43(17)
C(6)-C(7)-C(8)	112.62(18)	C(8)-C(14)-H(14)	105.5
C(6)-C(7)-H(7A)	109.1	C(15)-C(14)-H(14)	105.5
C(8)-C(7)-H(7A)	109.1	C(13)-C(14)-H(14)	105.5
C(6)-C(7)-H(7AB)	109.1	C(16)-C(15)-C(14)	100.33(18)
C(8)-C(7)-H(7AB)	109.1	C(16)-C(15)-H(15A)	111.7
H(7A)-C(7)-H(7AB)	107.8	C(14)-C(15)-H(15A)	111.7
C(14)-C(8)-C(7)	111.17(17)	C(16)-C(15)-H(15B)	111.7
C(14)-C(8)-C(9)	108.94(16)	C(14)-C(15)-H(15B)	111.7
C(7)-C(8)-C(9)	108.26(17)	H(15A)-C(15)-H(15B)	109.5
C(14)-C(8)-H(8)	109.5	C(17)-C(16)-C(15)	112.5(2)
C(7)-C(8)-H(8)	109.5	C(17)-C(16)-H(16)	123.7
C(9)-C(8)-H(8)	109.5	C(15)-C(16)-H(16)	123.7
C(10)-C(9)-C(11)	112.17(17)	C(16)-C(17)-C(20)	131.1(2)
C(10)-C(9)-C(8)	112.03(17)	C(16)-C(17)-C(13)	109.06(18)
C(11)-C(9)-C(8)	113.76(17)	C(20)-C(17)-C(13)	119.67(18)
C(10)-C(9)-H(9)	106.1	C(10)-C(18)-H(18A)	109.5
C(11)-C(9)-H(9)	106.1	C(10)-C(18)-H(18B)	109.5
C(8)-C(9)-H(9)	106.1	H(18A)-C(18)-H(18B)	109.5
C(5)-C(10)-C(9)	109.53(17)	C(10)-C(18)-H(18C)	109.5
H(18A)-C(18)-H(18C)	109.5	C(25)-C(26)-H(26B)	109.5
H(18B)-C(18)-H(18C)	109.5	H(26A)-C(26)-H(26B)	109.5
C(13)-C(19)-H(19A)	109.5	C(25)-C(26)-H(26C)	109.5
C(13)-C(19)-H(19B)	109.5	H(26A)-C(26)-H(26C)	109.5
H(19A)-C(19)-H(19B)	109.5	H(26B)-C(26)-H(26C)	109.5
C(13)-C(19)-H(19C)	109.5	C(25)-C(27)-H(27A)	109.5
H(19A)-C(19)-H(19C)	109.5	C(25)-C(27)-H(27B)	109.5
H(19B)-C(19)-H(19C)	109.5	H(27A)-C(27)-H(27B)	109.5
C(17)-C(20)-C(21)	109.78(17)	C(25)-C(27)-H(27C)	109.5
C(17)-C(20)-C(22)	112.33(17)	H(27A)-C(27)-H(27C)	109.5
C(21)-C(20)-C(22)	113.94(18)	H(27B)-C(27)-H(27C)	109.5
C(17)-C(20)-H(20)	106.8	O(1)-C(28)-C(29)	108.62(18)
C(21)-C(20)-H(20)	106.8	O(1)-C(28)-H(28A)	110.0
C(22)-C(20)-H(20)	106.8	C(29)-C(28)-H(28A)	110.0

C(20)-C(21)-H(21A)	109.5	O(1)-C(28)-H(28B)	110.0
C(20)-C(21)-H(21B)	109.5	C(29)-C(28)-H(28B)	110.0
H(21A)-C(21)-H(21B)	109.5	H(28A)-C(28)-H(28B)	108.3
C(20)-C(21)-H(21C)	109.5	C(30)-C(29)-C(34)	118.3(2)
H(21A)-C(21)-H(21C)	109.5	C(30)-C(29)-C(28)	121.1(2)
H(21B)-C(21)-H(21C)	109.5	C(34)-C(29)-C(28)	120.6(2)
N(1)-C(22)-C(23)	111.69(16)	C(29)-C(30)-C(31)	121.3(2)
N(1)-C(22)-C(20)	110.12(16)	C(29)-C(30)-H(30)	119.4
C(23)-C(22)-C(20)	115.05(17)	C(31)-C(30)-H(30)	119.4
N(1)-C(22)-H(22)	106.5	C(32)-C(31)-C(30)	119.8(2)
C(23)-C(22)-H(22)	106.5	C(32)-C(31)-H(31)	120.1
C(20)-C(22)-H(22)	106.5	C(30)-C(31)-H(31)	120.1
C(24)-C(23)-C(22)	113.33(17)	O(2)-C(32)-C(31)	124.1(2)
C(24)-C(23)-H(23A)	108.9	O(2)-C(32)-C(33)	116.1(2)
C(22)-C(23)-H(23A)	108.9	C(31)-C(32)-C(33)	119.7(2)
C(24)-C(23)-H(23B)	108.9	C(34)-C(33)-C(32)	120.1(2)
C(22)-C(23)-H(23B)	108.9	C(34)-C(33)-H(33)	120.0
H(23A)-C(23)-H(23B)	107.7	C(32)-C(33)-H(33)	120.0
C(23)-C(24)-C(25)	114.35(18)	C(33)-C(34)-C(29)	120.8(2)
C(23)-C(24)-H(24A)	108.7	C(33)-C(34)-H(34)	119.6
C(25)-C(24)-H(24A)	108.7	C(29)-C(34)-H(34)	119.6
C(23)-C(24)-H(24B)	108.7	O(2)-C(35)-H(35A)	109.5
C(25)-C(24)-H(24B)	108.7	O(2)-C(35)-H(35B)	109.5
H(24A)-C(24)-H(24B)	107.6	H(35A)-C(35)-H(35B)	109.5
C(24)-C(25)-C(27)	109.70(18)	O(2)-C(35)-H(35C)	109.5
C(24)-C(25)-C(26)	111.14(19)	H(35A)-C(35)-H(35C)	109.5
C(27)-C(25)-C(26)	110.4(2)	H(35B)-C(35)-H(35C)	109.5
C(24)-C(25)-H(25)	108.5	C(37)-C(36)-C(41)	118.9(2)
C(27)-C(25)-H(25)	108.5	C(37)-C(36)-S(1)	124.31(17)
C(26)-C(25)-H(25)	108.5	C(41)-C(36)-S(1)	116.45(17)
C(25)-C(26)-H(26A)	109.5	C(38)-C(37)-C(36)	121.5(2)
C(38)-C(37)-N(2)	115.3(2)	O(7)-C(46)-H(46A	109.3
C(36)-C(37)-N(2)	123.19(19)	C(45)-C(46)-H(4A)	109.3
C(39)-C(38)-C(37)	118.7(2)	O(7)-C(46)-H(4B)	109.3
C(39)-C(38)-H(38)	120.6	C(45)-C(46)-H(46B)	109.3
C(37)-C(38)-H(38)	120.6	H(46A)-C(46)-H(46B)	107.9
C(40)-C(39)-C(38)	120.8(2)	O(9)-C(47)-O(8)	123.9(2)
C(40)-C(39)-H(39)	119.6	O(9)-C(47)-C(48)	125.5(2)
C(38)-C(39)-H(39)	119.6	O(8)-C(47)-C(48)	110.6(2)
C(39)-C(40)-C(41)	120.4(2)	C(47)-C(48)-H(48A)	109.5
C(39)-C(40)-H(40)	119.8	C(47)-C(48)-H(48B)	109.5
C(41)-C(40)-H(40)	119.8	H(48A)-C(48)-H(48B)	109.5
C(40)-C(41)-C(36)	119.7(2)	C(47)-C(48)-H(48C)	109.4
C(40)-C(41)-H(41)	120.1	H(48A)-C(48)-H(48C)	109.5
C(36)-C(41)-H(41)	120.1	H(48B)-C(48)-H(48C)	109.5
O(7)-C(42)-N(1)	109.90(17)	O(11)-C(49)-O(10)	124.1(2)
O(7)-C(42)-C(43)	108.80(16)	O(11)-C(49)-C(50)	125.5(2)

N(1)-C(42)-C(43)	116.59(18)	O(10)-C(49)-C(50)	110.5(2)
O(7)-C(42)-H(42)	107.0	C(49)-C(50)-H(50A)	109.5
N(1)-C(42)-H(42)	107.0	C(49)-C(50)-H(50B)	109.5
C(43)-C(42)-H(42)	107.0	H(50A)-C(50)-H(50B)	109.5
O(8)-C(43)-C(44)	107.91(17)	C(49)-C(50)-H(50C)	109.5
O(8)-C(43)-C(42)	107.90(17)	H(50A)-C(50)-H(50C)	109.5
C(44)-C(43)-C(42)	107.01(17)	H(50B)-C(50)-H(50C)	109.5
O(8)-C(43)-H(43)	111.3	O(13)-C(51)-O(12)	123.5(2)
C(44)-C(43)-H(43)	111.3	O(13)-C(51)-C(52)	125.5(2)
C(42)-C(43)-H(43)	111.3	O(12)-C(51)-C(52)	111.0(2)
O(10)-C(44)-C(43)	109.45(17)	C(51)-C(52)-H(52A)	109.5
O(10)-C(44)-C(45)	109.06(17)	C(51)-C(52)-H(52B)	109.5
C(43)-C(44)-C(45)	110.96(18)	H(52A)-C(52)-H(52B)	109.5
O(10)-C(44)-H(44)	109.1	C(51)-C(52)-H(52C)	109.5
C(43)-C(44)-H(44)	109.1	H(52A)-C(52)-H(52C)	109.5
C(45)-C(44)-H(44)	109.1	H(52B)-C(52)-H(52C)	109.5
O(12)-C(45)-C(46)	110.73(18)	C(1S)-O(1S)-H(1S)	112.0
O(12)-C(45)-C(44)	107.11(17)	O(1S)-C(1S)-H(1SA)	109.6
C(46)-C(45)-C(44)	109.98(18)	O(1S)-C(1S)-H(1SB)	109.5
O(12)-C(45)-H(45)	109.7	H(1SA)-C(1S)-H(1SB)	109.5
C(46)-C(45)-H(45)	109.7	O(1S)-C(1S)-H(1SC)	109.3
C(44)-C(45)-H(45)	109.7	H(1SA)-C(1S)-H(1SC)	109.5
O(7)-C(46)-C(45)	111.75(17)	H(1SB)-C(1S)-H(1SC)	109.5

N-glycosylated-disaccharide product **3.42**

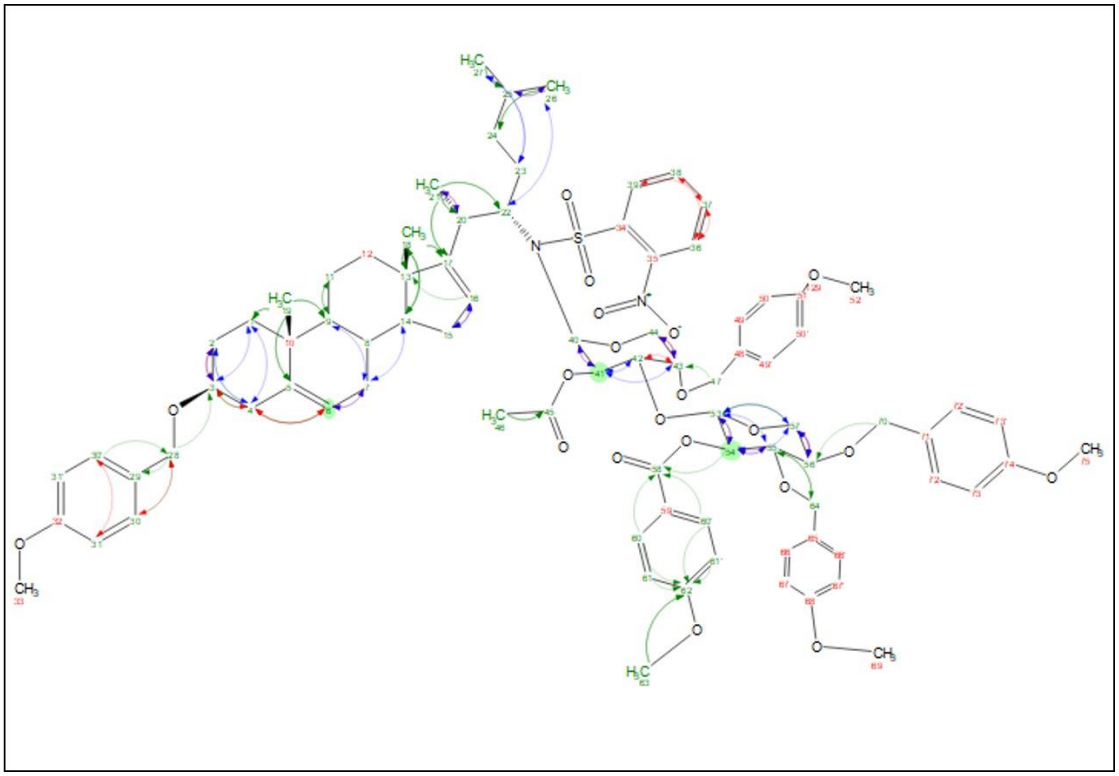

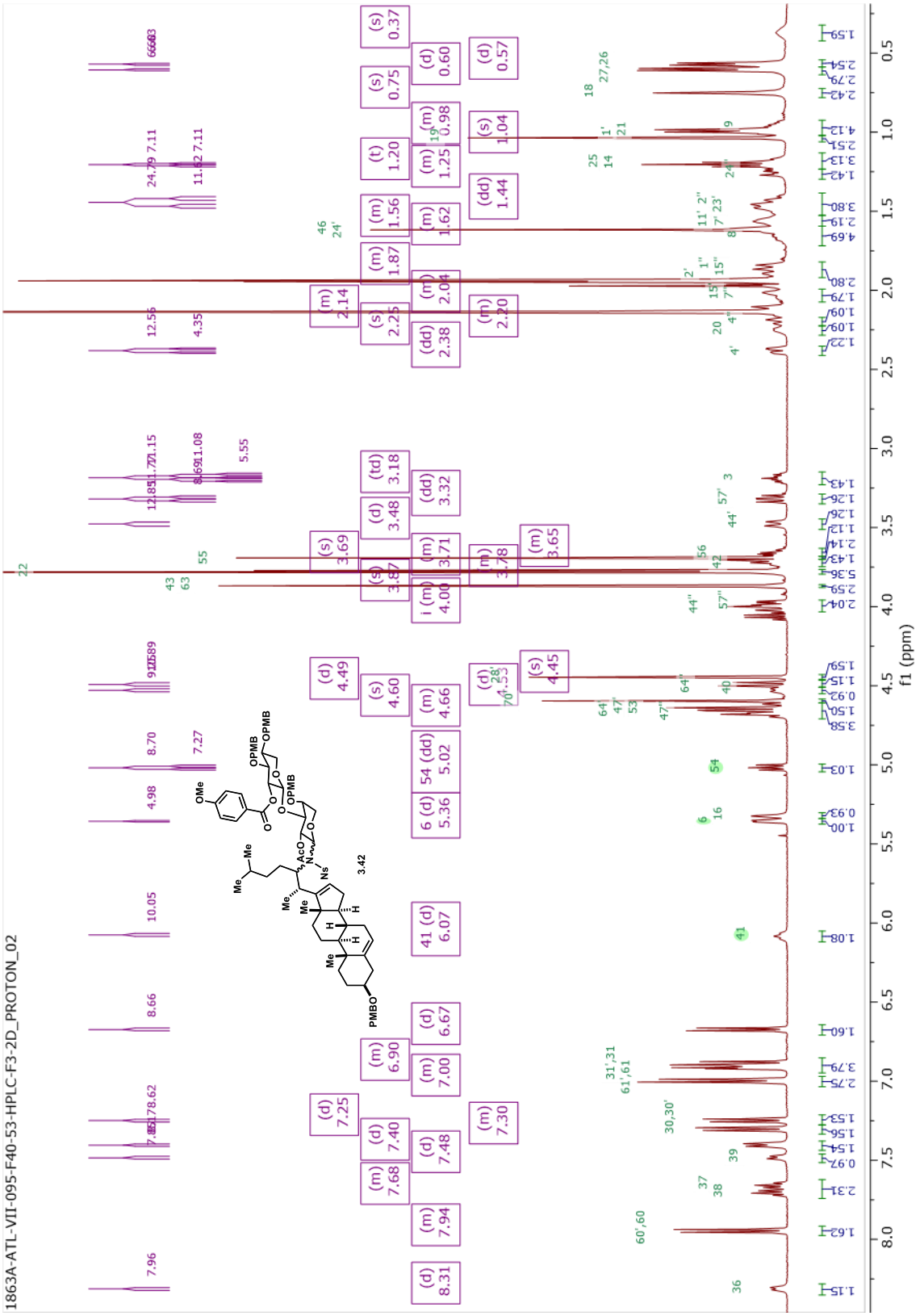
1863A-ATL-VII-095-F40-53-HPLC-F3-2D_PROTON_02
f1 (ppm)

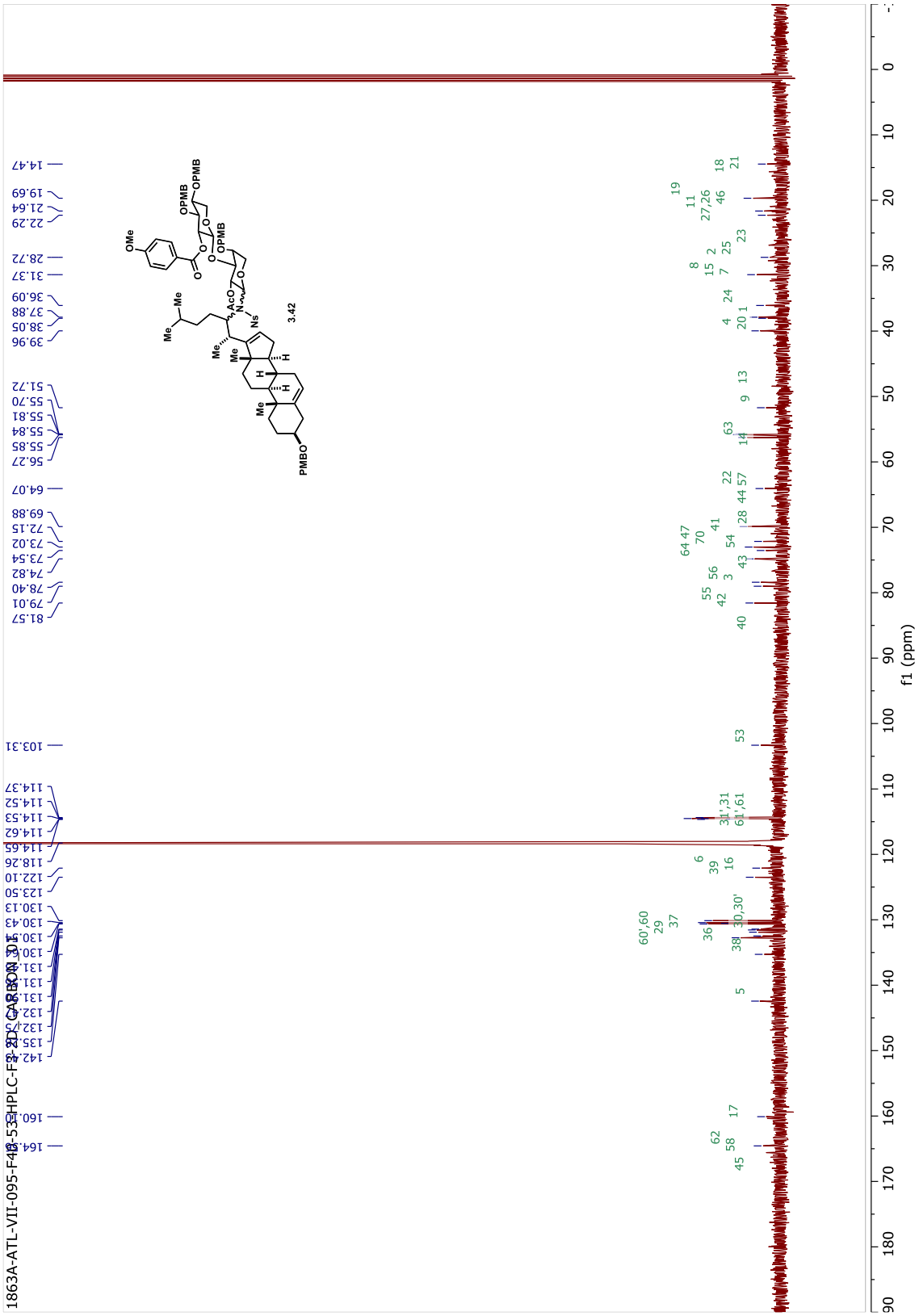
1863A-ATL-VII-095-F48-53-HPLC-F8-2D-CARBON-01
f1 (ppm)
3.42
OMe
OPMB
OPMB
OPMB
AcO
Ns
Me
Me
Me
Me
H
H
H
Me
PMBO

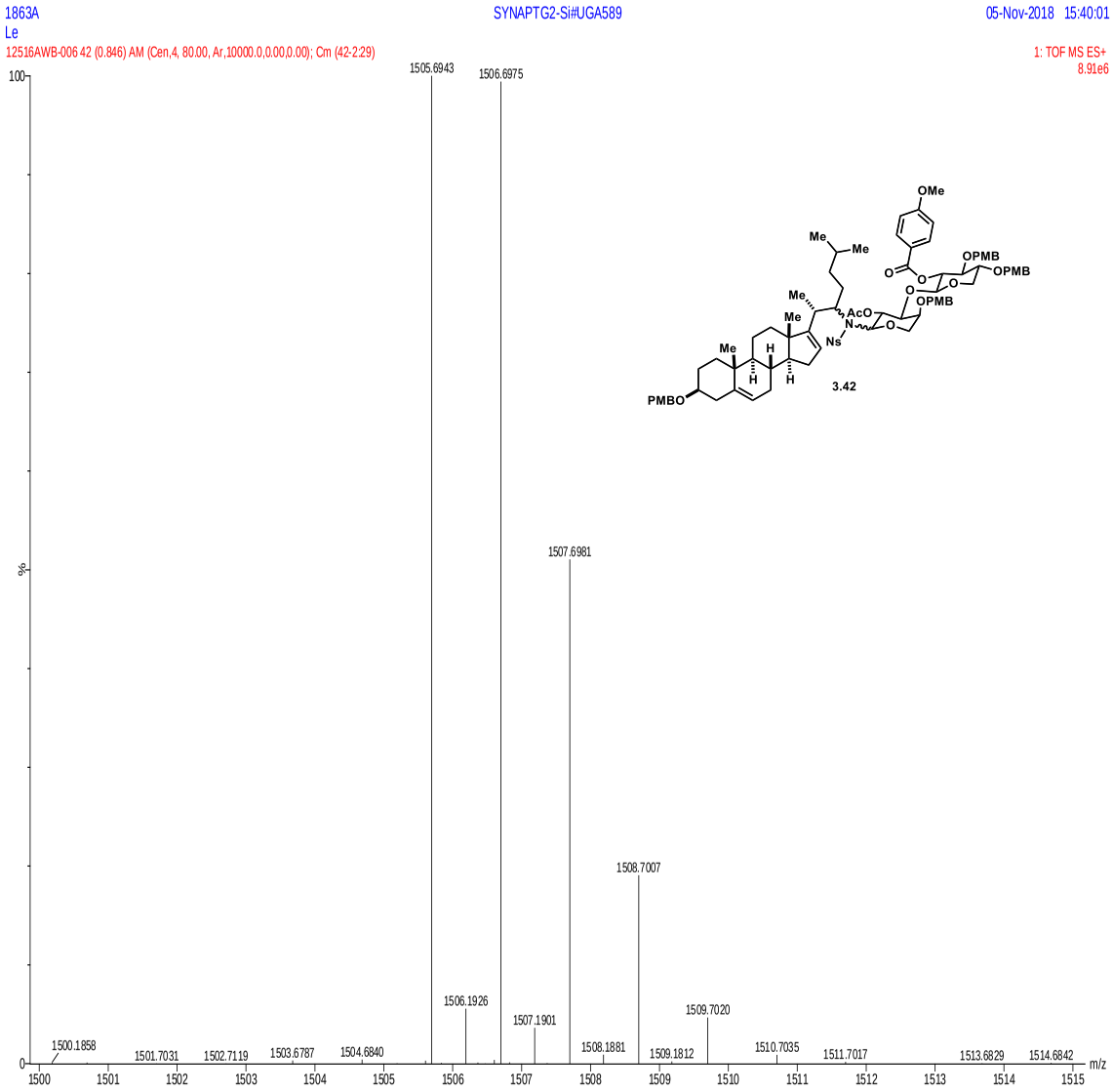
1863A
Le
SYNAPTG2-Si#UGA589
05-Nov-2018 15:40:01
12516AWB-006 42 (0.846) AM (Cen,4, 80.00, Ar,10000.0,0.00,0.00); Cm (42-2:29)
1: TOF MS ES+
8.91e6
100
%
0
1505.6943
1506.6975
1507.6981
1508.7007
1506.1926
1507.1901
1509.7020
1500.1858
1501.7031
1502.7119
1503.6787
1504.6840
1508.1881
1509.1812
1510.7035
1511.7017
1513.6829
1514.6842
1500
1501
1502
1503
1504
1505
1506
1507
1508
1509
1510
1511
1512
1513
1514
1515
m/z
OMe
Me
Me
OPMB
OPMB
OPMB
Me
Me
AcO
N
Ns
Me
H
H
H
PMBO
3.42

Chapter IV : Synthesis, Characterization and Evaluation of Stable-isotopically Labeled Anti-cancer Compounds for Precision Medicine

Abstract

Personalized cancer medicine has emerged as a targeted and tailored treatment approach to maximize the treatment efficacy and reduce toxicity for individual patients. Great advances in sequencing of cancer genomes and characterization of cancer biomarkers allowed for a more targeted cancer treatment [58]. However, patient-tailored administration of chemotherapeutic agents is still in its infancy due to the limitations in robust bioanalytical methods for therapeutic drug monitoring [87]. Here, the synthesis and characterization of stable-isotopically labeled anti-cancer compounds (OSW-1, gemcitabine, and cisplatin) allowed for absolute quantification of the compounds in single, living cells through the development of Single-probe quantitative Single Cell Mass Spectrometry (qSCMS). Utilizing the stable-isotopically labeled anti-cancer compounds, Single-probe qSCMS methodology successfully measured the concentration of the therapeutic agents inside both adherent and suspension cell lines. Based on the success of these in vitro cell line experiments, the qSCMS methodology was successfully used to quantify the intracellular gemcitabine drug levels in bladder cancer cells isolated from patients undergoing chemotherapy. This is perhaps the first instance of using SCMS to quantify the intracellular drug level in a patient cancer cell. The success of the Single-probe qSCMS method will advance personalized cancer medicine forward with a more customizable chemotherapeutic treatment course.

IV.1 Introduction

IV.1.1 Personalized medicine in cancer therapy

Recent advances of personalized cancer medicine entail not only targeted therapy but also focus on personalized and responsive course of treatments with interpatient differences taken into account.[44] Targeted cancer treatments have made great progress with high-throughput sequencing of cancer genomes, along with identification and characterization of cancer biomarkers.[58] However, personalized cancer medicine must also extend to development of a patient-tailored chemotherapy regimen. The conventional method for cancer treatment does not allow for patient-customized therapeutic process, mainly due to the restraint of the bioanalytical capabilities to provide informative patient analyses in a timely manner. Physicians typically determine drug-dosage for patients using mainly their physical characteristics, such as weight or body surface area[88], rather than biological or cancer-specific criteria. The prescribed chemotherapeutic agents are then administered following a pre-established schedule, usually without any real-time bioanalytical method to examine patient's response to the drugs or the efficacy of the treatment. At the end of the treatment course (weeks or months after the first medication administration), physicians conduct end-point analysis, such as an imaging study, to determine the efficacy of the treatment. By this time, patients may have endured an extended period of chemotherapy treatment along with the associated serious side effects, to only then learn that the treatment was not effective.

Therapeutic drug monitoring (TDM) emerged as a method that allows physician to measure the therapeutic agent concentration in biological samples such as serum throughout the course of treatment.[87] TDM provides feedback for the adjustment of the

following dosage to maintain a constant concentration of specific drugs in the patient's bloodstream.[89] Even though TDM enables a more customized dosage for the patient, it suffers the drawback results from inter-individual pharmacokinetic/pharmacodynamics where the amount of drug present in the patient serum might not reflect the amount of drug present at the tumor site.[87] Alternatively, TDM can be performed on tumor biopsies obtained from accessible tumors sites. This would involve invasive methods, and furthermore, the concentration of drugs at the tumor site doesn't necessarily give true validation of therapeutically-relevant concentration of the drug inside of the cancer cells.

The observation of heterogeneity in cancer biology has led the cancer research and anti-cancer therapeutic development to focus on biology at the single cell level. Recent advances in investigation of intratumor-heterogeneity[90], development of cancer stem cells[91], and identification of circulating tumor cells[92,93] have elevated cancer research to a more focused single-cell-level. These developments require methodologies to perform meaningful bioanalysis of patient-isolated cancer cells, which often cannot be easily propagated. A clinical bioanalytical method that allows the concentration of chemotherapeutic agents to be measured from inside of a patient's individual cancer cells would improve therapeutic drug monitoring significantly. This will help physicians to establish optimal dosing regimens that maximize the therapeutic effects while minimize the toxicities. Furthermore, performing single cell analysis on cancer cells isolated from patients undergoing chemotherapy would provide real-time relevant information about the therapeutic efficacy.

IV.1.2 Single Cell Mass Spectrometry and its application in personalized cancer medicine

Within the past two decades, Single Cell Analysis (SCA) has grown exponentially as a new approach that allows the investigation of biology in the individual cells.[94] SCA techniques can now detect and analyze many different classes of biomolecules, including genes, transcripts, proteins and metabolites.[94] Mass spectrometry (MS) has become an important methodology for single cell proteomics and metabolomics with its sensitive ability to simultaneously analyze a large number of molecules.[95] To improve the application of single cell mass spectrometry (SCMS) in biological research, recent advances have been focused on increasing detection sensitivity and mass resolution with novel sampling and ionization techniques.[94] The laboratory of Dr. Zhibo Yang at the University of Oklahoma (OU) has developed a novel SCMS sampling technology named the Single-probe.[45] The Single-probe can sample the intracellular constituents of live single eukaryotic cells for real-time MS analysis under ambient conditions without sample preparation.[45] The fabricated single probe consists of one fused silica capillary that carries solvent, and one nano-ESI emitter embedded in a laser-pulled dual-bore quartz needle (**Figure 12**).[45] For real-time MS analysis, the single-probe is inserted into a live and unaltered cell in order to sample the cell contents and ionize the intracellular components. The analytes are then delivered directly into a Thermo LTQ Orbitrap XL mass spectrometer through the nano-ESI emitter for high-resolution mass spectrometry analysis.

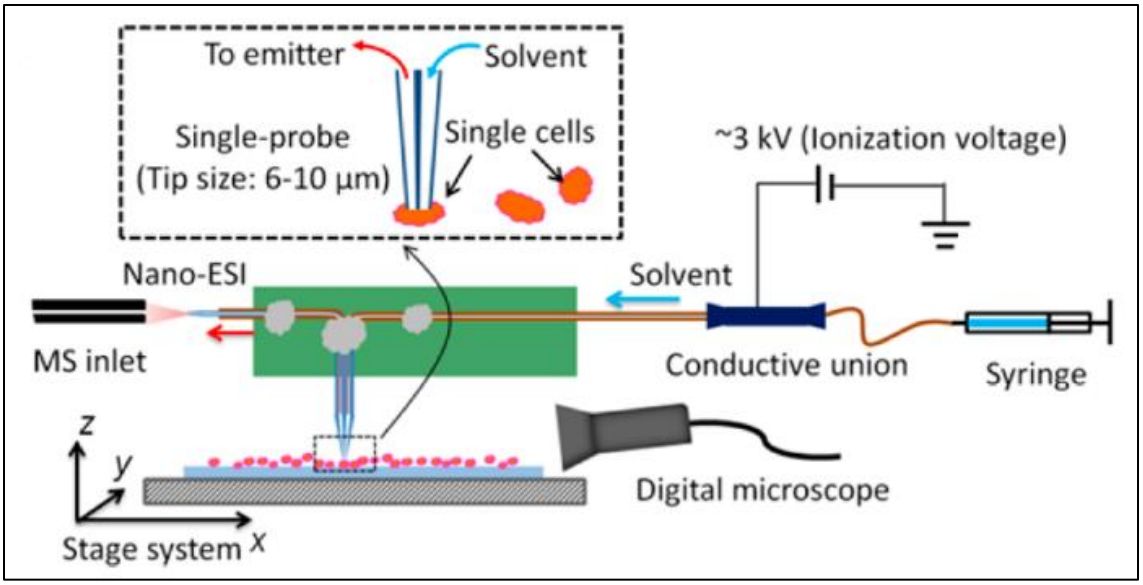

Figure 12. Set up schematic of a single cell MS analysis.
Figure is adapted from Pan *et al.* [45]

The Single-probe MS technique has been used successfully to analyze individual cervical cancer HeLa cells.[45] Multiple cellular metabolites and lipids were detected and identified in both negative and positive modes including ATP, ADP, AMP, phosphatidylcholines, and sphingomyleins.[45,95] When HeLa cells were treated with anticancer compounds such as Doxorubicin (Adriamycin), paclitaxel (Taxol), and OSW-1, the compounds and their metabolites can be detected inside the single cells [45]. Furthermore, the anti-cancer drugs inside of the single cancer cells can potentially be absolutely quantified with quantitative single cell mass spectrometry (qSCMS). The Single-probe qSCMS methodology can be utilized to determine the concentration of drugs inside the single cancer cells, including those from patient-isolated bladder cancer cells. Bladder cancer is an ideal candidate for development of Single-probe qSCMS. Bladder cancer cells are excreted in the urine and can be positively identified from no-cancerous cells based on overall morphology. Moreover, Single-probe qSCMS could also be applied

for other disease states in which the patient's cells can be easily accessed. With the ability to quantify the amounts of small molecules inside the single cells, Single-probe qSCMS will improve therapeutic drug monitoring (TDM) application for physicians and patients, and it will also be a powerful bioanalytical tool in basic biomedical research, especially for hard-to-propagate primary and patient-isolated cell populations.

IV.1.3 Anti-cancer compounds used in qSCMS studies

The experimental protocols for qSCMS methodology can be first established *in vitro* using the Single-probe technology on bladder cancer cell lines treated with anti-cancer compounds cisplatin[96], gemcitabine[97] and OSW-1[10] (**Figure 13**). Cisplatin and gemcitabine are well-established anti-cancer drugs used in treatment of bladder cancer.[97] Both of these drugs work through inducing DNA damage in cells. OSW-1 is a cytotoxic natural product with a unique mechanism of action.[10] By using these structurally diverse compounds, the generality of Single-probe qSCMS application to analyze small molecules will be evaluated.

Absolute quantification of a compound through mass spectrometry (MS) is only possible with the use of an internal standard compound. The ideal MS internal standards are stable-isotopically labeled (deuterated, carbon-13, or nitrogen-15) analogs of the compound of interest (**Figure 13**), which should possess the similar ionization characteristics with a different molecular weight. During the Single-probe qSCMS experiment, the isotopically labeled internal standard compounds will be added at a fixed concentration to the sampling solvent that goes through the Single-probe and carried the analytes from the single cell (**Figure 12**). The MS signal that corresponds to the internal standard will be used to calculate the concentration of the analyte present.

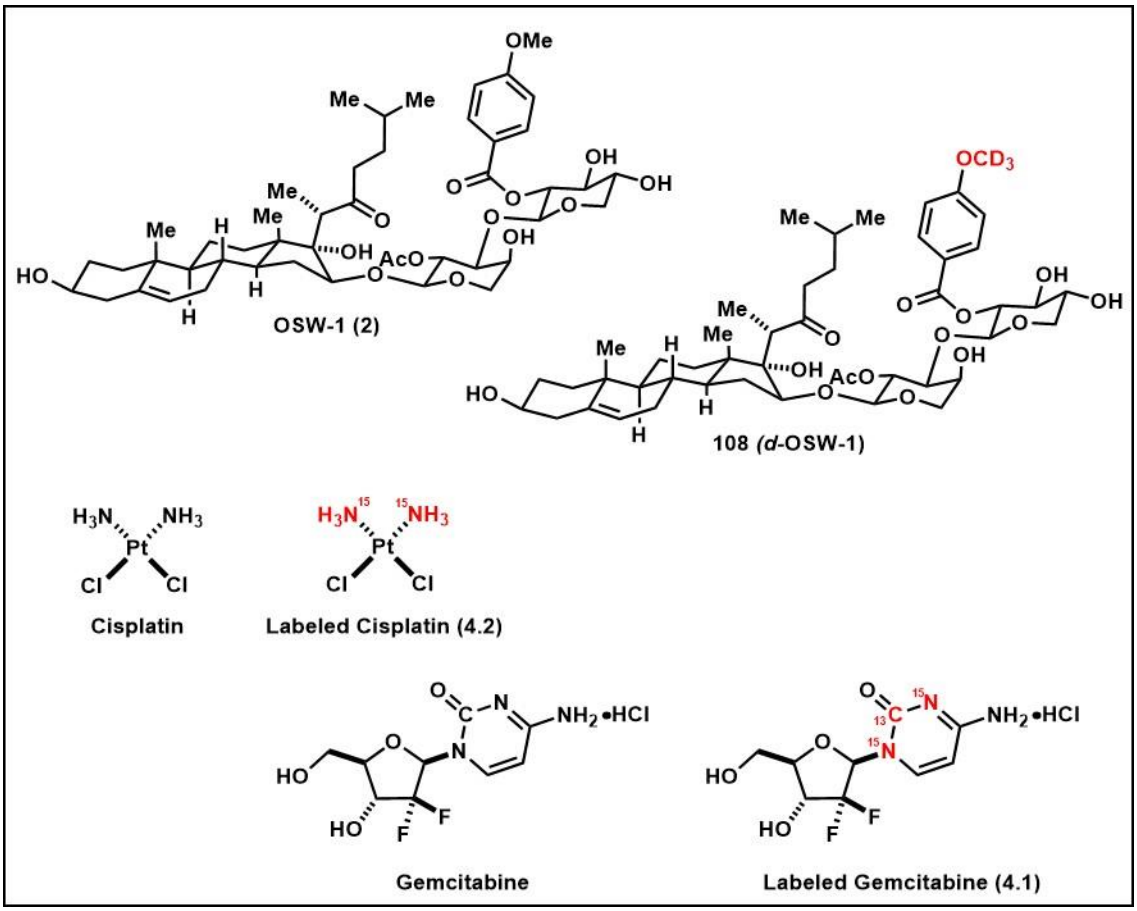

Figure 13. Anti-cancer compounds in qSCMS studies and their stable-isotopically labeled analogs

IV.2 Results and discussion

Isotopically-labeled OSW-1, gemcitabine, and cisplatin were synthesized following the established total synthesis of each compound, with adaptations to incorporate the isotopic labels.[98,99] Once the compounds were successfully synthesized, the labeled compounds underwent full characterization (2D NMR, IR, HR-MS, and biological assays) to validate the presence of stable isotopes at the desired location, and that incorporation of the stable isotopes did not change the bioactivity of the anti-cancer compounds. Then, the labeled compounds were employed as internal standard in Single-probe quantitative Single Cell Mass Spectrometry in Dr. Yang's Lab. Here, the syntheses and characterization of the

stable-isotopically labeled anti-cancer compounds will be described in detail, and their application in Single-probe qSCMS will be highlighted.

IV.2.1 Syntheses of stable-isotopically labeled anti-cancer compounds

IV.2.1.1 Synthesis and characterization of d-OSW-1

The synthesis and characterization of deuterated OSW-1 has been presented in detail in Chapter II (Section **II.3.1** to Section **II.3.4**).

IV.2.1.2 Synthesis and characterization of $^{15}N,^{13}C$-labeled Gemcitabine

Stable-isotopically labeled gemcitabine was accessed through a short sequence of reactions following the synthetic route that scientists at Eli Lily published in 1991 [98]. The starting material 3,5-di-O-benzoate-2-deoxy-2,2-difluoro-D-ribofuranose **4.3** (**Scheme 35**) was purchased commercially as a mixture of both anomers. The hemiacetal mixture was then activated as glycosyl donor by conversion of the free hydroxyl group to a mesyl group in **4.4** with good yield (82%). The glycosyl acceptor was prepared from commercially available 2-^{13}C, 1,3-$^{15}N_2$ cytosine **4.5** (**Scheme 35**). Glycosyl acceptor **4.6** was prepared *in situ* from heating the mixture of cytosine **4.5** and hexamethyldisilane to reflux in presence of ammonium sulfate for 45 minutes. Utilizing the Vorbrueggen glycosylation method, the mesylated glycosyl donor **4.4** was reacted with silylated glycosyl acceptor **4.6** and trimethylsilyl trifluoromethanesulfonate as the activator in refluxing 1,2-dichloroethane for 48 hours. This reaction produced a mixture of protected isotopically labeled gemcitabine **4.7** (76% yield). The glycosylation reaction was presumed to proceed through an S_N1 pathway involving an oxonium ion intermediate, which resulted in a mixture of nucleoside anomers with the ratio of $\alpha : \beta$ being 1.3 : 1 as measured through ^1H NMR.

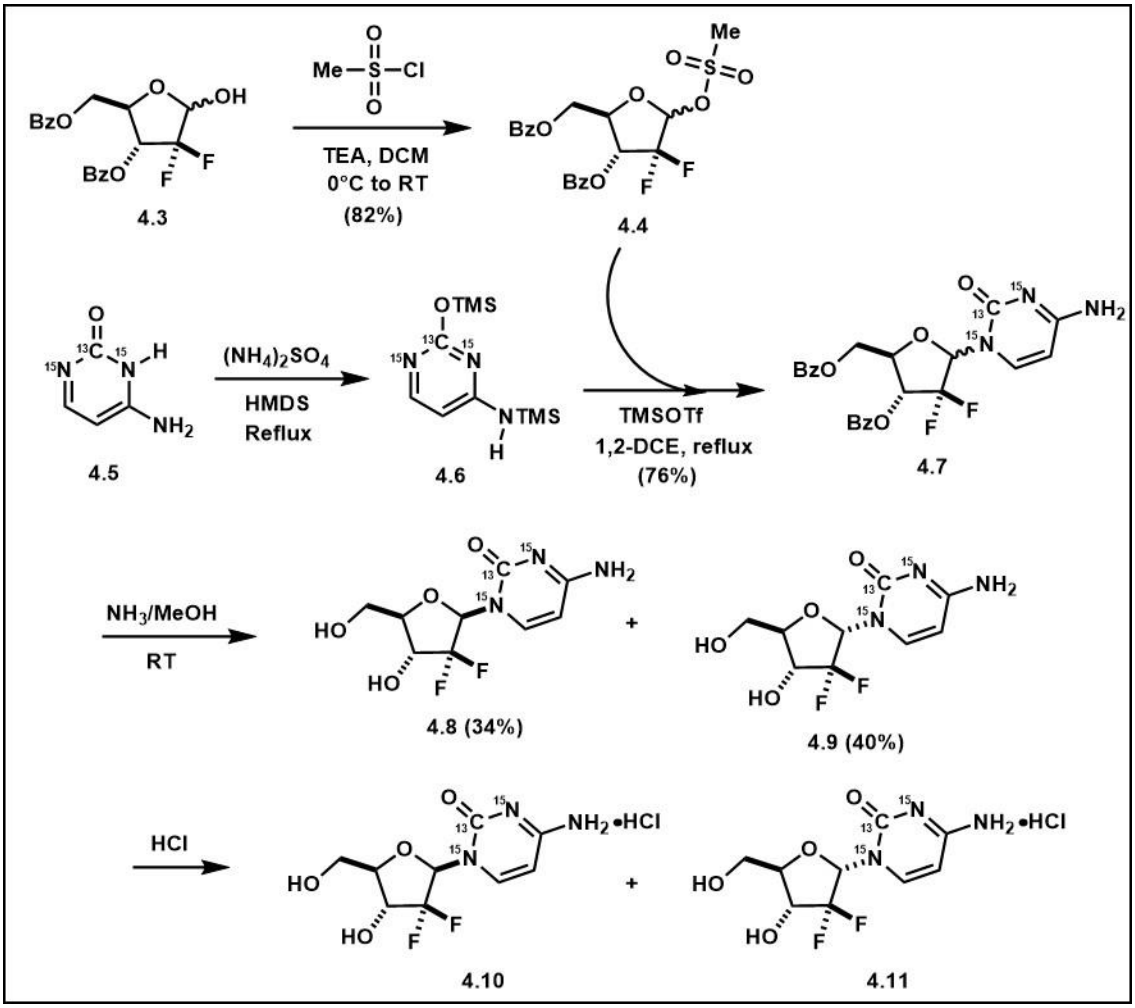

Scheme 35. Synthesis of stable-isotopically labeled Gemcitabine

Treating the mixture **4.7** with ammonia in anhydrous methanol effectively removed both benzoyl protecting groups. The anomeric mixture of deprotected nucleoside were successfully separated through semi-preparative reverse-phase HPLC to afford desired β-anomer (**4.8** in 34% yield) and α-anomer (**4.9** in 4.0% yield). The desired β-nucleoside **4.8** was then converted to the hydrochloride salt of gemcitabine **4.10** in the presence of equimolar HCl in isopropanol. The molecular weight of the stable-isotopically labeled gemcitabine **4.10** was confirmed through high resolution mass spectrometry.

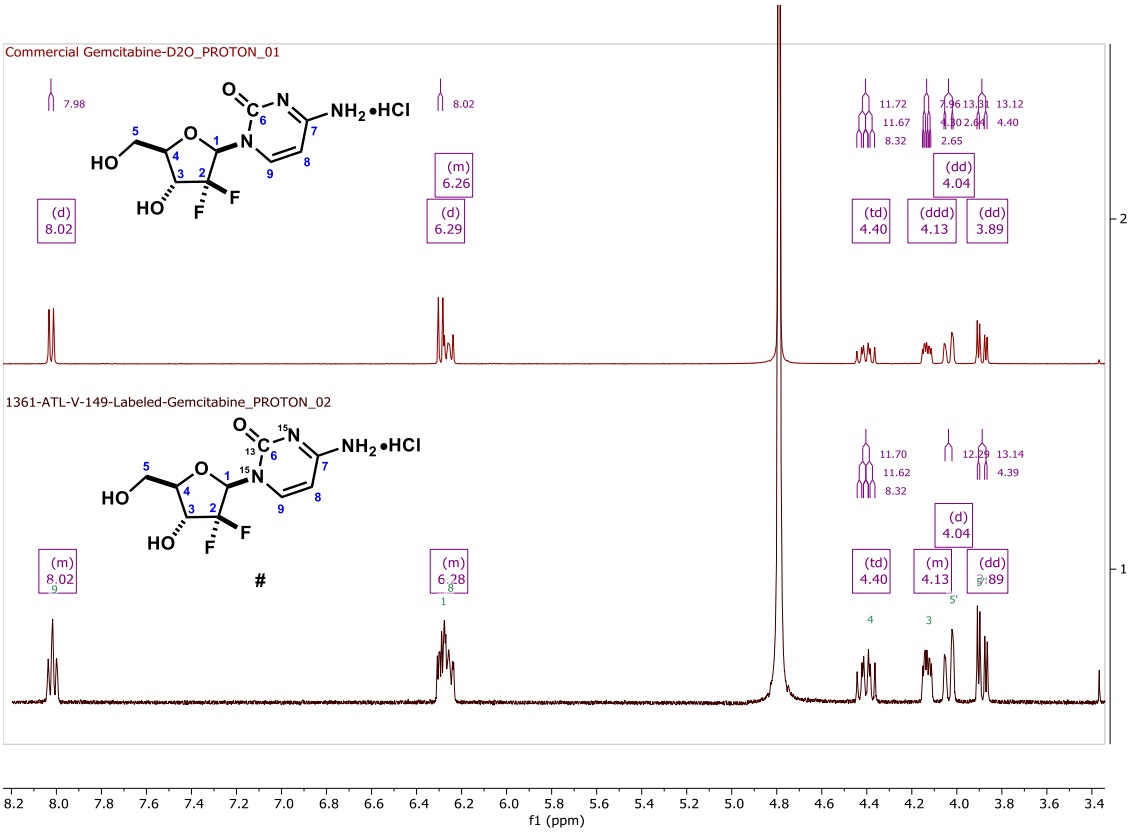

Figure 14. ^{1}H NMR spectra of non-labeled gemcitabine (top) and labeled gemcitabine (bottom)

Since both ^{15}N and ^{13}C are NMR active, the differences observed in the NMR spectra of labeled gemcitabine **4.10** and non-labeled gemcitabine can be used to confirm the presence and placement of the stable isotopes (**Figure 14**). As shown in **Figure 14**, the ^{1}H NMR signals of labeled gemcitabine matched up perfectly with the signals of non-labeled gemcitabine. The differences lie in the splitting patterns of the signals, especially the ones in proximity of ^{15}N and ^{13}C. The most downfield signal (at 8.02 ppm) was assigned to the proton on C-9. In the spectrum of non-labeled gemcitabine, this signal appears as a doublet, since the proton on C-9 can be split by proton on C-8. The signal at 8.02 ppm in the labeled-gemcitabine spectrum displays a different splitting pattern. C-9 in the labeled gemcitabine is adjacent to ^{15}N, which is NMR active. The coupling between proton on C-

9 and this ^{15}N resulted in the more complex splitting pattern observed. Similar patterns can be observed at around 6.28 ppm where two signals corresponding to C-1 and C-8 protons. In the non-labeled gemcitabine spectrum, the signal for C-1 proton appears as a clear doublet, while the signal for C-1 proton of the ^{15}N-labeled-gemcitabine shows a much more complicated multiplicity. The splitting pattern observed in the NMR, along with the HRMS and IR confirmed the structure of stable-isotopically labeled gemcitabine **4.10**.

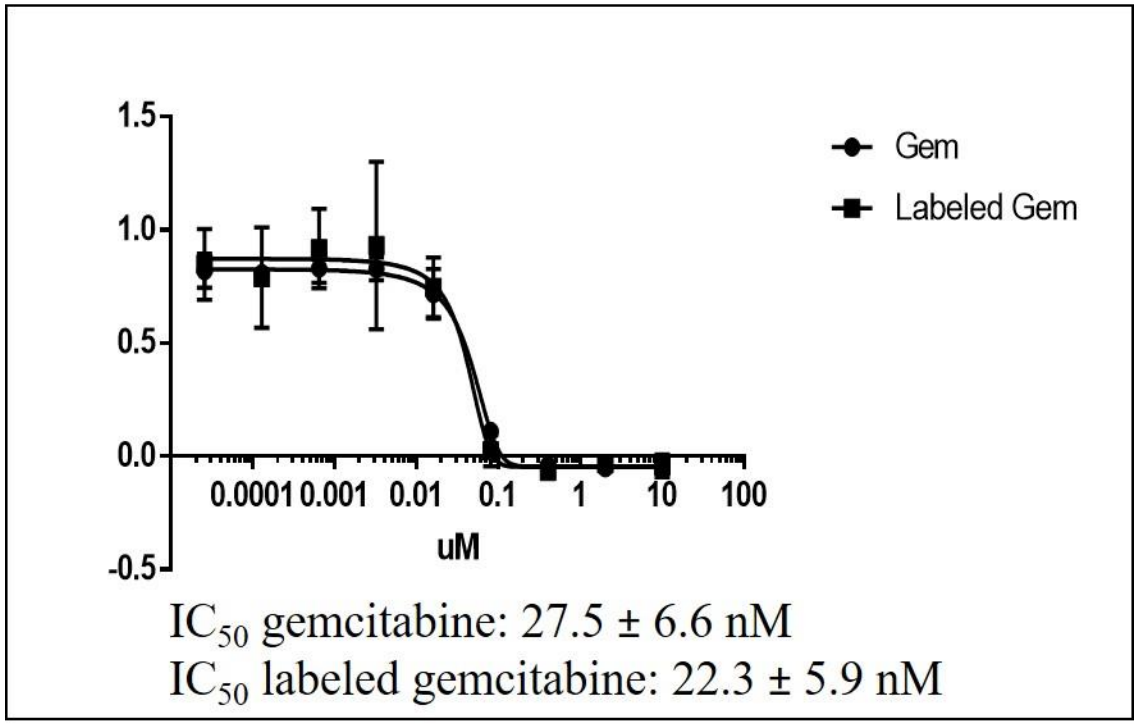

Figure 15. Cytotoxicity assay of non-labeled gemcitabine (Gem) and stable-isotopically labeled Gemcitabine (Labeled Gem) on T-24 cell line

The stable-isotopically labeled gemcitabine was evaluated, along with non-labeled gemcitabine, for their cytotoxicity in the adherent T-24 (bladder cancer) cell line (**Figure 15**). The IC_{50} value obtained for stable-isotopically labeled gemcitabine was 22.3 ± 5.9 nM, while that of non-labeled gemcitabine was 27.5 ± 6.6 nM. These identical values indicate that the presence of stable isotopes of nitrogen and carbon did not alter the

bioactivity of gemcitabine. The Single-probe qSCMS studies utilizing stable-isotopically labeled gemcitabine as the internal standard are underway.

IV.2.1.3 Synthesis and characterization of ^{15}N-labeled Cisplatin

Scheme 36. Synthesis of ^{15}N-labeled cisplatin

The cis-dichlorodiamineplatinum(II) (cisplatin) complex was synthesized following the rapid and facile one-step synthesis adapted from Lebedinsky's method [99] (**Scheme 36**). The ^{15}N-label was incorporated through the use of ^{15}N-labeled ammonium acetate. Potassium tetrachloroplatinate(II) (K_2PtCl_4) was heated in water to reflux in the presence of ^{15}N-labeled ammonium acetate and potassium chloride for 2 hours. After quick filtration of the hot reaction mixture, the desired cisplatin crystallized from the reaction mixture upon cooling. Pure cisplatin was obtained through recrystallization of crude product from 0.1M aqueous HCl in 25% yield. The incorporation of ^{15}N-labeled was confirmed through high resolution mass spectrometry (See **IV.4.2**. Compound data).

The presence of ^{15}N-label can also be observed through ^{1}H NMR (**Figure 16**). In the ^{1}H NMR spectrum of non-label cisplatin, the -NH_3 moiety shows up as a broad singlet at 4.17 ppm, since protons on nitrogen are exchangeable. For the ^{15}N-labeled cisplatin, the signal for -NH_3 group shows up as a doublet at 4.17 ppm with coupling constant of 72.30 Hz. This coupling constant is within range of the reported $J(^{15}N\text{-}^{1}H)$ [100]. The chemical shift of 4.17 ppm was reported to be from cisplatin, since ^{1}H signal for *trans*-platin would be observed at 3.74 ppm [101]. Both non-labeled and ^{15}N-labeled cisplatin were analyzed by 2D NMR (^{15}N – ^{1}H HSQC experiment) to show they have essentially the same chemical shifts

for both proton and nitrogen-15 (See **IV.5**.Chapter Appendix). X-ray crystallography analysis was attempted on ^{15}N-labeled cisplatin, but the crystals could not be grown to the sufficient size for the analysis.

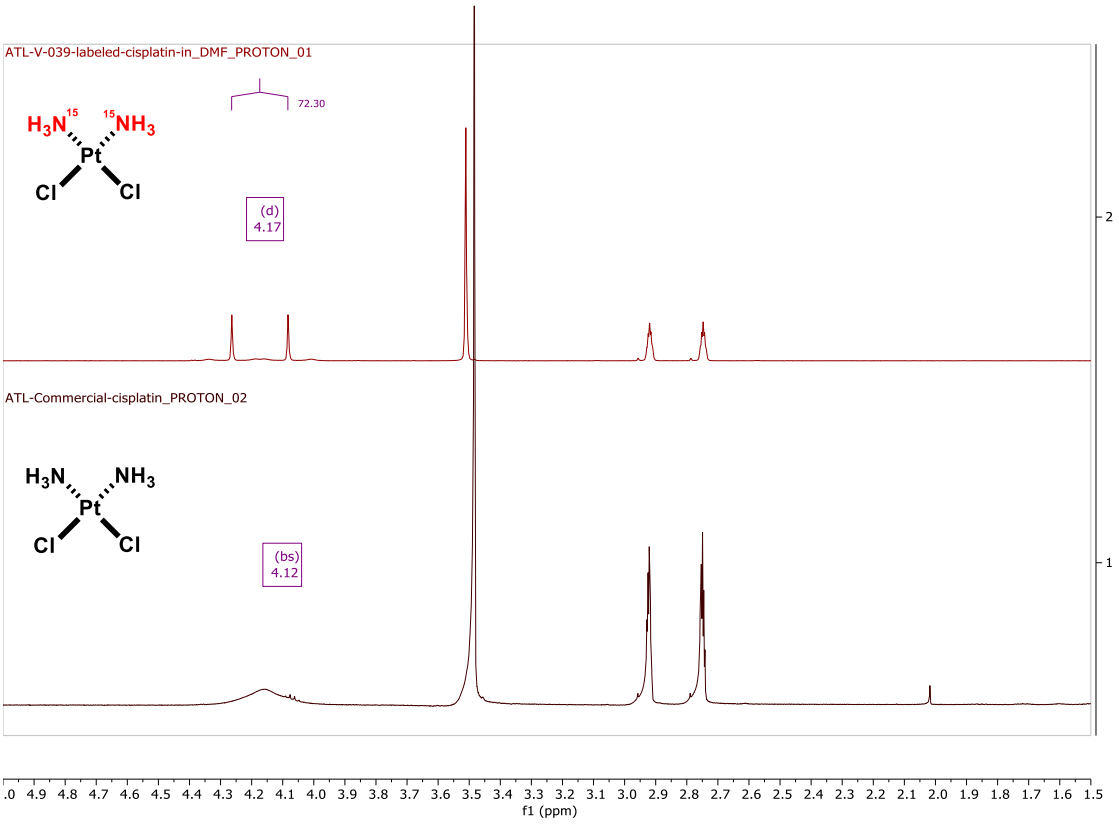

Figure 16. ^{1}H NMR spectra of ^{15}N-labeled cisplatin (top) and non-labeled cisplatin (bottom)

Cisplatin can undergo modifications inside of cells to form other platinum complexes through substitution of the chlorine with water or DMSO.[102] This interferes with the ability to use ^{15}N-labeled cisplatin as internal standard in qSCMS. Therefore, different technologies to detect and quantify platinum are being investigated and developed for qSCMS

IV.2.2 Application of stable-isotopically labeled anti-cancer compounds in qSCMS

Both deuterated OSW-1 and labeled gemcitabine were employed as the internal standards for the development and application of Single-probe qSCMS technology. As

demonstrated in **Figure 17**, a fixed concentration of the internal standard is added to the sampling solvent that goes through the Single-probe to then carry the cellular contents, along with the internal standard, to the mass spectrometry inlet for detection and analysis. The absolute concentration of the compound of interest was calculated based on the average cell volume, the sampling solvent flow rate and the concentration of the internal standard.

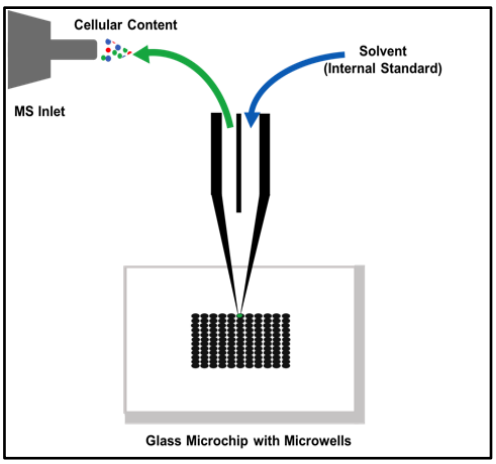

Figure 17. Schematic of real-time SCMS sampling with the Single-probe (courtesy of Shawna Standke)

Deuterated OSW-1 was used for the development and validation of the Single-probe qSCMS technique. **Figure 18** shows a representative mass spectrum of a single cell analysis utilizing the internal standard d-OSW-1. T-24 (bladder cancer) cells were treated for two hours with 1 µM OSW-1. Then the cells underwent single cell analysis with the Single-probe, with 100 nM of *d*-OSW-1 internal standard in the sampling solvent. In the mass spectrum of cellular contents (**Figure 18**), OSW-1 and the internal standard d-OSW-1 were clearly observed. The intensity of the peaks was then used to calculate the moles of OSW-1 present inside the cells.

Using the Single-probe qSCMS technology, the pharmacokinetic and pharmacodynamic properties of compounds of interest can be determined. The concentration of the molecule can be determined immediately at various time points after drug treatment through qSCMS, with minimal sample preparation. This shows a big advantage over the traditional methods of cellular analysis, which includes the preparation

of cell lysate from the samples and analysis through Liquid Chromatography-Mass Spectrometry (LCMS).

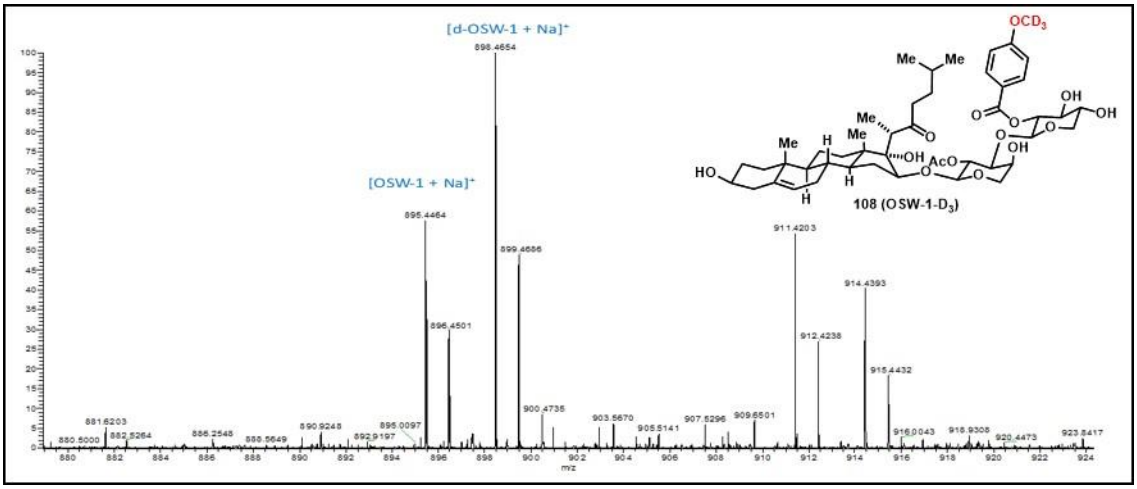

Figure 18. SCMS spectrum of T-24 (bladder cancer) cells after 2 hours treatment of 1µM OSW-1 with 100nM d-OSW-1 in the sampling solvent (courtesy of Shawna Standke and Ryan Bensen)

Similar to d-OSW-1, stable-isotopically labeled gemcitabine was employed as the internal standard for Single-probe qSCMS analysis. **Figure 19** presents the mass spectrum of a T-24 cell following a one-hour treatment with 0.1 µM gemcitabine, with 100 nM of labeled gemcitabine in the sampling solvent. The peaks for both gemcitabine and the internal standard are clearly observed in the spectrum, and their intensities can be used to calculate the moles of gemcitabine present inside the cell after treatment. With the collaboration between Burgett's and Yang's labs, the methodology has been optimized for both adherent cell lines (i.e. T-24 and SW-780-bladder cancer cell lines) and suspension cell lines (i.e. K562-human chronic myeloid leukemia).

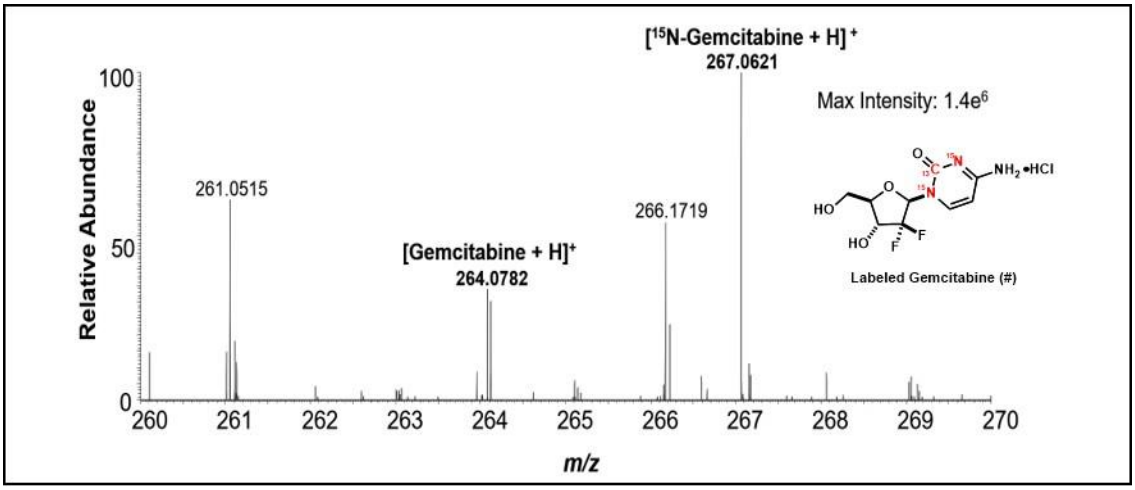

Figure 19. SCMS spectrum of T-24 (bladder cancer) cells after 1-hour treatment of 0.1µM gemcitabine with 100nM labeled gemcitabine in the sampling solvent (courtesy of Shawna Standke and Ryan Bensen)

Gemcitabine is an FDA-approved anti-cancer drug that is used currently in treating bladder cancer [97]. This presents the opportunity to apply Single-probe qSCMS technology to the clinical settings, which could later be adapted for personalized cancer medicine. Urine samples were collected from patients following infusion of gemcitabine as part of standard of care chemotherapy. Cells from patient urine were isolated, and the bladder cancer cells were identified via examination of morphology during the Single-probe analysis. Intracellular gemcitabine was quantified the Single-probe qSCMS method (example result, see **Figure 20**). This could mark the first reported time intracellular chemotherapy drug levels have been measured inside of single cancer cell isolated from a patient. The next stage of research will be to tract the intracellular levels of gemcitabine in bladder cancer cells of patient undergoing active chemotherapy. In the future, physicians could conceivable use the intracellular drug concentrations in a patient's individual cancer cells to adjust and optimize chemotherapy dosage to maximize the treatment efficacy.

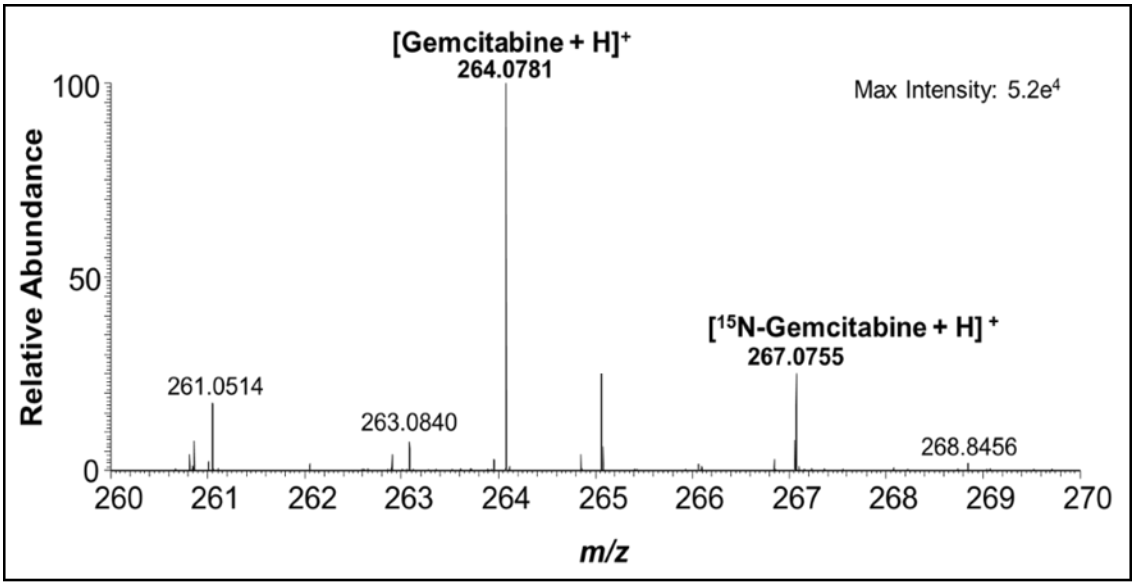

Figure 20. Mass spectrum of gemcitabine and ^{15}N-labeled-gemcitabine (1 µM) from an individual cell isolated from the urine of a bladder cancer patient (courtesy of Shawna Standke and Ryan Bensen)

IV.3 Conclusion

The development of personalized cancer medicine needs to extend beyond patient-matched-targeted treatment to include a more-tailored, and responsive chemotherapeutic administration that will maximize the benefit to the individual patient. The Single-probe quantitative Single Cell Mass Spectrometry emerged as a robust bioanalytical method that allows for the real-time analysis to measure the absolute concentration of therapeutic agent inside the single cells with minimal sample preparation. The synthesis and characterization of stable-isotopically labeled analogs of the anti-cancer compounds (OSW-1, gemcitabine and cisplatin) enabled the absolute quantification of the drugs through the Single-probe methodology. This method has been applied successfully to quantify the amount of drug in both adherent and suspension cell lines. Furthermore, Single-probe qSCMS effectively measured the concentration of gemcitabine, using the produced isotopically-labeled gemcitabine, in bladder cancer cells isolated from patients. This advancement could

develop into powerful too in cancer medicine to provide personalized, adaptable chemotherapy treatments.

IV.4 Experimental section

IV.4.1 General methods

All reactions were performed in oven-dried glassware under a positive pressure of nitrogen unless noted otherwise. Flash column chromatography was performed as described by Still *et al*.[55] employing E. Merck silica gel 60 (230-400 mesh ASTM). TLC analyses and preparative TLC (pTLC) purification was performed on 250µm Silica Gel 60 F254 plates purchased from EM Science and Fluka Analytical. All solvents and chemicals were used as purchased without further purification. Solvents used in the reactions were collected under nitrogen from a Pure Solv 400-5-MD Solvent Purification System (Innovative Technology). Infrared spectra were recorded on a Shimadzu IRAffinity-1 instrument, or Bruker Tensor 27 spectrometer, and IR spectra peaks are reported in terms of frequency of absorption (cm-1). ^{1}H and ^{13}CNMR spectra were recorded on VNMRS 300, VNMRS 400, VNMRS 500 or VNMRS 600 MHz-NMR Spectrometer. Chemical shifts for proton and carbon resonances are reported in ppm (δ) relative to the residual proton or the specified carbon in chloroform (δ 7.26, proton; 77.16, carbon). High-resolution mass spectrometry (HRMS) analysis was performed using Agilent 6538 high-mass-resolution QTOF mass spectrometer. HPLC purification was performed on Shimadzu LCMS 2020 system [LC-20AP (pump), SPD-M20A (diode array detector), LCMS-2020 (mass spectrometer)]. Semi-preparative HPLC purification was performed using Phenomenex Luna C-18(2) column, 5µm particle size (250 mm x 4.6 mm), supported by Phenomenex Security Guard cartridge kit C18 (4.0 mm x 3.0 mm); Phenomenex Luna C-8(2) column, 5µm particle size

(250 mm x 4.6 mm), supported by Phenomenex Security Guard cartridge kit C8 (4.0 mm x 3.0 mm) and HPLC-grade solvents.

IV.4.2 Compound data

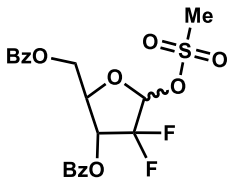

4.4

Compounds **4.4** was synthesized as previously describe.[98] To a solution of 2-Deoxy-2,2-difluoro-D-ribofuranose-3,5-dibenzoate (200.0 mg, 0.529 mmol) in anhydrous DCM (2 mL, 0.26 M) at 0°C was added triethylamine (103 µL, 0.74 mmol), followed by methanesulfonyl chloride (49 µL, 0.634 mmol). The reaction mixture was stirred at RT for 4h15m, when it was completed base on TLC analysis. The reaction mixture was diluted with DCM (20 mL), washed with 1N HCl (15 mL), 5% $NaHCO_3$ solution (15 mL), DI H_2O (15 mL), and brine. The organic phase was dried over Na_2SO_4, and filtered. The solvent was removed in vacuo to afford mixture of products (α:β = 1.3:1) as a sticky yellow gel (200 mg, 82% yield). Products **4.4** was used in the next step without further purification. ^{1}H NMR (400 MHz, Chloroform-d) δ 8.07 (dt, J = 8.5, 1.5 Hz, 5H), 8.05 – 8.02 (m, 2H), 7.66 – 7.61 (m, 2H), 7.58 (td, J = 7.5, 1.4 Hz, 2H), 7.46 (dtd, J = 15.6, 7.7, 2.4 Hz, 9H), 6.13 (d, J = 6.3 Hz, 1H), 6.03 (d, J = 6.5 Hz, 0H), 5.93 (dd, J = 15.0, 6.8 Hz, 1H), 5.57 (dd, J = 16.4, 4.3 Hz, 1H), 4.85 (q, J = 4.1 Hz, 1H), 4.79 – 4.70 (m, 2H), 4.70 – 4.57 (m, 3H), 3.17 (s, 3H), 3.02 (s, 3H). ^{13}C NMR (101 MHz, Chloroform-d) δ 166.01, 165.92, 165.09, 164.95, 134.35, 134.29, 133.74, 133.60, 130.26, 130.19, 129.86, 129.23, 129.16, 128.85, 128.82, 128.79, 128.64, 128.14, 127.98, 123.49, 123.13, 121.01, 120.74, 120.61, 120.45, 118.26, 117.93, 99.99, 99.74, 99.52, 99.28, 99.21, 98.96, 98.79, 98.54, 82.83, 82.80, 82.77,

79.84, 79.76, 71.34, 71.17, 70.98, 70.81, 69.75, 69.60, 69.49, 69.34, 63.06, 62.55, 40.42, 40.30. See **Chapter appendix** for NMR spectra.

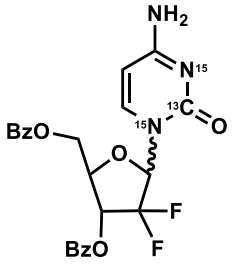

4.7

Compounds **4.7** were synthesized with procedure adapted from Chou *et al*.[98] A suspension of isotopically labeled cytosine **4.5** (25.0 mg, 0.219 mmol), ammonium sulfate (1.2 mg, 0.009 mmol) in hexamethyldisilazane (300 µL, 1.4 mmol) was heated under reflux (130°C) for 45 minutes. The reaction mixture was then cooled to RT. Under N_2 atmosphere, to this reaction mixture was added 1,2-dichloroethane (0.75 mL, 0.3 M) and trimethylsilyl trifluoromethanesulfonate (40 µL, 0.144 mmol). The clear, colorless solution was stirred at RT for 45 minutes. To the reaction mixture was then added SM (66 mg, 0.144 mmol, dissolved in 0.66 mL 1,2-dichloroethane). The reaction mixture was heated under reflux (90°C). The reaction progress was monitored by TLC (5% MeOH/$CHCl_3$, UV). 1,2-DCE was added periodically to keep the same reaction concentration. After 72 hours, the reaction was completed based on TLC analysis. The reaction mixture was cooled to RT, the solvent was removed *in vacuo* to afford a thick gel, which was dissolved in EtOAc (40 mL), washed with DI H_2O (5 mL x 3), 5% $NaHCO_3$ solution (5 mL). The organic phased was dried over Na_2SO_4 and filtered. The solvent was removed *in vacuo* to afford crude mixture (64.8 mg), which was purified through silica gel column chromatography (eluted with MeOH/$CHCl_3$ gradient, 2% to 10% MeOH) to afford desired products **4.7** as a white powder (52.7 mg, 76% yield). ^{1}H NMR (500 MHz, Chloroform-d) δ 8.10 – 8.03 (m, 6H),

8.03 – 7.99 (m, 2H), 7.67 – 7.56 (m, 4H), 7.51 – 7.41 (m, 10H), 6.68 (t, J = 7.0 Hz, 1H), 6.56 (bs, 1H), 5.83 (dd, J = 7.6, 3.6 Hz, 1H), 5.78 (dt, J = 10.3, 5.2 Hz, 1H), 5.70 (dd, J = 7.6, 3.7 Hz, 1H), 5.64 (d, J = 13.1 Hz, 1H), 4.86 – 4.75 (m, 2H), 4.68 (dd, J = 12.4, 4.6 Hz, 1H), 4.64 (d, J = 5.0 Hz, 2H), 4.55 (td, J = 4.7, 3.3 Hz, 1H). See **Chapter appendix** for NMR spectra.

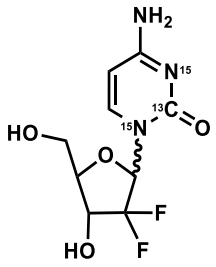

4.8

Compounds **4.8** and **4.9** were synthesized with procedure adapted from Chou *et al*.[98] To a suspension of **4.7** (47.6 mg, 0.10 mmol) in anhydrous MeOH (2 mL) at RT was added NH_3 solution in MeOH (100 µL, 7M solution). The reaction mixture was stirred at RT and the reaction progress was monitored by TLC (10% MeOH/$CHCl_3$, UV). The reaction was completed after 16h by TLC. The solvent was removed *in vacuo* to afford an oily residue, which was resuspended in DI H_2O (10 mL) and EtOAc (5 mL). The aqueous phase was extracted with EtOAc (5 mL) while the organic phase was washed with DI H_2O (5 mL). The combined aqueous phase was concentrated *in vacuo* to afford crude product as a clear gel (25 mg, 94%). The crude mixture was purified through LCMS (C18 column, condition) to afford **4.9** (α-anomer-10.5 mg, 39.5%) and **4.8** (β-anomer-9.0 mg, 33.9%).

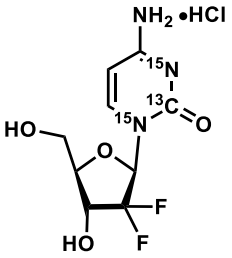

4.10

Compounds **4.10** were synthesized with procedure adapted from Chou *et al*.[98] Compound **4.8** (9.0 mg) was dissolved in DI H_2O (0.5 mL) and isopropanol (0.5 mL), then HCl solution (6 µL of 6N solution) was added. The mixture was mixed for 5 minutes, then the solvent was removed in vacuo to afford **4.10** as a white solid (10.1 mg).

^{1}H NMR (400 MHz, Deuterium Oxide) δ 8.06 – 7.98 (m, 1H), 6.33 – 6.22 (m, 2H), 4.40 (td, J = 11.7, 8.3 Hz, 1H), 4.18 – 4.09 (m, 1H), 4.04 (d, J = 12.3 Hz, 1H), 3.89 (dd, J = 13.1, 4.4 Hz, 1H). ^{13}C NMR (101 MHz, Deuterium Oxide) δ 160.58 (d, J = 14.2 Hz), 144.62 (d, J = 12.6 Hz), 121.62 (t, J = 260.5 Hz), 96.44 (d, J = 3.7 Hz), 86.30 – 84.66 (m), 81.81 (d, J = 7.7 Hz), 71.46 – 68.07 (m), 60.12. ^{19}F NMR (376 MHz, Deuterium Oxide) δ -116.75 (dd, J = 13.0, 5.5 Hz), -117.39 (dd, J = 12.9, 5.4 Hz), -118.00, -118.64. IR (cm^{-1}) 3392.64 (N-H), 3116.57(O-H), 3078.27, 1686.92 (C=N), 1652.89 (C=O), 1258.8 (C-N). HRMS calcd for $C_8{}^{13}CH_{11}F_2N^{15}N_2O_4 + H^+$- $[M+H]^+$: 267.0765; found 267.0730. See **Chapter appendix** for NMR, IR and HRMS spectra.

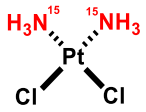

Labeled Cisplatin (4.2)

cis-dichlorodiammineplatinum(II) was synthesized with procedure adapted from Kukushkin *et al*.[99] A suspension of K_2PtCl_4 (100mg, 0.241 mmol), $^{15}NH_4OAc$ (80.9 mg, 1.04 mmol) and KCl (100.6 mg, 1.35 mmol) in DI H_2O (1.5 mL) was heated under reflux

(115°C) for 2 hours. During this period, the color of the reaction mixture changed from red to orange/brown (after 30 minutes), and then green-ish yellow (after 1 hour). After 2 hours, the hot reaction mixture was filtered through a cotton plug. The yellow filtrate was cooled in an ice bath and then stored at 4°C for 2 hours. The yellow precipitate was collected by centrifugation. The solid was washed with chilled DI H2O (3 mL x 3). The solid was then dried on hi-vac to afford crude product (58.6 mg). The crude product was purified through recrystallization in hot 0.1N HCl. The crude product was dissolved in sufficient amount of hot 0.1N HCl (~3.7 mL) to obtain a clear, yellow solution. The solution was immediately centrifuged for 30 seconds to separate any undissolved materials. The yellow supernatant was removed, then cooled in an ice bath for 15 minutes. To the mixture was added cold 200-proof EtOH (~12 mL). The yellow solid was collected by centrifugation, washed with cold EtOH (3 mL x 2), dried on hi-vac to afford the labeled cisplatin **4.2** (36.5 mg, 25% yield).

The NMR data (both ^{1}H and ^{15}N) matched perfectly with the commercially available cisplatin. In ^{1}H NMR spectrum of labeled cisplatin, a doublet with J-value of 72.3 Hz was observed, in comparison with a broad doublet in commercial cisplatin. This is due to N-15 being NMR active, therefore it splits the ^{1}H-NMR signal correspond to -NH_3 groups.

^{1}H NMR (500 MHz, DMF-d7) δ 4.16 (d, J = 72.3 Hz, 6H).^{15}N NMR (51 MHz, DMF-d7) δ -45.72. IR (cm_{-1}) 3278.39, 3200.45, 1618.74, 1536.15, 1307.72, 1292.16, 792.50. HRMS calcd for $Cl_2H_6{}^{15}N_2Pt + H^+$ $[M+H]^+$: 301.9569, found: 301.9534

IV.4.3 Cell cytotoxicity assay

T24 cell lines were grown in McCoy's medium supplemented with 10% synthetic fetal bovine serum and 1% penicillin-streptomycin. All cells were maintained in an incubator at

37°C under 5% CO_2, and they were passaged around 75% confluency. To avoid mutations, only cells under passage number 25 that were in culture less than 2 months were utilized in the experiments.

Cells (5000 cells/well) were plated into 96-well plates in 75 µl of medium. After 24 h, a time-zero plate was produced by adding 25 µL of medium and 20 µL of CellTiter-Blue (Promega) to the wells and then incubating the plates at 37 °C for 90 min. Fluorescence (560 nm excitation; 590 nm emission) was detected using a Tecan Infinite M200 to establish cell viability at time of dosing. Then, compounds were serially diluted in medium and delivered to the cells as 4× solutions in 25 µl of medium. At either 48 h or 72 h, CellTiter-Blue was added, and the fluorescence was recorded as described above. Growth relative to untreated cells was calculated, and this data was fitted to a four-parameter dose-response curve using GraphPad Prism 8.

IV.5 Chapter appendix

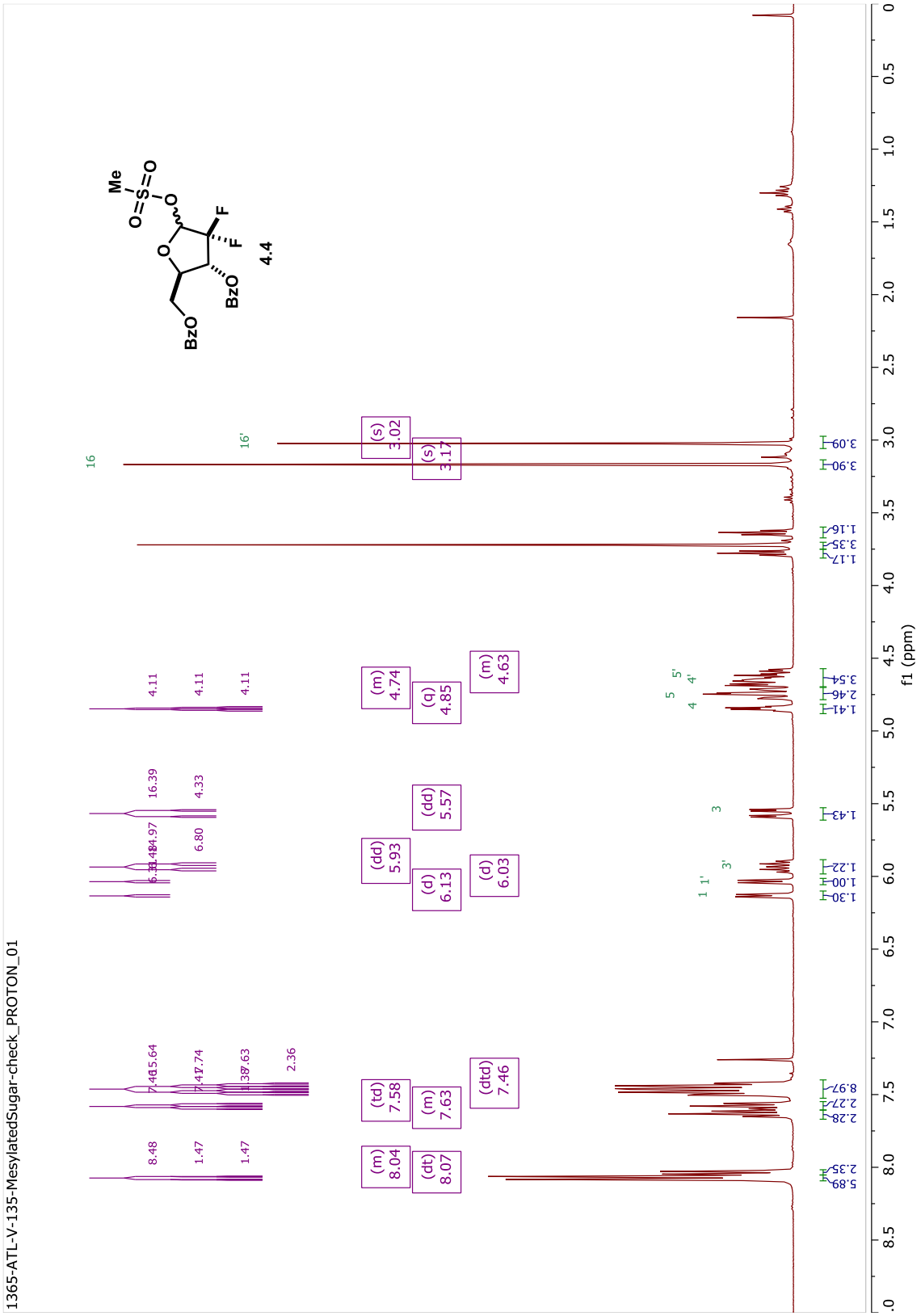

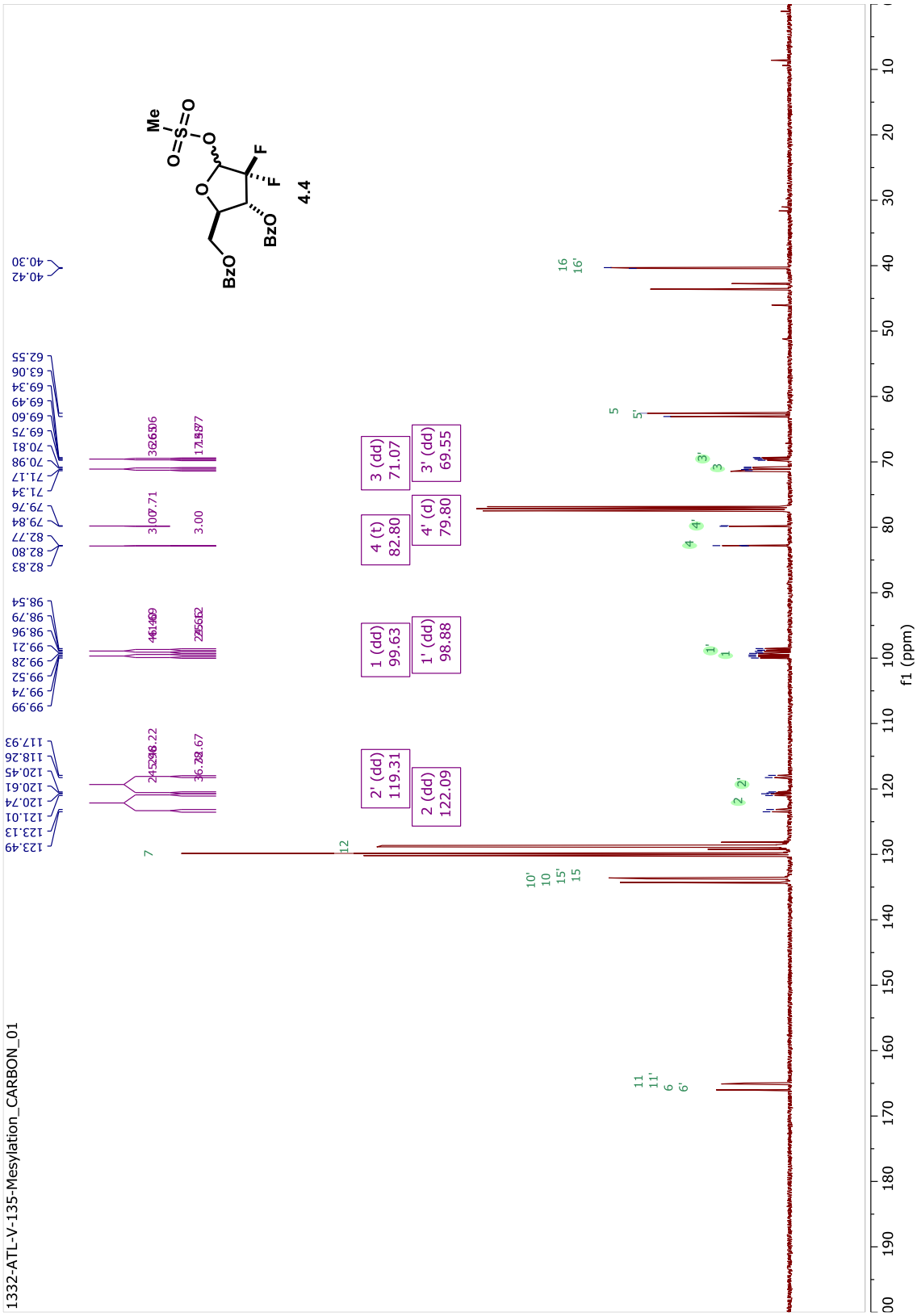
1332-ATL-V-135-Mesylation_CARBON_01
Me
O=S=O
O
O
F
F
BzO
BzO
4.4
f1 (ppm)
2' (dd)
119.31
2 (dd)
122.09
1 (dd)
99.63
1' (dd)
98.88
4 (t)
82.80
4' (d)
79.80
3 (dd)
71.07
3' (dd)
69.55

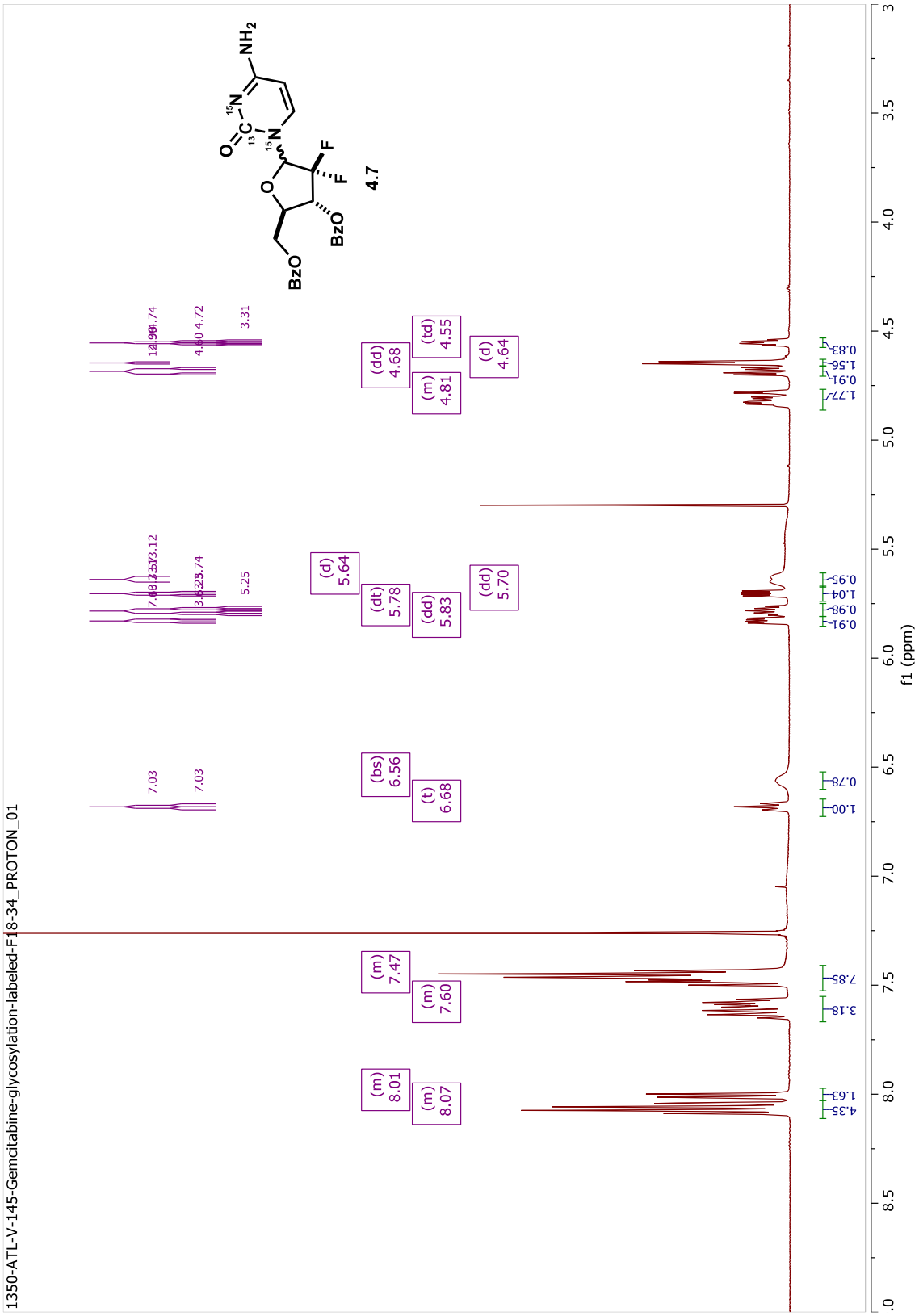
1350-ATL-V-145-Gemcitabine-glycosylation-labeled-F18-34_PROTON_01
4.7
f1 (ppm)

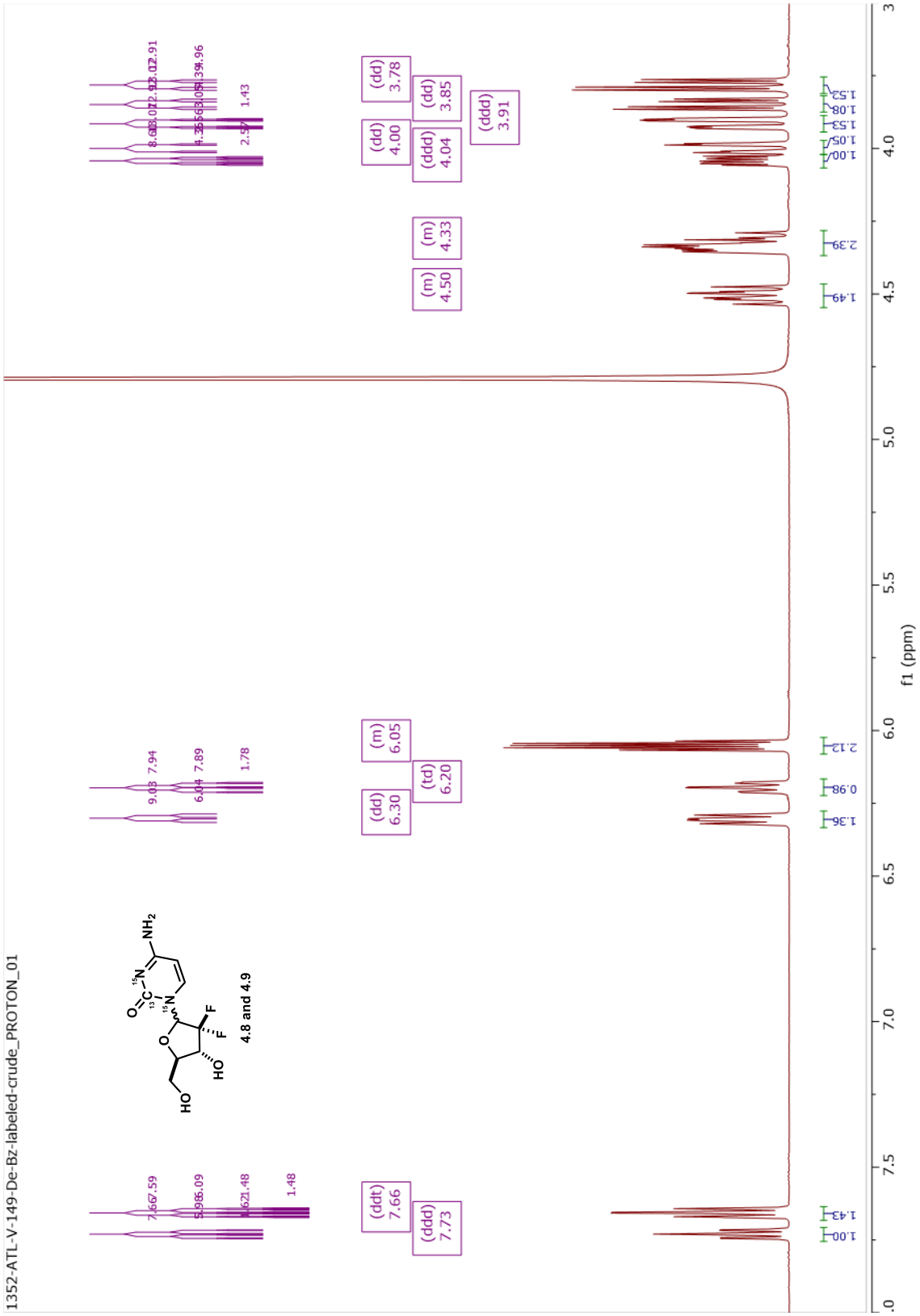
1352-ATL-V-149-De-Bz-labeled-crude_PROTON_01
4.8 and 4.9
f1 (ppm)

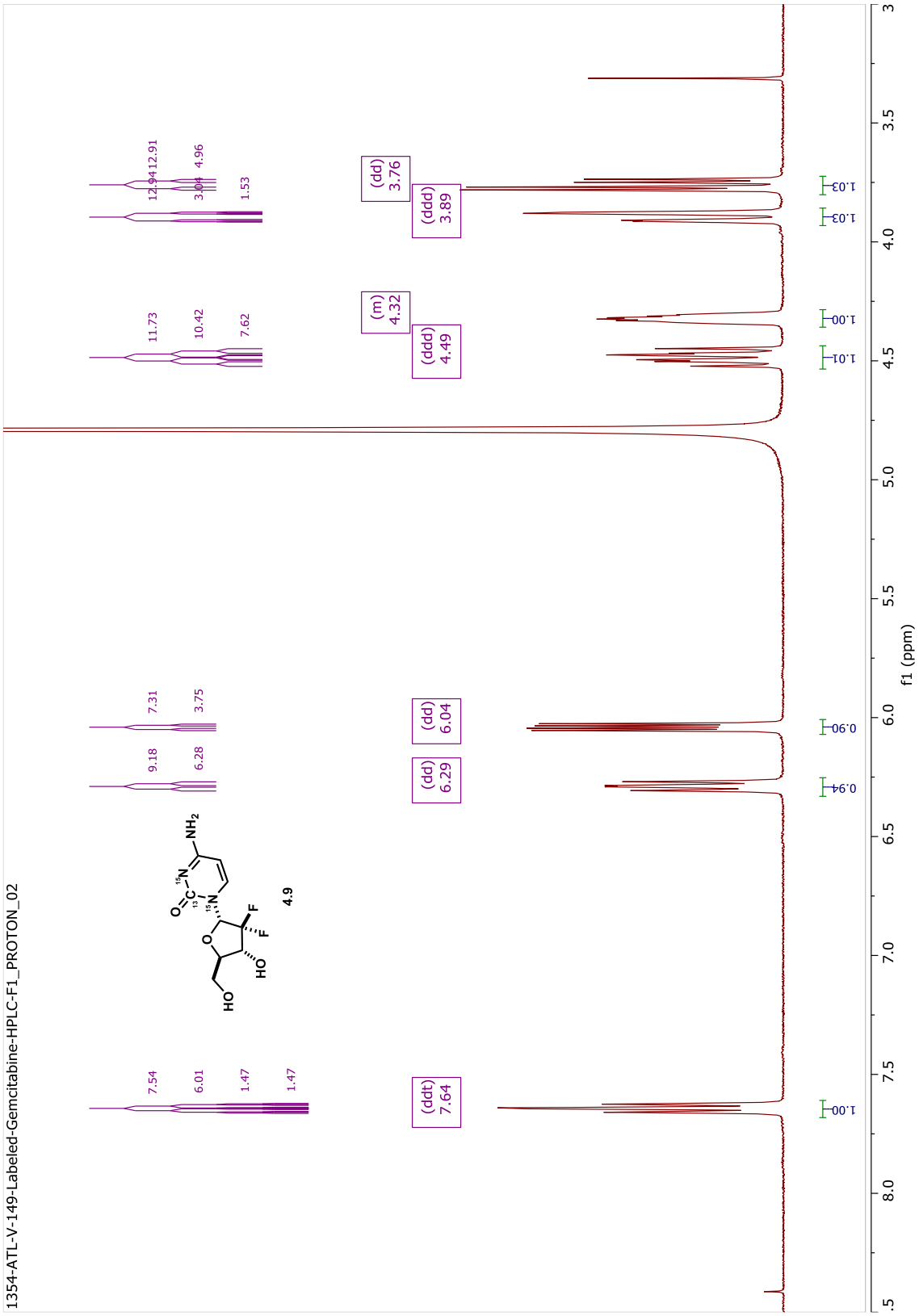
1354-ATL-V-149-Labeled-Gemcitabine-HPLC-F1_PROTON_02
4.9
(ddt) 7.64
(dd) 6.29
(dd) 6.04
(m) 4.32
(ddd) 4.49
(dd) 3.76
(ddd) 3.89
7.54
6.01
1.47
1.47
9.18
6.28
7.31
3.75
11.73
10.42
7.62
12.94
12.91
4.96
3.04
1.53
1.00
0.94
0.90
1.00
1.01
1.00
1.03
1.03
f1 (ppm)

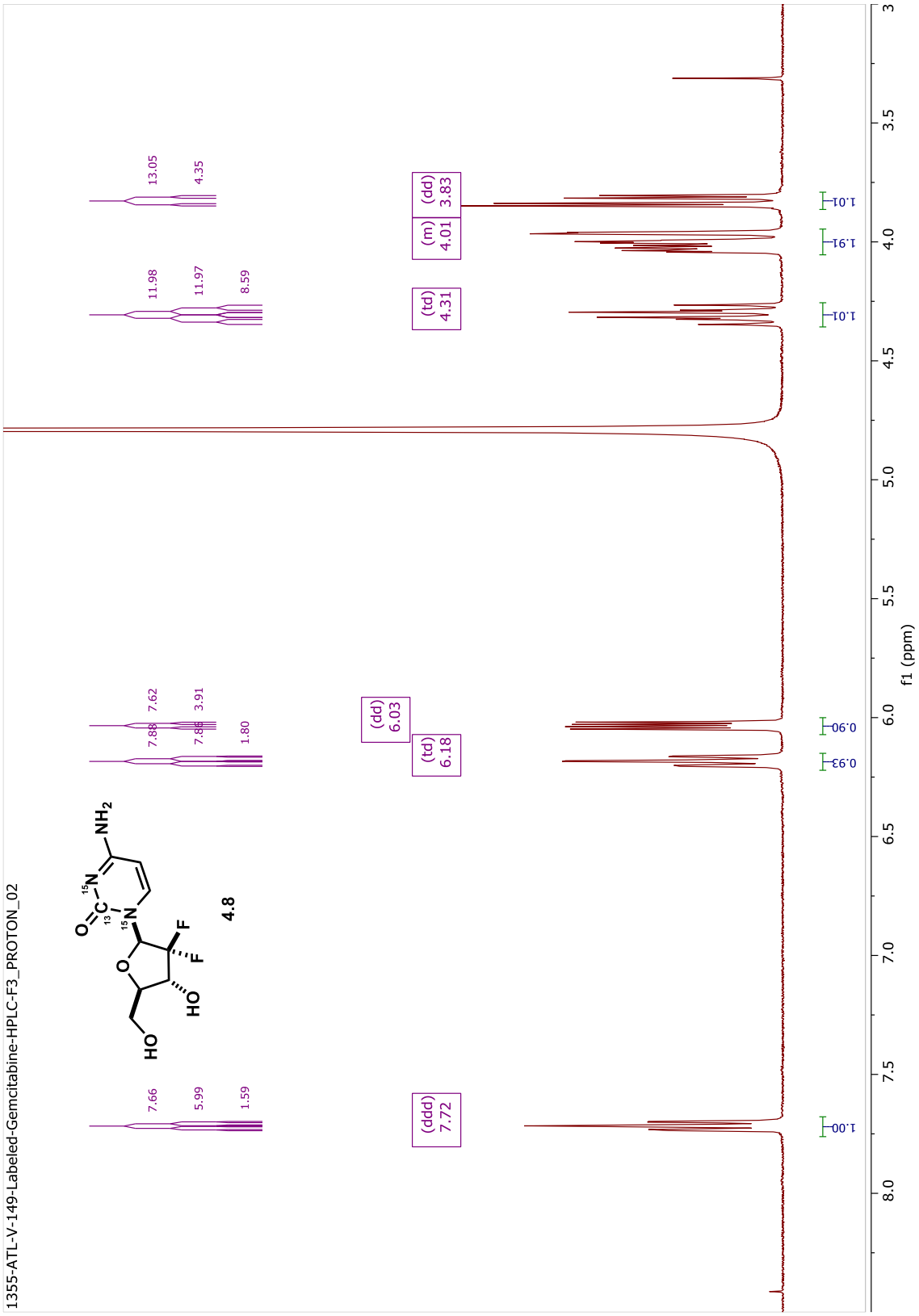
1355-ATL-V-149-Labeled-Gemcitabine-HPLC-F3_PROTON_02
4.8
7.66
5.99
1.59
7.88
7.62
7.88
3.91
1.80
11.98
11.97
8.59
13.05
4.35
(ddd)
7.72
(td)
6.18
(dd)
6.03
(td)
4.31
(m)
4.01
(dd)
3.83
1.00
0.93
0.90
1.01
1.91
1.01
f1 (ppm)

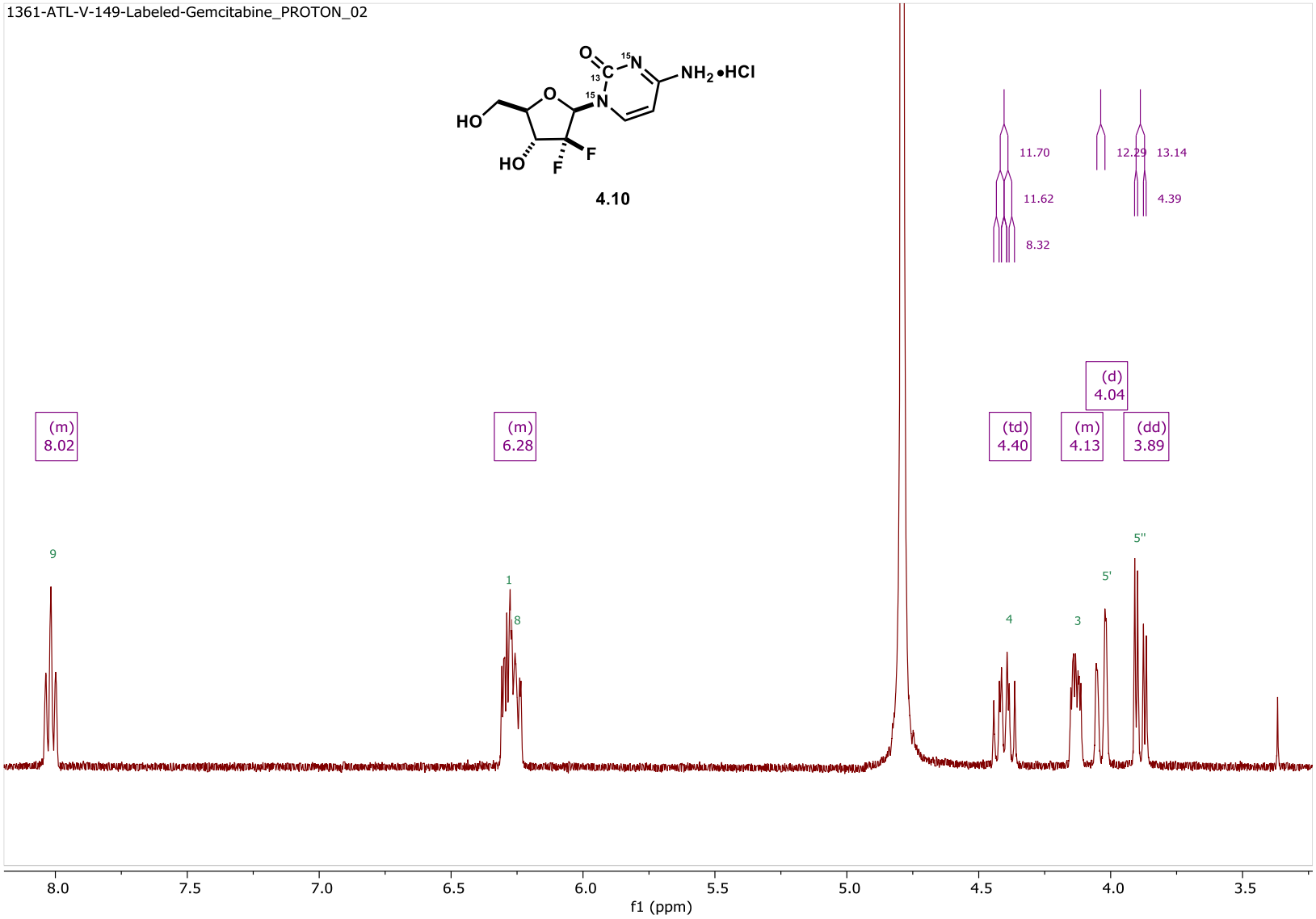
1361-ATL-V-149-Labeled-Gemcitabine_PROTON_02
4.10
11.70
11.62
8.32
12.29
13.14
4.39
(m)
8.02
(m)
6.28
(td)
4.40
(d)
4.04
(m)
4.13
(dd)
3.89
9
1
8
4
3
5'
5''
8.0
7.5
7.0
6.5
6.0
5.5
5.0
4.5
4.0
3.5
f1 (ppm)

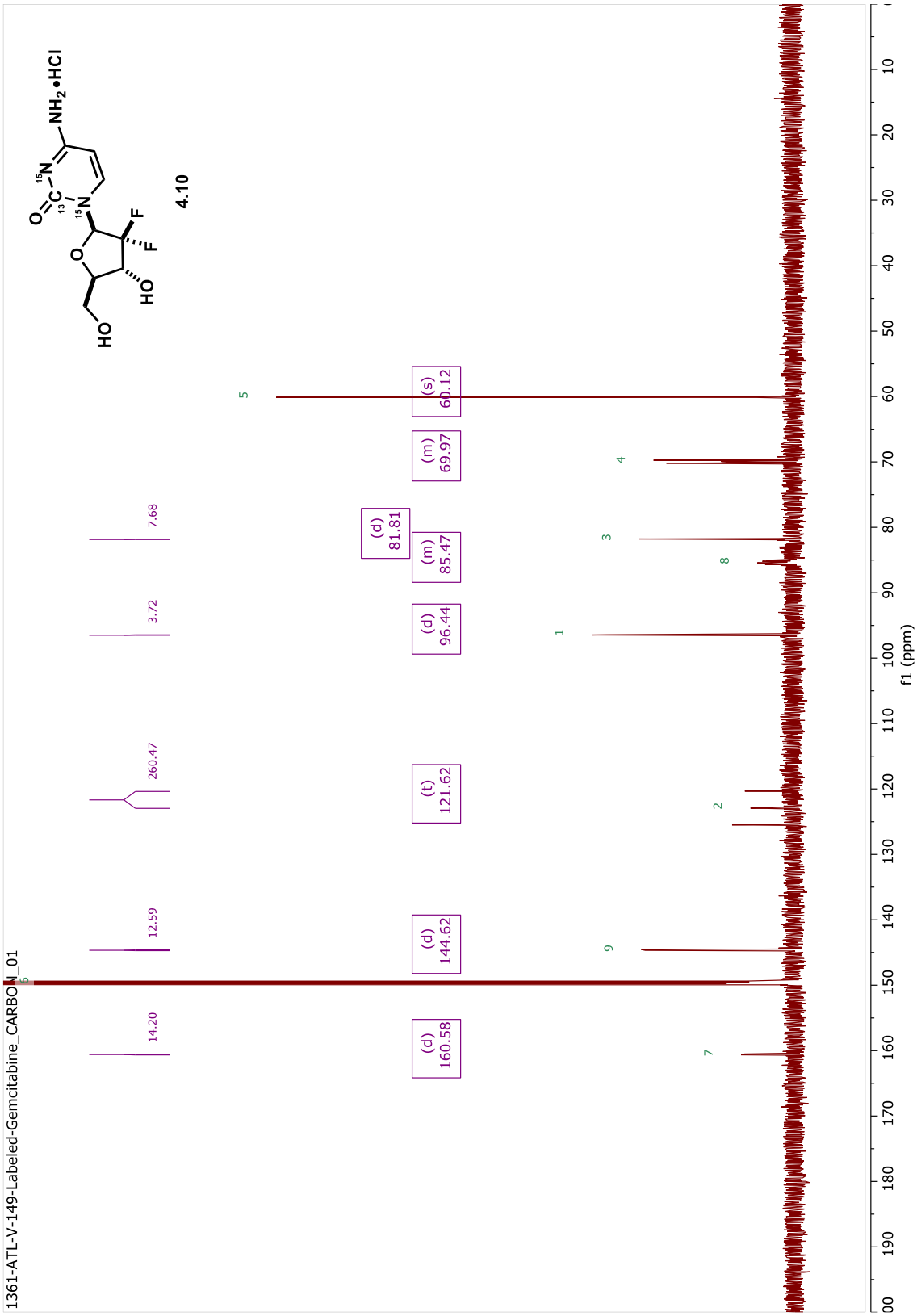
1361-ATL-V-149-Labeled-Gemcitabine_CARBON_01
4.10
14.20
12.59
260.47
3.72
7.68
(d) 160.58
(d) 144.62
(t) 121.62
(d) 96.44
(m) 85.47
(d) 81.81
(m) 69.97
(s) 60.12
f1 (ppm)

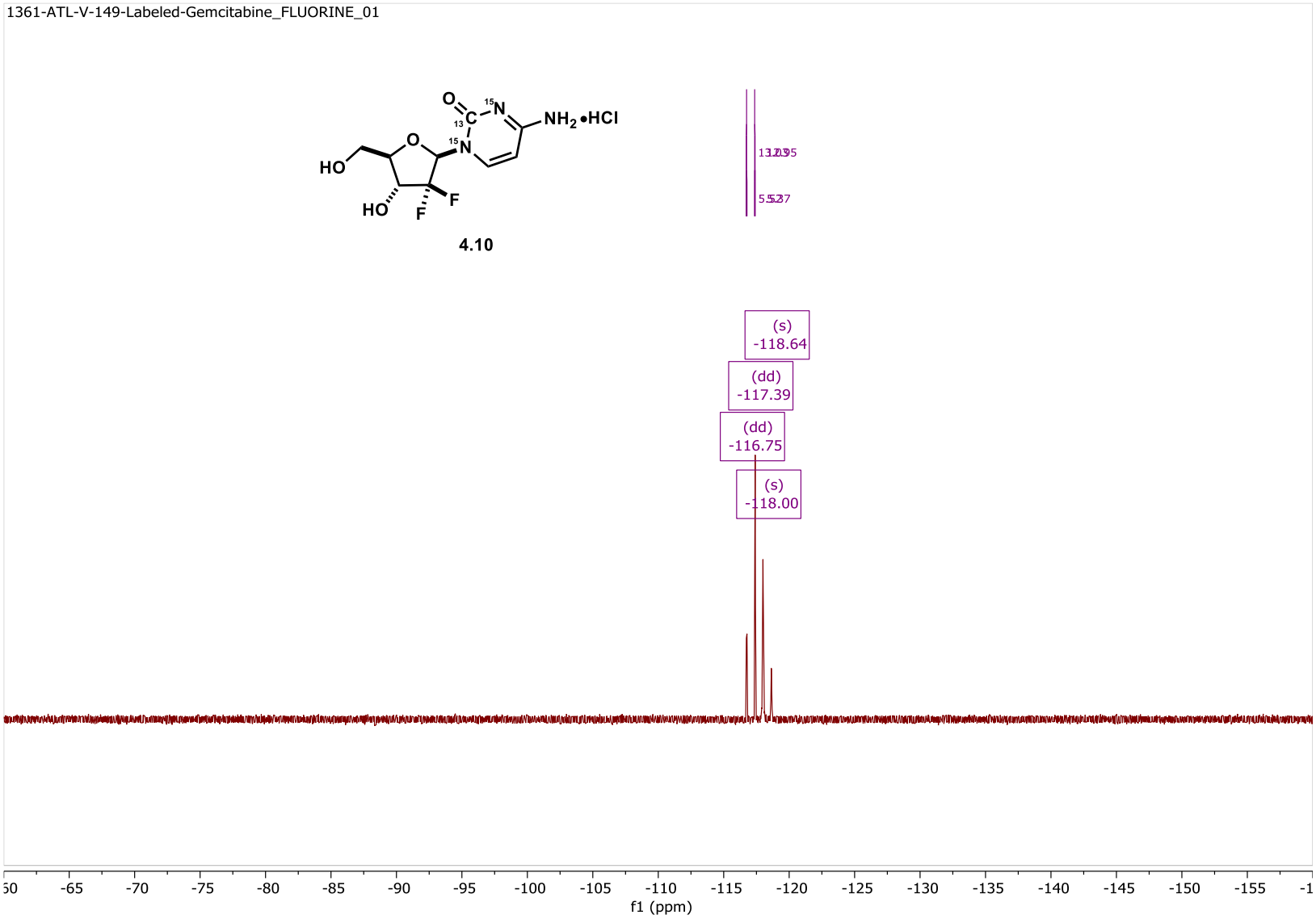
1361-ATL-V-149-Labeled-Gemcitabine_FLUORINE_01
4.10
(s)
-118.64
(dd)
-117.39
(dd)
-116.75
(s)
-118.00
f1 (ppm)

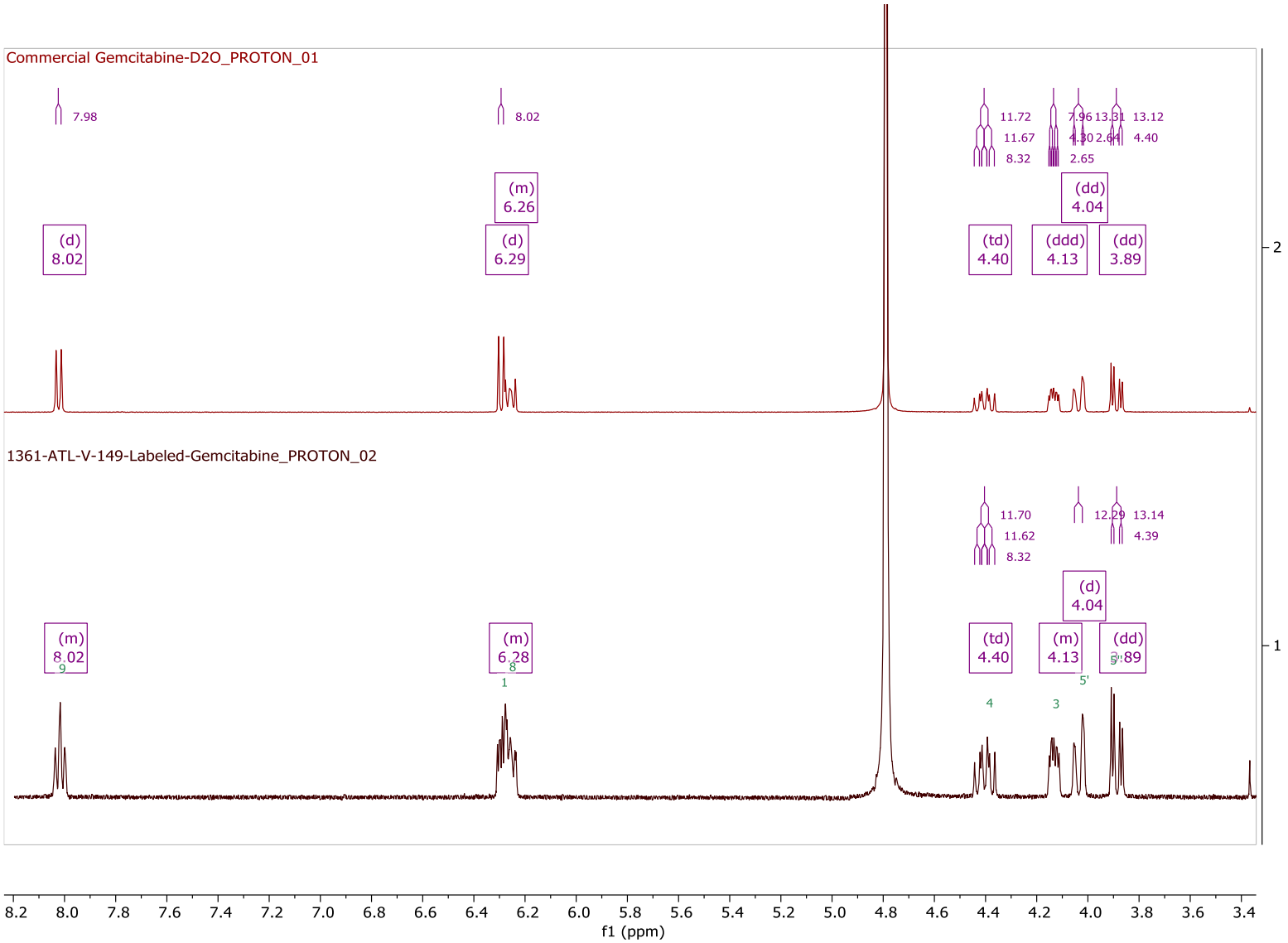
Commercial Gemcitabine-D2O_PROTON_01
7.98
8.02
11.72
11.67
8.32
7.96
13.31
13.12
4.30
2.64
4.40
2.65
(m)
6.26
(dd)
4.04
(d)
8.02
(d)
6.29
(td)
4.40
(ddd)
4.13
(dd)
3.89
2
1361-ATL-V-149-Labeled-Gemcitabine_PROTON_02
11.70
11.62
8.32
12.29
13.14
4.39
(d)
4.04
(m)
8.02
(m)
6.28
(td)
4.40
(m)
4.13
(dd)
3.89
1
f1 (ppm)

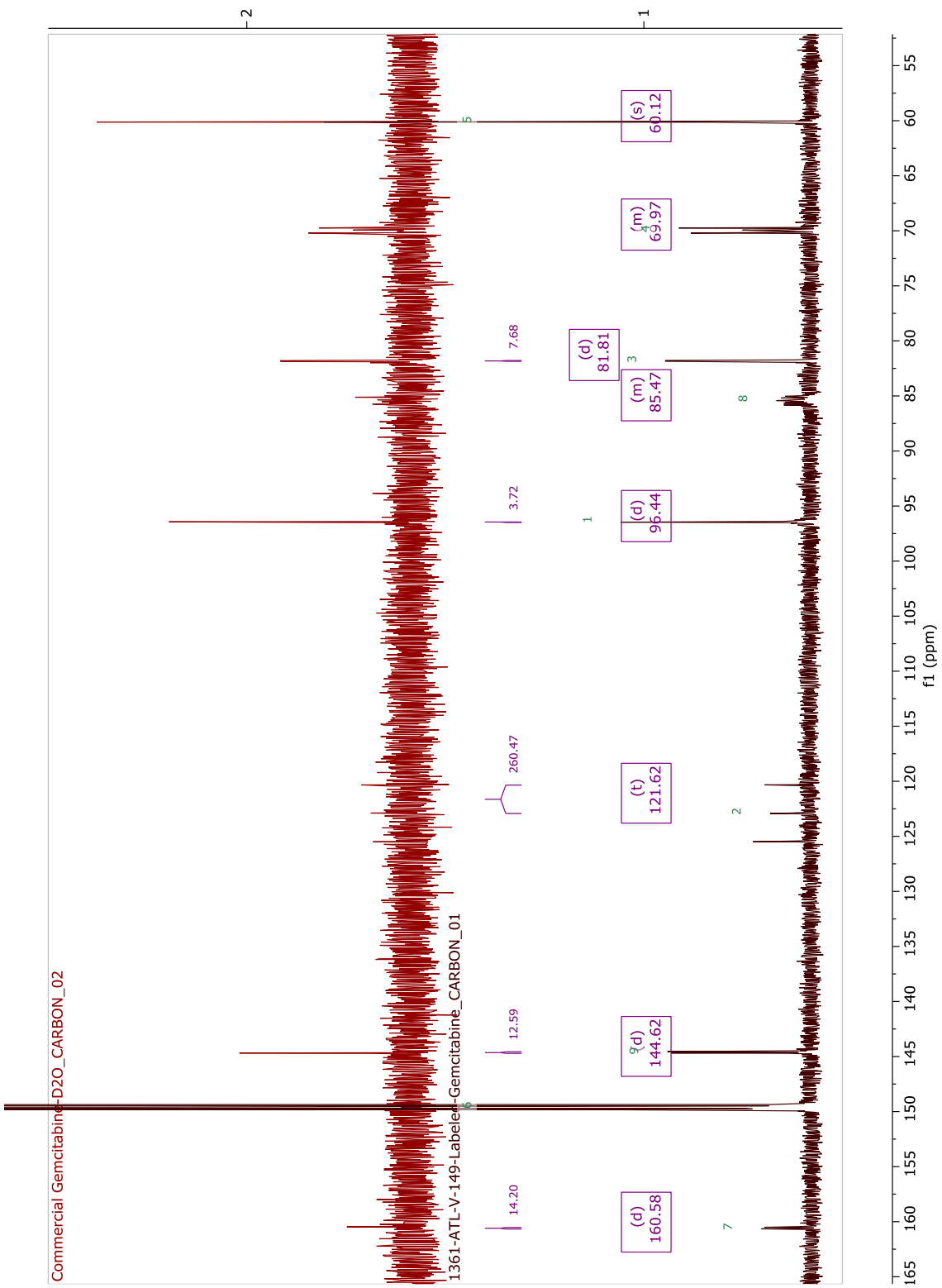
Commercial Gemcitabine-D2O_CARBON_02
1361-ATL-V-149-Labeled-Gemcitabine_CARBON_01
(d)
160.58
(d)
144.62
(t)
121.62
(d)
96.44
(m)
85.47
(d)
81.81
(m)
69.97
(s)
60.12
14.20
12.59
260.47
3.72
7.68
f1 (ppm)

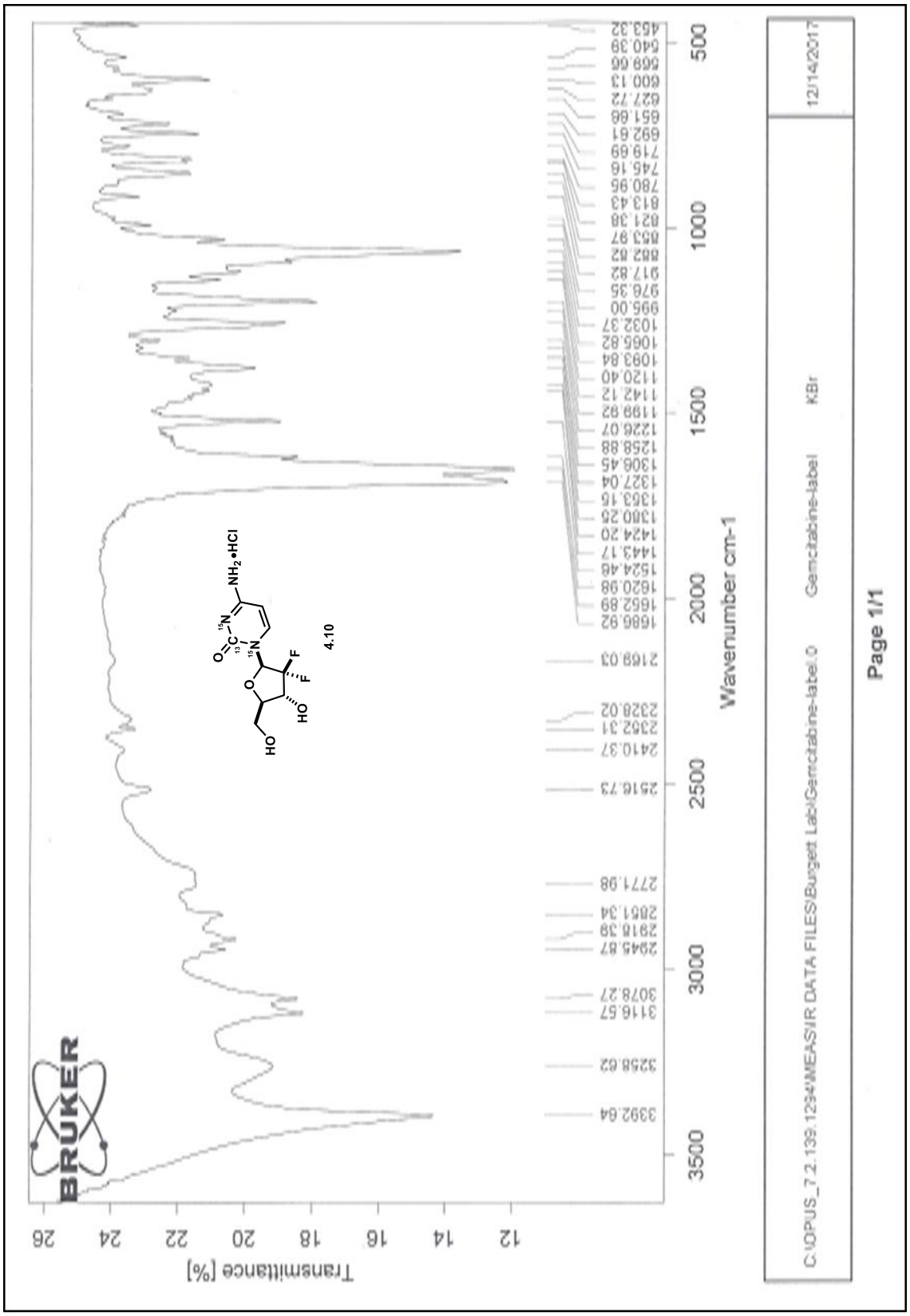
BRUKER
Transmittance [%]
Wavenumber cm-1
4.10
C:\OPUS_7.2.139.1294\MEAS\IR DATA FILES\Burgett Lab\Gemcitabine-label\0 Gemcitabine-label KBr
12/14/2017
Page 1/1

Sample Name	ATL-V-149-HPLC-F3	**Position**	p1a4	**Instrument Name**	Instrument 1
User Name	QTOF-PC\Admin	**Inj Vol**	5	**InjPosition**	
Sample Type	Sample	**IRM Calibration Status**	Success	**Data Filename**	12138AWB0005.d
ACQ Method	Pos-Loop-MS.m	**Comment**	0.1x	**Acquired Time**	12/19/2017 9:56:50 AM

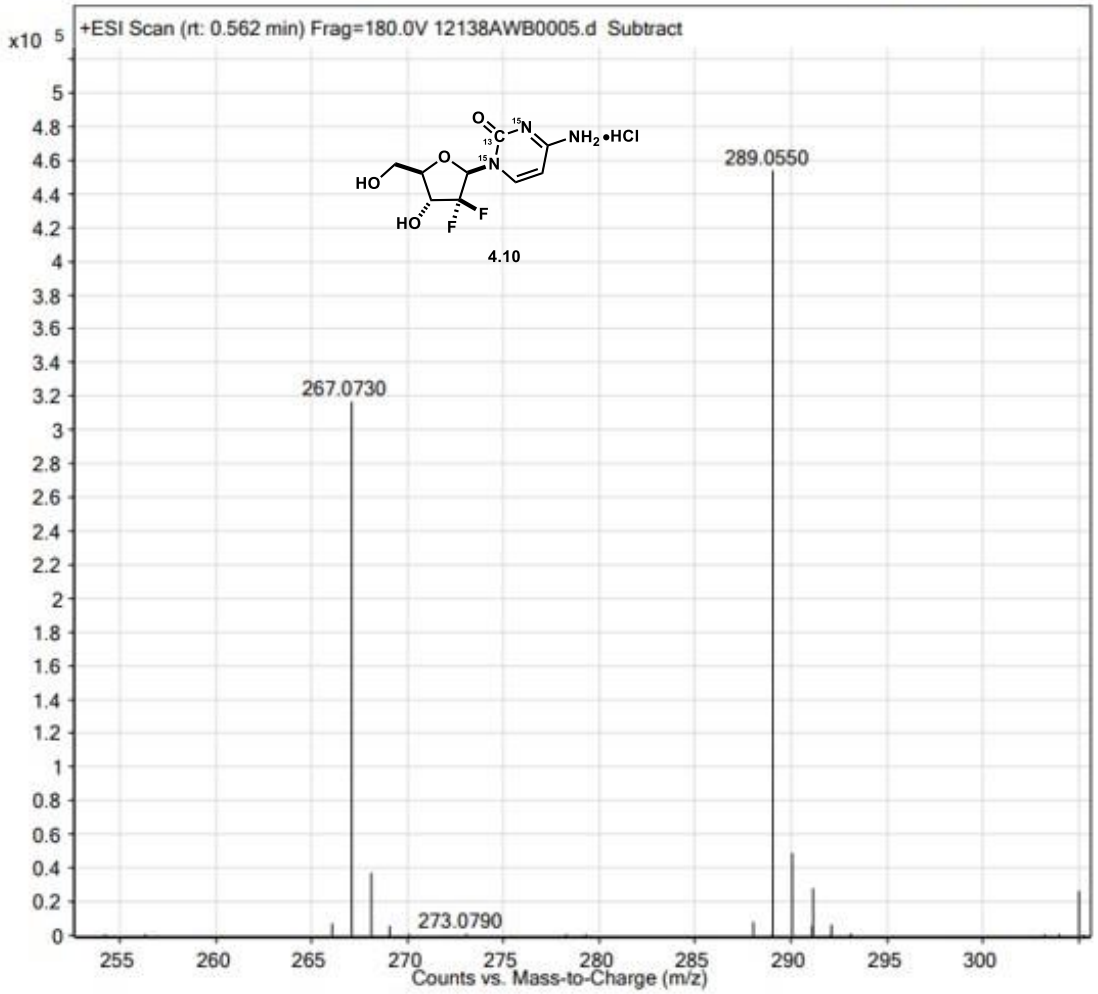

4.10

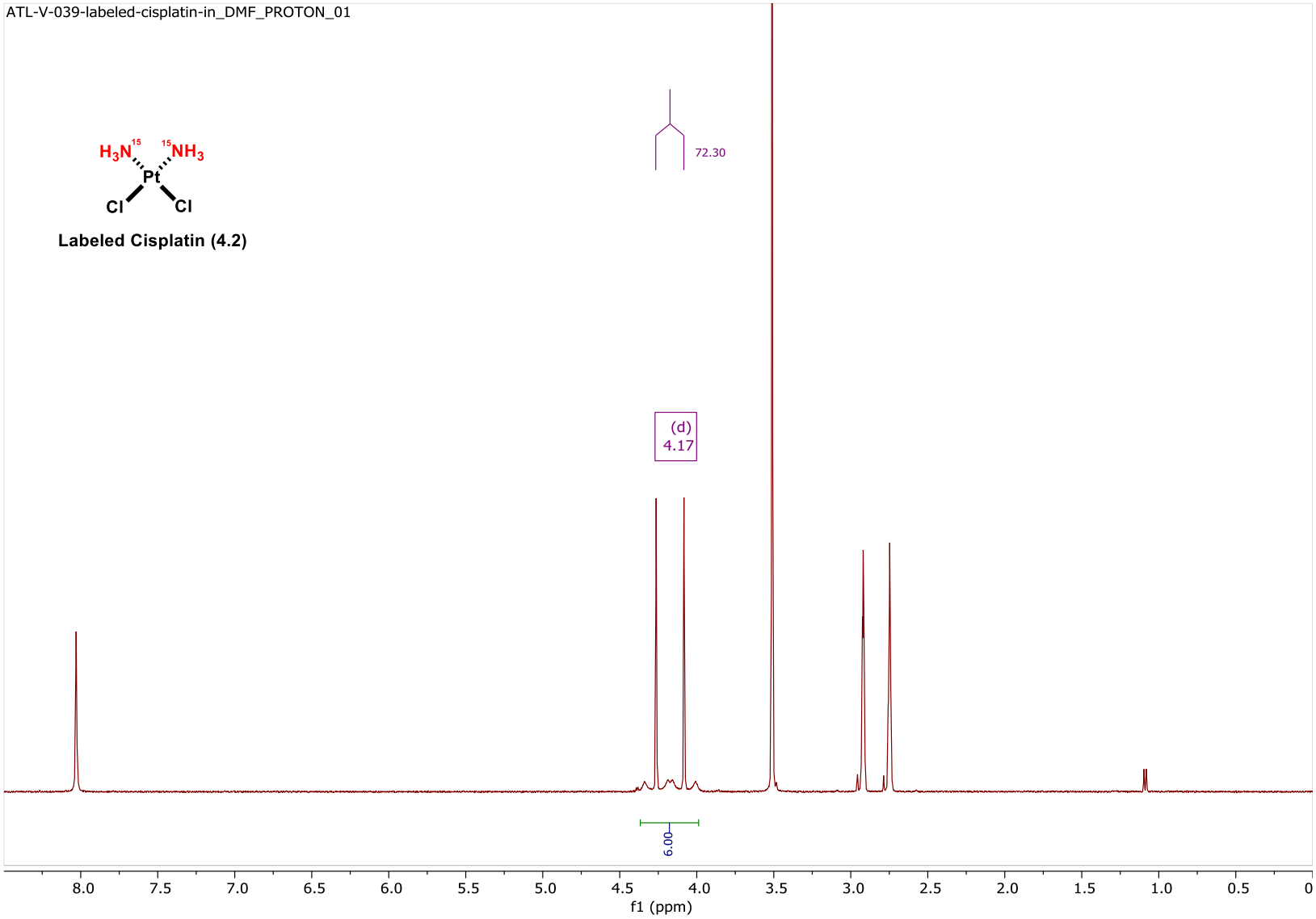
ATL-V-039-labeled-cisplatin-in_DMF_PROTON_01
H_3N^{15}
$^{15}NH_3$
Pt
Cl
Cl
Labeled Cisplatin (4.2)
72.30
(d)
4.17
6.00
8.0
7.5
7.0
6.5
6.0
5.5
5.0
4.5
4.0
3.5
3.0
2.5
2.0
1.5
1.0
0.5
0
f1 (ppm)

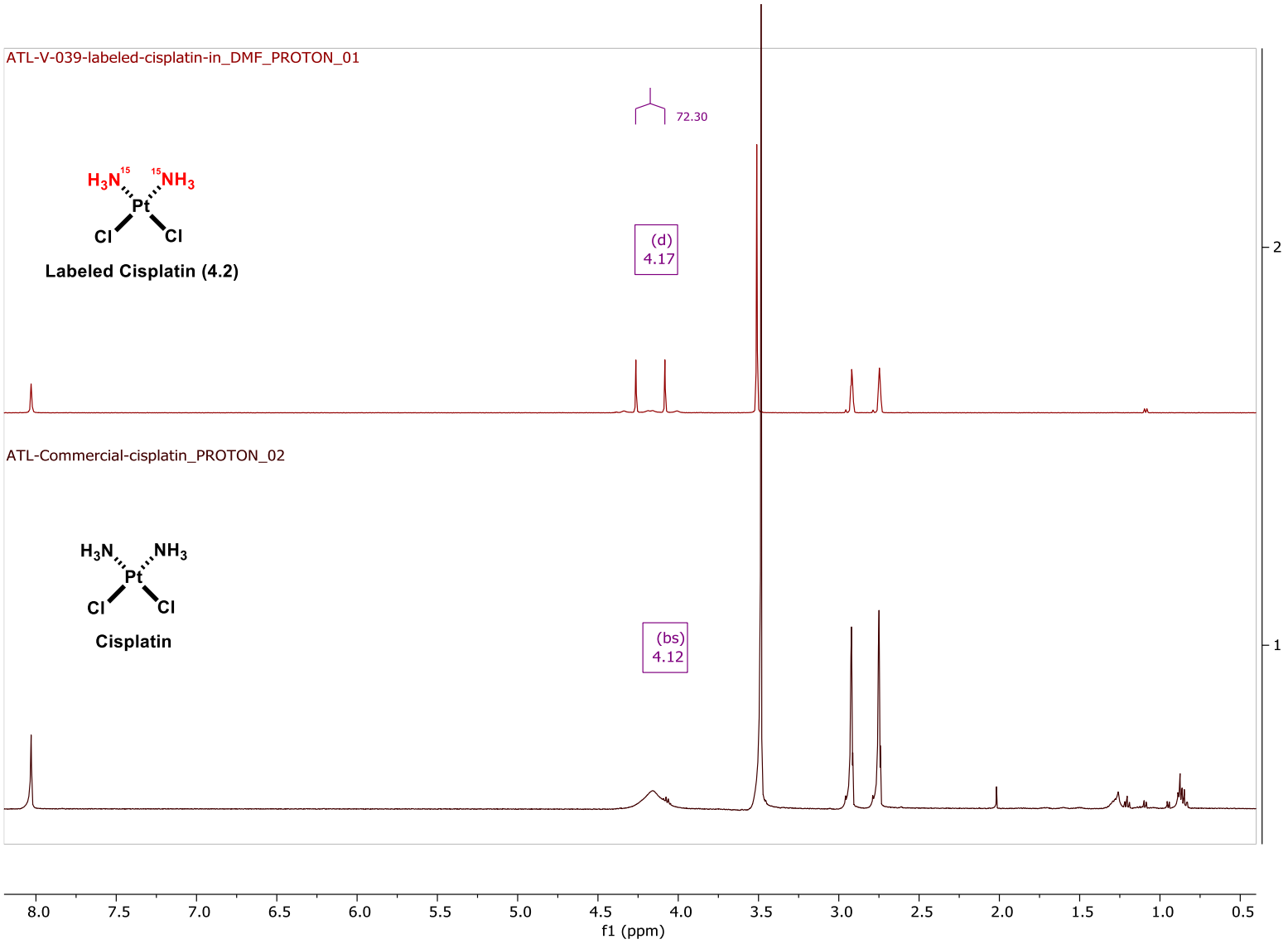
ATL-V-039-labeled-cisplatin-in_DMF_PROTON_01
72.30
H_3N^{15} $^{15}NH_3$
Pt
Cl Cl
Labeled Cisplatin (4.2)
(d)
4.17
2
ATL-Commercial-cisplatin_PROTON_02
H_3N NH_3
Pt
Cl Cl
Cisplatin
(bs)
4.12
1
8.0 7.5 7.0 6.5 6.0 5.5 5.0 4.5 4.0 3.5 3.0 2.5 2.0 1.5 1.0 0.5
f1 (ppm)

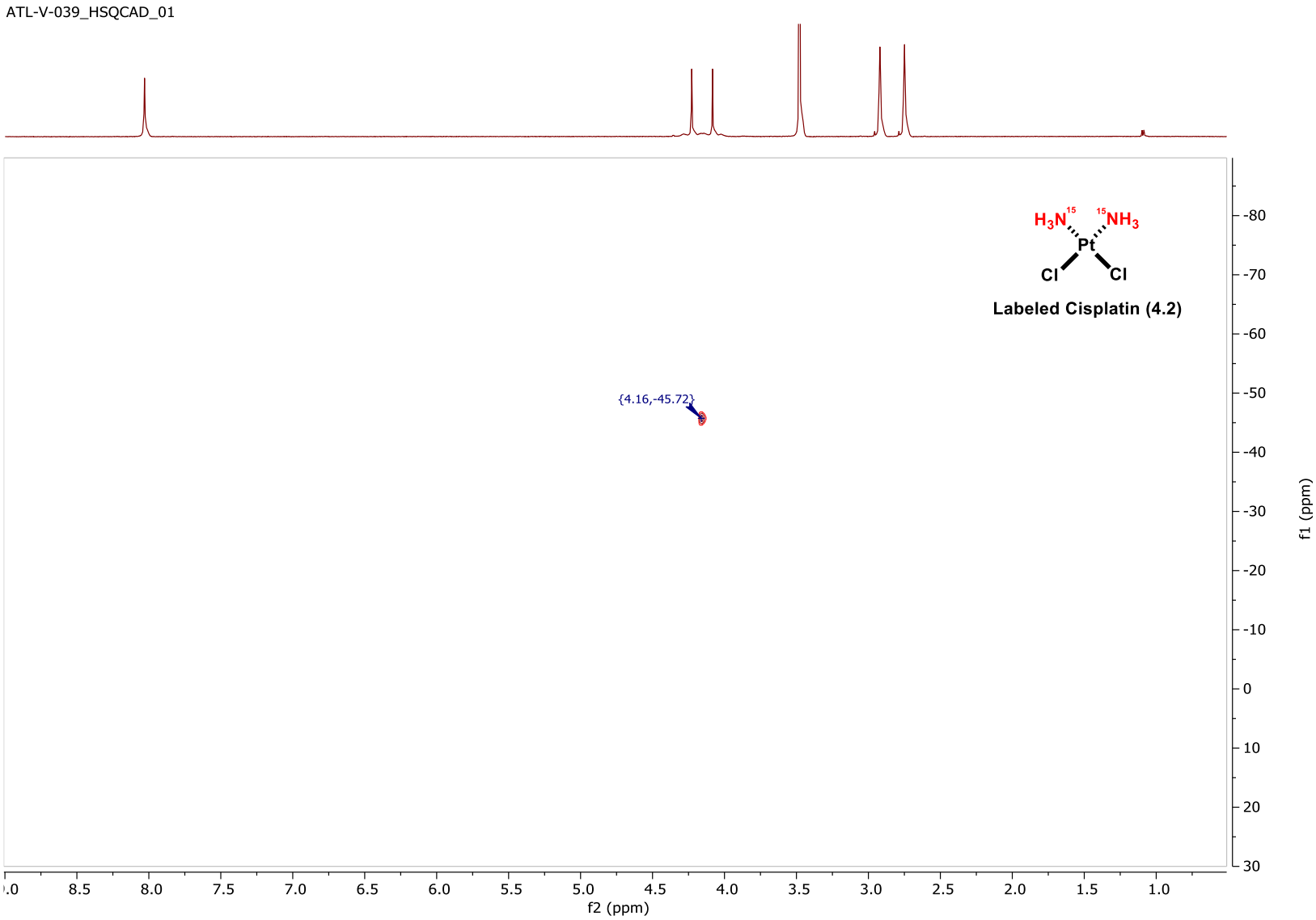
ATL-V-039_HSQCAD_01
{4.16,-45.72}
Labeled Cisplatin (4.2)
f2 (ppm)
f1 (ppm)

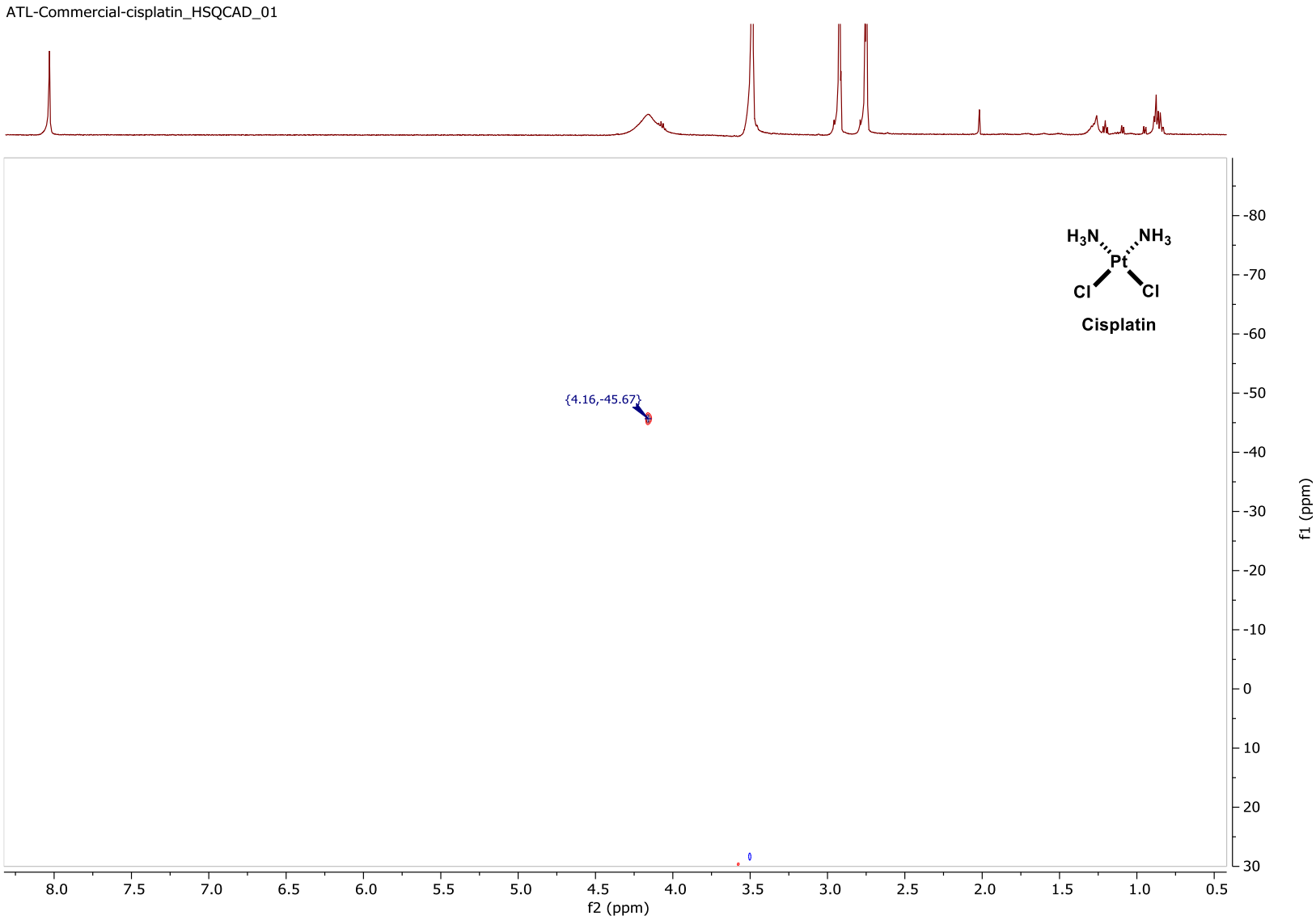
ATL-Commercial-cisplatin_HSQCAD_01
{4.16,-45.67}
Cisplatin
f2 (ppm)
f1 (ppm)

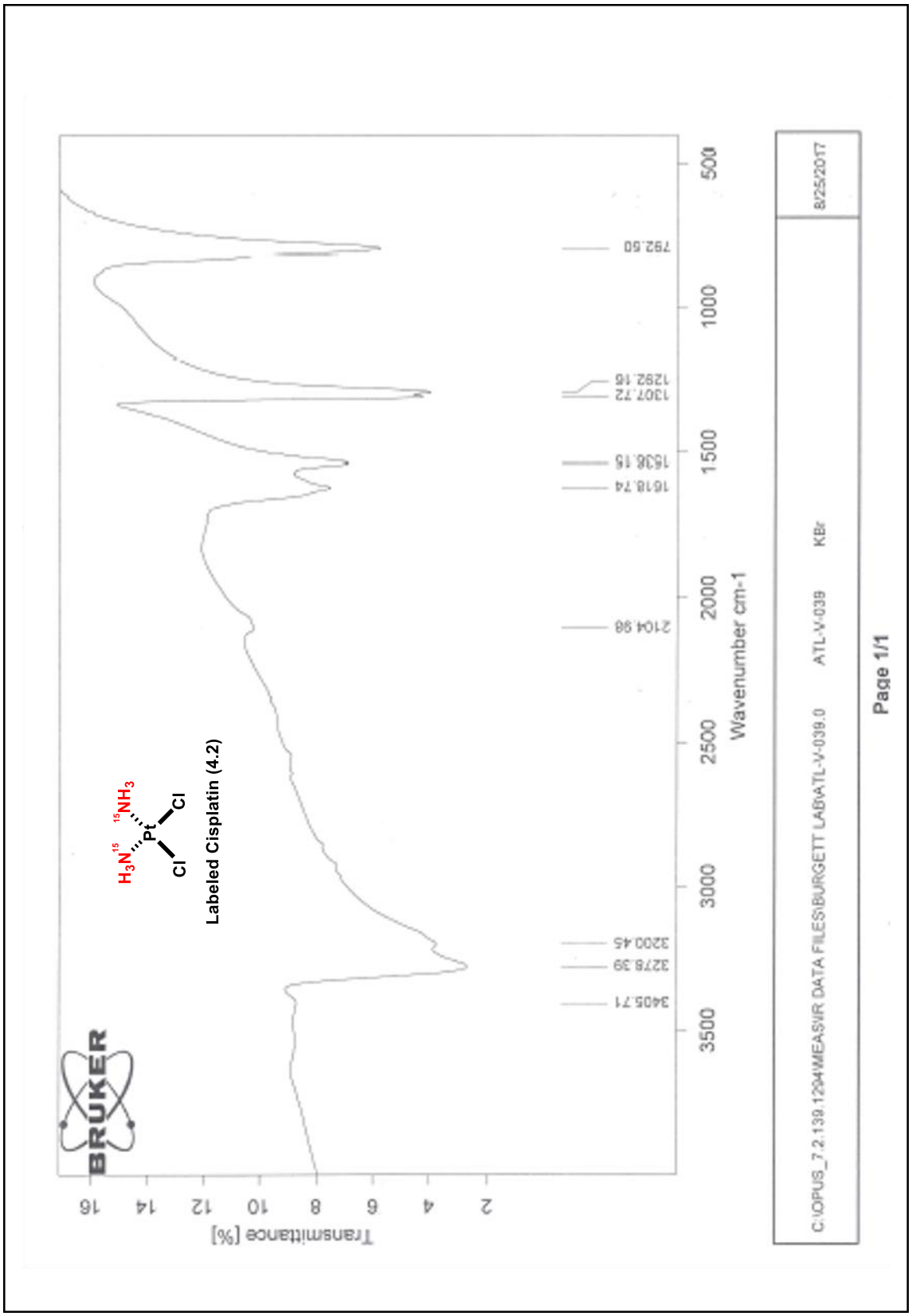
Labeled Cisplatin (4.2)
Transmittance [%]
Wavenumber cm-1
3405.71
3278.39
3200.45
2104.98
1618.74
1538.15
1307.72
1292.16
792.50
C:\OPUS_7.2.139.1294\MEASVR DATA FILES\BURGETT LAB\ATL-V-039.0 ATL-V-039 KBr
8/25/2017
Page 1/1

ATL-V-039-0.01x
Le

SYNAPTG2-Si#UGA589

28-Aug-2017 15:30:03

12053AWB-003 17 (0.364) AM (Cen,4, 80.00, Ar,10000.0,0.00,0.00); Sm (SG, 1x5.00); Cm (17:27)

1: TOF MS ES+
4.83e5

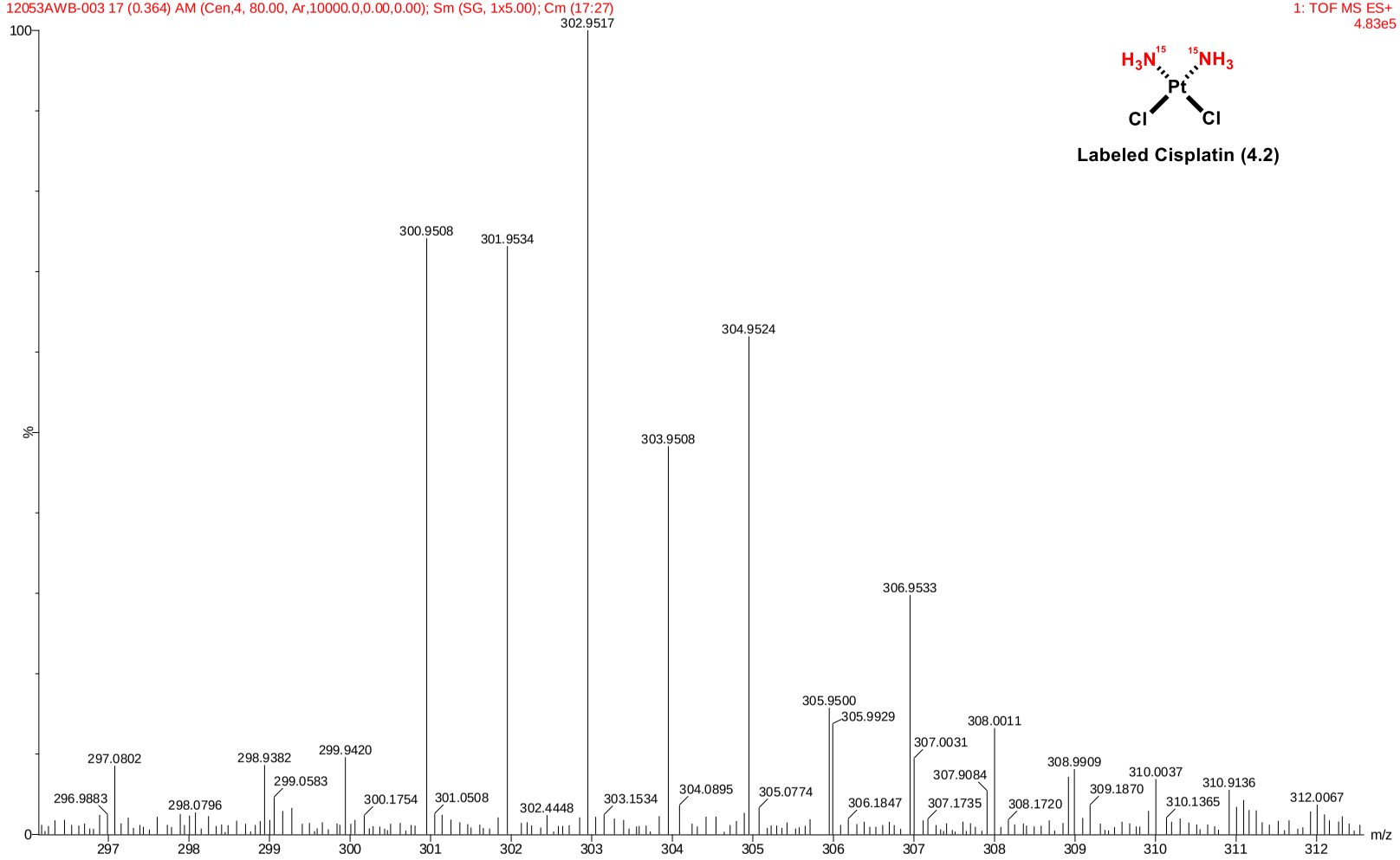

Labeled Cisplatin (4.2)

Chapter V : Synthesis, Characterization and Evaluation of α,α-Dichloro-all-trans-retinone (DAR) as a Selective Inhibitor for Retinaldehyde Dehydrogenase Enzymes

Abstract

The retinaldehyde dehydrogenase (RALDH) enzyme subfamily (which includes RALDH1, RALDH2, and RALDH3) catalyzes the irreversible oxidation of all-*trans*-retinaldehyde to all-trans-retinoic acid (atRA). Despite the importance of the RALDH enzymes in embryonic development and their association with different syndromes and diseases, no commercially available inhibitors that selectively target these enzymes are available. Utilizing a structure-based design strategy, α,α-dichloro-all-*trans*-retinone (DAR) was synthesized and characterized as a small molecule inhibitor that exhibited selectivity for RALDH1, 2, and 3, but not mitochondrial ALDH2. These results encourage the further development of DAR as a specific inhibitor for RALDH enzymes for use in experimental applications, and asvpotential therapeutic agents for many diseases.

V.1 Introduction and background

The aldehyde dehydrogenases (ALDHs) are a superfamily of proteins that catalyze the $NAD(P)^+$ dependent, irreversible oxidation of aldehydes to their respective carboxylic acids.[46] ALDH proteins have been shown to participate in a wide variety of physiological processes including aldehyde detoxification, alcohol metabolism, vision and neurotransmission.[103] Mutations in ALDH genes have been connected with various diseases such as brain, breast, and lung cancer [104,105], late-onset Alzheimer's disease [106], and alcohol flushing syndrome [107].

The retinaldehyde dehydrogenase (RALDH, also known as ALDH1A) subfamily consists of three members, RALDH1 (ALDH1A1), RALDH 2 (ALDH1A2) and RALDH 3 (ALDH1A3), which catalyze the oxidation of all-*trans*-retinoic acid (atRA) from retinaldehyde (both all-*trans*-retinaldehyde or 9-*cis*-retinaldehyde).[46] RALDH proteins are essential for regulating retinoic acid signaling prenatally and postnatally. In embryonic development, each RALDH is selectively expressed in targeted tissue to mediate organogenesis of the eye, brain, heart, kidney, lung, and reproductive organs.[108] Postnatally, RALDH proteins are involved in spermatogenesis[109], maintenance of lens transparency[110], and stem cell differentiation[111]. The RALDH subfamily has also been associated with a variety of diseases through the modulation of all-*trans*-retinaldehyde and all-*trans*-retinoic acid concentrations. RALDH1 has been linked to obesity [112] and inflammation[113], while RALDH2 has been associated with abnormal ocular growth (myopia)[114,115]. Therefore, RALDH 2 is a potential therapeutic target for the development of an effective therapy to slow or prevent the development of myopia.

Regardless the involvement of various ALDH family members in numerous diseases, pharmacological selective inhibitors have been developed for only two of the ALDH isozymes: ALDH1A1 (CM026, CM037) and ALDH3A1 (CB29) for treatment of oxazophosphorine resistant cancers.[116,117] Due to the similarities in protein structure, many inhibitors (reversible and irreversible) have been found to be non-specifically inhibit a range of ALDH family members.[117] Thus, studies utilizing these non-specific inhibitors to gain insights into the physiologic roles of ALDH isoenzyme activity may be complicated by inhibition of multiple proteins leading to off-target effects.

Recently, bisdichloroacetyldiamine (WIN 18446, commercially known as Fertilysin, (**Figure 21**) was shown to effectively and reversibly inhibit testicular all-*trans*-retinoic acid biosynthesis via the testes-specific enzyme RALDH2.[118,119] These findings led to WIN 18446 being employed as a male contraception in a number of mammals [119–121] and was tested for its potential as a male contraceptive in human volunteers [122]. Even though WIN 18446 was a promising candidate for male contraceptive, it was not introduced for the general public use because the disulfiram ethanol reaction (i.e. blurred vision, nausea, and flushing of the face) was observed upon patient consumption of alcohol while the compound was administered.[118] This observation indicated that WIN 18446 did not only interact with RALDH2, but also inhibited ALDH2 and possibly other ALDH enzymes, which was later confirmed *in vitro* .[119] These results demonstrate the importance of developing small molecule inhibitors that are specific and selective for the RALDH isozymes for treatment of diseases without unwanted and serious side effects. This chapter details the design, synthesis and evaluation of a novel inhibitor, [(3*E*,5*E*,7*E*,9*E*)-1,1-dichloro-4,8-dimethyl-10-(2,6,6-trimethylcyclohex-1-en-1-yl)deca-3,5,7,9-tetraene-2-one; "α,α-dichloro-all-*trans*-retinone" or DAR- **Figure 21**], for the retinaldehyde dehydrogenase (RALDH or ALDH1A) subfamily that is specific for RALDH1, RALDH2, and RALDH3, but has no activity on human mitochondrial ALDH2. This work resulted from a successful collaboration the Burgett's laboratory and the research group of Prof. Jody Summers' at OUHSC.

V.2 Results and discussion

V.2.1 Structure-based design of DAR

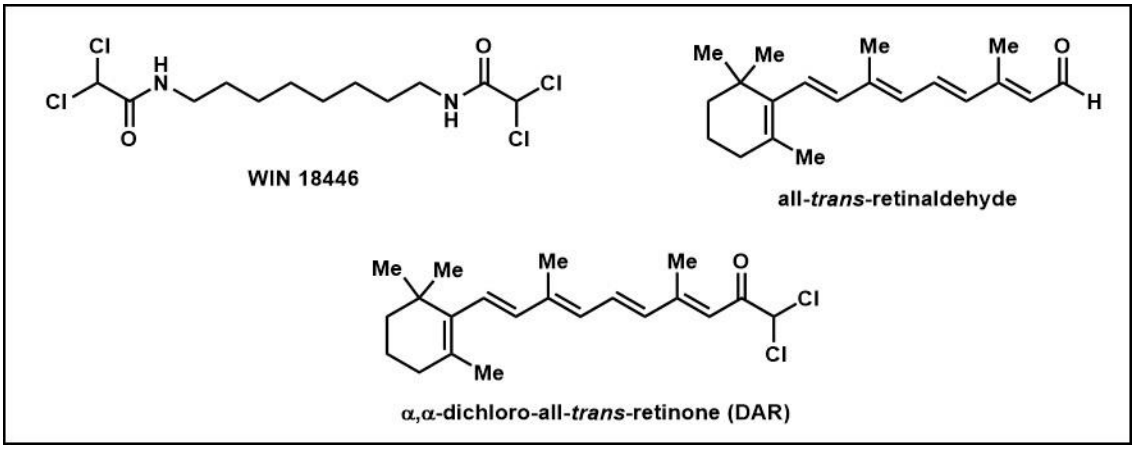

Figure 21. Structures of WIN 18446, all-*trans*-retinaldehyde, and DAR

α,α-dichloro-all-*trans*-retinone (DAR) was designed based on two results: 1) the covalent interaction of WIN 18446 with RALDH2; 2) the conformational differences in protein structure between the binding sites of RALDH enzymes and the other ALDH enzymes.[123] WIN 18446 has been shown to inhibit RALDH1, 2, and 3, as well as ALDH2 and other proteins of the ALDH superfamily.[122] WIN 18446 irreversibly binds to RALDH2 through a covalent modification as illustrated in the crystal structure of RALDH2 – WIN 18446 complex (**Figure 22**) [123]. The thiol group on residue cysteine 320 was proposed to undergo a S_N2 reaction to displace a chloride from WIN 18446 dichloro moiety to form the covalent adduct.[123] Furthermore, the substrate entrance tunnel for the RALDH enzymes are relatively larger than that of the other ALDH enzymes, as determined for ALDH2.[124] This difference in entrance tunnels size likely accounts for the specificity of retinaldehyde to the RALDH enzymes.[124] This research results suggests that a successful RALDH selective inhibitor could be a hybrid of the WIN 18446 and retinaldehyde. The DAR compound is

designed to contain the dichloromethyl moiety from WIN 18446 for irreversible interaction with the protein, and the large, rigid structure of retinaldehyde.

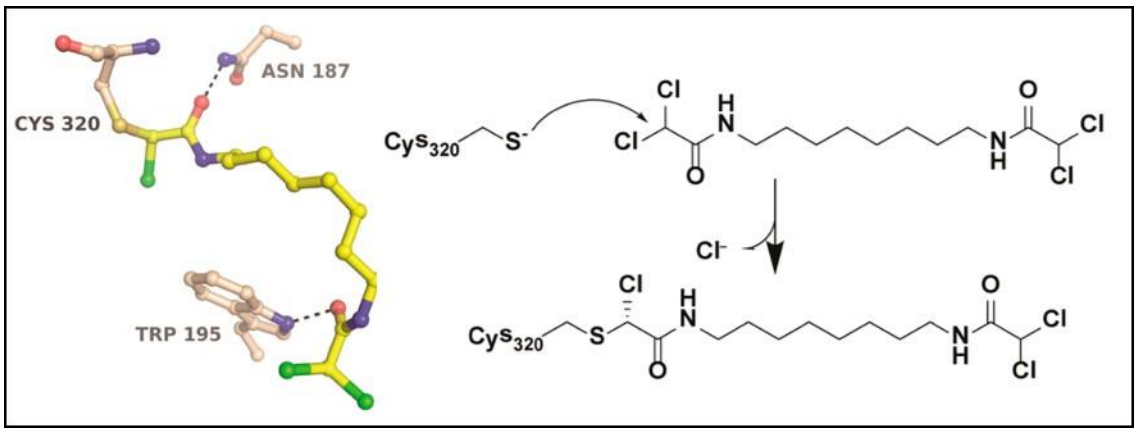

Figure 22. Crystal structure of the covalent adduct between Cys 320 and WIN 18446; proposed mechanism of adduct formation. Figure is adapted from Chen *et al.* [123]

V.2.2 Synthesis and characterization of DAR

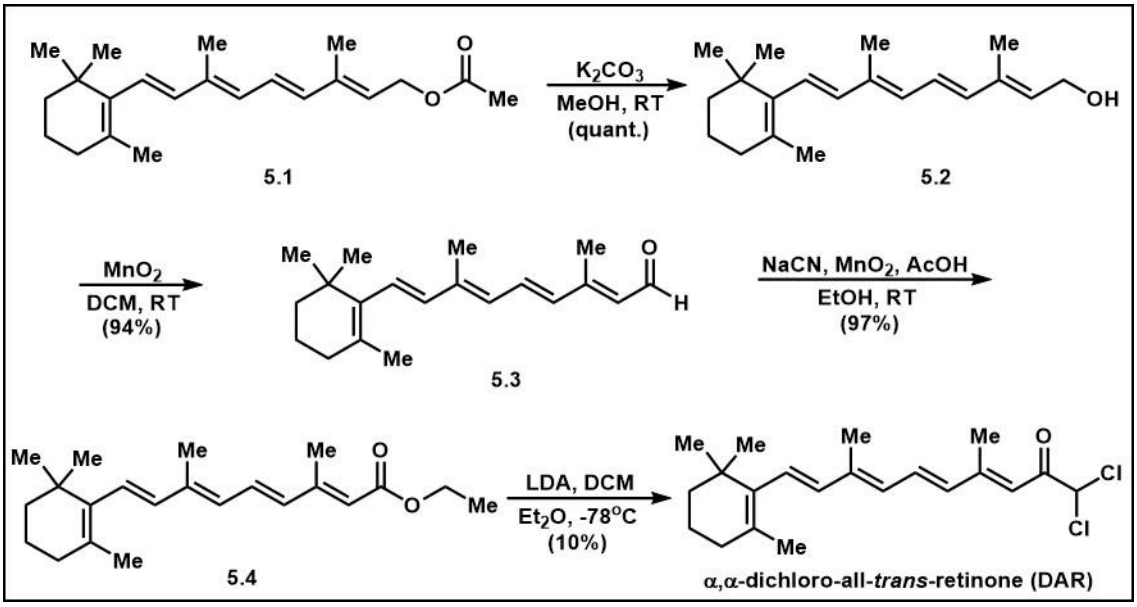

Scheme 37. Synthesis of α,α-dichloro-all-trans-retinone DAR

α,α-dichloro-all-trans-retinone (DAR) was synthesized in a one-step transformation of ethyl ester of retinoic acid **5.4** (**Scheme 37**). Since the availability of ethyl retinoate **5.4**

was rather limited commercially, it was synthesized in lab over two steps starting from commercially available retinyl acetate **5.1**. The all-*trans*-retinyl moiety, with the extended conjugation system, isomerizes very easily in light and acidic reaction conditions. All the reactions were carried out in a darkened fume hood, with reaction flasks wrapped in aluminum foil to limit the exposure of the compounds to ambient light. Reaction conditions were chosen carefully to lower the possibility of isomerization.

Saponification of retinyl acetate with a catalytic amount of potassium carbonate afforded retinol **5.2** in quantitative yield (**Scheme 37**). Retinol **5.2** was then oxidized to ethyl retinoate **5.4** through two steps.[125,126] First, oxidation of retinol **5.2** with manganese dioxide afforded all-*trans*-retinaldehyde **5.3**[125]. This reaction proceeded smoothly with excellent yield (94%). Retinaldehyde **5.3** was subjected to another oxidation condition with manganese dioxide in presence of cyanide ion to obtain ethyl retinoate **5.4**. In this process, retinaldehyde is converted to the cyanohydrin with the cyanide ion, which is susceptible to further oxidation by manganese dioxide to an acyl cyanide. Esterification of the acyl cyanide with the ethanol solvent produced ethyl ester **5.4** [126].

With ethyl retinoate prepared, the synthesis of α,α-dichloro-all-trans-retinone (DAR) was attempted. Dichloromethyllithium, generated *in situ* from a reaction of lithium diisopropylamide and dichloromethane, performed a nucleophilic addition to the carbonyl carbon of ethyl retinoate .[127] The adduct then underwent hydrolysis to afford the desired product **DAR** in fairly low yield (10%). A small amount of the starting ethyl retinoate was recovered, with the remaining mass balance of this reaction being comprised of a complex mixture of unidentified isomeric byproducts. Extensive purification, including preparative TLC and semi-preparative HPLC, produced analytically pure DAR, free from any

contaminating byproducts. The low yield of this reaction was not surprising given the combination of the inherent reactivity of the extended conjugated system in DAR and the highly reactive dichloromethyllithium species. DAR was characterized fully through HR-MS, 2D NMR spectroscopy and IR.

DAR is prone to photoisomerization, therefore was protected from ambient light at all times. DAR was dissolved in dimethylsulfoxide (DMSO) to produce 10 mM solution for biological testing. These stock solutions were protected from light and stored frozen at -20°C. Multiple small aliquots of DAR (10mM) were prepared and used for biological testing to prevent refreezing of sample as DAR will degrade upon frequent freeze/thaw cycles.

V.2.3 Biological evaluation of DAR

After DAR had been fully purified and characterized, evaluation of the compound commenced to determine its activity in biological systems. Dr. Angelica Harper (from Dr. Summers' lab) performed the majority of the biological assays. The concentration of all-*trans*-retinoic acid isolated from biological samples was measured and quantified using LCMS methods developed and optimized in Burgett lab.

V.2.3.1 Effects of DAR on aldehyde dehydrogenase activity

DAR was tested on recombinant chicken RALDH1, RALDH2, RALDH3, human RALDH2 (hRALDH2) and recombinant human mitochondrial ALDH2 (hALDH2) to examine the effects of DAR on aldehyde dehydrogenase activity (**Figure 23**). RALDH1, 2, 3, and hRALDH2 were pre-incubated with DAR (0 – 10 μM) for 20 minutes at 37°C, after which retinaldehyde (RAL, 250 μM) was added to the reaction mixture to initiate all-*trans*-retinoic acid (atRA) and NADH production. RALDH activity in the presence and

absence of DAR was measured by quantifying the synthesis of NADH, as both NADH and atRA are produced in equimolar amounts during the oxidation of all-*trans*-retinaldehyde.[46] DAR inhibited chicken RALDH1, 2, and 3 with IC_{50} values of 434.70 ± 99.70 nM, 55.00 ± 10.71 nM and 161.27 ± 16.57 nM, respectively, as well as human RALDH2 (hRALDH2, IC_{50} = 191.32 ± 36.77 nM) (**Figure 23A-D**). Using propionaldehyde as the substrate (5 mM) for human aldehyde dehydrogenase 2 (hALDH2), DAR (0 – 100 μM, 1 hour pre-incubation) did not have an inhibitory effect on hALDH2 (**Figure 23E**), while WIN 18446 inhibited hALDH2 with an observed IC_{50} of 229.33 ± 40.95 nM (**Figure 23E**). These results indicate that DAR has selectivity for RALDH enzymes with the most robust inhibition (lowest IC_{50}) observed for RALDH2 *in vitro* in the presence of the natural substrate, retinaldehyde (inhibition of RALDH2 > RALDH3 > RALDH1).

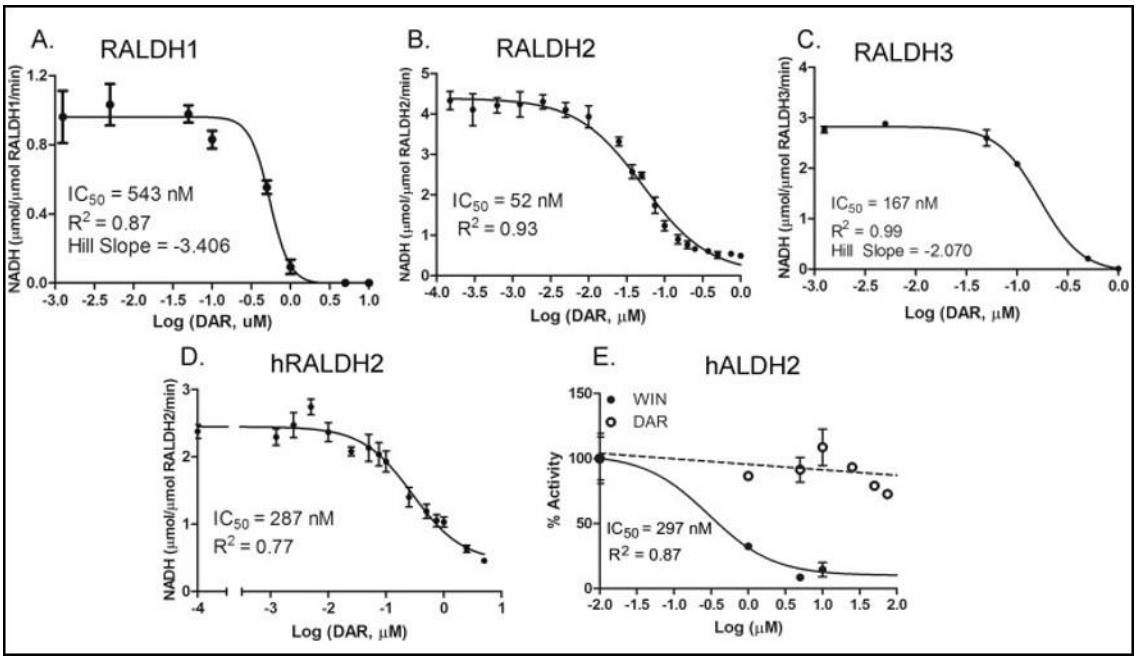

Figure 23. Dose response curves to compare the effect of DAR on chick and human RALDH1a isoforms and human mitochondrial ALDH2 (hALDH2). Data points (A-E) represent the average ± SEM for triplicate samples. Figure is adapted from Harper *et al*.[47]

V.2.3.2 DAR is an irreversible inhibitor of RALDH2

The mechanism of inhibition of DAR on recombinant chicken RALDH2 was investigated using various methods to determine if DAR acts as an irreversible inhibitor, since WIN 18446 inhibits human RALDH2 in a time-dependent and irreversible manner (**Figure 24**).[123]. Increasing concentrations of DAR in the enzyme reaction with RALDH2 resulted in a dose dependent decrease of V_{max} (**Figure 24A**). A hallmark of irreversible inhibition is the persistence of inhibition following removal of unbound inhibitor. When unbound inhibitor was removed by ultrafiltration (**Figure 24B**, "UF") prior to addition of cofactor and substrate, RADLH2 activity was not restored. The inhibition effects of DAR was observed similar to the results seen when unbound DAR remained present in the enzyme reaction (**Figure 24B**, " No UF"). In addition, the V_{max} for NADH synthesis was determined using increasing concentrations of RALDH2 (46 – 365 nM) in the presence of DAR (150 nM) (**Figure 24C**). A plot of V_{max} vs. RALDH2 concentration indicated that RALDH2 activity was completely inhibited when enzyme concentrations (46 – 91 nM) were less than the concentration of DAR [RALDH2] $\leq$ 150 nM). In the presence of 150 nM DAR, RALDH2 concentrations (183 – 365 nM) resulted in a linear increase in V_{max} for NADH synthesis (0.50 – 3.01 μM NADH/min). These results suggested that DAR irreversibly inhibits RALDH2. Similar experiments performed on RALDH1 and RALDH 3 also indicate that DAR is an irreversible inhibitor for chick RALDH1 and RALDH3 as well.

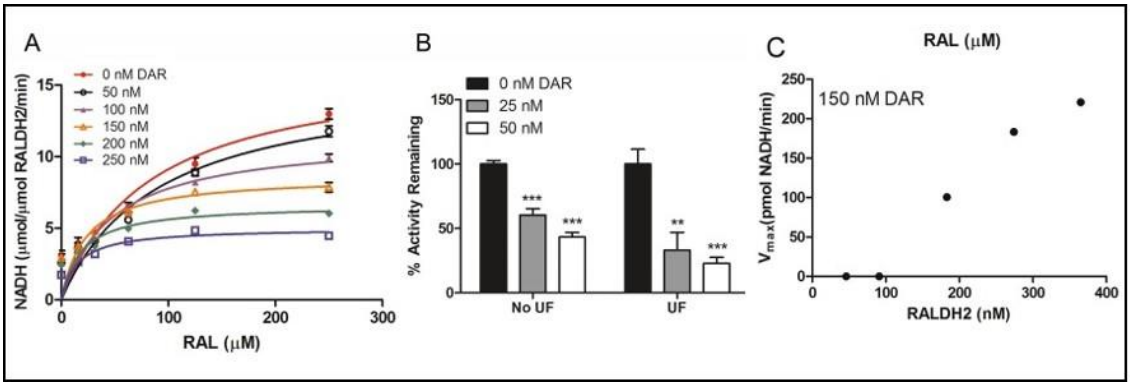

Figure 24. DAR is an irreversible inhibitor of RALDH2.
A) All-trans-retinaldehyde concentration-dependent RALDH2 (91 nM) activity in the presence of increasing concentration of DAR (0-250 nM; pre-incubated with RALDH2 for 20 minutes prior to addition of substrate and cofactor). B) RALDH2 activity measured before and after ultrafiltration of DAR-inactivated RALDH2 (0-50 nM DAR). C) Maximal rate (V_{max}) of enzyme activity was determined at increasing concentrations of RALDH2 (46-365 nM) with DAR concentration remaining constant (150 nM). Figure is adapted from Harper *et al*.[47]

V.2.3.3 DAR inhibits all-*trans*-retinoic acid synthesis in a RALDH2 expressing cell line

$^{(Dox)}$RALDH2-eGFP, a HEK-293 cell line expressing doxycycline (DOX)-inducible chicken RALDH2 was employed to assess the effect of DAR on intracellular RALDH2 activity (**Figure 25**). Treatment of the $^{(Dox)}$RALDH2-eGFP cells with DOX (5 µg/mL; 24 hours) resulted in the induction of RALDH2-eGFP expression as compared to non-induced $^{(Dox)}$RALDH2-eGFP cells (**Figure 25A**). In order to determine the toxicity of DAR on the $^{(Dox)}$RALDH2-eGFP cells, cell viability assays measuring DNA content and ATP production were performed (**Figure 25B**). Following treatment with DAR (0 – 50 µM) for 24 hrs, toxicity curves were determined with IC_{50} values of 2.94 ± 1.58 µM and 3.09 ± 0.48 µM, for DNA and ATP production, respectively.

Next, *ex vivo* effects of DAR on cells was investigated. DOX-induced RALDH2-eGFP expressing cells were treated with DAR (0 – 2 µM for 24 hrs). Following isolation

of cell lysates, the enzyme reaction was initiated by addition of NAD^+ and the substrate all-*trans*-retialdehyde (25 µM). All-*trans*-retinoic acid (atRA) was then extracted in hexanes from the enzyme reaction, dried and resuspended in acetonitrile to prepare samples for Liquid Chromatography Mass Spectrometry (LCMS) quantification. The concentration of atRA was determined from a calibration curve generated by LCMS using known concentrations of atRA (See **V.4.3**). Treatment of DOX-induced RALDH2-eGFP expressing cells with DAR (0 – 2 µM for 24 hours) resulted in a significant inhibition of all-trans-retinoic acid synthesis at 0.05 µM (↓42%, $p<0.01$), 0.50 µM (↓47%, $p<0.001$), 1 µM (↓92%, $p<0.001$), and 2 µM (↓93%, $p<0.001$) compared to the vehicle treated control (one-way ANOVA with Bonferroni's test for multiple comparisons) (**Figure 25B**). No atRA synthesis was detected in cells not induced with DOX (-DOX). Normalization of results in **Figure 25C** to RALDH2 protein expression in each sample (relative density quantified from western blot, *inset*) indicated a dose-dependent decrease in atRA synthesis with an IC_{50} value for the normalized inhibition curve calculated to be 187.20 ± 40.80 nM (**Figure 25D**).

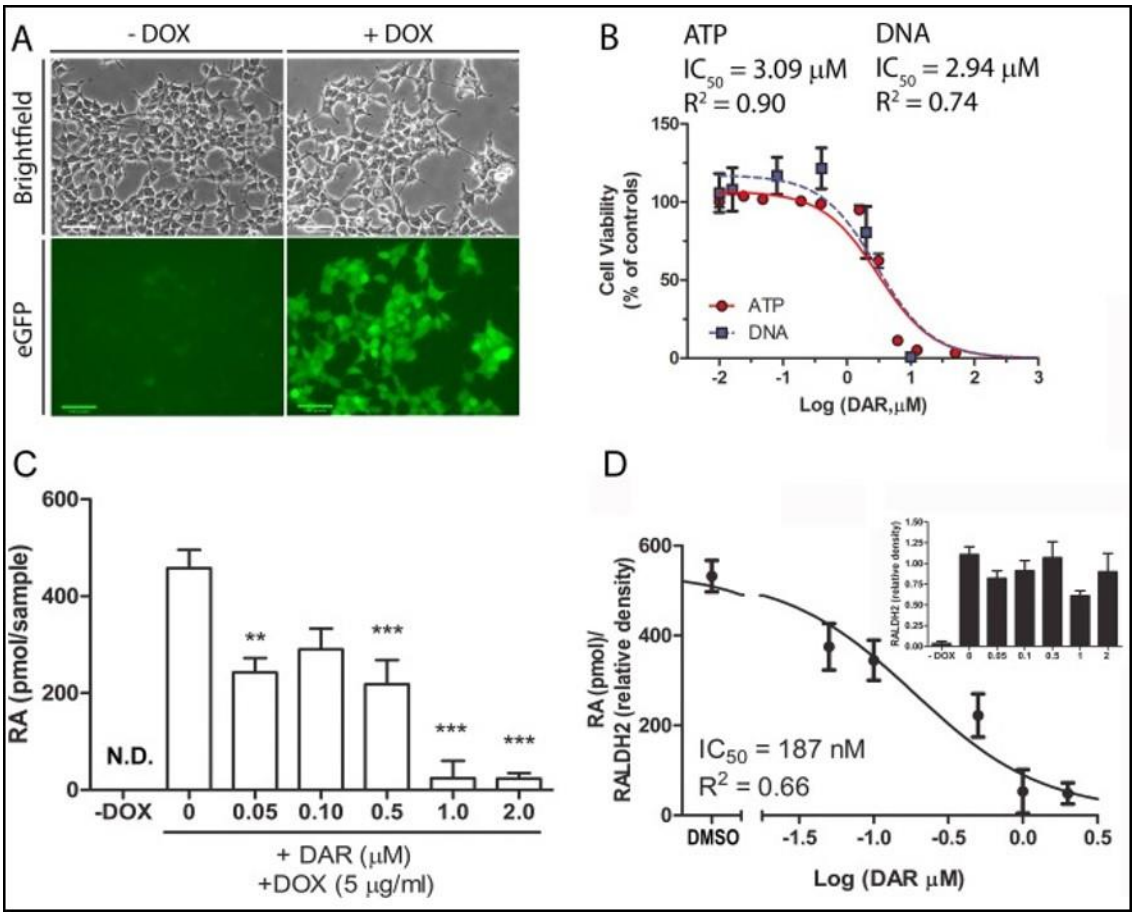

Figure 25. DAR inhibits all-*trans*-retinoic acid (atRA) synthesis in a RALDH2 expressing cell line.
A) Induction of chicken RALDH2-eGFP expression in a stably transfected, doxycycline (DOX)-inducible HEK 293 cell line ($^{(Dox)}$RALDH2-eGFP). RALDH2-eGFP expression is not detected in cell lysates not treated with DOX (-DOX). B) Toxicity curves measuring DNA content and ATP production in cells treated with DAR (- μM) for 24h. C) Inhibition of atRA synthesis in $^{(Dox)}$RALDH2-eGFP cells treated with DAR (0.05-2 μM) or vehicle (DMSO) for 24h. Following isolation of cell lysates, the enzyme reaction was initiated by addition of NAD+ and all-trans-retinaldehyde (25 μM). All-trans-retinoic acid was quantified by HPLC in Burgett lab. No atRA synthesis was detected in cells not induced with DOX (-DOX). D) Results in C normalized to RALDH2 protein expression. Relative RALDH2 expression was quantified from western blots of $^{(Dox)}$RALDH2-eGFP cell lysates (*inset*). Figure is adapted from Harper *et al*.[47]

Overall, the novel compound α,α-dichloro-all-trans-retinone (DAR) has been shown to selectively inhibit the RALDH isozymes *in vitro* (chicken RALDH2, RALDH3, RALDH1, and human RALDH2) and *ex vivo* in the nanomolar range in an irreversible

manner. DAR has superior selectivity compared to WIN 18446 as it did not have an inhibitory effect on the human mitochondrial ALDH2 enzyme.

V.3 Conclusions

The lack of selective inhibitors for the important and disease-relevant retinaldehyde dehydrogenase (RALDH) isozymes subfamily inspired the design and synthesis of α,α-dichloro-all-*trans*-retinone (DAR) using an intelligent drug design approach based on enzyme structure and substrate affinity. DAR was synthesized and purified from a complex mixture of products due to the high reactivity of the retinyl moiety and the dichloromethyllithium reagent. After successful structure characterization of DAR, its biological activity was examined through several experiments. The results showed that DAR inhibits chicken RALDH1, 2, 3, and human RALDH2 in an irreversible manner, but has no inhibitory effect on human mitochondrial ALDH2. These results are promising for the development of a therapeutic agent selective for the RALDH enzymes, specifically RALDH2 for the treatment of myopia [114,115]. The structure of DAR will require optimization to improve compound stability and yield of the synthetic route.

V.4 Experimental section

V.4.1 General methods

All reactions were performed in oven-dried glassware under a positive pressure of nitrogen unless noted otherwise. Flash column chromatography was performed as described by Still *et al*.[55] employing E. Merck silica gel 60 (230-400 mesh ASTM). TLC analyses and preparative TLC (pTLC) purification was performed on 250µm Silica Gel 60 F254 plates purchased from EM Science and Fluka Analytical. All solvents and chemicals were used as purchased without further purification. Solvents used in the reactions were

collected under nitrogen from a Pure Solv 400-5-MD Solvent Purification System (Innovative Technology). Infrared spectra were recorded on a Shimadzu IRAffinity-1 instrument, or Bruker Tensor 27 spectrometer, and IR spectra peaks are reported in terms of frequency of absorption (cm^{-1}). ^{1}H and ^{13}CNMR spectra were recorded on VNMRS 300, VNMRS 400, VNMRS 500 or VNMRS 600 MHz-NMR Spectrometer. Chemical shifts for proton and carbon resonances are reported in ppm (δ) relative to the residual proton or the specified carbon in chloroform (δ 7.26, proton; 77.16, carbon). High-resolution mass spectrometry (HRMS) analysis was performed using Agilent 6538 high-mass-resolution QTOF mass spectrometer. HPLC purification was performed on Shimadzu LCMS 2020 system [LC-20AP (pump), SPD-M20A (diode array detector), LCMS-2020 (mass spectrometer)]. Semi-preparative HPLC purification was performed using Phenomenex Luna C-18(2) column, 5µm particle size (250 mm x 4.6 mm), supported by Phenomenex Security Guard cartridge kit C18 (4.0 mm x 3.0 mm); Phenomenex Luna C-8(2) column, 5µm particle size (250 mm x 4.6 mm), supported by Phenomenex Security Guard cartridge kit C8 (4.0 mm x 3.0 mm) and HPLC-grade solvents.

V.4.2 Compound data

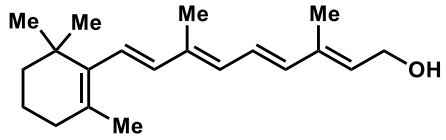

5.2

Compounds **5.2** were synthesized with procedure adapted from Solladie *et al.*[125] Retinyl acetate **5.1** (520.1 mg, 1.58 mmol) was dissolved in methanol (6.6 mL) under nitrogen at room temperature to afford a light yellow, cloudy mixture. To the stirring mixture was added K_2CO_3 (109.4 mg, 0.79 mmol). After 45 minutes, the reaction was completed based on TLC analysis (30% EtOAc/hexanes). The mixture was filtered through a cotton plug.

The solvent was removed in vacuo to afford a thick, orange oil, which was dissolved in DCM (50 mL). The organic layer was washed with saturated $NaHCO_3$ solution (30 mL), DI water (20 mL x 2). The combined aqueous layer was back extracted with DCM (20 mL x 2). The combined organic layer was washed with brine, dried over Na_2SO_4, and filtered. The solvent was removed in vacuo to afford the desired product **5.2** as an opague, yellow gel, which was used without purification (453 mg, quantitative yield). ^{1}H NMR (400 MHz, Chloroform-d) δ 6.62 (dd, J = 15.2, 11.2 Hz, 1H), 6.29 (d, J = 15.1 Hz, 1H), 6.22 – 6.05 (m, 3H), 5.69 (t, J = 7.0 Hz, 1H), 4.31 (t, J = 6.2 Hz, 2H), 2.01 (t, J = 6.4 Hz, 2H), 1.96 (s, 3H), 1.87 (s, 3H), 1.71 (s, 3H), 1.66 – 1.57 (m, 3H), 1.49 – 1.44 (m, 2H), 1.24 (t, J = 5.6 Hz, 1H), 1.02 (s, 6H). See **Chapter appendix** for NMR spectra.

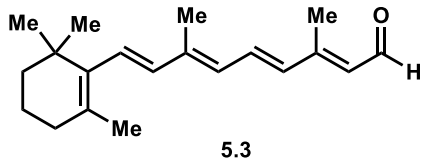

5.3

Compounds **5.3** were synthesized with procedure adapted from Solladie *et al*.[125] Retinol **5.2** (453 mg, 1.58 mmol) was dissolved in dry DCM (8.2 mL) at room temperature. To the stirring mixture was added activated MnO_2 (1.42 g, 16.3 mmol) as solid. After one hour, the reaction was completed based on TLC analysis (20% EtOAc/hexanes). The MnO_2 was removed by centrifugation (4300G, 5 minutes). The solvent was then removed in vacuo to afford desired product **5.3** as a thick, dark orange oil, which was used without purification (422.8 mg, 1.49 mmol, 94% yield). The NMR data agreed with published reference[125]. ^{1}H NMR (400 MHz, Chloroform-d) δ 10.10 (d, J = 8.1 Hz, 1H), 7.14 (dd, J = 15.1, 11.5 Hz, 1H), 6.35 (dd, J = 15.6, 10.9 Hz, 2H), 6.23 – 6.11 (m, 2H), 5.97 (d, J = 8.2 Hz, 1H), 2.33 (s, 3H), 2.07 – 1.99 (m, 5H), 1.72 (s, 3H), 1.67 – 1.59 (m, 2H), 1.51 – 1.43 (m, 2H), 1.03 (s, 6H). See **Chapter appendix** for NMR spectra.

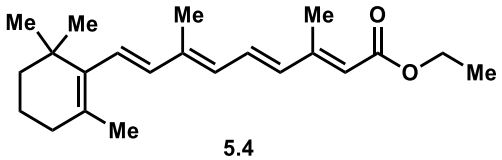

5.4

Compounds **5.4** were synthesized with procedure adapted from Solladie *et al* and Corey *et al*.[125,126] Retinal **5.3** (422.8 mg, 1.49 mmol) was dissolved in dry EtOH (15 mL) at room temperature. To the reaction mixture was added NaCN (72.8 mg, 1.49 mmol) as a solid and glacial acetic acid (128 µL, 2.23 mmol) dissolved in EtOH (0.5 mL). After 45 minutes, to the mixture was added activated MnO_2 (1.29 g, 14.9 mmol). The mixture was stirred at room temperature and the progress was followed by TLC (10% EtOAc/hexanes). After 24h, to the reaction mixture was added more MnO_2 (388 mg, 4.47 mmol). After 48h, the reaction was completed based on TLC analysis. The MnO_2 was removed by centrifugation (4300G, 5 minutes). The black residue was washed with DCM (30 mL x3). The supernatant was washed with saturated $NaHCO_3$ (30 mL), DI water (30 mL x2). The aqueous layer was back extracted with DCM (30 mL). The combined organic layer was washed with brine (50 mL), dried over Na_2SO_4, and filtered. The solvent was removed to afford desired product **5.4** as a dark orange oil, which was used without purification (476.2 mg, 97% yield). ^{1}H NMR (400 MHz, Chloroform-d) δ 6.99 (dd, J = 15.1, 11.4 Hz, 1H), 6.34 – 6.23 (m, 2H), 6.18 – 6.09 (m, 2H), 5.77 (s, 1H), 4.17 (q, J = 7.1 Hz, 2H), 2.35 (s, 3H), 2.10 – 1.94 (m, 5H), 1.71 (s, 3H), 1.66 – 1.56 (m, 2H), 1.52 – 1.44 (m, 2H), 1.29 (t, J = 7.2 Hz, 3H), 1.03 (s, 6H). See **Chapter appendix** for NMR spectra.

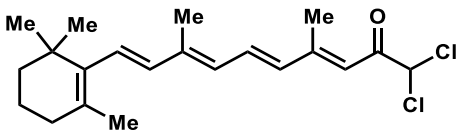

α,α-dichloro-all-*trans*-retinone (DAR)

Ethyl retinoate **5.4** (69.5 mg, 0.211 mmol) was dissolved in dry ethyl ether (0.9 mL) under nitrogen. Dichloromethane (19.0 µL, 0.296 mmol) was added via syringe. The dark yellow solution was cooled down to -78˚C. LDA solution (2.0M in THF, 170 µL, 0.338 mmol) was added dropwise slowly over 5 minutes. Upon the addition of LDA, the color of the reaction mixture turned dark red/brown. The progress of the reaction was monitored by TLC (10% EtOAc/hexanes, CAM stain) every 2 minutes. The reaction mixture was stirred at -78˚C for additional 10 minutes, when no further reaction progress was observed on TLC. To the reaction mixture, 400 µL of 6N HCl was added to quench the reaction. The mixture was warmed to room temperature, diluted with ethyl ether (30 mL), washed with 1N HCl (15 mL x 2) and with distilled water (15 mL x 2). The combined aqueous phase was back extracted with ethyl ether (5 mL x 2). The combined organic phase was washed with brine (20 mL) and dried over Na_2SO_4, and filtered. The solvent was removed under reduced pressure to afford crude product as a dark brown oil (70 mg).

The reaction did not go to completion, and produced multiple products based on TLC analysis showing multiple spots. The crude mixture was then separated by pTLC (3 plates) eluted with 4.5% EtOAc/hexane. The pTLC plates were covered with multiple thin, inseparable bands. Four main, separable bands were collected: band 1 (Rf=0.54, 12.8 mg, desired product 5); band 2 (Rf=0.48, 14.9 mg, recovered 4); band 3 (Rf=0.37, 7 mg, tetrachloro-adduct possible); band 4 (Rf=0.22, 2.8 mg, mixture of compounds).

The desired product from fraction 1 was further purified by HPLC using a Phenomenex C18(2) Luna semiprep column, 96-98% MeCN/water with 0.1% formic acid gradient (2.5 mL/min flow rate, start with 3 minutes of 96%, gradient 96-98% in 9 minutes, hold at 98% for 8 minutes). This resulted in the pure desired product **DAR** (yellow oil, 7.7 mg, 10%

yield, 12.6% borsm) with retention time at 16.7 minute. See **Chapter appendix** for NMR spectra.

^{1}H NMR (500 MHz , CDCl3): δ = 7.21 (dd, J = 15.0, 11.5 Hz, 1H, H6), 6.49 (s, 1H, H3), 6.42 (d, J = 15.1 Hz, 1H, H5), 6.37 (d, J = 18.0 Hz, 1H, H7), 6.20 (d, J = 11.5 Hz, 1H, H9), 6.17 (d, J = 15.9 Hz, 1H, H10), 5.84 (s, 1H, H1), 2.44 (s, 3H, H17), 2.05 (s, 3H, H18), 2.04 (m, 2H, H13), 1.68 - 1.59 (m, 2H, H14), 1.52-1.46 (m, 2H, H15), 1.05 (s, 6H, H20). ^{13}C NMR (126 MHz, CDCl3): δ = 186.46 (C2), 159.02 (C4), 141.93 (C8), 137.63 (C11), 137.05 (C10), 134.81 (C5), 134.38 (C6), 130.63 (C12), 130.03 (C7), 129.40 (C9), 118.02 (C3), 71.02 (C1), 39.60 (C15), 34.28 (C16), 33.17 (C13), 28.97 (C10), 21.77 (C19), 19.18 (C14), 14.96 (C17), 13.05 (C18). IR (NaCl, cm^{-1}): 3440 (Csp3-H), 2920 (Csp2-H), 1680 (C=O), 1558 (C=C), 785 (C-Cl). HRMS (ESI): m/z calculated for $C_{21}H_{28}Cl_2O + H^+$ [M + H^+]: 367.1595, found: 367.1596, Δ = 0.27ppm.

V.4.3 LCMS calibration curve for all-*trans*-retinoic acid

all-*trans*-retinoic acid (atRA) was quantified as previously described with the following modifications: a Shimadzu LCMS 2020 (Shimadzu; Kyoto, Japan) with a Cortecs C18 column [2.7 μm particle size with VanGuard Cartridge (Waters; Milford, MA)] was used to achieve atRA separation. The column compartment was maintained at 25 °C, and the autosampler was maintained at 10 °C. The following solvents were used: A, H_2O with 0.1% formic acid; B, acetonitrile. The column was equilibrated in 70% acetonitrile prior to sample loading. 25 μL of sample was injected into the column, and separation was achieved at 400 μL/min with the following gradient: 0–3 min, hold at 70% B; 3–15 min, 70% B to 95% B; 15–20 min, hold at 95% B; 20–21 min, 95% B to 70% B; 21–37 min, re-equilibrate at 70% B. Elution of atRA was monitored using a photodiode array detector at 350 nm,

followed by MS detection. Retention time of atRA was 20.6 min with an m/z of 300.25. atRA was quantified from a calibration curve (**Figure 26**) generated using known amounts of atRA (0–1500 pmol) eluted with the above gradient.

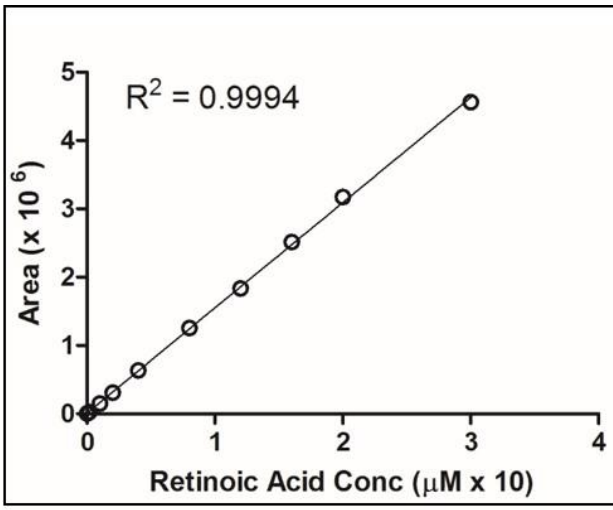

Conc (µM)	pmol/25 µl	Peak Area
0	0	5148
0.1	2.5	14410
0.1	5	29031
1	25	151775
2	50	311833
4	100	634454
8	200	1255511
12	300	1835030
16	400	2513543
20	500	3171768
30	750	4559262

Figure 26. all-trans-retinoic acid LCMS calibration curve

V.5 Chapter appendix

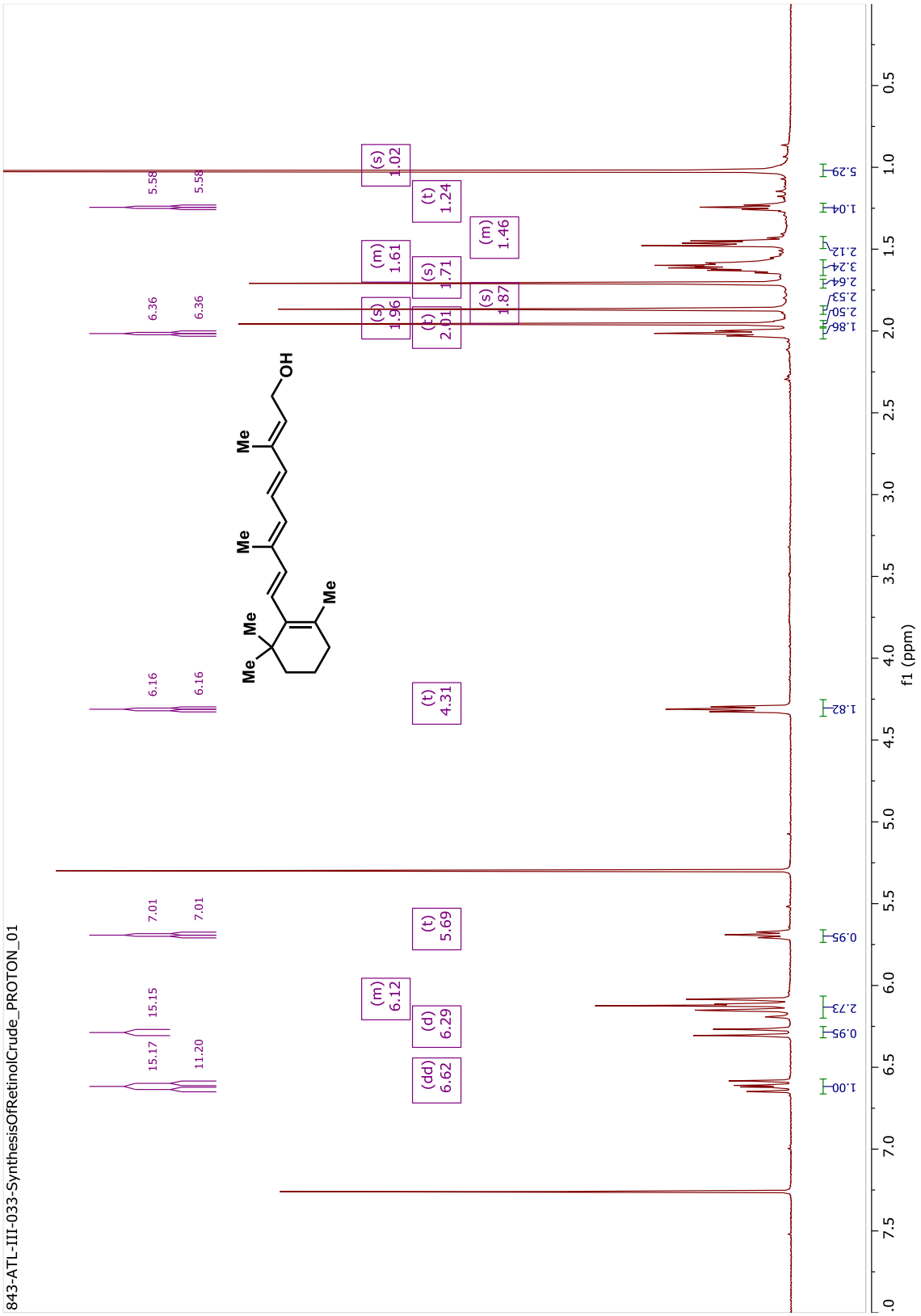

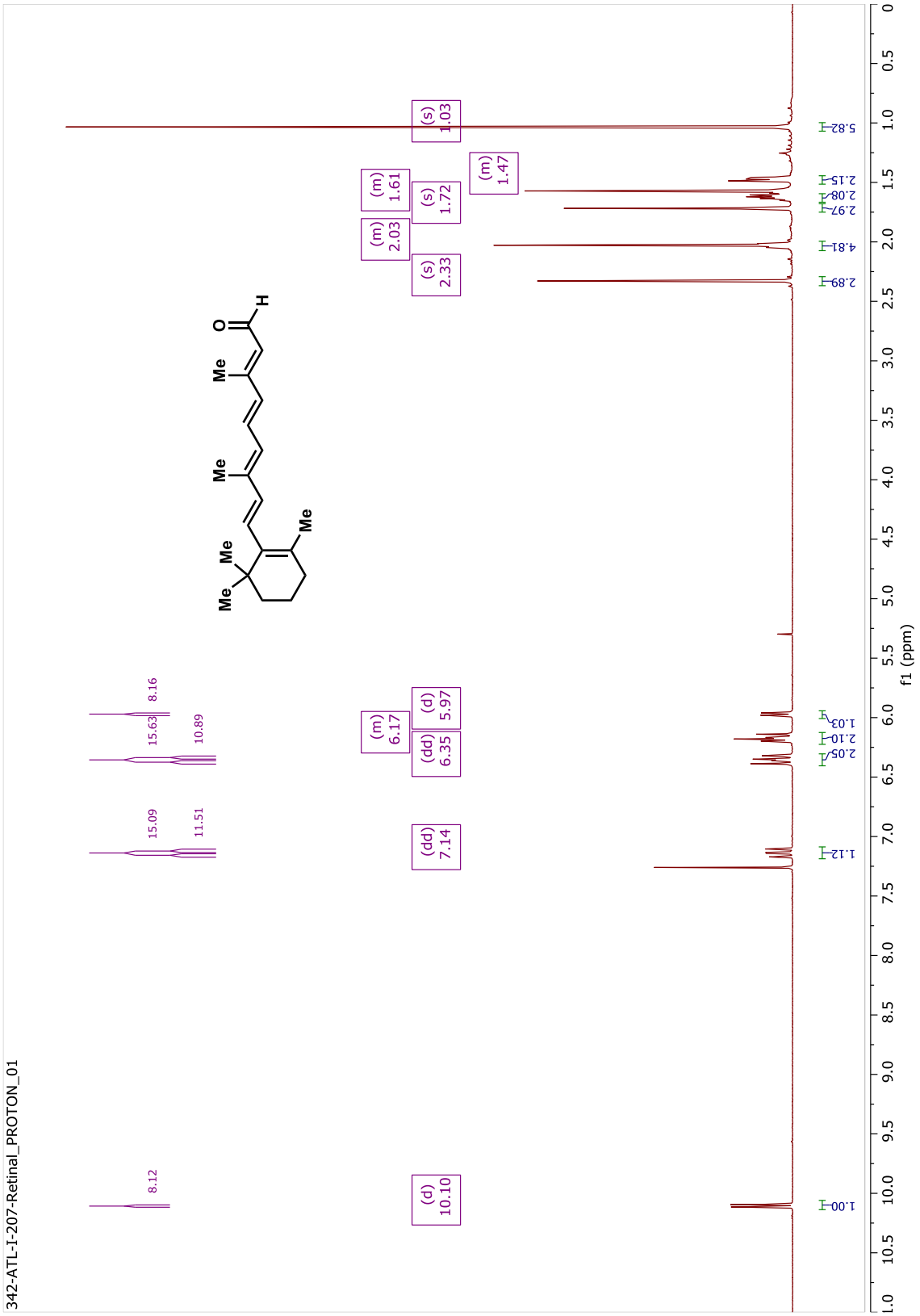
342-ATL-I-207-Retinal_PROTON_01
Me
Me
Me
Me
Me
O
H
(s) 1.03
(m) 1.47
(m) 1.61
(s) 1.72
(m) 2.03
(s) 2.33
(m) 6.17
(d) 5.97
(dd) 6.35
(dd) 7.14
(d) 10.10
8.12
8.16
15.63
10.89
15.09
11.51
5.82
2.15
2.08
2.97
4.81
2.89
1.03
2.10
2.05
1.12
1.00
f1 (ppm)

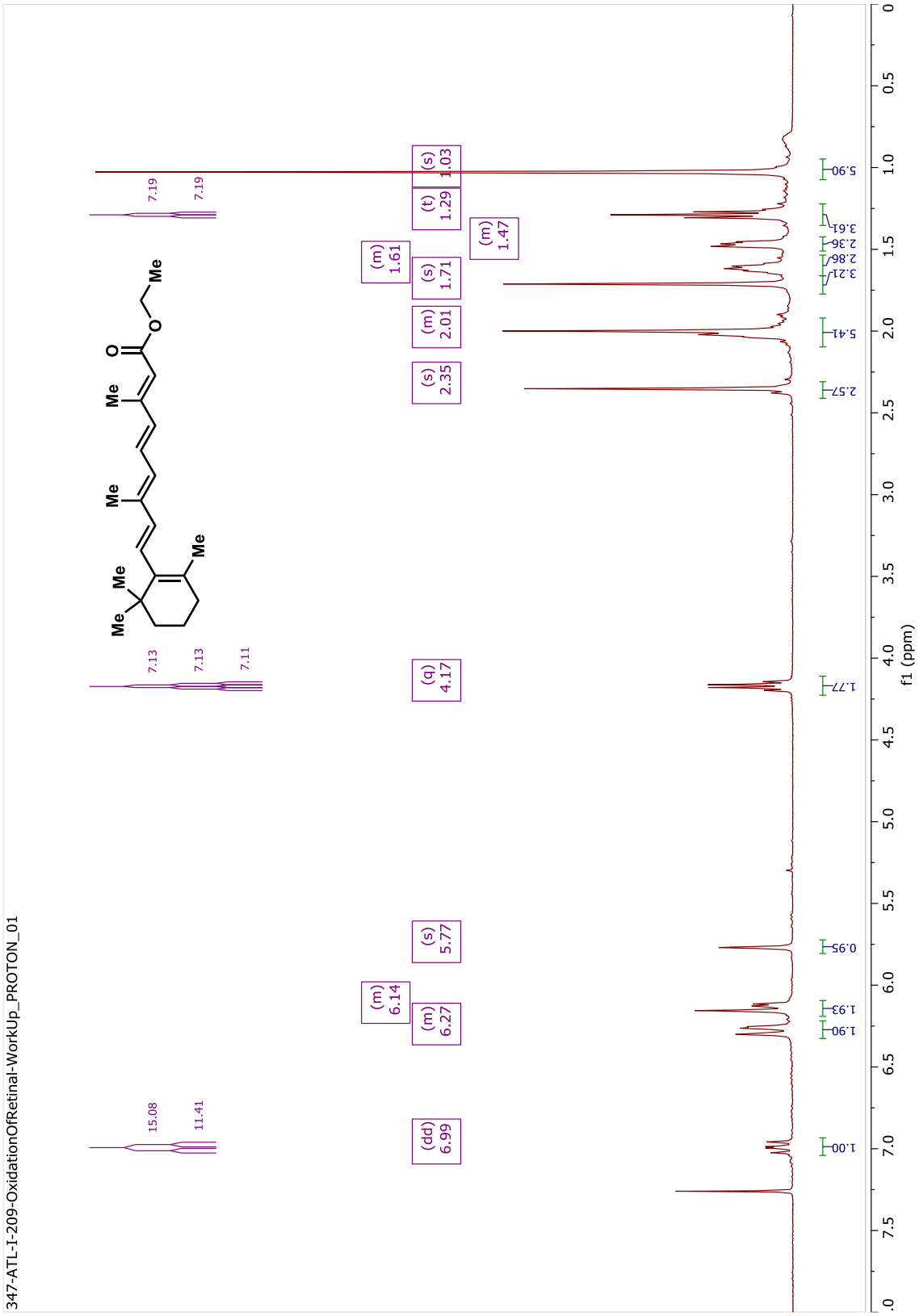
347-ATL-I-209-OxidationOfRetinal-WorkUp_PROTON_01
Me
Me
Me
Me
O
O
Me
7.19
7.19
7.13
7.13
7.11
15.08
11.41
(s) 1.03
(t) 1.29
(m) 1.47
(m) 1.61
(s) 1.71
(m) 2.01
(s) 2.35
(q) 4.17
(s) 5.77
(m) 6.14
(m) 6.27
(dd) 6.99
5.90
3.61
2.36
2.86
3.21
5.41
2.57
1.77
0.95
1.93
1.90
1.00
f1 (ppm)

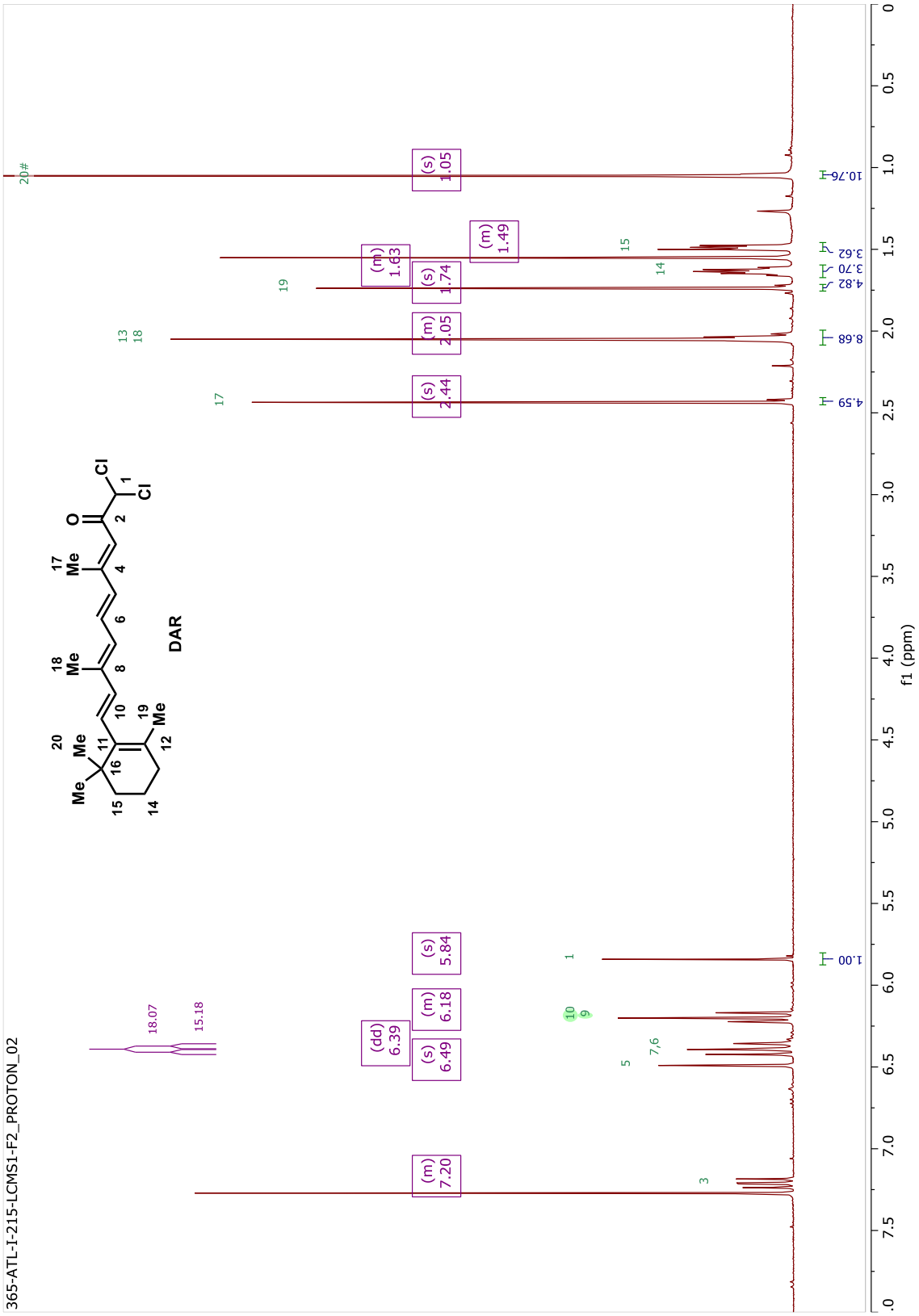
365-ATL-I-215-LCMS1-F2_PROTON_02
DAR
f1 (ppm)

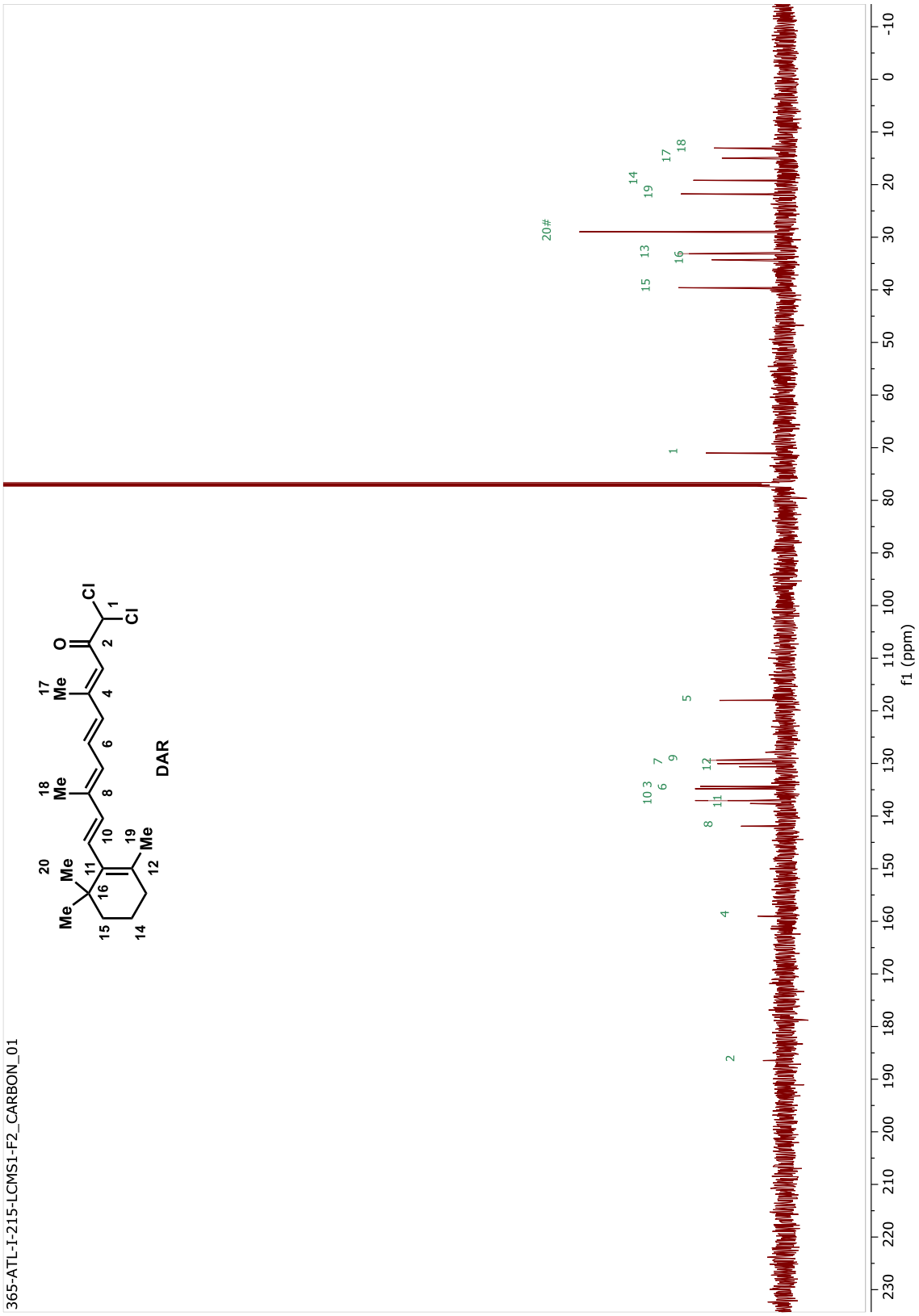
365-ATL-I-215-LCMS1-F2_CARBON_01
DAR
f1 (ppm)

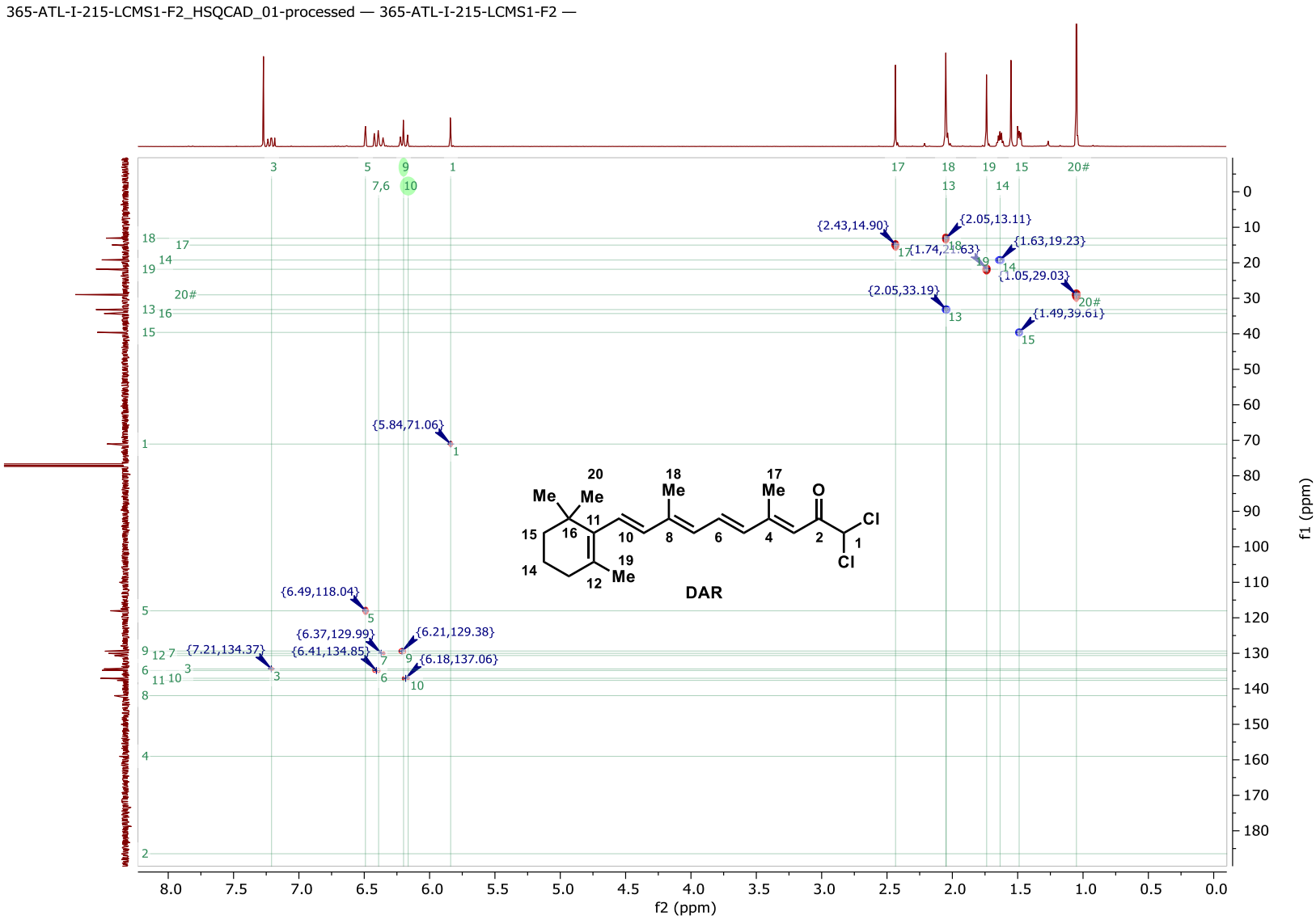
365-ATL-I-215-LCMS1-F2_HSQCAD_01-processed — 365-ATL-I-215-LCMS1-F2 —
{2.43,14.90}
{2.05,13.11}
{1.74,21.63}
{1.63,19.23}
{1.05,29.03}
{2.05,33.19}
{1.49,39.61}
{5.84,71.06}
{6.49,118.04}
{6.37,129.99}
{6.21,129.38}
{7.21,134.37}
{6.41,134.85}
{6.18,137.06}
DAR
f2 (ppm)
f1 (ppm)

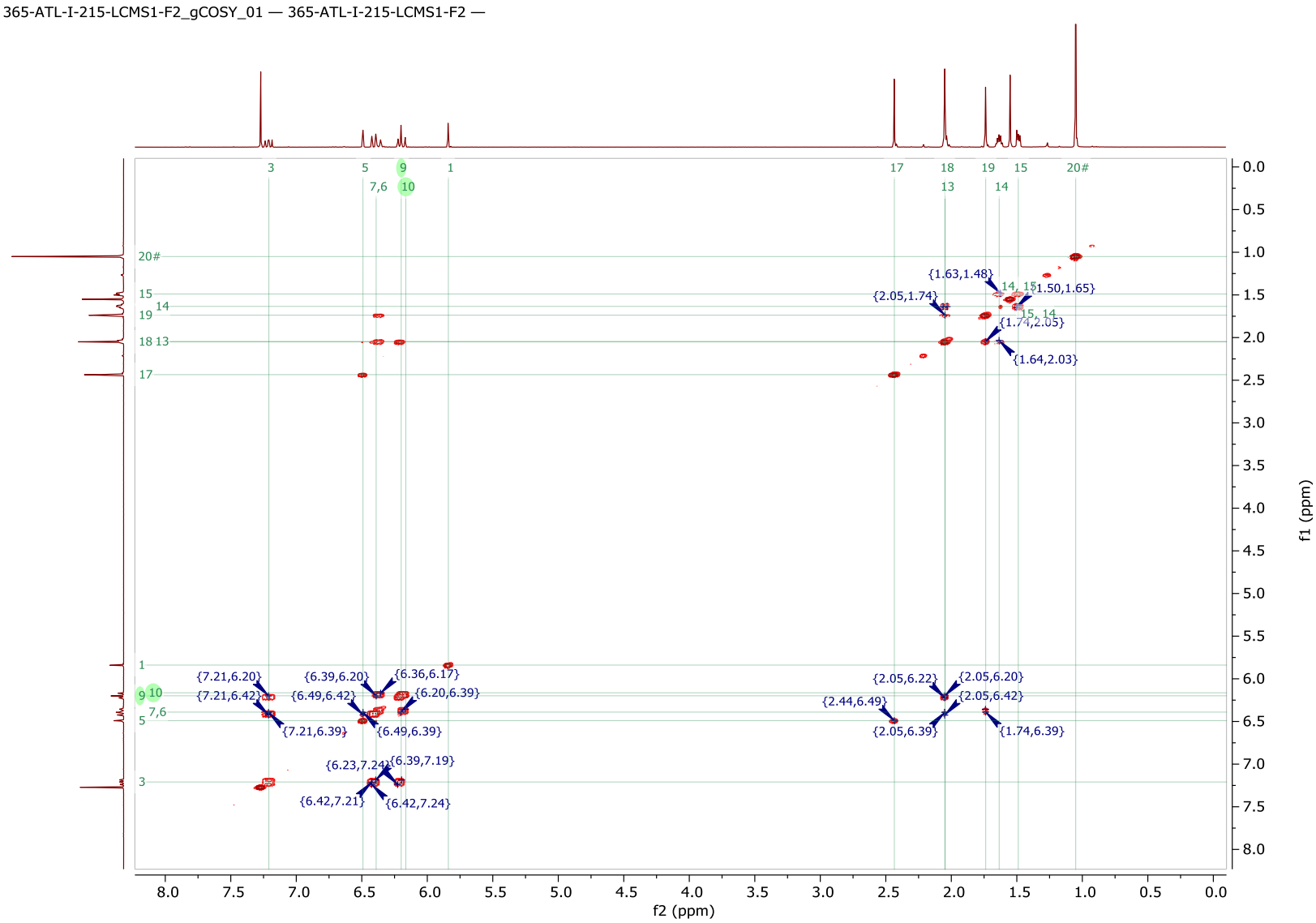
365-ATL-I-215-LCMS1-F2_gCOSY_01 — 365-ATL-I-215-LCMS1-F2 —
f2 (ppm)
f1 (ppm)
{7.21,6.20}
{7.21,6.42}
{7.21,6.39}
{6.39,6.20}
{6.49,6.42}
{6.49,6.39}
{6.36,6.17}
{6.20,6.39}
{6.23,7.24}
{6.39,7.19}
{6.42,7.21}
{6.42,7.24}
{1.63,1.48}
{2.05,1.74}
{1.50,1.65}
{1.74,2.05}
{1.64,2.03}
{2.05,6.22}
{2.05,6.20}
{2.44,6.49}
{2.05,6.42}
{2.05,6.39}
{1.74,6.39}

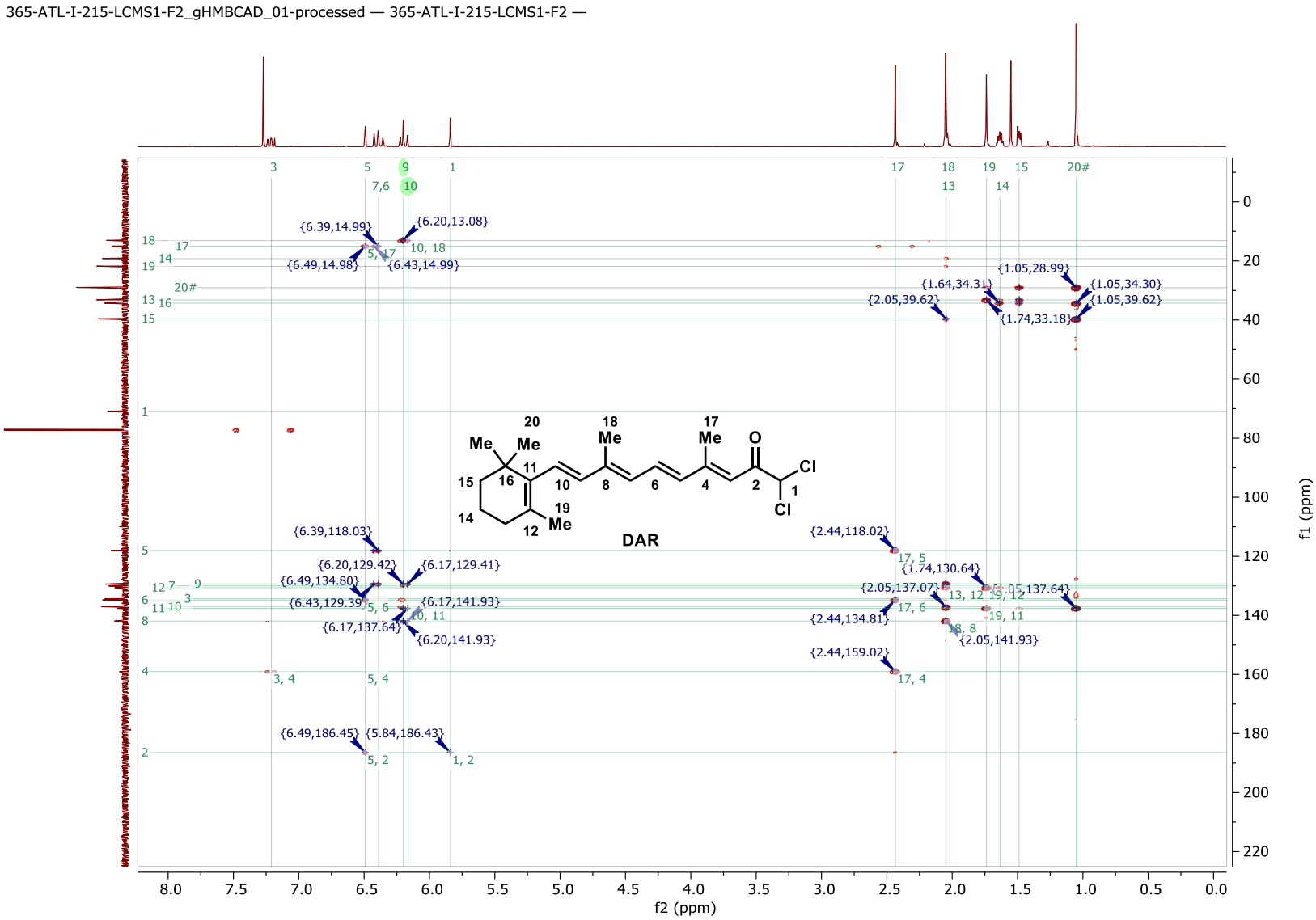
365-ATL-I-215-LCMS1-F2_gHMBCAD_01-processed — 365-ATL-I-215-LCMS1-F2 —
DAR
f2 (ppm)
f1 (ppm)

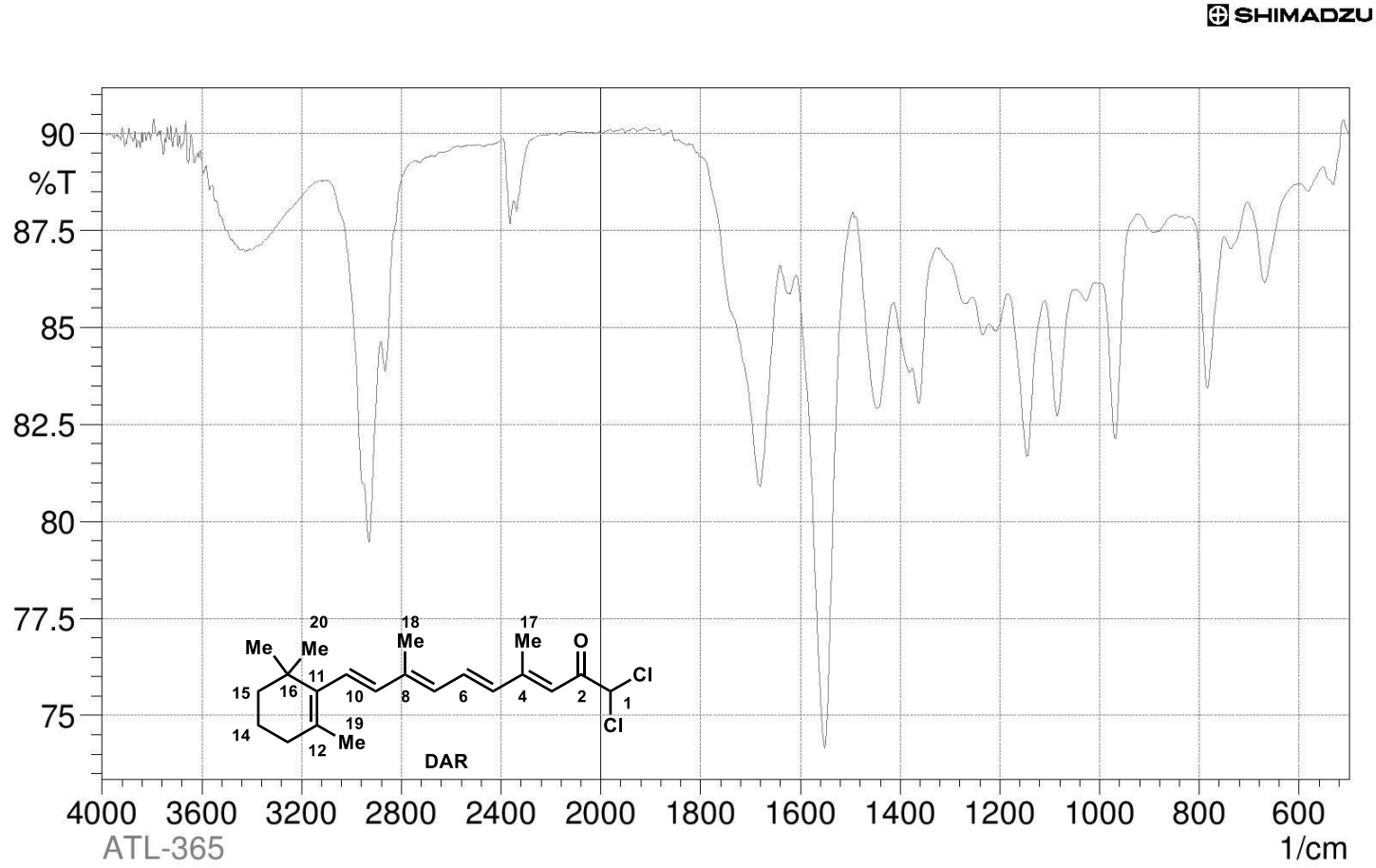

Comment;
ATL-365

No. of Scans;
Resolution;
Apodization;

Date/Time; 7/3/2015 3:55:09 PM
User; Nicholas-IR

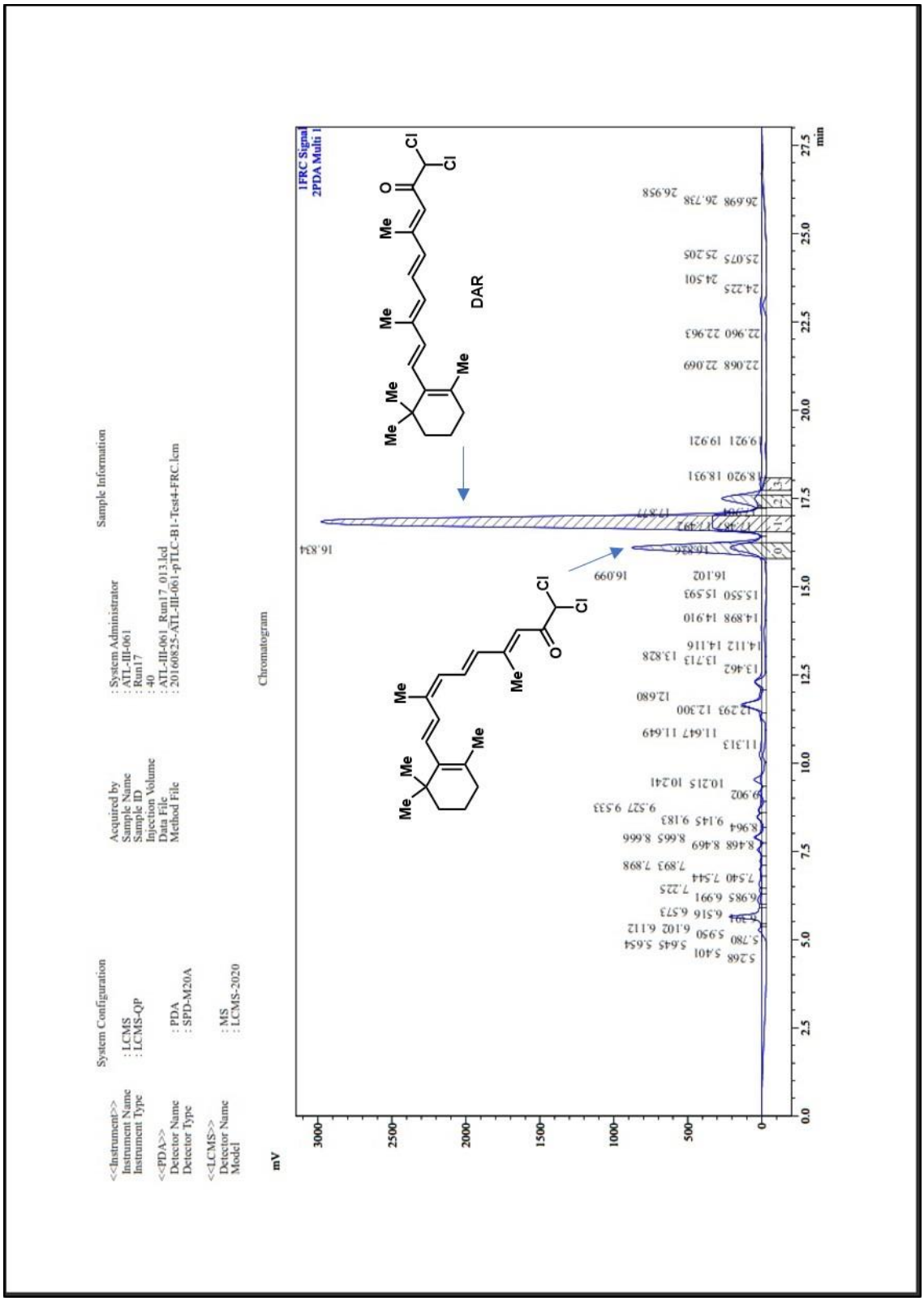
System Configuration
<<Instrument>>
Instrument Name : LCMS
Instrument Type : LCMS-QP
<<PDA>>
Detector Name : PDA
Detector Type : SPD-M20A
<<LCMS>>
Detector Name : MS
Model : LCMS-2020
Acquired by : System Administrator
Sample Name : ATL-III-061
Sample ID : Run17
Injection Volume : 40
Data File : ATL-III-061_Run17_013.lcd
Method File : 20160825-ATL-III-061-pTLC-B1-Test4-FRC.lcm
Sample Information
Chromatogram
mV
min
1FRC Signal
2PDA Multi 1
DAR
16.834
16.099
17.877
26.958
26.738
26.698
25.205
25.075
24.501
24.225
22.963
22.960
22.069
22.068
19.921
19.921
18.931
18.920
16.826
16.102
15.593
15.550
14.910
14.898
14.116
14.112
13.828
13.713
13.462
12.680
12.300
12.293
11.649
11.647
11.313
10.241
10.215
9.902
9.533
9.527
9.183
9.145
8.964
8.666
8.665
8.469
8.468
7.898
7.893
7.544
7.540
7.225
6.991
6.985
6.573
6.516
6.112
6.102
5.950
5.780
5.654
5.645
5.401
5.268
Me
Me
Me
Me
Me
Me
O
Cl
Cl

Chapter VI : Conclusions and Outlooks

Since the identification of OSW-1's cellular targets as disease-relevant proteins OSBP and ORP4, the natural product OSW-1 has shown significant potential for therapeutic applications. The OSW-1 compound exhibits broad-spectrum anti-viral activity through its inhibition of OSBP, and potent anti-cancer activity through its interaction with ORP4. The comparable binding affinity of the OSW-1 compound to both OSBP and ORP4 incumbers its development as effective therapeutic agents. Furthermore, the mechanism of action of the OSW-1 compound still remains unclear.

To gain further insights to the OSW-1 compound's mechanism of action, a set of OSW-1 probe analogs were designed and synthesized, including 1) a deuterated OSW-1 analog useful for mass spectrometry (MS) quantification of OSW-1; 2) a biologically inactive OSW-1 analog useful for serving as a negative control compound, and 3) a series of OSW-1 analogs with an introduced amine linker that retains the biological activity of OSW-1 while allowing for direct further derivatization. These compounds were prepared through either total synthesis and direct derivatization of the OSW-1 compound.

The deuterated OSW-1 analog was accessed through the total synthesis route, with the deuterium labeled installed on the C-3'' of OSW-1 xylose moiety. This process was proven to be lengthy, with the multistep synthesis required from each moiety, and low-yield, mainly due to the late-stage, low-yielding Schmidt glycosylation reaction utilized to assemble the molecule. Once synthesized, the deuterated OSW-1 analog was employed as an internal standard to measure the concentration of the OSW-1 compound inside the living cells through the Single-probe quantitative Single-Cell Mass Spectrometry. This deuterated

OSW-1 analog can be further applied in the future for different mass spectrometry studies to probe the mechanism of action of OSW-1.

The set of OSW-1 analogs with amine linker that retain the biological activity of OSW-1 will allow for further direct and selective derivatization of the OSW-1 compound for desirable biological studies. These analogs were accessed through two-steps synthesis that installed the linker on the OSW-1 molecule and revealed the free amine handle. The installation of the linker resulted in two products, C-3" and C-4" linker, in approximately equal amount. The analogs with C-3" linker retained the binding affinity of OSW-1 to OSBP protein, while the analogs with C-4" linker showed a significant decrease in bioactivity as compared to OSW-1. Therefore, alternative methodologies to install the linker selectively on C-3" of the OSW-1 molecule should be investigated to limit the formation of the biologically inactive C-4" linker. The free amine moiety then allows for selective derivatization, since the OSW-1 compound possesses several hydroxyl groups. The OSW-1 analogs with C-3" linker can now be derivatized for further studies, such as conjugation with a cancer-specific antibody [antibody-drug conjugate (ADC)] to increase the selectivity of the OSW-1 compound to cancer cells.

To increase OSW-1's potential as therapeutic agent, a new and concise two-component approach to different OSW-1 scaffolds with an E-ring bridge were proposed to allow for the rapid assembly to OSW-1 analogs with increased affinity to OSBP or ORP4. Through performing total synthesis of OSW-1, it became apparent that the total synthesis route does not allow for rapid derivatization of the OSW-1 structure, since each moiety requires several synthetic steps, and the low-yielding assembly of the molecule through Schmidt glycosylation. In this new approach, the OSW-1 steroidal aglycon component will

be joined with an imine component carrying the side chain and saccharide moieties through an imino-ene and cyclization tandem reaction to form the E-ring bridge. This approach was demonstrated successfully with the aldehyde to provide the foundation for development of the reactions involving the imines.

A set of OSW-1 analogs with the E-ring modifications are being synthesized through the conventional OSW-1 total synthesis route to provide validation for the proposed two-component approach. The analogs were assembled through *N*-glycosylation reaction of a steroidal amine moiety containing the side chain, and the OSW-1 disaccharide moiety. The Schmidt glycosylation condition failed to produce any glycosylated product. Through screening of many glycosylation methodologies, the Fukuyama Mitsunobu reaction with mild condition yielded the desired *N*-linked glycosylated product. Moving forward, this glycosylated product will need to be deprotected to remove all the protecting groups on the disaccharide moiety, and then cyclized to form the E-ring.

Beside the main projects involving the natural product OSW-1 described above, side projects focused on the development of potential therapeutic applications were carried out with quantitative Single-Cell Mass Spectrometry (qSCMS). Stable isotopically-labeled anti-cancer drugs cisplatin and gemcitabine were synthesized. These compounds will be used as internal standards for the quantification of these drugs in isolated cells from patients who are undergoing chemotherapy treatments. This will allow for a personalized treatment approach that maximizes the drug's efficacy while minimizing the toxicity for the patients.

Through a collaboration project, the first selective inhibitor for retinaldehyde dehydrogenase (RALDH) enzymes, α,α-dichloro-all-*trans*-retinone (DAR), were designed and synthesized for potential development of therapeutic treatments for myopia. DAR was

evaluated through multiple biological assays to determine that it acts as a selective irreversible inhibitor for RALDHs. Even though DAR was successfully synthesized, its synthesis suffered from low yield due to the high reactivity of the reagents. Furthermore, the DAR compound is quite labile due to the photoisomerization ability of the highly conjugated moiety of DAR. Therefore, DAR serves as a great starting point but more development to increase the synthetic yield and the stability of the compound is desired for the development of therapeutic treatments for myopia.

Appendix

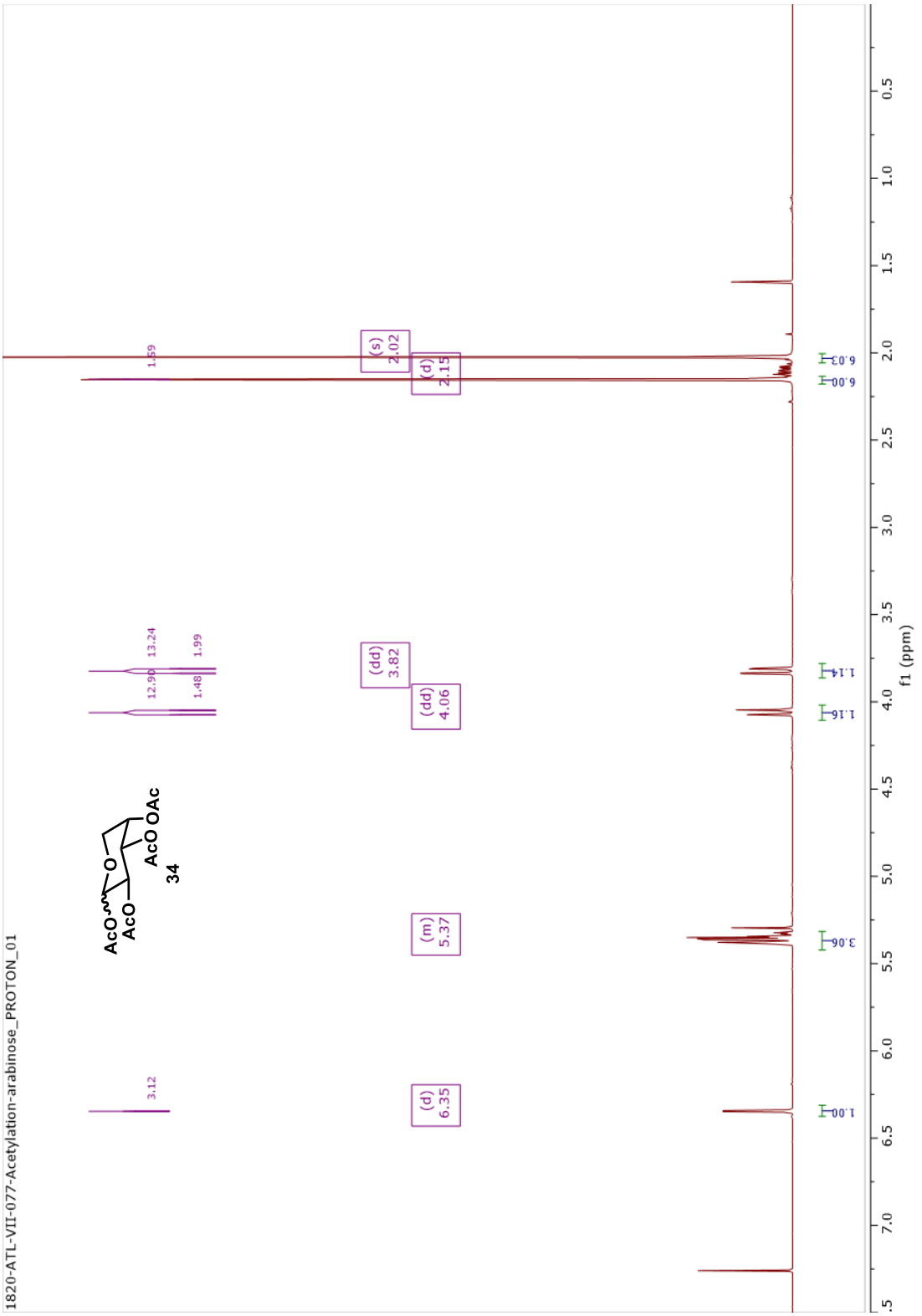
1820-ATL-VII-077-Acetylation-arabinose_PROTON_01
AcO
AcO
O
AcO
OAc
34
3.12
12.90
13.24
1.48
1.99
1.59
(d)
6.35
(m)
5.37
(dd)
4.06
(dd)
3.82
(d)
2.15
(s)
2.02
1.00
3.06
1.16
1.14
6.00
6.03
f1 (ppm)

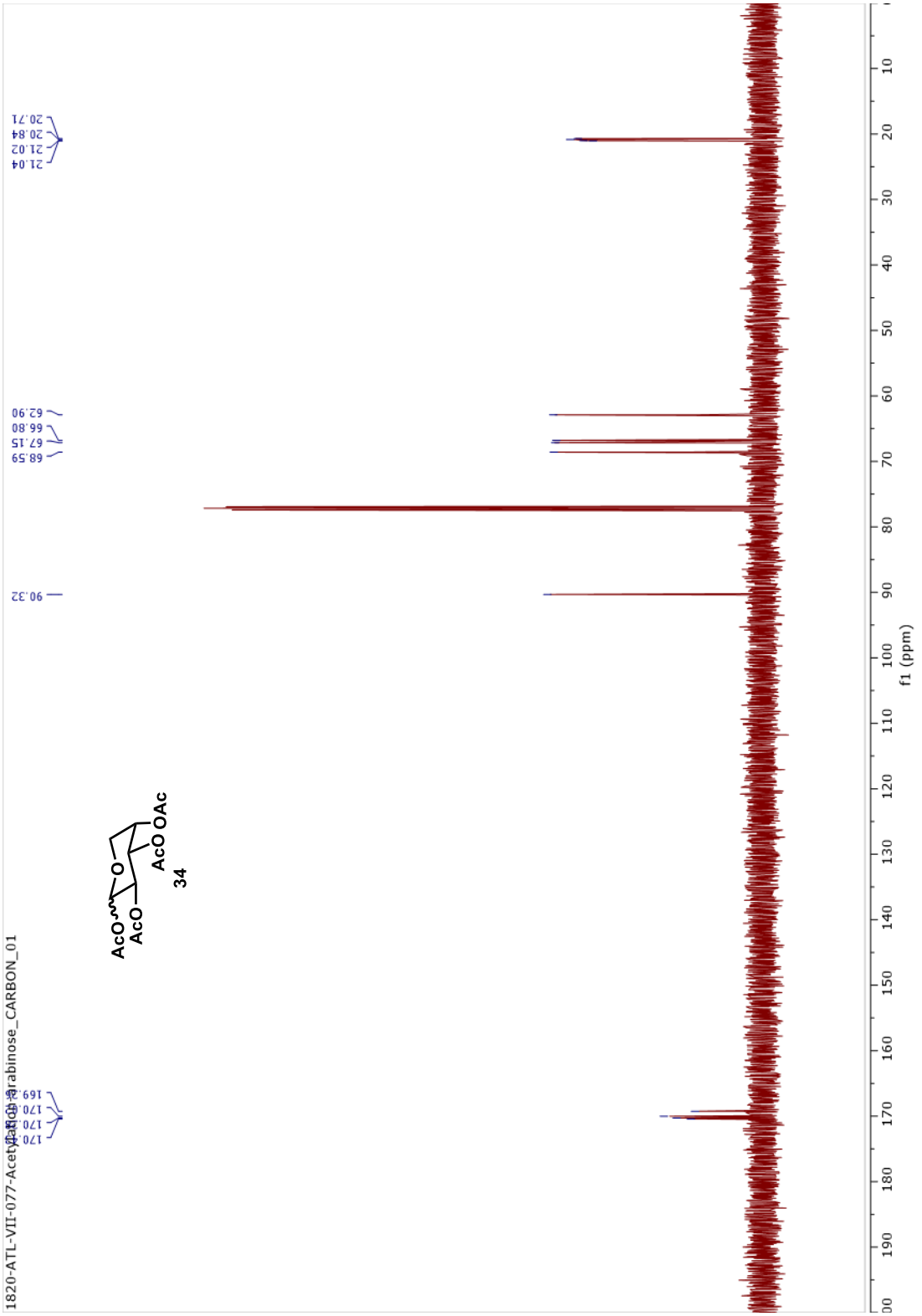
1820-ATL-VII-077-Acetylated-Arabinose_CARBON_01
AcO
AcO
O
AcO
OAc
34
20.71
20.84
21.02
21.04
62.90
66.80
67.15
68.59
90.32
f1 (ppm)

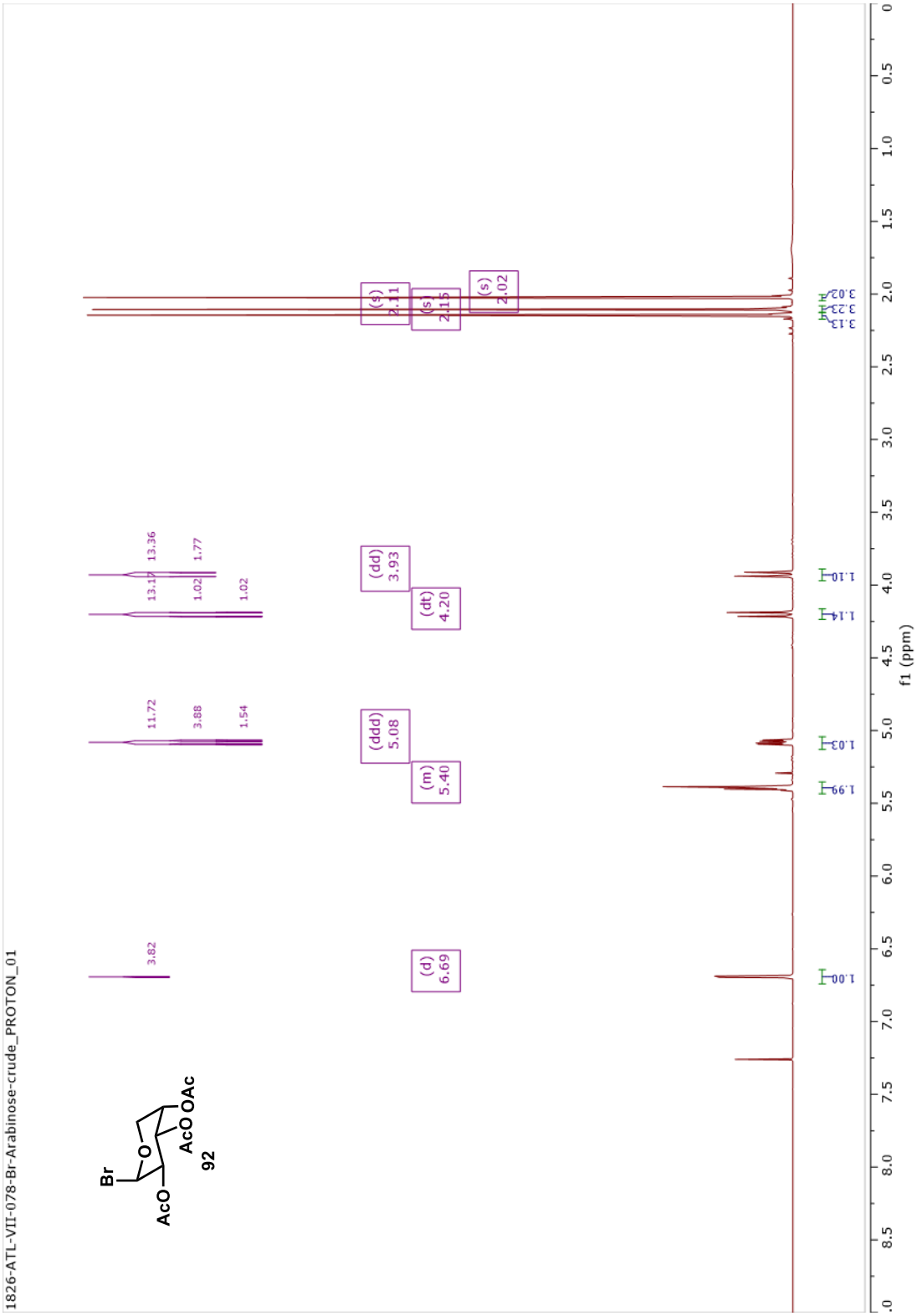
1826-ATL-VII-078-Br-Arabinose-crude_PROTON_01
Br
AcO
O
AcO
OAc
92
3.82
11.72
3.88
1.54
13.36
13.19
1.77
1.02
1.02
(d)
6.69
(m)
5.40
(ddd)
5.08
(dt)
4.20
(dd)
3.93
(s)
2.11
(s)
2.15
(s)
2.02
1.00
1.99
1.03
1.14
1.10
3.02
3.23
3.13
f1 (ppm)

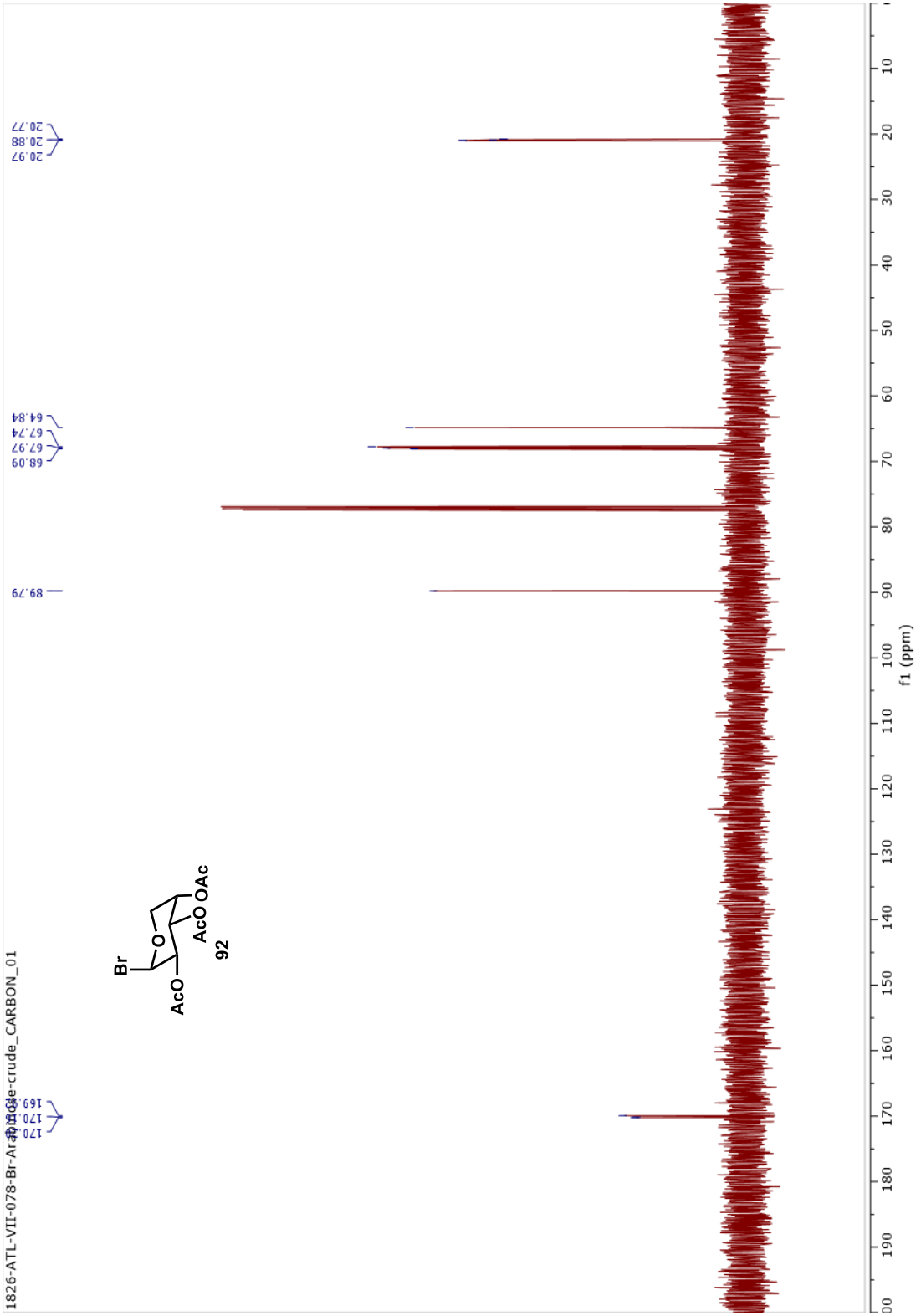
1826-ATL-VII-078-Br-Ara-Diole-crude_CARBON_01
20.77
20.88
20.97
64.84
67.74
67.97
68.09
89.79
169.83
170.11
170.46
Br
AcO
O
AcO
OAc
92
f1 (ppm)

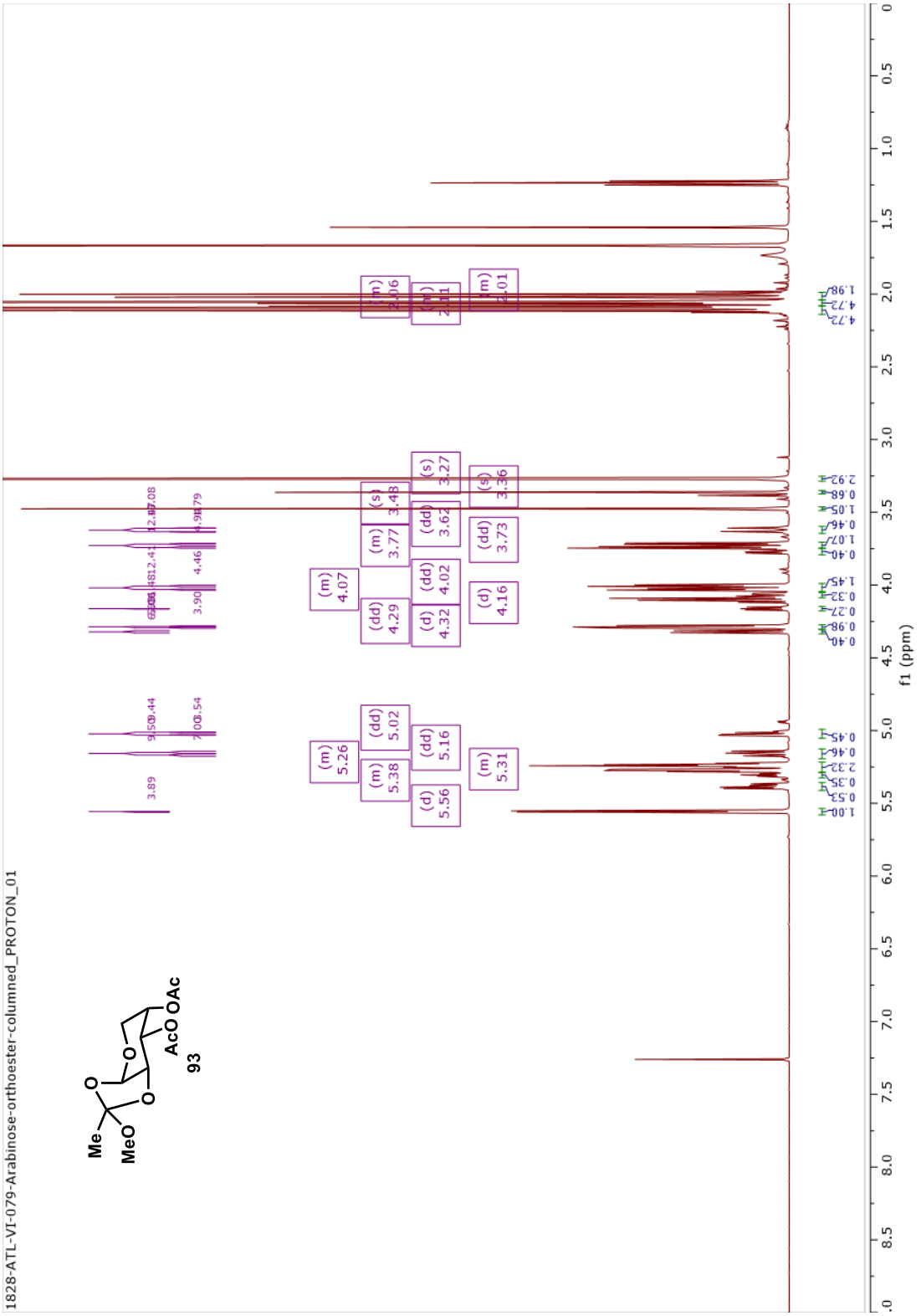
1828-ATL-VI-079-Arabinose-orthoester-columned_PROTON_01
Me
MeO
O
O
O
AcO OAc
93
f1 (ppm)

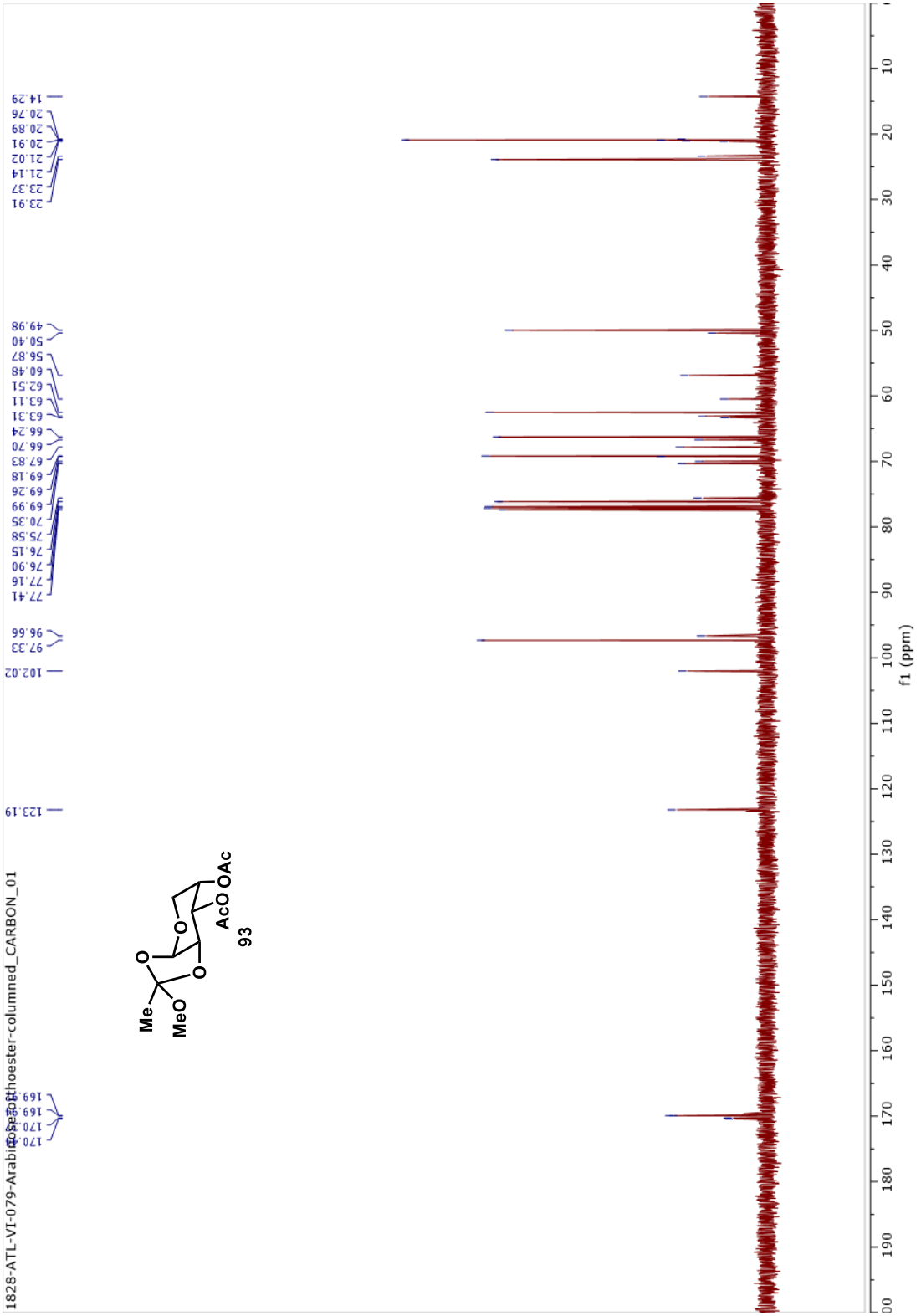
1828-ATL-VI-079-Arabinose-diethoester-columned_CARBON_01
14.29
20.76
20.89
20.91
21.02
21.14
23.37
23.91
49.98
50.40
56.87
60.48
62.51
63.11
63.31
66.24
66.70
67.83
69.18
69.26
69.99
70.35
75.58
76.15
76.90
77.16
77.41
96.66
97.33
102.02
123.19
169.11
169.41
170.03
170.18
Me
MeO
O
O
O
AcO
OAc
93
f1 (ppm)

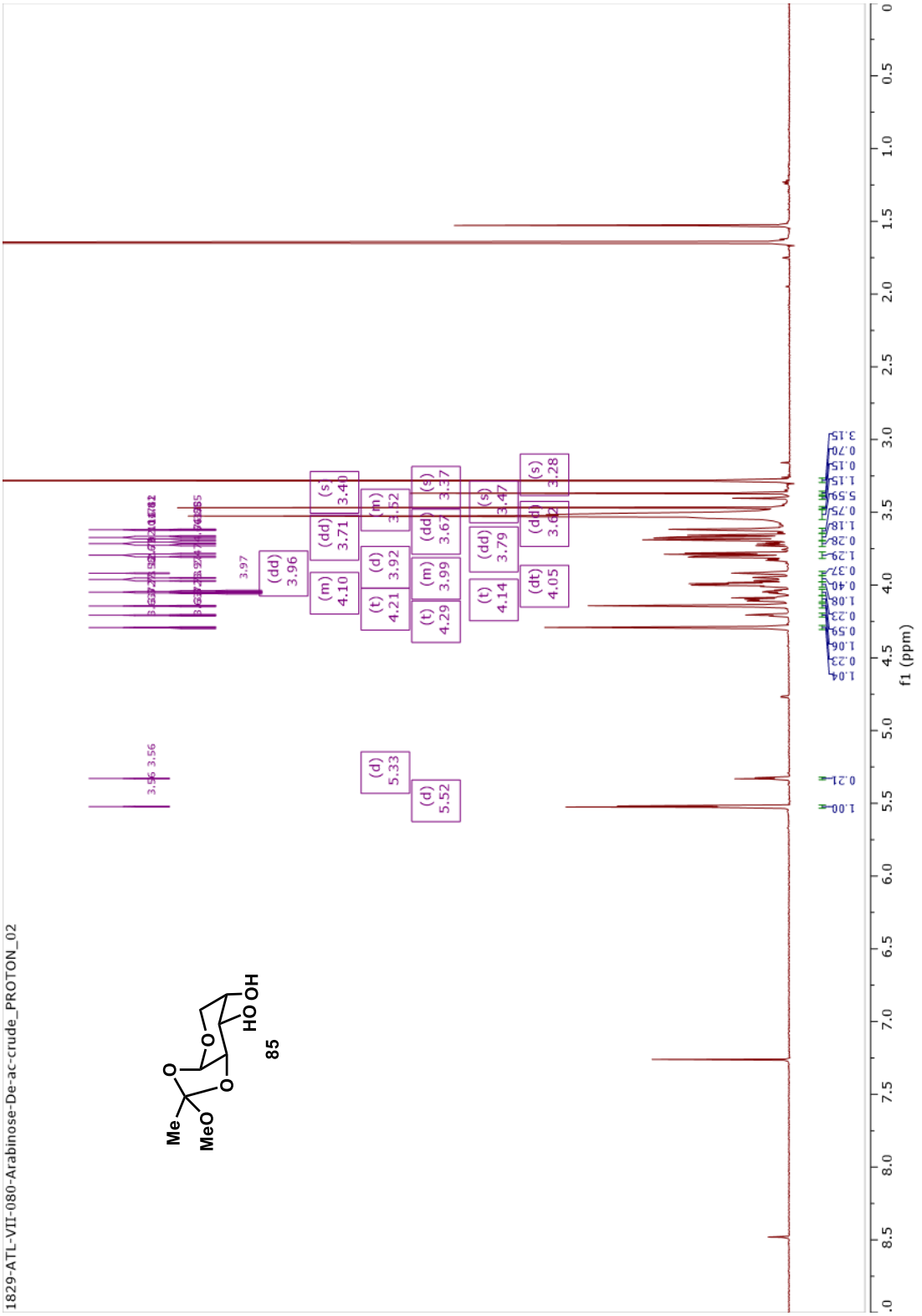
1829-ATL-VII-080-Arabinose-De-ac-crude_PROTON_02
HO OH
O
O
O
Me
MeO
85
3.56
3.97
(dd) 3.96
(m) 4.10
(t) 4.21
(d) 5.33
(d) 5.52
(t) 4.29
(m) 3.99
(dd) 3.71
(d) 3.92
(dd) 3.67
(s) 3.40
(m) 3.52
(s) 3.37
(t) 4.14
(dd) 3.79
(s) 3.47
(dt) 4.05
(dd) 3.62
(s) 3.28
f1 (ppm)

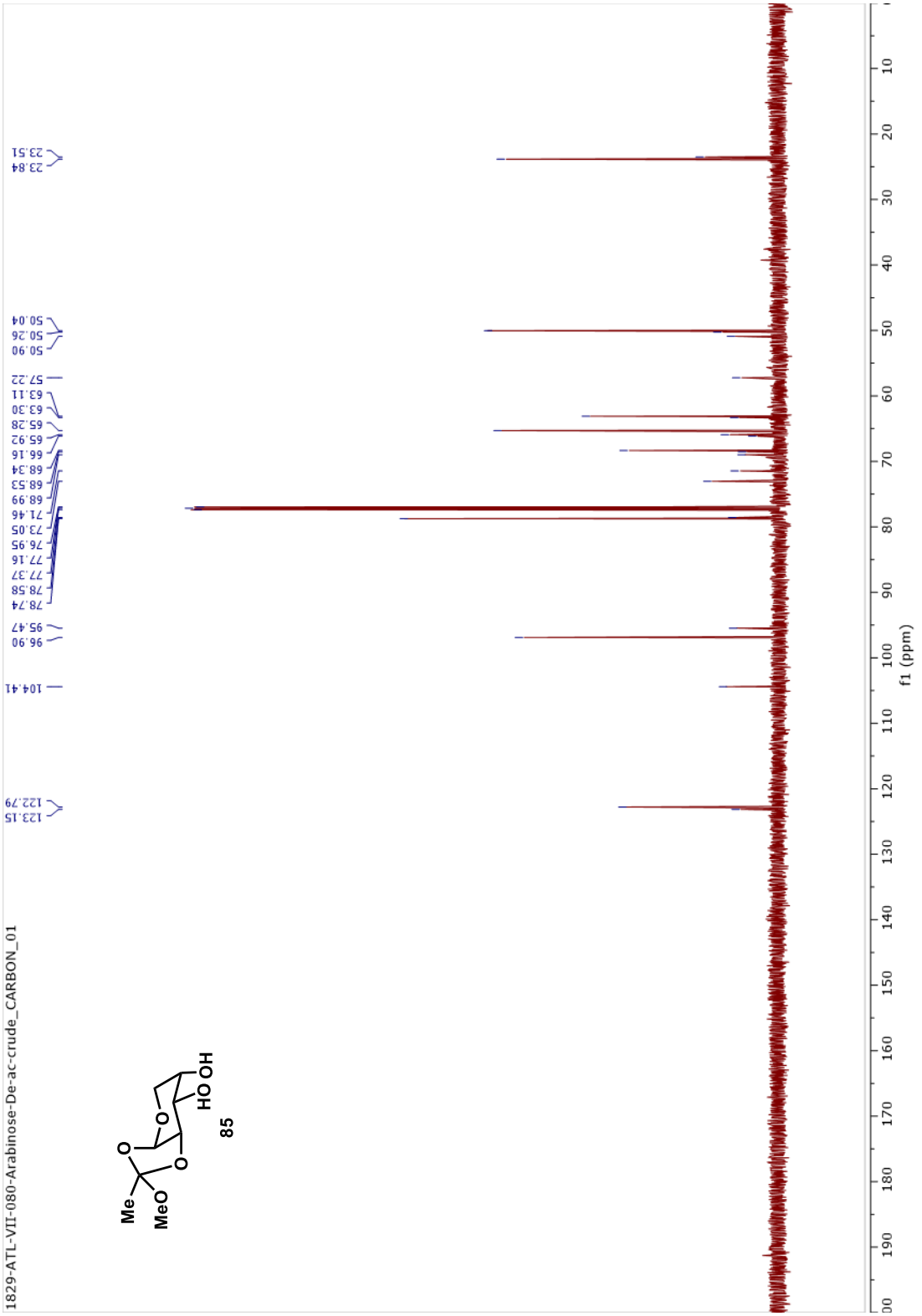
1829-ATL-VII-080-Arabinose-De-ac-crude_CARBON_01
23.51
23.84
50.04
50.26
50.90
57.22
63.11
63.30
65.28
65.92
66.16
68.34
68.53
68.99
71.46
73.05
76.95
77.16
77.37
78.58
78.74
95.47
96.90
104.41
122.79
123.15
Me
MeO
O
O
O
HO OH
85
f1 (ppm)

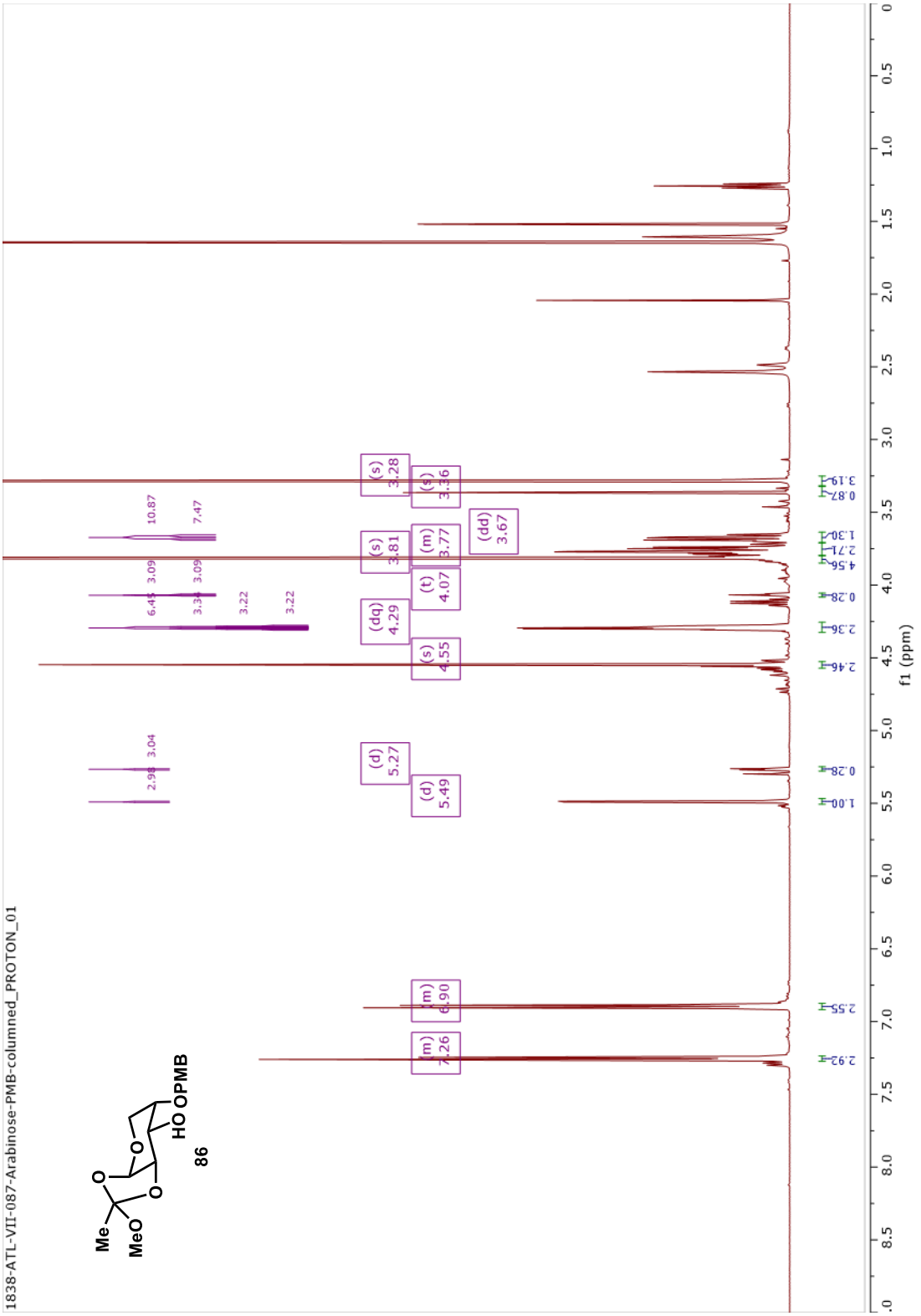
1838-ATL-VII-087-Arabinose-PMB-columned_PROTON_01
Me
MeO
HO
OPMB
86
f1 (ppm)

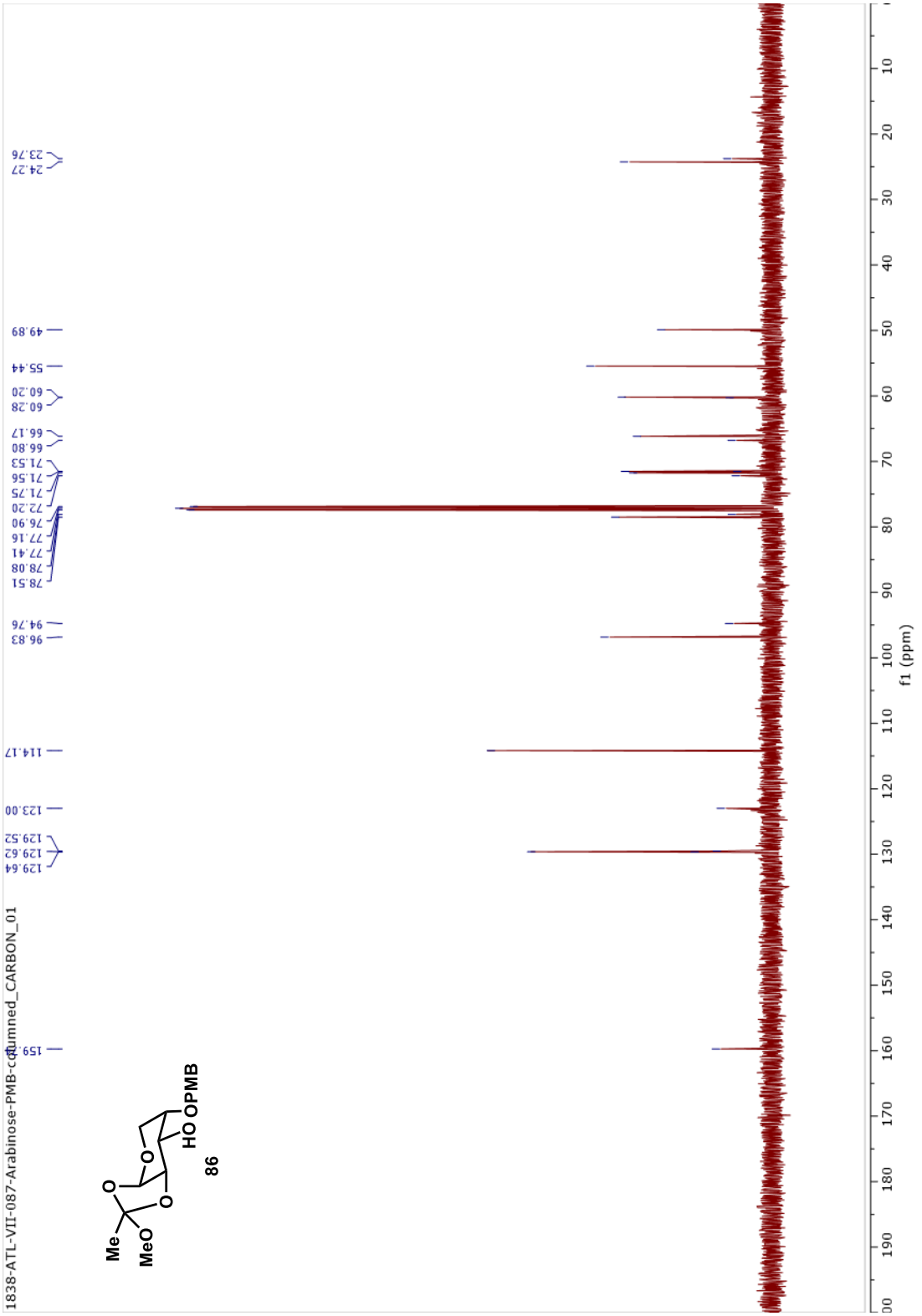
1838-ATL-VII-087-Arabinose-PMB-co...umned_CARBON_01
159.77
129.64
129.62
129.52
123.00
114.17
96.83
94.76
78.51
78.08
77.41
77.16
76.90
72.20
71.75
71.56
71.53
66.80
66.17
60.28
60.20
55.44
49.89
24.27
23.76
Me
MeO
HO
OPMB
86
f1 (ppm)

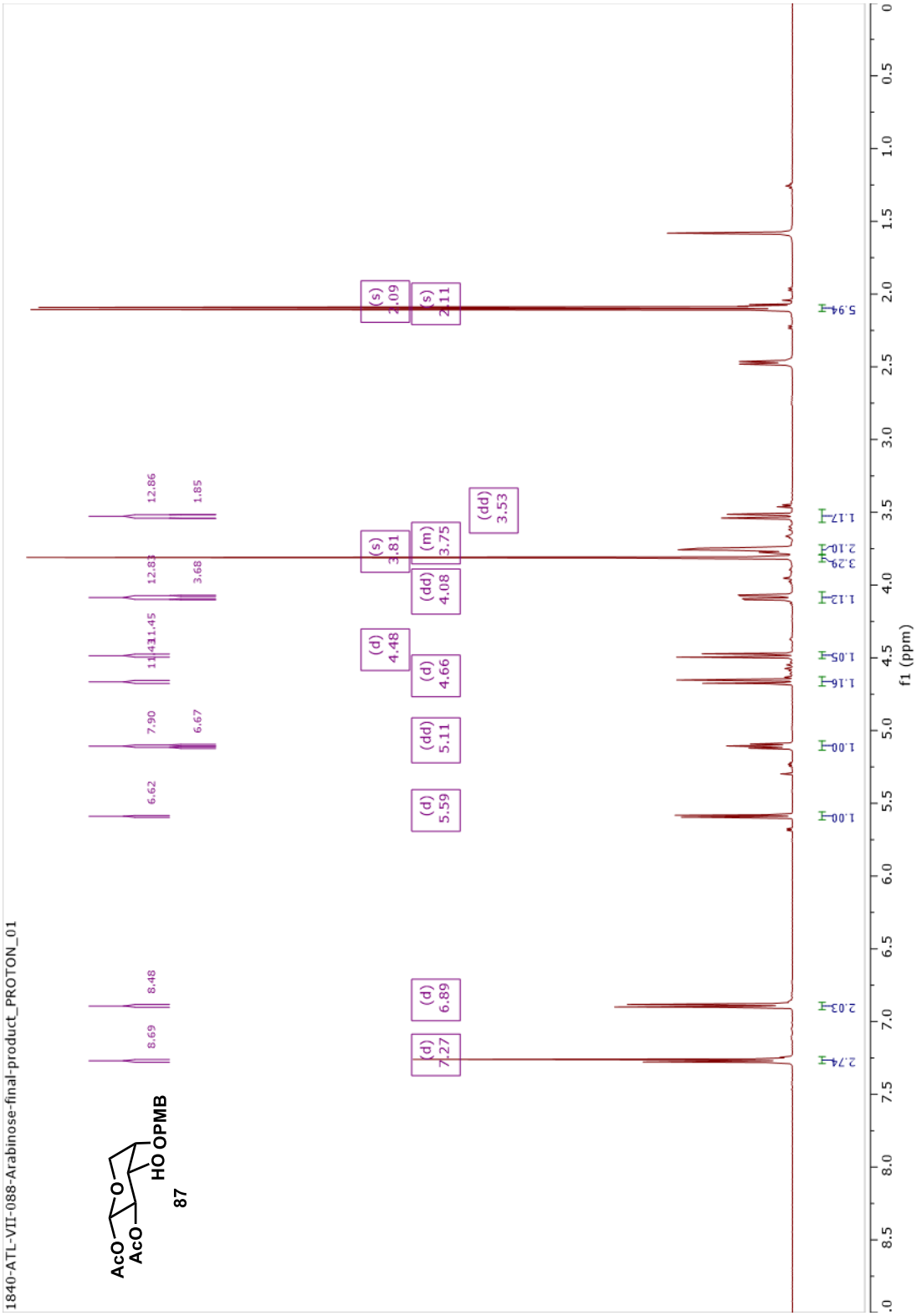
1840-ATL-VII-088-Arabinose-final-product_PROTON_01
AcO
AcO
O
HO
OPMB
87
8.69
8.48
7.90
6.67
6.62
12.86
1.85
12.83
3.68
11.45
(d) 7.27
(d) 6.89
(d) 5.59
(dd) 5.11
(d) 4.66
(d) 4.48
(dd) 4.08
(m) 3.75
(s) 3.81
(dd) 3.53
(s) 2.09
(s) 2.11
5.94
2.74
2.03
1.00
1.00
1.00
1.16
1.05
1.12
3.29
2.10
1.17
f1 (ppm)

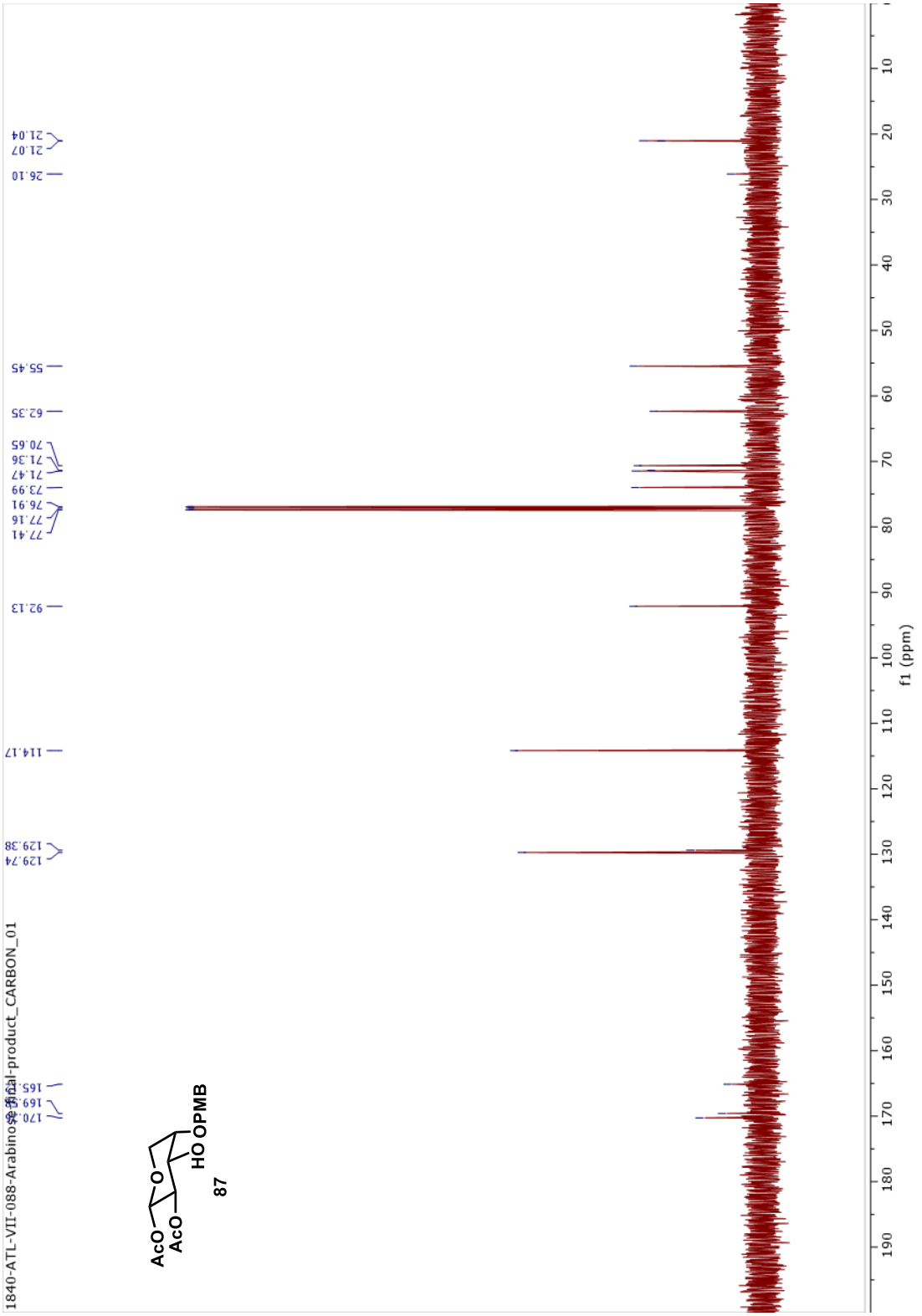
1840-ATL-VII-088-Arabinose final-product_CARBON_01
21.04
21.07
26.10
55.45
62.35
70.65
71.36
71.47
73.99
76.91
77.16
77.41
92.13
114.17
129.38
129.74
165.15
169.58
170.25
AcO
AcO
O
HO
OPMB
87
f1 (ppm)

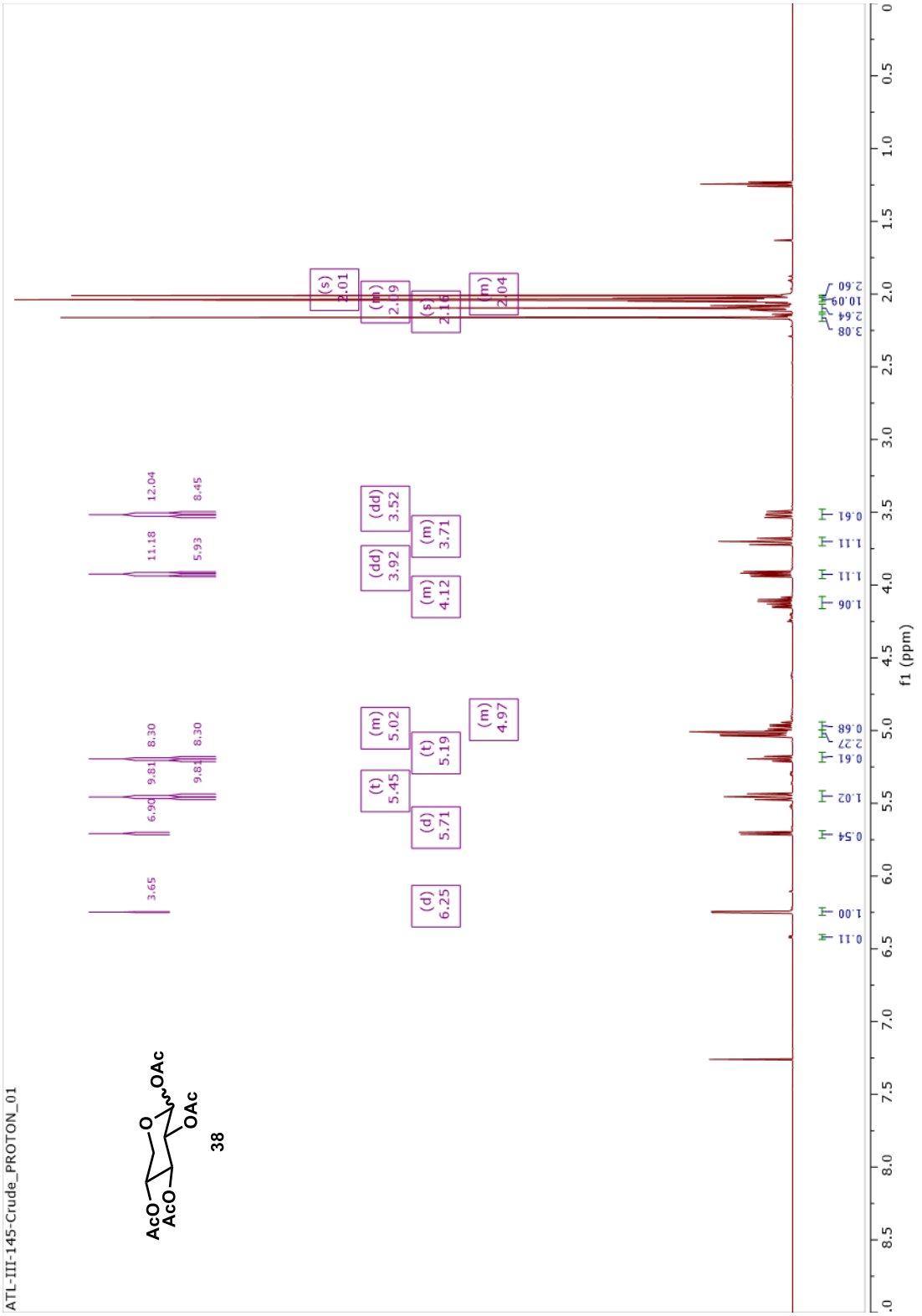
ATL-III-145-Crude_PROTON_01
AcO
AcO
OAc
OAc
O
38
f1 (ppm)

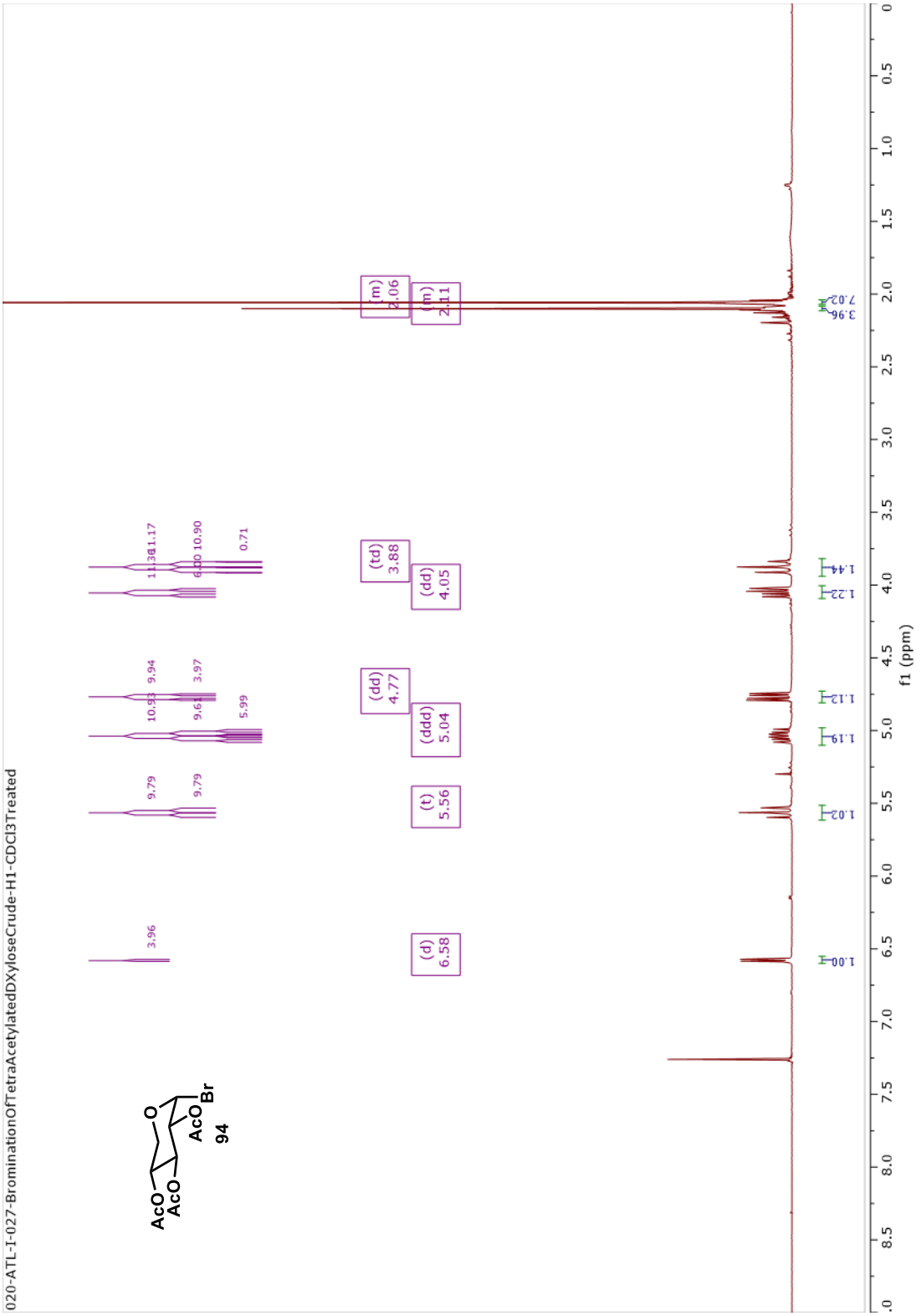
020-ATL-I-027-BrominationOfTetraAcetylatedDXyloseCrude-H1-CDCl3Treated
AcO
AcO
O
AcO
Br
94
(d)
6.58
(t)
5.56
(ddd)
5.04
(dd)
4.77
(td)
3.88
(dd)
4.05
(m)
2.11
(m)
2.06
f1 (ppm)

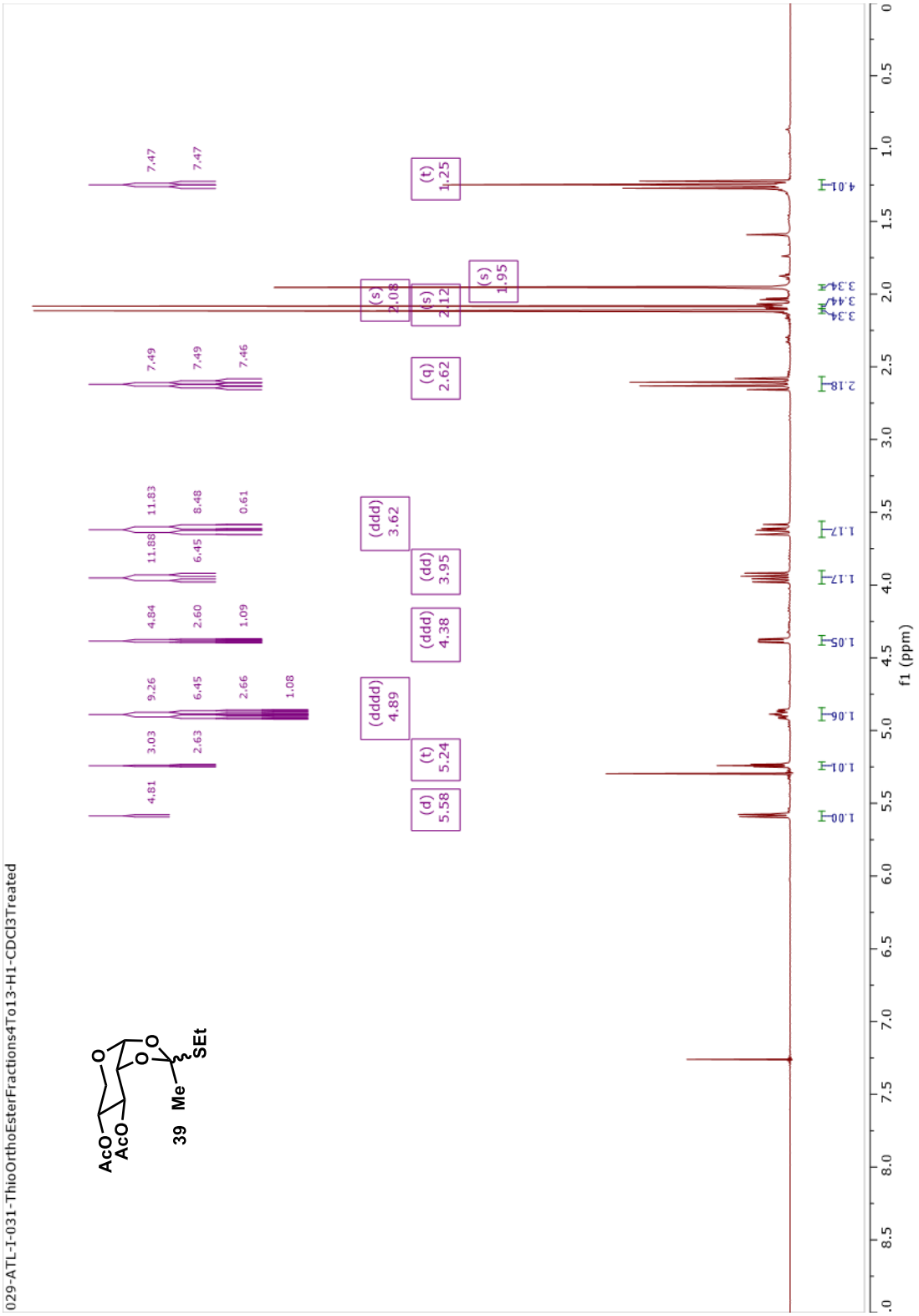
029-ATL-I-031-ThioOrthoEsterFractions4To13-H1-CDCl3Treated
AcO
AcO
39 Me
SEt
f1 (ppm)

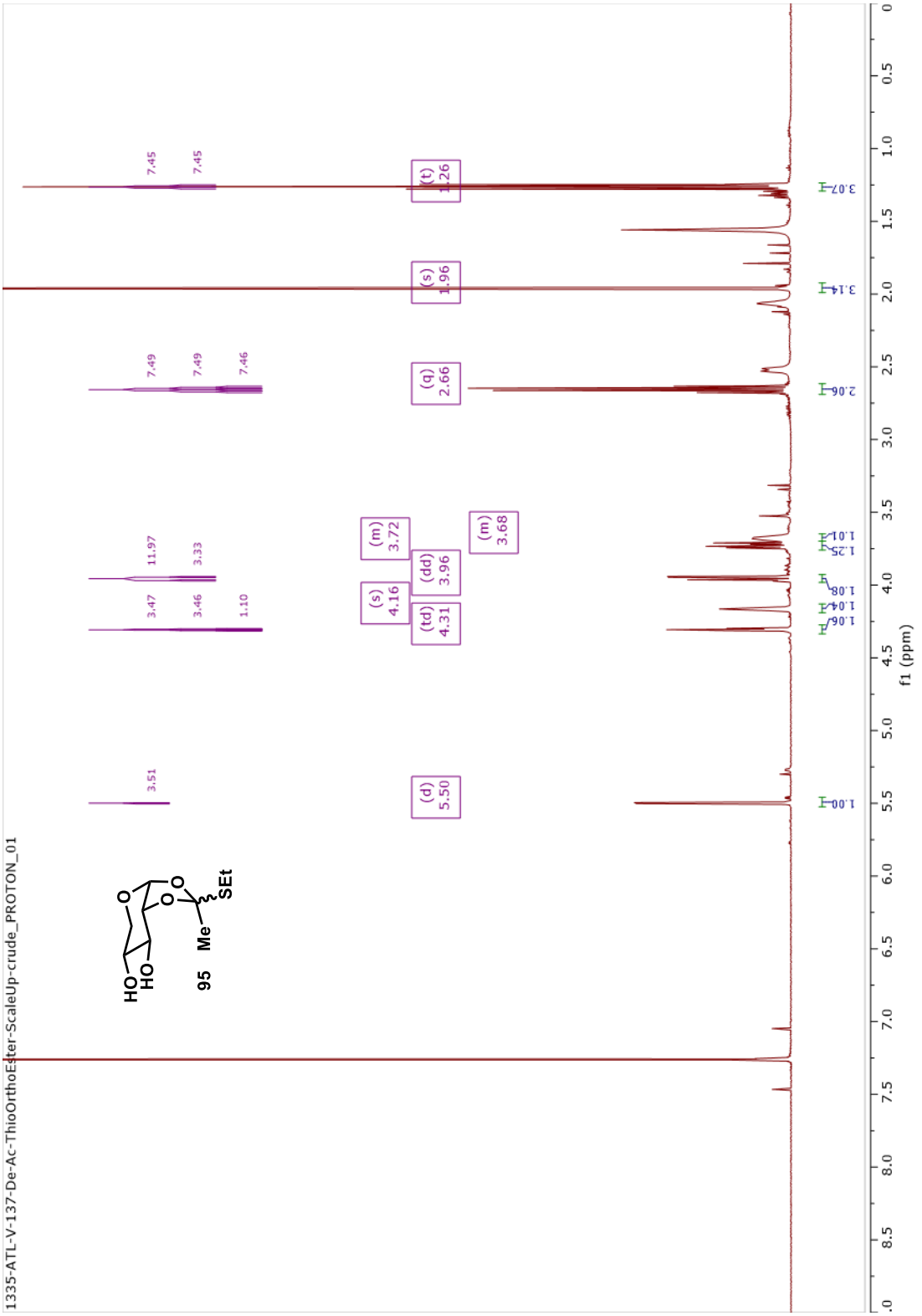
1335-ATL-V-137-De-Ac-ThioOrthoEster-ScaleUp-crude_PROTON_01
HO
HO
O
O
O
95
Me
SEt
(d) 5.50
(td) 4.31
(s) 4.16
(m) 3.72
(dd) 3.96
(m) 3.68
(q) 2.66
(s) 1.96
(t) 1.26
3.51
3.47
3.46
11.97
3.33
1.10
7.49
7.49
7.46
7.45
7.45
1.00
1.06
1.04
1.08
1.25
1.01
2.06
3.14
3.07
f1 (ppm)

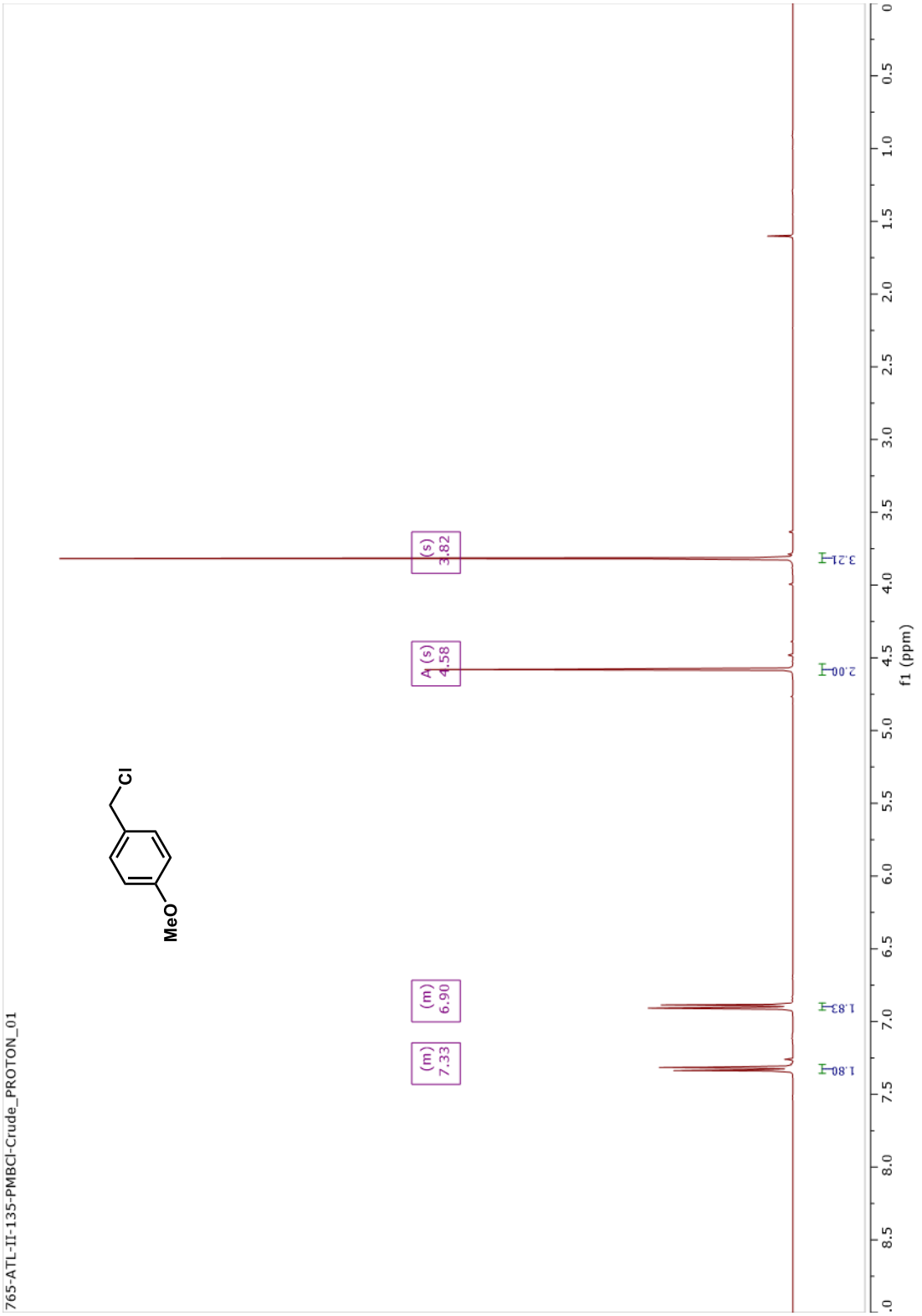
765-ATL-II-135-PMBCl-Crude_PROTON_01
Cl
MeO
(m) 7.33
(m) 6.90
A (s) 4.58
(s) 3.82
1.80
1.83
2.00
3.21
f1 (ppm)

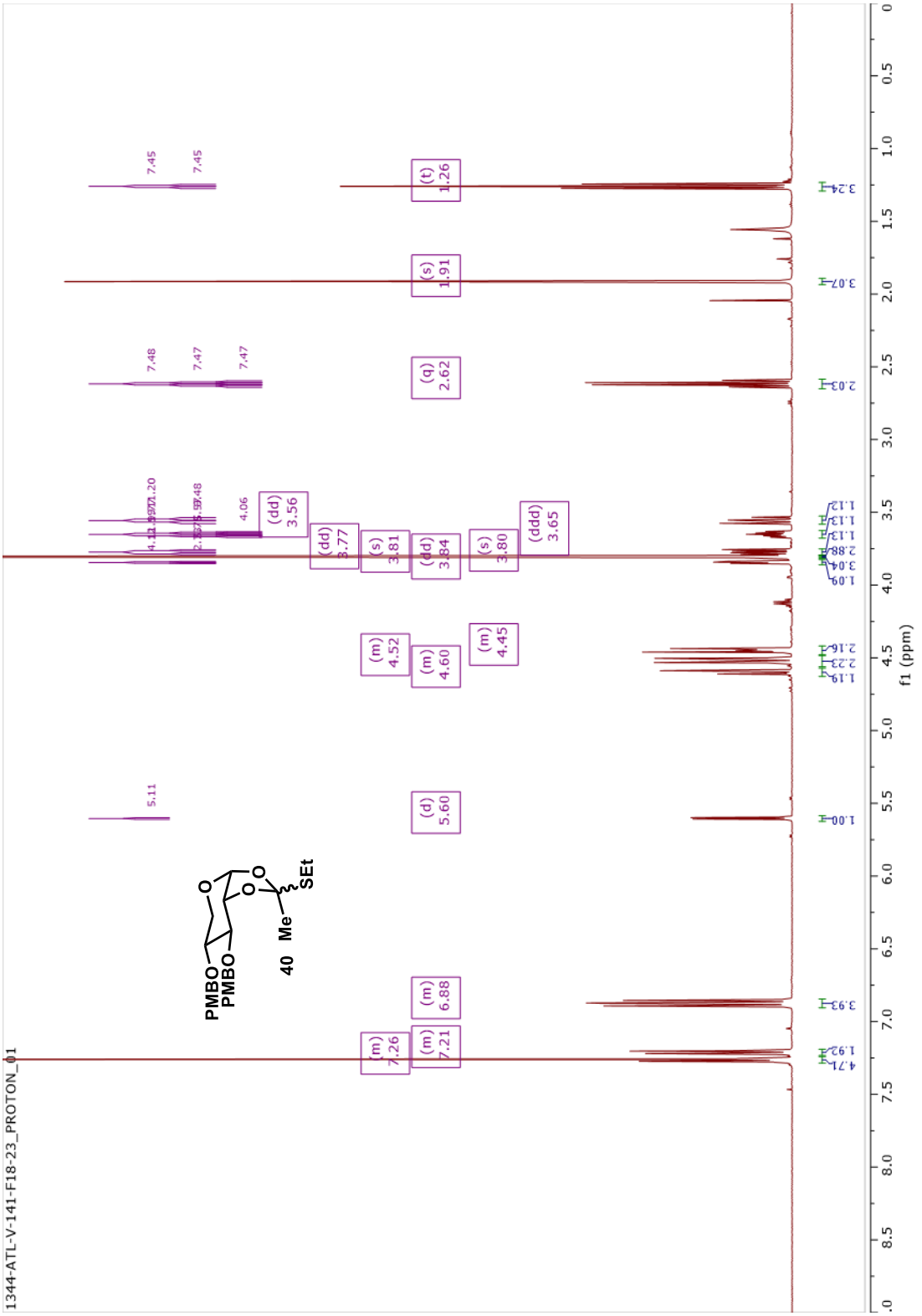
1344-ATL-V-141-F18-23_PROTON_01
PMBO
PMBO
40 Me
SEt
f1 (ppm)

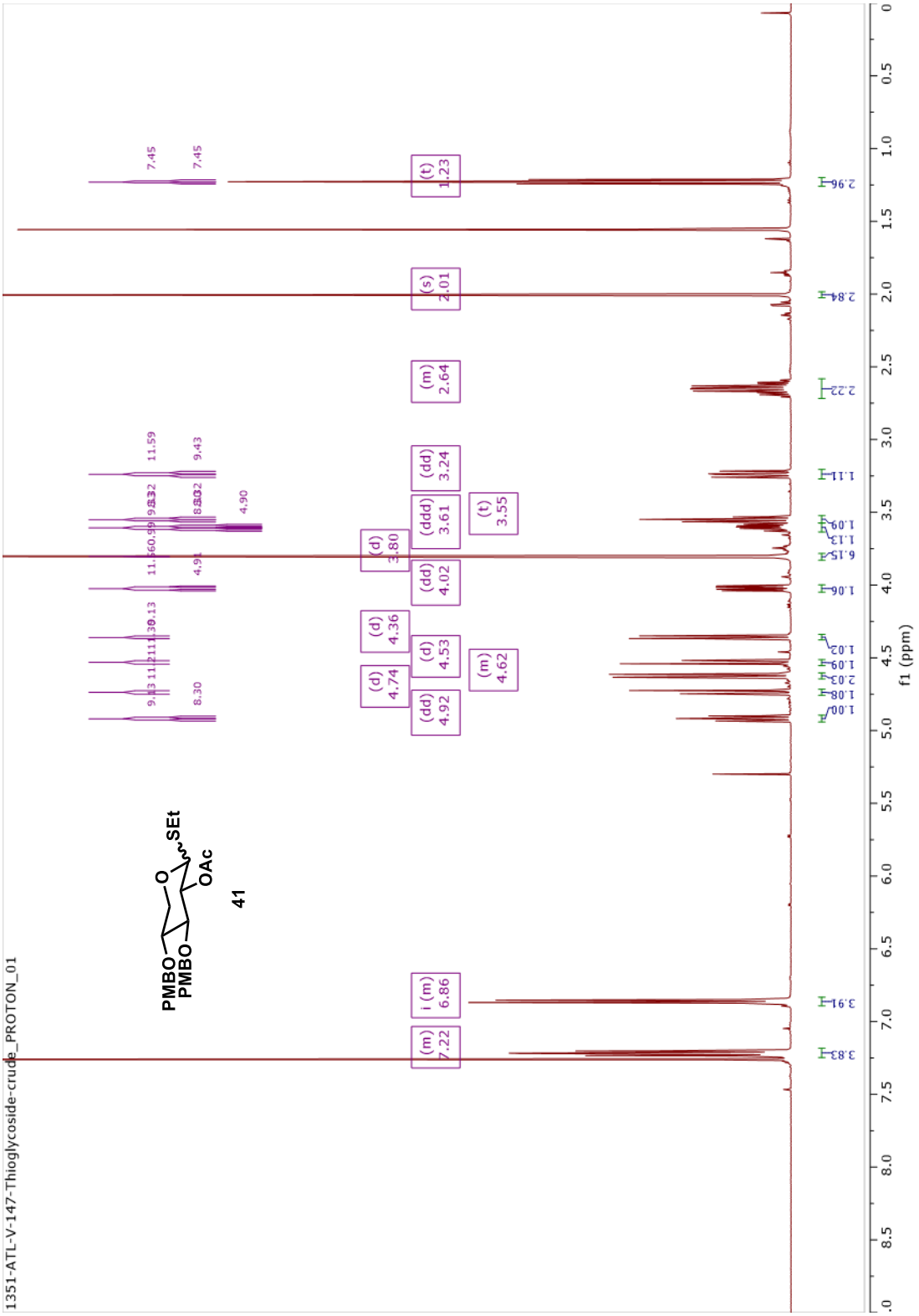
1351-ATL-V-147-Thioglycoside-crude_PROTON_01
PMBO
PMBO
SEt
OAc
41
f1 (ppm)

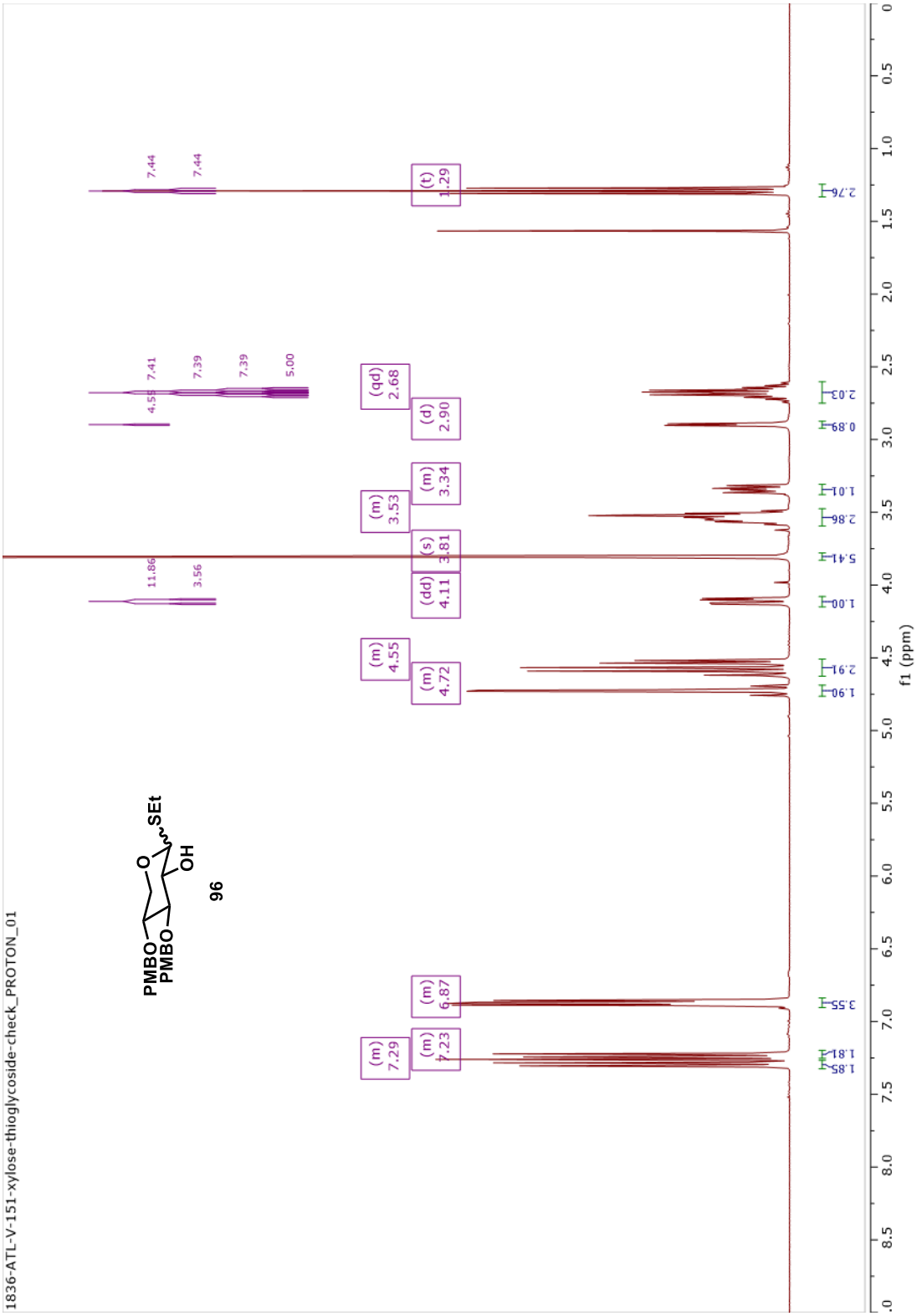
1836-ATL-V-151-xylose-thioglycoside-check_PROTON_01
PMBO
PMBO
O
SEt
OH
96
11.86
3.56
7.44
7.44
4.58
7.41
7.39
7.39
5.00
(m) 7.29
(m) 7.23
(m) 6.87
(m) 4.72
(m) 4.55
(dd) 4.11
(s) 3.81
(m) 3.53
(m) 3.34
(qd) 2.68
(d) 2.90
(t) 1.29
2.76
2.03
0.89
1.01
2.86
5.41
1.00
2.91
1.90
3.55
1.81
1.85
f1 (ppm)

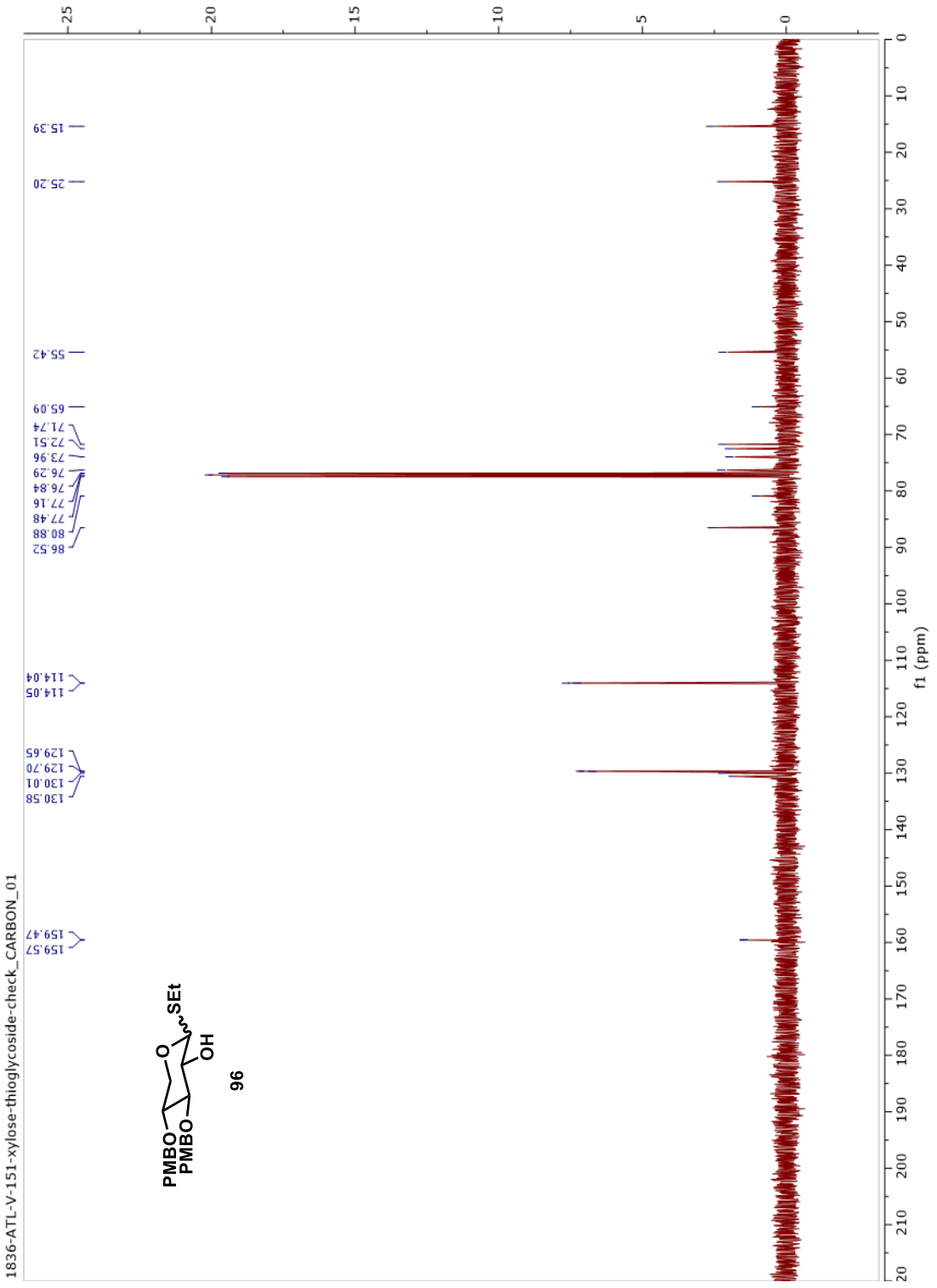
1836-ATL-V-151-xylose-thioglycoside-check_CARBON_01
159.57
159.47
130.58
130.01
129.70
129.65
114.05
114.04
86.52
80.88
77.48
77.16
76.84
76.29
73.96
72.51
71.74
65.09
55.42
25.20
15.39
PMBO
PMBO
O
SEt
OH
96
f1 (ppm)

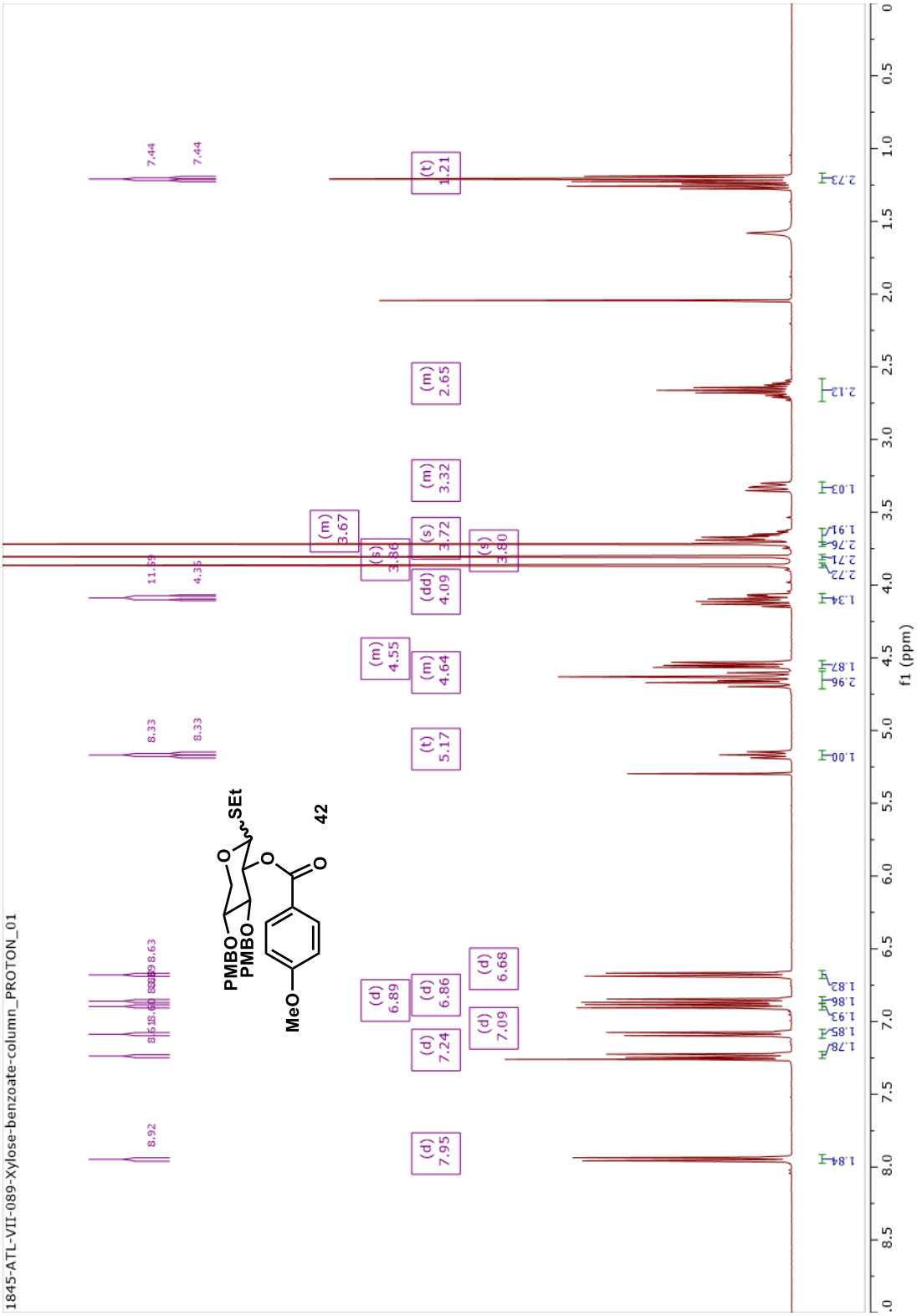
1845-ATL-VII-089-Xylose-benzoate-column_PROTON_01
PMBO
PMBO
SEt
MeO
42
f1 (ppm)

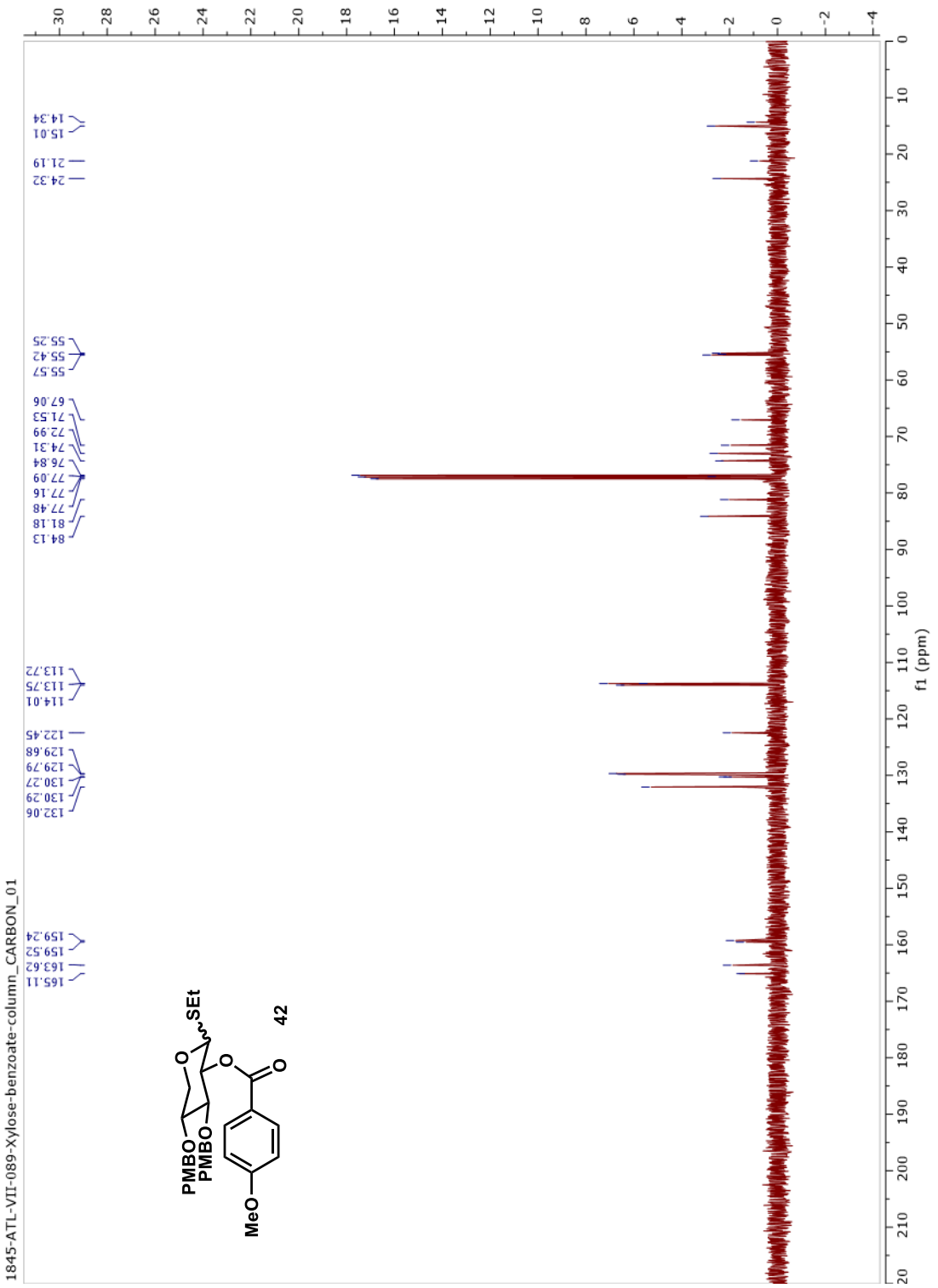
1845-ATL-VII-089-Xylose-benzoate-column_CARBON_01
f1 (ppm)
PMBO
PMBO
SEt
MeO
42

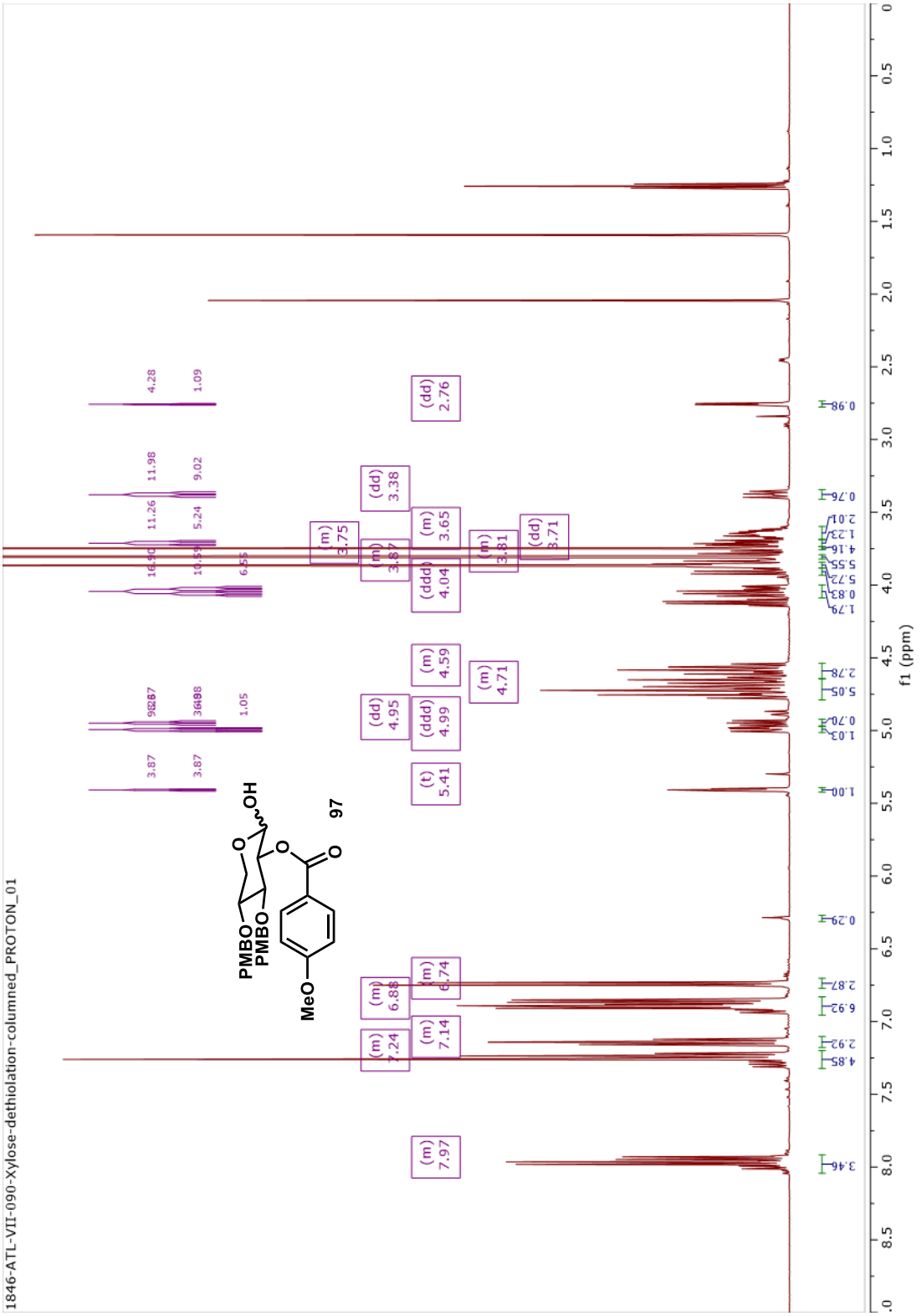
1846-ATL-VII-090-Xylose-dethiolation-columned_PROTON_01
PMBO
PMBO
OH
O
O
O
MeO
97
(m) 7.97
(m) 7.24
(m) 7.14
(m) 6.88
(m) 6.74
(t) 5.41
(dd) 4.95
(ddd) 4.99
(m) 4.59
(m) 4.71
(ddd) 4.04
(m) 3.87
(m) 3.75
(m) 3.81
(m) 3.65
(dd) 3.71
(dd) 3.38
(dd) 2.76
f1 (ppm)

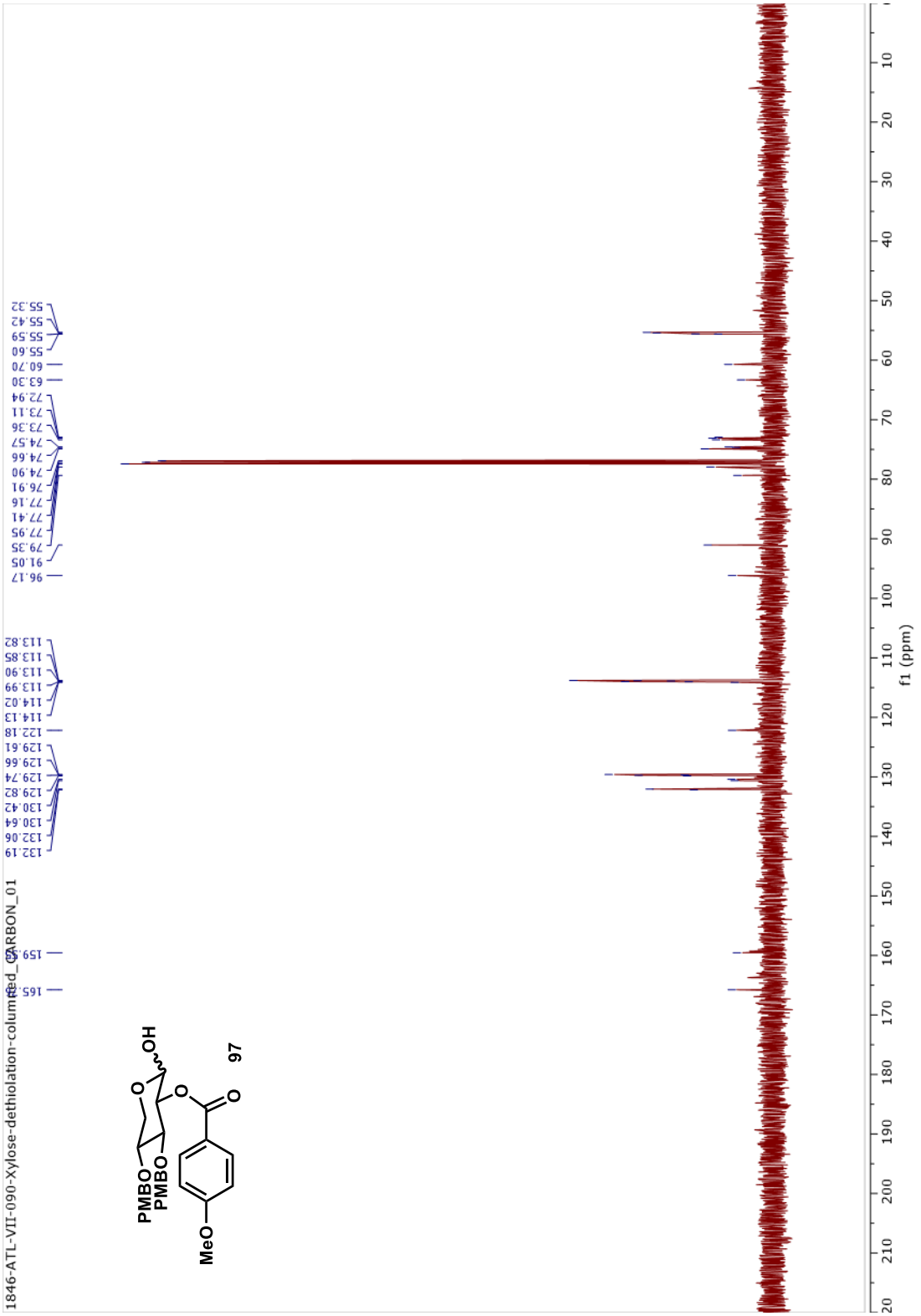
1846-ATL-VII-090-Xylose-dethiolation-columned_CARBON_01
165.37
159.47
132.19
132.06
130.64
130.42
129.82
129.74
129.66
129.61
122.18
114.13
114.02
113.99
113.90
113.85
113.82
96.17
91.05
79.35
77.95
77.41
77.16
76.91
74.90
74.66
74.57
73.36
73.11
72.94
63.30
60.70
55.60
55.59
55.42
55.32
PMBO
PMBO
OH
O
O
O
MeO
97
f1 (ppm)

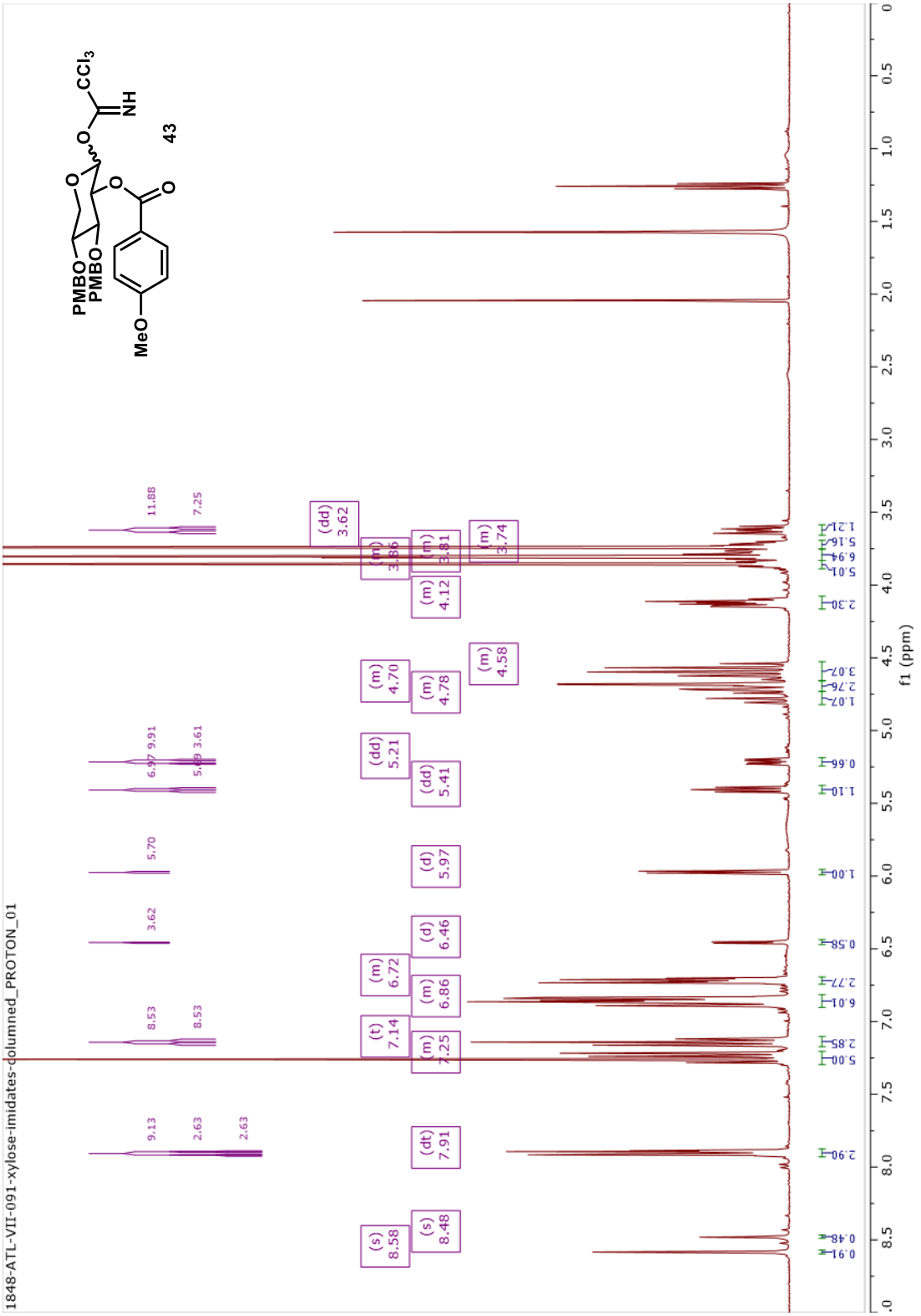
1848-ATL-VII-091-xylose-imidates-columned_PROTON_01
PMBO
PMBO
MeO
CCl3
NH
43
f1 (ppm)

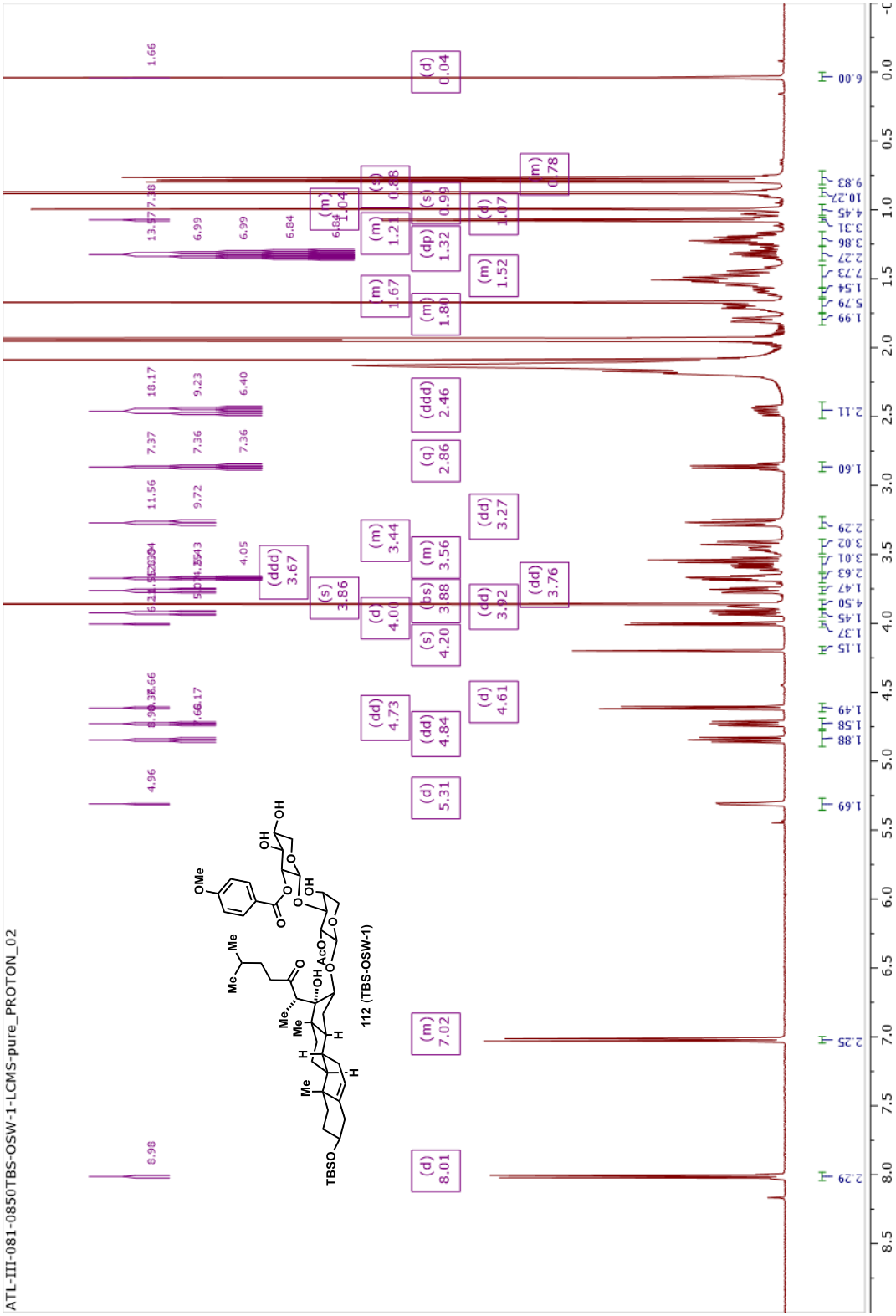
ATL-III-081-0850TBS-OSW-1-LCMS-pure_PROTON_02
112 (TBS-OSW-1)
f1 (ppm)

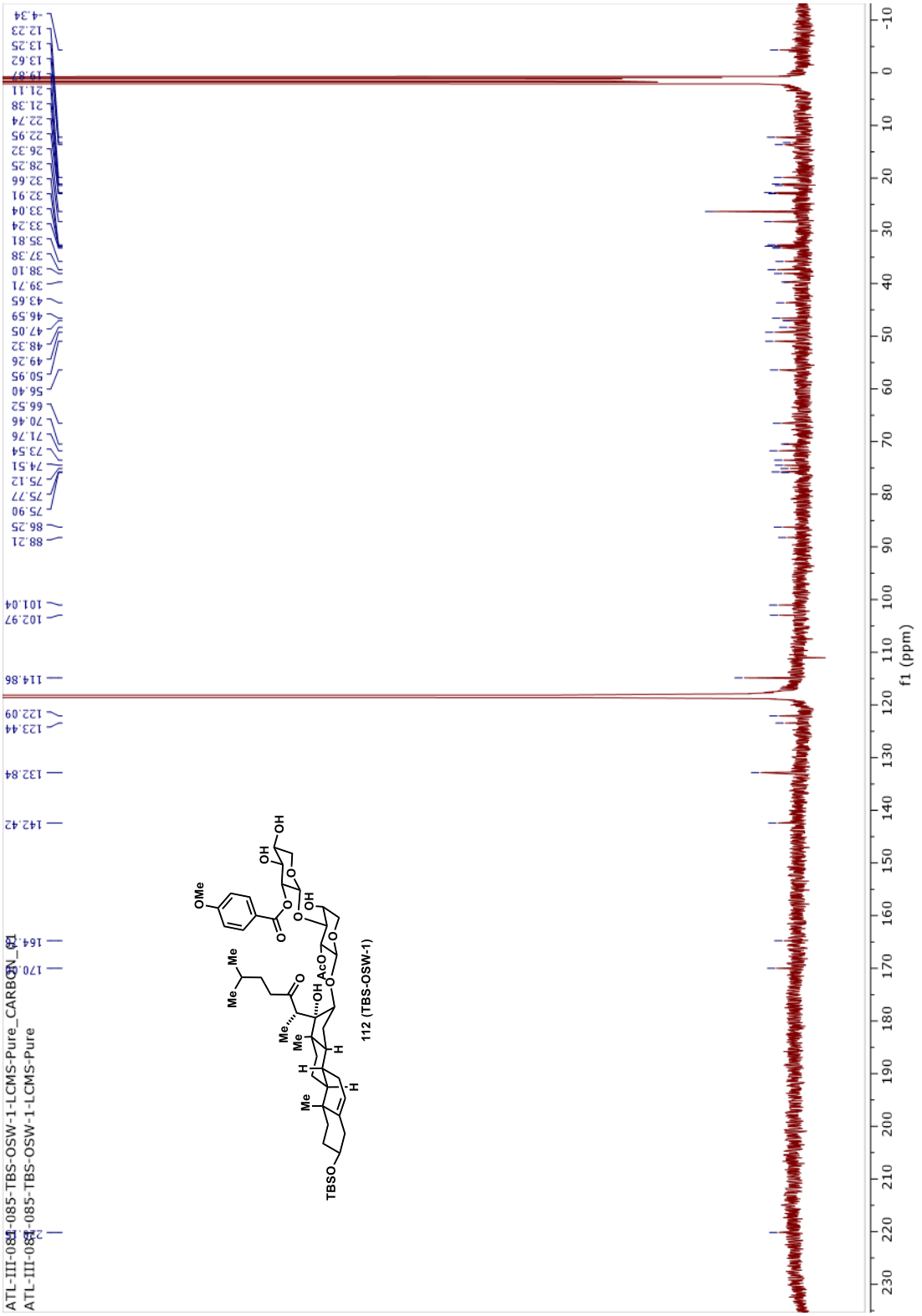
ATL-III-085-TBS-OSW-1-LCMS-Pure_CARBON_01
ATL-III-085-TBS-OSW-1-LCMS-Pure
f1 (ppm)
112 (TBS-OSW-1)

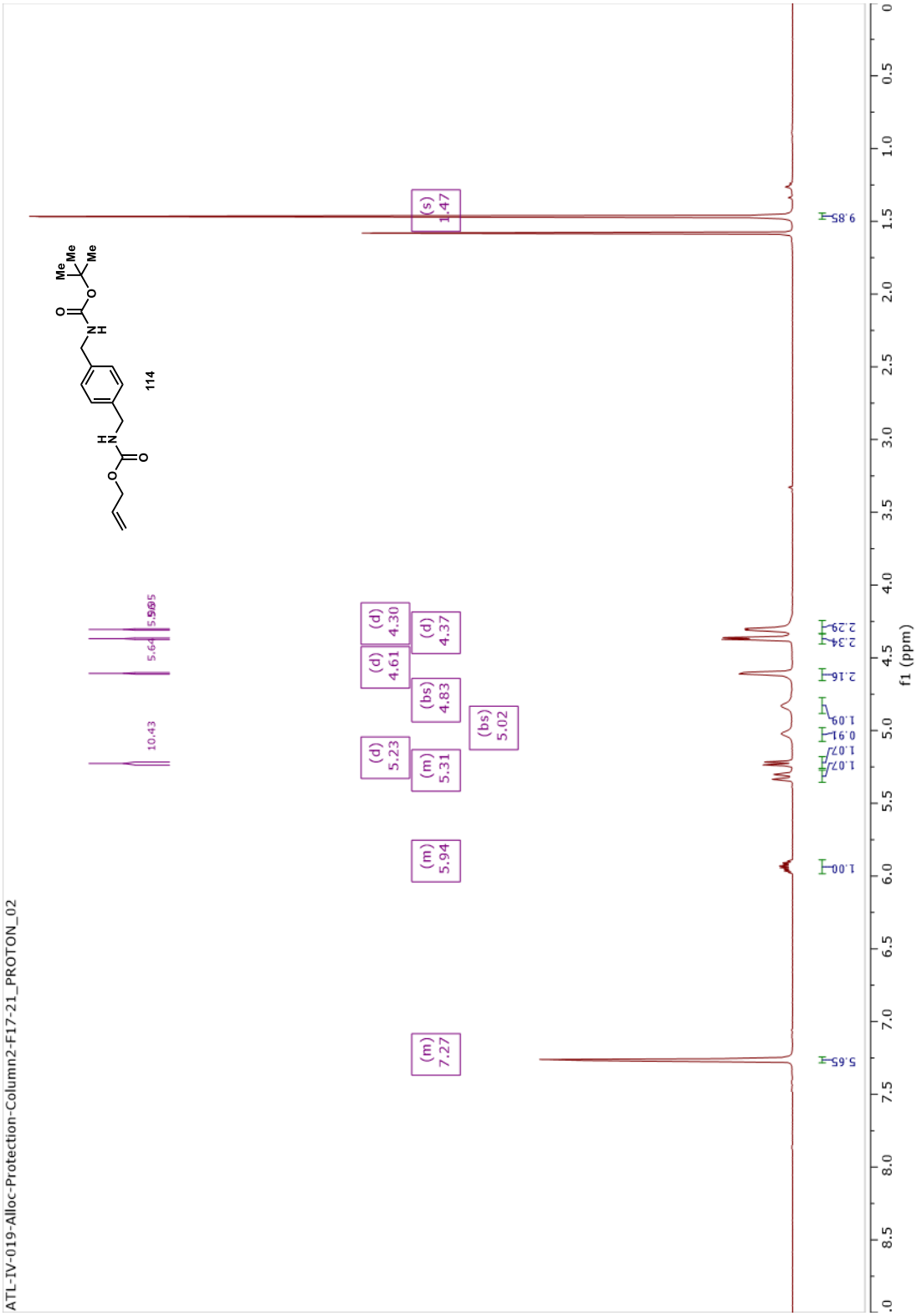
ATL-IV-019-Alloc-Protection-Column2-F17-21_PROTON_02
114
(s) 1.47
(d) 4.30
(d) 4.37
(d) 4.61
(bs) 4.83
(bs) 5.02
(d) 5.23
(m) 5.31
(m) 5.94
(m) 7.27
10.43
5.64
5.65
9.85
2.29
2.34
2.16
1.09
0.91
1.07
1.07
1.00
5.65
f1 (ppm)

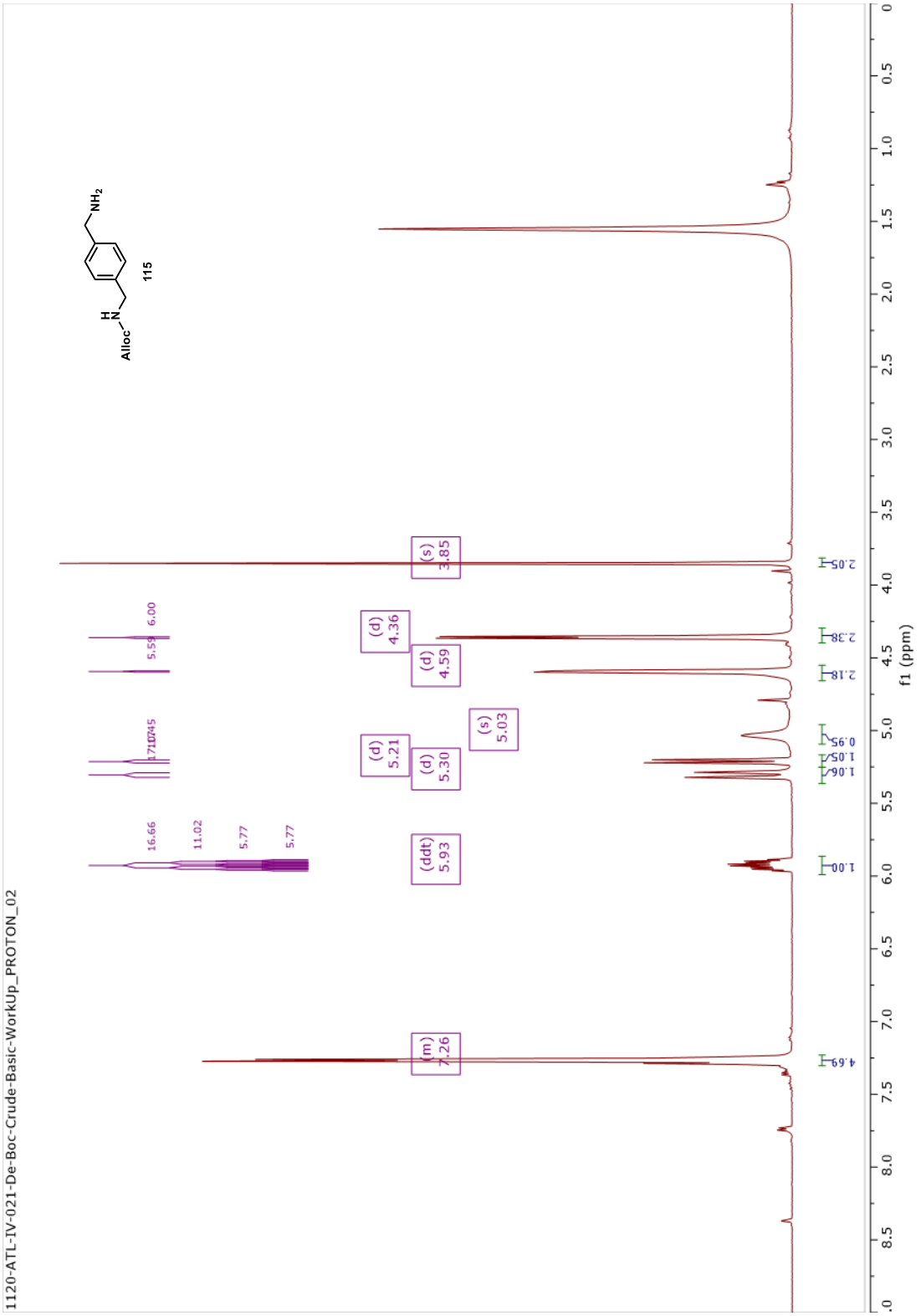
1120-ATL-IV-021-De-Boc-Crude-Basic-WorkUp_PROTON_02
NH2
H
N
Alloc
115
(m) 7.26
(ddt) 5.93
(d) 5.30
(d) 5.21
(s) 5.03
(d) 4.59
(d) 4.36
(s) 3.85
16.66
11.02
5.77
5.77
5.59
6.00
1.71
1.45
4.69
1.00
1.06
1.05
0.95
2.18
2.38
2.05
f1 (ppm)

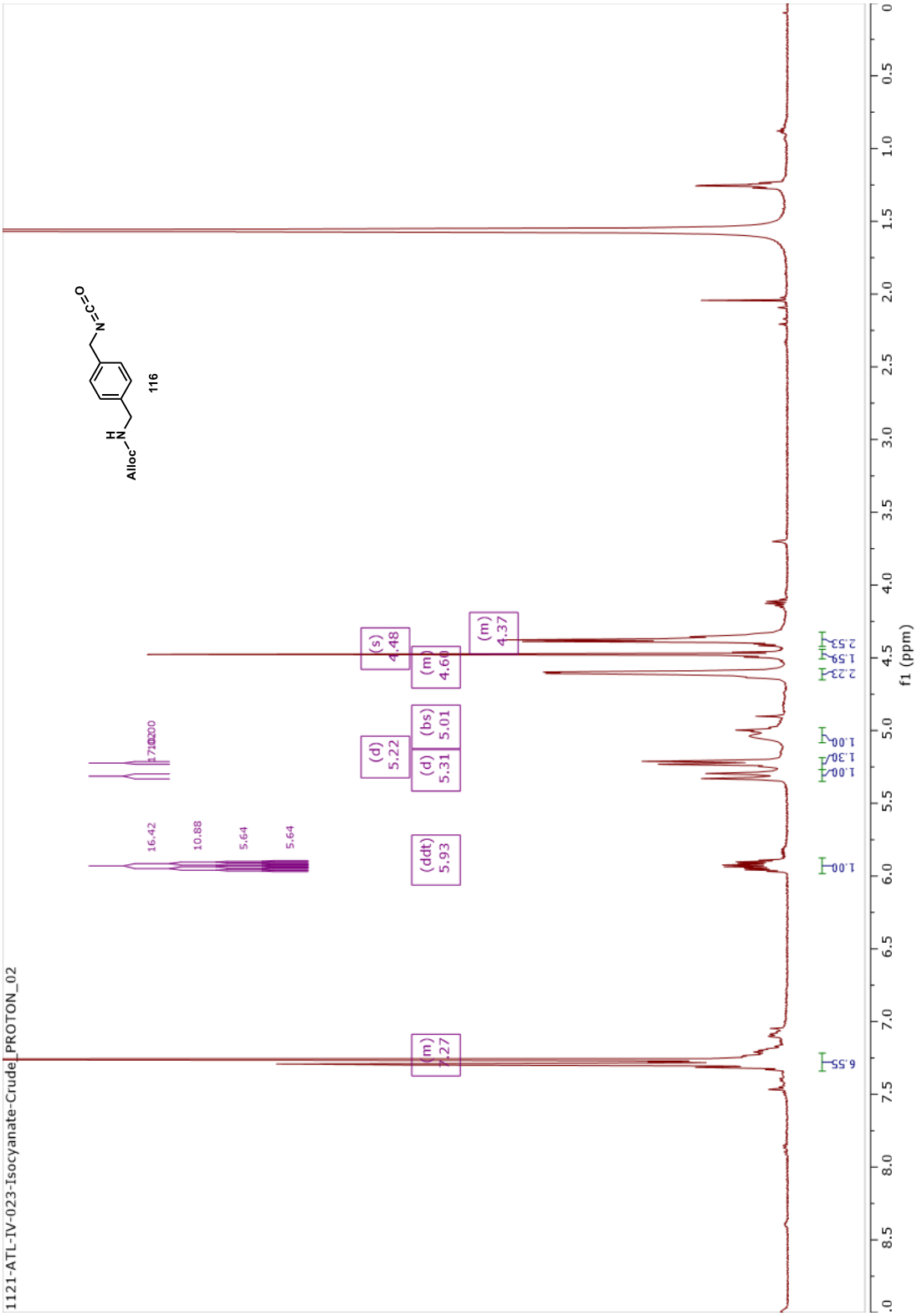
1121-ATL-IV-023-Isocyanate-Crude_PROTON_02
116
Alloc
(m) 7.27
(ddt) 5.93
(d) 5.22
(d) 5.31
(bs) 5.01
(m) 4.66
(s) 4.48
(m) 4.37
16.42
10.88
5.64
5.64
6.55
1.00
1.00
1.30
1.00
2.53
1.59
2.23
f1 (ppm)

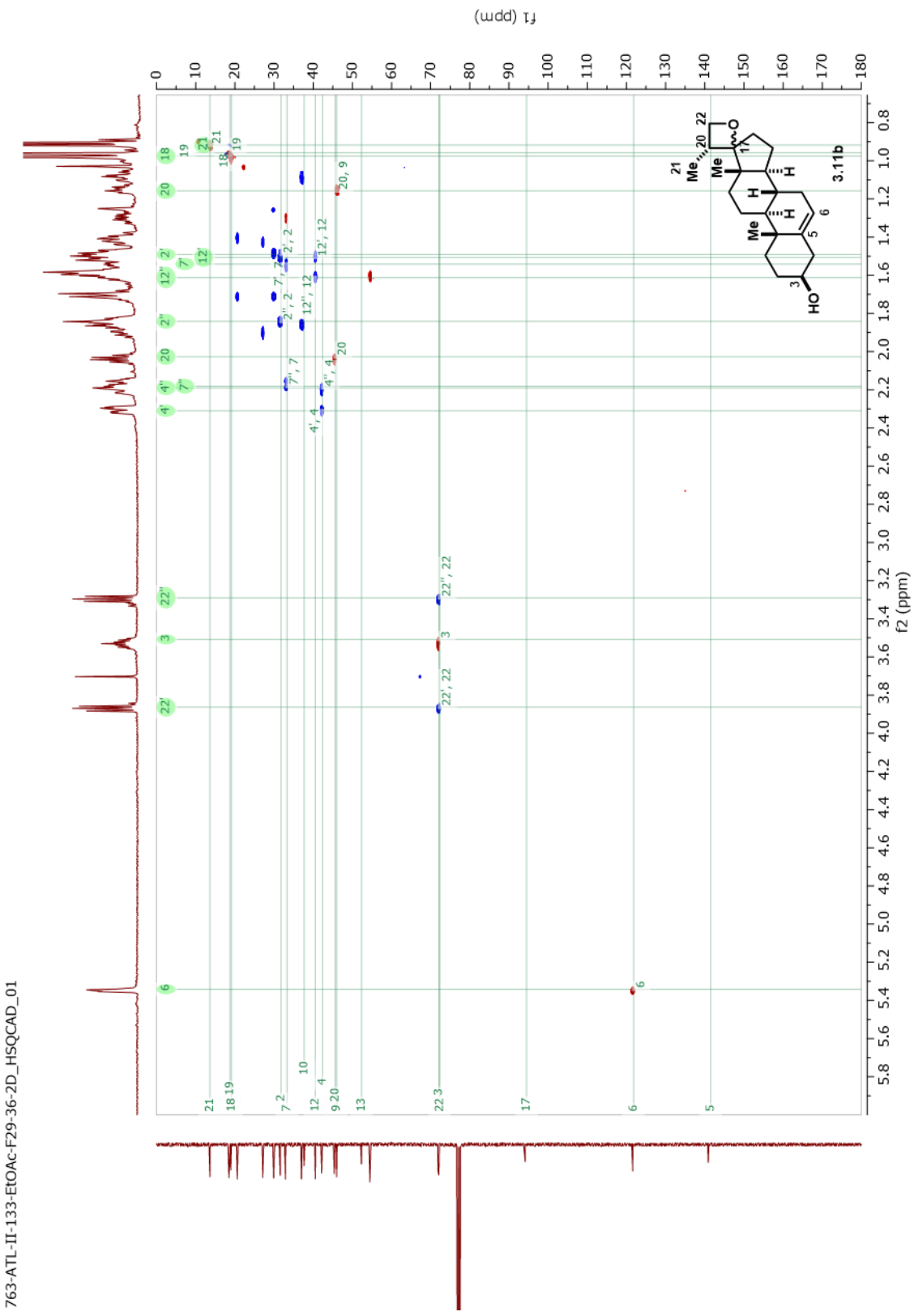
763-ATL-II-133-EtOAc-F29-36-2D_HSQCAD_01
f1 (ppm)
f2 (ppm)
3.11b

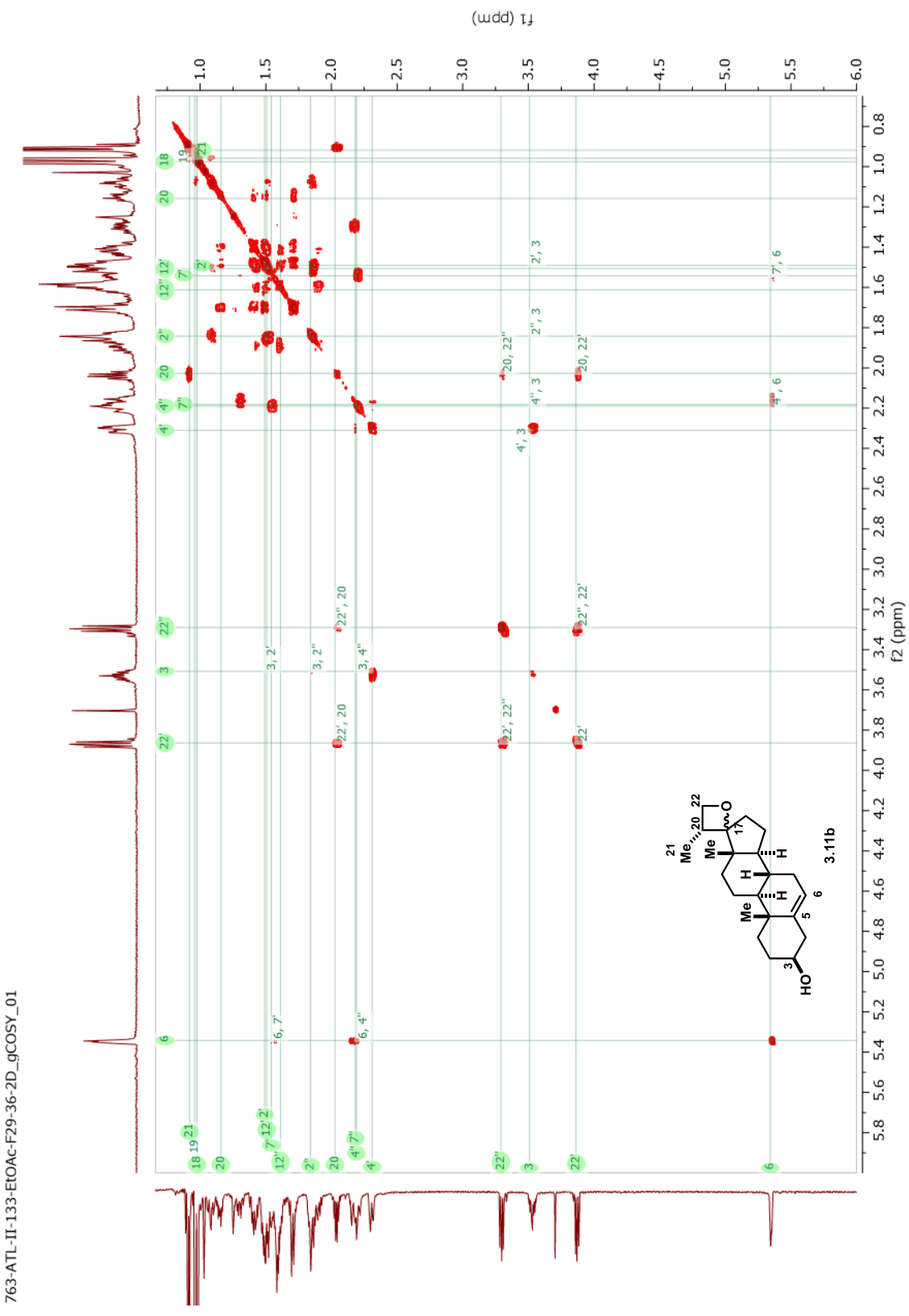
763-ATL-II-133-EtOAc-F29-36-2D_gCOSY_01
f2 (ppm)
f1 (ppm)
3.11b

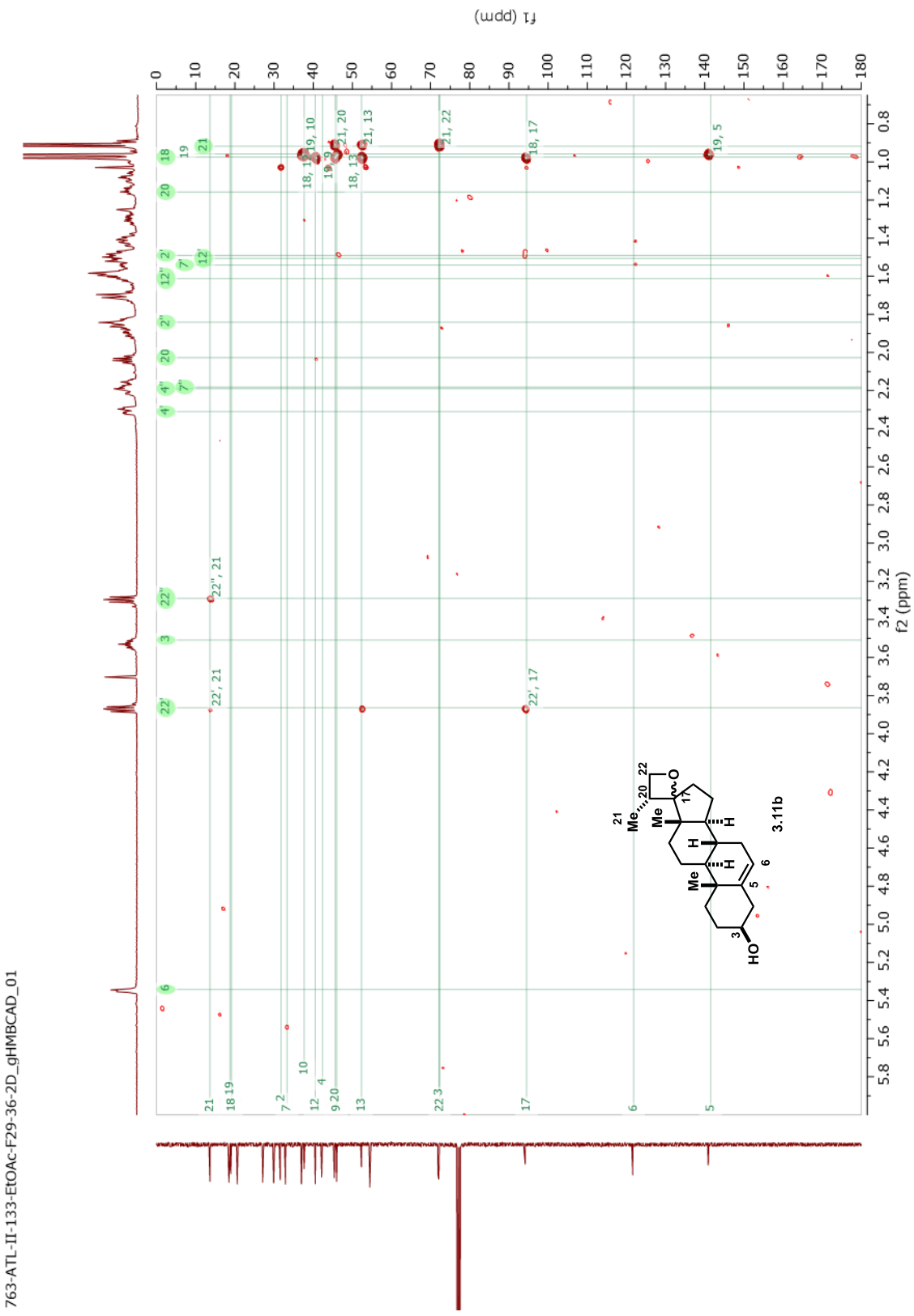
763-ATL-II-133-EtOAc-F29-36-2D_gHMBCAD_01
f1 (ppm)
f2 (ppm)
3.11b

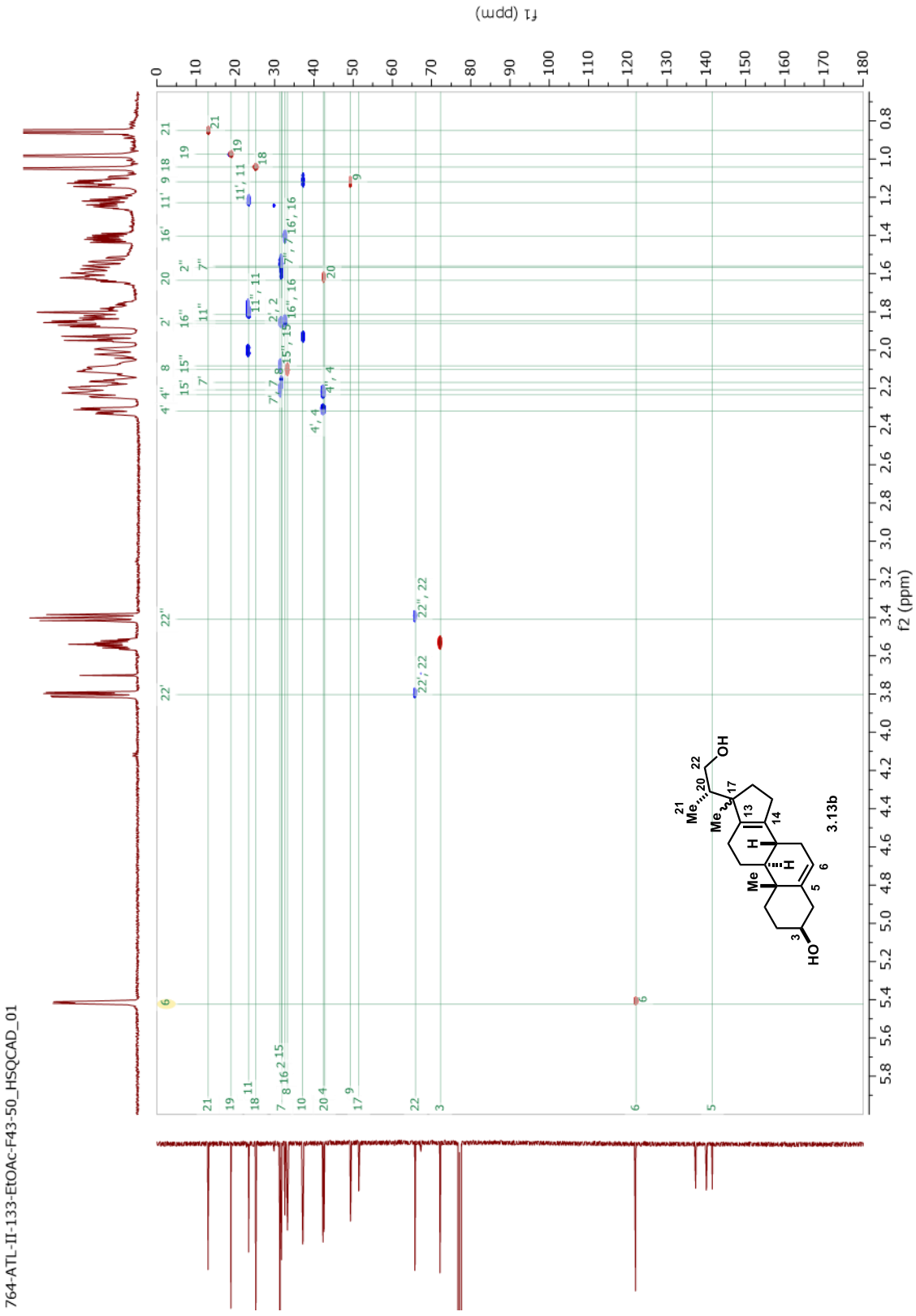
764-ATL-II-133-EtOAc-F43-50_HSQCAD_01
f2 (ppm)
f1 (ppm)
3.13b

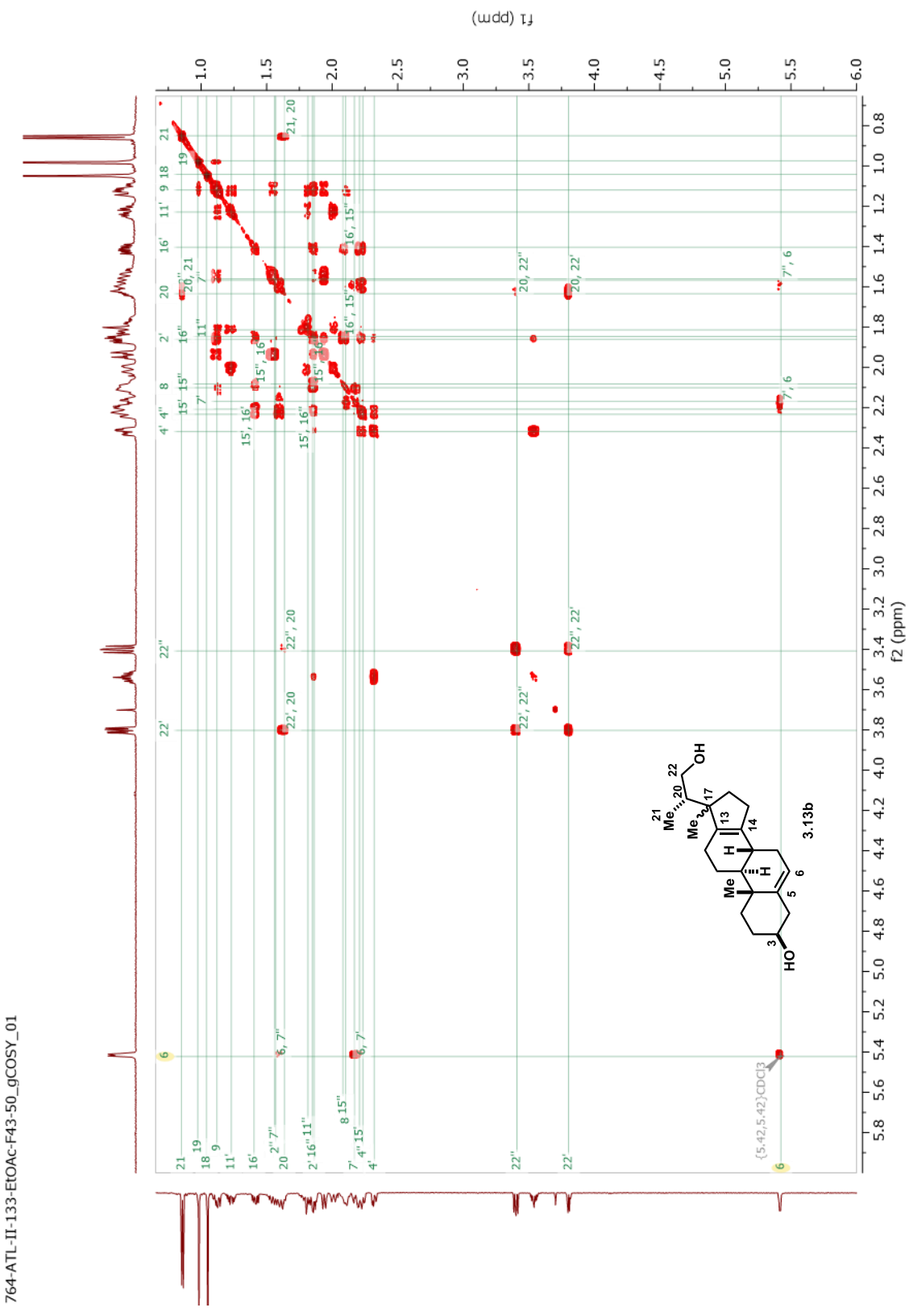
764-ATL-II-133-EtOAc-F43-50_gCOSY_01
f1 (ppm)
f2 (ppm)
3.13b
{5.42,5.42}CDCl3

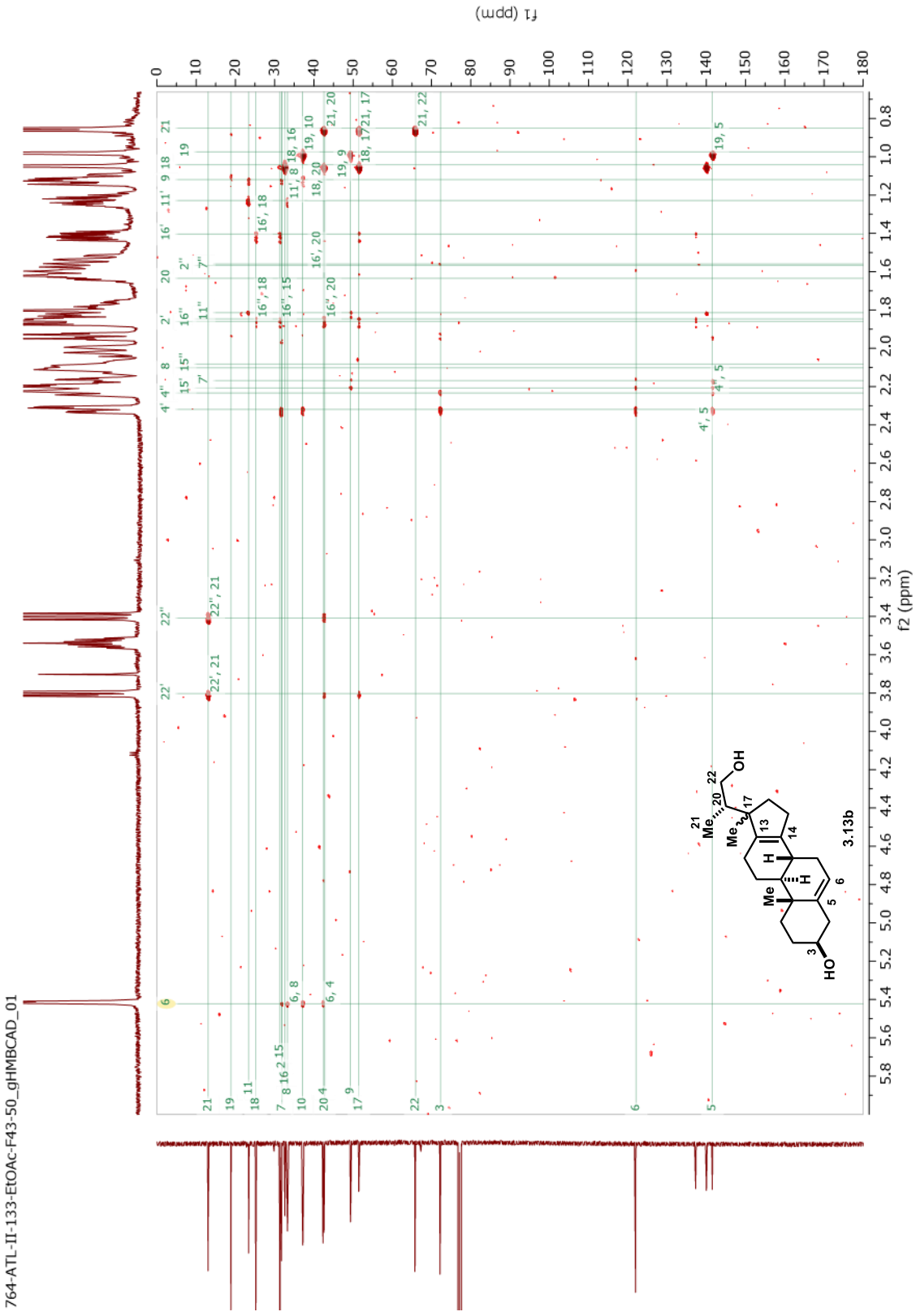
764-ATL-II-133-EtOAc-F43-50_gHMBCAD_01
f2 (ppm)
f1 (ppm)
3.13b

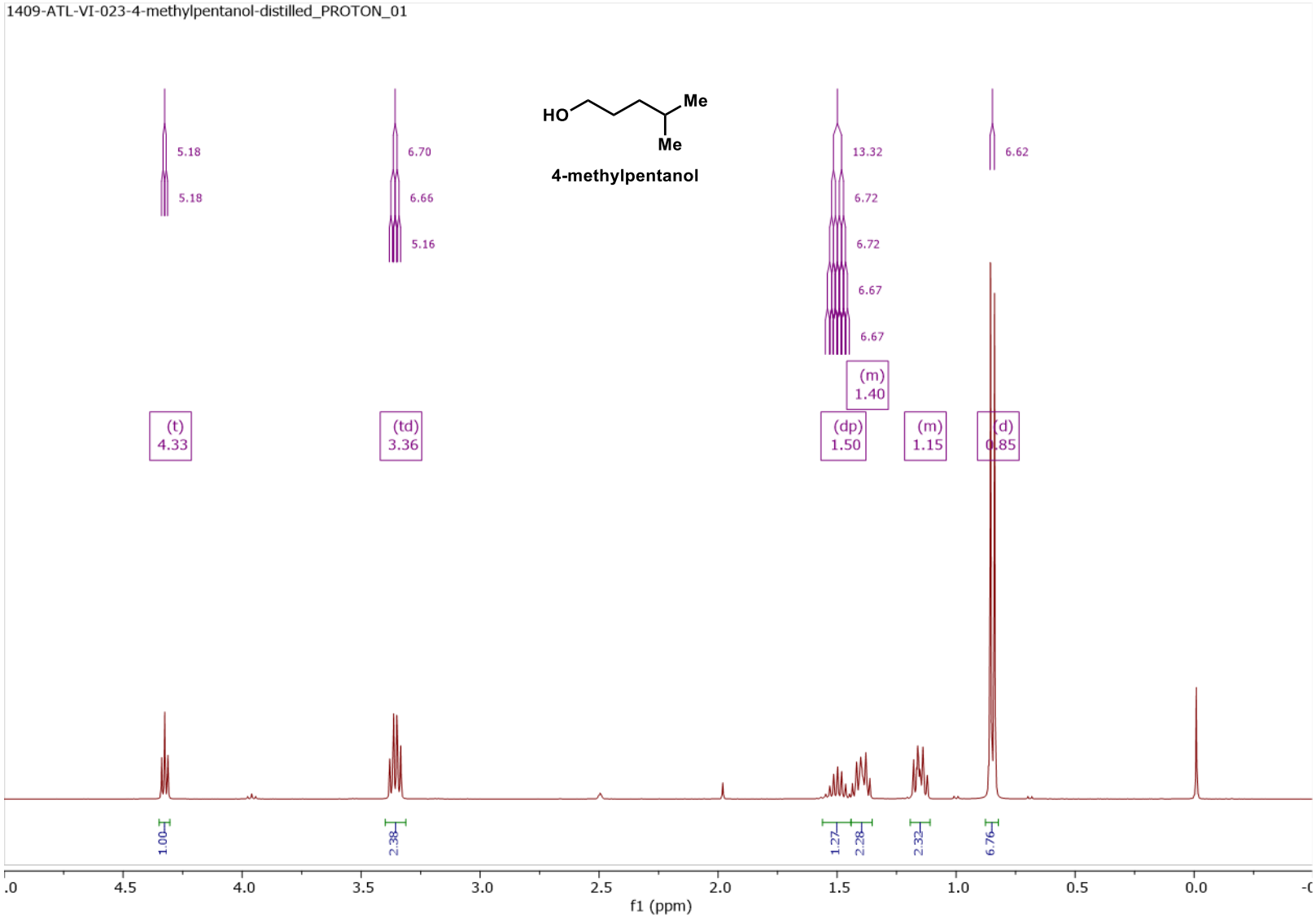
1409-ATL-VI-023-4-methylpentanol-distilled_PROTON_01
HO
Me
Me
4-methylpentanol
5.18
5.18
6.70
6.66
5.16
13.32
6.72
6.72
6.67
6.67
6.62
(t)
4.33
(td)
3.36
(m)
1.40
(dp)
1.50
(m)
1.15
(d)
0.85
1.00
2.38
1.27
2.28
2.32
6.76
f1 (ppm)

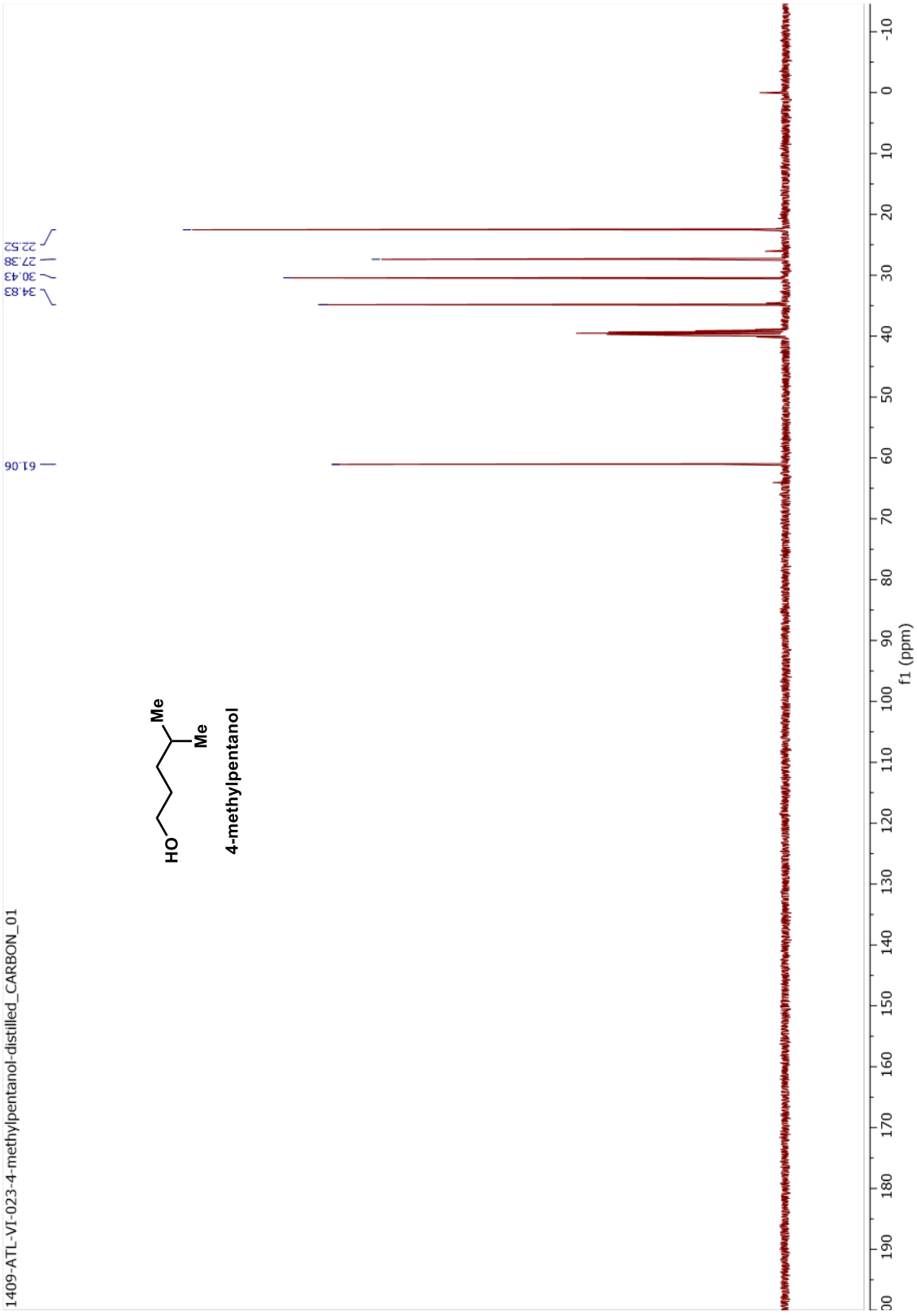
1409-ATL-VI-023-4-methylpentanol-distilled_CARBON_01
4-methylpentanol
HO
Me
Me
61.06
34.83
30.43
27.38
22.52
f1 (ppm)

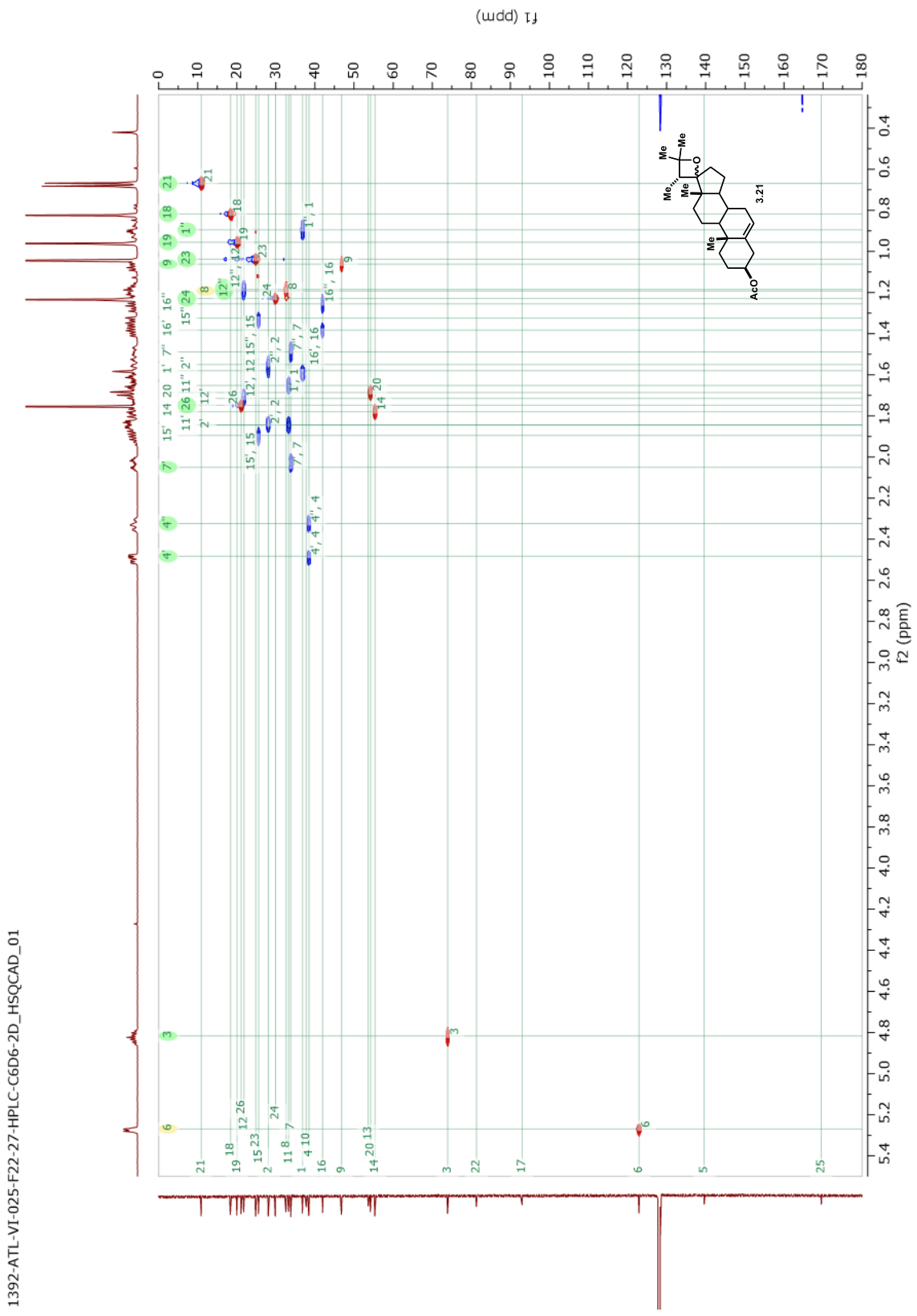
1392-ATL-VI-025-F22-27-HPLC-C6D6-2D_HSQCAD_01
f1 (ppm)
f2 (ppm)
Me
Me
Me
Me
O
AcO
3.21

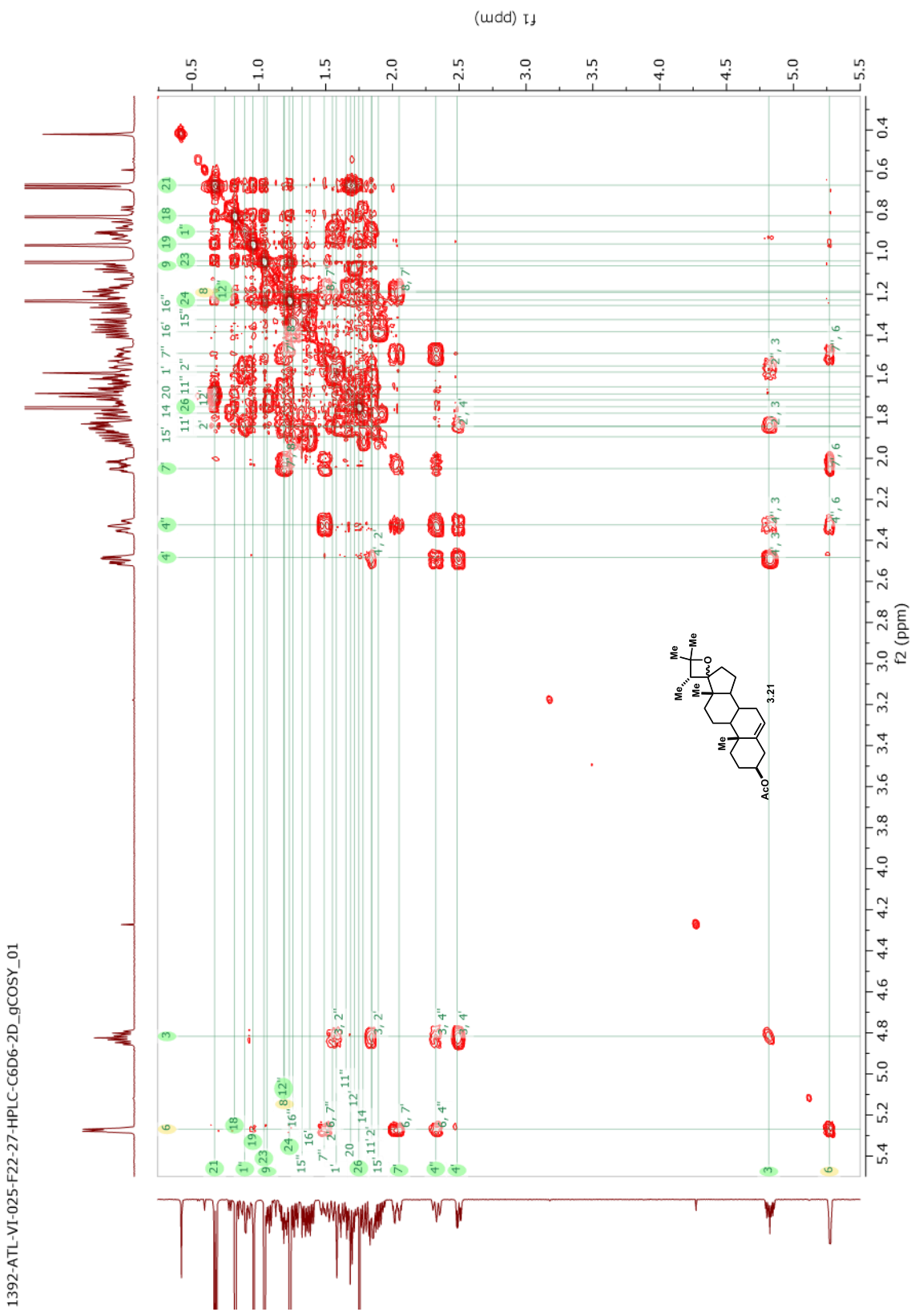
1392-ATL-VI-025-F22-27-HPLC-C6D6-2D_gCOSY_01
f1 (ppm)
f2 (ppm)
Me
Me
Me
Me
Me
AcO
3.21

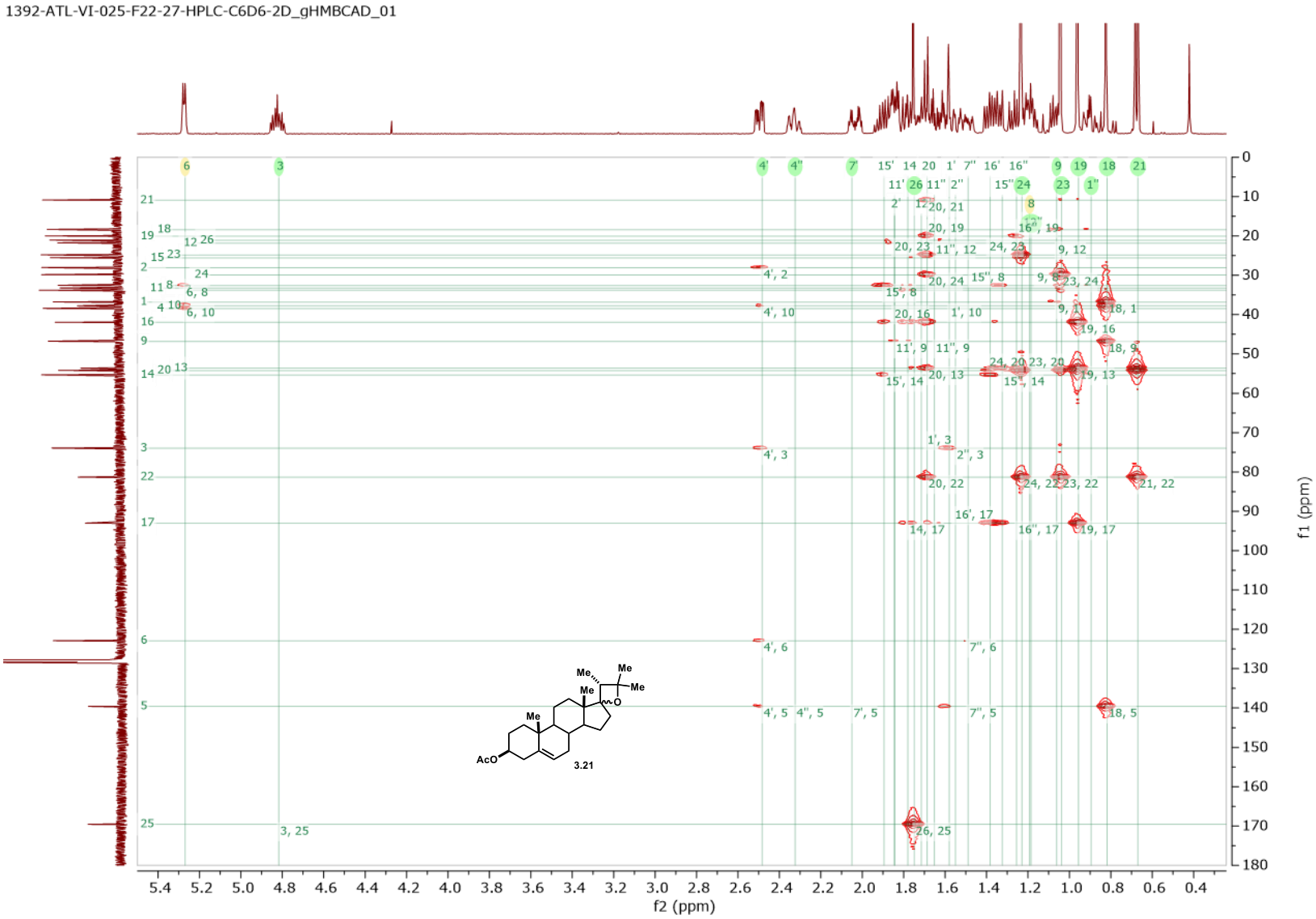
1392-ATL-VI-025-F22-27-HPLC-C6D6-2D_gHMBCAD_01
f2 (ppm)
f1 (ppm)
AcO
Me
3.21

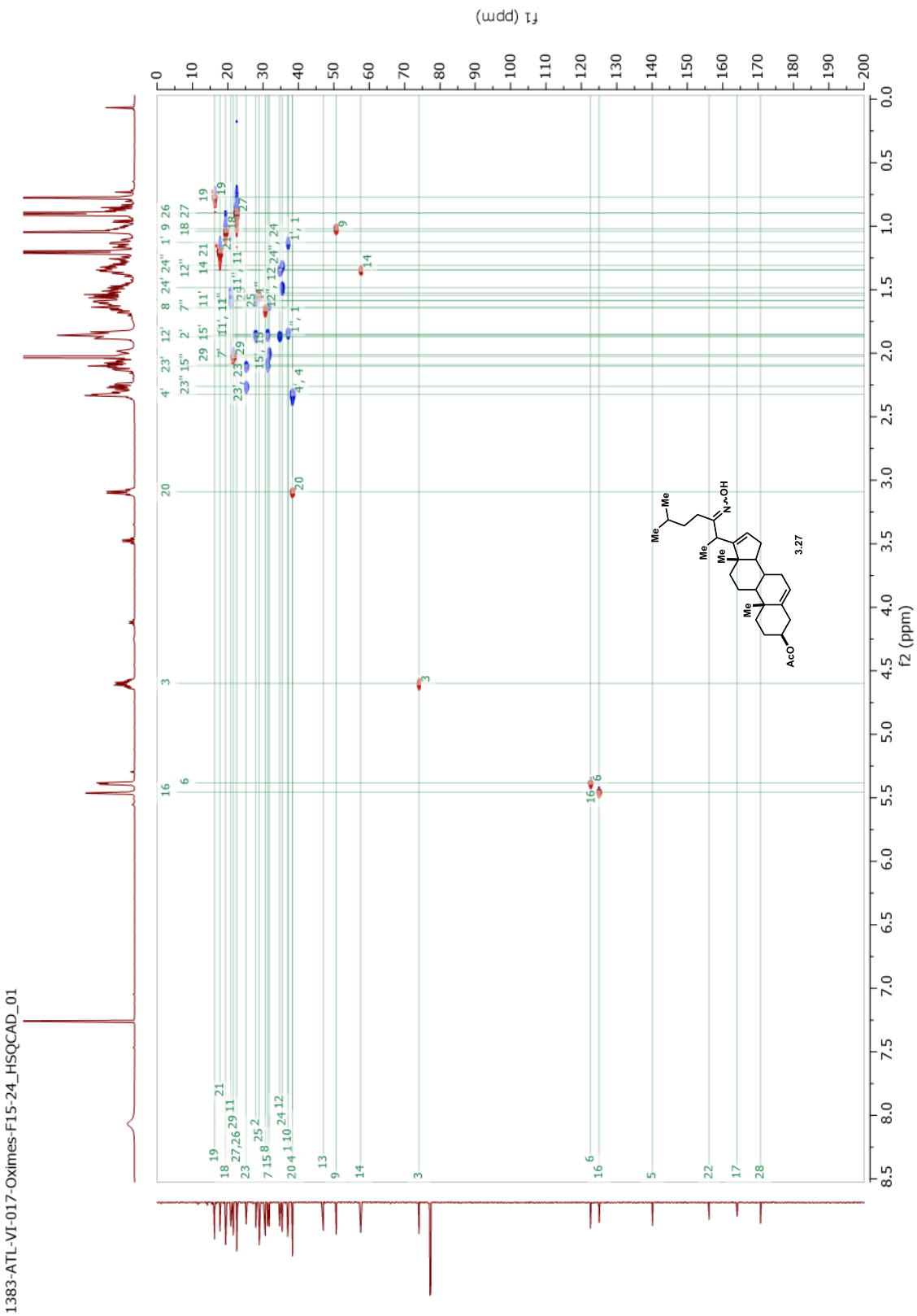
1383-ATL-VI-017-Oximes-F15-24_HSQCAD_01
f1 (ppm)
f2 (ppm)
3.27

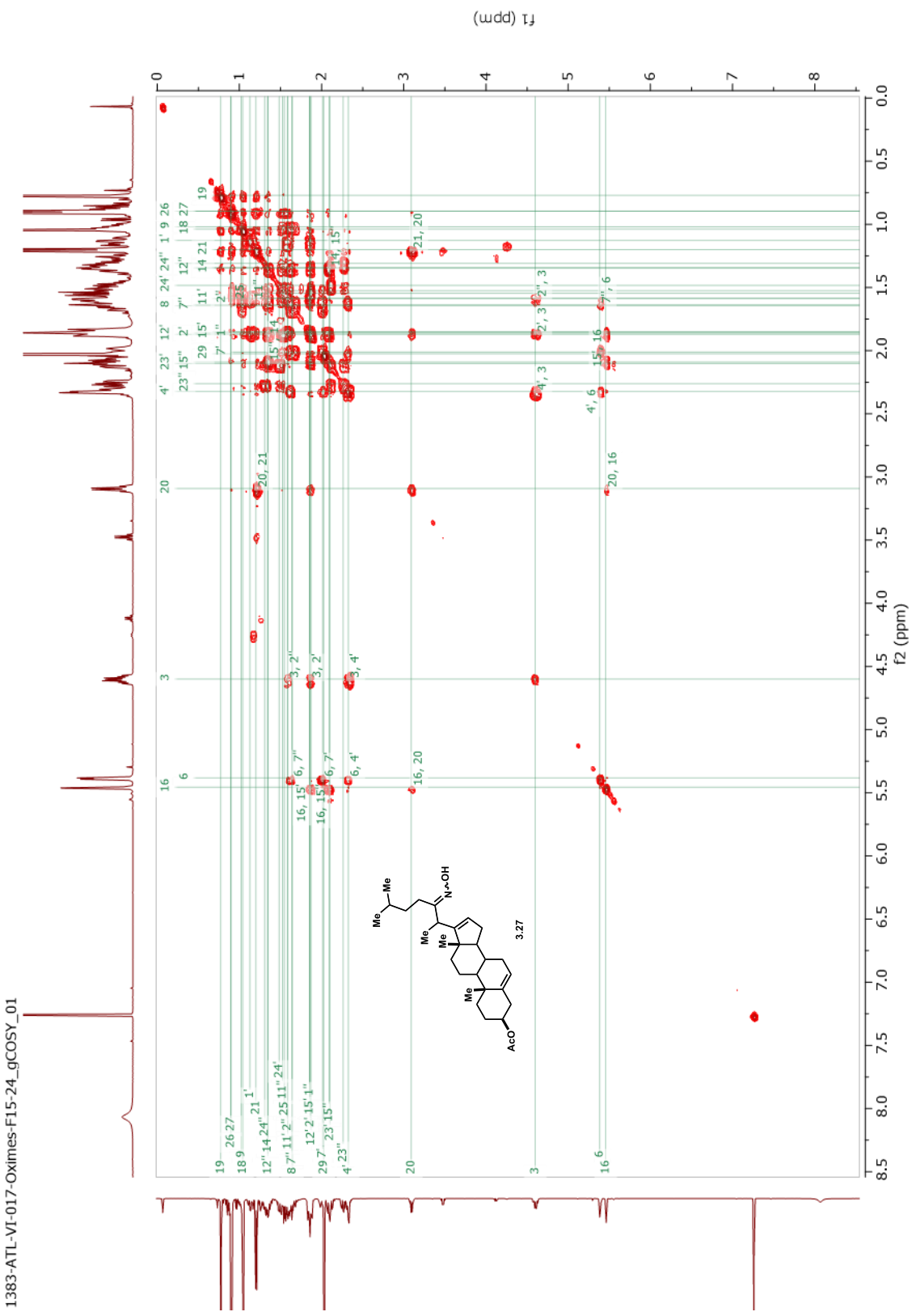
1383-ATL-VI-017-Oximes-F15-24_gCOSY_01
f2 (ppm)
f1 (ppm)
3.27

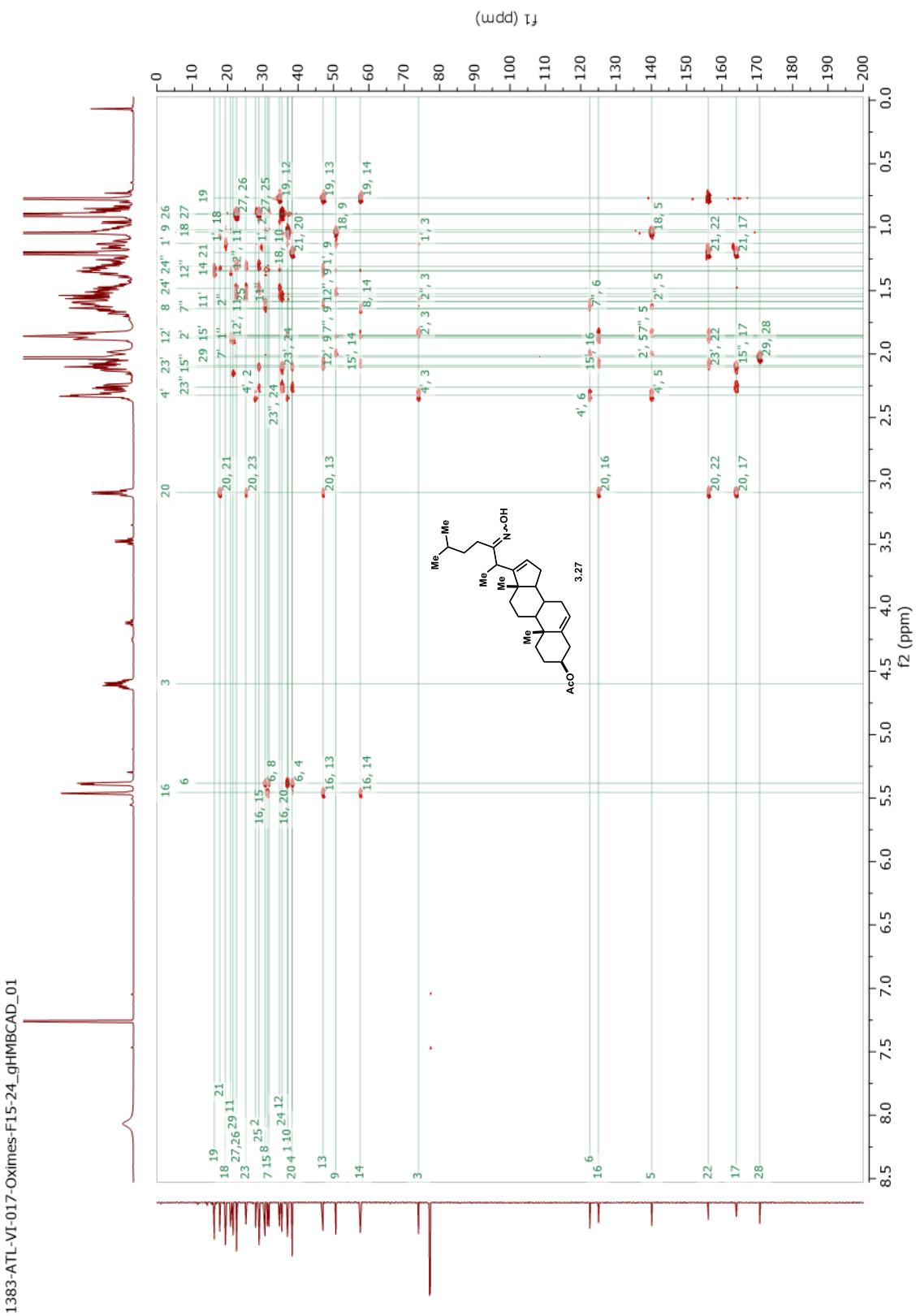
1383-ATL-VI-017-Oximes-F15-24_gHMBCAD_01
f2 (ppm)
f1 (ppm)
3.27

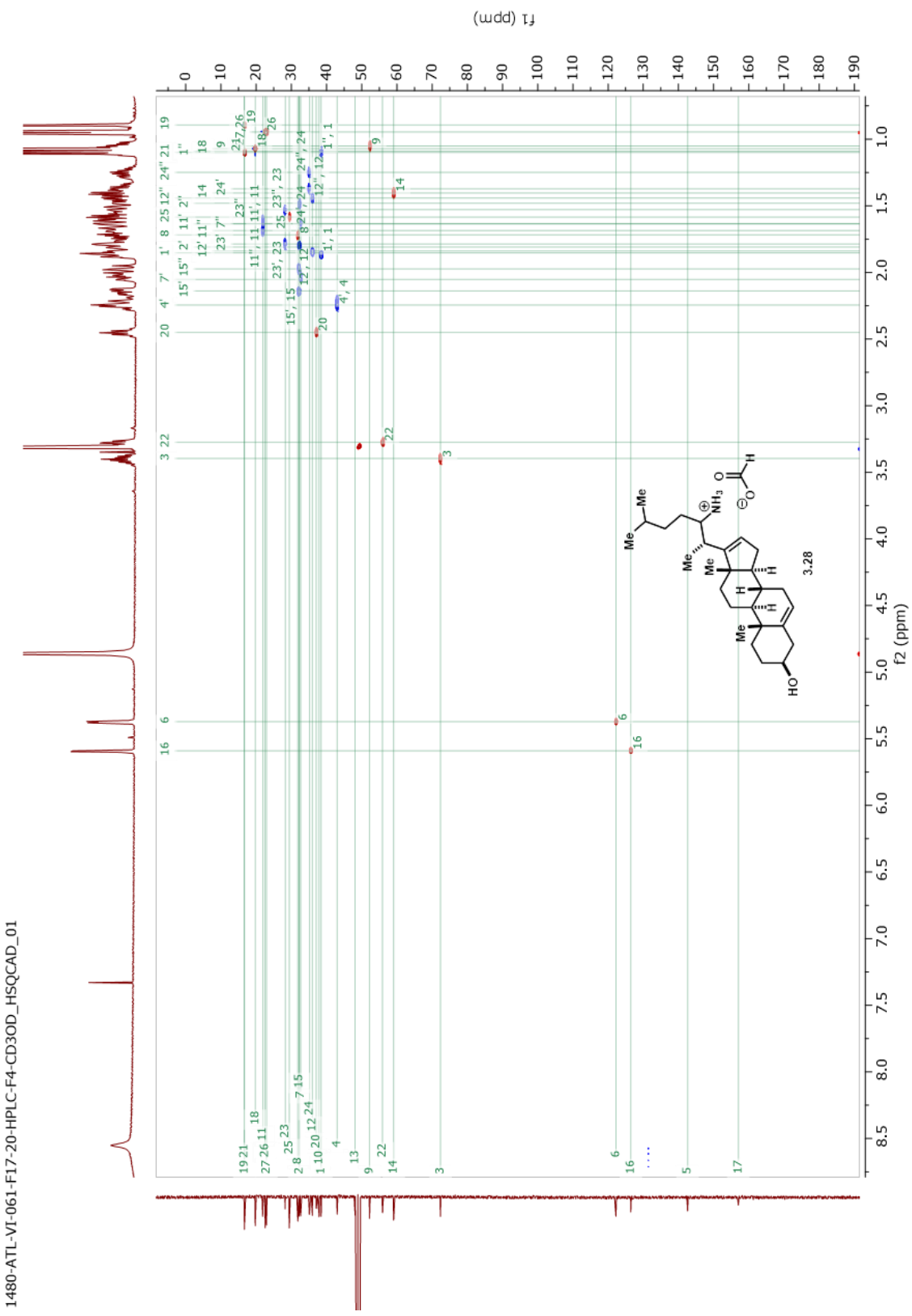
1480-ATL-VI-061-F17-20-HPLC-F4-CD3OD_HSQCAD_01
f2 (ppm)
f1 (ppm)
3.28

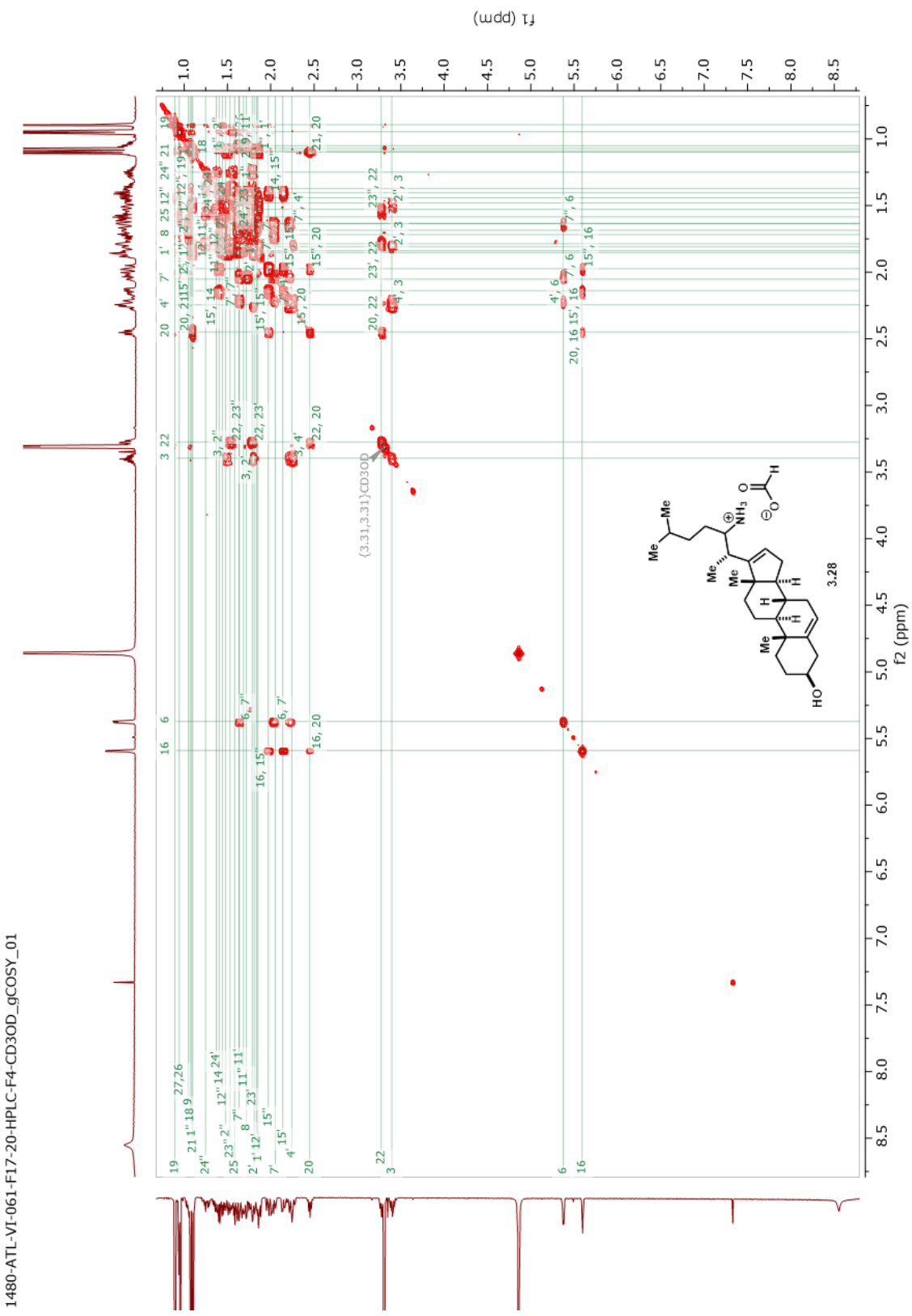
1480-ATL-VI-061-F17-20-HPLC-F4-CD3OD_gCOSY_01
f2 (ppm)
f1 (ppm)
{3.31,3.31}CD3OD
3.28

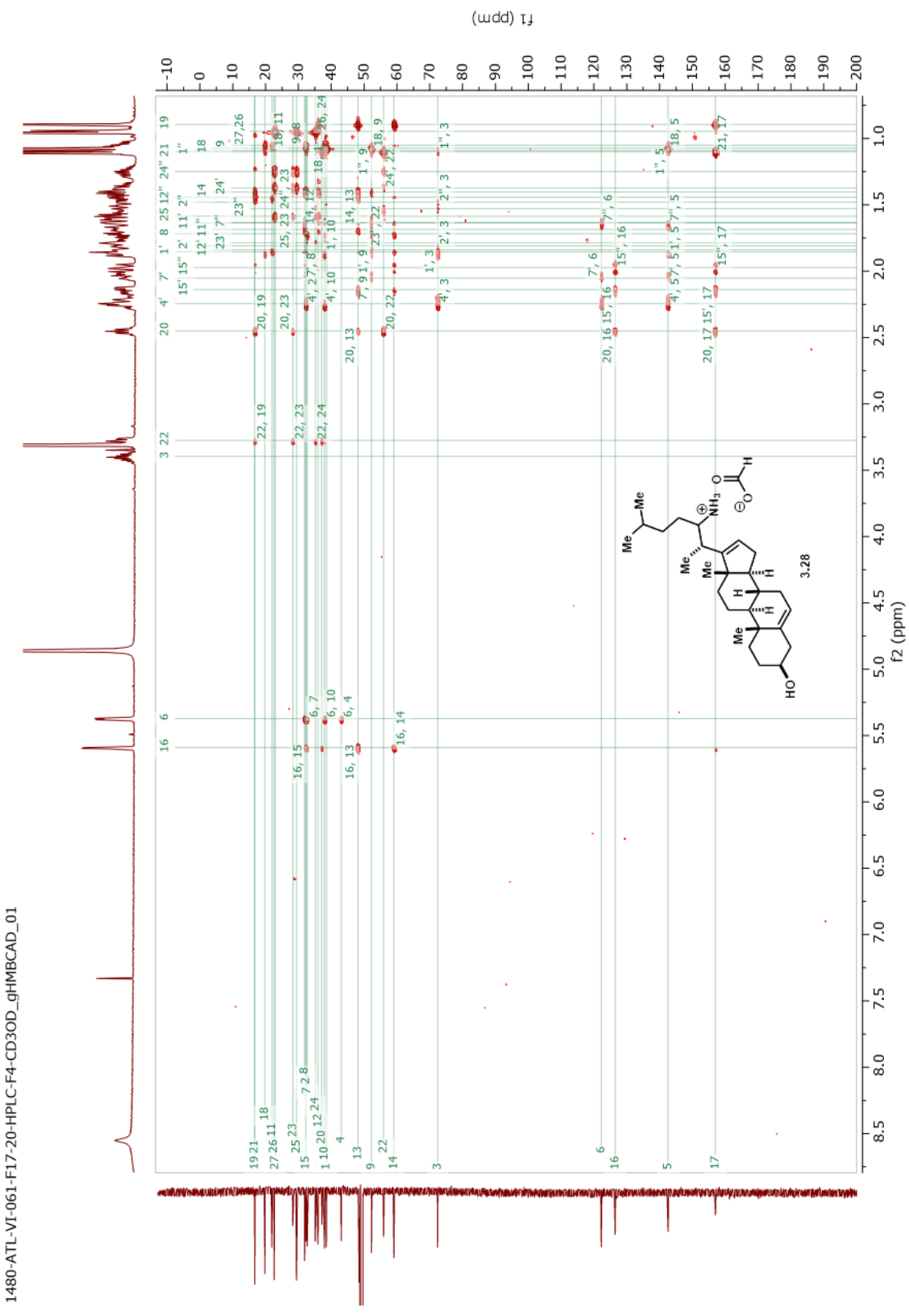
1480-ATL-VI-061-F17-20-HPLC-F4-CD3OD_gHMBCAD_01
f2 (ppm)
f1 (ppm)
3.28

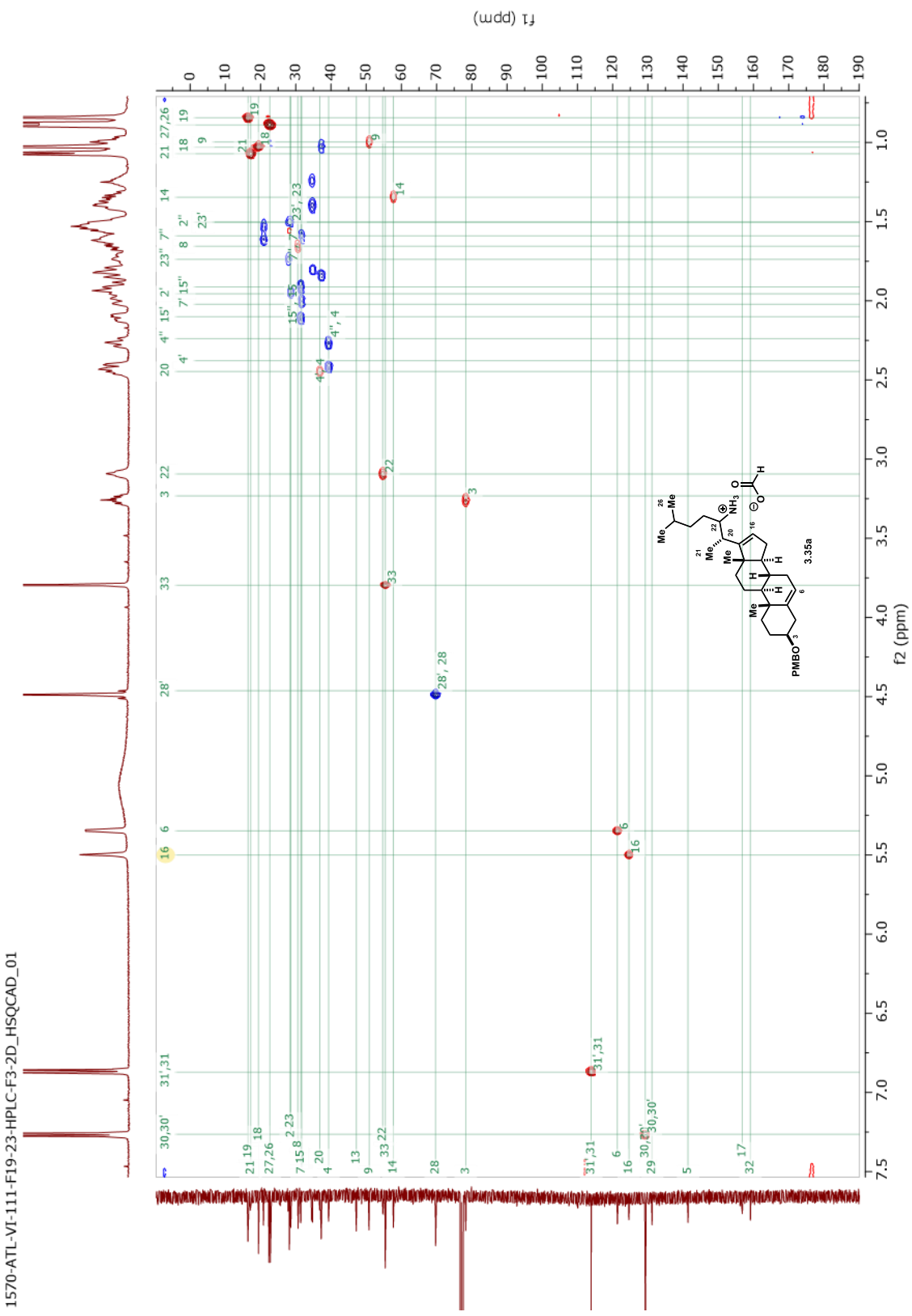
1570-ATL-VI-111-F19-23-HPLC-F3-2D_HSQCAD_01
f1 (ppm)
f2 (ppm)
3.35a
PMBO

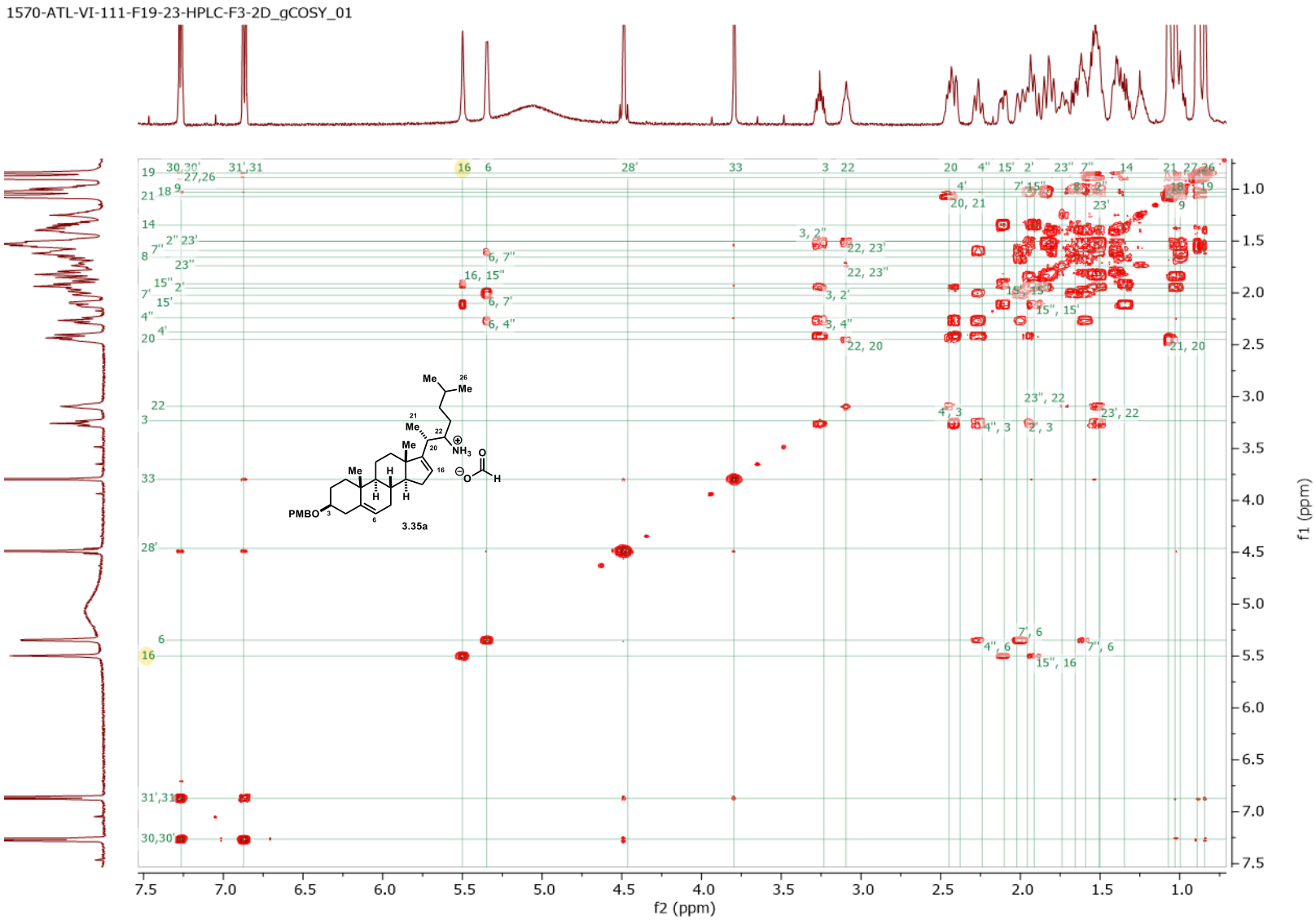
1570-ATL-VI-111-F19-23-HPLC-F3-2D_gCOSY_01
f2 (ppm)
f1 (ppm)
3.35a

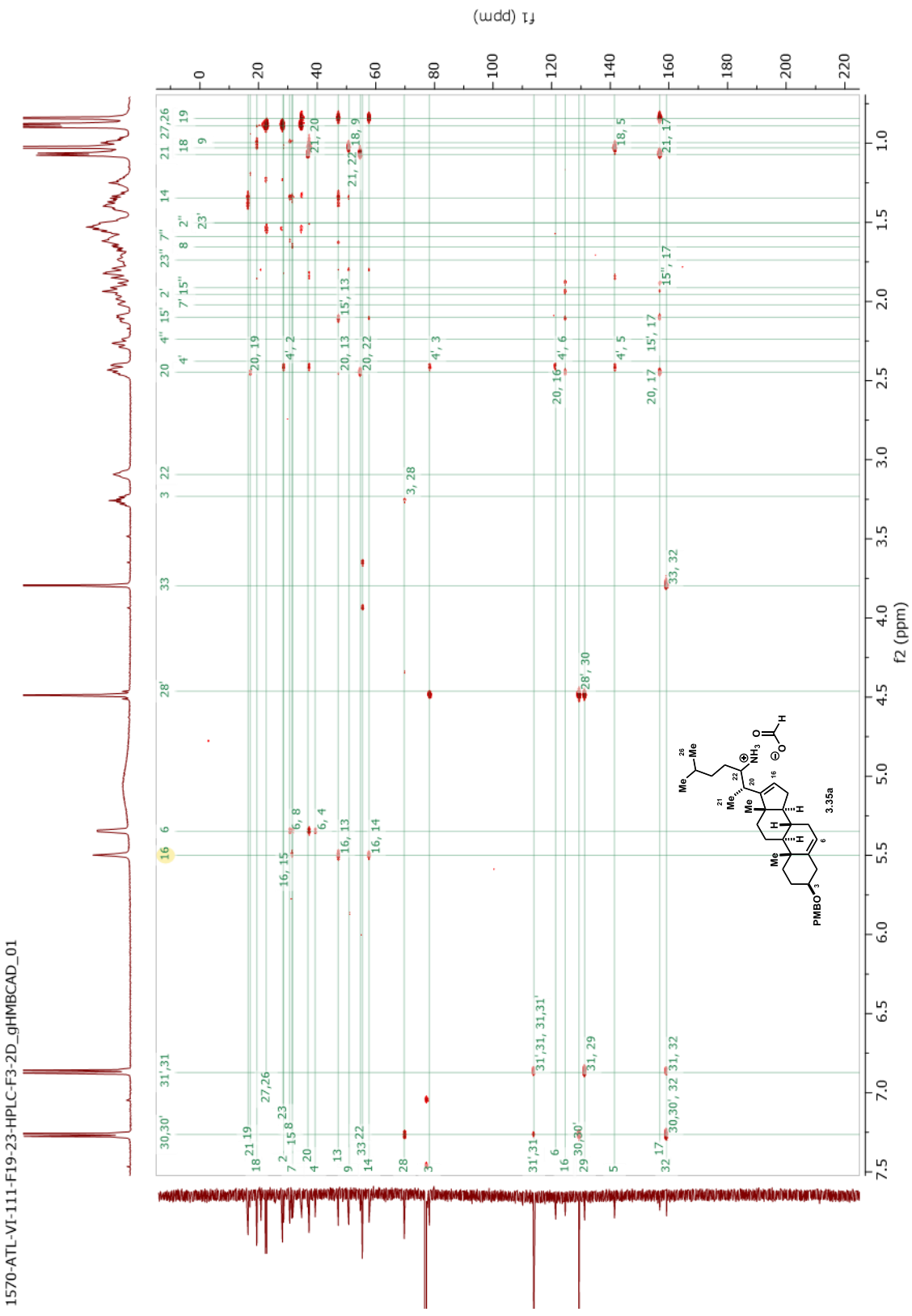
1570-ATL-VI-111-F19-23-HPLC-F3-2D_gHMBCAD_01
f1 (ppm)
f2 (ppm)
3.35a
PMBO

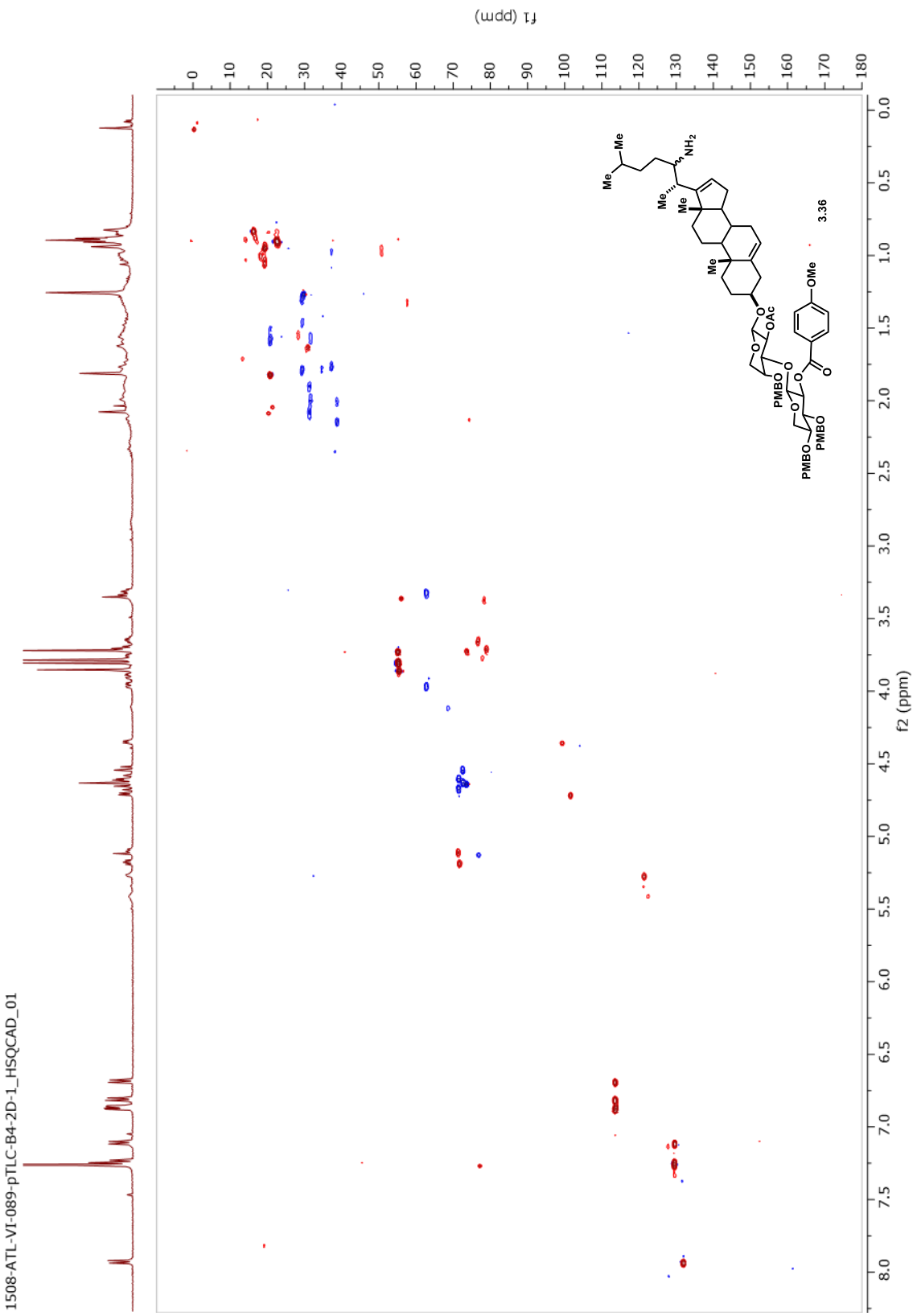
1508-ATL-VI-089-pTLC-B4-2D-1_HSQCAD_01
f1 (ppm)
f2 (ppm)
3.36
Me
Me
NH2
Me
Me
Me
OAc
O
PMBO
PMBO
PMBO
OMe
O

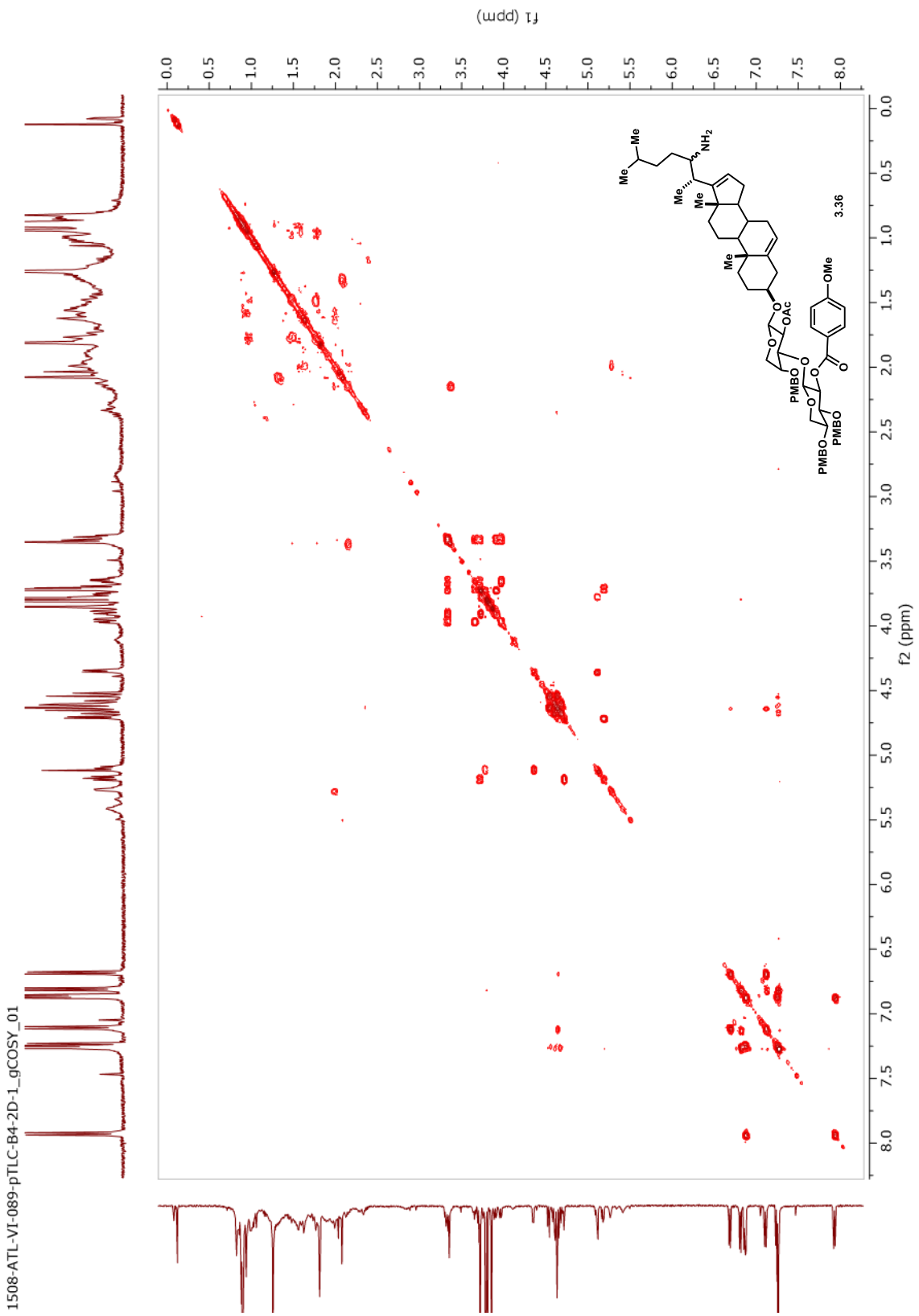
1508-ATL-VI-089-pTLC-B4-2D-1_gCOSY_01
f1 (ppm)
f2 (ppm)
0.0
0.5
1.0
1.5
2.0
2.5
3.0
3.5
4.0
4.5
5.0
5.5
6.0
6.5
7.0
7.5
8.0
Me
Me
NH2
Me
Me
Me
OAc
O
PMBO
PMBO
PMBO
OMe
3.36

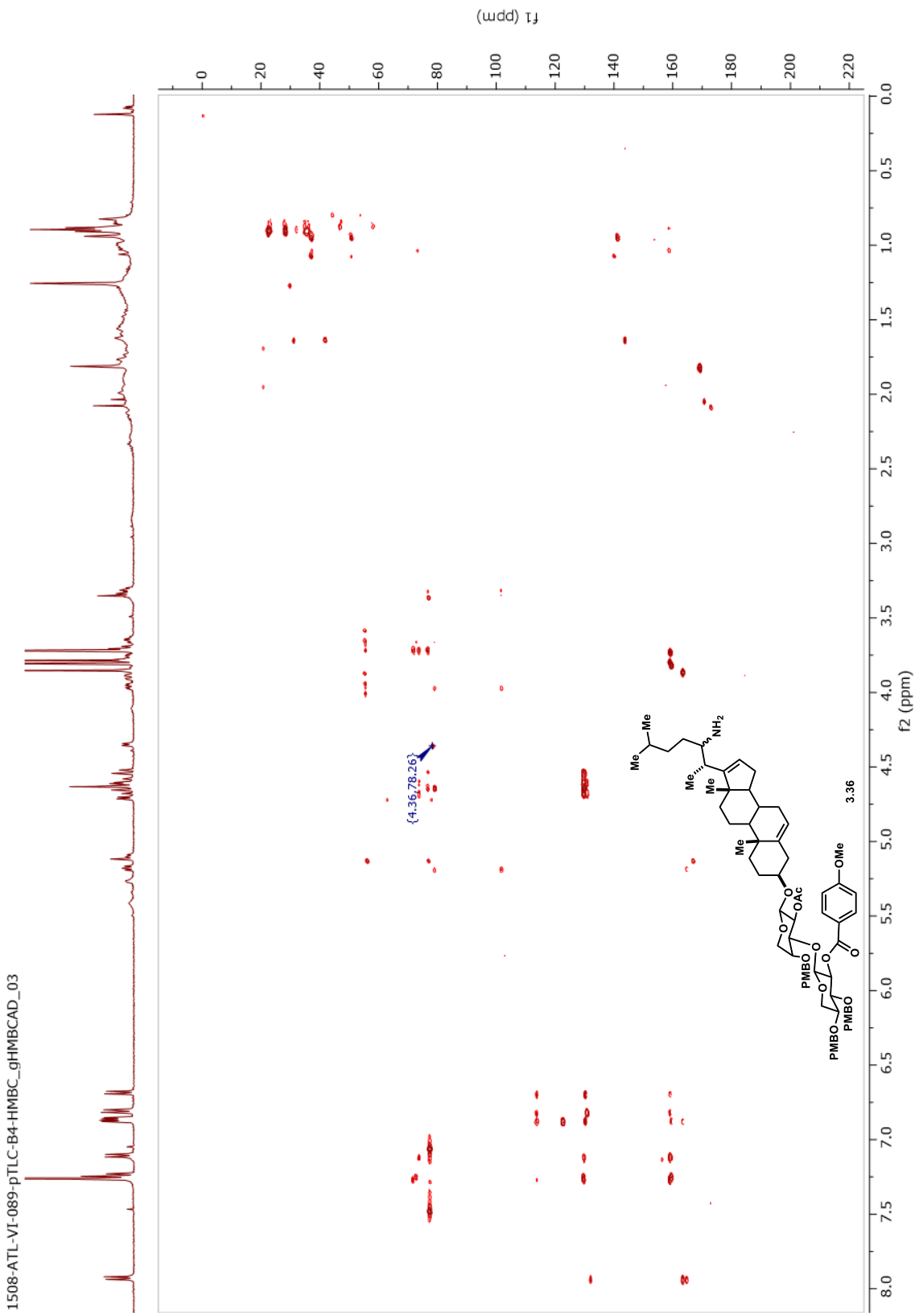
1508-ATL-VI-089-pTLC-B4-HMBC_gHMBCAD_03
f1 (ppm)
f2 (ppm)
{4.36,78.26}
Me
Me
NH2
Me
Me
Me
OAc
PMBO
PMBO
PMBO
OMe
3.36

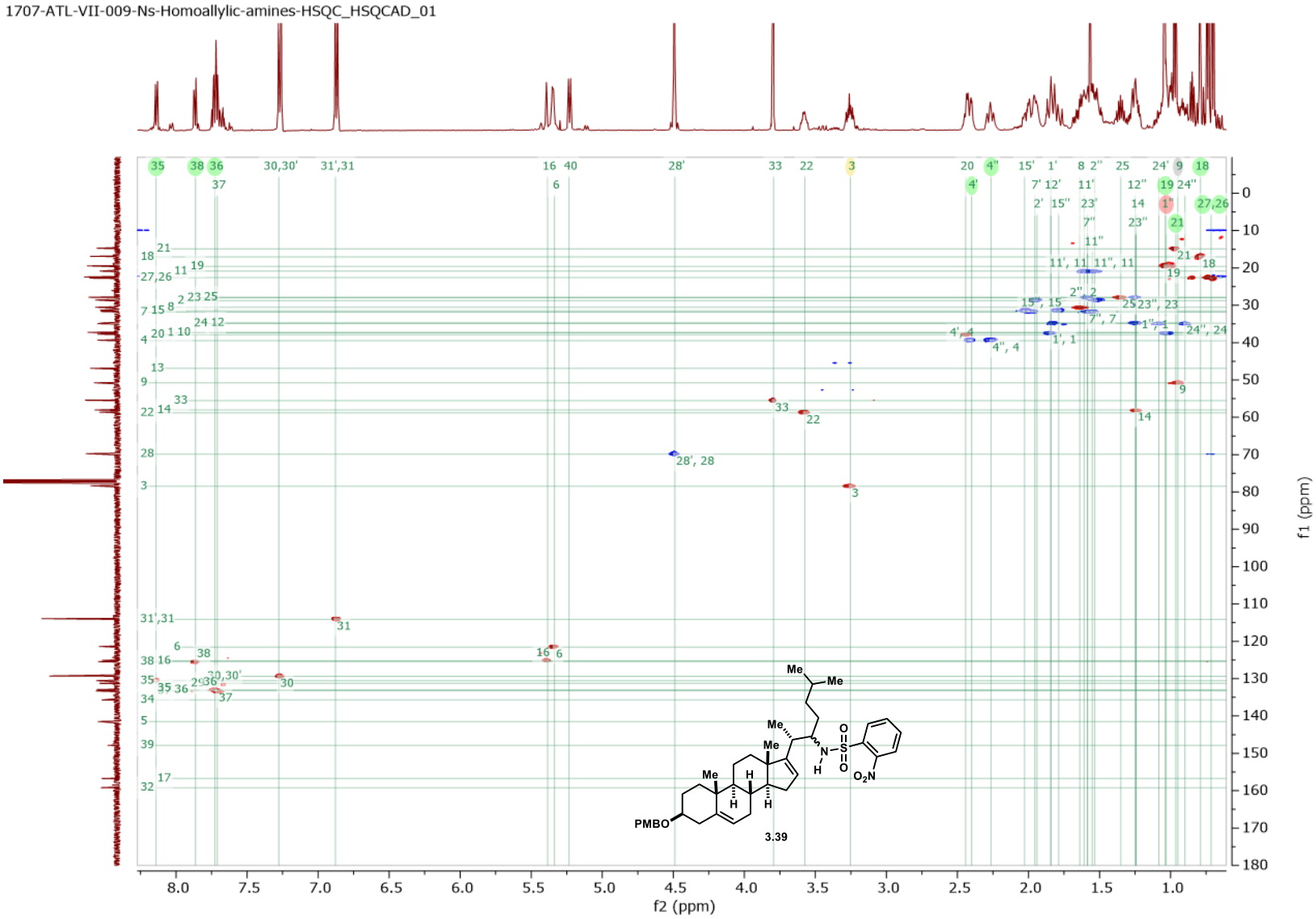
1707-ATL-VII-009-Ns-Homoallylic-amines-HSQC_HSQCAD_01
f2 (ppm)
f1 (ppm)
PMBO
3.39

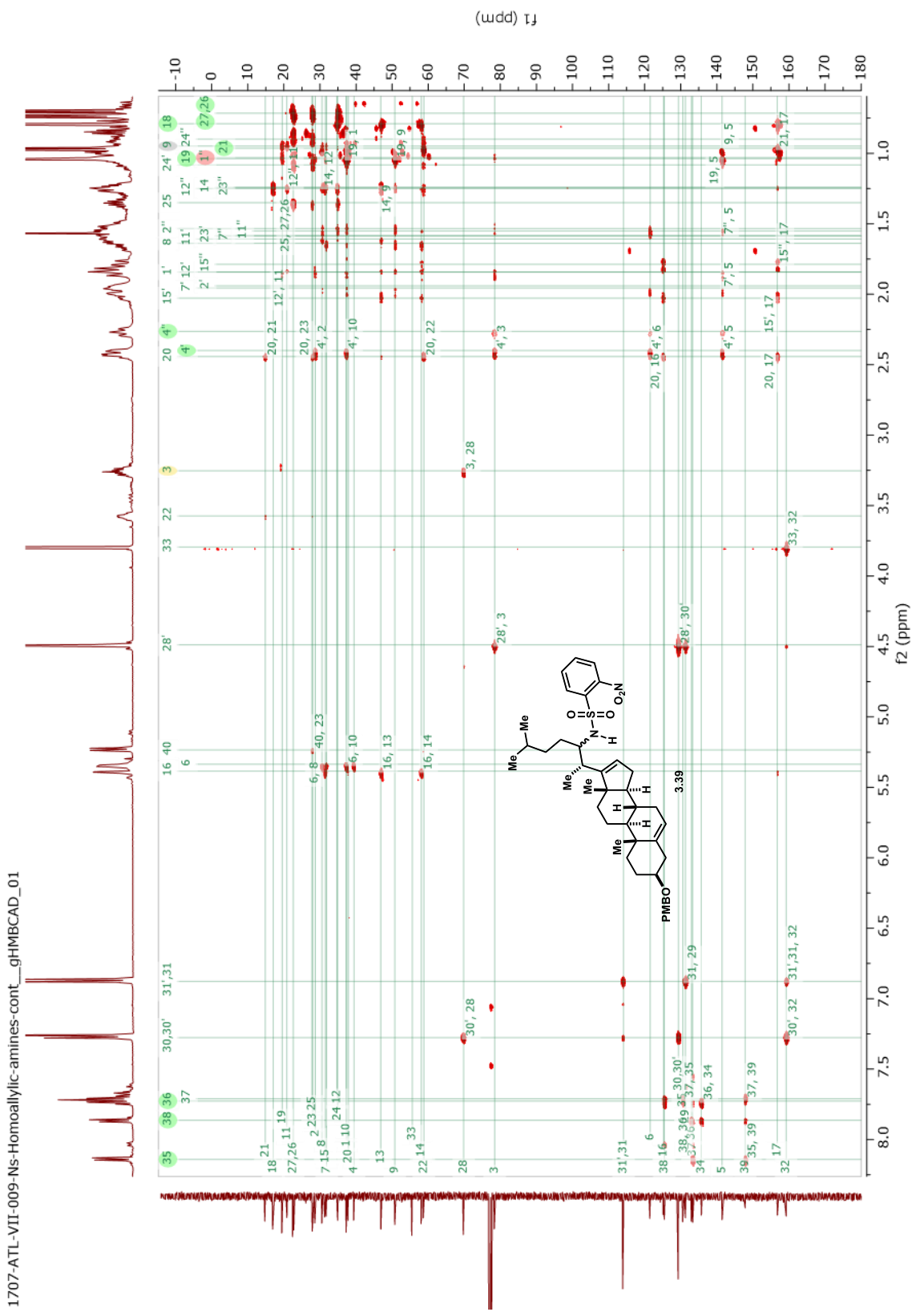
1707-ATL-VII-009-Ns-Homoallylic-amines-cont__gHMBCAD_01
f1 (ppm)
f2 (ppm)
PMBO
3.39

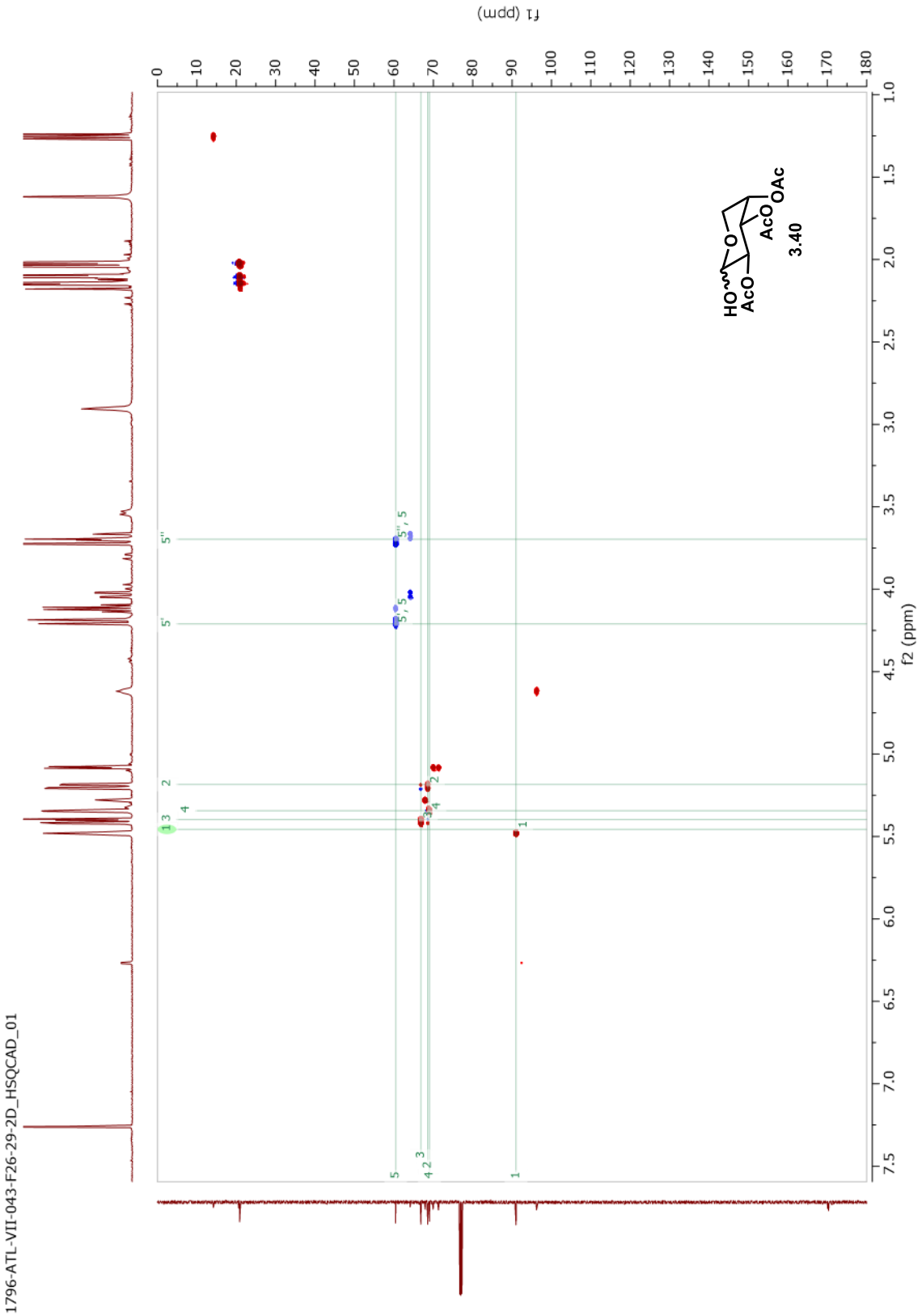
1796-ATL-VII-043-F26-29-2D_HSQCAD_01
f1 (ppm)
f2 (ppm)
HO
AcO
AcO
OAc
O
3.40

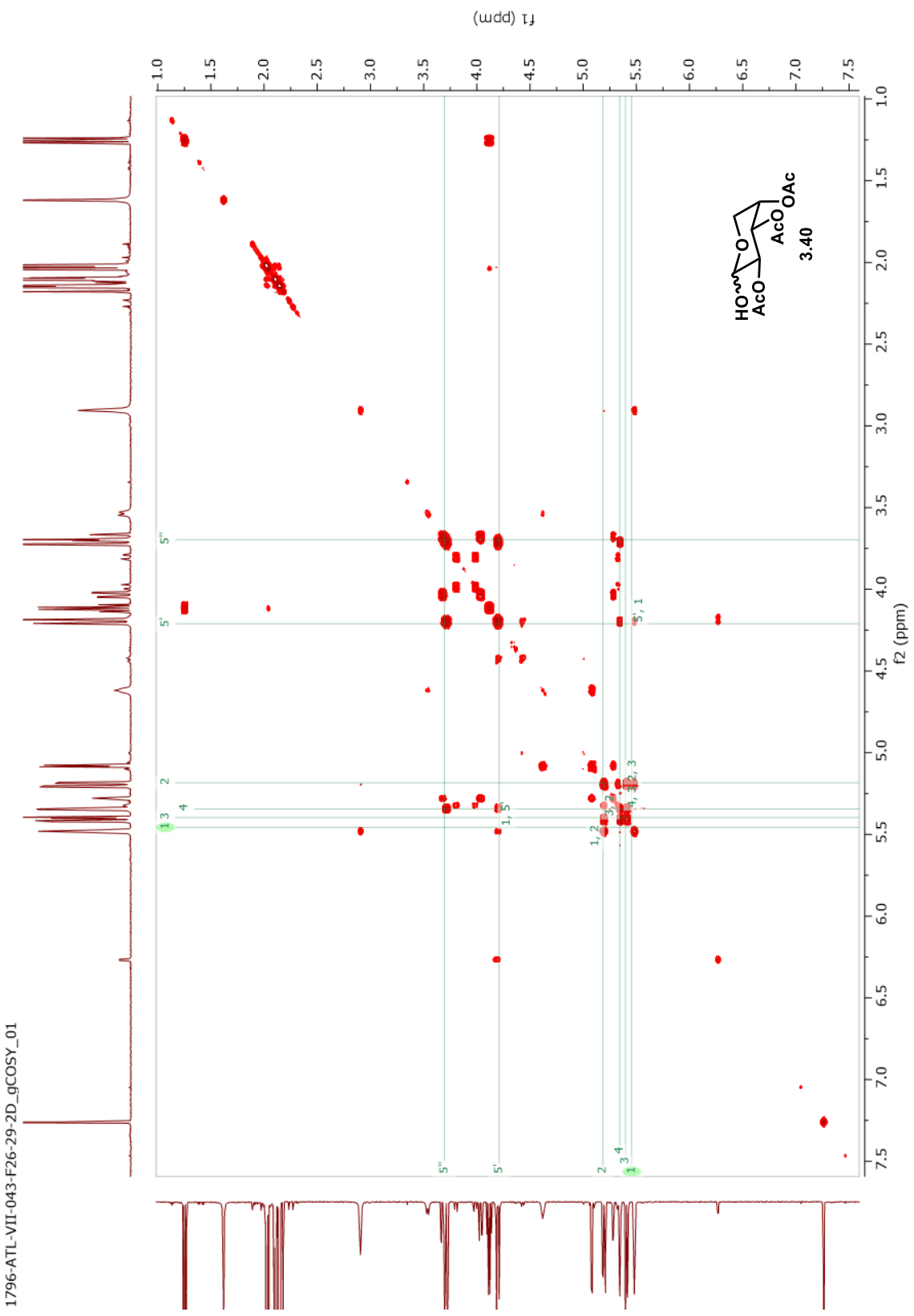
1796-ATL-VII-043-F26-29-2D_gCOSY_01
f1 (ppm)
f2 (ppm)
HO
AcO
O
AcO
OAc
3.40

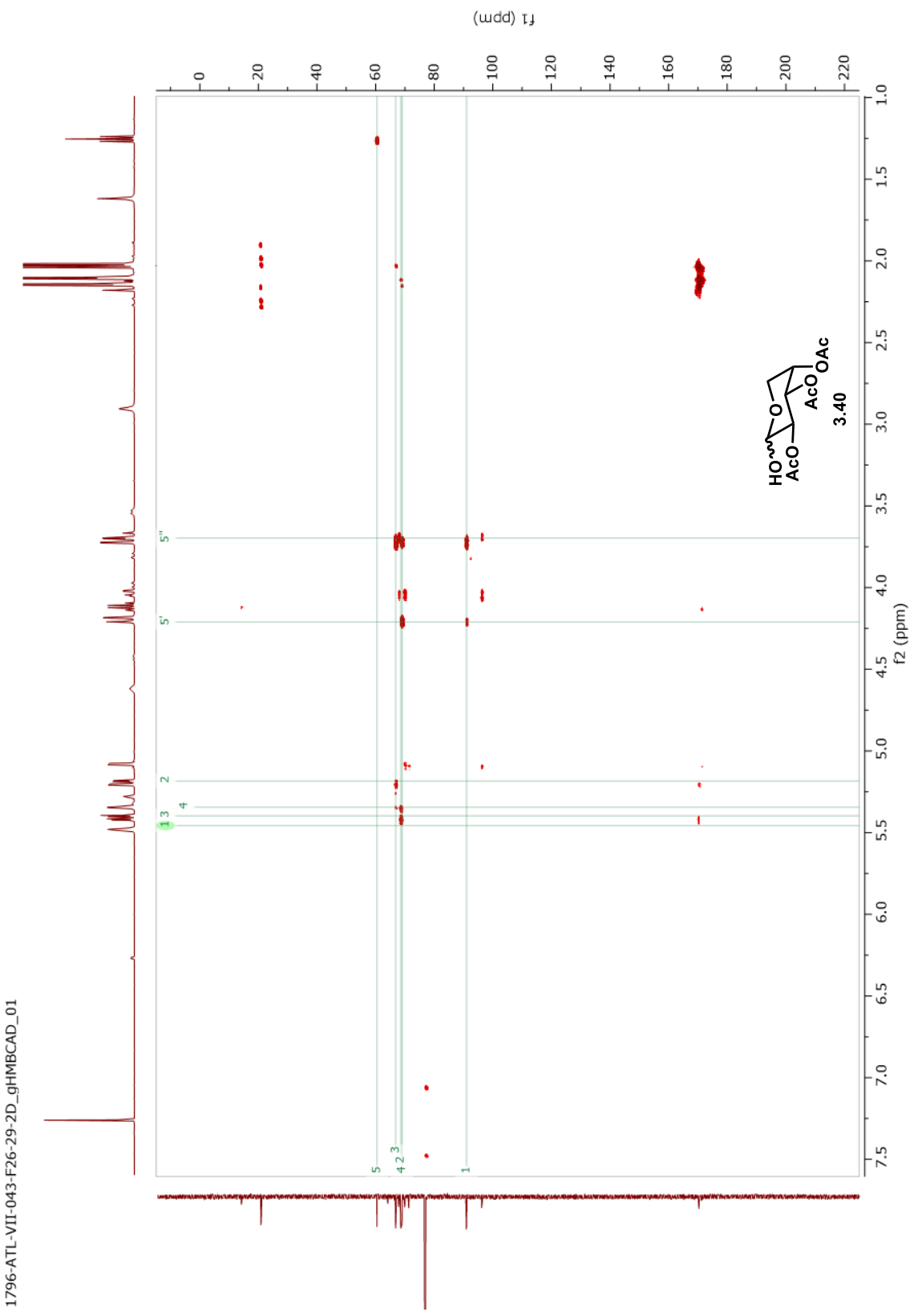
1796-ATL-VII-043-F26-29-2D_gHMBCAD_01
f1 (ppm)
f2 (ppm)
HO
AcO
O
AcO
OAc
3.40

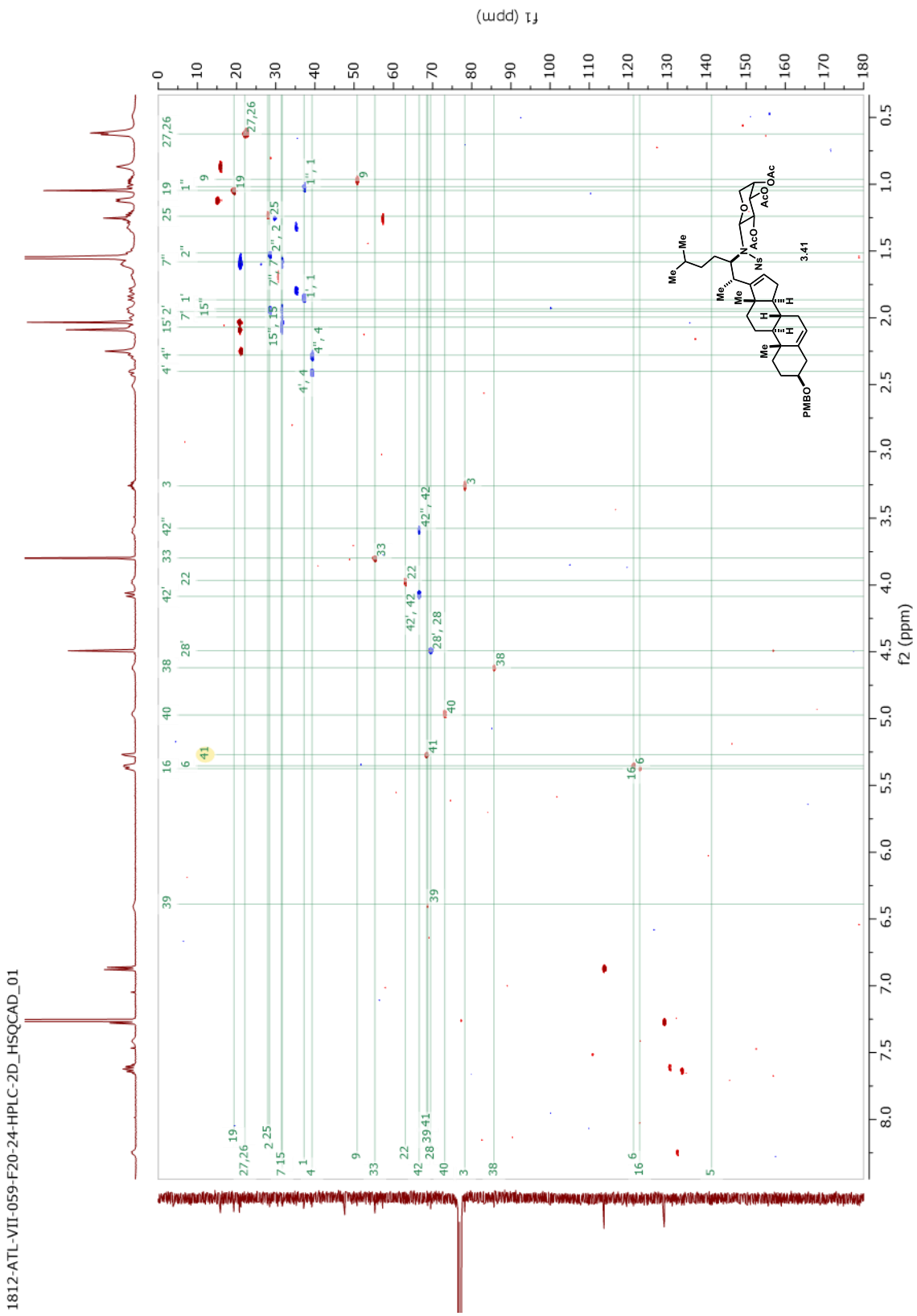
1812-ATL-VII-059-F20-24-HPLC-2D_HSQCAD_01
f1 (ppm)
f2 (ppm)
3.41
PMBO
Ns
AcO
OAc
Me
H

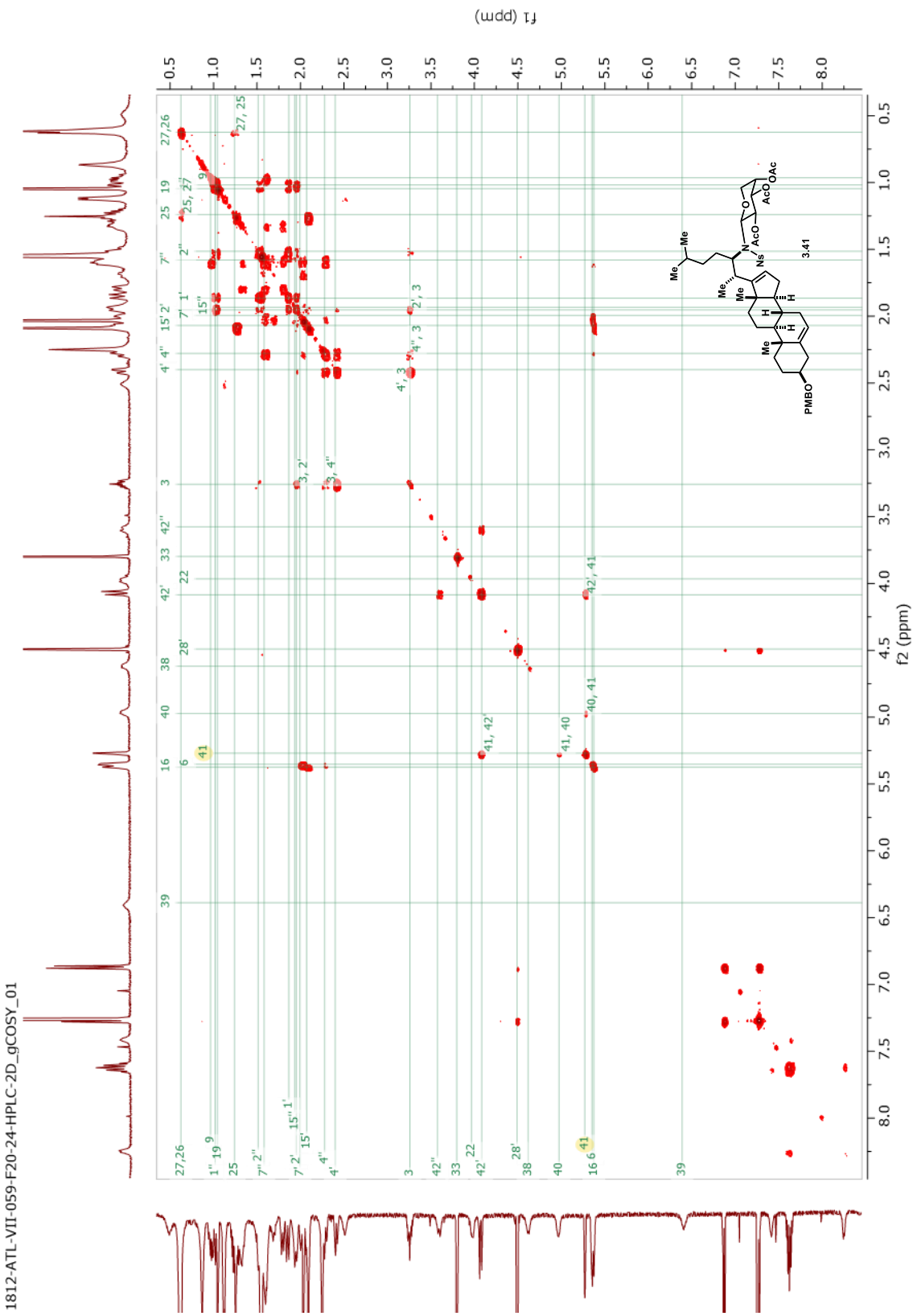
1812-ATL-VII-059-F20-24-HPLC-2D_gCOSY_01
f2 (ppm)
f1 (ppm)
PMBO
3.41

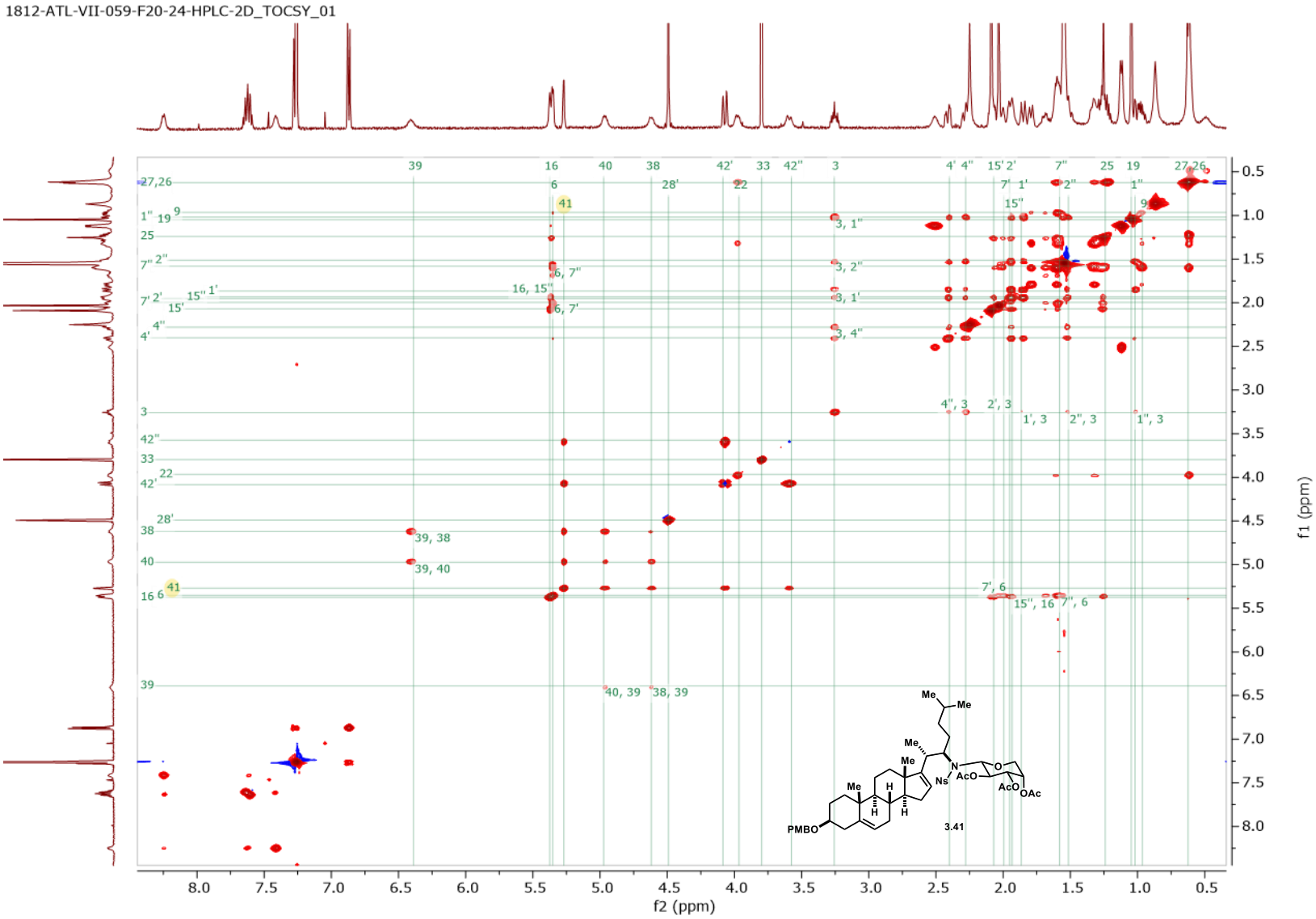
1812-ATL-VII-059-F20-24-HPLC-2D_TOCSY_01
f2 (ppm)
f1 (ppm)
PMBO
Ns
AcO
AcO
OAc
3.41

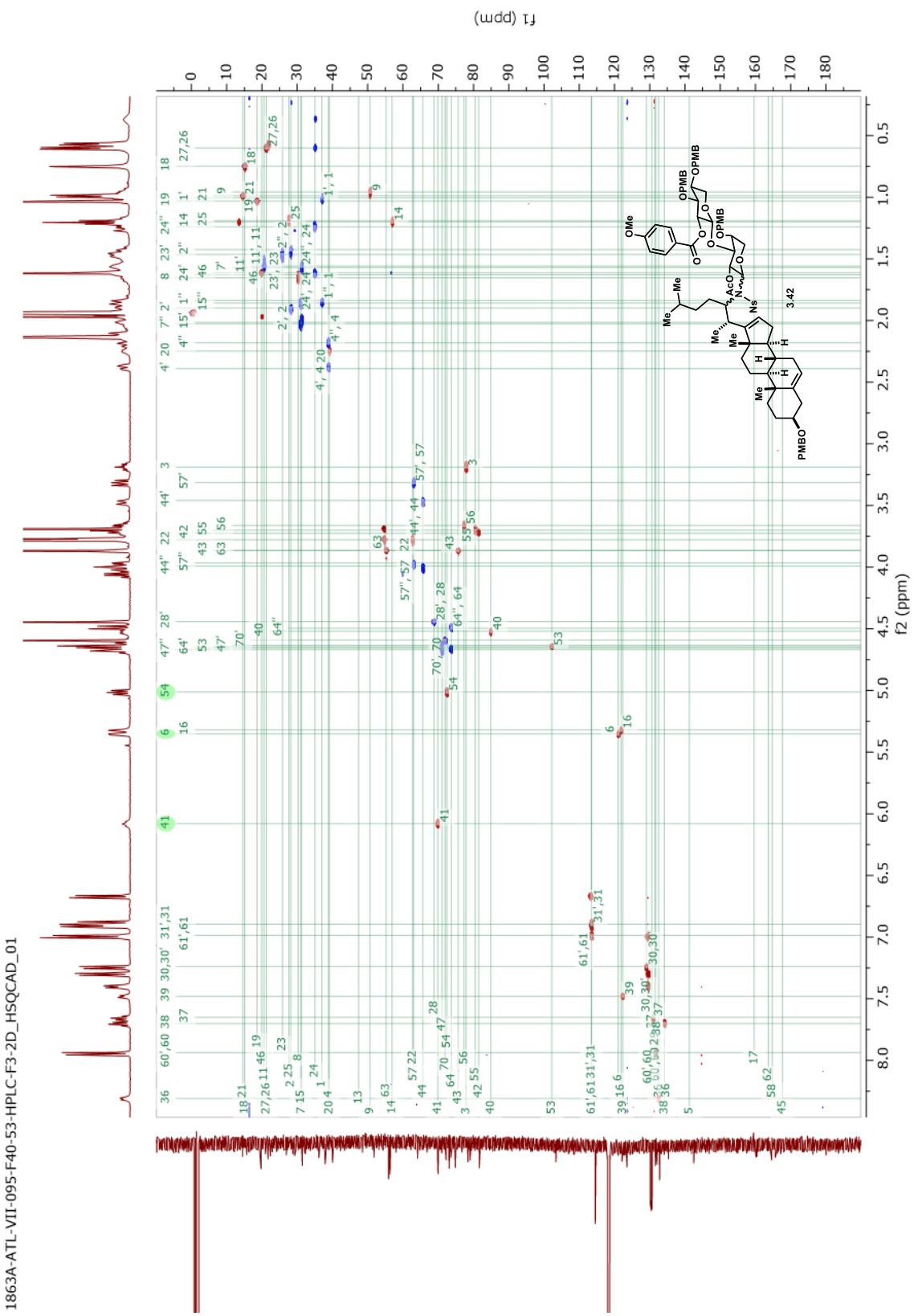
1863A-ATL-VII-095-F40-53-HPLC-F3-2D_HSQCAD_01
f2 (ppm)
f1 (ppm)
OPMB
OMe
PMBO
Ns
AcO
Me
H
3.42

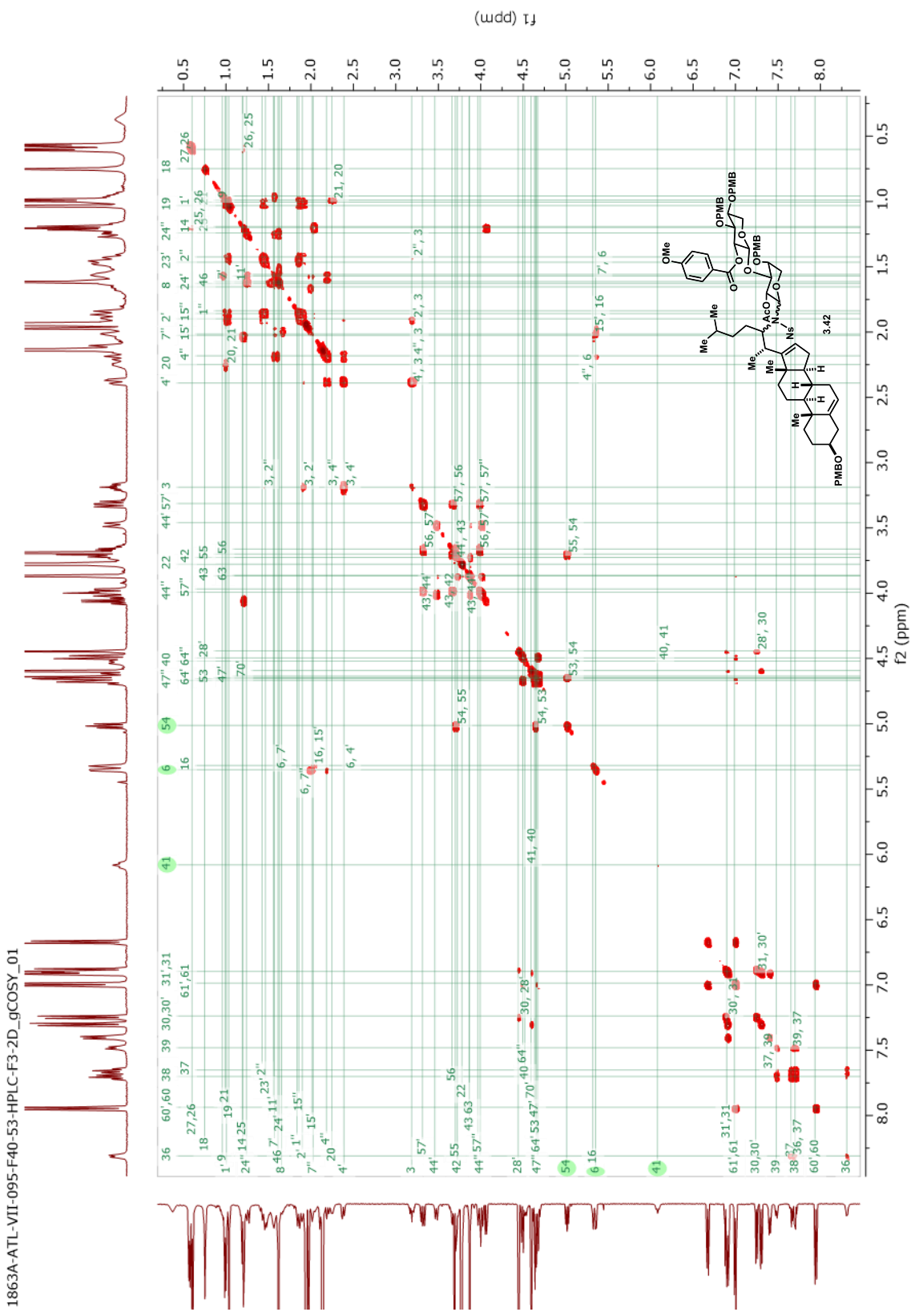
1863A-ATL-VII-095-F40-53-HPLC-F3-2D_gCOSY_01
f2 (ppm)
f1 (ppm)
OMe
OPMB
OPMB
OPMB
AcO
Ns
Me
Me
Me
Me
Me
H
H
H
3.42
PMBO

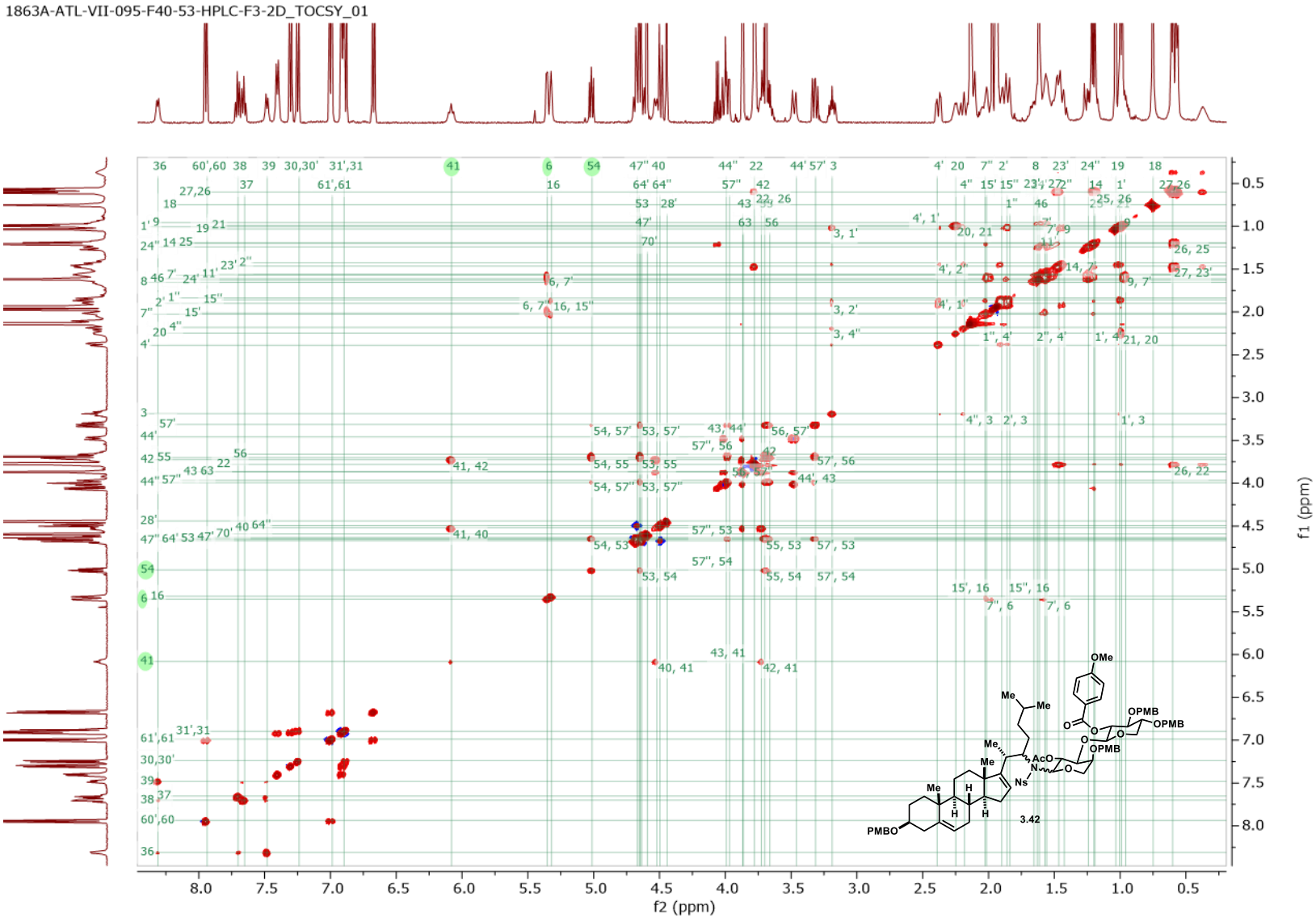
1863A-ATL-VII-095-F40-53-HPLC-F3-2D_TOCSY_01
f2 (ppm)
f1 (ppm)
3.42

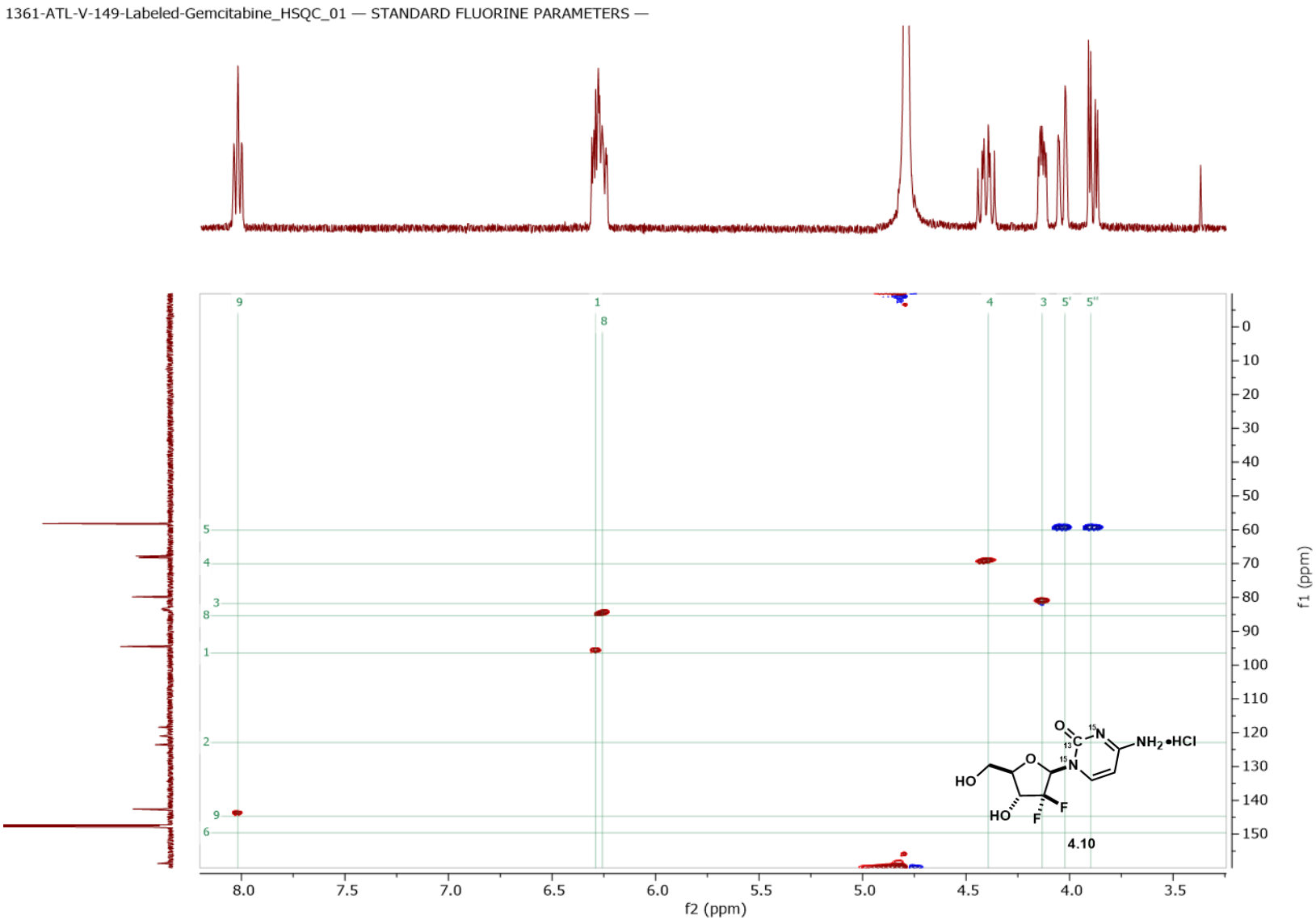
1361-ATL-V-149-Labeled-Gemcitabine_HSQC_01 — STANDARD FLUORINE PARAMETERS —
f2 (ppm)
f1 (ppm)
4.10

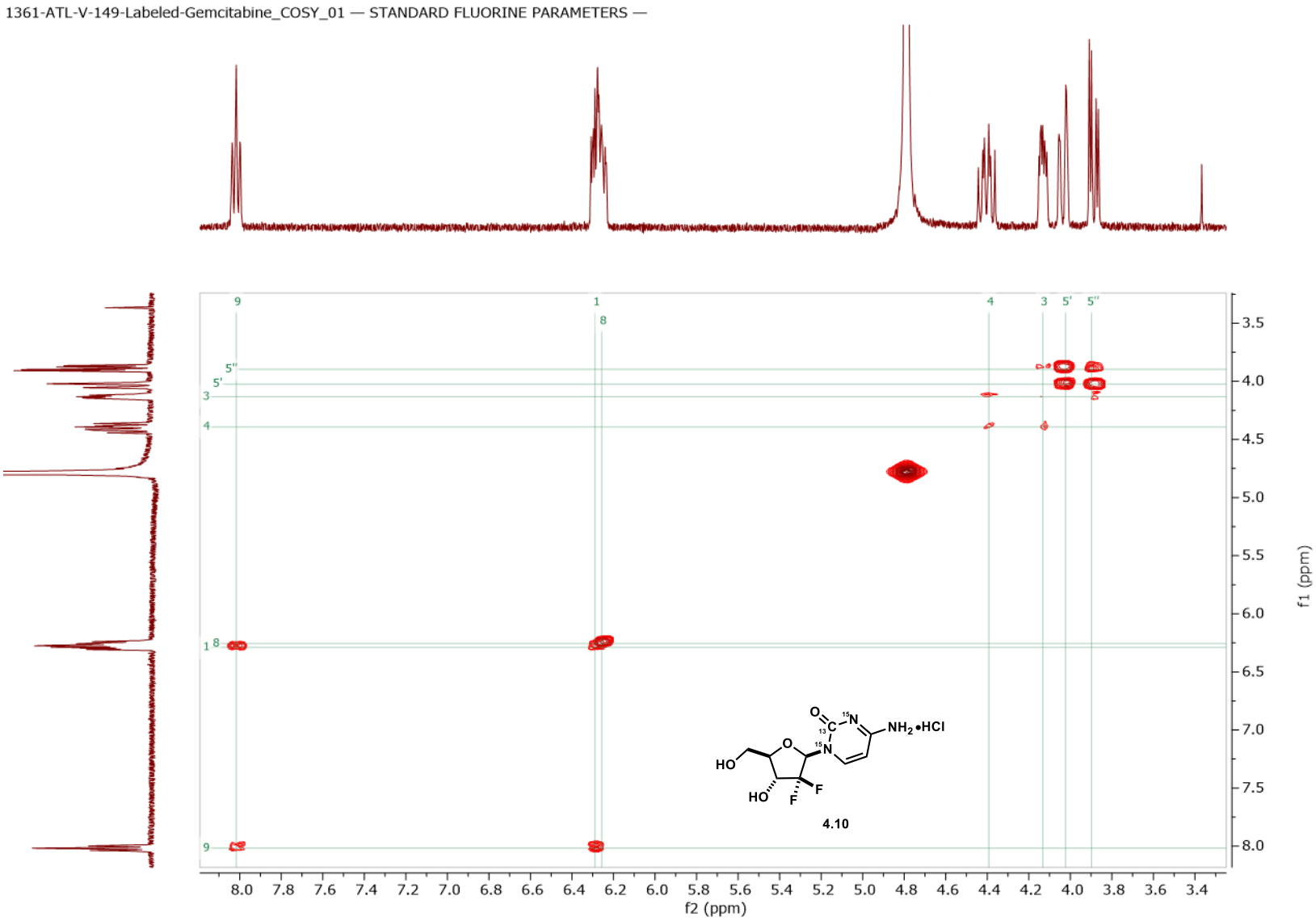
1361-ATL-V-149-Labeled-Gemcitabine_COSY_01 — STANDARD FLUORINE PARAMETERS —
9
1
8
4
3
5'
5''
3
4
1
8
9
HO
HO
F
F
NH2•HCl
4.10
f2 (ppm)
f1 (ppm)

References

1. Sparg, S. G., Light, M. E. & Van Staden, J. Biological activities and distribution of plant saponins. *J. Ethnopharmacol.* **94,** 219–243 (2004).
2. Challinor, V. L. & De Voss, J. J. Open-chain steroidal glycosides, a diverse class of plant saponins. *Nat. Prod. Rep.* **30,** 429–454 (2013).
3. Kubo, S., Mimaki, Y., Terao, M. & Sashida, Y. Acylated cholestane glycosides from the bulbs of. *Phytochemistry* **31,** 3969–3973 (1992).
4. Tang, Y., Li, N., Duan, J. & Tao, W. Structure, bioactivity, and chemical synthesis of OSW-1 and other steroidal glycosides in the genus Ornithogalum. *Chem. Rev.* **113,** 5480–514 (2013).
5. Iguchi, T. *et al.* Structural characterization of cholestane rhamnosides from ornithogalum saundersiae bulbs and their cytotoxic activity against cultured tumor cells. *Molecules* **22,** 1–21 (2017).
6. Kuroda, M., Mimaki, Y., Yokosuka, A., Hasegawa, F. & Sashida, Y. Cholestane glycosides from the bulbs of Ornithogalum thyrsoides and their cytotoxic activity against HL-60 leukemia cells. *J. Nat. Prod.* **65,** 1417–1423 (2002).
7. Kuroda, M., Mimaki, Y. & Sashida, Y. Cholestane rhamnosides from the bulbs of Ornithogalum saundersiae. *Phytochemistry* **52,** 445–452 (1999).

8. Mimaki, Y. *et al.* A New Cytotoxic Cholestane Bisdesmoside from *Ornithogalum saundersiae* Bulbs. *Biosci. Biotechnol. Biochem.* **60,** 1049–1050 (1996).

9. Mimaki, Y. *et al.* Cholestane Glycosides with Potent Cytostatic Activites on Various Tumor Cells from Ornithogalum saundersiae Bulbs. *Bioorg. Med. Chem. Lett.* **7,** 633–636 (1997).

10. Burgett, A. W. G. *et al.* Natural products reveal cancer cell dependence on oxysterol-binding proteins. *Nat. Chem. Biol.* **7,** 639–47 (2011).

11. Albulescu, L. *et al.* Broad-range inhibition of enterovirus replication by OSW-1, a natural compound targeting OSBP. *Antiviral Res.* **117,** 110–114 (2015).

12. Schenk, T. *et al.* Screening of Natural Products Extracts for the Presence of Phosphodiesterase Inhibitors Using Liquid Chromatography Coupled Online to Parallel Biochemical Detection and Chemical Characterization. *J. Biomol. Screen.* **8,** 421–429 (2003).

13. Rabow, A. A., Shoemaker, R. H., Sausville, E. A. & Covell, D. G. Mining the National Cancer Institute's Tumor-Screening Database: Identification of Compounds with Similar Cellular Activities. *J. Med. Chem.* **45,** 818–840 (2002).

14. Pettit, G. R. *et al. Isolation and Structure of the Powerful Cell Growth*

Inhibitor Cephalostatin. *J. Am. Chem. Soc* **110,** (Academic Press, 1988).

15. Komiya, T. *et al.* Ritterazine B, a new cytotoxic natural compound, induces apoptosis in cancer cells. *Cancer Chemother. Pharmacol.* **51,** 202–208 (2003).
16. Beutler, J. A., Shoemaker, R. H., Johnson, T. & Boyd, M. R. Cytotoxic Geranyl Stilbenes from Macaranga schweinfurthii. *J. Nat. Prod.* **61,** 1509–1512 (1998).
17. Tasdemir, D. *et al.* Bioactive Isomalabaricane Triterpenes from the Marine Sponge Rhabdastrella globostellata. *J. Nat. Prod.* **65,** 210–214 (2002).
18. Weber-Boyvat, M., Zhong, W., Yan, D. & Olkkonen, V. M. Oxysterol-binding proteins: functions in cell regulation beyond lipid metabolism. *Biochem. Pharmacol.* **86,** 89–95 (2013).
19. Kentala, H., Weber-Boyvat, M. & Olkkonen, V. M. OSBP-Related Protein Family: Mediators of Lipid Transport and Signaling at Membrane Contact Sites. *Int. Rev. Cell Mol. Biol.* **321,** 299–340 (2016).
20. Kandutschs, A. A. & Thompson, E. B. Cytosolic Proteins That Bind Oxygenated Sterols- Cellular Distribution, Specificity, and some

Properties. *J. Biol. Chem.* **255,** 10813–10826 (1980).

21. Jaworski, C. J., Moreira, E., Li, A., Lee, R. & Rodriguez, I. R. A Family of 12 Human Genes Containing Oxysterol-Binding Domains. *Genomics* **78,** 185–196 (2001).
22. Olkkonen, V. M., Zhou, Y., Yan, D. & Vihervaara, T. Oxysterol-binding proteins-emerging roles in cell regulation. *Eur. J. Lipid Sci. Technol.* **114,** 634–643 (2012).
23. Olkkonen, V. M. & Li, S. Oxysterol-binding proteins: Sterol and phosphoinositide sensors coordinating transport, signaling and metabolism. *Prog. Lipid Res.* **52,** 529–538 (2013).
24. Maeda, K. *et al.* Interactome map uncovers phosphatidylserine transport by oxysterol-binding proteins. *Nature* **501,** 257–261 (2013).
25. Tong, J., Yang, H., Yang, H., Eom, S. H. & Im, Y. J. Structure of Osh3 Reveals a Conserved Mode of Phosphoinositide Binding in Oxysterol-Binding Proteins. *Struct. Des.* **21,** 1203–1213 (2013).
26. Lehto, M. *et al.* The OSBP-related protein family in humans. *J. Lipid Res.* **42,** 1203–13 (2001).
27. Moreira, E. F., Jaworski, C., Li, A. & Rodriguez, I. R. Molecular and Biochemical Characterization of a Novel Oxysterol-binding Protein (OSBP2) Highly Expressed in Retina*. *J. Biol. Chem.* **276,** 18570–

18575 (2001).

28. Wyles, J. P., Perry, R. J. & Ridgway, N. D. Characterization of the sterol-binding domain of oxysterol-binding protein (OSBP)-related protein 4 reveals a novel role in vimentin organization. *Exp. Cell Res.* **313,** 1426–1437 (2007).

29. Strating, J. R. P. M. *et al.* Intraconazole Inhibits Enterovirus Replication by Targeting the Oxysterol-binding Protein. *Cell Rep.* **10,** 600–615 (2015).

30. Tapparel, C., Siegrist, F., Petty, T. J. & Kaiser, L. Picornavirus and enterovirus diversity with associated human diseases. *Infect. Genet. Evol.* **14,** 282–293 (2013).

31. Lugo, D. & Krogstad, P. Enteroviruses in the early 21st century: new manifestations and challenges. *Curr. Opin. Pediatr.* **28,** 107–113 (2016).

32. Meutiawati, F. *et al.* Posaconazole inhibits dengue virus replication by targeting oxysterol-binding protein. *Antiviral Res.* **157,** 68–79 (2018).

33. Charman, M., Colbourne, T. R., Pietrangelo, A., Kreplak, L. & Ridgway, N. D. Oxysterol-binding Protein (OSBP)-related Protein 4 (ORP4) Is Essential for Cell Proliferation and Survival. *J. Biol. Chem.* **289,** 15705–15717 (2014).

34. Zhong, W. *et al.* ORP4L is essential for T-cell acute lymphoblastic leukemia cell survival. *Nat. Commun.* **7,** 1–14 (2016).

35. Deng, S., Yu, B., Lou, Y. & Hui, Y. First Total Synthesis of an Exceptionally Potent Antitumor Saponin, OSW-1. *J. Org. Chem.* **64,** 202–208 (1998).

36. Yu, W. & Jin, Z. Total synthesis of the anticancer natural product OSW-1. *J. Am. Chem. Soc.* **124,** 6576–83 (2002).

37. Morzycki, J. W., Gryszkiewicz, A. & Jastrz, I. Neighboring group participation in epoxide ring cleavage in reactions of some 16??,17??-oxidosteroids with lithium hydroperoxide. *Tetrahedron* **57,** 2185–2193 (2001).

38. Ibuka, T. *et al.* New Stereoselective Synthesis of 20S and 20R Steroidal Side Chains. Remarkable Stereoselectivity Differences between Saturated and αβ-Unsaturated Steroidal Esters. *J. Org. Chem.* **53,** 3947–3952 (1988).

39. Morzycki, J. W. & Wojtkielewicz, A. Synthesis of a cholestane glycoside OSW-1 with potent cytostatic activity. *Carbohydr. Res.* **337,** 1269–1274 (2002).

40. Morzycki, J. W., Wojtkielewicz, A. & Wołczyński, S. Synthesis of analogues of a potent antitumor saponin OSW-1. *Bioorganic Med.*

Chem. Lett. **14,** 3323–3326 (2004).

41. Shi, B., Tang, P., Hu, X., Liu, J. O. & Yu, B. OSW saponins: facile synthesis toward a new type of structures with potent antitumor activities. *J. Org. Chem.* **70,** 10354–67 (2005).
42. Tsubuki, M., Matsuo, S. & Honda, T. A new synthesis of potent antitumor saponin OSW-1 via Wittig rearrangement. *Tetrahedron Lett.* **49,** 229–232 (2008).
43. Xue, J. *et al.* A Total Synthesis of OSW-1. *J. Org. Chem.* **2007,** 157–161 (2008).
44. Castro, D. G. De, Clarke, P. A. & Workman, P. Personalized Cancer Medicine : Molecular Diagnostics , Predictive biomarkers , and Drug Resistance. *Clin. Pharmacol. Ther.* **93,** 252–259 (2013).
45. Pan, N. *et al.* The Single-probe: A miniaturized multifunctional device for single cell mass spectrometry analysis. *Anal. Chem.* **86,** 9376–9380 (2014).
46. Koppaka, V. *et al.* Aldehyde Dehydrogenase Inhibitors: a Comprehensive Review of the Pharmacology, Mechanism of Action, Substrate Specificity, and Clinical Application. *Pharmacol. Rev.* **64,** 520–539 (2012).
47. Harper, A. R. *et al.* Design, synthesis, and ex vivo evaluation of a

selective inhibitor for retinaldehyde dehydrogenase enzymes. *Bioorg. Med. Chem.* **26,** 5766–5779 (2018).

48. Thomas, G. & Hall, M. N. TOR signalling and control of cell growth. *Curr. Opin. Cell Biol.* **9,** 782–787 (1997).

49. Zhou, J. & Giannakakou, P. Targeting Microtubules for Cancer Chemotherapy. *Curr. Med. Chem. -Anti-Cancer Agents* **5,** 65–71 (2005).

50. Garbaccio, R. M. & Parmee, E. R. The Impact of Chemical Probes in Drug Discovery: A Pharmaceutical Industry Perspective. *Cell Chem. Biol.* **23,** 10–17 (2016).

51. Herde, Z. D., John, P. D., Alvarez-Fonseca, D., Satyavolu, J. & Burns, C. T. Stereoselective acetylation of hemicellulosic C5-sugars. *Carbohydr. Res.* **443–444,** 1–14 (2017).

52. Maitani, Y., Asano, S., Takahashi, S., Nakagaki, M. & Nagai, T. Selective Monoalkylation of Acyclic Diols by Means of Dibutyltin Oxide and Fluoride Salts. *Chem. Pharm. Bull.* **39,** 1972–1982 (1991).

53. Schmidt, R. R. & Toepfer, A. Glycosylation with highly reactive glycosyl donors: efficiency of the inverse procedure. *Tetrahedron Lett.* **32,** 3353–3356 (1991).

54. Guo, J. & Ye, X. Protecting Groups in Carbohydrate Chemistry:

Influence on Stereoselectivity of Glycosylations. *Molecules* **15,** 7235–7265 (2010).

55. Still, W. C., Kahn, M. & Mitra, A. Rapid chromatographic technique for preparative separations with moderate resolution. *J. Org. Chem.* **43,** 2923–2925 (1978).

56. Magnus, V., Vikić-Topić, D., Iskrić, S. & Kveder, S. Competitive formation of peracetylated α-l-arabinopyranosides and β-l-arabinopyranose 1,2-(alkyl orthoacetates) in Koenigs-Knorr condensations. *Carbohydr. Res.* **114,** 209–224 (1983).

57. Collins, F. S. & Varmus, H. A New Initiative on Prescision Medicine. *N. Engl. J. Med.* **372,** 793–795 (2015).

58. Roychowdhury, S. & Chinnaiyan, A. M. Advancing Precision Medicine for Prostate Cancer Through Genomics. *J. Clin. Oncol.* **31,** 1866–1873 (2018).

59. Li, J.-W. *et al.* Oxysterol-binding protein-related protein 4L promotes cell proliferation by sustaining intracellular Ca 2+ homeostasis in cervical carcinoma cell lines. *Oncotarget* **7,** 65849–65861 (2016).

60. Fournier, M. V *et al.* Identification of a Gene Encoding a Human Oxysterol-binding Protein-Homologue: A Potential General Molecular Marker for Blood Dissemination of Solid Tumors. *Cancer Res.* **59,**

3748–3753 (1999).

61. Henriques Silva, N. *et al.* HLM/OSBP2 is expressed in chronic myeloid leukemia. *Int. J. Mol. Med.* **12,** 663–666 (2003).

62. Arita, M. *et al.* Oxysterol-Binding Protein Family I Is the Target of Minor Enviroxime-Like Compounds. *J. Virol.* **87,** 4252–4260 (2013).

63. Shim, A. *et al.* Therapeutic and prophylactic activity of itraconazole against human rhinovirus infection in a murine model OPEN. *Sci. Rep.* **6,** 23110 (2016).

64. Yang, C. G., Reich, N. W., Shi, Z. & He, C. Intramolecular additions of alcohols and carboxylic acids to inert olefins catalyzed by silver(I) triflate. *Org. Lett.* **7,** 4553–4556 (2005).

65. Sultana, S., Devi, N. R. & Saikia, A. K. Synthesis of Substituted Tetrahydropyrans and Tetrahydrofurans via Intramolecular Hydroalkoxylation of Alkenols. *Asian J. Org. Chem.* **4,** 1281–1288 (2015).

66. Beesley, R. *et al.* Intramolecular Hydroalkoxylation of Unactivated Alkenes Using Silane–Iodine Catalytic System. *Org. Lett.* **17,** 4377–4383 (2015).

67. Morrow, D. F., Culbertson, T. P. & Hofer, R. M. Synthesis of 17-Disubstituted Steroids by the Claisen Rearrangement. *J. Org. Chem.*

32, 361–369 (1967).

68. Scheer, I., Kohen, F. & Mallory, R. A. Rearrangement of 20-substituted bisnorallocholanes and derivatives. *J. Org. Chem.* **36,** 716–718 (1971).

69. Okachi, T., Fujimoto, K. & Onaka, M. Practical Carbonyl-Ene Reactions of r-Methylstyrenes with Paraformaldehyde Promoted by a Combined System of Boron Trifluoride and Molecular Sieves 4A. *Org. Lett.* **4,** 1667–1669 (2002).

70. Houston, T. A., Tanaka, Y. & Koreeda, M. Stereoselective Construction of 22-Oxygenated Steroid Side-Chains by Dimethylaluminum Chloride-Mediated Ene Reactions of Aldehydes. *J. Org. Chem.* **58,** 4287–4292 (1993).

71. Tate, D. J. *et al.* Improved syntheses of high hole mobility phthalocyanines: A case of steric assistance in the cyclo-oligomerisation of phthalonitriles. *Beilstein J. Org. Chem* **8,** 120–128 (2012).

72. Høgmoen Åstrand, O. A. *et al.* Development of new LXR modulators that regulate LXR target genes and reduce lipogenesis in human cell models. *Eur. J. Med. Chem.* **74,** 258–263 (2014).

73. William A. Waters, M.A, SC.D., F. R. S. Mechanisms of Oxidation by

Compounds of Chromium and Manganese. *Q. Rev. Chem. Soc.* **12,** 277–300 (1958).

74. Sager, W. F. & Bradley, A. Oxidation of Triethylmethane and Other Hydrocarbons by Acidified Dichromate. *J. Am. Chem. Soc.* **78,** 1187–1190 (1956).

75. Lemoine, H. & Deguin, B. Mild and Chemoselective Lactone Ring-Opening with (TMS)ONa. Mechanistic Studies and Application to Sweroside Derivatives. *J. Org. Chem.* **79,** 4358–4366 (2014).

76. Jung, M. E. & Piizzi, G. gem-Disubstituent effect: Theoretical basis and synthetic applications. *Chem. Rev.* **105,** 1735–1766 (2005).

77. Maier, M. E. Product Class 6: Lactones. *Sci. Synth.* **20b,** 1421–1551 (2006).

78. Wuitschik, G. *et al.* Oxetanes in Drug Discovery: Structural and Synthetic Insights. *J. Med. Chem* **53,** 3227–3246 (2010).

79. Yamada, K., Fujita, H., Kitamura, M. & Kunishima, M. A practical method for p -methoxybenzylation of hydroxy groups using 2,4,6-tris(p -methoxybenzyloxy)-1,3,5-triazine (TriBOT-PM). *Synth.* **45,** 2989–2997 (2013).

80. Li, B., Zhang, B., Zhang, X. & Fan, X. Synthesis of 3-Cyano-1 *H* -indoles and Their 2′-Deoxyribonucleoside Derivatives through One-

Pot Cascade Reactions. *J. Org. Chem.* **81,** 9530–9538 (2016).

81. Huo, C., Wang, C., Zhao, M. & Peng, S. Stereoselective synthesis of natural N-(1-deoxy-D-β-fructos-1-yl)-L- amino acids and their effect on lead decorporation. *Chem. Res. Toxicol.* **17,** 1112–1120 (2004).
82. Petermichl, M., Loscher, S. & Schobert, R. Total Synthesis of Aurantoside G, an N-β-Glycosylated 3-Oligoenoyltetramic Acid from Theonella swinhoei. *Angew. Chem. Int. Ed.* **55,** 10122–10125 (2016).
83. Kurosawa, W., Kan, T. & Fukuyama, T. Preparation of Secondary Amines From Primary Amines Via 2-Nitrobenzenesulfonamides: N-(4-Methoxybenzyl)-3-Phenylpropylamine. *Org. Synth.* **79,** 186 (2002).
84. Kan, T. & Fukuyama, T. Ns strategies: A highly versatile synthetic method for amines. *Chem. Commun.* **4,** 353–359 (2004).
85. Fletcher, S. The Mitsunobu reaction in the 21 st century. *Org. Chem. Front.* **2,** 739–752 (2015).
86. Watt, G. M., Flitsch, S. L., Fey, S., Elling, L. & Kragl, U. The preparation of deoxy derivatives of mannose-1-phosphate and their substrate specificity towards recombinant GDP-mannose pyrophosphorylase from Salmonella enterica, group B. *Tetrahedron Asymmetry* **11,** 621–628 (2000).
87. Bardin, C. *et al.* Therapeutic drug monitoring in cancer – Are we

missing a trick ? *Eur. J. Cancer.* **50,** 2005–2009 (2014).

88. Sawyer, M. & Ratain, M. J. Body surface area as a determinant of pharmacokinetics and drug dosing. *Invest. New Drugs.* **19**, 171–177 (2001).

89. Kang, J. & Lee, M. Overview of Therapeutic Drug Monitoring. *Korean J. Intern. Med.* **24**, 1–10 (2009).

90. Marusyk, A., Almendro, V. & Polyak, K. Intra-tumour heterogeneity: a looking glass for cancer? *Nat. Publ. Gr.* **12,** 323–334 (2012).

91. Nguyen, L. V, Vanner, R., Dirks, P. & Eaves, C. J. Cancer Stem Cells: An Evolving Concept. *Nat. Rev. Cancer* **12,** 133–143 (2012).

92. Cristofanilli, M. Circulating Tumor Cells, Disease Progression, and Survival in Metastatic Breast Cancer. *Semin. Oncol.* **33,** 9–14 (2006).

93. Balic, M., Williams, A., Lin, H., Datar, R. & Cote, R. J. Circulating Tumor Cells: From Bench to Bedside. *Annu. Rev. Med.* **64,** 31–44 (2013).

94. Zhang, L. & Vertes, A. Single-Cell Mass Spectrometry Approaches to Explore Cellular Heterogeneity. *Angew. Chem. Int. Ed.* **57,** 4466–4477 (2018).

95. Pan, N., Rao, W., Standke, S. J. & Yang, Z. Using dicationic ion-pairing compounds to enhance the single cell mass spectrometry

analysis using the single-probe: A microscale sampling and ionization device. *Anal. Chem.* **88,** 6812–6819 (2016).

96. Dasari, S. & Tschounwou, P. B. Cisplatin in cancer therapy : molecular mechanisms of action. *Eur. J. Pharmacol.* **740,** 364–378 (2015).
97. Dash, A. *et al.* A role for neoadjuvant gemcitabine plus cisplatin in muscle-invasive urothelial carcinoma of the bladder: A retrospective experience. *Cancer* **113,** 2471–2477 (2008).
98. Chou, T. S., Heath, P. C., Poteet, L. M., Lakin, R. E. & Hunt, A. H. Stereospecific Synthesis of 2-Deoxy-2,2-difluororibonolactone and Its Use in the Preparation of 2'-Deoxy-2',2'-difluoro-β-D-ribofuranosyl Pyrimidine Nucleosides: The Key Role of Selective Crystallization. *Synthesis (Stuttg).* 565–570 (1992).
99. Kukushkin, V. Y., Oskarsson, A., Elding, L. I. & Farrell, N. Transition metal complexes and precursors. *Inorg. Synth. Vol 32* **32,** 141–228 (1998).
100. Berners-Price, S. J., Ronconi, L. & Sadler, P. J. Insights into the mechanism of action of platinum anticancer drugs from multinuclear NMR spectroscopy. *Prog. Nucl. Magn. Reson. Spectrosc.* **49,** 65–98 (2006).
101. Petruzzella, E., Chirosca, C. V., Heidenga, C. S. & Hoeschele, J. D.

Microwave-assisted synthesis of the anticancer drug cisplatin, *cis*-[$Pt(NH_3)_2Cl_2$]. *Dalt. Trans.* **44,** 3384–3392 (2015).

102. Appleton, T., Hall, J. & Ralph, S. Nitrogen-15 and platinum-195 NMR spectra of platinum ammine complexes: trans- and cis-influence series based on platinum-195-nitrogen-15 coupling constants and nitrogen-15 chemical shifts. *Inorg. Chem.* **24,** 4685–4693 (1985).
103. Jackson, B. *et al.* Update on the aldehyde dehydrogenase gene (ALDH) superfamily. *Hum. Genomics* **5,** 283–303 (2011).
104. Januchowski, R., Wojtowicz, K. & Zabel, M. The role of aldehyde dehydrogenase (ALDH) in cancer drug resistance. *Biomed. Pharmacother.* **67,** 669–680 (2013).
105. Jelski, W. & Szmitkowski, M. Alcohol dehydrogenase (ADH) and aldehyde dehydrogenase (ALDH) in the cancer diseases. *Clin. Chim. Acta* **395,** 1–5 (2008).
106. Grünblatt, E. & Riederer, P. Aldehyde dehydrogenase (ALDH) in Alzheimer's and Parkinson's disease. *J. Neural Transm.* **123,** 83–90 (2016).
107. Thomasson, H. R., Crabb, D. W., Edenberg, H. J. & Li, T. K. Alcohol and aldehyde dehydrogenase polymorphisms and alcoholism. *Behav. Genet.* **23,** 131–136 (1993).

108. Niederreither, K., Fraulob, V., Garnier, J. M., Chambon, P. & Dollé, P. Differential expression of retinoic acid-synthesizing (RALDH) enzymes during fetal development and organ differentiation in the mouse. *Mech. Dev.* **110,** 165–171 (2001).

109. Chung, S. S. W. & Wolgemuth, D. J. Role of retinoid signaling in the regulation of spermatogenesis. *Cytogenet. Genome Res.* **105,** 189–202 (2004).

110. Chen, Y., Thompson, D. C., Koppaka, V., Jester, J. V. & Vasiliou, V. Ocular aldehyde dehydrogenases: Protection against ultraviolet damage and maintenance of transparency for vision. *Prog. Retin. Eye Res.* **33,** 28–39 (2013).

111. Chanda, B., Ditadi, A., Iscove, N. N. & Keller, G. Retinoic acid signaling is essential for embryonic hematopoietic stem cell development. *Cell* **155,** 215–227 (2013).

112. Ziouzenkova, O. *et al.* Retinaldehyde represses adipogenesis and diet-induced obesity. *Nat. Med.* **13,** 695–702 (2007).

113. Ito, K., Zolfaghari, R., Hao, L. & Ross, A. C. Inflammation rapidly modulates the expression of ALDH1A1 (RALDH1) and vimentin in the liver and hepatic macrophages of rats in vivo. *Nutr. Metab.* **11,** (2014).

114. Summers Rada, J. A., Hollaway, L. R., Lam, W., Li, N. & Napoli, J. L. Identification of RALDH2 as a visually regulated retinoic acid synthesizing enzyme in the chick choroid. *Investig. Ophthalmol. Vis. Sci.* **53,** 1649–1662 (2012).

115. Harper, A. R., Wang, X., Moiseyev, G., Ma, J. X. & Summers, J. A. Postnatal chick choroids exhibit increased retinaldehyde dehydrogenase activity during recovery from form deprivation induced myopia. *Investig. Ophthalmol. Vis. Sci.* **57,** 4886–4897 (2016).

116. Parajuli, B., Georgiadis, T. M., Fishel, M. L. & Hurley, T. D. Development of selective inhibitors for human aldehyde dehydrogenase 3A1 (ALDH3A1) for the enhancement of cyclophosphamide cytotoxicity. *ChemBioChem* **15,** 701–712 (2014).

117. Morgan, C. A. & Hurley, T. D. Characterization of two distinct structural classes of selective aldehyde dehydrogenase 1A1 inhibitors. *J. Med. Chem.* **58,** 1964–1975 (2015).

118. Amory, J. K. *et al.* Suppression of spermatogenesis by bisdichloroacetyldiamines is mediated by inhibition of testicular retinoic acid biosynthesis. *J. Androl.* **32,** 111–119 (2011).

119. Paik, J. *et al.* Inhibition of retinoic acid biosynthesis by the bisdichloroacetyldiamine WIN 18,446 markedly suppresses

spermatogenesis and alters retinoid metabolism in mice. *J. Biol. Chem.* **289,** 15104–15117 (2014).

120. Asa, C. S. *et al.* Efficacy, Safety, and Reversibility of a Bisdiamine Male-Directed Oral Contraceptive in Gray Wolves (Canis lupus). *J. Zoo Wildl. Med.* **27,** 501–506 (1996).
121. Munson, L., Chassy, L. M. & Asa, C. Efficacy, safety and reversibility of bisdiamine as a male contraceptive in cats. *Theriogenology* **62,** 81–92 (2004).
122. Heller, C. G., Moore, D. J. & Paulsen, C. A. Suppression of spermatogenesis and chronic toxicity in men by a new series of bis(dichloroacetyl) diamines. *Toxicol. Appl. Pharmacol.* **3,** 1–11 (1961).
123. Chen, Y. *et al.* Structural Basis of ALDH1A2 Inhibition by Irreversible and Reversible Small Molecule Inhibitors. *ACS Chem. Biol.* **13,** 582–590 (2018).
124. Moore, S. A. *et al.* Sheep liver cytosolic aldehyde dehydrogenase: The structure reveals the basis for the retinal specificity of class I aldehyde dehydrogenases. *Structure* **6,** 1541–1551 (1998).
125. Solladie, G. & Girardin, A. Synthesis of New Aromatic Retinoid Analogues by Low-Valent Titanium Induced Reductive Elimination. *J.*

Org. Chem. **54,** 2620–2628 (1989).

126. Corey, E. J., Gilman, N. W. & Ganem, B. E. New Methods for the Oxidation of Aldehydes to Carboxylic Acids and Esters. *J. Am. Chem. Soc.* **90,** 5616–5617 (1968).

127. Barluenga, J., Llavona, L., Yus, M. & Concellon, J. M. Reactivity of in situ generated dihalomethyllithium towards dicarboxylic acid diesters and lactones: Synthetic applications. *Tetrahedron* **47,** 7875–7886 (1991).